5 17 p

# Recent Experiences in Multidisciplinary Analysis and Optimization

# Recent Experiences in Multidisciplinary Analysis and Optimization

*Compiled by*
Jaroslaw Sobieski
*Langley Research Center*

# PREFACE

This conference publication contains the papers presented at the NASA Symposium on Recent Experiences in Multidisciplinary Analysis and Optimization, held at NASA Langley Research Center, Hampton, Virginia, April 24-26, 1984. The purposes of the symposium were to exchange information about the status of the application of optimization and associated analyses in industry or research laboratories to real life problems, and to examine the directions of future developments.

Within the broad statement of the symposium's purposes, information exchange has encompassed the following:

Examples of successful applications

"Attempt and failure" examples, particularly to describe the reasons for failure and lessons learned

Identification of potential applications and benefits, even though no attempt to apply optimization may have been made as yet

Synergistic effects of optimized interaction and trade-offs occurring among two or more engineering disciplines (e.g., structural engineering and aerodynamics) and/or subsystems in a system (e.g., propulsion and airframe in aircraft)

Traditional organization of a design process as a vehicle for or an impediment to the progress in the design methodology

Computer technology in the context of the foregoing

This information exchange has covered aerospace and other industries as well as universities and government agencies.

The goal of the meeting was to reach a better understanding of the extent to which optimization and the associated analyses are being used, development directions, the future potential, and actions that ought to be taken to realize the potential sooner. That goal was attained and the symposium showed through both the diversity and quality of papers and the active participation of the attendees that the activities in the subject area are vigorous beyond the initial expectations. There was a consensus that multidisciplinary analysis and optimization have an important potential as aids to human intellect in the design process, and that cooperation of industry, academia, and government, under NASA leadership, is needed to realize that potential.

PRECEDING PAGE BLANK NOT FILMED

iii

# CONTENTS

## Part 1

### SESSION 1: INTRODUCTION AND GENERAL CONSIDERATIONS
#### Co-Chairmen: L. A. McCullers and J. Sobieski

### SESSION 2: OPTIMIZATION IN VARIOUS INDUSTRIES
#### Chairman: W. J. Stroud

SESSION 3A:  APPLICATIONS 1
Chairman:  J. H. Starnes, Jr.

SESSION 3B:  APPLICATIONS 2
Chairman:  I. Abel

SESSSION 4:  METHODS AND TOOLS 1
Co-Chairmen:  R. T. Haftka and H. Miura

Part 2*

SESSION 5A:  ROTORCRAFT APPLICATIONS
Co-Chairmen:  C. E. Hammond and R. J. Huston

*Part 2 is presented under separate cover.

---

†Paper not available for publication.

STRUCTURAL SYNTHESIS –
PRECURSOR AND CATALYST

L. A. Schmit
University of California, Los Angeles
Los Angeles, California

## STRUCTURAL SYNTHESIS PROBLEM STATEMENT

Almost 25 years have elapsed since it was recognized that a rather general class of structural design optimization tasks could be posed as nonlinear mathematical programming problems (Ref. 1). Figure 1 shows the nonlinear programming problem statement and its geometric interpretation in terms of a hypothetical two-dimensional design space plot. The use of inequality concepts is essential to the proper statement of most design optimization problems because at the outset it is not usually known how many or which constraints will be critical at the final design. In other words, the design drivers are not known with certainty in advance. In a structural context the constraints represented by Eq. 1 usually include: (A) one behavior constraint for each failure mode in each load condition; (B) side constraints that introduce fabrication and analysis validity limitations as well as "rules of thumb." Posing the structural design optimization task as a nonlinear programming problem makes it possible to consider: multiple load conditions; a wide variety of failure modes (e.g. limitations on stress, strain, displacement, buckling load, natural frequencies, etc.); side constraints; and objective functions other than weight minimization. During the past two decades a great deal of effort has been devoted to learning how to solve the structural synthesis problem efficiently for systems of practical interest. The main theme of this presentation will be to suggest that many of the key ideas that have helped advance the state of the art in structural synthesis may provide useful guidelines for the development of analysis and design tools in other disciplines.

Given the pre-assigned parameters and the load conditions

find the vector of design variables $\vec{D}$ such that

$$g_q(\vec{D}) \geq 0 \; ; \; q\varepsilon Q \quad (1)$$

and

$$M(\vec{D}) \to Min \quad (2)$$

where

$$\vec{D}^T = \lfloor D_1, D_2 \ldots D_I \rfloor \quad (3)$$
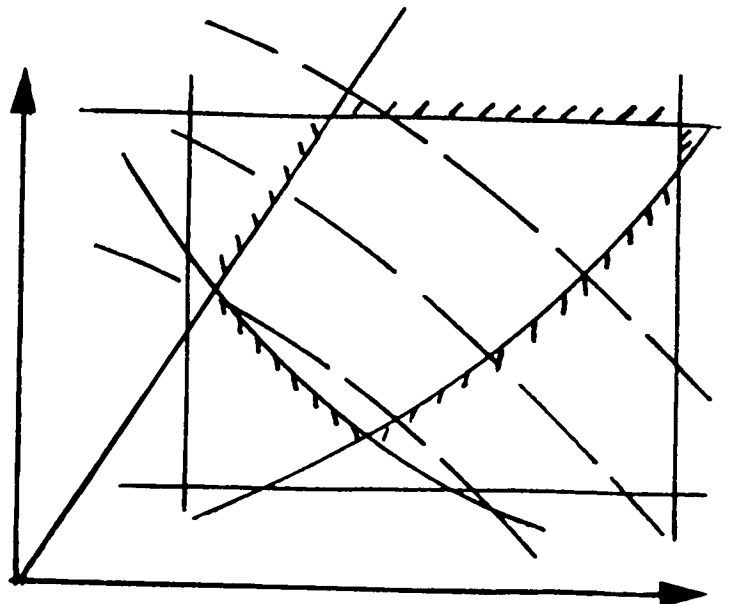


Figure 1

# STRUCTURAL COMPONENT SYNTHESIS (1968)

During the 1960's the structural synthesis concept was successfully applied to structural components of a fundamental and recurring nature (e.g. stiffened plates (see Ref. 2 and 3) and stiffened cylindrical shells (see Ref. 4 and 5)). The structural synthesis capability reported in Ref. 5 for minimum weight optimum design of integrally stiffened clyindrical shells (see Fig. 2a) was state of the art in 1968. In a philosophical sense, it was a precursor of the approximation concepts approach that was to emerge during the 1970's. This problem involved seven design variables (see Fig. 2b), multiple load conditions ($N_k$, $p_k$, $\Delta T_k$,), a rather extensive set of strength and buckling failure modes, and minimum gage and other side constraints. The mathematical programming problem statement was transformed into a sequence of unconstrained minimizations using the Fiacco-McCormick interior penalty function formulation (see Eq. 4, 5 and 6). The constraint repulsion characteristic of this penalty function formulation leads to a sequence of non-critical designs that tend to "funnel down the middle" of the feasible region in design space (see Fig. 2c). This observation led to the idea that approximate analyses could be used during each unconstrained minimization stage, with good expectations that the sequence of designs generated would remain in the actual feasible region. By doing a complete buckling analysis at the beginning of each stage and retaining only the critical and potentially critical mode shapes during each unconstrained minimization, computational efficiency was improved by a factor of 75 while still generating a sequence of positive margin designs with decreasing weight. Dynamically updated constraint deletion techniques that retain only design drivers and potentially critical constraints have and will continue to play an important role in the development of optimum design capabilities for structures as well as multidisciplinary systems.



(a)

(b)

(c)

$$\phi(\vec{D}, r_p) \to \text{Min} \quad (4)$$

$$\phi(\vec{D}, r_p) = M(\vec{D}) + r_p \sum_{q \in Q_R} [1/g_q(\vec{D})] \quad (5)$$

$$r_{p+1} \leftarrow c r_p \quad ; \quad c < 1 \quad (6)$$
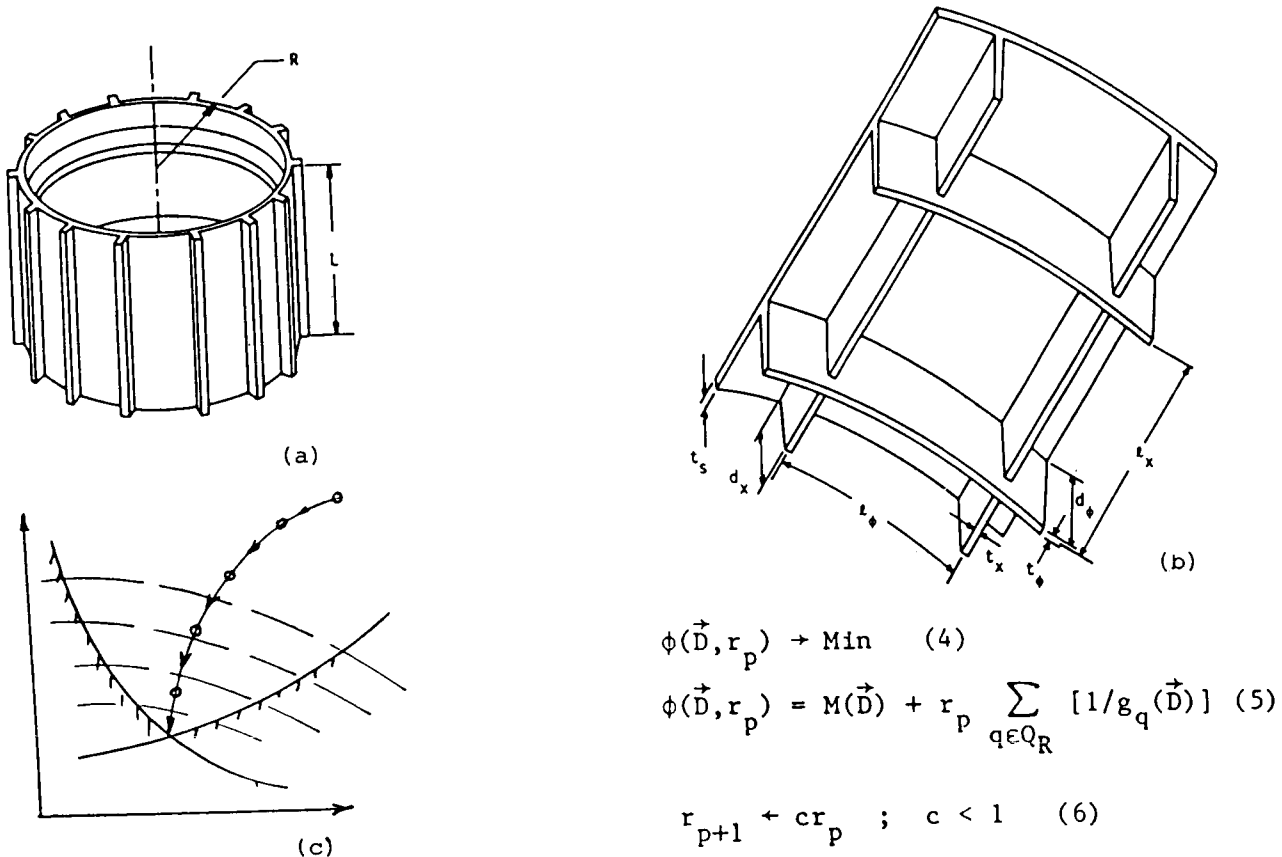
Figure 2

# DESIGN ORIENTED STRUCTURAL ANALYSIS

Interest in developing efficient system level structural synthesis capabilities based on finite element analysis models stimulated research on design oriented structural analysis (DOSA) during the 1965-1975 time period (e.g. see Ref. 6-14). This work was based on the idea that in a design context the objective of structural analysis should be to generate with minimum effort an estimate of the critical and potentially critical response quantities adequate to guide the design modification process. Developments in DOSA fall into three main catagories: (1) behavior sensitivity analysis; (2) reduced basis methods for structural analysis; and (3) reorganization of finite element analysis methods to serve the special characteristics of the design optimization task (see Fig. 3). The basic goal of behavior sensitivity analysis is to obtain information about rates of change of response quantities with respect to changes in design variables. The key to accomplishing this involves implicit differentiation of the governing analysis equations with respect to the design variables, as illustrated by Eqs. 7 and 8 in Fig. 3 for the case of linear static structural analysis via the finite element (displacement) method. When sensitivity derivatives are needed for only a small subset of displacement components, it will be more efficient to employ adjoint methods (see Refs. 15-17). Reduced basis methods in static structural analysis are analogous to the common practice in dynamic analysis of using a reduced set of generalized coordinates and normal mode basis vectors. The basic idea, illustrated by Eqs. 9-12 in Fig. 3 is to use a relatively small number of well chosen basis vectors $\vec{u}_n$ to drastically reduce the number of unknowns in the analysis from J to N. Finite element analysis can be better matched to the needs of the design optimization task. For example, the stiffness matrix K can be formed using precalculated and stored invariant parts $K_0$ and $K_i$ as illustrated by Eq. 12 in Fig. 3. This organization also makes the $\partial K/\partial D_i$ (see Eq. 14), needed for behavior sensitivity analysis (see Eq. 8). already available in storage.

Behavior Sensitivity (Static)

$$K\vec{u} = P \tag{7}$$

$$K\frac{\partial \vec{u}}{\partial D_i} = \frac{\partial \vec{P}}{\partial D_i} - \frac{\partial K}{\partial D_i}\vec{u} \tag{8}$$

Reduced Basis (Analysis)

$$\vec{u} \approx \vec{u}_A = \sum_{n=1}^{N} r_n \vec{u}_n = B\vec{r} \tag{9}$$

$N \ll J = $ DOF's

$$\pi_p \approx \tilde{\pi}_p = \frac{1}{2}\vec{u}_A^T K \vec{u}_A - \vec{u}_A^T \vec{P} \tag{10}$$

$$\pi_p = \frac{1}{2}\vec{r}^T B^T K B\vec{r} - \vec{r}^T B^T \vec{P} \tag{11}$$

$$\delta\tilde{\pi}_p = 0 \rightarrow B^T K B\vec{r} = B^T\vec{P} \tag{12}$$

Finite Element

$$K = K_0 + \sum_{i=1}^{I} D_i K_i \tag{13}$$

Analysis Organization

$$\frac{\partial K}{\partial D_i} = K_i \text{ (invariant)} \tag{14}$$

Figure 3

## ANALYSIS MODEL - DESIGN MODEL

When dealing with large system level design optimization problems it is very important to distinguish between the analysis model and the design model. While Fig. 4 illustrates this idea in terms of a structural system, it should be apparent that analogous distinctions exist in other areas (e.g. aerodynamic design, thermal design, etc.). Generating a structural analysis model usually involves idealization and discretization. In the context of the finite element method, idealization refers to selecting the kinds of elements and discretization refers to deciding on the number and distribution of finite elements and displacement degrees of freedom (DOF's) (see Fig. 4a). Once these decisions have been made, the structural analysis problem has a definite mathematical form. Establishing the design model involves another important set of decisions, namely: (1) deciding on the kind, number, and distribution of design variables; (2) identifying the load conditions and constraints to be considered during the design optimization; and (3) selecting the objective function. This process may be viewed as somewhat analogous to making the judgements that lead to the analysis model. A schematic representation of three alternate skin design models is shown in Fig. 4b. Limitations on the number of independent design variables are often imposed by symmetry, fabrication, and cost control considerations. In many structural design optimization problems the number of finite elements needed in the analysis model (to adequately predict behavior) is much larger than the number of design variables required to describe the practical design problem of interest. In some problems involving substantial changes in configuration it may be necessary to dynamically update the analysis model as the design evolves (e.g. see Ref. 18). In any event, it should be recognized that analysis modeling and design modeling involve two distinct but interrelated sets of decisions.
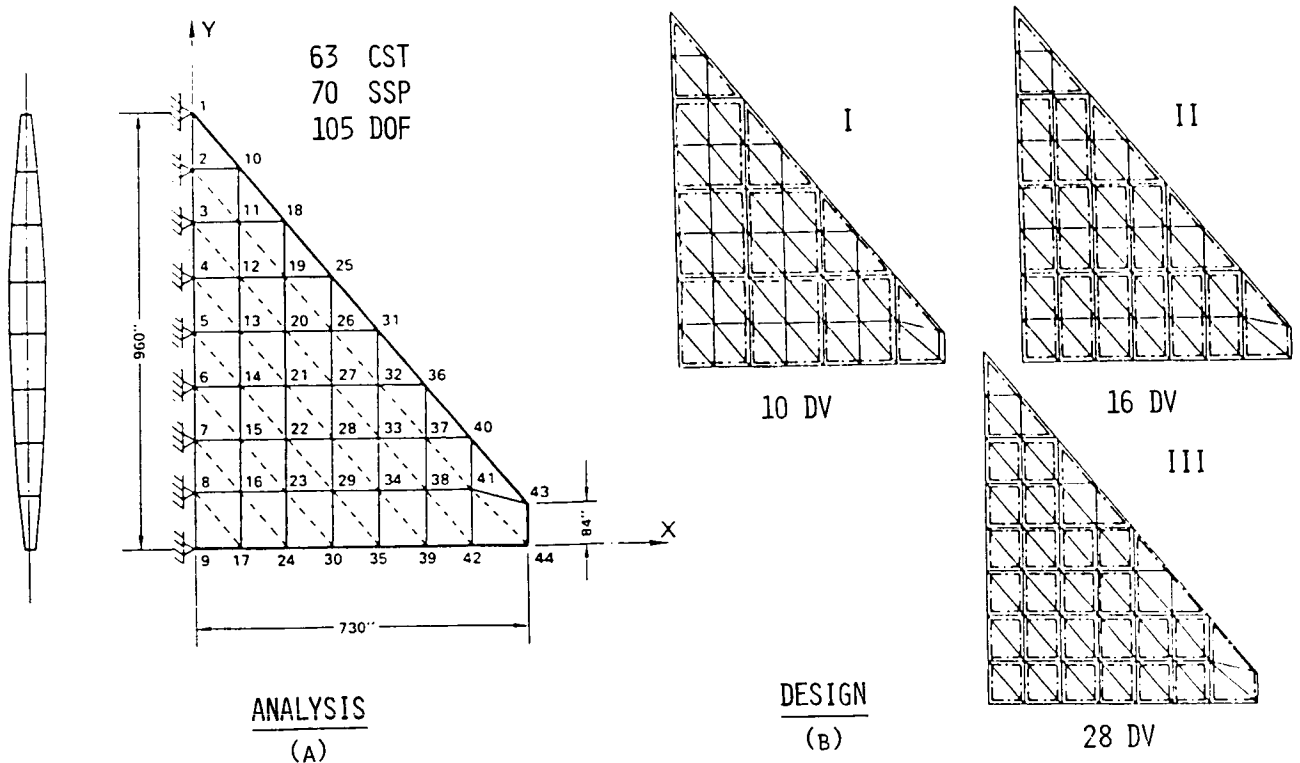
Figure 4

## KEY TO A TRACTABLE FORMULATION

Prior to 1970, the main obstacles to the development of large scale structural synthesis capabilities were associated with the fact that the general formulation (see Fig. 1, Eqs. 1 and 2) involved: (1) large numbers of design variables; (2) large numbers of inequality constraints; and (3) many behavior constraint functions that are computationally burdensome implicit functions of the design variables. During the 1970's these obstacles were overcome by replacing the initial problem statement with a sequence of relatively small, algebraically explicit, approximate problems that preserve the essential features of the original design optimization task (e.g. see Refs. 19 - 25). As indicated schematically in Fig. 5 this was accomplished through the coordinated use of approximation concepts such as: (1) reducing the number of independent design variables by linking and/or basis reduction; (2) reducing the number of constraints considered at each stage by temporary deletion of inactive or redundant constraints; and (3) constructing high quality explicit approximations for retained constraint functions (via the use of Taylor series expansions in terms of insightfully selected intermediate variables).

Find $\vec{D}$ such that

$g_q(\vec{D}) \geq 0$ ; $q \epsilon Q$

and

$M(D) \to MIN$

__Basic Problem__

→

Linking

Basis Reduction

Constraint

Deletion

Explicit

Constraints

__Approximation__

__Concepts__

→

Find $\vec{\delta}$ such that

$\tilde{h}_q^{(p)}(\vec{\delta}) \geq 0$ ; $q \epsilon Q_R^{(p)}$

and

$W(\vec{\delta}) \to MIN$

__Approximate__

__Problem__
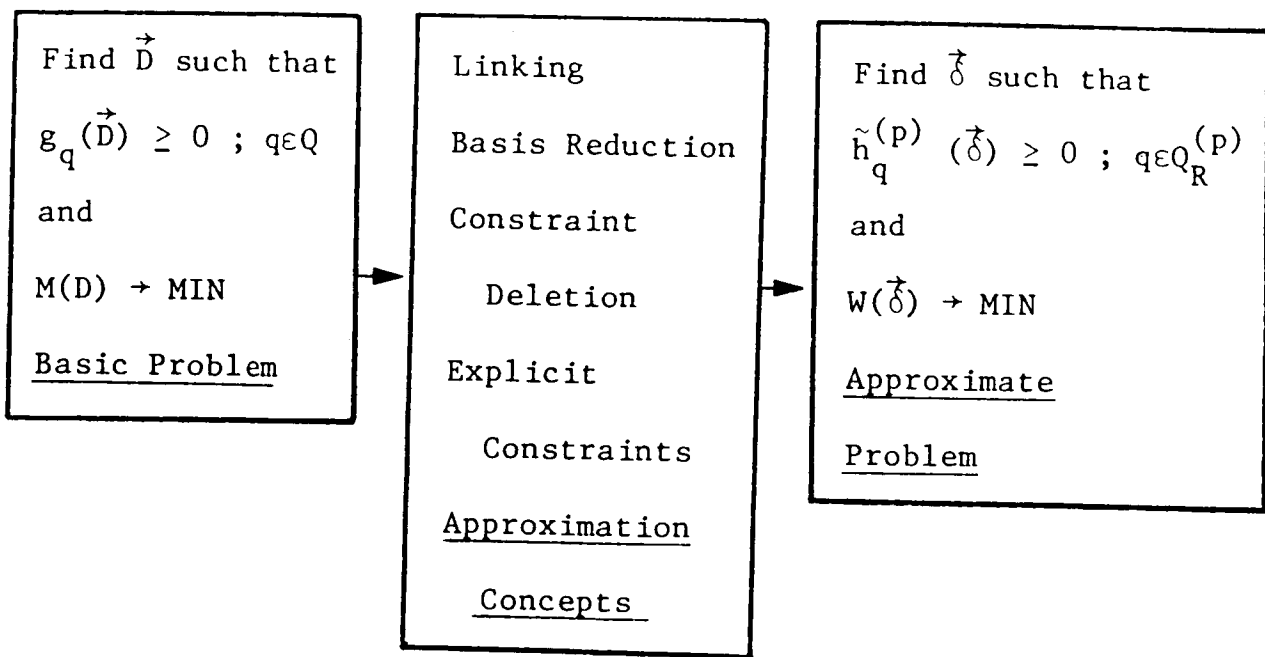
Figure 5

## APPROXIMATION CONCEPTS

In its simplest form, design variable linking fixes the relative sizes of some preselected group of finite elements. The reduced basis concept in design space further reduces the number of independent design variables by expressing the vector of I design variables $\vec{D}$ as a linear combination of B prelinked basis vectors $\vec{T}_b$, where B<<I (see Eq. 15, Fig. 6). Constraint deletion techniques such as **regionalization** and **truncation** represent computer implementation of conventional design practice. Regionalization is a scheme in which, for a specified region (e.g., all those elements linked to a particular design variable $\delta_b$), only one constraint (the most critical) is retained for each loading condition. The truncation idea simply involves temporary deletion of constraints for which the response ratio $R_q(\vec{D})$ (see Eq. 16, Fig. 6) is so low that the corresponding constraint will be inactive. In Eq. 16, Fig. 6) only those behavior constraints with response ratios greater than c are retained in the reduced set of constraints denoted by $q\epsilon Q_R^{(p)}$. Also, in the case of linear constraints it is often possible to identify strictly critical constraints and they can be permanently deleted. When seeking high quality explicit approximations it is important to appreciate the flexibility offered by Taylor series expansions in terms of insightfully selected intermediate variables $[x_b=f_b(\delta_b)]$. Equation 17, Fig. 6 shows a general **second-order** Taylor series expansion for the constraint $g_q$ in terms of intermediate design variables $\vec{X}$. This expression can be specialized and in the context of structural systems, **first-order, second-order diagonal (separable), and full second-order** approximations have been used. The use of reciprocal design variables has been notably successful in generating high quality explicit approximations for displacement constraints. Finally, it should be noted that in some instances it may be preferable to generate Taylor series expansions for response quantities while preserving the explicit nonlinearity inherent to the constraint function when it is expressed in terms of response quantities.

## Linking and Basic Reduction

$$\vec{D} = [L][R]\vec{\delta} = [T]\vec{\delta} = \sum_{b=1}^{B} \vec{T}_b \, \delta_b \qquad (15)$$

## Constraint Deletion

$$g_q(\vec{D}) = 1 - R_q(\vec{D}) \geq 0 \quad ; \quad R_q(\vec{D}) = \frac{f_q(\vec{D})}{f_{qa}} \geq c \quad ; \quad q\epsilon Q_R^{(p)} \qquad (16)$$

## Explicit Constraints

$$g_q(\vec{X}) \approx \tilde{g}_q(\vec{X}) = g_q(\vec{X}^{(p)}) + (\vec{X} - \vec{X}^{(p)})^T \, \nabla g_q(\vec{X}^{(p)})$$

$$+ \frac{1}{2} (\vec{X} - \vec{X}^{(p)})^T \, [\frac{\partial^2 g_q}{\partial x_b \partial x_c} (\vec{X}^{(p)})] \, (\vec{X} - \vec{X}^{(p)}) \qquad (17)$$

Figure 6

## APPROXIMATION CONCEPTS BLOCK DIAGRAM

The approximation concepts approach to design optimization is shown in Fig. 7. This basic approach has been and continues to be used in developing modern structural design optimization capabilities; however it is potentially applicable to a much wider range of engineering design optimization problems. The approach outlined in Fig. 7 is modular and it combines the previously discussed approximation concepts and existing nonlinear programming algorithms. The "preprocessor" computes and stores all necessary information that is independent of the design variable values. A typical stage in the iterative design process begins with the control block supplying a "trial design" to the "approximate problem generator" (APG). Upon leaving the APG block, the current approximate problem statement is passed through "design process control" and handed off to the "optimization algorithm" block, along with a set of trial values for the design variables. This approximate problem is explicit and relatively small, therefore it can be solved using well-established algorithms. Furthermore, the approximate problem often has a special algebraic structure (e.g. convex, separable, quadratic, linear, etc.) which facilitates efficient solution via the use of special purpose techniques such as dual method algorithms (e.g. see Refs. 26-30). Once the "optimization algorithm" block has generated an improved design, it is passed back to the "design process control" block where it becomes the trial design for the next stage of the iterative design process outlined in Fig. 7. The multistage process is usually terminated by a diminishing returns criterion with respect to further improvement in the objective function. For a significant class of minimum weight structural sizing problems, it has been shown that practical convergence can be achieved using only 5 to 10 full finite element analyses.
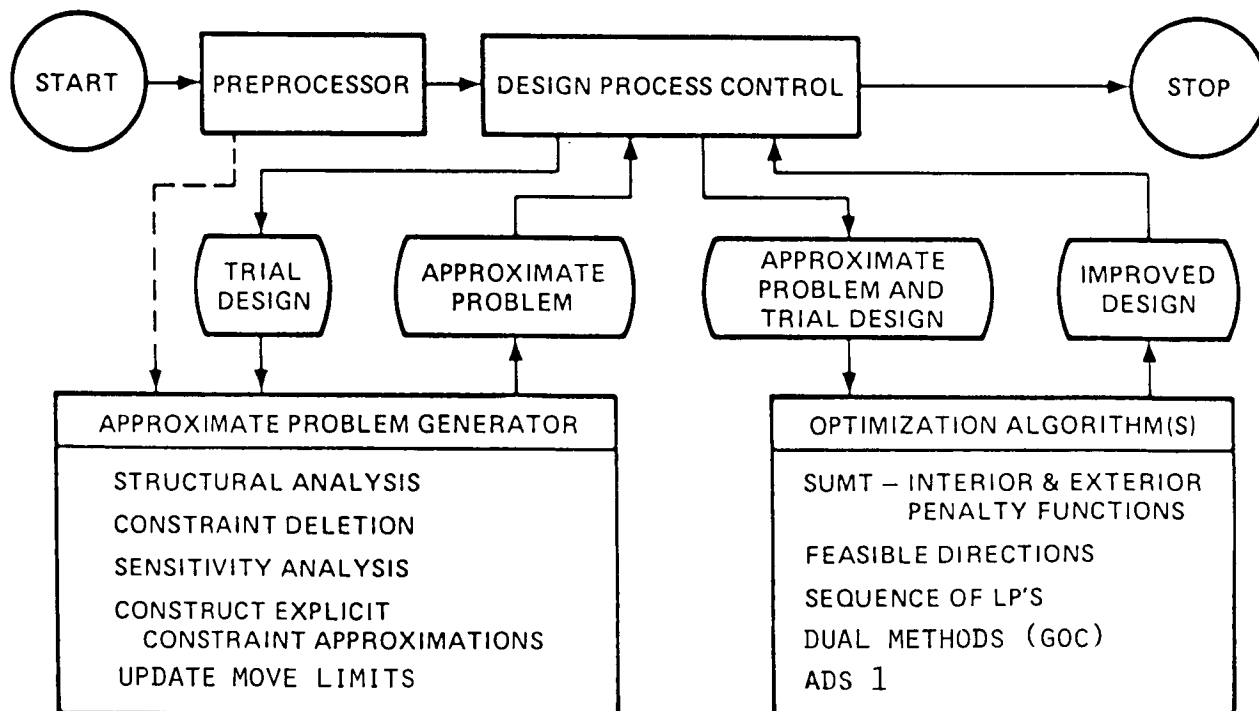


Figure 7

## SENSITIVITY ANALYSIS ANALOGY

While the use of behavior sensitivity analysis has become common practice during the past decade, the importance of optimum design sensitivity analysis has only recently been recognized by the structural optimization community (see Ref. 31 and subsequent work Refs. 32-35). Figure 8 outlines a useful analogy. In the analysis context, rates of change for behavior response quantities (e.g., displacements, stresses, natural frequencies, normal modes, etc.) with respect to design variables are obtained via implicit differentiation of the pertinent analysis equations (see Eq. 18, Fig. 8). In the optimum design context, rates of change for optimum design variable values (primal and dual) with respect to problem parameters (e.g., allowable displacement, allowable stress, applied load, etc.) are obtained via implicit differentiation of the necessary conditions characterizing the base optimum design (see Eq. 19, Fig. 8). Behavior sensitivity derivatives represent valuable quantitative information that can be used to: (1) help guide redesign via man-machine interaction; (2) construct explicit approximations for response quantities in terms of design variables ($n.b. \alpha_b = 1/\delta_b$). These explicit approximations can often be used to bypass the actual analyses for alternative designs in the neighborhood of the base design. Optimum design sensitivity derivatives represent valuable quantitative information that can be used to: (1) help guide higher level trade-off studies via man-machine interaction; (2) construct explicit approximations for optimum design variable values in terms of problem parameters ($p_k$). These explicit approximations can be used to bypass the actual optimization for modest changes in the problem parameters (assuming no shift in critical constraint set $Q_{cr}$, see Eq. 19, Fig. 8). The quality of the explicit approximations generated by behavior sensitivity/optimum design sensitivity analysis can often be improved by thoughtful selection of intermediate design variables/problem parameters. Also, optimum design sensitivity is important in the development of multi-level methods (see Ref. 36).

| Behavior Response Sensitivity | Optimum Design Sensitivity |
|---|---|
| $\dfrac{\partial \vec{u}}{\partial \alpha_b}$   rates of change of response quantities w.r.t. design variables | $\dfrac{\partial \vec{\alpha}^*}{\partial p_k}$ , $\dfrac{\partial \vec{\lambda}^*}{\partial p_k}$   rates of change of optimum primal and dual variables w.r.t. problem parameters |
| Implicit differentiation of pertinent analysis Eqs. $$\frac{\partial}{\partial \alpha_b}\left\{\begin{array}{c} K\,\vec{u} = \vec{P} \\ \text{or} \\ K\,\vec{v} = \lambda M \vec{v} \\ \text{etc} \end{array}\right\} \quad (18)$$ | Implicit differentiation of necessary conditions at optimum $$\frac{\partial}{\partial p_k}\left\{\begin{array}{l} \dfrac{\partial M}{\partial \alpha_b} - \sum_{q \in Q_{cr}} \lambda_q \dfrac{\partial g_q}{\partial \lambda_b} = 0;\ b \epsilon \tilde{B} \\ g_q = 0\ ;\ q \epsilon Q_{cr} \end{array}\right\} (19)$$ |
| man-machine interaction   select intermediate DV's   explicit approximations   bypass analysis | trade-off studies   select intermediate PP's   explicit approximations   bypass optimization |

Figure 8

# AIRFOIL OPTIMIZATION

Many of the ideas that have played a key role in advancing the state of the art in structural synthesis are potentially transferable to design optimization tasks in other discipline areas. For example, in Refs. 37 and 38 numerical airfoil optimization is carried out using reduced basis concepts and Taylor series approximations. Various airfoil optimization tasks can be formulated as nonlinear programming problems. For instance the objective may be to minimize the drag coefficient $C_D$ or maximize the lift coefficient $C_L$. Typically the constraints may include limits on lift, drag, pitching moment, thickness, and camber. The airfoil shape is defined as a linear combination of basis vectors $\vec{Y}^{(1)}$, $\vec{Y}^{(2)}$, $...\vec{Y}^{(n)}$, some or all of which may represent other airfoils (see Fig. 9a and Eq. 20). The scalars $a_1$, $a_2, ...a_n$ in Eq. 20 can be thought of as participation coefficients and they are taken to be components of the vector of design variables $\vec{X}$ (see Eq. 21). This reduced basis approach, first used for airfoil optimization in 1976 (see Ref. 39), provides good airfoil definition without having to use large numbers of design variables to define the airfoil thickness distribution. In Refs. 37 and 38 an innovative approximation concepts approach is used to reduce the number of aerodynamic analyses needed for design optimization by a factor of 2 or more. The basic idea used is to gradually develop second-order Taylor series approximations (see Eq. 22) for both the objective function $F(\vec{X})$ and the constraint functions $G_j(\vec{X})$ by using existing data or data generated earlier in the design optimization process. Each approximation generated for the $F(\vec{X})$ (and the $G_j(\vec{X})$) is used to improve the design (see Fig. 9b). This is followed by a full aerodynamic analysis which adds a new data point to the currently available set of data points. Examples reported in Refs. 37 and 38, as well as recent results (Ref. 40) using more realistic aerodynamics and spline function representation of airfoil shape, illustrate that approximation concepts can be successfully adapted to airfoil optimization.



(a) Basis Shapes
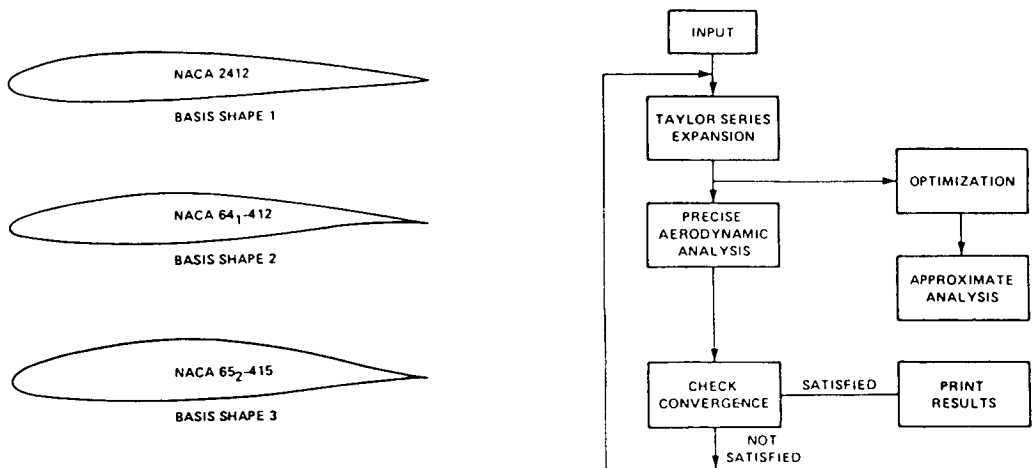
(b) Approximate Analysis

$$\vec{Y} = a_1\vec{Y}^{(1)} + a_2\vec{Y}^{(2)} \ ... \ a_n\vec{Y}^{(n)} \qquad (20)$$

$$\vec{X}^T = \left\lfloor a_1, a_2, ......a_n \right\rfloor \qquad (21)$$

$$F(\vec{x}) = F^0 + \Delta\vec{X}^T \ \nabla F$$

$$+ \frac{1}{2} \ \Delta\vec{X}^T \ [H] \ \Delta\vec{X} \qquad (22)$$

Figure 9

10

# THERMAL OPTIMIZATION

Thermal analysis and design is another area in which structural synthesis has served as a catalyst. For example in Refs. 41 and 42 techniques for computing the sensitivity of temperatures (steady state and transient) with respect to design variables that define a thermal protection system (and associated structure) have been developed and assessed. Also, in Ref. 43, explicit thermal response approximations based on first-order Taylor series expansions as well as constraint deletion techniques are successfully applied to some component level thermostructural design optimization problems (e.g. the thermostructural panel shown in Fig. 10a). The constraints for this problem are time parametric since the thermal behavior is transient (see Eq. 23). Instead of replacing the time parametric constraint (Eq. 23) with a large number of regular constraints representing the response at closely spaced time points $t_j$ (Eq. 24), the response is monitored only at the most critical points (see Fig. 10b, points A, B, C, and Eq. 25). As the design changes during optimization the critical time points drift; however, it is shown in Ref. 43 that drift does not affect the first derivatives of the critical constraints (Eq. 25) with respect to design variables. During each stage in the approximation concepts approach employed in Ref. 43, the critical time points are frozen and Taylor series constraint approximations are generated only for that reduced set of constraints. The critical time points and the constraint approximations are updated periodically. It is reported in Ref. 43 that the combined use of these two approximation concepts produced an order of magnitude reduction in computational time required for convergence of the design optimization process. Finally, it should be noted that the reduced-basis method is also being applied to transient thermal analysis problems (see Ref. 44).



$$g(\vec{D},t) \geq 0 \quad ; \quad 0 \leq t \leq t_{max} \qquad (23)$$

$$g(\vec{D},t_j) \geq 0 \quad ; \quad j = 1,2,\ldots n \qquad (24)$$

$$g(\vec{D},t_{cr}) \geq 0 \quad ; \quad cr = A,B,C \qquad (25)$$
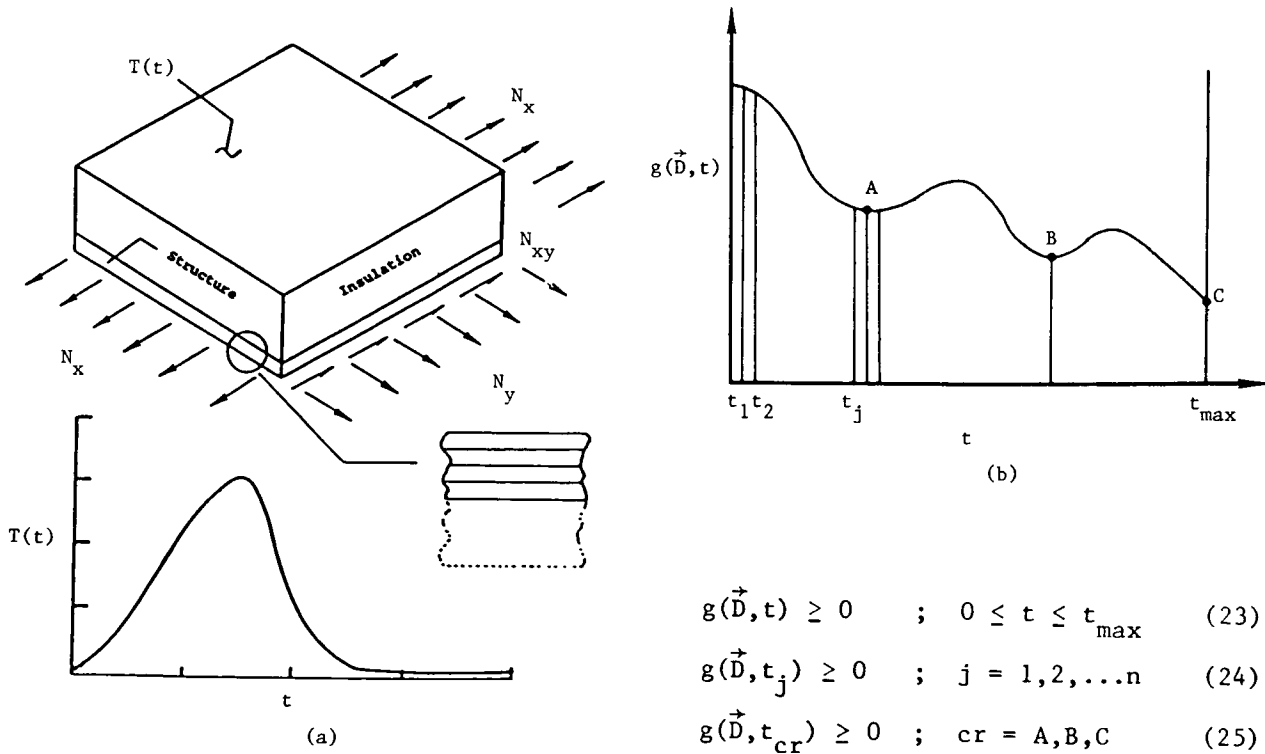
Figure 10

# OPTIMIZATION OF COMPRESSOR VANE SETTINGS

Gas turbine engines for jet aircraft must maintain high performance over a wide range of flight conditions; therefore variable-geometry configurations and bleed systems are built into components such as the fan and the compressor. During development many compressors are built with all vane rows variable, even though only a few rows may be left variable in the final design configuration. Primary compressor performance goals $(M(\vec{D}))$ include: maximum efficiency, maximum stall margin, maximum flow range, and maximum pressure ratio. Furthermore, there will always be constraints $g_q(\vec{D}) \geq 0$. For instance one might want to maximize efficiency while maintaining a minimum acceptable stall margin and also satisfying stress limitations. In Refs. 45-47 a sequence of approximate problems approach has been applied to the optimization of compressor vane settings. The block diagram shown in Fig. 11a (taken from Ref. 48) outlines the general approach. The basic idea is to gradually refine the approximations generated as more experimental data is accumulated. A particularly interesting part of the work reported in Ref. 45 involved optimization of a three-stage compressor with four rows of variable vanes. Optimization of compressor efficiency was carried out experimentally by both the traditional approach (sequentially opening and closing each vane row) and the sequence of approximate optimization problems approach. Vane settings were optimized for 8 different operating speeds (see Fig. 11b) and in each case the improvement in compressor efficiency achieved via the sequence of approximate optimization problems approach exceeds that obtained by the traditional approach. Furthermore, 40% fewer test points were required to obtain these superior results. The results reported in Ref. 45 support the contention that the approximations concepts approach to design optimization can be used to find better designs at significantly lower cost, even when the objective and constraint functions must be evaluated experimentally.
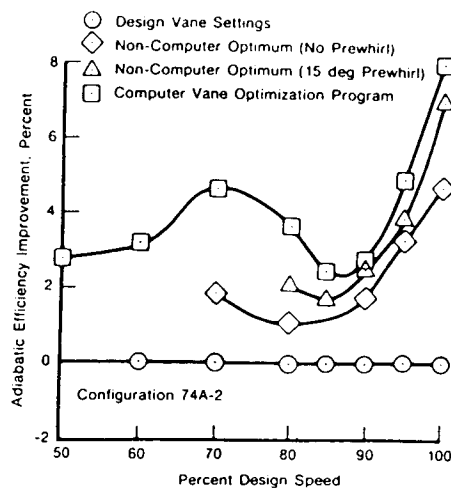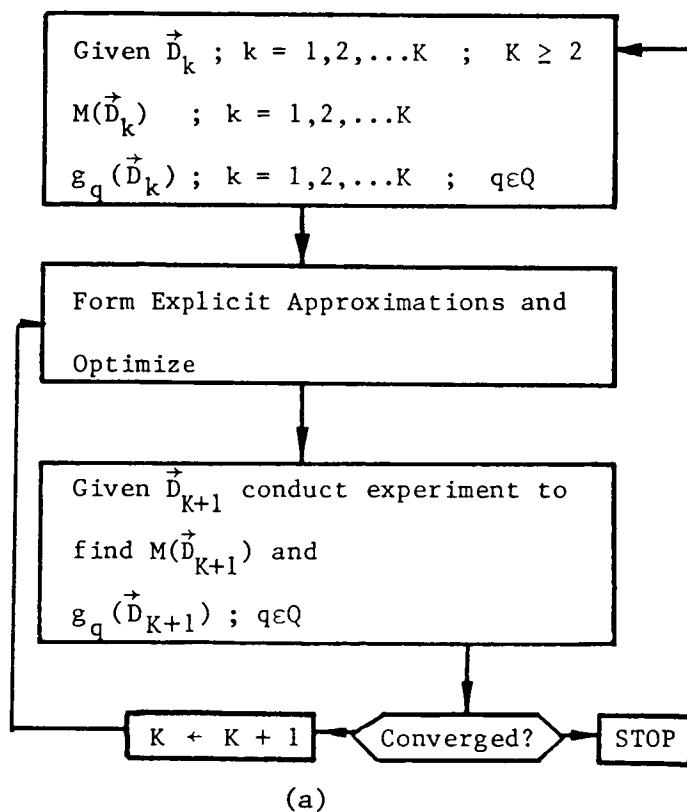


Figure 11

## MULTILEVEL METHODS AND DECOMPOSITION

The basic objective of multilevel methods is to break down a large unmanageable design optimization problem into a hierarchy of interconnected smaller problems that are tractable. When a large design optimization problem is naturally explicit (e.g. see Ref. 49) or when it can be replaced by a sequence of explicit approximations it may be possible to apply formal decomposition algorithms drawn from the mathematical programming literature. However the current limitations of formal decomposition algorithms are such that interest has been stimulated in the generation of heuristic decomposition techniques (e.g. see Refs. 50-54). In the structural synthesis context multilevel methods have been of continuing interest since the early 1970's (e.g. see Refs. 50 and 51). Almost all of the multilevel work in structural synthesis has focused on two-level systems such as that depicted schematically in Fig. 12. In Refs. 52 and 53 the multilevel method was improved by using: (1) a nonlinear programming formulation at both the component and the system level; (2) approximation concepts (linking, constraint deletion, and explicit constraint approximations) to facilitate efficient solution of the system level problems; (3) change in stiffness as the component level objective function to be minimized. Recently a general method for breaking large multidisciplinary problems down into several levels of subproblems was proposed (Ref.36). This general method was subsequently implemented for two-level structural optimization and successfully applied to a portal frame type structure (see Ref. 54). A key feature of this work is that it makes use of optimum design sensitivity analysis to convey to the system level coupling information about how the cumulative measure of component constraint violation (for each component) will react to changes in the system level design variables. Multilevel methods and formal decomposition are areas of continuing research activity that are likely to have significant influence on the development of multidisciplinary design optimization.
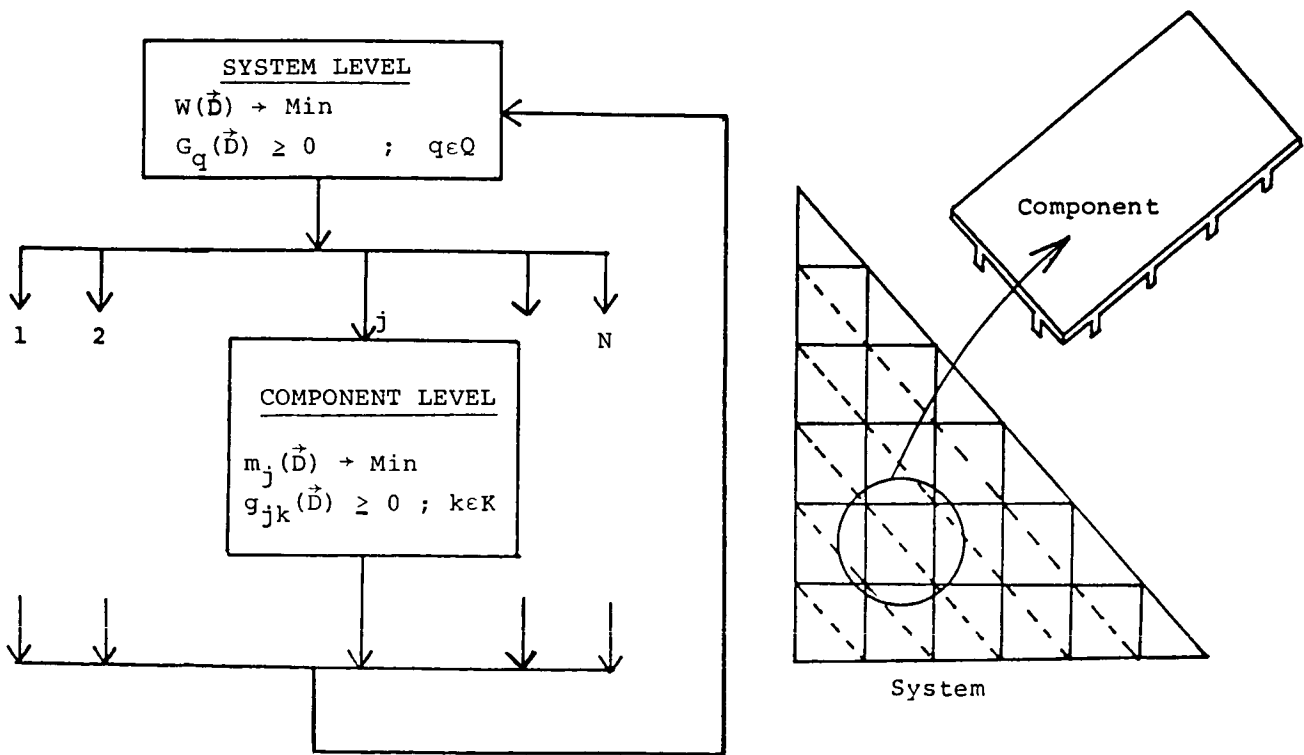


Figure 12

## SUMMARY

More than twenty five years have elapsed since it was recognized that a rather general class of structural design optimization tasks could be properly posed as an inequality constrained minimization problem. Figure 13 summarized several ideas that have played a key role in advancing the state of the art in structural synthesis. As indicated by the airfoil, thermal, and compressor vane examples some of these ideas are already being transferred or extended to other discipline areas. It is suggested that, independent of primary discipline area, it will be useful to think about: (1) posing design problems in terms of an objective function and inequality constraints; (2) generating design oriented approximate analysis methods (giving special attention to behavior sensitivity analysis); (3) distinguishing between decisions that lead to an analysis model and those that lead to a design model; (4) finding ways to generate a sequence of approximate design optimization problems that capture the essential characteristics of the primary problem, while still having an explicit algebraic form that is matched to one or more of the established optimization algorithms; (5) examining the potential of optimum design sensitivity analysis to facilitate quantitative trade-off studies as well as participation in multilevel design activities. An open-minded and imaginative quest for parallel opportunities in other disciplines offers significant potential for advancing the state of the art in multidisciplinary analysis and design. It should be kept in mind that multilevel methods are inherently well suited to a parallel mode of operation in computer terms or to a division of labor between task groups in organizational terms. Based on structural experience with multilevel methods the following general guidelines are suggested: (1) seek to weaken coupling between levels via basic organization, selection of intermediate level objective functions and the use of move limits; (2) whenever possible try to satisfy local constraints through local design variable changes; (3) for noncritical components seek a balanced design with uniform positive margins. Multilevel methods and decomposition can be expected to play a vital role in the development of multidisciplinary design optimization capabilities.

●NLP Formulation - Inequality Constraints

●DOSA : Behavior Sensitivity Analysis

      Reduced Basis in Analysis

      Organization of Analysis

●Analysis Model - Design Model

●Approximation Concepts

      Linking and Basis Reduction

      Constraint Deletion Techniques

      Explicit Constraints (Taylor series)

●Match Optimization Algorithm◄───►Approximate Problem

●Optimum Design Sensitivity Analysis

●Multilevel Methods and Decomposition

Figure 13

## REFERENCES

1. Schmit, L.A., "Structural Design by Systematic Synthesis," Proceedings, 2nd Conference on Electronic Computation, ASCE, New York, 1960, pp. 105-122.

2. Schmit, L.A. and Kicher, T.P., "Structural Synthesis of Symmetric Waffle Plate," NASA TN D-1691, Dec. 1962.

3. Schmit, L.A., Kicher, T.P., and Morrow, W.W. "Structural Synthesis Capability for Integrally Stiffened Waffle Plates", AIAA Journal, Vol. 1, Dec. 1963, pp 2820-2836.

4. Kicher, T.P., "Structural Synthesis of Integrally Stiffened Cylinders," Journal of Spacecraft and Rockets, Vol. 5, Jan. 1968, pp. 62-67.

5. Morrow, W.M. and Schmit, L.A., "Structural Synthesis of a Stiffened Cylinder," NASA CR-1217, 1968.

6. Melosh, R.J. and Luik, R., "Approximate Multiple Configuration Analysis and Allocation for Least Weight Structural Design," AFFDL-TR-67-29, 1967.

7. Fox, R.L., "Constraint Surface Normals for Structural Synthesis Techniques," AIAA Journal, Vol. 3, Aug. 1965, pp. 1516-1517.

8. Fox, R.L. and Kapoor, M.P., "Rates of Change of Eigenvalues and Eigenvectors," AIAA Journal, Vol. 6, Dec. 1968, pp. 2426-2429.

9. Storaasli, O.O. and Sobieszczanski, J., "On the Accuracy of the Taylor Approximation for Structural Resizing," AIAA Journal, Vol. 12, Feb. 1974, pp. 231-233.

10. Fox, R. L. and Miura, H., "An Approximate Analysis Technique for Design Calculations," AIAA Journal, Vol. 9, Jan. 1971, pp. 177-179.

11. Noor, A.K. and Lowder, H.E., "Approximate Techniques of Structural Reanalysis," Computers and Structures, Vol. 4, Aug. 1974, pp. 801-812.

12. Noor, A.K. and Lowder, H.E., "Structural Reanalysis Via a Mixed Method," Computers and Structures, Vol. 5, April 1975, pp. 9-12.

13. Noor, A.K., "Multiple Configuration Analysis Via Mixed Method," Journal of the Structural Division, ASCE, Vol. 100, No. ST9, 1974, pp. 1991-1997.

14. Bhatia, K.G., "Rapid Iterative Reanalysis for Automated Design," NASA TN D-6534, 1971.

15. Fleury, C. and Sander, G., "Structural Optimization by Finite Element," University of Liege, Belgium, LTAS Report SA-58, Jan. 1978.

16. Arora, J.S. and Haug, E.J., "Methods of Design Sensitivity Analysis in Structural Optimization," AIAA Journal, Vol. 17, September 1979, pp. 970-974.

17. Vanderplaats, G.N., "Comment on Methods of Design Sensitivity Analysis in Structural Optimization," AIAA Journal, Vol. 18, No. 11, November 1980, pp. 1406-1407.

18. Bennett, J.A. and Botkin, M.E, "Shape Optimization of Two-Dimensional Structures with Geometric Problem Description and Adaptive Mesh Refinement," Proceedings, AIAA/ASME/ASCE/AHS 24th Structures, Structural Dynamics and Materials Conference, Lake Tahoe, Nevada, May 1983, pp. 422-431.

19. Schmit, L.A. and Farshi, B., "Some Approximation Concepts for Structural Synthesis," AIAA Journal, Vol. 12, May 1974, pp 692-699.

20. Haftka, R. T., "Automated Procedure for Design for Wing Structures to Satisfy Strength and Flutter Requirements," NASA TN D-7264, 1973.

21. Haftka, R.T. and Starnes, J.H., "Applications of a Quadratic Extended Interior Penalty Function for Structural Optimization," AIAA Journal, Vol. 14, June 1976, pp. 718-724.

22. Starnes, J.H. and Haftka, R.T., "Preliminary Design of Composite Wings for Buckling, Strength and Displacement Constraints," Proceedings, AIAA/ASME 19th Structures, Structural Dynamics and Materials Conference, Bethesda, MD, April 1978, pp. 1-13.

23. Schmit, L.A. and Miura, H., "Approximation Concepts for Efficient Structural Synthesis," NASA CR-2552, March 1976.

24. Schmit, L.A. and Miura, H., "A New Structural Analysis/Synthesis Capability - ACCESS 1", AIAA Journal, Vol. 14, May 1976, pp. 661-671.

25. Schmit, L.A. and Miura, H., "An Advanced Structural Analysis/Synthesis Capability - ACCESS 2," *International Journal of Numerical Methods in Engineering*, Vol. 12, Feb. 1978, pp. 353-377.

26. Fleury, C., "Structural Weight Optimization by Dual Methods of Convex Programming," *International Journal of Numerical Methods in Engineering*, Vol. 14, No. 12, 1979, pp. 1761-1783.

27. Schmit, L.A. and Fleury, C., "Structural Synthesis by Combining Approximation Concepts and Dual Methods," *AIAA Journal*, Vol. 18, Oct. 1980, pp. 1252-1260.

28. Schmit, L.A. and Fleury, C., "Discrete-Continuous Variable Structural Synthesis Using Dual Methods," *AIAA Journal*, Vol. 18, Dec. 1980, pp. 1515-1524.

29. Fleury, C. and Schmit, L.A., "Dual Methods and Approximation Concepts in Structural Synthesis," NASA CR-3226, Dec. 1980.

30. Fleury, C. and Braibant, V., "An Approximation Concepts Approach to Shape Optimal Design," Report SA-112, Aerospace Laboratory, University of Liege, Belgium, January 1984.

31. Sobieszczanski-Sokieski, J., "Optimum Design Sensitivity," Research in Progress Presentation, AIAA/ASME/ASCE/AHS 21st Structures, Structural Dynamics and Materials Conference, Seattle, Washington, May 1980.

32. Sobieszczanski-Sobieski, J., Barthelemy, J.-F., and Riley, K.M., "Sensitivity of Optimum Solutions to Problem Parameters," Proceedings of the AIAA/ASME/ASCE/AHS 22nd Structures, Structural Dynamics and Materials Conference, Atlanta, Georgia, April 1981, AIAA Paper No. 81-9548 (see also NASA TM-83134, May 1981 and *AIAA Journal*, Vol. 20, No. 9, September 1982, pp. 1291-1299).

33. Barthelemy, J.F. and Sobieszczanski-Sobieski, J., "Extrapolation of Optimum Design Based on Sensitivity Derivatives," *AIAA Journal*, Vol. 21, No. 5, May 1983, pp. 797-799.

34. Barthelemy, J.F. and Sobieszczanski-Sobieski, J., "Optimum Sensitivity Derivatives of Objective Functions in Nonlinear Programming," *AIAA Journal*, Vol. 21, No. 6, June 1983, pp. 913-915.

35. Schmit, L.A. and Chang, K.J., "Optimum Design Sensitivity Based on Approximation Concepts and Dual Methods," *Int. J. for Numerical Methods in Engineering*, Vol. 20, No. 1, January 1984, pp. 39-75.

36. Sobieszczanski-Sobieski, J., "A Linear Decomposition Method for Large Optimization Problems - Blueprint for Development," NASA TM-83248, February 1982.

37. Vanderplaats, G.N., "Efficient Algorithm for Numerical Airfoil Optimization," *Journal of Aircraft*, Vol. 16, No. 12, December 1979, pp. 842-847.

38. Vanderplaats, G. N., "Approximation Concepts for Numerical Airfoil Optimization," NASA TP-1370, March 1979.

39. Vanderplaats, G.N. and Hicks, R.M., "Numerical Airfoil Optimization Using Reduced Number of Design Coordinates," NASA TMX-73, 151, July 1976.

40. Misegades, K.P., "Airfoil Optimization," AIAA Paper No. 84-0053, AIAA 22nd Aerospace Sciences Meeting, Reno, Nevada, January 1984.

41. Haftka, R.T., "Techniques for Thermal Sensitivity Analysis," *Int. J. for Numerical Methods in Engineering*, Vol. 17, No. 1, January 1981, pp. 71-80.

42. Haftka, R.T. and Malkus, D.S., "Calculation of Sensitivity Derivatives in Thermal Problems by Finite Differences," *Int. J. for Numerical Methods in Engineering*, Vol. 17, No. 12, December 1981, pp. 1811 - 1821.

43. Haftka, R.T. and Shore, C.P., "Approximation Methods for Combined Thermal/Structural Design," NASA TP-1428, June 1979.

44. Shore, C.P., "Application of the Reduced Basis Method to Nonlinear Transient Thermal Analysis," Research in Structural and Solid Mechanics - 1982, NASA Conference Publication 2245, 1982, pp. 49-65.

45. Garberoglio, J.E., Song, J.O. and Boudreaux, W.L., "Optimization of Compressor Vane and Bleed Settings," ASME Paper No. 82-GT-81, Proceedings of 27th International Gas Turbine Conference and Exhibit, London, England, April 1982.

16

46. Garberoglio, J.E., Song, J.O. and Boudreaux, W.L., "Optimization of Compressor Vane and Bleed Settings," AFWAL - TR - 2046, June 1981.

47. Garberoglio, J.E., Song, J.O. and Boudreaux, W.L., "Optimization of Compressor Vane and Bleed Settings - Users Manual," Report FR-13996, Pratt & Whitney Aircraft Group, AFWAL contract no. F33615-79-C-2013, 1981.

48. Vanderplaats, G.N., "Numerical Optimization Techniques for Engineering Design," McGraw Hill Book Co., New York, 1984.

49. Woo, T.H. and Schmit, L.A., "Decomposition in Optimal Plastic Design of Structures," Int. J. of Solids and Structures, Vol. 17, No. 1, January 1981, pp. 39-56.

50. Giles, G.L., "Procedure for Automating Aircraft Wing Structural Design," Journal of the Structural Division, ASCE, Vol. 97, No. ST 1, January 1971, pp. 99-113.

51. Sobieszczanski, J. and Leondorf, D., "A Mixed Optimization Method for Automated Design of Fuselage Structures," Journal of Aircraft, Vol. 9, December 1972, pp. 805-822.

52. Schmit, L.A. and Ramanathan, R.K., "Multilevel Approach to Minimum Weight Design Including Buckling Constraints," AIAA Journal, Vol. 16, February 1978, pp. 97-104.

53. Schmit, L.A. and Mehrinfar, M., "Multilevel Optimum Design of Structures with Fiber-Composite Stiffened-Panel Components," AIAA Journal, Vol. 20, January, 1982, pp. 138-147.

54. Sobieszczanski-Sobieski, J., James, B., and Dovi, A., "Structural Optimization by Multilevel Decomposition," AIAA Paper No. 83-0832, Proceedings of the AIAA/ASME/ASCE/AHS 24th Structures, Structural Dynamics, and Materials Conference, Part I, Lake Tahoe, Nevada, May 1983, pp. 369-382.

# OPTIMIZATION
# IN THE
# SYSTEMS ENGINEERING PROCESS

Loren A. Lemmerman
Lockheed-Georgia Company

ABSTRACT

The objective of this paper is to look at optimization as it applies to the design
process at a large aircraft company. I hope to describe the design process at
Lockheed-Georgia, give some examples of the impact that optimization has had on that
process and then indicate some areas that must be considered if optimization is to
be successful and supportive in the total design process.

All of us here support optimization enthusiastically, and I am no exception. I in-
tend to show great improvements in our design process in my presentation. In a
following paper, my colleague, Gary Gabriele, will amplify on the same theme and
provide technical details for our activities (ref. 1). However, the tone of my
presentation may come across as being somewhat cautionary. This is deliberate.
I feel that proper design of an optimization approach to design is mandatory, and
that failure to do so will result in rejection of a highly beneficial tool.

OVERVIEW

To make my case, I will proceed along the following path. I will first define the
design process at Lockheed-Georgia, and I will give examples of how optimization
fits into that process. Then I will relate the design facets affected by optimi-
zation to the total design process to outline some considerations that I feel are
important.

- DEFINE DESIGN PROCESS

- PROVIDE EXAMPLES OF IMPACT OF
  OPTIMIZATION

- DISCUSS TASKS REMAINING TO
  COMPLETE DESIGN PROCESS

# DESIGN PROCESS

The essential elements of the design process consist of the mission definition phase that provides the system requirements, leading to the conceptual design, the preliminary design, and finally the detail design. Mission definition is performed largely by operations analysts in conjunction with the customer. The result of their study is handed off to the systems engineers for documentation as the systems requirements. The document that provides these requirements is the basis for the further design work of the design engineers.

The design phase actually begins with conceptual design, which is generally conducted by a small group of engineers using multidisciplinary design programs. Because of the complexity of the design problem, the analyses are relatively simple and generally dependent on parametric analyses of the configuration. The result of this phase is a baseline configuration from which preliminary design may be initiated.

Preliminary design is far more complicated, both because the analysis techniques are more complex, and also because these techniques require specialized knowledge. The objective of this step is to refine the design estimates made during conceptual design and to add additional detail to the description of the configuration. At the conclusion of this phase, the airplane is defined well enough so that a company can comfortably bid the cost of producing the new airplane.

Detail design is largely mechanical in nature, and normally occurs after receipt of an order for production. This is not an area of concentration in the context of today's subject, and I will ignore it for the remainder of the presentation.

```
      CONTRACTED                  PROPOSAL      CONTRACT
       STUDIES                    REQUESTED      AWARD


       1-3 YEARS          1-2 YEARS        1 YEAR


 ┌──────────┐  ┌──────────┐  ┌──────────┐  ┌──────────┐  ┌────────┐
 │MISSION   │──│SYSTEM    │──│CONCEPTUAL│──│PRELIMINARY│─│DETAIL  │──→ MANUF.
 │DEFINITION│──│REQUIREMENTS│─│DESIGN   │──│DESIGN    │──│DESIGN  │
 └──────────┘  └──────────┘  └──────────┘  └──────────┘  └────────┘

 MARKET RESEARCH      ADVANCED DESIGN      AERODYNAMICS      PROJECT ENG.
 OPERATIONS ANALYSIS  SYSTEMS ENGINEERING  STRUCTURES        DETAIL DESIGN
                                           PROPULSION        STRESS
                                           AIRCRAFT SYS.     SUBSYSTEMS
                                           SUPPORTABILITY    WEIGHTS
                                                             VALUE ENG
                                                             TEST
```

## CONCEPTUAL DESIGN - A DEFINITION

To provide a basis for amplification of the conceptual design process, look at the figure below. The function of the conceptual design process is to conduct a multidisciplinary analysis of an airplane to produce values of parameters that describe an airplane. These parameters are top level descriptions that leave most of the actual configuration details undefined. However, implicit in this process is the trading of factors that relate to the performance of the configuration. The trades I mean are typified by the thinness of a wing desired by an aerodynamicist versus the thickness of a wing as desired by a structural analyst.

Typical parameters defined at this stage are fuselage length and width, wing area, sweep, aspect ratio, and, to a limited extent, control surface.

MISSION → MULTIDISCIPLINARY ANALYSIS → PARAMETERS DESCRIBING A/C

(
FUSELAGE DIMENSIONS

WING DIMENSIONS

CONTROL SURFACES
)
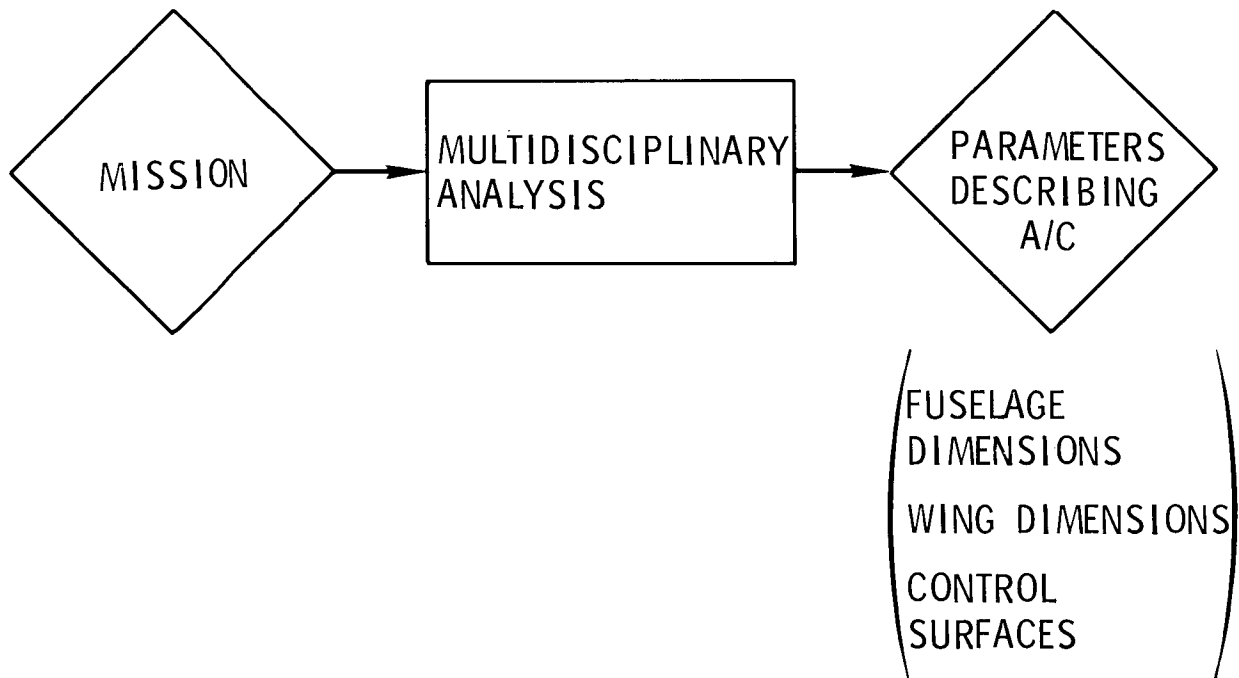
## CURRENT CONCEPTUAL DESIGN PROCESS

In former times, conceptual design was manually directed and highly iterative. The process consisted of guessing an initial configuration, analyzing that configuration, and then systematically varying each of several design parameters to examine a design space within which manual optimization could be done. Normally the number of parameters examined did not exceed four, because of the human limitations in absorbing more variations than that. There were several disadvantages to the former approach. This process was time consuming, fallible, and tedious. It was time consuming because the answer depended on many executions of a computer code. It was fallible because the choice of the parameter variation to be examined was entirely at the discretion of the designer. Thus, the quality of the answers was directly dependent on the skill of that designer. In addition, no one could be sure that a large enough design space has been investigated to ensure that a true optimum had been found. This old procedure was also tedious. All data had to be manipulated manually. Although this did provide useful insight to the designer, the cost was a further delay. Dozens of computer runs had to be scanned, the results judged for correctness, and the results plotted on carpet plots. Many hours of talented labor were consumed performing menial tasks.

The former process was basically eliminated at Lockheed-Georgia several years ago, in favor of the approach shown here, based entirely on numerical optimization. The new process is described schematically here. The former process was usually completed in one day. Many of the manual actions have been eliminated. Now, a given study may consume as much time as formerly, but a much larger range of design variables has been included.
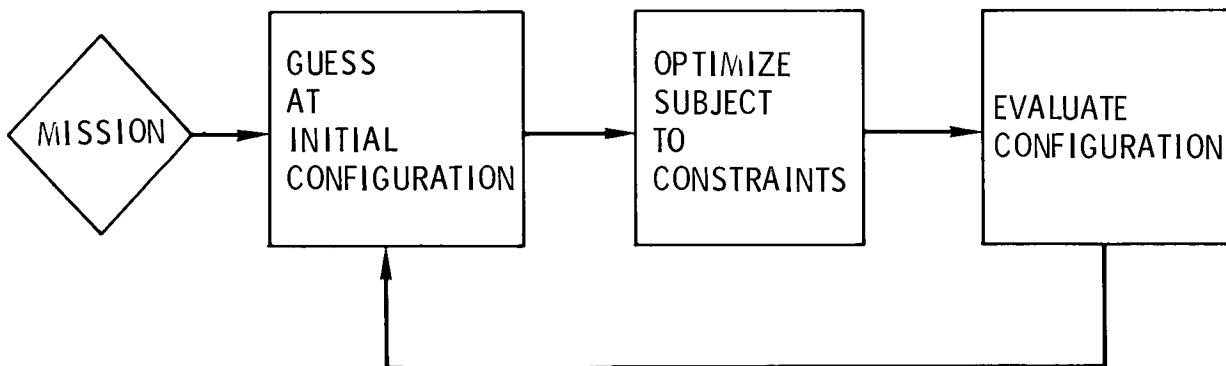
# PRELIMINARY DESIGN PROCESS (PARTIAL)

The next step in the design process is preliminary design. This is the process, partially illustrated here, by which the conceptual design baseline is analyzed in greater depth to confirm the design or provide foundation for changing the design. This process is typified by the more or less simultaneous execution of many detailed design codes in several disciplines. Obviously, the communication during the process is difficult, and the designs proposed by each discipline are frequently inconsistent. Iterative loops, while very common, cannot be represented because of the indeterminate sequence of such iteration.

As an example of the type of analysis conducted in this phase, consider aerodynamics for a moment. The codes frequently applied in this phase consist of full potential subsonic or transonic codes for configuration analysis, full potential codes for direct design, and Navier-Stokes codes for highly complex viscous flow analyses. As a result of the aerodynamic analysis done during this phase of design, the wing external contours are fully defined and more reliable estimates of the vehicle performance are available. Similar refinements and definition are added by each of the participating disciplines.

The deficiencies of the current approach are immediately obvious. First and foremost, the result is a suboptimal configuration. Even though optimization may be used within isolated analyses, the difficulty of communication in real time and the lack of available trade-off criteria mean that no global, rigorous optimization occurs.
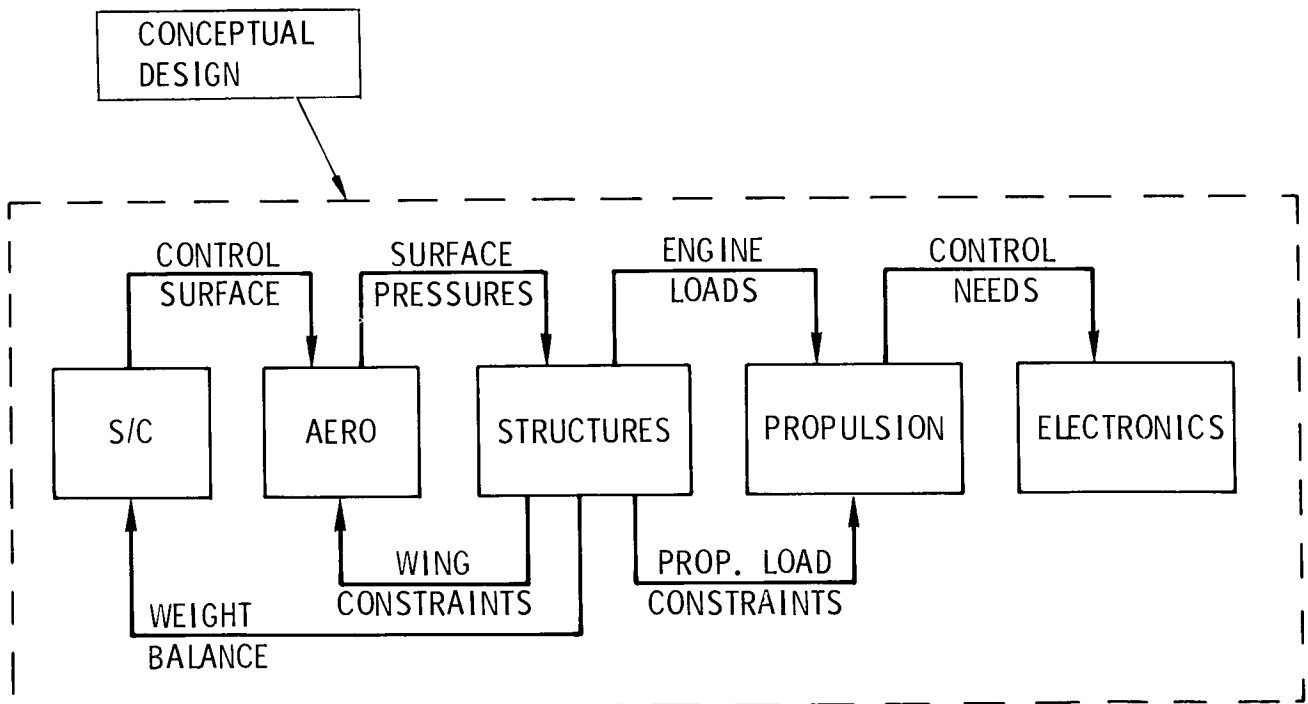
## CURRENT USE OF OPTIMIZATION IN PRELIMINARY DESIGN

I have already alluded to the use of optimization on individual analyses in this phase. Here are some examples of such optimizations. The aerodynamics discipline has been very active in developing optimization techniques for the design of wings in transonic flow, largely based on FLO codes. These methods provide a wing shape, starting with a specification of a desirable pressure distribution. Using such methods, the wing contour and twist distribution may be calculated directly.

Subsonic optimization techniques have generally been limited to the design of high lift systems. In this case, the optimal location of a slotted trailing edge flap can be found by optimizing on the axial force for the system and by using panelling methods for calculating the flap system pressure distribution.

Structural optimization has been done for minimizing structural weight, given loading conditions. In this case, the structure is modeled using finite element techniques, with element geometries such as thicknesses or cross sectional areas taken as design variables. Another example of structural optimization is in the design of composite panels. The objective is to determine the ply orientation to respond to specific loading conditions.

- **WING AERODYNAMICS**

  - TRANSONIC

  - SUBSONIC

- **WING STRUCTURES**

  - STRUCTURAL WEIGHT

  - PANEL DESIGN

# CURRENT PRELIMINARY DESIGN OPTIMIZATION

If I were to summarize the preliminary design optimization work currently being done at Lockheed-Georgia, I would have to say that its use is relatively new, that it has been very well accepted, and that its use is certainly increasing. But this may eventually become a severe problem for us, since the optimization is being applied to subprocesses within design. Worse yet, it is being applied to old design philosophies. The result has to be suboptimal designs.

- RELATIVELY NEW

- WELL ACCEPTED

- USE IS INCREASING

BUT

- OPTIMIZATION IS BEING APPLIED TO OLD THINKING

## PROPOSED PRELIMINARY DESIGN PROCESS

The preliminary design process is clearly another candidate for improvement by optimization. The technical challenge of this problem is much greater than that of the conceptual design process, but the potential payoff is also much larger. The challenge comes, in part, from the large number of individuals and computer programs normally invoked at this design state, and the current dearth of technology available to solve the very different problems thus posed.

One possible way to apply optimization in the preliminary design process is shown here. The fundamental idea is that candidate design parameters flow downward to the individual analysis modules and the result of the analysis flows back up to the optimizer.

Obviously, such a system is far from reality. The technical challenges outweigh those of optimization itself. The analysis methods normally used in preliminary design are state-of-the-art methods that are time consuming, user-sensitive, and modeling sensitive. Because of this, not only will new optimization techniques be needed, but so will entirely new operational procedures. For example, optimization now is executed mostly as a black box program. The analysis points provided by support codes are considered to be correct and not subject to code sensitivities. In the preliminary design process illustrated here, the former approach clearly will not work. The new process must include a method for disciplinary engineers to examine the analysis code results as they are being generated to ensure that the optimized results are valid. When such an optimization method is available, however, I submit that the problem is far from finished. This is so because people inevitably are the designers, and the design techniques, whether through optimization or not, must take the human element into consideration.
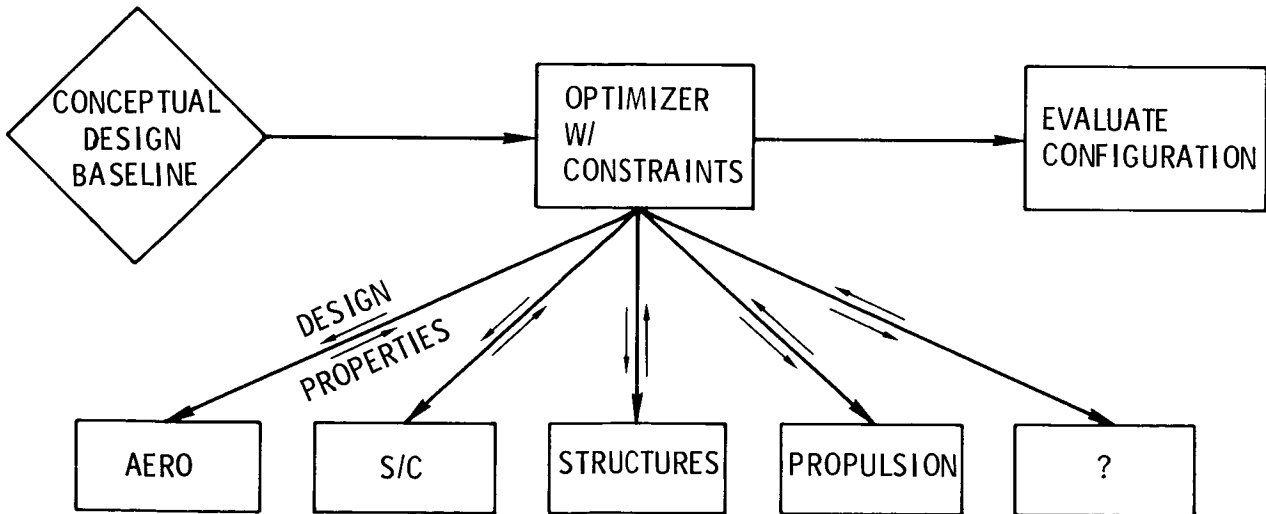
To expand on this theme, let me begin by giving you my orientation.  I am in the Systems Engineering Department at Lockheed-Georgia.  This slide gives a reasonable definition of what Systems Engineering means to us.  By its very definition, it is a process of dealing with people in a large design operation.  As such, our interest is not in the internal workings of design codes, but rather in how individuals use given design codes to produce designs, and then how those individuals transmit their information to other designers in the organization.

# A DISCIPLINE THAT COORDINATES THE ENGINEERING ACTIVITIES WITHIN LARGE ORGANIZATIONS TO HELP PRODUCE A SUPERIOR, COST-EFFECTIVE, TIMELY PRODUCT

## TASKS OF SYSTEMS ENGINEERING

Let me illustrate these ideas by presenting the four main tasks of the Systems Engineering operation. As illustrated, they involve the management of trade studies, requirements, interfaces, and technical risk. Another way to express these four tasks is Communication, Communication, Communication, Communication. I will now pick a couple of these tasks to show you what I mean.

- **TRADE STUDY MANAGEMENT**

- **REQUIREMENTS MANAGEMENT**

- **INTERFACE MANAGEMENT**

- **RISK MANAGEMENT AND DECISION SUPPORT**

Decisions <u>are</u> the design process. By its very nature, design requires definition of some configuration from an infinity of possibilities. The best design is some compromise of many and widely varying constraints. Many times the choices to be made are aesthetic, or subjective, or not amenable to computer analysis. In these situations, and sometimes even in well-defined engineering choices, trade studies must be performed that are outside the domain of the optimization process.

The illustration here is a simple representation of the decisions that might be made to select a navigation system for an airplane. These choices are displayed as a hierarchy, beginning with the top level vehicle considerations, and then working downward to finer levels of detail. Systems Engineering is responsible for generating such a trade tree to illustrate the decisions to be made, defining the design groups to be involved, coordinating the studies needed, and documenting the results.

Some of the decisions illustrated in this trade tree are supported by optimized methods. For example, the vehicle may be initially sized with optimization and components may also be designed with optimized methods. Nonetheless, when design decisions are to be made, there is a high likelihood that not all the decisions will have been supported through optimization. The point is, optimization methods are imbedded in the total design process, and this must be taken into account in the development of these optimization methods.
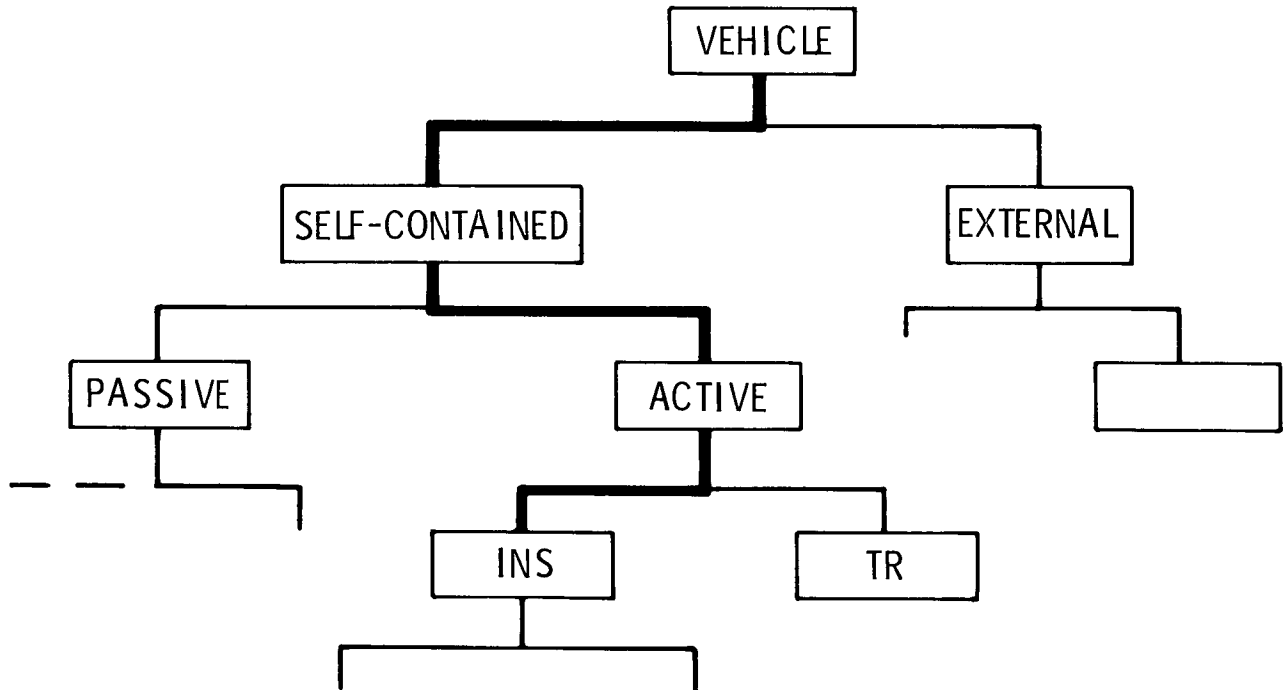
## TRADE STUDIES WITH OPTIMIZATION

This last feature is what I am trying to illustrate here. Some decisions of the design process will be made within the optimization process. Some will not. But those that do not must have information available from the optimization to assist the manual decision-making process. This is true whether the outside decision is being made concurrently with the optimization or whether it lags the optimization by days, weeks, or months.

The implication is that information that is more comprehensive than just the final optimized configuration must be provided and stored. Possible information needs include sensitivities around the optimal point and the optimization history. In addition, it will be necessary to provide a way to interrupt the optimization process as it is occurring to input new information to the optimization process and to influence, on the fly, the outcome.
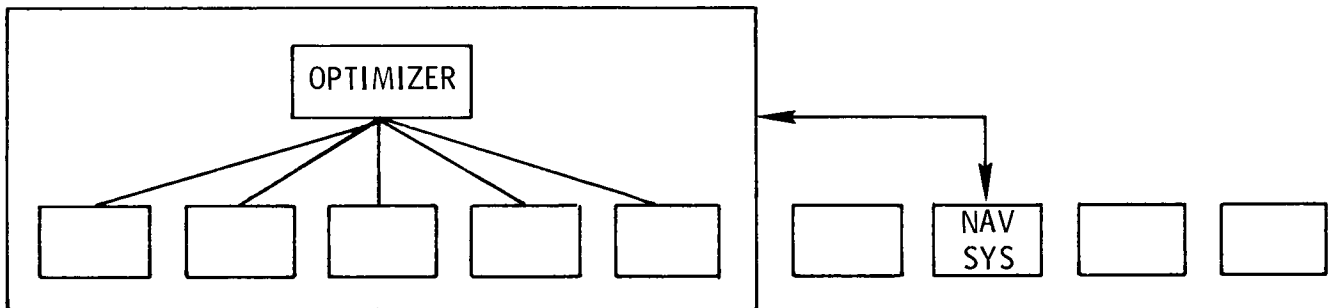
# REQUIREMENTS FLOWDOWN

Let me provide one more example, that of requirements flowdown. This is another example of the communication involved in the design process. In this case, the objective is to communicate to each individual designer the importance of his design in meeting the top level performance requirements. This is done by analyzing the top level system requirements and assigning or allocating these top level requirements to the next lower level to determine the drivers in the system. This process is repeated to successively lower levels until the final objective is accomplished. That is, the question "What is each individual's contribution to the total system performance?" is answered at the lowest logical level.

A specific performance might be maintenance manhours per flight hour, or it might be minimum range requirements. Whatever the requirement, this process allocates it to the lowest level of the configuration, maintains the traceability to the top level requirement, and assures that the total system requirement will be met.

```
                      ┌──────────────┐
                      │ SYSTEM LEVEL │
                      │ PERFORMANCE  │
                      │ REQUIREMENTS │
                      └──────────────┘
              ┌──────────────┐        ┌──────────────┐
              │ ALLOCATABLE  │        │ UNIQUE TO    │
              │ BTWN ELEMENTS│        │ ELEMENT      │
              └──────────────┘        └──────────────┘
        ┌──────────────┐    ┌──────────────┐
        │ ALLOCATABLE  │    │ UNIQUE TO    │
        │ BTWN SUBSYS  │    │ SUBSYSTEM    │
        └──────────────┘    └──────────────┘
  ┌──────────────┐    ┌──────────────┐
  │ ALLOCATABLE  │    │ UNIQUE TO    │
  │ BTWN COMP    │    │ COMPONENT    │
  └──────────────┘    └──────────────┘
```
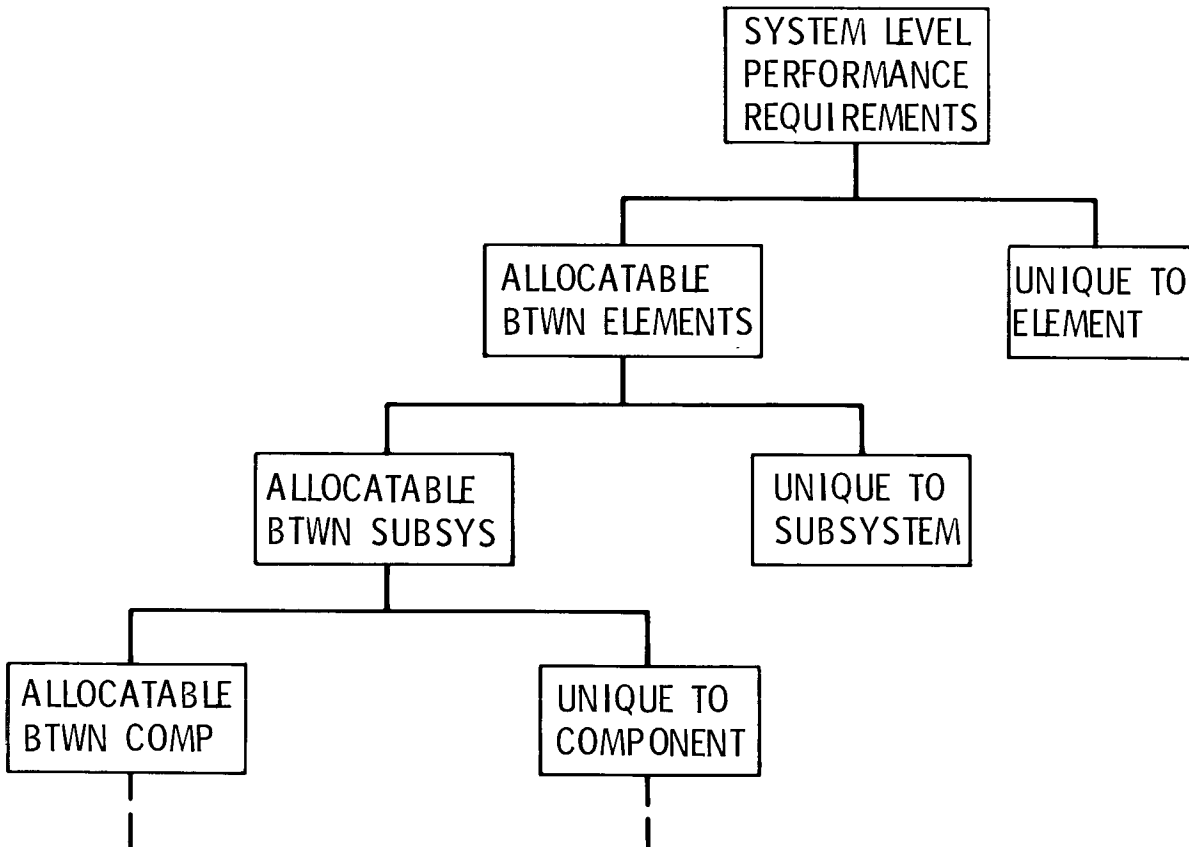
# REQUIREMENTS ANALYSIS

The question is, "What is a proper allocation?" If a top level requirement is rippled to the lowest level, which functional area should contribute what proportion to the final performance? If we rely on an optimization process that merely gives a final answer, we are blind. This is another case of not all functions being included in the optimization process. For these "outside" functions, we have no sensitivity information upon which to base realistic allocations. The actual situation might be as illustrated here, where the cost of attaining a given level of performance varys greatly from one discipline to another. I have used cost as the measure, but I could have used any measure of merit. For the illustration I have given, the optimal allocation of the requirement is that which simultaneously attains the top level system performance and minimizes the cost. In the future, our optimization processes must provide visibility for such data.

## OPTIMIZE ALLOCATIONS
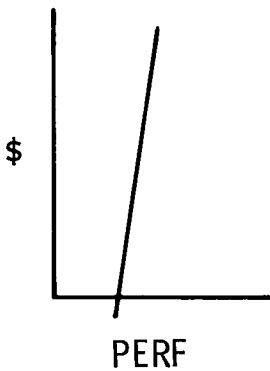


| ALLOCATION 1 | ALLOCATION 2 | ALLOCATION 3 | ALLOCATION 4 |
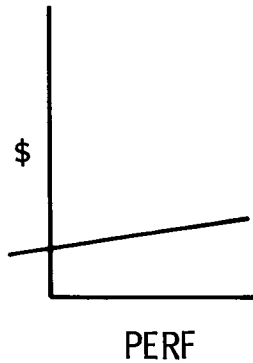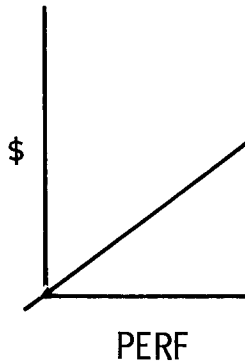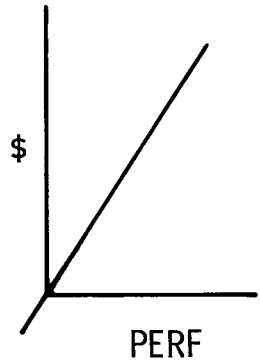
## SUMMARY

I have attempted to illustrate that optimization has a role in our design process, both today and in the future. The benefits are well known already, but I believe that we are only seeing the proverbial tip of the iceberg.

Optimization must, however, continue to be sold and this selling is best done by consistent good performance. For this good performance to occur, the future approaches must be clearly thought out so that the optimization methods solve the problems that actually occur during design. The visibility of the design process must be maintained as further developments are proposed. Careful attention must be given to the management of data in the optimization process, both for technical reasons and for administrative purposes. Finally, to satisfy program needs, provisions must be included to give data to support program decisions, and to communicate with design processes outside of the optimization process.

If we fail to adequately consider all of these needs, the future acceptance of optimization will be impeded. We simply cannot allow that to happen. Optimization is too important.

- **OPTIMIZATION HAS A ROLE IN OUR DESIGN PROCESS**

- **DEVELOPMENT OF OPTIMIZATION METHODS MUST REFLECT NEEDS OF TOTAL DESIGN PROCESS**

# PRACTICAL CONSIDERATIONS
# IN AEROELASTIC DESIGN

Bruce A. Rommel and Alan J. Dodd
Douglas Aircraft Company
McDonnell Douglas Corporation

## ABSTRACT

This paper examines the structural design process for large transport aircraft. Practical considerations include design criteria to satisfy certification requirements of FAR Part 25 and selected JAR requirements. Critical loads must be determined from a large number of load cases within the flight maneuver envelope. The structural design is also constrained by considerations of producibility, reliability, maintainability, durability, and damage tolerance, as well as impact dynamics and multiple constraints due to flutter and aeroelasticity. Aircraft aeroelastic design considerations in three distinct areas of product development (preliminary design, advanced design, and detailed design) are presented and contrasted. The present state of the art is challenged to solve the practical difficulties associated with design, analysis, and redesign within cost and schedule constraints. The current practice consists of largely independent engineering disciplines operating with unorganized data interfaces. The need is then demonstrated for a well-planned computerized aeroelastic structural design optimization system operating with a common interdisciplinary data base. This system must incorporate automated interfaces between modular programs. In each phase of the design process, a common finite-element model for static and dynamic optimization is required to reduce errors due to modeling discrepancies. As the design proceeds from the simple models in preliminary design to the more complex models in advanced and detailed design, a means of retrieving design data from the previous models must be established.

The past 20 years have seen spectacular advances in the methodology for computer-aided design of aerospace structures. However, the gap between theoretical and pilot program development and the practical application to hardware development has remained significant. This paper examines the practical aspects of the aircraft structural design process and attempts to define areas of research needed to close the gap between theory and application. This discussion will illustrate why the gap exists and why the traditional organization of the design process has not led to the new technologies needed to close the gap.

The process of aircraft structural design has traditionally been one of sizing and drawing by the designer. This is followed by analytical and test verification of the design throughout the design development process. The aircraft structural design must, of course, sustain the aeroelastic loads throughout the flight envelope, including dynamic landing and taxi loads, impact dynamics, and acoustics. The aircraft structural design must also be able to prevent the aeroelastic instabilities of flutter and divergence. As shown in Figure 1, the first step in the design process is to establish the design criteria necessary to satisfy the certification requirements for the Federal Aviation Administration, the Joint Airworthiness Requirements, or Military Procurement Specifications. Included in these design requirements are considerations of flutter and aeroelasticity, durability and damage tolerance, and the less tangible requirements stemming from company experience, philosophy, and economics. The purpose of these requirements is to ensure product safety and reliability.
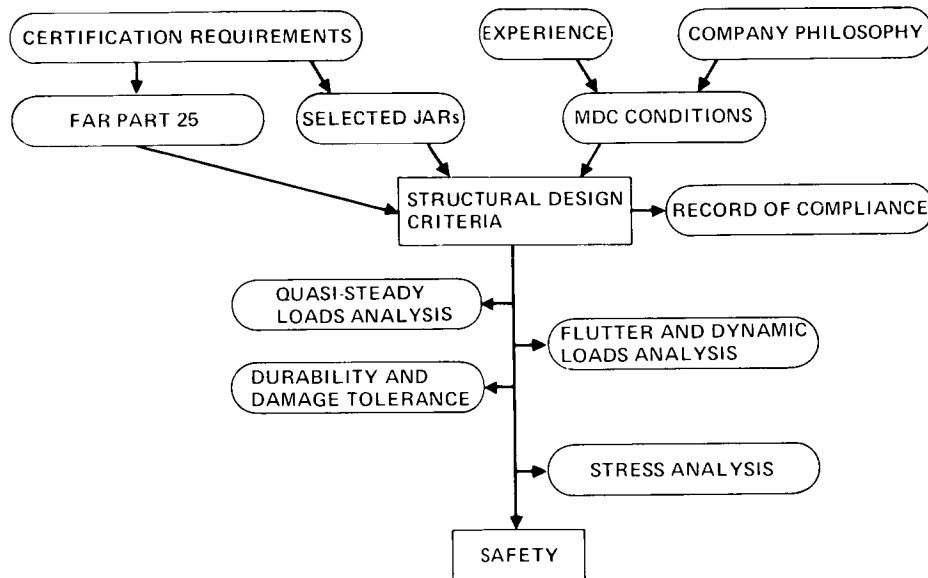


FIGURE 1. DESIGN CRITERIA – THE FIRST STEP

Figure 2 shows a basic breakdown of loads analyses required to satisfy the design requirements of a typical commercial transport aircraft. These analyses include flexibility effects for both steady and dynamic flight loading conditions. Loads induced by balanced maneuvers in flight, as well as dynamic landing and taxi loads and PSD gust loads, must be investigated to ensure that worst-case design loads for a specific aircraft have been found. In addition to the loads induced by normal operation, the off-limits performance induced by possible malfunctions of automated control systems must also be accounted for. Life-cycle loads spectra must provide design criteria for durability and damage tolerance to ensure an adequate service life. The purpose of all of these loads predictions is to provide structural design integrity for strength, fatigue, damage-tolerant, and fail-safe design of the aircraft structure. The "Catch-22" is that most of these loads evaluations require a structural model to predict the load redistribution that takes place due to aeroelastic effects. That is, some design cycle iteration is required between the loads prediction and the structural design before the design loads can be established.
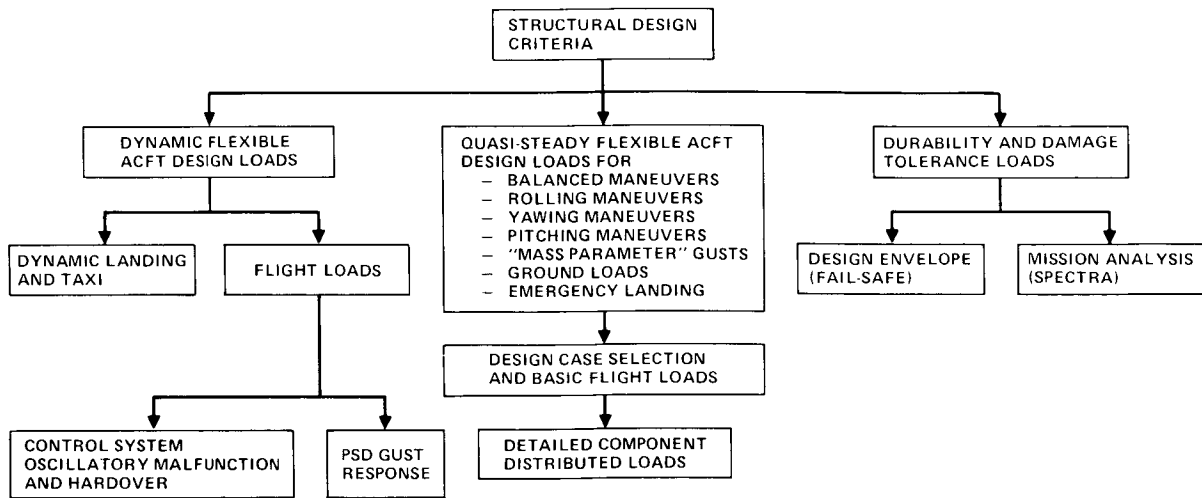
**FIGURE 2. LOADS ANALYSIS SUMMARY**

Figure 3 shows the primary critical load conditions established for the design of a typical commercial aircraft. Each of these load conditions must be examined for a number of variations of flight parameters. Figure 4 shows that, even for a relatively small number of flight parameter variations, a very large number of flight load conditions will result. These loads must then be evaluated to select the critical design loads for structural analysis and design. To accomplish this, most airframe manufacturers use box beam models of the aircraft for loads and dynamics analysis.

Figure 5 shows the critical design considerations for the fuselage of a commercial aircraft. These considerations include impact dynamics for a number of scenarios of survivable crashes. These impact dynamics studies are nonlinear dynamic analyses of a portion of the aircraft. The purpose of these studies is to provide design criteria, such as frame spacing, to limit the damage in these events. An entirely different type of analysis is required to determine fuselage design criteria to limit cabin interior noise due to acoustic effects. These design considerations, coupled with producibility, repairability, durability, damage tolerance, and other factors, make it impossible to achieve minimum weight for fuselage flight design loads.
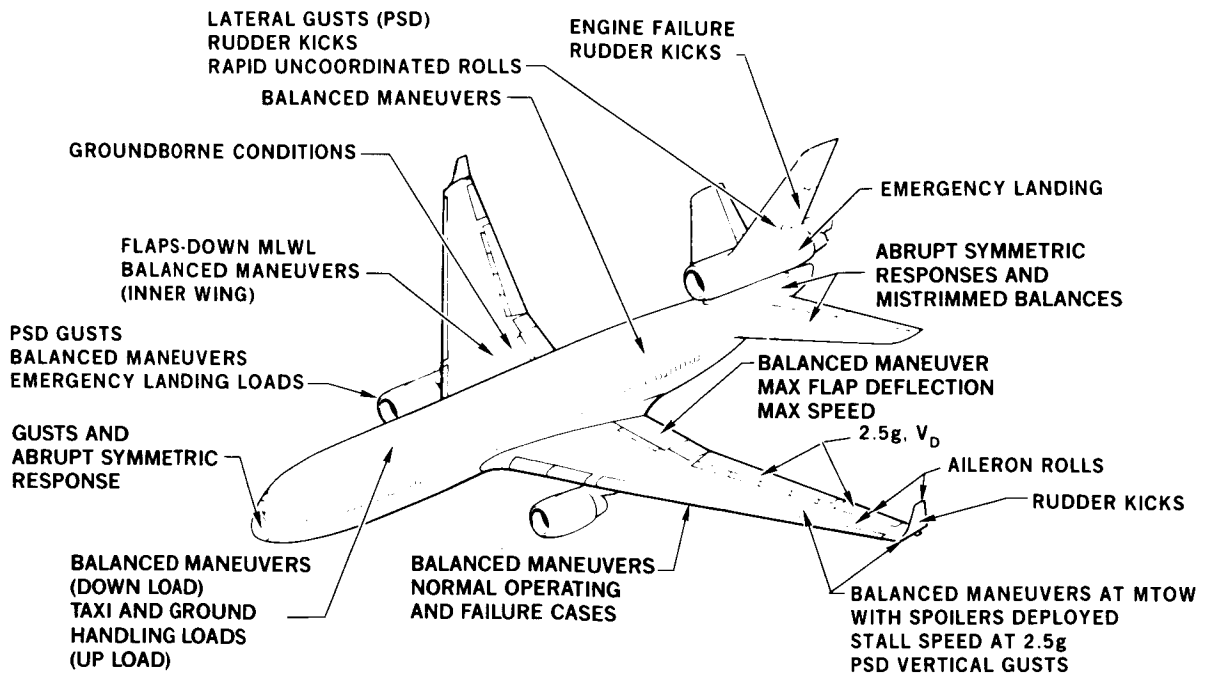


**FIGURE 3. PRIMARY CRITICAL LOADING CONDITIONS**

## BALANCED MANEUVER DESIGN ENVELOPE

| PARAMETER | TYPICAL NUMBER OF VALUES USED |
|---|---|
| SPEED | 5 |
| MACH NO. (ALTITUDE) | x 10 |
| WEIGHT | x 4 |
| CENTER OF GRAVITY | x 2 |
| WING FUEL QUANTITY | x 2 |
| SPEED-BRAKE SPOILER | x 2 |
| THRUST MAX/MIN | x 2 = 3,200 CONDITIONS |

FLAPS DOWN BALANCED MANEUVER SURVEY = 1,600 CONDITIONS

## TOTAL 4,800 CONDITIONS

LARGE NUMBER OF ANALYSIS CONDITIONS MADE POSSIBLE BY USE OF
COMPUTER-BASED METHODS

FIGURE 4. COMPREHENSIVE SURVEY FOR CRITICAL CASE SELECTION

INSPECTABILITY

PRODUCIBILITY

DAMAGE TOLERANCE

DURABILITY

IMPACT DYNAMICS

CUTOUTS

WEIGHT

ACOUSTIC EFFECTS

JOINTS AND SPLICES

REPAIRABILITY
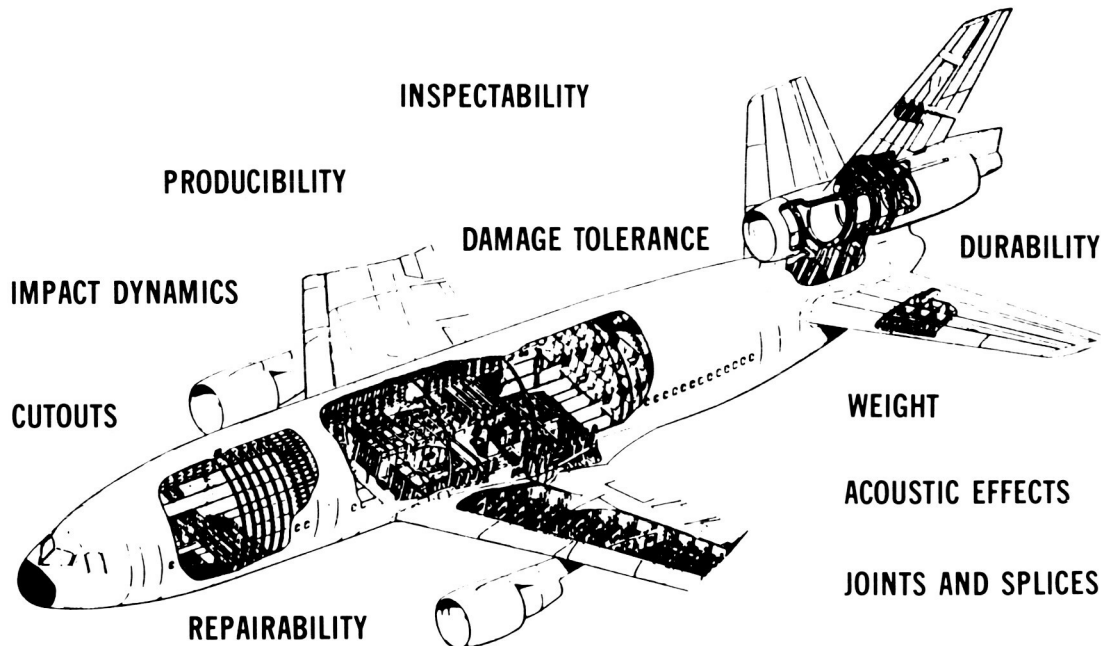
FIGURE 5. CRITICAL FUSELAGE DESIGN CONSIDERATIONS

Figure 6 shows typical service and fatigue life design criteria for a commercial aircraft. Typically, these aircraft are designed for a service life of 20 years or 60,000 flight hours. The fatigue life goal is typically twice the normal service life.

A commercial aircraft, like a combat aircraft, must tolerate a certain amount of damage without being unsafe to fly. Figure 7 shows some of the fail-safe and damage tolerance considerations in use at Douglas Aircraft Company. The fuselage must be able to sustain full design limit loads with a skin crack passing through two bays, including a break in the central longeron or crack stopper. Damage tolerance analysis of composite materials is still immature. There is no universal agreement on failure criteria or even what constitutes a failure in composite materials. Other fail-safe and damage tolerance considerations include maintaining adequate flutter margin after failures in the engine mounts or pylons.

| | FLIGHT STRUCTURE | LANDING GEAR | |
|---|---|---|---|
| | FAIL-SAFE STRUCTURE | SAFE-LIFE STRUCTURE | |
| | MEDIUM AND LONG RANGE | MEDIUM RANGE | LONG RANGE |
| DESIGN SERVICE LIFE (20 YEARS) | 60,000 FLIGHT HOURS 30,000 FLIGHTS/LANDINGS | 50,000 LANDINGS | 33,300 LANDINGS |
| FATIGUE LIFE GOAL (DESIGN MEAN LIFE) | 120,000 FLIGHT HOURS 60,000 FLIGHTS/LANDINGS | 150,000 LANDINGS | 100,000 LANDINGS |

FIGURE 6. SERVICE LIFE AND STRUCTURAL FATIGUE DESIGN CRITERIA

PRIMARY FLIGHT STRUCTURE IS DESIGNED TO BE FAIL-SAFE SO AIRCRAFT MAY BE SAFELY OPERATED AFTER FAILURE OF ANY PRINCIPAL STRUCTURAL MEMBER

DOUGLAS CRITERIA EQUAL OR EXCEED FAR REQUIREMENTS

FUSELAGE SHELL WILL SUSTAIN DESIGN LIMIT LOADS AFTER A FULL TWO-SKIN-BAY CRACK LENGTH IN ANY DIRECTION (WITH CENTRAL CRACK STOPPER OR CENTRAL LONGERON BROKEN)

WING WILL SUSTAIN DESIGN LIMIT LOADS AFTER A FULL TWO-BAY CRACK IN THE SKIN WITH CENTRAL STRINGER BROKEN

ALL PRIMARY CONTROL SURFACES WILL SUSTAIN DESIGN LIMIT LOADS AFTER FAILURE OF ANY HINGE FITTING OR SUPPORT MEMBER
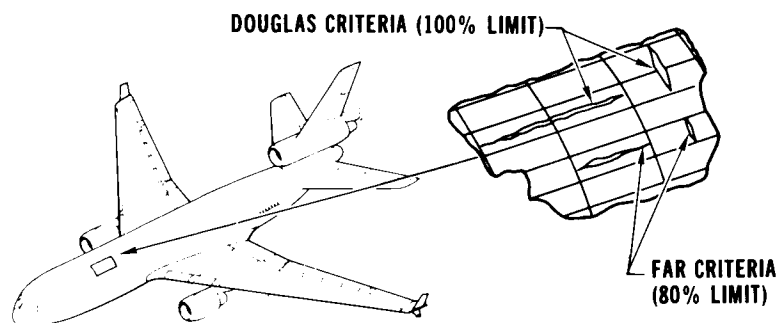


FIGURE 7. DAMAGE TOLERANCE

Figure 8 shows some of the parameter variations that must be studied to certify that a commercial airliner will meet FAA requirements. The basic flutter design requirements permit no flutter, buzz, or divergence below $1.2 V_D$ and no flutter below $V_D$ after any single mechanical failure or any combination of extremely improbable failures, including dual hydraulic system failures. Most of these events can be certified by adequate analysis, but some must be substantiated by testing. Flutter speeds are highly dependent on aircraft geometry as well as the distribution of weight and stiffness. If the flutter margin is negative for any fuel weight, payload configuration, or other parameter variation, a structural redesign is required to raise the flutter speed. About 60 percent of the weight of a commercial aircraft is due to nonstructural components, and not all of the remaining 40 percent is represented in any finite-element model of the aircraft. To account for the difference, the total weight must be estimated from semiempirical data. The weight of material in the finite-element model may be subtracted from the total weight, and the remainder may be distributed to the nodes and elements in the finite-element model.
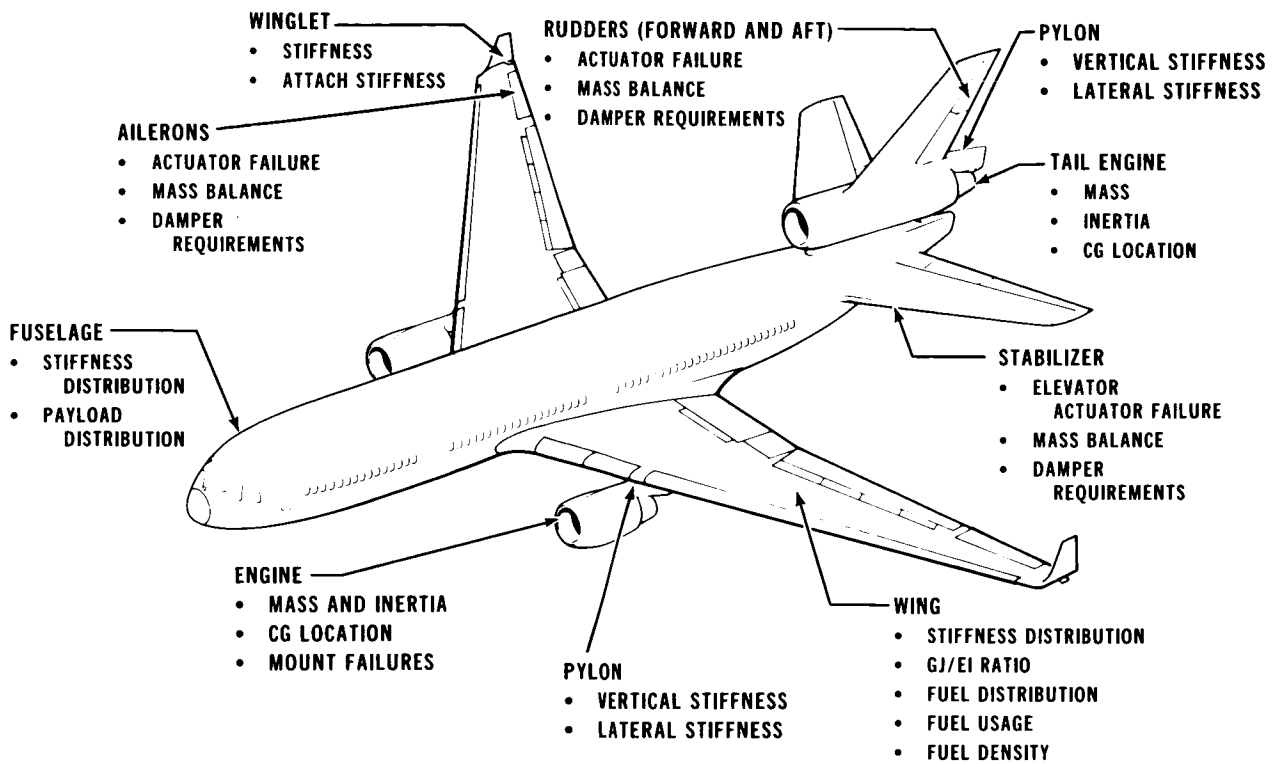
FIGURE 8. PARAMETERS INVESTIGATED FOR FLUTTER

As shown in Figure 9, aeroelastic structural design is constrained by the basic "abilities" — producibility, reliability (fail-safe and safe-life), maintainability, durability and damage tolerance, and inspectability. It may be argued that since the design is not optimum anyway, there is no need to optimize the aircraft structure. The answer is that while the "abilities" constrain the design, satisfying these constraints alone does not ensure that an optimum design has been found. The "abilities" are an important consideration in the design process, but are not the only binding constraints. These constraints may be considered as a set of side constraints that determine upper and lower bounds on the geometric and behavior variables.

As has been shown, the aeroelastic design process is necessarily an iterative process. For example, if analysis shows any part of the structure to be under-strength or vastly over-strength, then design changes are required. Following the design change, new loads are required based on the revised flexibility of the structure. Perhaps a new structural model will be created at this time. In a large aerospace organization, these changes often involve many groups of specialists, each of which has a detailed knowledge of a specific task but little or no knowledge of related tasks. This traditional organization of the design process is slow and unresponsive to the rapid design changes required in preliminary and advanced aircraft design. Furthermore, different structural models are used by different groups for the special needs of each group.

# PRODUCIBILITY

# RELIABILITY (FAIL-SAFE AND SAFE-LIFE)

# MAINTAINABILITY

# DURABILITY (AND DAMAGE TOLERANCE)

# INSPECTABILITY

FIGURE 9. AEROELASTIC STRUCTURAL DESIGN IS CONSTRAINED BY THE BASIC "ABILITIES"

Figure 10 shows some of the organizational constraints imposed on the aeroelastic design process by the traditional approach. These constraints include (1) the multiplicity of structural models, (2) inconsistency in data requirements, (3) lack of interdisciplinary awareness, (4) vesting of traditional values, and (5) loss of communication in the data flow. The use of different structural models by different groups leads to a basic difficulty that must be dealt with in the design optimization process. The problem is in relating the results from one structural representation to the results from another structural representation. For example, the Loads group wants a beam model so that it can find the worst load cases in a set of 4,800 load conditions. Using the beam model, the stress resultants of shear, moment, and torque provide a quick and easy discriminant. On the other hand, the Stress or Strength group needs a finite-element model to perform an adequate stress analysis. The Stress group needs the loads, but frequently it will get the shear, moments, and torques instead. Worse yet, these stress resultants may not be self-consistent, since they may only represent an envelope of the flight load conditions. Adding to the difficulty is the vesting of traditional values by each group and the loss of communication in the data flow. Frequently, data requirements are passed between groups by a trail of interoffice memos rather than the orderly flow of structured data files.

## MULTIPLICITY OF STRUCTURAL MODELS
## INCONSISTENCY IN DATA REQUIREMENTS
## LACK OF INTERDISCIPLINARY AWARENESS
## VESTING OF TRADITIONAL VALUES
## LOSS OF COMMUNICATION IN THE DATA FLOW

FIGURE 10. ORGANIZATIONAL CONSTRAINTS ON AEROELASTIC DESIGN

As shown in Figure 11, the aircraft design development process may proceed in several phases. The first is the initial design phase, in which the aircraft configuration is selected. The second phase is advanced design, where trade studies are performed on a few candidate configurations, and the primary structure is designed and analyzed. Proposal activities are supported by trade studies in the advanced design phase. Source selection and procurement of long-lead-time items may have to be based solely on the results from the advanced design studies. In the third phase, we have the detail design activity. In this stage, a single aircraft configuration has been selected, and detailed design and analysis leading to drawing release and tooling for manufacture are completed. In the fourth phase, we have the growth design stage of the aircraft design cycle. In this last phase, modifications to an existing design (fuselage stretch, re-engine, wing extensions, etc.) lead back to Phase III activities.

**PHASE I**    **CONFIGURATION DESIGN**
INITIAL PRELIMINARY DESIGN EFFORT. CONFIGURATION
ANALYSES. BASIC WEIGHTS BREAKDOWN.
THREE-VIEW DRAWING.

**PHASE II**    **ADVANCED DESIGN**
ADDITIONAL POINT DESIGNS. TRADEOFF STUDIES.
PRIMARY STRUCTURE LAYOUT AND ANALYSIS.
PROPOSAL EFFORTS.

**PHASE III**    **DETAIL DESIGN**
DETAILED DESIGN AND ANALYSIS LEADING TO
DRAWING RELEASE.

**PHASE IV**    **GROWTH DESIGN**
MODIFICATIONS OF EXISTING DESIGNS (FUSELAGE
STRETCH, RE-ENGINE, WING EXTENSION, ETC).
PROPOSALS. TRADEOFFS. FOLLOWED BY PHASE III
ACTIVITY.

FIGURE 11. BASIC AREAS OF DESIGN ACTIVITY

In the initial or configuration design stage of the aircraft design process, weights are determined by semi-empirical data, and the preliminary aerodynamic design is optimized. A preliminary structural model like the box beam model of Figure 12 may be constructed for aeroelastic loads and flutter analysis. These models usually will involve no more than 300 to 500 degrees of freedom (DOF). Flexibility effects that result from changes in direction in the elastic axis and wing-fuselage or tail-fuselage intersections may be estimated or ignored. At a later stage in the design process, these "stick" models may be corrected using the results from finite-element models of local portions of the aircraft structure as shown in Figure 13.

**300 DEGREES OF FREEDOM**

REQUIRES A BOX BEAM
ANALYSIS TO DETERMINE
EI, GJ, AND AE
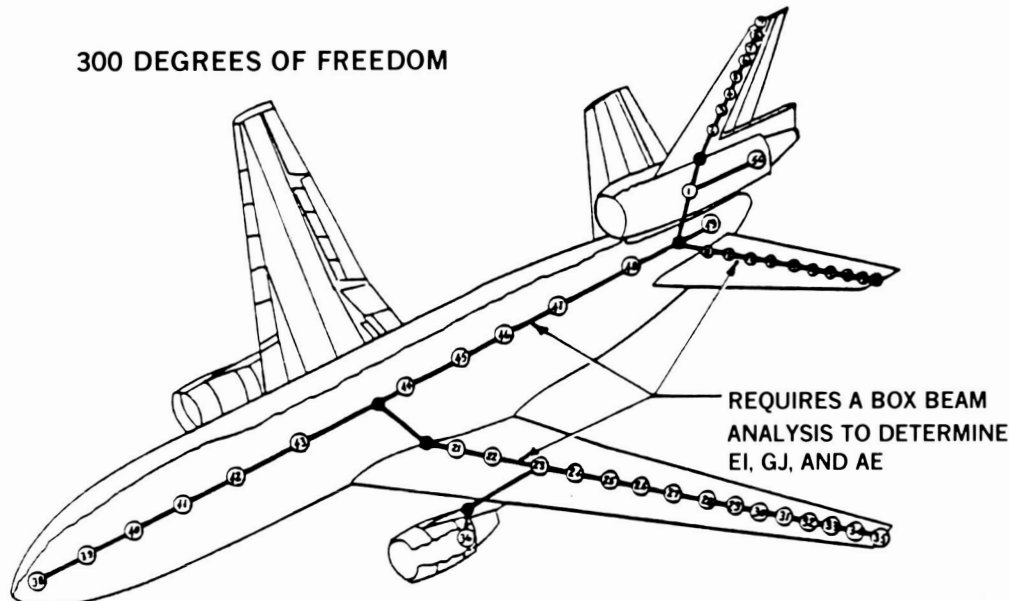
FIGURE 12. BEAM-STICK MODELS MAY BE USED IN PRELIMINARY DESIGN
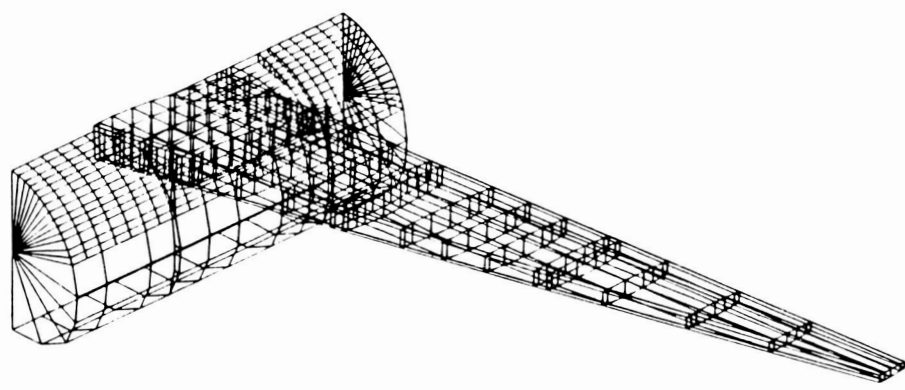
FIGURE 13. WING/FUSELAGE INTERSECTION FINITE-ELEMENT MODEL

In the advanced design phase, these stick models and local structures models may be replaced by coarse-grid finite-element models like that shown in Figure 14. Typically, these coarse-grid models may employ 3,000 to 5,000 DOF. The beam stick models may still be used for loads and dynamic modal analysis of high-aspect-ratio-wing aircraft. For these configurations, beam models are adequate, providing allowances are made for flexibility effects that result from stress redistributions. These stress redistributions, which are a secondary effect in the loads and modal analyses, are of primary importance to the static strength analyses. For this reason, the structural model for static strength analyses includes structural details often omitted or only grossly represented in the dynamics and loads model.

To automate the design process, one must use common structural models at each stage of the design process and provide a uniform if not consistent means of relating the results from one structural model to those of another. This is true for both the sequential design and the simultaneous design process.
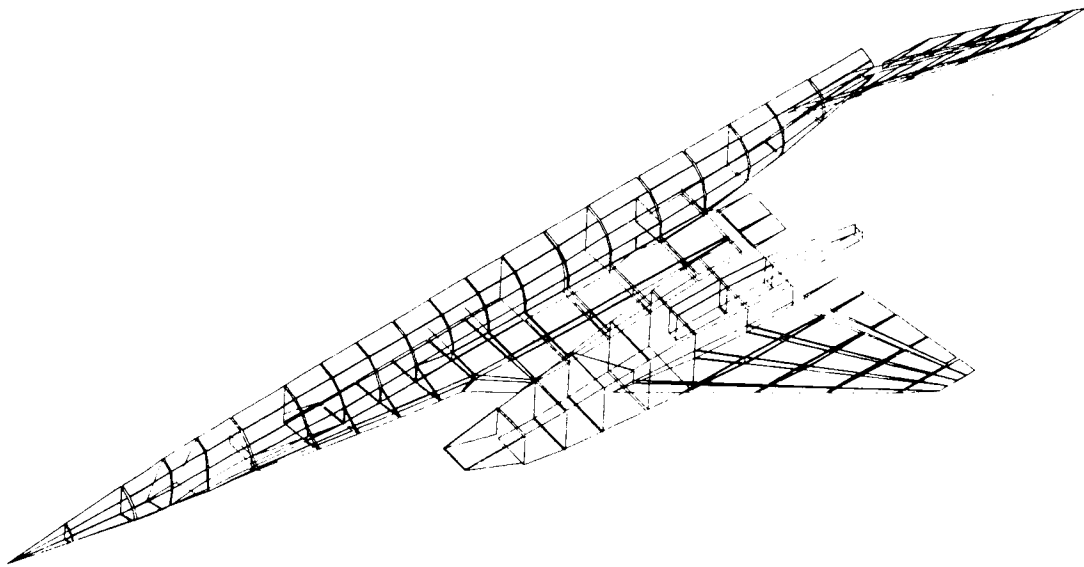
FIGURE 14. FINITE-ELEMENT AIRCRAFT MODEL USED IN ADVANCED DESIGN

In the sequential design process, a suboptimization is performed to satisfy a subset of the constraints. For example, one may perform a static strength optimization to resize the structure for a number of the most critical load conditions. This process may be followed by a flutter optimization to increase the flutter speed for a number of different payloads and fuel weight conditions. To avoid violating the static strength constraints during the flutter resizing, one may use the structural sizes found by the static strength optimization as minimum gauge constraints in the flutter optimization. However, if one is using a detailed finite-element model for static strength optimization and a beam stick model for flutter optimization, then one is faced with the very difficult task of converting the finite-element model into an equivalent beam representation and defining the minimum gauge constraints. Also, the joint flexibility that results from stress redistribution at discontinuities in the elastic axis will be altered by the flutter resizing process. These problems can be eliminated if one uses the same structural model for both static strength and flutter optimization.

In the simultaneous design process, both strength and flutter constraints must be satisfied at the same time. It seems apparent that simultaneous design requires common models for both strength and dynamics work. This, too, is not without difficulty.

Figure 15 shows one of the models used in a recent Phase III design study. In the detailed design phase, structural models may use 20,000 to 60,000 DOF, which will pose great challenges for the dynamic and loads analysis. Figure 16 shows some of the approaches to modal analysis of very large models. These approaches include direct methods, such as subspace iteration and the Lanczos algorithm, as well as indirect methods, such as component mode synthesis and successive mesh refinement (modal assembler solver).

Most of these techniques have been used on models as large as that shown in Figure 15. However, the cost of these analyses continues to be a significant factor. Until these techniques are in routine use on super computers or low-cost "super-mini's," there will be strong opposition to using these models in automated aeroelastic design.

Figure 17 summarizes some of the challenges that must be met in developing a practical aeroelastic design optimization system. These challenges are as follows:

Fatigue and Damage Tolerance Design Criteria — To begin with, one must determine fatigue and damage tolerance design criteria for use in the preliminary and advanced design phases of the aircraft design process.

Finite-Element Modeler (FEM) Extensions — FEM programs developed for conventional analysis do not provide details such as design vector definition and design variable linkage data, nor do they provide for broken member element groups.

44

**Damage Tolerance in Design** — Special analysis procedures must be developed to handle damage tolerance considerations within the design cycle. In principle, some aspects of damage tolerance analysis can be handled as a sensitivity analysis. This simple strategy is complicated by a large combination of member groups and load sets.

**Aeroelastic Tailoring with Composite Materials** — The strength and stiffness of composite materials may be tailored to achieve desired aeroelastic characteristics. However, this advantage of composite materials will not be fully realized until experimentally verified failure criteria can be agreed upon.
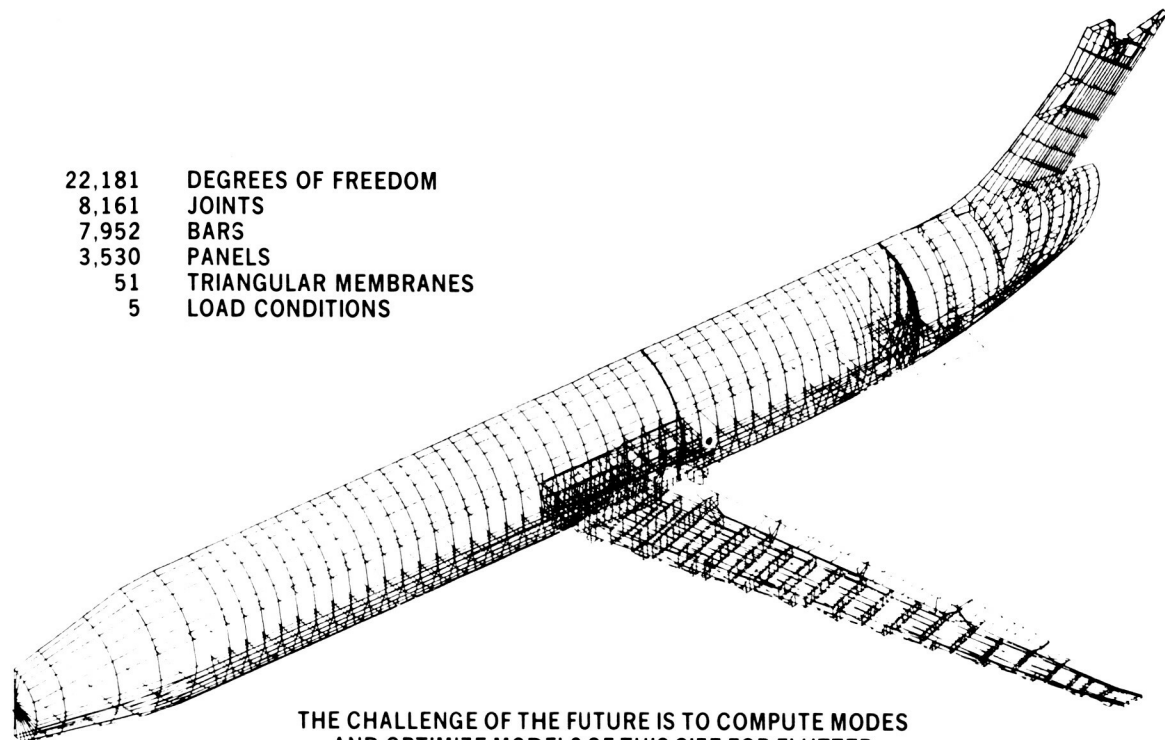
|        |                       |
|--------|-----------------------|
| 22,181 | DEGREES OF FREEDOM    |
| 8,161  | JOINTS                |
| 7,952  | BARS                  |
| 3,530  | PANELS                |
| 51     | TRIANGULAR MEMBRANES  |
| 5      | LOAD CONDITIONS       |

THE CHALLENGE OF THE FUTURE IS TO COMPUTE MODES
AND OPTIMIZE MODELS OF THIS SIZE FOR FLUTTER

FIGURE 15. FINITE-ELEMENT AIRCRAFT MODEL USED IN DETAILED DESIGN STUDIES

## DIRECT METHODS
- ### SUBSPACE ITERATION
- ### LANCZOS ALGORITHM

## INDIRECT METHODS
- ### COMPONENT MODE SYNTHESIS
- ### SUCCESSIVE MESH REFINEMENT (MODAL ASSEMBLER SOLVER)

FIGURE 16. APPROACHES TO MODAL ANALYSIS OF VERY LARGE MODELS

DETERMINATION OF FATIGUE ALLOWABLES AND DAMAGE
TOLERANCE CRITERIA FOR PRELIMINARY AND ADVANCED
DESIGN STRUCTURAL OPTIMIZATION

FINITE-ELEMENT MODELER EXTENSIONS

DAMAGE TOLERANCE IN DESIGN

AEROELASTIC TAILORING WITH COMPOSITE MATERIALS

DETERMINATION OF BUCKLING AND CRIPPLING ALLOWABLES

MODAL ANALYSIS OF VERY LARGE STRUCTURAL MODELS

SPECIAL FINITE ELEMENTS

DEFINITION OF CRITICAL AEROELASTIC LOAD CASES FOR
STATIC STRENGTH

SIMULTANEOUS DESIGN FOR STRENGTH AND FLUTTER

FIGURE 17. AEROELASTIC STRUCTURAL OPTIMIZATION CHALLENGES

Determination of Buckling and Crippling Allowables — Compression allowables may be determined by buck-ling stress, which is dependent on the design variables. When buckled skin models are used for static strength analysis, a model dependency results that is inappropriate in modal analysis for dynamics and loads work.

Modal Analysis of Very Large Structural Models — If common models are to be used for static strength and dynamics, then highly efficient means of modal analysis of very large structural models will have to be devised.

Special Finite Elements — Special finite elements are required for preliminary and advanced design as well as for structures that use composite materials.

Critical Aeroelastic Load Cases for Static Strength — The determination of critical aeroelastic loads for static strength involves a large number of load conditions and load cycling.

Simultaneous Design for Strength and Flutter — Sequential and simultaneous design both require common structural models or complex means of relating modeling parameters from different models.

Added to the above technical challenges are the organizational constraints discussed earlier and the reluctance to accept change.

The practical stituations described in this paper are changing. Comprehensive computer data bases are being developed to formalize and speed the transfer of data between engineering disciplines. To do this requires a dialogue between disciplines and a definition and awareness of common goals. AFFDL and NASA, among others, are funding development of program systems for automated aeroelastic design. On the horizon loom the super com-puters, holding out the prospect of eliminating most practical constraints on problem size and computing cost.

The challenge today is not how to solve the engineering problems as much as how to organize the solving of the engineering problems to take full advantage of the tools that are available.

FLUTTER OPTIMIZATION

IN

FIGHTER AIRCRAFT DESIGN

William E. Triplett
McDonnell Aircraft Company
St. Louis, MO

# OPTIMIZATION APPLICATIONS

The efficient design of aircraft structure involves a series of compromises among various engineering disciplines. These compromises are necessary to ensure the best overall design. To effectively reconcile the various technical constraints requires a number of design iterations, with the accompanying long elapsed time. Automated procedures can reduce the elapsed time, improve productivity and hold the promise of optimum designs which may be missed by batch processing.

This presentation includes several examples of optimization applications including aeroelastic constraints. Particular attention is given to the success or failure of each example and the lessons learned. The specific applications are shown in Figure 1. The final two applications were made recently.

| Program | Design Phase | Configuration |
|---------|--------------|---------------|
| COPS | Conceptual | F-15 Stabilator[1-2] |
| TSO | Preliminary | Various Configurations[3-4-5] |
| FASTOP | Preliminary | NASTRAN Beam-Rod Wing[6-7] |
| NASTRAN "Sensitivity" | Detail | NASTRAN Beam-Rod Stabilator |

Figure 1

# COPS ANALYTICAL MODEL

Figure 2 illustrates the modeling of the stabilator in the Computerized Optimization Procedure for Stabilators (COPS); Reference 1 describes the procedure. The analytical model is a single-cell torque box idealized by eight discrete rigid chord streamwise sections with three mass points per section. Quasi-steady aerodynamic forces act at user specified locations in each section. Nondimensional geometrical design parameters may be specified for taper ratio, thickness ratios at root and tip chords, aspect ratio, leading edge sweep angle, tip cut-off angle, pitch axis hinge line angle, pitch axis intersection with the mean aerodynamic chord (MAC), and spar locations.
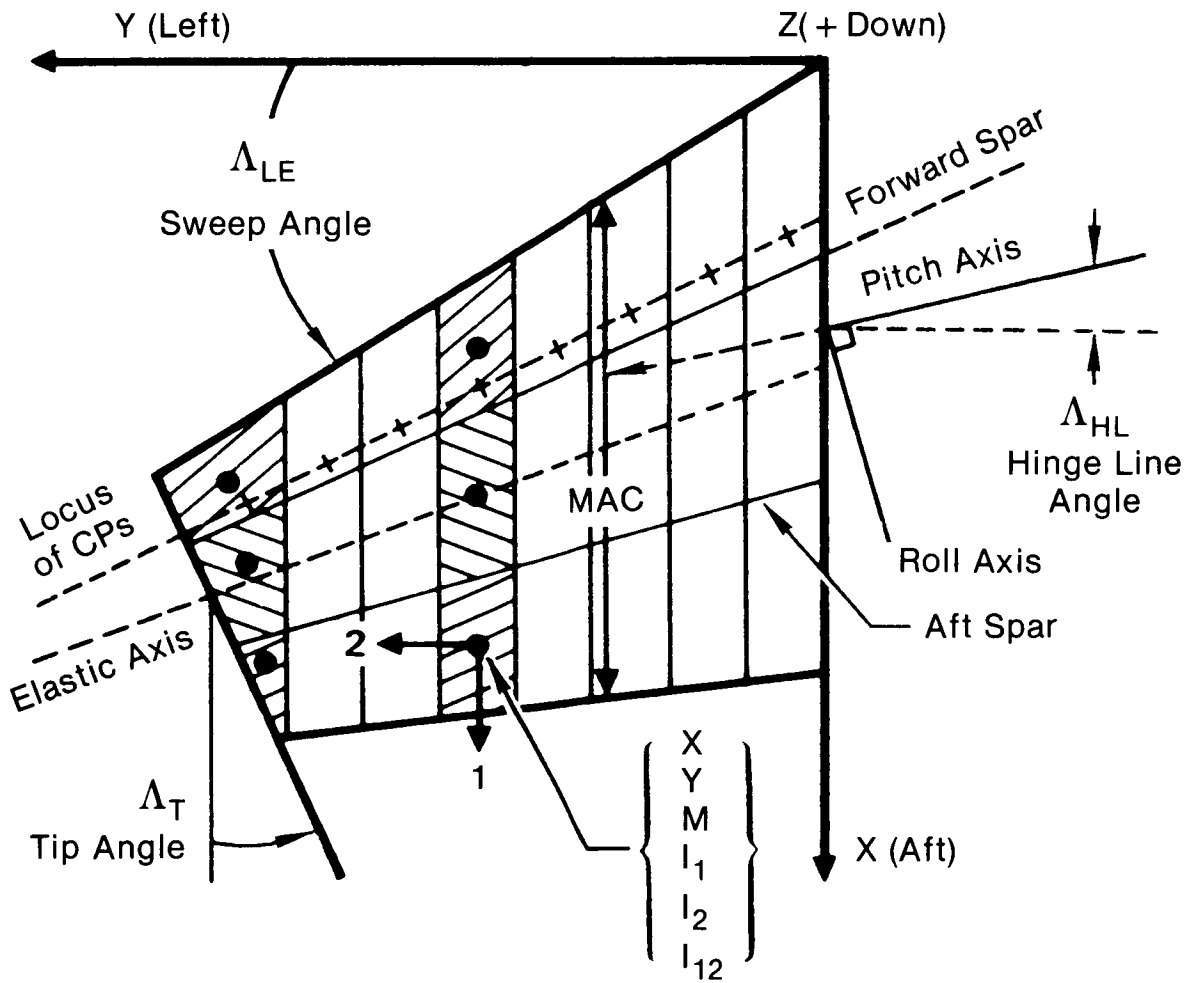
Figure 2

# COPS CONCEPTUAL FLOW DIAGRAM

A greatly simplified flow diagram is shown in Figure 3. The procedure synthesizes, from the input data, a stabilator which satisfies all system constraints except those for flutter and divergence. A systematic perturbation of design variables for 1) torsional stiffness, 2) balance weight, 3) pitch restraint and 4) roll restraint follows until the aeroelastic constraint is satisfied for minimum additional weight. The procedure may be used in its basic sequential optimization scheme, where a new dynamic system is established after each iteration step. It may alternately be used in its simultaneous optimization mode, where each design variable is individually and exclusively evaluated from the same initial design point. The basic COPS program contains a realistic representation for every significant aspect of a believable stabilator flutter analysis and is fast enough, on the computer, to be used as an integral part of more encompassing aircraft systems optimization programs, as shown in the figure.
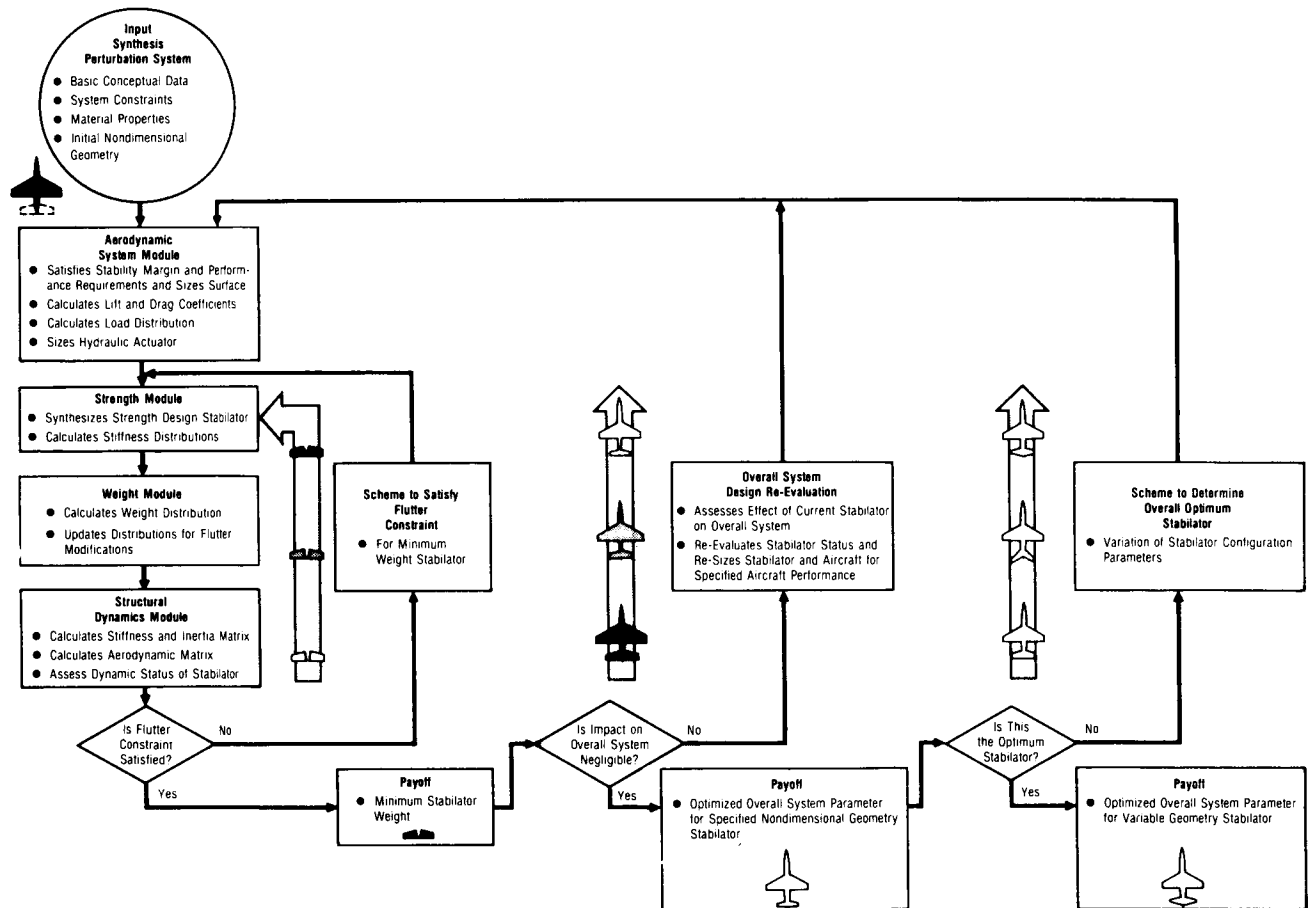


Figure 3

# COPS EXAMPLE - EARLY CONCEPTUAL DESIGN FOR F-15 STABILATOR

Using the semi-automatic "simultaneous" procedure, the COPS program was used to calculate the ratios of the change of flutter dynamic pressure to weight change $(\Delta Q/\Delta W)$ for separate perturbations of stiffness at each of the elastic axis stations, as shown in Figure 4a. Flutter was calculated for specified levels of $\Delta Q/\Delta W$ and compared, in Figure 4b, with optimization runs based on a torsional stiffness distribution proportional to the fourth power of the local chord and separately by balance weights at the tip leading edge. The balance weight of approximately 15 lb is the minimum weight solution. Figure 4c shows the stiffness distributions for both the $C^4$ and sensitivity approaches.

**Sensitivities for Separate Perturbations of Stiffness**

**Comparison of Weight for Flutter**

**Comparison of Stiffness Distributions for Flutter**



(a)

(b)

(c)
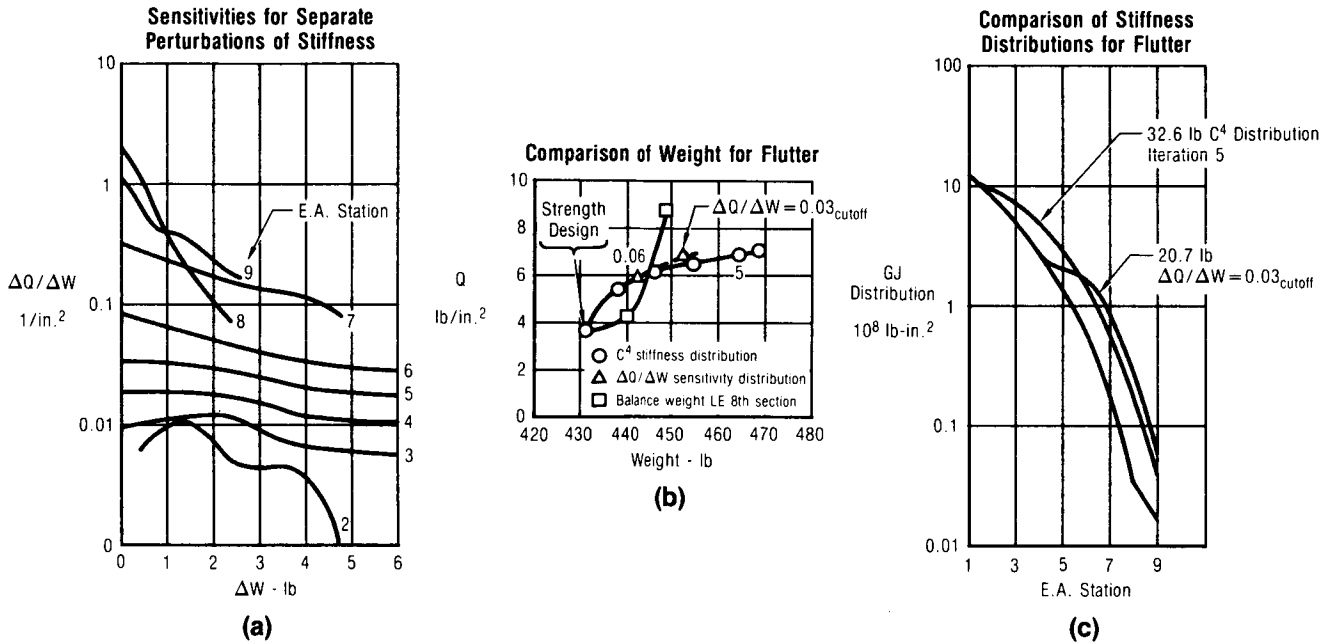
Figure 4

# DETAIL DESIGN OF OPTIMUM F-15 STABILATOR

Two separate configurations were considered for the final F-15 detail design, as shown in Figure 5a and discussed in Reference 2. The flutter model test results are summarized in Figure 5b. The 15-lb balance weight produces an overall increase in flutter speed with Mach number. The snag leading edge produces an overall increase in flutter speed, similar to that for the balance weight, at low speeds. However, the speed variation with Mach number is quite different, with the snag showing an initial sharper drop with increasing Mach number followed by a subsequent sharper rise with further Mach number increase. Analyses indicated the favorable sharper rise to be associated primarily with the aft shift in stabilator aerodynamic center attributable to the area removed by the snag. The snag offered a significant weight savings over the balance weight with no effect on subsonic drag, aircraft stability or flying qualities. A small supersonic drag penalty was offset by the attendant weight reduction.

**Alternate Configurations**

Snag
Leading
Edge

Squared Tip for 15 lb
Outboard Leading
Edge Balance Weight

**(a)**

**Flutter Velocity
vs
Mach Number**

Balance Weight
Snag
Unstable
Stable
Aircraft Envelope
15% Flutter
Margin

Normalized
Velocity

Normalized Mach Number

**(b)**
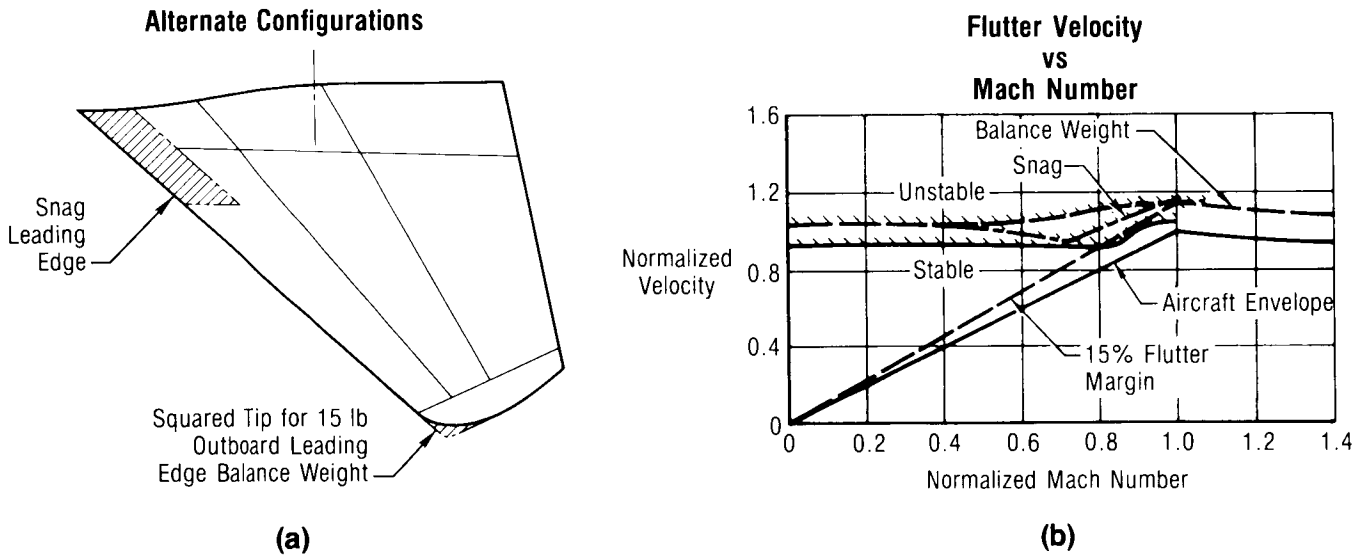
Figure 5

## AEROELASTIC TAILORING STUDY CONFIGURATIONS

Studies have been conducted on the use of the directional properties of composite material to provide design improvements for fighter aircraft as discussed in Reference 3. The TSO (Aeroelastic Tailoring and Structural Optimization) computer program, Reference 4, which was developed by the Air Force Flight Dynamics Laboratory (AFFDL), was used in these investigations. The configurations evaluated, shown in Figure 6, covered a wide spectrum of fighter aircraft aerodynamic surfaces, including 1) the F-15 composite wing, 2) a preliminary design horizontal tail, 3) a prototype aircraft movable outer panel, and 4) a conceptual wing for a future aircraft. The TSO program was validated with the F-15 composite wing which was designed to have the same distributed stiffness characteristics as the production metal wing. In spite of the structural approximations required by the TSO program, the predicted aeroelastic properties were surprisingly close to measured values.
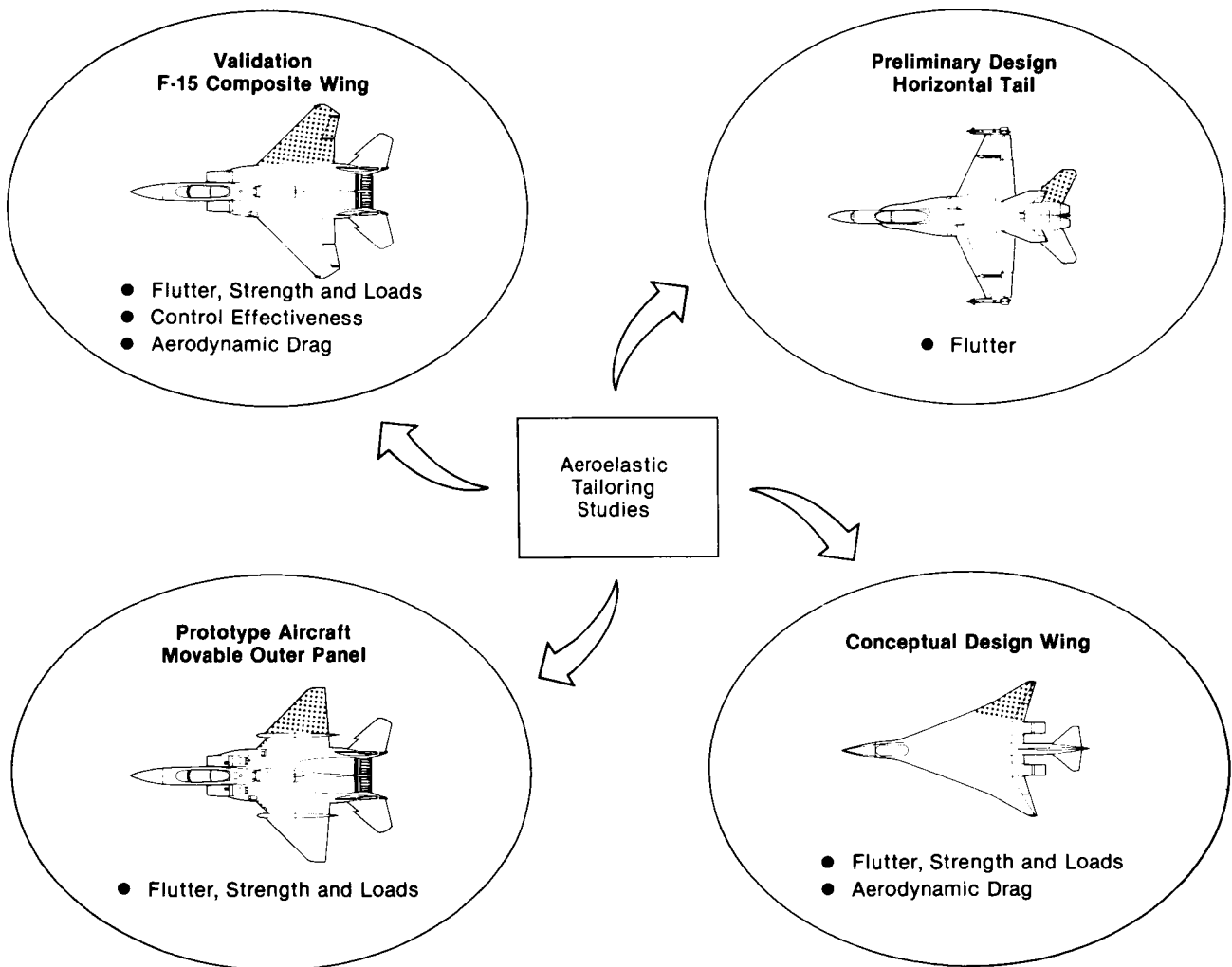


Figure 6

Aeroelastic tailoring can play a significant role in the design of aircraft in various ways, as indicated in Figure 7. Specific detail is given for each configuration in References 3 and 5.

As currently configured, the TSO computer program is appropriate for use primarily in preliminary design. The restrictive structural modeling requirements of TSO lead to converged results which are generally qualitative and which must be liberally interpreted when converting to a design that can be built. The experience gained in the validation studies of the F-15 composite wing design, however, indicates that skillful use of the procedure can also yield good results in final detail design.

### F-15 Composite Wing

- Drag Reduction and Increased Roll Effectiveness With No Weight Cost

### Preliminary Design Horizontal Tail

- Composite Material Performs Dual Function of Strength and Flutter Balance Weight

### Prototype Aircraft Movable Outer Panel

- Optimum Solution Based on Wing Root Pitch Restraint Increases

### Conceptual Design Wing

- Significant Wing Twist Offering Potential Aerodynamic Benefits

### Forward Swept Wing

- Zero Weight Cost for Divergence

Figure 7

## EQUIVALENT AFT SWEPT WING MODELS

The optimized forward swept wing (FSW) was compared with three equivalent aft swept wings (ASW),shown in Figure 8,and evaluated for the same design constraints,as discussed in Reference 5. They are 1) an Equivalent Leading Edge sweep, where the ASW leading edge sweep angle is the negative of the FSW leading edge sweep angle, 2) an Equivalent Elastic Axis sweep, and 3) a Flipped Wing. The wing geometry applies to all four wings. The wings were shifted longitudinally to give the same locations for the mean aerodynamic chords (MAC). The same aerodynamic and structural models were used for all four wings. One of the apparent effects of the equivalent leading edge design is a structural bending axis that is about 20% shorter than the axis of the FSW. The bending axis for the flipped wing design, on the other hand, is about 12% longer.

BL 60.8

$\Lambda_{LE} = -30.30°$
$\Lambda_{TE} = -53.72°$
$L_{EA} = 221$ in.

$X_0$

MAC

**Equivalent Leading Edge**
$\Lambda_{LE} = 30.30°$
$\Lambda_{TE} = -10.98°$
$L_{EA} = 176$ in.

**Equivalent Elastic Axis**
$\Lambda_{LE} = 48.45°$
$\Lambda_{TE} = 19.31°$
$L_{EA} = 221$ in.

**Flipped Wing**
$\Lambda_{LE} = 53.72°$
$\Lambda_{TE} = 30.30°$
$L_{EA} = 248$ in.

| Wing Geometry NACA 64A0XX | |
|---|---|
| Theo Area | 382.92 ft$^2$ |
| Aspect Ratio | 3.80 |
| Taper Ratio | 0.15 |
| Span/2 | 228.9 in. |
| $C_R$ (Theo) | 209.5 in. |
| $C_T$ | 31.4 in. |
| Mean Aero Chord $\bar{c}$ | 142.5 in. |
| $\bar{Y}_{MAC}$ | 86.3 in. |
| t/c (Root) | 0.052 |
| t/c (Tip) | 0.050 |
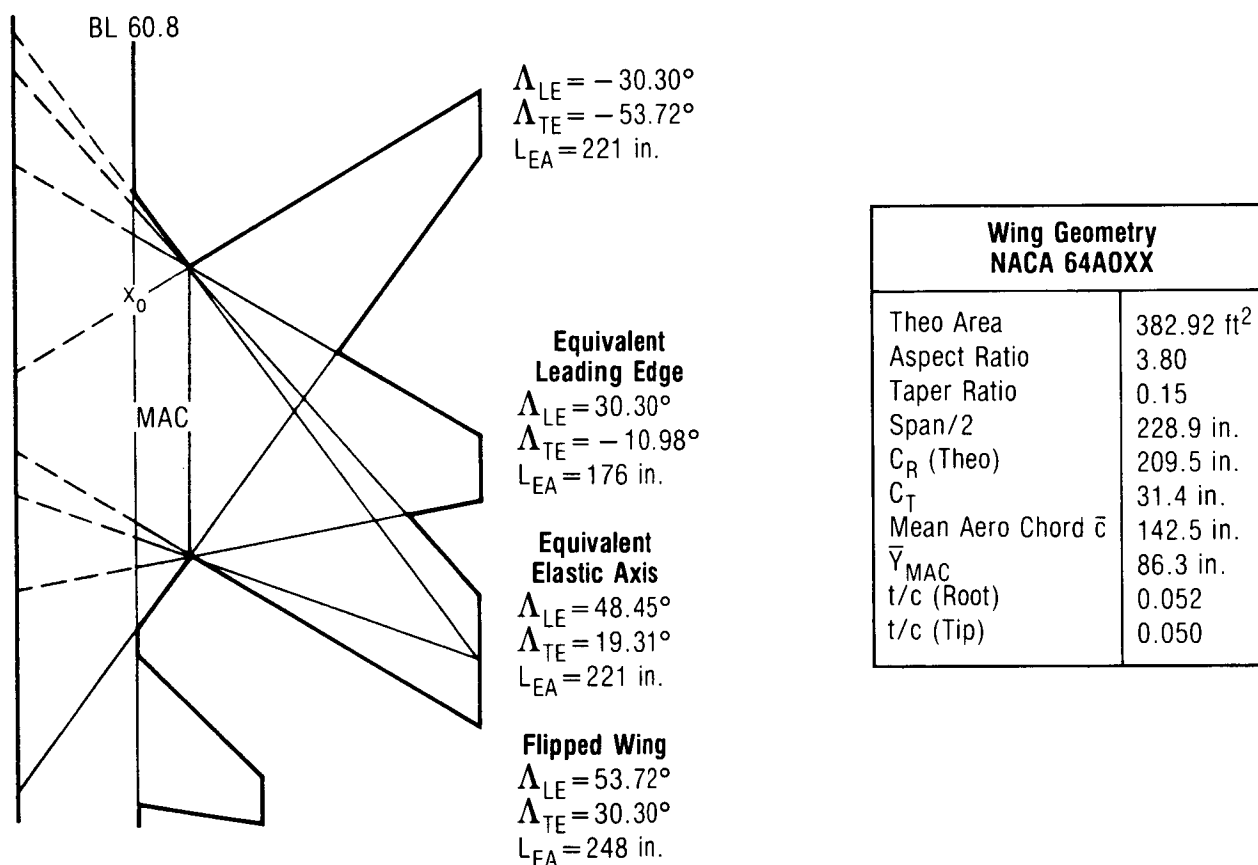
Figure 8

## COMPARISON OF FORWARD SWEPT WING WITH
## THREE EQUIVALENT AFT SWEPT WINGS

Each of the ASWs was optimized by TSO and the results are shown in Figure 9. The FSW has the highest torque box skin weight and the Equivalent LE ASW, which is essentially a straight wing such as on the F-18, has the lowest weight. This weight advantage of the nearly straight wing is a direct result of the reduced structural axis length, which can be seen by comparing the bending moment normal to the elastic axis at the fuselage moldline. The air loading is also most favorable for the design of the fuselage carry-through structure on the FSW and the straight wing, as shown by considering both pitch and roll moments at the wing root. The ASWs are divergence free but have an active flutter constraint. The FSW has favorable flutter properties, primarily because the frequency of the wing bending mode changes very little with increasing airspeed. Coupling with the torsion mode still occurs, but at a higher velocity than for the ASWs.

| | FSW Optimum | ASW Equivalent Leading Edge | ASW Equivalent Elastic Axis | ASW Flipped Wing |
|---|---|---|---|---|
| Composite Layer Orientation - deg ($\theta_1$, $\theta_2$, $\theta_3$ With Respect to Bending Axis) | $-80.9$, $+11.1$, $+14.5$ | $-45$, $0$, $+45$ | $-45$, $0$, $+45$ | $-45$, $0$, $+45$ |
| Torque Box Skin Weight - lb | 227.5 | 118.9 | 162.1 | 158.9 |
| Wash-in Angle at Tip - deg (Elastic) | 5.1 | $-0.2$ | $-5.1$ | $-7.6$ |
| Total Panel II Load | 59,159 | 64,973 | 62,240 | 59,604 |
| Roll Moment at Panel II Root About BL 60.8 - in.-lb $\times 10^6$ | 4.03 | 4.51 | 4.10 | 3.78 |
| Pitch Moment at Panel II Root About $X_0$ - in.-lb $\times 10^6$ | $-1.65$ | 3.56 | 5.63 | 6.08 |
| Bending Moment Normal to Elastic Axis at Moldline - in.-lb $\times 10^6$ | 6.32 | 4.27 | 4.47 | 4.54 |
| Divergence Velocity - kt (Required Velocity $=912$) | 936 | NA | NA | NA |
| Flutter Velocity - kt | 1,050 | 810 | 820 | 760 |
| Aileron Roll Effectiveness $=$ Total RM / Rigid RM | 1.13 | 0.43 | 0.35 | 0.29 |
| Flexible / Rigid Panel II Lift Ratio | 1.19 | 1.01 | 0.85 | 0.80 |

**Mach 0.9, Sea Level, 7.33 g**

Figure 9

56

# FASTOP APPLICATION TO NASTRAN BEAM-ROD
## DYNAMIC MODEL

The FASTOP (Flutter and Strength Optimization Program) computer program (Reference 6) which was developed by the AFFDL, has been applied to a beam-rod vibration and flutter idealization of a wing/store flutter model. The chosen configuration for this detail design application was a wind tunnel model with two stores on an outboard pylon and wing tip missile on, as described in Reference 7. The NASTRAN model is shown in Figure 10. The NASTRAN beam elements are based on GJ and EI stiffness distributions, referred to an elastic axis, with similar distributions for the leading and trailing edge control surfaces and the missile. There are rigid bars to connect the various components with the proper boundary conditions. Concentrated-elasticity members are used to represent integral springs, e.g. actuators, wing fold, missile/launcher/wing interfaces and wing/fuselage attachment. Structural optimization is not feasible because FASTOP does not calculate stresses in the beam elements. Steady air loads are not required because the starting point is an existing strength design. It was felt that the chances for success would be excellent for this simple straightforward model which has only 147 structural members.
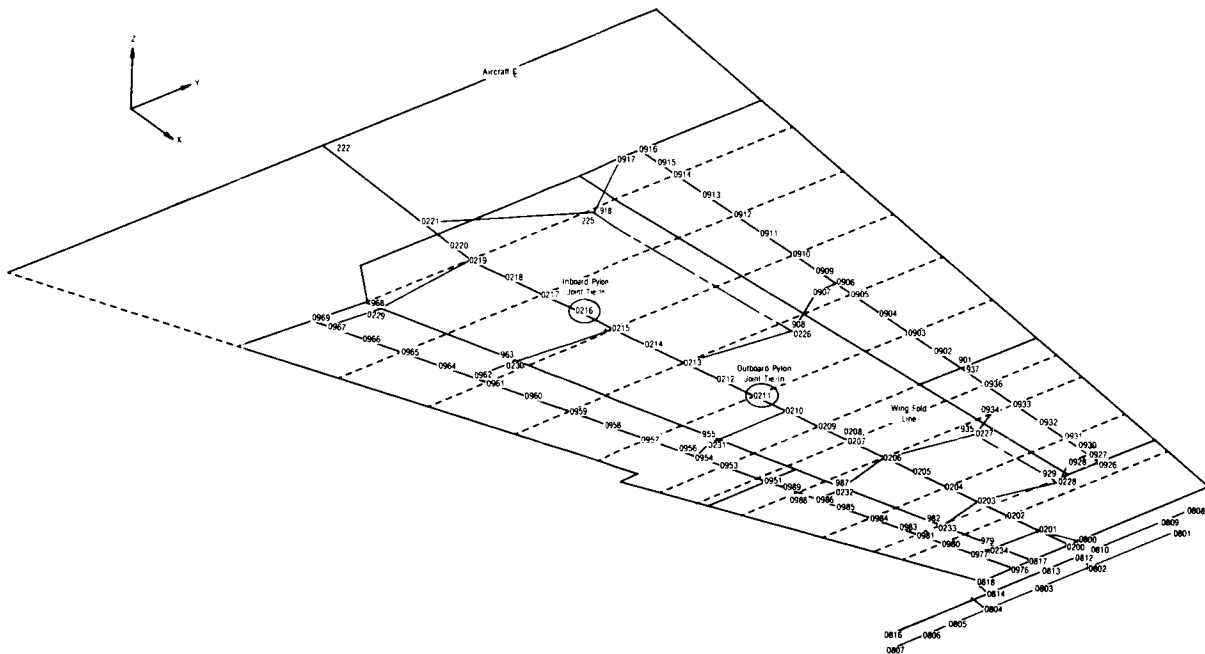


Figure 10

# FASTOP ANALYTICAL CONSIDERATIONS

Many approximations and computational difficulties were encountered in converting the NASTRAN model to FASTOP, as indicated in Figure 11.

## Strength Analysis
- Concentrated Elasticity Converted to Pseudo Rigid Beams
- Rigid Bars Converted to Pseudo Rigid Beams
- Grid Points Renumbered to Satisfy Bandwidth Requirement
- Trailing Edge Control Surface Actuator Beams Placed in Plane of the Wing
- Pylon and Stores Eliminated From Analysis

## Vibration Analysis
- Diagonal Inertia Matrix to Satisfy Positive Definite Check
- Vibration Calculated for Only 20 Normal Modes
- Frequency Comparison Better Than Expected Considering Structural Compromises

## Unsteady Aerodynamics
- Three-Dimensional Missile Model Converted to Flat Plate to Satisfy Interpolation Procedure

## Flutter Analysis
- Non-Optimum Weight Factors Defined for Each Beam Element
- Resizing Permitted Only for Main Torque Box and Control Surfaces

Figure 11

## FASTOP FLUTTER OPTIMIZATION RESULTS

The results shown in Figure 12 look promising until one examines the redesign changes in the individual elements. The first 3 design cycles add increments of weight to the structural elements in proportion to their flutter velocity derivatives, $\partial V_f / \partial W_i$, provided the derivatives are larger than an arbitrary minimum. This arbitrary minimum, which is not specified by the user, leads to an uneven spanwise distribution with peaks and valleys. It suffers from the lack of a built-in French Curve, which would smooth out the peaks and valleys to create a near-optimum design that could be built. The design cycles 4-10 continue the optimization by adjusting the weight distribution, while maintaining the desired flutter velocity. This weight adjustment reduces the increments along the wing torque box and builds up a large mass at the leading edge of the wing. The final design has only a large mass at the leading edge, near mid span, much like a forward mounted engine on a transport aircraft wing.
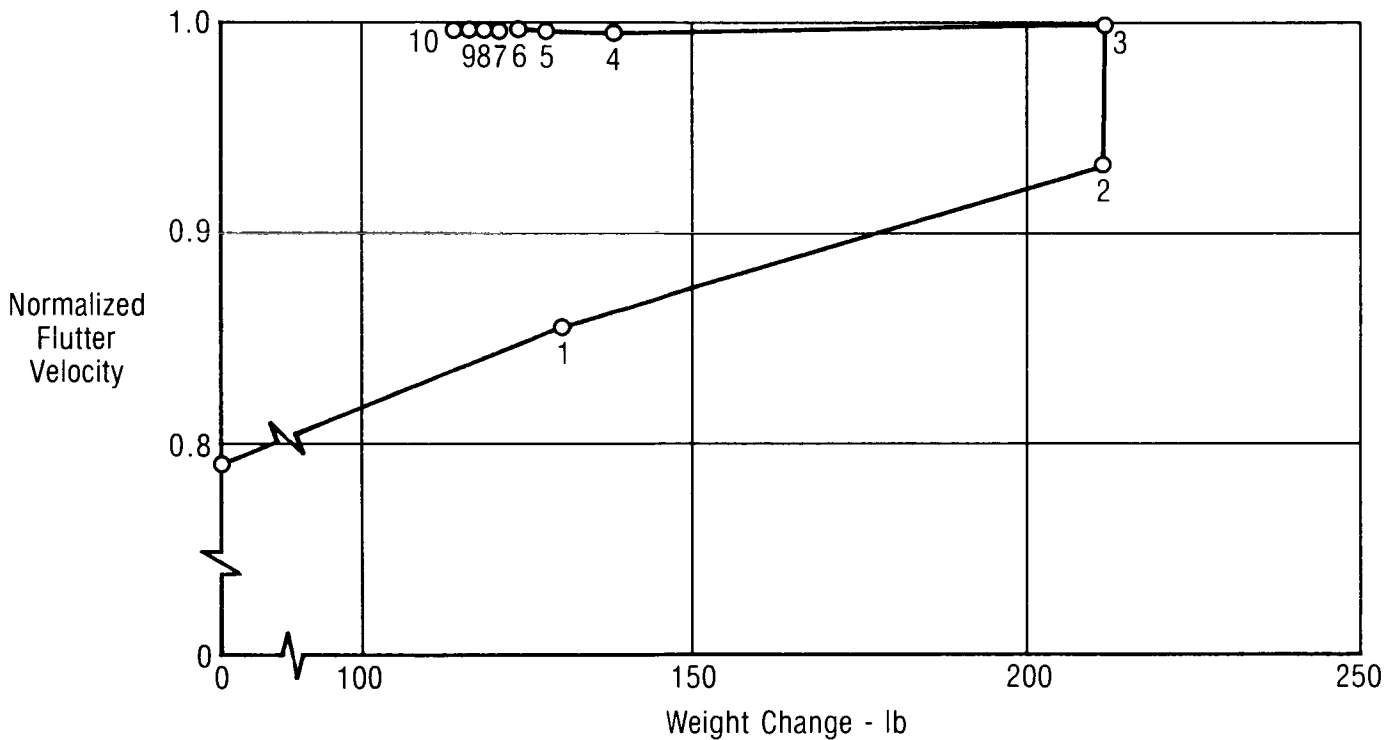


Figure 12

# SENSITIVITY ANALYSIS DATA PREPARATION

This approach to flutter optimization is based on a "sensitivity" technique similar to that first explored in conjunction with the development of the COPS program, which is described in Figure 4. The study was done in an extremely short elapsed time using existing flutter data sets for a beam-rod stabilator idealization based on NASTRAN and Doublet lattice. The only new data required are the GJ versus number of 45° plies per skin for several elastic axis (EA) stations, as shown in Figure 13a. With these data the change in GJ versus elastic axis station can be calculated for various weight increments, as shown in Figure 13b.
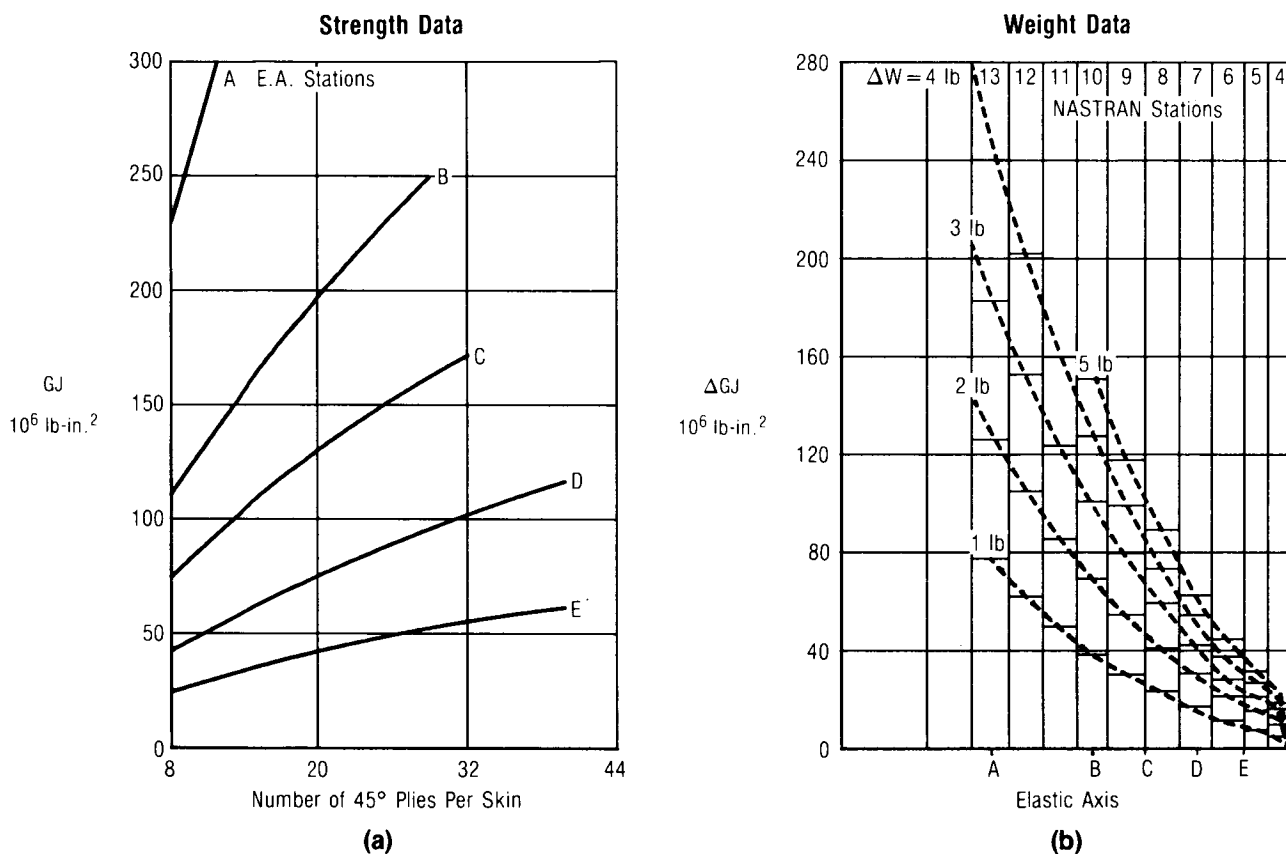


Figure 13

## SENSITIVITY OPTIMIZATION RESULTS

The steps in the sensitivity optimization study are given in Figure 14. Each step of the redesign is based on batch submittals of the NASTRAN flutter routines, followed by a conscious choice for the elements to be used in the subsequent step. After step 4 it is possible, by the use of engineering judgment, to specify a redesign distribution which satisfies the flutter requirement and is practical to build. These studies are state of the art in all respects and are quicker, cheaper and more accurate than possible with any currently available automatic optimization procedure.

**Step 1**
**Initial Design**
$\Delta W = 2$ lb Increments

| Station | $V_F$* | Redesign W |
|---------|--------|------------|
| 13 | 0.864 | |
| 12 | 0.865 | |
| 11 | 0.868 | |
| 10 | 0.868 | |
| 9 | 0.873 | |
| 8 | 0.872 | |
| 7 | 0.879 | 2 |
| 6 | 0.877 | 2 |
| 5 | 0.881 | 2 |
| 4 | 0.878 | 2 |
| Redesign 1 | | 8 lb |

(Choose 7, 6, 5, 4)

**Step 2**
**Redesign 1 (8 lb)**
$\Delta W = 2$ lb Increments

| Station | $V_F$ | Redesign W |
|---------|-------|------------|
| 13 | 0.936 | |
| 12 | 0.937 | |
| 11 | 0.940 | |
| 10 | 0.940 | |
| 9 | 0.945 | 2 |
| 8 | 0.943 | 2 |
| 7 | 0.939 | 2 |
| 6 | 0.939 | 2 |
| 5 | 0.943 | 2 |
| 4 | 0.944 | 2 |
| Redesign 2 | | 12 lb |

(Choose 9, 8, 7)

**Step 3**
**Redesign 2 (12 lb)**
$\Delta W = 2$ lb Increments

| Station | $V_F$ | Redesign W |
|---------|-------|------------|
| 13 | 0.961 | |
| 12 | 0.963 | |
| 11 | 0.965 | |
| 10 | 0.965 | |
| 9 | 0.961 | 2 |
| 8 | 0.961 | 2 |
| 7 | 0.964 | 2 |
| 6 | 0.964 | 2 |
| 5 | 0.968 | 4 |
| 4 | 0.969 | 4 |
| Redesign 3 | | 16 lb |

(Choose 5, 4)

**Step 4**
**Redesign 3 (16 lb)**
$\Delta W = 1$ lb Increments

| Station | $V_F$ | Redesign W |
|---------|-------|------------|
| 13 | 0.983 | |
| 12 | 0.984 | |
| 11 | 0.986 | 1 |
| 10 | 0.985 | 1 |
| 9 | 0.982 | 2 |
| 8 | 0.982 | 2 |
| 7 | 0.983 | 2 |
| 6 | 0.983 | 2 |
| 5 | 0.984 | 4 |
| 4 | 0.984 | 4 |
| Redesign 4 | | 18 lb |

(Choose 11, 10)

*$V_F$ is normalized to $V_{required}$

**Step 5**
**Engineering Judgment**
**Test Case**

| Station | $V_F$ | Redesign W |
|---------|-------|------------|
| 13 | | |
| 12 | | |
| 11 | | 1 |
| 10 | | 1 |
| 9 | | 2 |
| 8 | | 2 |
| 7 | | 3 |
| 6 | | 3 |
| 5 | | 4 |
| 4 | | 4 |
| Redesign 5 | | 20 lb |

$V_F = 1.0$

**Step 6**
**Verification**
**Redesign 5 (20 lb)**
$\Delta W = 1$ lb Increments

| Station | $V_F$ | Redesign W |
|---------|-------|------------|
| 13 | 1 003 | |
| 12 | 1.004 | |
| 11 | 1.003 | |
| 10 | 1.003 | |
| 9 | 1.003 | Step 5 is OK |
| 8 | 1.002 | |
| 7 | 1.002 | |
| 6 | 1.002 | |
| 5 | 1.003 | |
| 4 | 1.004 | |
| | | |

Figure 14

## CONCLUSIONS AND RECOMMENDATIONS

The following conclusions are appropriate in the area of flutter optimization.

1) COPS, or a similar routine, is suitable for use in conceptual design for individual lifting surfaces when the geometry is undefined.

2) TSO is suitable for use in preliminary design for individual lifting surfaces when the geometry is defined but there is still no well-defined structural model. Limitations in the structural model allow only limited use in detail design.

3) FASTOP is based on a sound concept but is not general enough for use in detail design and is too difficult to use in preliminary design.

4) NASTRAN based semi-automatic sensitivity techniques are the preferred approach for detail designs when the structural model is well defined but the flutter speed is deficient.

Since NASTRAN is the accepted industry standard for structural analyses it seems appropriate to either 1) incorporate flutter optimization routines in NASTRAN or 2) ensure that any alternate program developments have a complete one-to-one relationship to NASTRAN in all respects, and are designed to include generation of input data by graphics procedures.

## *Conclusions*

- COPS Is Suitable for Conceptual Design

- TSO Is Suitable for Preliminary Design

- NASTRAN Sensitivity Technique Is Suitable for Detail Design

## *Recommendations*

- Incorporate Flutter Optimization in NASTRAN

- If Alternate Procedure, Ensure Complete One-to-One Relationship to NASTRAN Including Graphics Generation of Bulk Data

Figure 15

# REFERENCES

1.  Triplett, W. E., and Ising, K. D., "Computer Aided Stabilator Design Including Aeroelastic Constraints," Journal of Aircraft, July 1971.

2.  Shelton, J. D., and Tucker, P. B., "Minimum Weight Design of the F-15 Empennage for Flutter," AIAA/ASME/SAE 16th Structures, Structural Dynamics and Materials Conference (SSDM), Denver, Colorado, 27-29 May 1975.

3.  Triplett, W. E., "Aeroelastic Tailoring Studies in Fighter Aircraft Design," Journal of Aircraft, July 1980.

4.  Lynch, R. W., Rogers, W. A., and Braymen, W. W., "Aeroelastic Tailoring of Advanced Composite Structures for Military Aircraft," AFFDL-TR-76-100, Vol. III, February 1978.

5.  Triplett, W. E., "Aeroelastic Tailoring of a Forward Swept Wing and Comparisons with Three Equivalent Aft Swept Wings," AIAA/ASME/ASCE/AHS 21st Structures, Structural Dynamics and Materials Conference (SSDM), Seattle, Wash., 12-14 May, 1980.

6.  Markowitz, J., and Isakson, G., "FASTOP-3: A Strength, Deflection, and Flutter Optimization Program for Metallic and Composite Structures," AFFDL-TR-78-50, May 1978.

7.  Triplett, W. E., "Wind Tunnel Correlation Study of Aerodynamic Modeling for F/A-18 Wing-Store Tip-Missile Flutter," AIAA/ASME/ASCE/AHS 24th Structures, Structural Dynamics and Materials Conference (SSDM), Lake Tahoe, Nev., 2-4 May 1983. (Journal of Aircraft, Spring 1984)

# APPLICATION OF THE GENERALIZED REDUCED GRADIENT METHOD TO CONCEPTUAL AIRCRAFT DESIGN

Gary A. Gabriele
Lockheed-Georgia Company

# AIRCRAFT DESIGN PHASES

The complete aircraft design process can be broken into three phases of increasing depth: conceptual design, preliminary design, and detail design. Conceptual design consists primarily of developing general arrangements and selecting the configuration that optimally satisfies all mission requirements. The result of the conceptual phase is a conceptual baseline configuration that serves as the starting point for the preliminary design phase.

The conceptual design of an aircraft involves a complex trade-off of many independent variables that must be investigated before deciding upon the basic configuration. Some of these variables are discrete (number of engines), some represent different configurations (canard vs conventional tail) and some may represent incorporation of new technologies (aluminum vs composite materials). A particular combination of these choices represents a concept; however there are additional variables that further define each concept. These include such independent variables as engine size, wing size, and mission performance parameters, which must be selected before a particular configuration can be evaluated. Generally, these additional variables are chosen to optimize each concept before selecting a final configuration.

Mission Requirements

Conceptual Design

Conceptual Baseline

● General Arrangement & Performance
● Representative Contours
● General Internal Arrangement

● Optimization
● Parametric
● 1st Level Analysis

Preliminary Design

Allocated Baseline

● System Specifications
● Detail Contour
● Internal Arrangement

● Sophisticated Analysis
● Multi-Discipline
● Optimization

Detailed Design

Production Baseline

● Part Drawing

Production & Support

Advanced Design

Project Design

## OPTIMAL VEHICLE SELECTION BY PARAMETRIC DESIGN

The principal analysis tool used during the conceptual design phase is the sizing program. At Lockheed-Georgia, the sizing program is known as GASP (Generalized Aircraft Sizing Program). GASP is a large program containing analysis modules covering the many different disciplines involved in defining the aircraft, such as aerodynamics, structures, stability and control, mission performance, and cost. These analysis modules provide first-level estimates the aircraft properties that are derived from handbook, experimental, and historical sources.

To make a run of the sizing program, the engineer develops a data set defining the fuselage geometry, the mission profile, a candidate propulsion system, the general arrangement of the components, the extent of new technologies to be incorporated into the design, and the values for the independent design variables. The sizing program provides a complete weight breakdown of the airplane, aerodynamic properties, mission and airport performance, center of gravity ranges, and cost data.

To optimize a design, the engineer must choose a selection criteria such as minimum weight and determine design constraints that define feasible designs. He is then faced with the classical design optimization problem: find the optimal values of the independent design variables that minimize the selection criteria and satisfy the design constraints. Without some automated optimization method, this process is generally performed by plotting the results of the sizing program obtained by parametically varying the independent variables throughout their ranges. For a problem involving 4 design variables, this may result in as many as 256 runs of the sizing program. This can be a very time-consuming process when many different designs must be investigated.

① Cruise-Sized Airplane

Gross Wt
Wing Area
Rated Thrust
OWE
Mission Fuel
DOC
Field Performance

② Field Performance

③ Mission-Compatible Airplane

④ Optimal Cruise

Min DOC

⑤ Optimum Configuration

Min DOC

Optimum Airplane
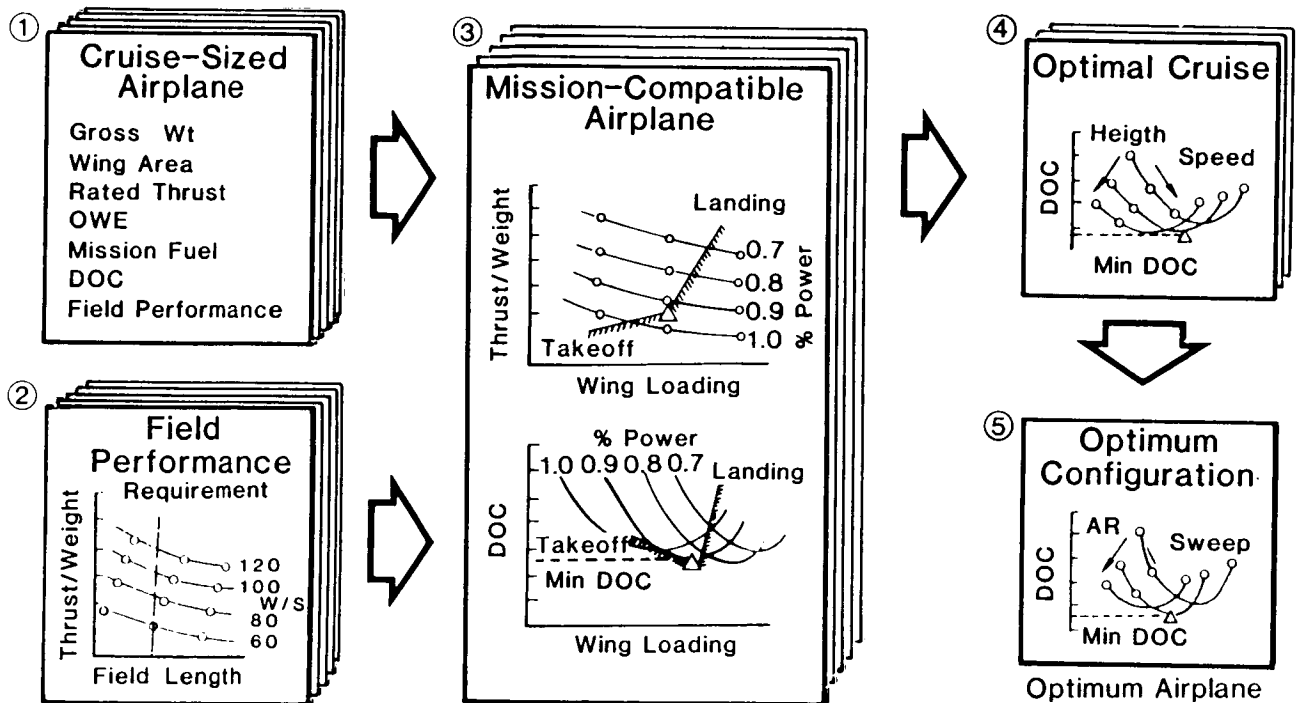
# AUTOMATED CONCEPTUAL DESIGN SYSTEM

This paper describes our experiences in combining a numerical optimization algorithm with the aircraft sizing program to obtain an automated conceptual design system. The structure of the system is shown below indicating that the optimizer functions as a black box interacting with the sizing program, which provides the required function values. Such a structure allows substitution of any appropriate optimization algorithm with very little impact on the sizing program, or changes to the sizing program with very little effect on the optimizer.

In the past decade, advances in optimization methods have produced several algorithms that have proven to be both reliable and robust in a number of engineering applications. One of these is the Generalized Reduced Gradient (GRG) method. The GRG method is an extension of the reduced gradient method for linear constraints to the nonlinear case from which highly robust and efficient implementations (refs. 1, 2, 3) have been produced. It is this method that we have chosen for the optimizer.
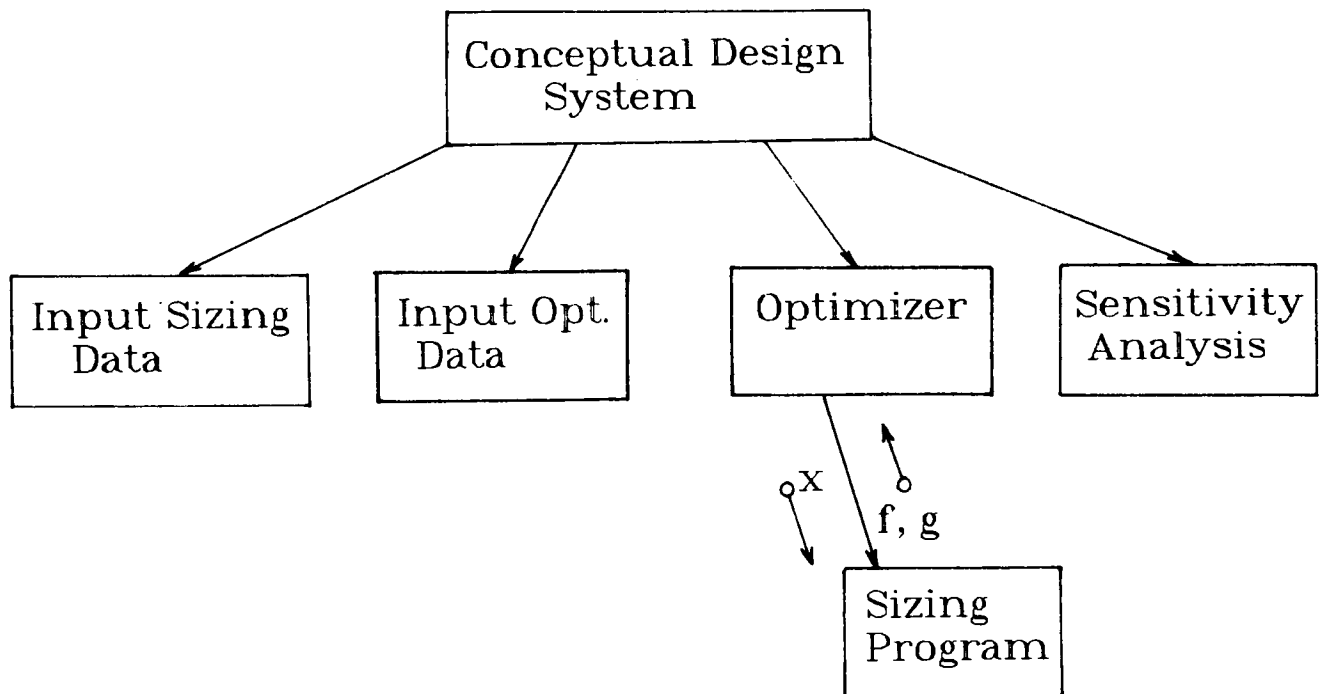
## THE NONLINEAR PROGRAMMING PROBLEM

The general nonlinear programming problem (NLP) can be stated as shown below. The function f(x) is a scalar function representing the criteria to be optimized and x is a vector of design variables. The h(x) functions represent equality constraints that require specific combinations of the design variables, and the g(x) functions represent inequality constraints that define feasible regions in the design space. All functions are assumed to be nonlinear.

$$\text{Minimize} \quad f(x); \quad x = [\, x_1, x_2, \dots, x_N \,]^T$$

**Subject To**

$$g_j(x) \geq 0 \quad j = 1, 2, \dots, J$$

$$h_k(x) = 0 \quad k = 1, 2, \dots, K$$

**Where**

$f(x)$ = Objective Function

$x$ = A Column Vector Of Design Variables

$g_j(x)$ = Inequality Constraints

$h_k(x)$ = Equality Constraints

$x^O$ = Starting Point

$x^k$ = Candidate Point

70

## GENERALIZED REDUCED GRADIENT METHOD

The GRG method restates the NLP in the form shown below, where the vectors $x^L$ and $x^0$ represent the lower and upper bounds on the design variables x. The inequality constraints are included as equality constraints through the addition of slack variables. The parameter M represents the total number of constraints. The constraints include only the functional constraints; variable bounds are accounted for separately to allow for a more efficient handling of this special class of constraints.

The basic strategy of the GRG method is derived from trying to use each equality constraint $h_m(x)$ to eliminate a design variable from the problem. However, for most engineering problems, the constraints are too complex to allow this substitution. The GRG method accomplishes this by employing the Implicit Function Theorem.

Minimize $\quad f(x), \; x = [x_1, x_2, ..., x_N]^T$

Subject to

$\quad h_m(x) = 0 \qquad m = 1, 2, ..., M$

$\quad x^L < x < x^U$

Strategy:

Solve each $h_m(x)$ explicity for a Variable and Substitute into $f(x)$.

Problem:   Not always Possible for Complex Engineering Functions or Simulations.

Solution:   Do It Implicity.

# DERIVATION OF THE REDUCED GRADIENT

Consider the following strategy, whose foundations can be found in the simplex method of linear programming. Divide the design vector x into two classes, non-basic or independent (z) variables and basic or dependent (y) variables, as shown in the figure, where $Q = N - M$. The search for the optimum will occur by searching in the design space of the nonbasic variables and the basic variables will be used to satisfy the constraints. A gradient vector for this new problem can be obtained by introducing the division of the design variables into the objective and constraint functions and following the steps shown in equations (1) to (3).

The reduced gradient defines the rate of change of the objective function with respect to the nonbasic variables with the basic variables adjusted to maintain feasibility. In the presence of linear constraints, equation (3) represents the changes necessary in the basic variables for a given change in the nonbasic variables. Additional adjustment is necessary in the nonlinear situation. Conceptually, the above derivation corresponds to a transformation of the GRG problem into one having the following form:

Minimize: $F(z)$  $z = (z_1, z_2, \ldots, z_q)^T$

Subject to: $z^l \leq z \leq z^u$

where the basic variables y have been eliminated from the original problem by using the constraints $h_m(z,y) = 0$ to solve for y in terms of z. The gradient of $F(z)$ is represented by the reduced gradient, and the necessary equations for y in terms of z represented by equation (3).

Divide X into two classes, dependent and independent

$X = [y,z]^T$

$Y = [y_1, y_2, \ldots, y_M]^T$  Dependent Variables

$Z = [z_1, z_2, \ldots, z_q]^T$  Independent Variables

Calculate the first variation of $f(X)$ and $H(x)$ using Z and Y

$df(x) - \nabla_z f(x)^T dz + \nabla_y f(x)^T dy$       (1)

$dH(x) = \nabla_z H(x)\, dz + \nabla_y H(x)\, dy = 0$       (2)

Solve (2) for dy

$dy = - [\nabla_y H(x)]^{-1} \nabla_z H(x)\, dz$       (3)

Substitute (3) for dy in (1) to arrive at the REDUCED GRADIENT

Reduced Gradient $\nabla_R F(z)$

$\nabla_R F(z)^T = \nabla_z f(x)^T - \nabla_y f(x)^T \nabla_y H(x)^{-1} \nabla_z H(x)$       (4)

The Reduced Gradient defines the gradient for the new *reduced* problem

Minimize     $F(z)$, $z = [z_1, z_2, \ldots, z_q]^T$

Subject to     $z^l \leq z \leq z^u$

the change in Y necessary to maintain feasibility is defined by equation (3) for linear constraints.

A necessary condition for the existence of a local minimum of an unconstrained nonlinear function is that the elements of the gradient vanish. Similarly, a local minimum of the reduced problem shown in the previous figure occurs when the elements of the reduced gradient satisfy the conditions shown below.

Points that satisfy these conditions satisfy the Kuhn-Tucker conditions for the existence of a constrained relative minimum of the original NLP problem (ref. 3). An additional benefit of this method is that the Lagrange multipliers are calculated in the course of calculating the reduced gradient vector.

## Convergence Conditions

$$
\nabla_R F(z)_i \quad \begin{cases} < 0 & \text{if } z_i = z_i^{u} \\ \\ > 0 & \text{if } z_i = z_i^{1} \\ \\ = 0 & \text{otherwise} \end{cases}
$$

$$i = 1, 2, 3, \ldots, Q$$

When this conditon holds, the corresponding point X satisfies the Kuhn-Tucker conditions for the existence of a local constrained minimum of the original problem.

# GENERALIZED REDUCED GRADIENT ALGORITHM

The basic steps of the GRG algorithm are given in this figure. The method looks very much like any gradient based method, with some exceptions. The search directions for the nonbasic variables are based on the reduced gradient vector and initial directions for the basic variables are then calculated from equation (3). In the calculation of the nonbasic direction any gradient-based search method, such as conjugate gradient or variable metric, may be used.

The line search phase is also similar, except additional logic is also required to adjust the basic variables and determine when a new constraint is encountered. The basic variable adjustment occurs in the presence of nonlinear constraints. As we move along the search direction defined for the nonbasic variables and calculated from equation (3) for the basics, we can expect, for nonlinear constraints, that the trial points will violate the constraints. To maintain feasibility, an adjustment of the basic variables at each trial point is undertaken to get back to the constraint surface before evaluating the objective function. During this adjustment the independent variables are held constant. The line search is terminated by one of the following conditions: a relative local minimum was located along that search direction, a new constraint was encountered which limited the search, or adjustment of the basic variables to maintain feasibility was not possible at some trial points.
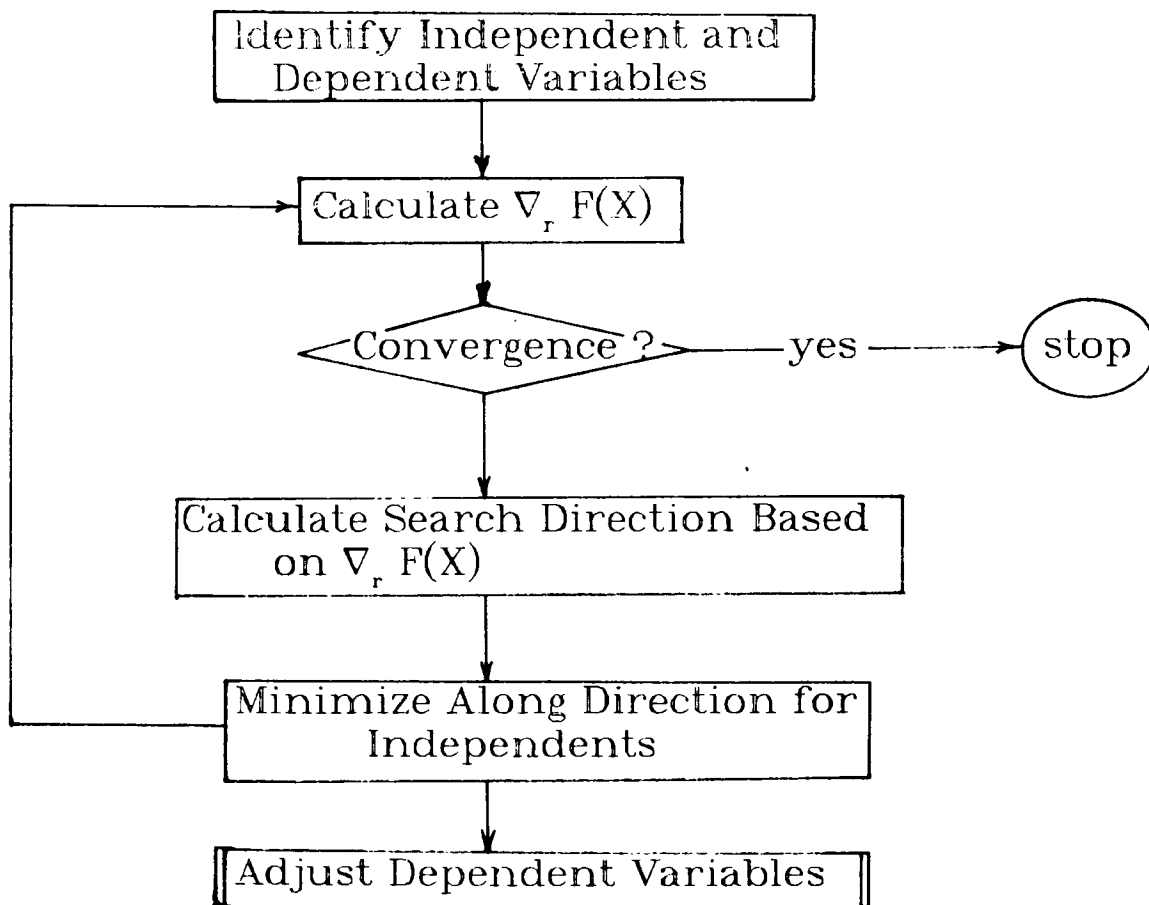
# DEPENDENT VARIABLE ADJUSTMENT

This figure depicts the adjustment of the dependent variable $y_1$ during the line search phase of the GRG algorithm. Here we have taken a step along the search direction from $x^0$. Holding the independent variable $z_1$ constant, we now adjust $y_1$ to get back to the constraint $h(x)$.

A modified Newton method is usually employed to adjust the basic variables during the line search. The iteration sequence is given below, where $A_0$ is the initial inverse of $\nabla_y h(x)$ used at the start of the GRG iteration to calculate the reduced gradient and t is an iteration of Newton's method.

The modified Newton method has been used in all current implementations of the GRG algorithm. This is due primarily to the substantial savings in computation time obtained by avoiding successive reformulations of the Jacobian inverse. However, the major drawback of the method is that it does not possess the convergence rate of the classical method obtained by evaluating the Jacobian and its inverse at every Newton iteration. Poor convergence of the Newton method can lead to insufficient progress being made during a line search, which may hinder convergence of the algorithm to the optimal solution.

Two factors that have a major influence on the convergence are the approximations to the basic variables during the line search and the inaccuracies of using the inverse $A_0$. Suggestions for improving the former have appeared in Lasdon (ref. 2), and Gabriele and Ragsdell (ref. 3), and both offer improvements in convergence.

Techniques for improving the inverse $A_0$ have appeared in the literature for solving nonlinear systems of equations. Broyden's method (ref. 4) is one of these methods and is summarized below. This method is used in our implementation of the GRG algorithm.

## MODIFIED NEWTON METHOD

$$y^{t+1} = y^t - A_0 H(z^k, y^t)$$

$$z^k = \text{fixed values of independents}$$

$$A_0 = \text{initial inverse of } \nabla_y H(x) \text{ used in calculating } \nabla_r f(x)$$

## BROYDEN'S METHOD

The inverse Jacobian matrix A is updated at each iteration by

$$A_{i+1} = A_i - (A_{i+1} v^T - p_i s_i) p_i^T A_i / (p_i^T A_i v_i)$$

$$v_i = H(z^k, y^{t+1}) - H(z^k, y^t)$$

$$p_i = -A_i H(z^k, y^t)$$

$$y^{t+1} = y^t + s_i p_i$$

# CONCEPTUAL AIRCRAFT DESIGN PROBLEM 1

We will now discuss two example problems that demonstrate the effectiveness of this method for conceptual aircraft design. The first problem is typical of the type of problem that is generally solved very early in a conceptual study. The number of design parameters and constraints is small (ref. 5) but is large enough to preclude the use of graphical techniques.

In this problem we are required to minimize the takeoff gross weight (TOGW) of a transport aircraft that will be required to fly a simple climb-cruise mission. The design variables are cruise altitude (H), wing loading (W/S), wing aspect ratio (AR), engine cruise power setting (PS), and wing sweep (SWEEP). The constraints and variable bounds are shown in the figure.

This problem posesses some interesting scaling problems that must be addressed before we can be sure a numerical optimization technique can be effectively applied. The variable scales range from multiples of 1000 for altitude to less than 1 for power setting. The constraints range from values less than 1 for lift coefficient to thousands of feet for takeoff distance. The engineer must be sensitive to these differences when establishing convergence criteria and constraint tolerances. The algorithm should be able to provide some help and should be as insensitive to scale as possible. This is more true of the GRG algorithm than some other available algorithms such as the penalty function based methods.

## Minimize: TOGW(H, W/S, AR, PS, SWEEP)

## Subject to:

$$\text{Cruise } C_L \leq C_L \text{ limit}$$

$$\text{Fuel Volume Ratio} \geq 1.05$$

$$\text{Take off Distance} \leq 10500 \text{ ft.}$$

$$\text{Rate of Climb} \geq 300 \text{ fpm.}$$

$$\text{Approach Speed} \leq 150 \text{ knots}$$

$$31000 \leq H \leq 40000 \text{ ft}$$
$$90 \leq W/S \leq 190$$
$$6 \leq AR \leq 14$$
$$.7 \leq PS \leq 1.$$
$$10 \leq \text{Sweep} \leq 35 \text{ deg.}$$

The results shown in the figure were obtained using a modified version of the OPT program (ref. 5). All variables were scaled between 0. and 10. followed by a scaling of the objective and constraint partials using the approach developed by Root and Ragsdell (ref. 6). Each constraint was scaled by the engineer to avoid trying to obtain unreasonable values when the constraints were active.

The final solution has three functional constraints active and one variable bound active, leaving one degree of freedom. The problem terminated with the norm of the reduced gradient below the tolerance.

The functions evaluation refers to the number of times the sizing program was called. This is an important quantity because the time spent performing a function evaluation using the sizing program far outweighs the time spent by the optimizer generating trial points. This number compares favorably with that required to perform the analysis graphically. This solution required about 2-3 hours of elapsed time.

To solve this problem using a graphical technique such as carpet plotting would require approximately 4 calls to the sizing program for each design variable, or 1024 aircraft sizings. Even if we were to solve this problem using only 4 design variables, we would require about 256 calls to the sizing program. In addition to this, we would have to add the time required to plot and solve for the optimum. For a problem of this size we can expect an experienced engineer to take 1 to 2 days.

|  | Start Pt | Final |
| --- | --- | --- |
| H | 33000 | 31000 |
| W/S | 120 | 154.1 |
| AR | 9 | 7.6 |
| PS | .9 | .91 |
| SWEEP | 20 | 25.5 |
| | | |
| TOGW | 530,278 | 500,727 |

| | |
| --- | --- |
| Iterations | 7 |
| Functions Eval. | 73 |

Active Constraints: $x_1^L$, constraints 2,4,5

78

# PROBLEM 1 ITERATION HISTORY

As can be seen from this figure, the progress to the optimum was fairly rapid. A review of the output produced by the optimizer would show that each 'kink' in the curve (iterations 1, 3 and 4) corresponds to one of the constraints being encountered. This points to the strength of the GRG method for engineering problems; as it locates a constraint or the intersection of two or more constraints, it can easily track or follow that constraint to an optimum. In aircraft design, our optimal design points generally lie on one or more constraints.
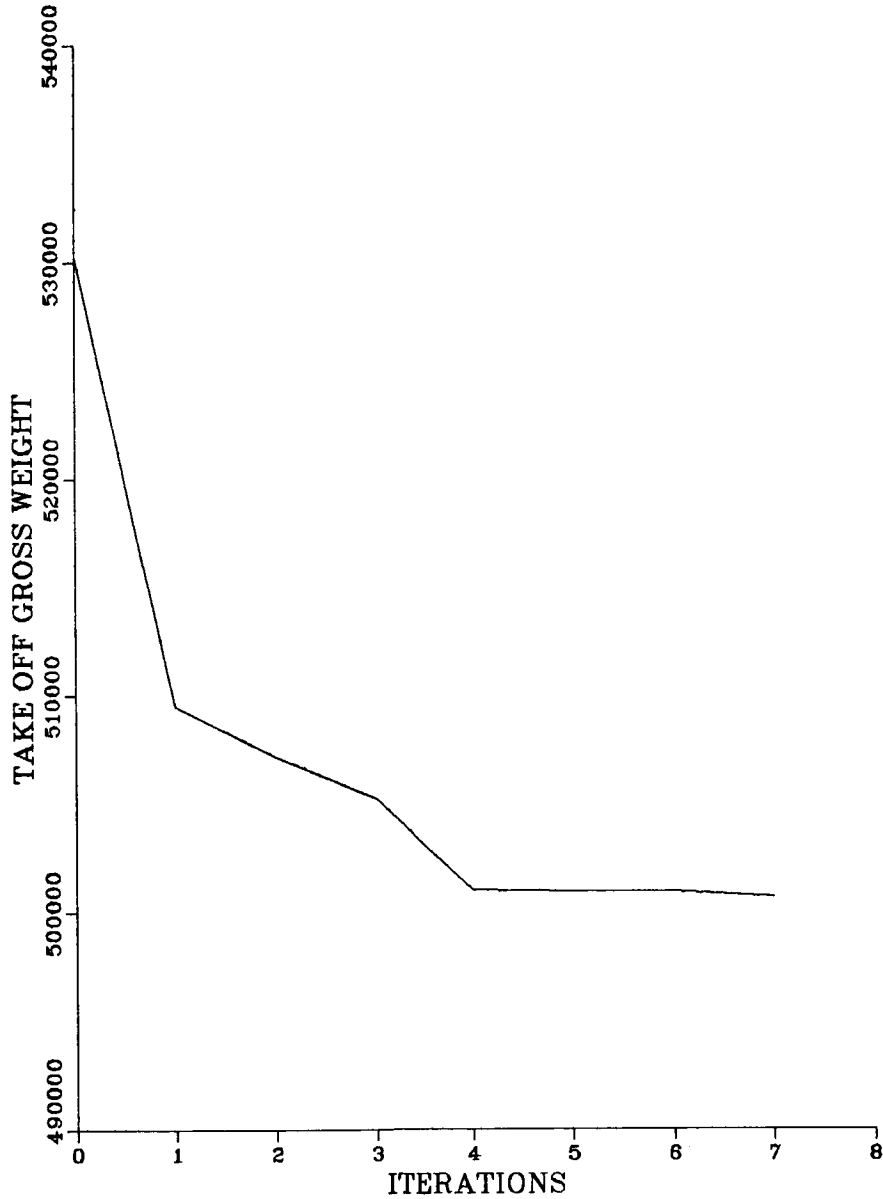
Another important feature of the GRG algorithm is the generation of the Lagrange multipliers. The Lagrange multipliers allow the engineer to check the sensitivity of the objective function to changes in the active constraints. For this problem, the lower limit on cruise altitude was set at 31000 feet, and the resultant optimum altitude was at this limit. Using the Lagrange multiplier printed for this constraint, the engineer can use the procedure shown below to estimate how much the optimum objective function value would change if he were to lower the limit to 30000 feet. We see that the estimated change from the sensitivity analysis is 499,251 lb, which compares favorably with the result (498,945 lb) obtained by re-optimizing the problem with the new lower limit. Making the Lagrange multipliers available to the engineer allows him to interpret the results of his optimization more effectively and have more confidence in the results produced by the optimizer.

Change in optimal value of f(x) can be estimated by:

$$\Delta f = \mu_j \, \Delta g_j$$

where $\mu_j$ = Lagrange multiplier

$\Delta g_j$ = change in active constraint

For our problem, lower bound on $x_1$ is active with a corresponding multiplier value

$$\mu_1 = 1.47531$$

Change lower bound from 31000 to 30000, $\Delta g_1 = -1000$

New optimal f(x) = 499,251 lb. from above analysis

Re-optimization produces f(x) = 498,945 lb. ( 0.06 % difference)

The second example problem demonstrates an expansion of the original problem to allow for optimizing and balancing of the aircraft in one step. In the first problem we presented, the balance and loadability of the aircraft were ignored. Usually the engineer fixes values for the variables that effect the balance of the aircraft at the start of the optimization, performs the optimization, then checks the balance of the aircraft. If the aircraft is not balanced, changes in the balance parameters are made and the problem is re-optimized. This continues until he produces a balanced, optimal design. For most conventional configurations, this occurs in about 2-3 cycles of this process. For unconventional configurations for which there is little experience, balancing may take considerably longer.

In this problem we have included the balance parameters, wing position, main gear position, and horizontal and vertical tail coefficients as design variables. We also have included eight additional constraints that will define the balance of the aircraft. This problem will allow us to balance the aircraft at the same time that we optimize the other system parameters. This eliminates the need to perform the above cycle of re-optimization and provides an effective method by which stability and control requirements and loadability requirements can be integrated within the sizing process. The disadvantage to this approach is that we have almost doubled the number of variables and possible active constraints that the optimizer must handle.

Minimize: TOGW (H, W/S, AR, PS, SWEEP, WING POSITION, MAIN GEAR POSITION, HORIZONTAL AND VERTICAL TAIL COEFFICIENTS )

Subject to:

Cruise $C_L \leq C_L$ limit

Fuel Volume Ratio $\geq 1.05$

Take off Distance $\leq 10500$ ft.

Rate of Climb $\geq 300$ fpm.

Approach Speed $\leq 150$ knots

Forward and Aft C.G. limits required for S&C

Minimum Vertical Tail Size for Engine Out and Control

Minimum Nose Gear Load under Critical Loading Conditions   (5)

The results for this larger problem are shown below. (The design concept is different from the previous example, therefore comparison of weight is meaningless.) Again, this problem presents a challenge in variable and constraint scaling for the optimizer that was handled in the same manner as for problem 1.

As can be seen, the number of function evaluations is still low relative to the size of the problem. The majority (117) of the evaluations were spent calculating the numerical gradients.

In addition to the lower limit on altitude and the rate of climb specification, the active constraints for this problem were the three stability and control constraints (6, 7 and 8) on the tail sizes, and the minimum nose gear load under one of the 5 critical loading conditions (constraint 13). This last constraint contributes mostly to limiting the main gear location. This solution corresponds to within .5% of a result obtained using the old method described earlier.

|  | Start Pt | Final Pt |
|---|---|---|
| H | 32000 | 31000 |
| W/S | 140 | 154.1 |
| AR | 6.5 | 7.6 |
| PS | .9 | .91 |
| SWEEP | 20 | 25.5 |
| WING POS. | .463 | .479 |
| M.G. POS. | .697 | .652 |
| $V_H$ | .655 | .524 |
| $V_V$ | .090 | .079 |
| TOGW | 1,146,220 | 1,108,335 |

| Iterations | 13 |
|---|---|
| Functions Eval. | 189 |

Active Constraints: $x_1^L$,

constraints 4, 6, 7, 8, 13

## PROBLEM 2 ITERATION HISTORY

The figure below illustrates that the method made good progress toward the optimum and was close after about seven iterations.  The problem terminated again with the norm of the reduced gradient below the selected criterion.  The elapsed time for this problem was between 3-4 hours.  The advantage here is that the final optimal design is also an aircraft that is acceptable with respect to stability and control and loadability requirements.  This provides a valuable design tool for those new concepts or configurations that prove difficult to balance.
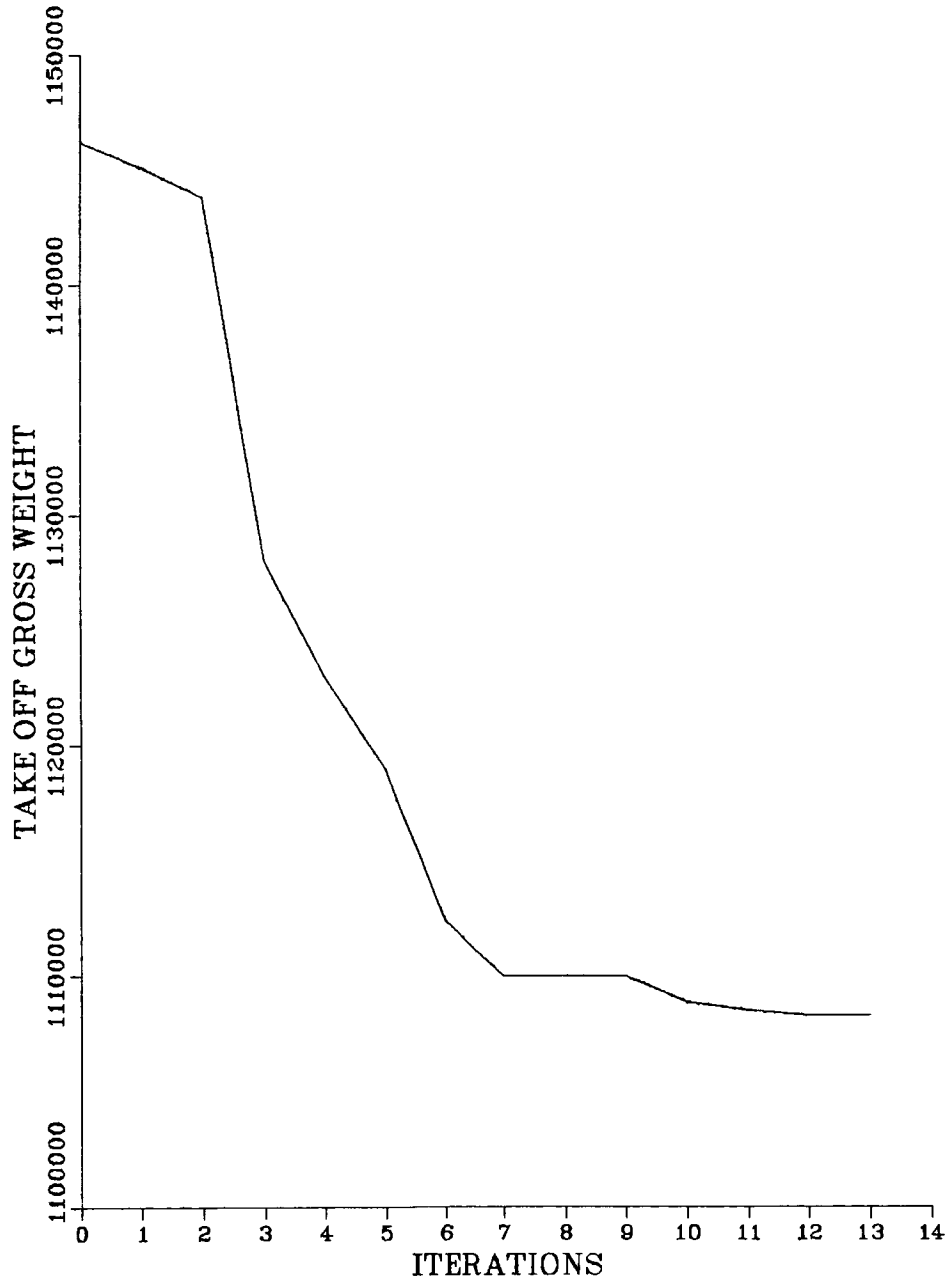
## CONCLUSIONS

We have seen from these two examples that numerical optimization provides substantial improvements in designer productivity over graphical techniques. This allows the designer to investigate many more designs and concepts at a very crucial time during the design process.

In our experience, the GRG algorithm provides a very reliable method for conceptual aircraft optimization. The automated conceptual design system is used on a daily basis at Lockheed in all conceptual design studies. The basic ability of the method to easily locate optimum points that lie on constraint boundaries appears to be well suited to this type of problem.

We have seen in the second design example that optimization can be used to help solve design problems in which we have limited design experience. In fact, we can now use optimization to formulate new design methods in areas in which it is difficult to understand the interaction among design parameters and new technologies or concept. This is particularly true in conceptual aircraft design, in which innovation is more or less the rule.

The automated conceptual design system is used by engineers who are not optimization experts. These engineers have been trained in how the optimizer works and how to evaluate the results. But they often still require help in the development of new formulations or in resolving whether the optimizer has truly reached a solution. For these situations our experience suggests that someone with a strong optimization background should be a member of any conceptual design study.

- Numerical optimization provides substantial improvements in designer efficiency over manual techniques.

- The GRG method is a reliable method for conceptual aircraft optimization.

- Numerical optimization can help solve difficult design problems where conventional wisdom is lacking.

- A team concept employing an optimization expert and an experienced designer is essential.

# REFERENCES

1.  Abadie, J., and J. Carpenter, "The Generalization of the Wolfe Reduced Gradient Method to the Case of Nonlinear Constraints," in _Optimization_ (R. Fletcher, Ed.), Academic Press, New York, 1969.

2.  Lasdon, L. S., A. D. Waren, A. Jain, and M. Ratner, "Design and Testing of a Generalized Reduced Gradient Code for Nonlinear Programming," _ACM Trans. Math. Software_, Vol. 4, No. 1, pp. 34-50, 1978.

3.  Gabriele, G. A. and K. M. Ragsdell, "The Generalized Reduced Gradient Method: A Reliable Tool for Optimal Design," _ASME J. Eng. Ind._, Vol. 99, No. 2, pp. 384-400, May 1977.

4.  Broyden, C. G., "A Class of Methods for Solving Nonlinear Simultaneous Equations," _Math. Comp._, Vol. 21, pp. 368-381, 1965.

5.  Gabriele, G. A. and K. M. Ragsdell, "OPT: A Nonlinear Programming Code in Fortran IV - User's Manual," Purdue Research Foundation, West Lafayette, IN, Jan. 1976.

6.  Root, R. R., and K. M. Ragsdell, "Computational Enhancements of the Method of Multipliers," _ASME J. Mech. Des._, Vol. 102, pp. 517-523, 1970.

# EXPERIENCES PERFORMING CONCEPTUAL DESIGN OPTIMIZATION OF TRANSPORT AIRCRAFT

P. Douglas Arbuckle and Steven M. Sliwa
NASA Langley Research Center
Hampton, Virginia

C-2

## OPTIMUM PRELIMINARY DESIGN OF TRANSPORTS

OPDOT (Optimum Preliminary Design of Transports) is a computer program developed at NASA Langley Research Center for evaluating the impact of new technologies upon transport aircraft (Ref. 1). For example, it provides the capability to look at configurations which have been resized to take advantage of active controls and provide an indication of economic sensitivity to its use. Although this tool returns a conceptual design configuration as its output, it does not have the accuracy, in absolute terms, to yield satisfactory point designs for immediate use by aircraft manufacturers. However, the relative accuracy of comparing OPDOT-generated configurations while varying technological assumptions has been demonstrated to be highly reliable. Hence, OPDOT is a useful tool for ascertaining the synergistic benefits of active controls, composite structures, improved engine efficiencies and other advanced technological developments.
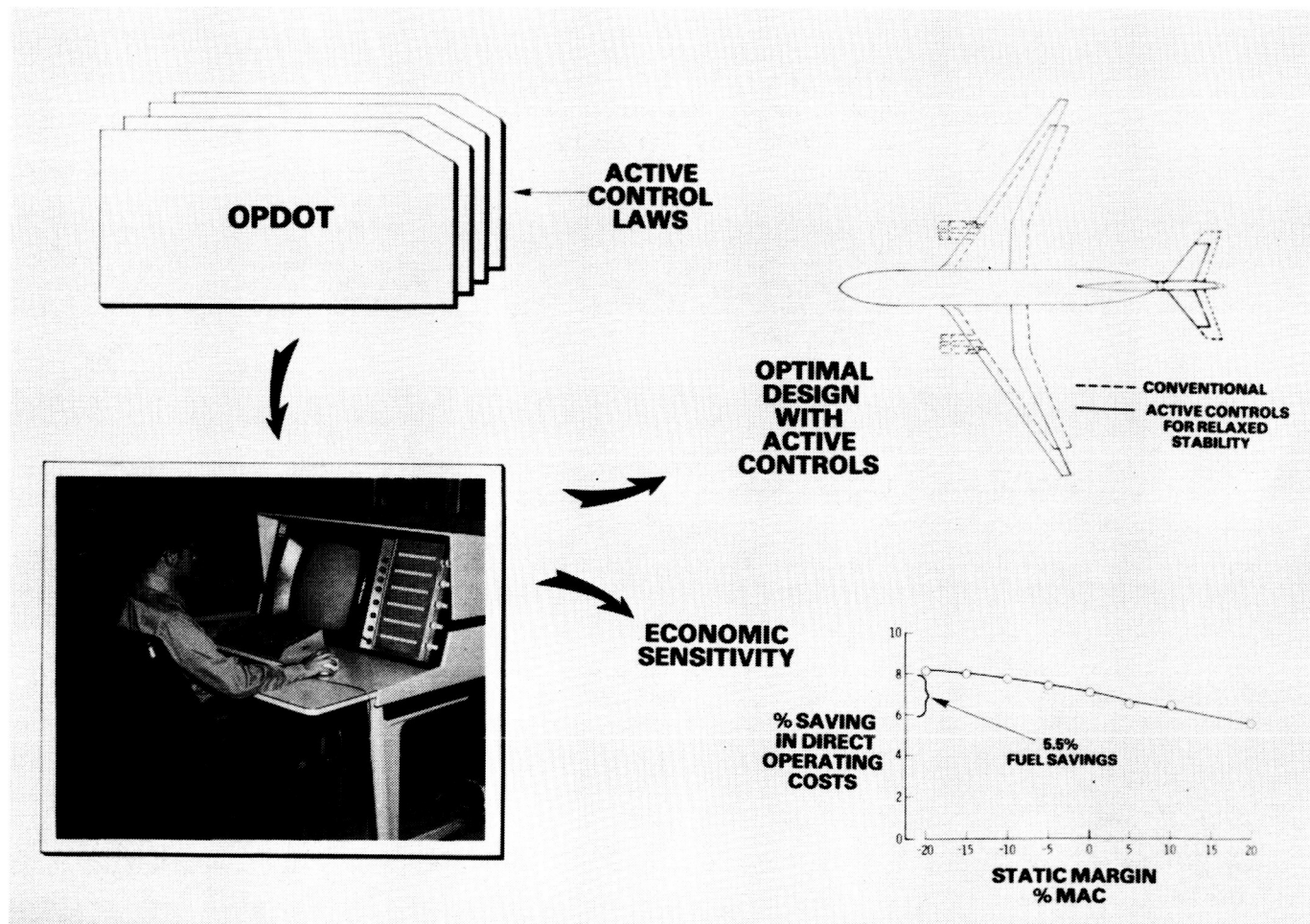
# OPTIMAL DESIGN METHODOLOGY

The approach used by OPDOT is a direct numerical optimization of an economic performance index. A set of independent design variables is iterated, given a set of design constants and data. The design variables include wing geometry, tail geometry, fuselage size, and engine size. This iteration continues until the optimum performance index is found which satisfies all the constraint functions. The analyst interacts with OPDOT by varying the input parameters to either the constraint functions or the design constants. Note that the optimization of aircraft geometry parameters is equivalent to finding the ideal aircraft size, but with more degrees of freedom than classical design procedures will allow.

```
┌─────────┐     WING AREA                              ┌──────────┐  ECONOMICS
│ DESIGN  │     WING ASPECT RATIO                      │ DESIGN   │  FIXED GEOMETRIES
│         │     FUSELAGE LENGTH                        │          │  TECHNOLOGY LEVEL
│VARIABLES│     HORIZONTAL TAIL AREA                   │CONSTANTS │  NON-LINEAR AERO.
└─────────┘     TAIL ASPECT RATIO                      └──────────┘  BASELINE ENGINE
     DOC        C.G.                                                  ETC.
     ROI        THRUST
     FARE       ETC.
     L/D   ┌────────────┐                               ┌────────┐
     WT.   │PERFORMANCE │◄──────────────────────────────│        │
     FUEL  │ FUNCTION   │──────────────────────────────►│  DATA  │
     ETC.  └────────────┘        ┌────────────┐         │  BASE  │
                                 │ CONSTRAINT │◄────────│        │
                                 │ FUNCTIONS  │────────►└────────┘
                                 └────────────┘  ENGINE OUT PERF.
          ┌────────────┐                          FIELD LENGTH
          │ AUGMENTED  │                          FLYING QUALITIES
          │ FUNCTION   │                          GEOMETRY CONSTRAINTS
          └────────────┘                          CONTROL POWER
                                                  ETC.
          ◄───┐OPTIMIZER
           NO │ LOGIC
              │YES
          ┌────────────┐
          │CONSTRAINED │
          │ SOLUTION   │
          └────────────┘
```

89

Numerical optimization logic has been the focus of research in many disciplines for some time. For OPDOT, an algorithm was desired that would not require the constant supervision of the designer. A variety of gradient methods applicable to aircraft design, as well as a feasible direction/search method coupled with a gradient method for the final stage, were considered. But studies indicated that most methods suffered from numerical difficulties when analytical equations were not available to provide gradients, as well as initialization problems when the number of constraints was large with respect to the number of design variables. To overcome these difficulties, a direct sequential search simplex algorithm (the Nelder-Mead simplex procedure, Refs. 2 and 3) was utilized. This procedure is characterized by its adaptive nature, which enables the simplex to either reflect, extend, contract, or shrink to conform to the properties of the optimized function. Further, unlike most optimization procedures, this procedure approaches the optimum by moving away from "bad" values of the objective function, as opposed to trying to move directly towards the optimum. The most appealing features of the procedure from the designer's point of view are its reliability and its robust convergence (except in regions of the design variables with low gradients of the performance index).
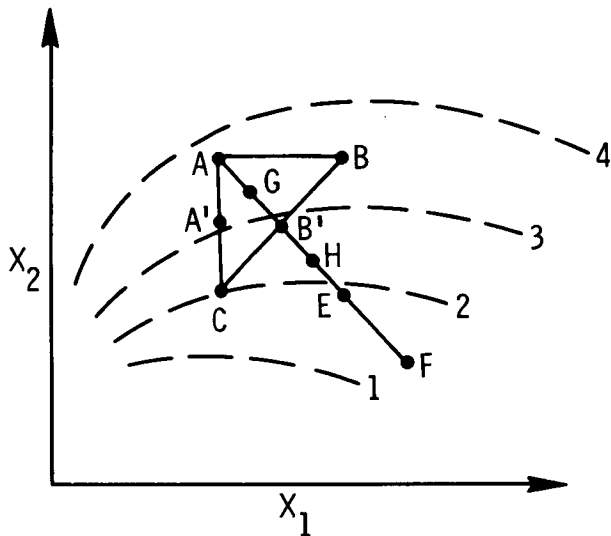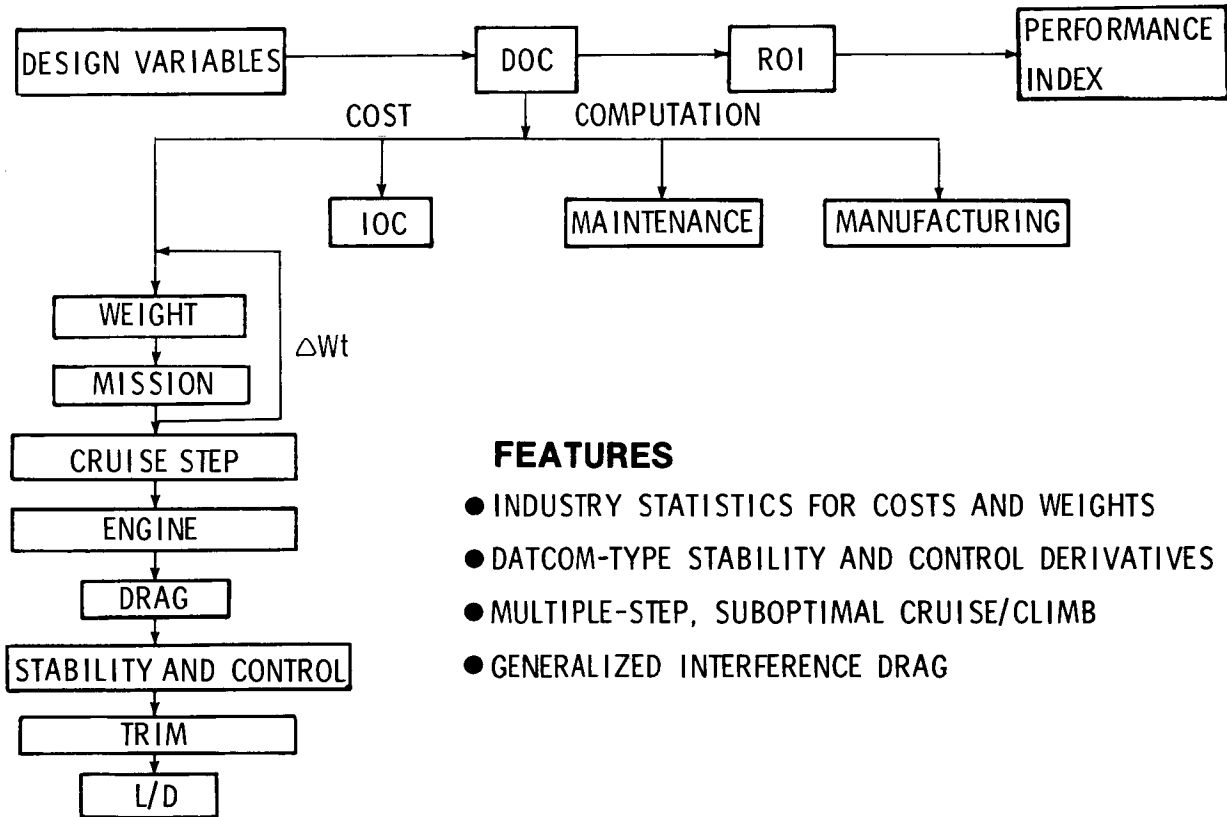


## CHARACTERISTICS:

- DIRECT NUMERICAL PROCEDURE REQUIRING NO GRADIENTS

- MINIMUM APPROACHED BY MOVING AWAY FROM HIGH VALUES OF FUNCTION

- EXTREMELY RELIABLE, REQUIRING LITTLE "FINE-TUNING"

- ROBUST IN TERMS OF CONVERGENCE

90

The performance index in OPDOT is computed by having a candidate configuration "fly" an entire mission while satisfying reserve fuel requirements. Industry statistics are used for estimating weights and costs. The stability and control analysis used is similar to Datcom-type capabilities and the program computes the interference drag in a general way, making the performance index sensitive to tail sizing considerations. The flight profile is a multiple-step model of a suboptimal cruise/climb for best fuel efficiency.

```
 ┌────────────────┐      ┌───────┐      ┌──────┐           ┌─────────────┐
 │DESIGN VARIABLES│─────▶│  DOC  │─────▶│  ROI │──────────▶│PERFORMANCE  │
 └────────────────┘      └───────┘      └──────┘           │INDEX        │
                      COST    │    COMPUTATION              └─────────────┘
       ┌───────────────┬──────┼───────────────┬───────────────┐
       │               ▼      ▼               ▼               ▼
       │            ┌──────┐            ┌───────────┐   ┌──────────────┐
       │            │ IOC  │            │MAINTENANCE│   │MANUFACTURING │
       │            └──────┘            └───────────┘   └──────────────┘
       ▼
  ┌─────────────┐
  │   WEIGHT    │       △Wt
  └─────────────┘
  ┌─────────────┐
  │   MISSION   │
  └─────────────┘
  ┌─────────────┐
  │ CRUISE STEP │
  └─────────────┘
  ┌─────────────┐
  │   ENGINE    │
  └─────────────┘
  ┌─────────────┐
  │    DRAG     │
  └─────────────┘
┌───────────────────┐
│STABILITY AND CONTROL│
└───────────────────┘
  ┌─────────────┐
  │    TRIM     │
  └─────────────┘
  ┌─────────────┐
  │     L/D     │
  └─────────────┘
```

## FEATURES

- INDUSTRY STATISTICS FOR COSTS AND WEIGHTS
- DATCOM-TYPE STABILITY AND CONTROL DERIVATIVES
- MULTIPLE-STEP, SUBOPTIMAL CRUISE/CLIMB
- GENERALIZED INTERFERENCE DRAG

91

# METHODOLOGY FOR CONDUCTING SENSITIVITY STUDIES

A sensitivity study is performed by inputting a set of problem parameters and selecting an initial set of independent design variables. OPDOT finds a solution, and that configuration is saved for later comparison. The analyst then systematically varies a design constant or constraint function and saves each optimum design. A locus of these optimum designs can then be plotted as a function of the parameter in question. This plot is used to illustrate the sensitivity of a design to the application of a new technology, with each point representing a transport design which includes the maximum synergistic benefits available for the set of inputs specified.
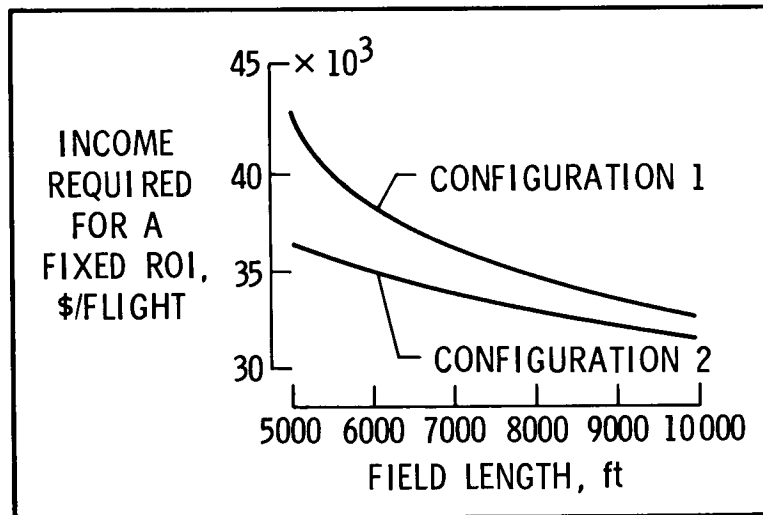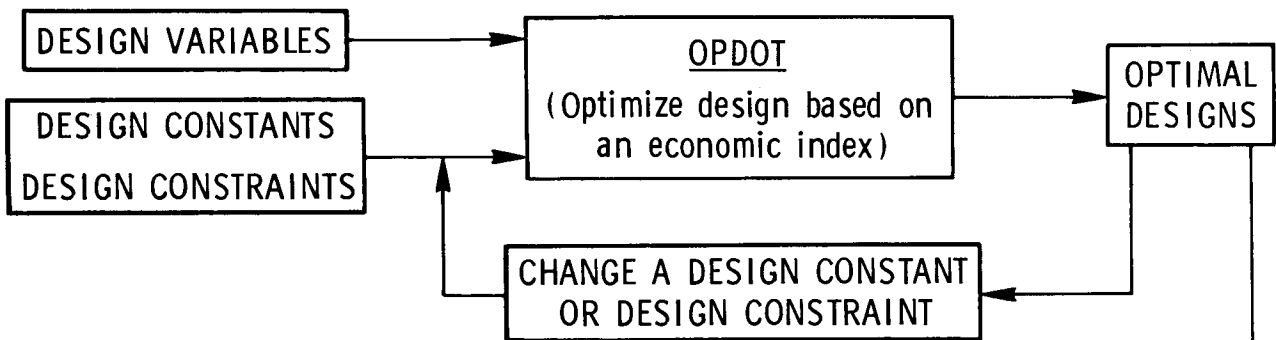
One study that was made using OPDOT (Refs. 4,5) was the evaluation of the impact of minimum acceptable flying qualities upon aircraft design.  This is the prime factor which influences aircraft design when RSSAS systems are considered.  It is assumed that an RSSAS system will augment the flying qualities up to more than acceptable levels, but provisions must be made in the event the autopilot/augmentation system fails.  Transport aircraft will generally have mechanical back-ups, so a given configuration should have sufficient unaugmented stability to ensure that a flight can be completed after a set of failures.  Clearly the unaugmented stability requirements, in effect, specify the inherent aerodynamic stability characteristics of a configuration.  OPDOT will give designers economic sensitivities to these criteria, enabling a proper compromise between safety and economy.  It was found that many of the criteria being considered for unaugmented flying qualities of transports with RSSAS were either inadequate or inappropriate for specifying airplane design parameters.

- **DEMONSTRATED USE OF CONSTRAINED OPTIMIZATION IN PRELIMINARY DESIGN**

- **RSSAS SHOULD YIELD ABOUT 1.5% SAVINGS IN DOC (3.5% FUEL SAVINGS)**

- **LONGITUDINAL FLYING QUALITIES DESIGN CRITERIA FOR UNAUGMENTED TRANSPORTS NEEDS FURTHER RESEARCH**

One design parameter considered in the flying qualities study was the impact of relaxing the natural static stability requirement for transport aircraft. A locus of optimum designs indicates that, for the configuration being considered, a savings of 2.5 percent in direct operating cost is possible when compared to a baseline configuration with 5 percent static margin. This corresponds to a fuel savings of 6 percent. At -7 percent static margin, reducing the static stability constraint yields no further improvements. This is because the control constraints (typically nose gear unstick during take-off) prevent the design from having a smaller horizontal stabilizer, since a minimum size tail is required for control and the center-of-gravity cannot be moved any further aft without sacrificing nose gear steering traction.
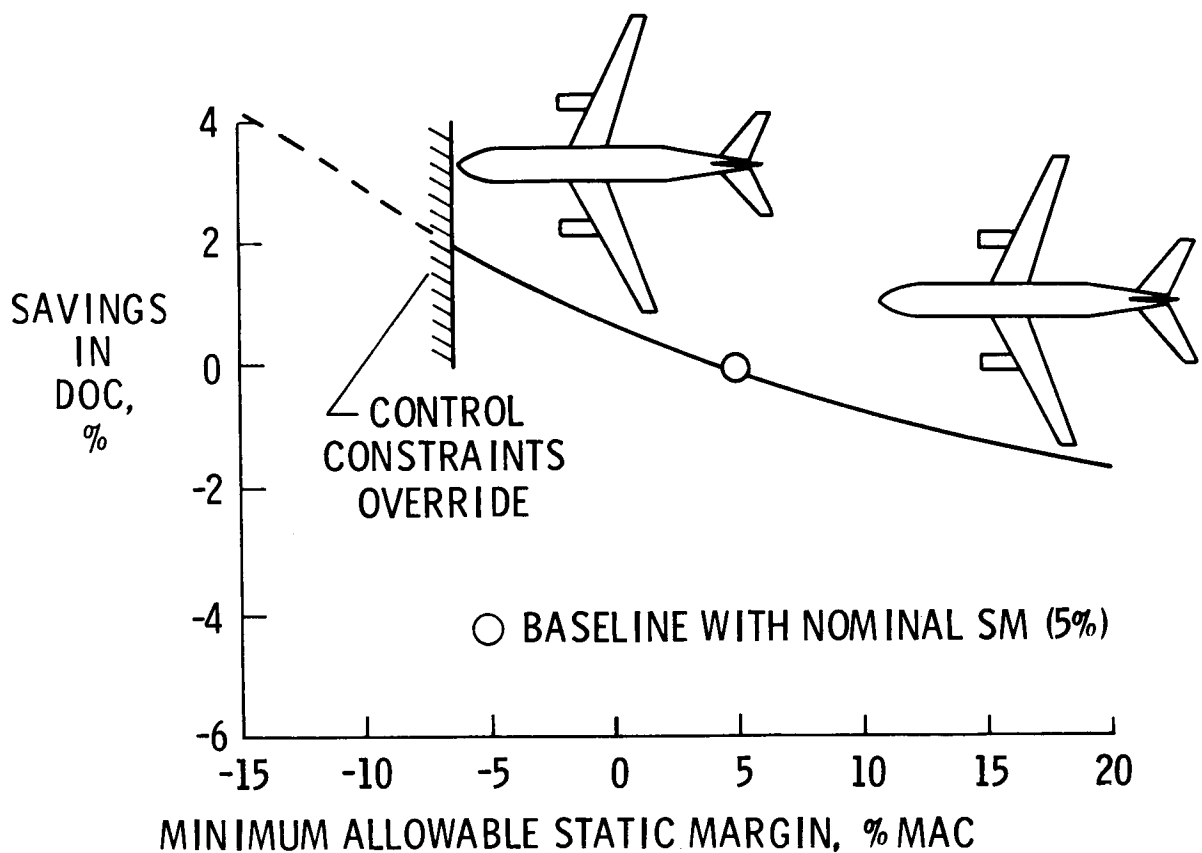
One unaugmented flying-qualities criterion of considerable interest is time-to-double amplitude. This plot illustrates the importance of economic sensitivity to a proposed criterion. If a designer is considering applying a constraint of 30 or 40 seconds, it is easy to see that arbitrarily relaxing the constraint from 30 to 40 seconds is of little economic consequence. However, the opposite is true when considering an arbitrary boundary ranging between 2 and 6 seconds. Economic sensitivity information should be considered before establishing the flying-qualities criteria since they significantly impact the aircraft design.
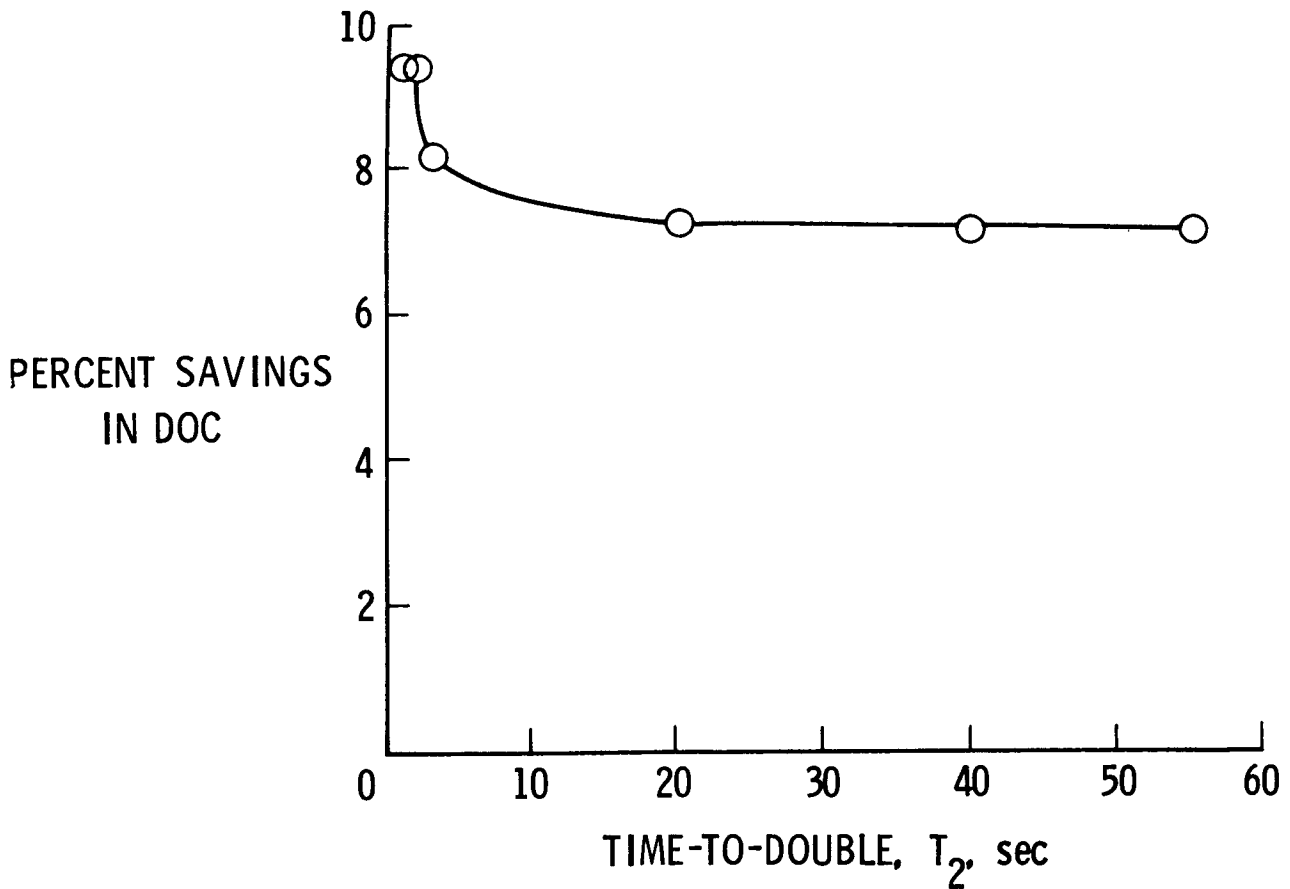
OPDOT was also used in a study (Refs. 6,7) evaluating the sensitivity of transport aircraft design to various design constraints and technology assumptions. During this study, the full benefits of resizing the design to take advantage of a new technology were demonstrated. Various performance indices were used to generate "optimal designs" in an effort to identify a robust and meaningful economic index. FARE (defined as the income required for a fixed return-on-investment) was chosen as the best performance index for use in this and future studies. The impacts (measured in FARE) of various mission, economic, production, and technological specifications upon transport design were evaluated. Sizable savings were possible with moderate enhancements in structural efficiency, fuel consumption, load alleviation, and maximum lift coefficient. Modest gains were observed with reductions in wing drag coefficient, pitching moments, and static margin.

- DEMONSTRATED THE BENEFITS FROM SYNERGISTIC RESIZING OF A TRANSPORT CONFIGURATION TO TAKE ADVANTAGE OF NEW TECHNOLOGIES OR NEW OPERATING ENVIRONMENTS

- EVALUATED THE OPTIMAL DESIGN SENSITIVITY TO SELECTION OF VARIOUS PERFORMANCE INDICES

- QUANTIFIED TRANSPORT AIRCRAFT DESIGN SENSITIVITIES TO VARIOUS OPERATIONAL AND TECHNICAL CONSTRAINTS

OPDOT has also been used in studies to evaluate and compare various proposed transport configurations. One of these studies was a comparison of a canard configuration with a conventional aft-tail configuration (Ref. 8). This study was initiated in response to the growing debate concerning the merits of canards and their impact on design. OPDOT was used to provide the following preliminary analyses: identifying critical design constraints, quantifying their impact on the design, comparing them with critical design constraints for aft-tail transports, and comparing the relative mission performance of canard and aft-tail transports. The canard study identified an unusually high canard $C_{L_{max}}$ requirement and an unconventional main gear location (out of the wing box structure) as critical design parameters for a canard transport.

Various assumptions were made in this study which may or may not be realistic. Further research into implementation of high lift devices on control surfaces and into quantification of the weight and drag penalties associated with an unconventional main gear location is required.

Designing for unstable static margins has been proposed to improve canard transport designs, but it was shown that a greater incremental benefit would be achieved by applying that technology to an aft-tail configuration.

- IDENTIFIED CANARD $C_{L_{MAX}}$ AND MAIN LANDING GEAR LOCATION AS CRITICAL DESIGN CONSTRAINTS FOR CANARD TRANSPORTS

- IF NOMINAL VALUES OF THE IDENTIFIED CRITICAL CONSTRAINTS CAN BE ACHIEVED WITH LITTLE PENALTY, THEN CANARD TRANSPORTS MAY EXHIBIT BETTER ECONOMIC PERFORMANCE

- DESIGNING FOR UNSTABLE STATIC MARGINS BENEFITS CONVENTIONAL TRANSPORT DESIGNS MORE THAN CANARD TRANSPORT DESIGNS

Among the ideas developed by NASA Langley researchers for improving transport efficiency is the proposed twin-fuselage transport configuration (Ref. 9). It is argued that the twin-fuselage configuration offers two key advantages over a comparable conventional configuration: a lighter, lower-drag fuselage per passenger, and a higher wing aspect ratio. However, twin-fuselage configurations introduce several new design problems that must be examined.

A study of twin-fuselage configurations using OPDOT was recently initiated, with a focus on obtaining quantitative economic and performance comparisons of twin-fuselage and conventional configurations as well as identifying key design parameters for the twin-fuselage transport. The preliminary results of the twin-fuselage configuration study show that a 250-passenger twin-fuselage transport is approximately 8 percent cheaper to operate than a comparable conventional transport. However, it is uncertain whether the statistical relationships used by OPDOT (especially for wing weight computations) remain valid for all of the twin-fuselage configurations studied. Typically, these configurations had wing aspect ratios of 11-12. Further, no consideration has been given to additional engineering, development, or certification costs that might be incurred by a twin-fuselage configuration. Even so, potential wing weight reductions show great promise and may determine the economic viability of typical twin-fuselage configurations. These potential wing weight reductions require more detailed study to firmly establish the advantage of a twin-fuselage configuration.

- A TWIN-FUSELAGE TRANSPORT MAY BE MORE ECONOMICAL THAN FUTURE CONVENTIONAL TRANSPORTS

- HYPOTHESIZED WING STRUCTURAL WEIGHT REDUCTIONS DUE TO TWIN-FUSELAGE CONCEPT SHOW PROMISE AND NEED FURTHER STUDY

During the course of the studies presented in this report, it became apparent that it is necessary to have a reliable optimization algorithm. Many optimizations need to be performed for such trade studies, and they should require as little "fine-tuning" from the designer as possible. Performing airplane design with computer optimization techniques places a burden on the designer to properly constrain the problem. This requires the analyst to carefully consider the fundamental factors which determine an aircraft's configuration.

OPDOT is very effective at maximizing the synergistic economic benefits of utilizing a new technology, since it provides an opportunity to integrate a new technology early into the design process. Because the accuracy of certain weight and cost statistics is expected to be of the order of 10 percent, OPDOT is viewed as being most useful in comparing various calculated designs to illustrate relative benefits, rather than in predicting absolute cost or performance figures of point designs. The inherent sensitivity of applying new technologies, changing mission constraints, or varying economic assumptions is of prime interest to the designer anyway. Experience has shown that if a design has not been properly constrained, it will often either diverge or converge to an impractical solution. Analysts using OPDOT must skim the intermediate calculations to assure that each set of designs is feasible. Tools like OPDOT can increase the productivity and accuracy of designers, but experience is still needed to properly plan a study and interpret the results. This is especially true since the region of validity of the statistical data must be considered. OPDOT is best viewed as an interpolation tool as opposed to an extrapolation tool.

- **USED RELIABLE DIRECT-SEARCH OPTIMIZATION ALGORITHM**

- **METHODICAL USE OF CONSTRAINTS REQUIRED**

- **VERY EFFECTIVE AT MAXIMIZING SYNERGISTIC BENEFITS OF APPLYING NEW TECHNOLOGIES**

- **PRIME USE IS FOR DETERMINING RELATIVE BENEFITS AS OPPOSED TO DETERMINING POINT DESIGN**

- **INTERMEDIATE RESULTS SHOULD BE REVIEWED BY KNOWLEDGEABLE DESIGNER FOR FEASIBILITY**

- **OPDOT IS MOST ACCURATE WHEN USED AS INTERPOLATION TOOL VERSUS EXTRAPOLATION TOOL**

SUMMARY

Since the synergistic benefits of a new technology are often twice (or more) the benefits obtainable from "adding" a new technology to an existing design, the integration of new technologies or relaxed design constraints should occur early in the design process so that the maximum advantages may be obtained. A computer program (OPDOT) has been developed at NASA Langley which utilizes optimization techniques to evaluate economic sensitivities of applying new technologies at the preliminary design level for transport aircraft. In this presentation, results from studies conducted with OPDOT have been summarized to illustrate the benefits of this approach.

- IT IS ESSENTIAL TO INTEGRATE NEW TECHNOLOGY CONSIDERATIONS IN THE BEGINNING OF THE DESIGN PROCESS TO REALIZE FULL POTENTIAL BENEFITS

- DEVELOPED RESEARCH TOOL FOR COMPARING EFFECTS OF TECHNOLOGY AND OTHER CONSTRAINTS ON TRANSPORT SIZING AND ECONOMICS

- CONDUCTED STUDIES TO QUANTIFY THESE EFFECTS

- CONDUCTED STUDIES TO PROVIDE PRELIMINARY ANALYSES OF PROPOSED NEW TRANSPORT CONFIGURATIONS

# REFERENCES

1. Sliwa, Steven M.; and Arbuckle, P. Douglas: OPDOT: A Computer Program for the Optimum Preliminary Design of a Transport Airplane. NASA TM-81857, 1980.

2. Olsson, D. M.: A Sequential Simplex Program for Solving Minimization Problems. Journal of Quality Technology, Vol. 6, No. 1, Jan. 1974, pp. 53-57.

3. Olsson, Donald M.; and Nelson, Lloyd S.: The Nelder-Mead Simplex Procedure for Function Minimization. Technometrics, Vol. 17, No. 1, Feb. 1975, pp. 45-51.

4. Sliwa, Steven M.: Economic Evaluation of Flying-Qualities Design Criteria for a Transport Configured with Relaxed Static Stability. NASA TP-1760, 1980.

5. Sliwa, Steven M.: Impact of Longitudinal Flying Qualities Upon the Design of a Transport With Active Controls. AIAA Paper No. 80-1570, 1980.

6. Sliwa, Steven M.: Use of Constrained Optimization in the Conceptual Design of a Medium-Range Subsonic Transport. NASA TP-1762, 1980.

7. Sliwa, Steven M.: Sensitivity of the Optimal Design Process to Design Constraints and Performance Index for a Transport Airplane. AIAA Paper No. 80-1895, 1980.

8. Arbuckle, P. Douglas; and Sliwa, Steven M.: Parametric Study of Critical Constraints for a Canard Configured Medium Range Transport Using Conceptual Design Optimization. AIAA Paper No. 83-2141, 1983.

9. Houbolt, John C.: Why Twin Fuselage Aircraft? Aeronautics and Astronautics, Vol. 20, No. 4, April 1982, pp. 26-35.

# THE ROLE OF OPTIMIZATION IN STRUCTURAL MODEL REFINEMENT

L. L. Lehman

Integrated Systems, Inc.
Palo Alto, California

# TRADITIONAL STRUCTURAL ANALYSIS/REFINEMENT CYCLE

To evaluate the role that optimization can play in structural model refinement, it is necessary to examine the existing environment for the structural design/structural modification process. The traditional approach to design, analysis, and modification is illustrated in Figure 1. Typically, a cyclical path is followed in evaluating and refining a structural system, with parallel paths existing between the real system and the analytical model of the system. The major failing of the existing approach is the rather weak link of communication between the cycle for the real system and the cycle for the analytical model. Only at the expense of much human effort can data sharing and comparative evaluation be enhanced for the two parallel cycles. Much of the difficulty can be traced to the lack of a user-friendly, rapidly reconfigurable engineering software environment for facilitating data and information exchange. Until this type of software environment becomes readily available to the majority of the engineering community, the role of optimization will not be able to reach its full potential and engineering productivity will continue to suffer.
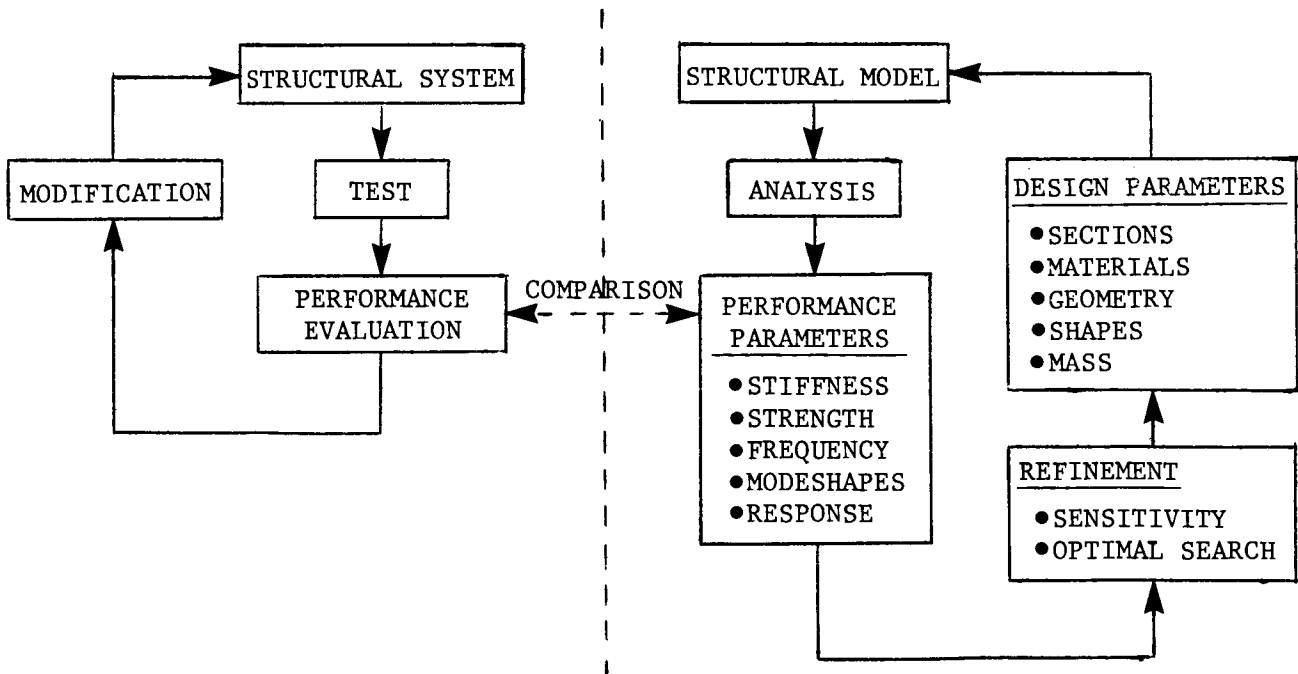
Figure 1.

# INTEGRATED ANALYSIS/REFINEMENT SYSTEM

A key issue in current engineering design, analysis, and test is the definition
and development of an integrated engineering software support capability.  The data
and solution flow for this type of integrated engineering analysis/refinement system
is shown in Figure 2.  Such a system should be capable of providing a wide variety of
reconfigurable software tools that support the analysis/refinement cycle and allow
flexible data handling.  Through careful specification of modular, plug-compatible
software interfaces, an engineering analysis system can flexibly support a wide
variety of capabilities while providing individual users with a powerful, consistent
support environment for their own privately developed software.  Support tools that
allow user reconfiguration of the application interface should be provided with the
core of such a system.  Within this type of integrated analysis environment, optim-
ization utilities can be readily combined with analysis tools to more effectively
support various stages of the design cycle.
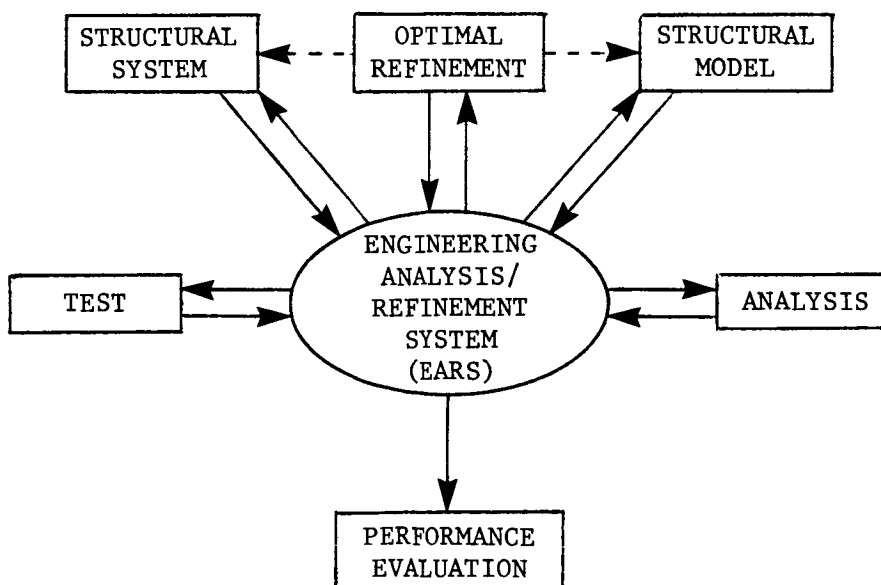
Figure 2.

## ARCHITECTURE OF AN ENGINEERING ANALYSIS/REFINEMENT SYSTEM

The general architecture of an engineering analysis/refinement system is shown in Figure 3. The system consists of three major classes of "toolkits" that can interact through well defined interfaces. The toolkits accept input data from the local Engineering Data System and in turn generate output data that is sent back to the local data system. The local data system consists of an engineering data base for permanent data as well as "data stack" handlers that accommodate temporary data. The entire analysis system is driven by a simple but powerful interpretive programming language that controls both execution and data handling.

Within this framework, optimization capability is considered as a general purpose tool that can be used to support the analysis/refinement cycle. An isolated optimization capability is often of limited utility in obtaining rapid problem solutions, but becomes quite useful when it can be readily combined with powerful modeling and analysis tools. In the current context, structural model refinement capability is assembled from a collection of fundamental tools. This type of capability can be made available as part of a preprogrammed (but reconfigurable) application library.
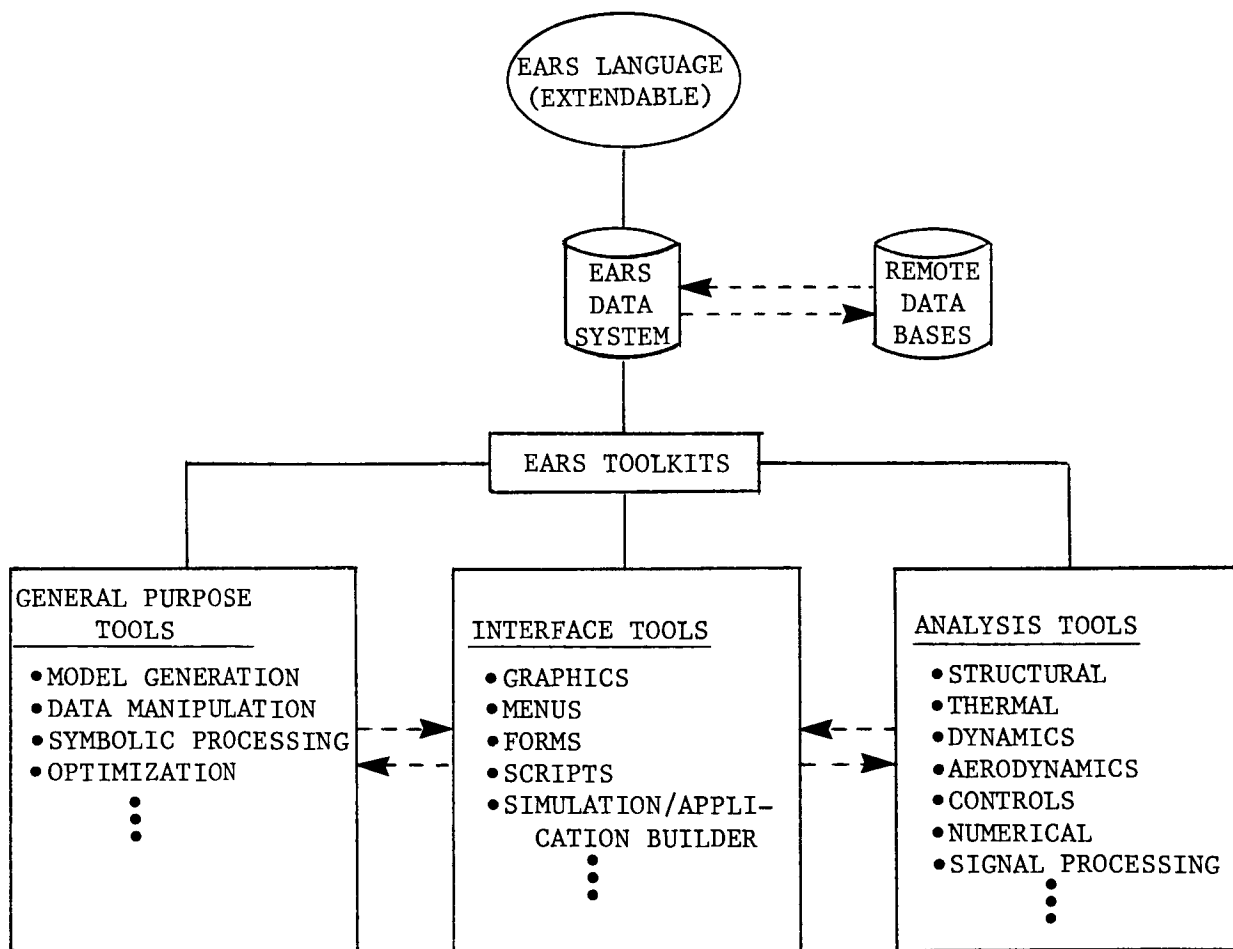


Figure 3.

# TOOLKIT SUPPORT FOR STRUCTURAL MODEL REFINEMENT

Support for structural model refinement requires consideration of optimization, structural modeling, and data handling capability. A number of desired capabilities that contribute to the refinement steps of the design cycle are given in Figure 4. As shown in this figure, support for the refinement process is provided both by special tools and by additional capability during the model generation phase. For example, the model generation tools provide not only for various types of models, but also for optimal model reduction and parameter sensitivity. Special capabilities are needed to define measures for model observability and model error. Nonlinear signal processing is needed to detect and quantify nonlinearities in test data before the model identification phase. In addition, special simulation capabilities are required for nonlinear model evaluation.

Optimization Tools

- Robust Algorithms
- Sensitivity/Gradient Calculation
- Design Variable Linking
- Multilevel Formulations
- Adaptive Objective Functions

Model Generation/Manipulation Tools

- Discrete Parameter Models
- Component Mode Models
- Damped Substructure Coupling
- Optimal Model Reduction
- Parameter Sensitivities

Special Tools

- Observability/Refinability Measures
- Model Error Measures
- Nonlinear Signal Processing
- Advanced Differential/Algebraic Simulation

Figure 4.

# A GENERAL MODEL FOR STRUCTURAL REFINEMENT

In order to integrate all of the tools needed to support structural model re-
finement, it is necessary to adhere to a consistent model for both formulation and
computation.  The diagram of a general model for supporting structural refinement is
shown in Figure 5.  The main feature of this approach is that parameter refinement is
defined in terms of a separate refinement model that isolates the parameters to be
modified from the nominal structural model.  The refinement model is a function of
the physical design variables and the physical system coordinates. Update of the
refinement model is achieved by optimal selection of the physical design variables.
Output of the refinement model can be interpreted as residuals to be applied to the
nominal system model.  Definition of the system model is in terms of either physical,
modal, or combined physical/modal coordinates. The system model is most often repre-
sented in state vector form, which is especially useful for damped systems.
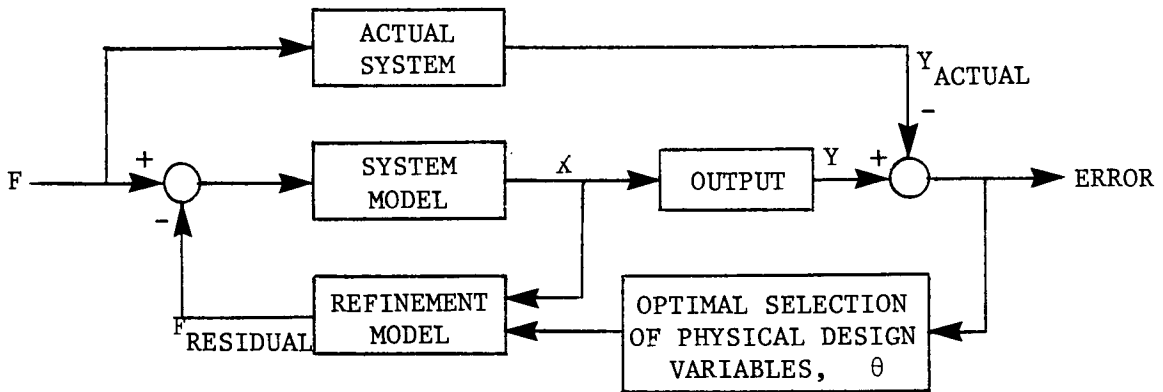


$$M\ddot{X} + C\dot{X} + KX = F - F_{RESIDUAL}$$

$$\ddot{Z} + 2\xi\omega\dot{Z} + \omega^2 Z = \mathscr{F} - \mathscr{F}_{RESIDUAL}, \quad X = \Psi Z, \quad \mathscr{F} = \Psi^T F$$

$$F_{RESIDUAL}(X, \theta)$$

Figure 5.

# A GRAPHICAL MODEL BUILDER INTERFACE

Much of the effort of combining optimization and analysis capability is associated with constructing, manipulating, and interconnecting various forms of software models. Traditionally, this process has been very time consuming and quite error prone. A graphical model builder based on functional diagrams can provide a far better user interface for model construction and linking. Such an approach can be used for building both analysis and simulation models and rapidly interconnecting them with optimization algorithms to form design and refinement packages. Functional "superblocks" representing either analysis or optimization algorithms can be constructed by assembling desired functions from a catalog of predefined primary functions. By allowing superblocks to be hierarchical, complex capabilities can be built up by following either a "top-down" or "bottom-up" approach. Both user-constructed and predefined functional blocks can be used. To aid in design and refinement of models, functional blocks can automatically provide parameter sensitivities. A schematic depicting the typical construction of performance index and constraint calculation superblocks is shown in Figure 6. By combining this type of problem-oriented graphical interface with flexible analysis "toolkits" containing state-of-the-art optimization tools, significant productivity advances can be achieved in the analysis/refinement cycle.



$$\begin{bmatrix} \theta_1 \\ \theta_2 \\ \vdots \\ \theta_n \end{bmatrix}$$

$C_i$ (or f)

Performance Index or Constraint Function Output From the Superblock
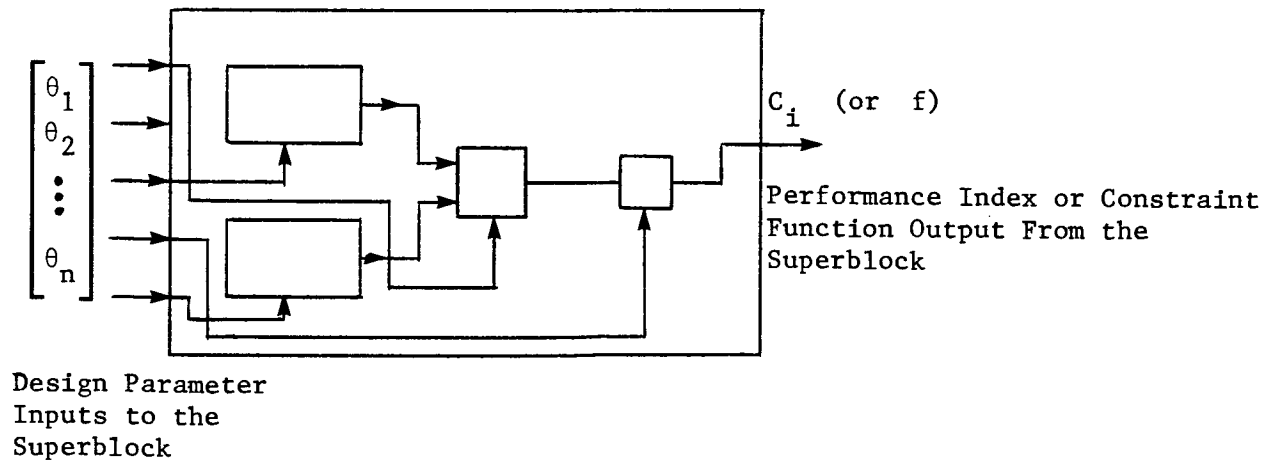
Design Parameter Inputs to the Superblock

Figure 6.

PIAS, A PROGRAM FOR AN
ITERATIVE AEROELASTIC SOLUTION

Marjorie E. Manro
Boeing Commercial Airplane Company
Seattle, Washington

## WHAT IS PIAS?

PIAS is the acronym for a Program for an Iterative Aeroelastic Solution. This will be a modular computer program that combines the use of a finite-element structural analysis code with any linear or nonlinear aerodynamic code (fig. 1). At this point in time, PIAS has been designed but the software has not been written. The idea for this development originated with P. J. (Bud) Bobbitt of the NASA Langley Research Center. There was initial interest in an aeroelastic solution for a separation-induced leading-edge vortex. Figures 2 and 3 show some examples of the flow patterns for a low aspect ratio wing and illustrate the need for a nonlinear aeroelastic solution. The development of PIAS by The Boeing Commercial Airplane Company was done under NASA contract NAS1-16740. The engineering and software specifications for PIAS are documented in NASA CR-172200 (ref. 1). The Leading-Edge Vortex Program, which calculates pressure distributions including the effects of a separation-induced leading-edge vortex, uses an iterative solution method. This led to the concept of an iteration cycle on configuration shape external to the aerodynamic code.

- **Program for an Iterative Aeroelastic Solution**

- **Modular computer program to combine:**
  - **Finite-element structural analysis code**
  - **Any linear or nonlinear aeroelastic code**

- **Development:**
  - **Initiated by NASA Langley**
  - **Designed by The Boeing Commercial Airplane Company**
  - **Under NASA contract NAS1-16740**
  - **Reported in NASA CR-172200**

- **Leading-Edge Vortex Program**
  - **Separation-induced leading-edge vortex**
  - **Iterative solution**

Figure 1

# EFFECT OF ANGLE OF ATTACK ON FLOW PATTERN, FLAT WING, M = 0.40

The flow patterns shown in figures 2 and 3 are based on experimental data obtained under several NASA contracts and summarized in references 2 through 4. An extensive data base was acquired for three wings that have the same planform and thickness distribution but different shapes — flat, twisted, and cambered-twisted. Figure 2 shows a comparison of the flow patterns on the planform of the flat wing at two angles of attack at a Mach number of 0.40. The flow pattern is illustrated by lines of constant pressure with the pressure difference between adjacent lines also being a constant. At the moderate angle of attack shown on the left side of the figure, a vortex has developed along the entire leading edge, but attached flow is still apparent on the aft inboard half of the wing. At the high angle of attack shown on the right side of the figure, the vortex has moved inboard with very little of the flow on the inboard wing still attached.

$$\alpha = 8^{\circ} \qquad\qquad \alpha = 16^{\circ}$$
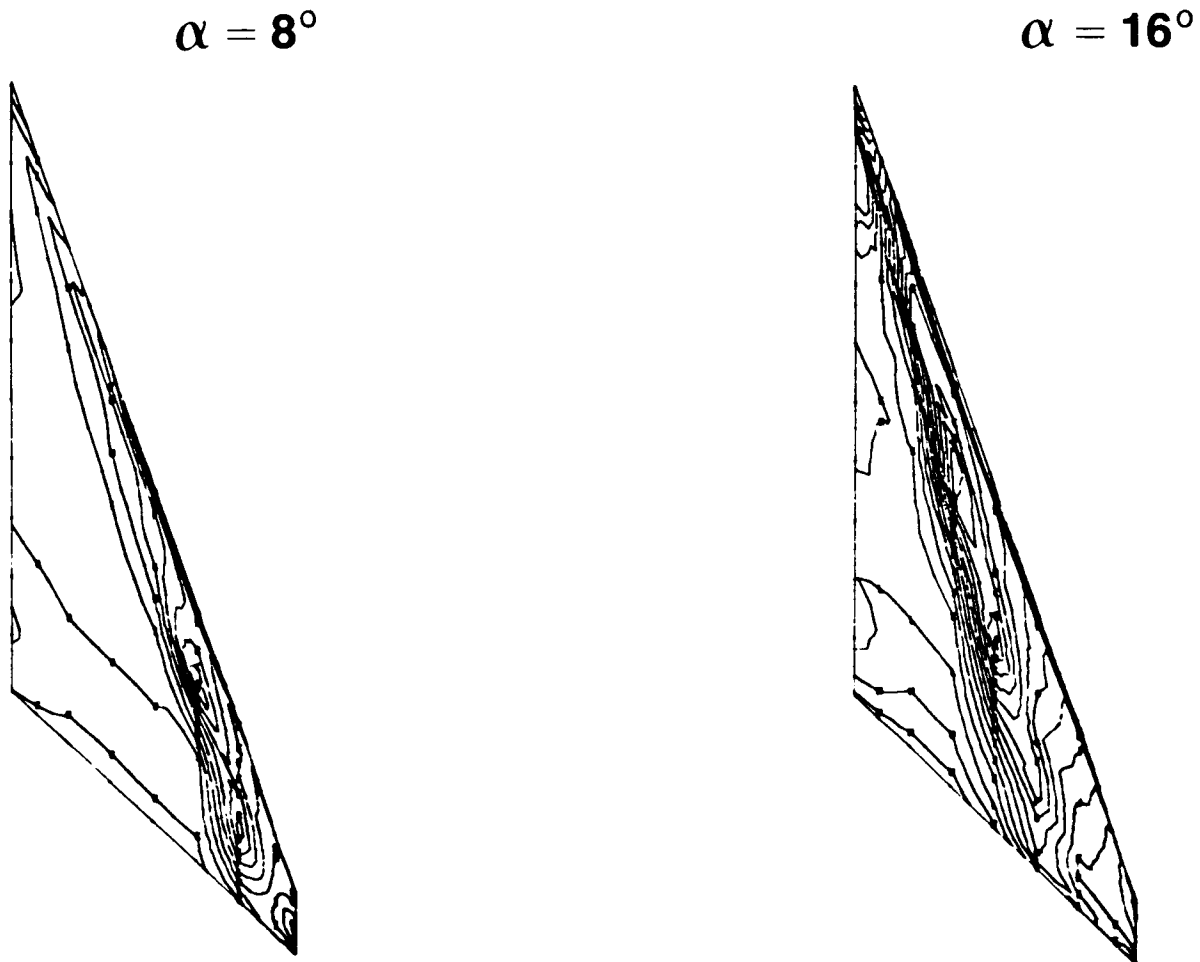


Figure 2

In figure 3, data are shown at Mach number = 0.40 for only one angle of attack, but for two wing shapes. The flow pattern on the left side of the figure — for the flat wing — is the same data as shown at $8^\circ$ angle of attack on the previous figure. The flow pattern on the twisted wing on the right side of the figure is quite different. The vortex has just started at the wing tip at this angle of attack. There is $4.5^\circ$ washout at the tip of the twisted wing and the flow pattern shown here closely resembles the pattern on the flat wing at an angle of attack of 4 degrees. The futility of using a linear method to predict these flow patterns is clearly illustrated in these figures.

**Flat wing**                    **Twisted wing**

Figure 3

114
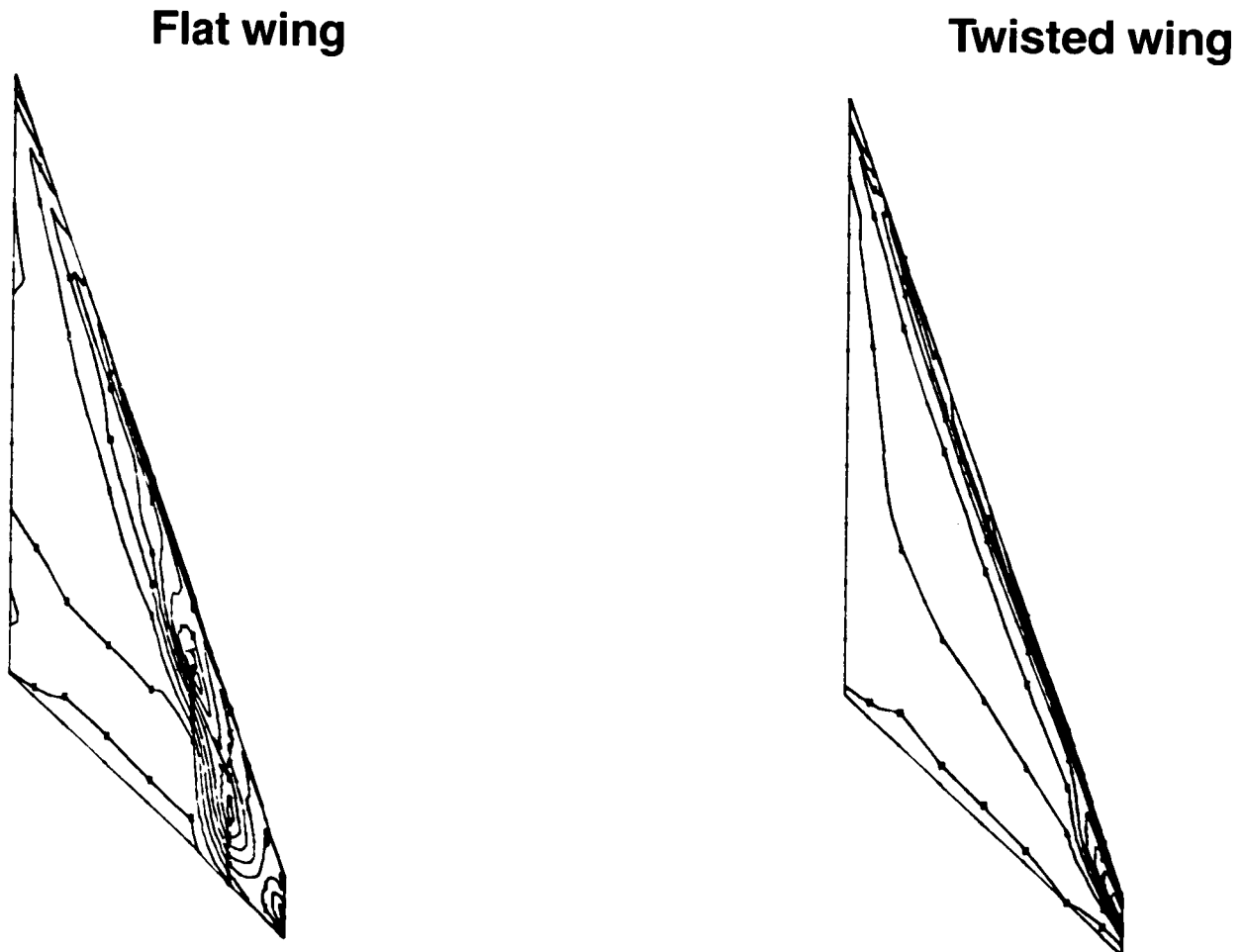
## RATIONALE FOR SELECTING AN ITERATIVE PROCEDURE

A review of the attributes of closed form and iterative solutions was made to confirm the decision to select an iterative procedure (see fig. 4). In a closed form solution, the structural flexibility terms are an integral part of the aerodynamic code. This works well when the aerodynamic solution is linear. If the aerodynamic solution is nonlinear, it is difficult if not impossible to include the flexibility terms in the formulation. In any case, the development would have to be done for each aerodynamic theory. In an iterative solution, the terms for structural flexibility are kept separate from the aerodynamic code. The approach used to obtain aeroelastic loads at a specified design load factor is the alternate execution of two codes: one to calculate the aerodynamic loads on a specific shape and the other to calculate the deflected shape under load. This alternate execution is continued until the wing shape is compatible with the applied loads. The development, applied to one nonlinear aerodynamic program, will address the logic to obtain both convergence to a deformed shape at each angle of attack and convergence to the design load factor. The data management scheme developed for one aerodynamic module will accomodate another theory with minor changes.

- **Closed form solution**
  - **Structural flexibility terms in aerodynamic code**
  - **Straightforward for linear aerodynamic methods**
  - **Difficult for nonlinear aerodynamic methods**
  - **Separate development for <u>each</u> nonlinear aerodynamic theory**

- **Iterative solution**
  - **Structural flexibility terms separate from aerodynamic solution**
  - **Existing structural program can be used to calculate deflected shape under load**
  - **Alternate execution of code to calculate:**
    - **Aerodynamic loads on a specific shape**
    - **Deflected shape under load**
  - **Development for one aerodynamic theory addresses:**
    - **Logic for solution convergence**
    - **Data management**
  - **Other aerodynamic theories**
    - **Should be added easily**
    - **Would require minor changes to data management**

Figure 4

Having established that the iterative form for an aeroelastic solution was preferred, a review was made to determine the general need for an iterative aeroelastic solution (see fig. 5). Generally, the aircraft configurations that are currently in design exhibit nonlinear flow because of either the physical config- uration or the flight domain, or both. The high costs of fuel and increased airline competition due to deregulation have made more efficient aircraft and therefore more realistic design load prediction a necessity. In the past, it has been necessary to augment the use of linear theories with experimental data for structural design. As the costs of wind tunnel testing increase, it is not reasonable to test the many points in the flight envelope that are necessary to support this effort. Many computer programs are being developed that address particular types of nonlinear flow now that computer power is increasing. Both the speed of computations and the available in-core storage have influenced this progress.

- **Current aircraft exhibit nonlinear flow**
  - **Physical configuration**
  - **Flight domain**

- **More realistic design load prediction is required for efficient aircraft**
  - **High fuel costs**
  - **Airline competition due to deregulation**

- **Linear systems are inadequate without experimental augmentation**

- **Costs of wind tunnel testing are increasing**

- **Many theories for nonlinear aerodynamics are being developed**

- **More computer power is available**
  - **Faster**
  - **More in-core storage**

Figure 5

The basic flow of the proposed interative solution is shown in figure 6. The initial input includes the aerodynamic model, the structural and mass models, the flight condition description, and execution parameters for the solution. These parameters include the maximum number of iterative cycles, the acceptable tolerance on the change in deflection between cycles, and the acceptable tolerance on the design load factor. There are two levels of iteration. The outer level consists of solutions at several angles of attack. This approach is necessary because of the nonlinear nature of the solution. The procedure for determining the values of successive angles of attack is shown later. The inner level of iteration continues for each angle of attack until a wing shape is obtained that is compatible with the calculated airload. The acceptable tolerance on deflection may be less stringent for the initial stages of the solution than for the final solution. The aerodynamic and structural modules shown in this cycle are separate programs and the only requirement is that a specified minimum amount of data is written to a file for communication with PIAS. The other calculations and the interpolations are provided by new code that will also control the solution sequence.

- **Basic definition of model**
- **Initial condition**

**Revise angle of attack**

**AERODYNAMIC MODULE**
Calculate pressure
distribution

**Revise aero model
deflections**

no

no

**STRUCTURAL MODULE**
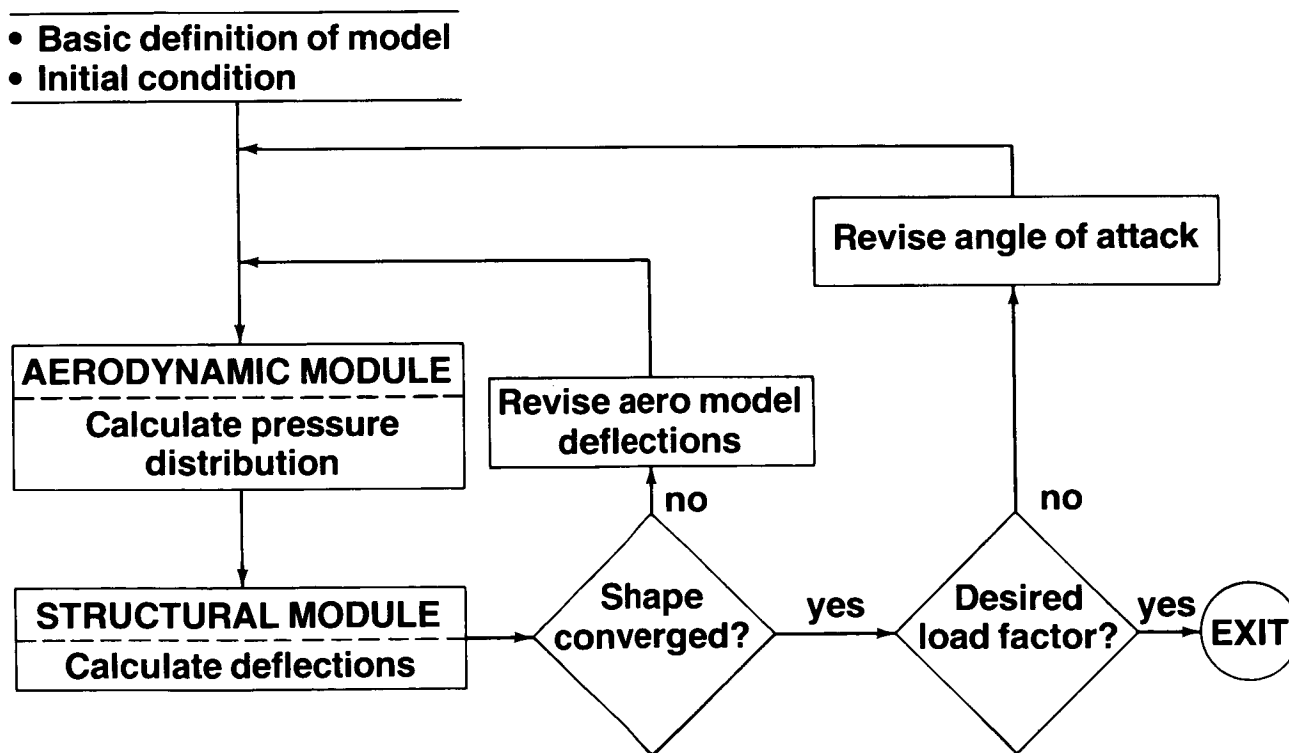Calculate deflections

Shape
converged?

yes

Desired
load factor?

yes

EXIT

Figure 6

117

The major problems that need to be solved before a viable aeroelastic solution is possible are shown in figure 7. The first of these is the difference between the grid used in the aerodynamic module and the model for structure and mass. Generally, the aerodynamic grid is tailored to be densest in areas where high pressure gradients are expected; the structural model is densest in regions of high stress/strain gradients. Usually, the mass model is compatable with the structural model. The pressure values calculated by the aerodynamic code are typically located at panel centroids. The code for structural analysis requires loads at the structural nodes, and for a realistic analysis the summation of these loads must represent the total load and distribution as obtained from the aerodynamic program. The conversion of one type of data to the other type is a required function. Code that is external to the functions already available in the aerodynamic and structural programs is needed to make additional calculations, to initiate execution of the existing codes as required by the algorithm, to determine when convergence within specified tolerances is achieved, and to manage the data flow and storage. The data management plan must allow for the changing nature of the data during the solution, as well as for the required checkpoint-restart capability. The design of PIAS stressed retention of adequate data so that the solution could be easily restarted from several points in the cycle. In addition to a continuous execution to the desired load factor, it is expected that the user will sometimes wish to pause periodically to review the results at selected steps in the cycle. There will also be times when a situation will be encountered for which a course of action was not defined.

- **Difference in aerodynamic and structural grids**
  - **Aerodynamic grid — dense in regions of high pressure gradients**
  - **Structural grid — dense in regions of high stress/strain gradients**

- **Code is required to provide:**
  - **Additional calculations**
  - **Data conversion**
  - **Selective execution of existing codes**
  - **Control of solution convergence**
    - **Configuration shape within specified tolerance**
    - **Load factor within specified tolerance**
  - **Data management**

- **Checkpoint-restart procedures**
  - **Planned pauses during solution**
  - **Restart after a situation is encountered for which a course of action was not defined**

Figure 7

DESIGN OF PIAS

The elements incorporated into the design of PIAS are shown in figure 8. The Leading-Edge Vortex (LEV) Program is used for the aerodynamic module. The output is pressure distributions at the centroids of panels representing the configuration surface. The LEV Program has the capability to calculate loads for either attached flow or for a separation-induced vortex. The ATLAS Integrated Structural Analysis and Design System is used for calculating the deformed shape of the wing under the combined effect of airload and inertia loads. ATLAS is a system of modules with a variety of capabilities. The ATLAS surface spline interpolation module uses the method of Desmarais (ref. 5). A sample of the results of an interpolation using this method is shown in figure 9. A recent development for potential enhancement of ATLAS uses the surface spline interpolation module to perform an exact integration of the pressure distribution over discrete areas of the wing to obtain forces and moments. From these forces and moments, equivalent nodal loads are calculated that represent the total load. The Execution Control Monitor (ECM) will direct the execution of these programs, including control of solution convergence. The ECM will also provide a data management scheme to transfer the data between the aerodynamic and structural modules. The few additional calculations that are required for an aeroelastic solution — but not for the aerodynamic and structural modules individually — are part of the function of the ECM. These calculations determine the vertical load factor, the revised angle of attack, and the origin of the vortex when using the separated-flow option of the LEV Program for the aerodynamic module.

- **Combine existing codes into an aeroelastic solution**
  - **Leading-Edge Vortex (LEV) Program**
    - **Separation-induced leading-edge vortex**
    - **Attached flow**
  - **ATLAS**
    - **Structural and mass modeling**
    - **Calculate structural deflection due to airload and inertia loads**
    - **Surface spline interpolation**
    - **Calculate equivalent nodal loads**

- **Execution Control Monitor (ECM)**
  - **Direct the overall aeroelastic solution process**
  - **Control of solution convergence**
  - **Data management**
    - **Transfer of data**
    - **Retention of results at each solution step for restart**
  - **Provide additional calculations**
    - **Load factor, $n_z = C_L \, q \, S/W$**
    - **Revised angle of attack**
    - **Origin of vortex for separated-flow option of LEV**

Figure 8

119

# RESULTS OF SURFACE SPLINE INTERPOLATION

The upper left portion of figure 9 shows an isometric drawing of an experimental upper surface pressure distribution on an arrow wing. The arrows show the locations of the measured data and, as indicated, the orifices were arranged in seven streamwise rows. Progressing from the inboard to the outboard section, the location of the peak pressure is a little farther aft at each spanwise section. In the lower right hand portion of this figure, an isometric drawing of the interpolated pressures is shown. The output points are arranged in rows that are perpendicular to the centerline of the model. The location of the peak pressures follows the same pattern as shown in the input distribution. In this case, the extrapolation in the wing tip area seems to be quite good, even though extrapolation is not recommended with this method.
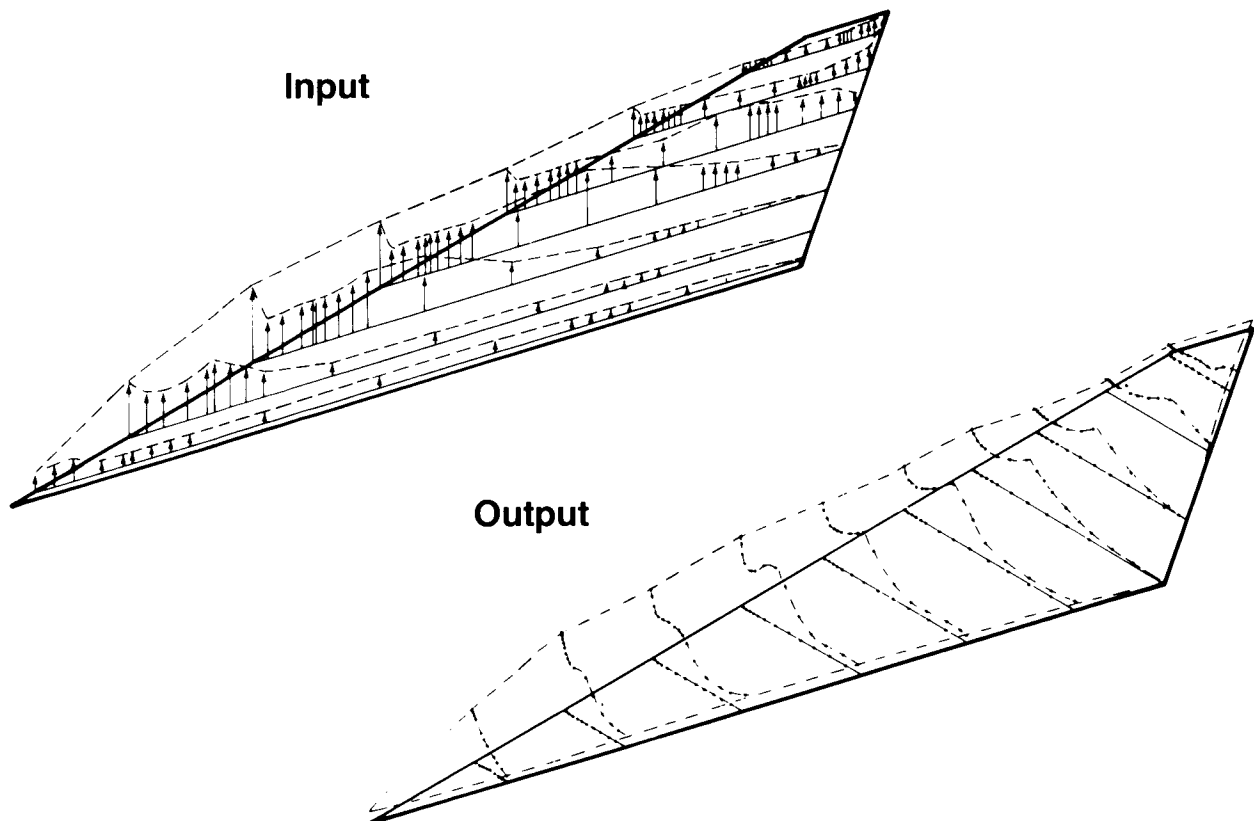
**Input**

**Output**

Figure 9

## ATLAS INTEGRATED STRUCTURAL ANALYSIS AND DESIGN SYSTEM

As shown in figure 10, ATLAS is based on the stiffness finite-element structural analysis method. The extensive library of structural finite elements allows modeling of configurations from the simple to the complex for both metalic and advanced composite structures. Capabilities are also provided for modeling structural, nonstructural, fuel, and payload mass distributions with the library of mass finite elements or by concentrated masses. Automatic grid generation from minimum user input simplifies both structural and mass modeling. A number of other features that are needed for the iterative process, as well as some that will make the process easier for the user, are available in ATLAS. The capability for using a combination of local coordinate systems — rectangular, cylindrical, and spherical — allows the aerodynamic and structural grids to be in different systems. The surface spline interpolation method and calculation of equivalent nodal loads, as previously described, are necessary to obtain the deflection of the wing at the structural nodes. The surface spline interpolation method will be used to calculate the modifications to the aerodynamic grid for the next execution of the aerodynamic code. There is the capability in ATLAS to have a control program which can be a combination of FORTRAN code, calls to execute other modules of ATLAS, and calls to execute codes that are not a part of ATLAS. This capability provides a convenient framework for developing the Execution Control Monitor (ECM).

- **Stiffness finite-element structural analysis method**

- **Structural modeling**
    - **Library of structural finite elements**
    - **Simple to complex configurations**
    - **Metallic and advanced composite structures**

- **Mass modeling**
    - **Library of mass finite elements or concentrated masses**
    - **Structural, nonstructural, fuel, and payload mass distributions**

- **Additional features**
    - **Automatic grid generation - minimum input**
    - **Capability to use a combination of local coordinate systems**
    - **Surface spline interpolation, calculation of equivalent nodal loads**
    - **Data management**
    - **Execution control modules**
        - **Perform problem-specific calculations**
        - **Execute selected modules of ATLAS**
        - **Execute other programs**

Figure 10

# DETERMINATION OF SECOND ANGLE OF ATTACK

As stated earlier, the ECM will calculate the revised angle of attack. A basic premise of this development is that the vertical load factor is not a linear function of the angle of attack $\alpha$. It is expected that solutions for four angles of attack will be necessary to achieve the design load factor $n_z$. The user specifies the first angle of attack for each case; the load factor for this angle of attack is then calculated from the predicted pressure distribution and is shown in figure 11 as a solid circle, labeled 1. The second angle of attack may be selected to correspond to the design load factor by temporarily assuming a linear variation between zero and the first calculated point as shown on the left, or the user may specify $\alpha_2$ directly as shown on the right. The load factor for the second point is obtained from the pressure distribution at this angle of attack and is shown as the solid circle labeled 2. It is clear that the assumption of linearity is only a convenience for estimating the next angle of attack to try.
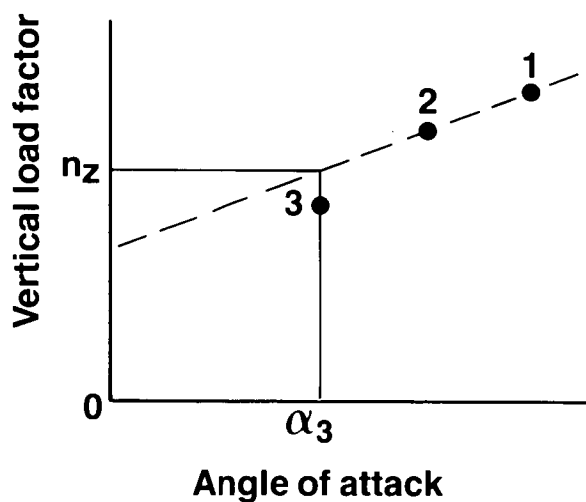


**Third angle of attack**　　　　　　**Fourth angle of attack**
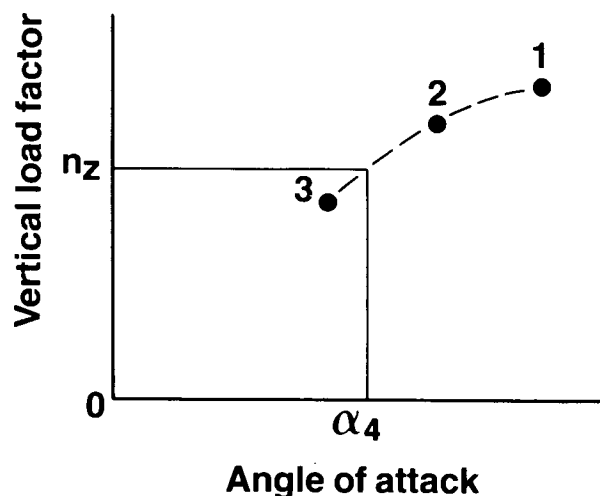
Figure 11

# DETERMINATION OF THIRD AND FOURTH ANGLES OF ATTACK

Again assuming a linear variation of load factor with angle of attack, these first two points are used to find the angle of attack for the design load factor by linear interpolation (or extrapolation) as shown in the left part of figure 12. The load factor is calculated using the pressure distribution from the third solution and is shown as a solid circle labeled 3. A curve fit through these three points is used to get the fourth angle of attack, which should be the final one. The logic in PIAS is such that as soon as the calculated load factor is within the user-specified tolerance for the desired load factor, the solution will stop.
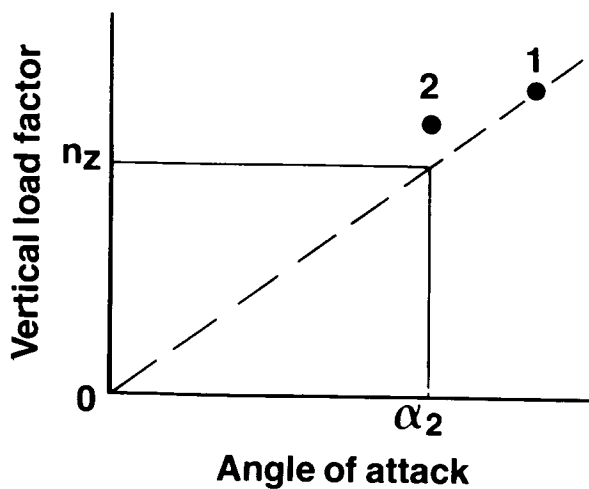


Default method                                        Input $\alpha_2$
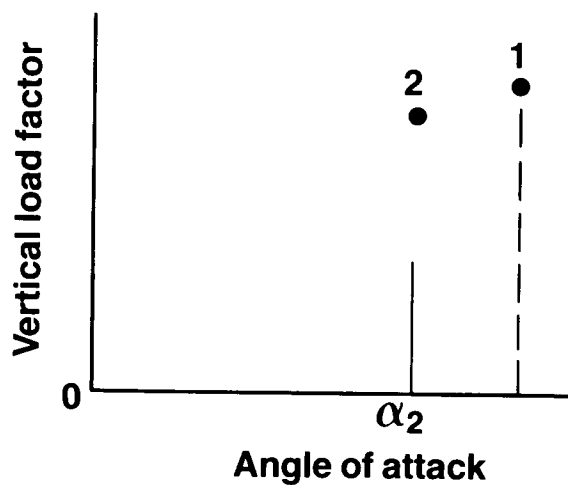
Figure 12

As the specification for PIAS was developed, some unexpected uses became apparent as listed in figure 13. The initial goal was to be able to calculate design load pressure distributions for a specific load factor. By stopping the solution after convergence on the wing shape at the first angle of attack, it will be possible to analyze flexible wind tunnel models for expected test conditions. The little-used capability to represent cases with attached flow in the LEV Program will allow analyses of a configuration that exhibits this phenomenon through part or all of its flight envelope. With the capabilities of ATLAS, it will be possible to calculate the internal stresses for the design load case. In addition, once the structure and mass of the aircraft are modeled, the user can take advantage of other ATLAS capabilities such as the vibration and flutter analyses and automated structural resizing. In respect to adding other aerodynamic codes to PIAS, it is interestng to note that advances are being made in nonlinear transonic codes — full potential and Euler — and in nonlinear supersonic codes.

- **Loads for wing with shape converged at a specific angle of attack**

- **Attached flow**

- **Internal stresses**

- **Other ATLAS capabilities**
  - **Vibration analysis**
  - **Flutter analysis**
  - **Automated structural resizing**

- **Nonlinear transonic codes**
  - **Full potential**
  - **Euler**

- **Nonlinear supersonic codes**

Figure 13

# REFERENCES

1. Manro, Marjorie E.; Donahue, Michael J.; Dreisbach, Rodney L.; and Bussoletti, John E.: Specification for a Program for an Iterative Aeroelastic Solution (PIAS). NASA CR-172200, 1983.

2. Manro, Marjorie E.; Manning, Kenneth J. R.; Hallstaff, Thomas H.; and Rogers, John T.: Transonic Pressure Measurements and Comparison of Theory to Experiment for an Arrow-Wing Configuration, Summary Report. NASA CR-2610, 1976.

3. Manro, Marjorie E.: Supersonic Pressure Measurements and Comparison of Theory to Experiment for an Arrow-Wing Configuration. NASA CR-145046, 1976.

4. Manro, Marjorie E.: Transonic Pressure Measurements and Comparisons of Theory to Experiment for Three Arrow-Wing Configurations, Summary Report. NASA CR-3434, 1982.

5. Harder, R. L.; and Desmarais, R. N.: Interpolation Using Surface Splines. Journal of Aircraft, vol. 9, no. 2, Feb. 1972, pp. 189-191.
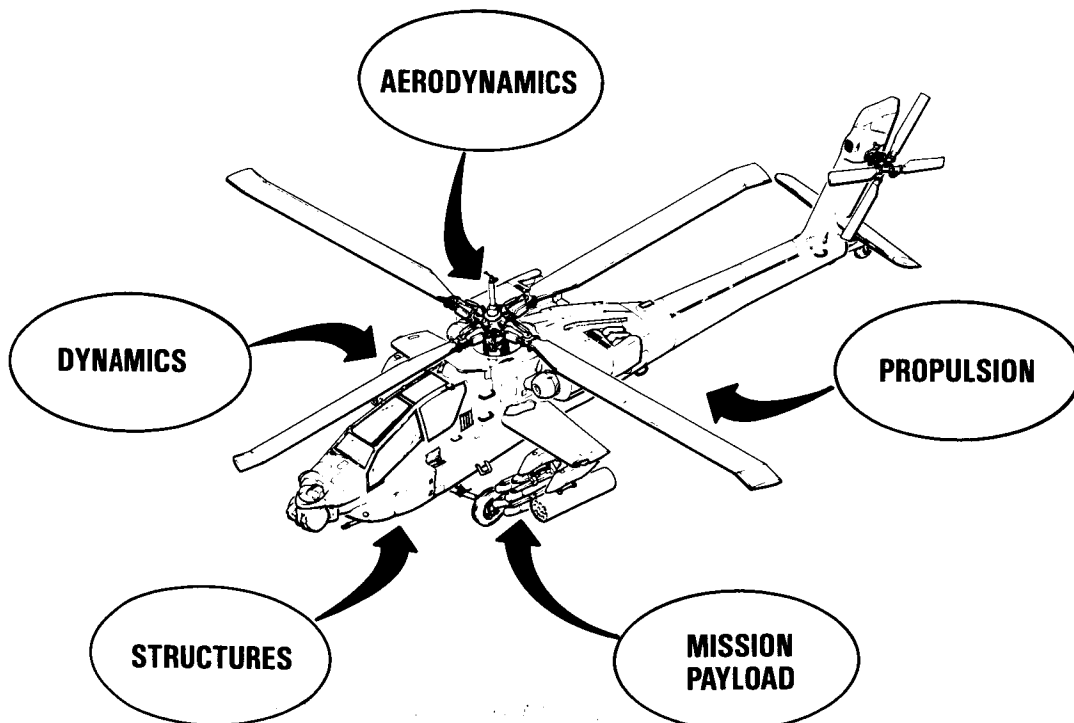
# OPTIMIZATION PROCESS IN
# HELICOPTER DESIGN

A. H. Logan and D. Banerjee
Hughes Helicopters, Inc.
Culver City, CA

# HELICOPTER DESIGN CONSIDERATIONS

Optimization is a technique for balancing values in a system against each other so that the overall value of the system is maximized or minimized toward a predefined end. In helicopter design, this optimization procedure generally involves the minimization of the airframe/propulsion system weight required to support a prescribed mission payload and profile. Minimum cost is also a requirement but this is generally related to weight and hence weight is the initial objective. The airframe/propulsion system weight is an interrelated function dependent on the requirements of several conflicting disciplines. For example, the aerodynamically optimum rotor system may be dynamically unstable unless advanced structural concepts such as composite materials are applied. Changes in the rotor system then influence the overall aircraft geometry due to clearance and internal volume requirements. Further, changes in mission profile may result in a different optimum configuration. All these considerations require a practical process of design optimization that achieves significant precision through use of computers and application of emerging mathematical tools.

At Hughes Helicopters, this process is currently applied at two distinct levels: total configuration and component. In total configuration, the issues to be resolved include sizing of various components to achieve a certain mission. In components, detailed shapes and sizes are determined to optimize component performance. At both levels, the process is both complicated and complex, involving the balancing of many disciplines and technologies including aerodynamics, dynamics, structures, and propulsion.

# METHODS OF OPTIMIZATION

In traditional design procedures, design optimization processes were inhibited by the difficulty of performing the calculations necessary to minimize (maximize) an objective function under constraints. Instead, typically, large systems of differential equations had to be solved in part; then experiments were performed on full or scale models in a cycle of hypothesis, test, and modification. Since the initial design definition was imprecise, a wide range of models had to be carried through test and modification to ensure that a near optimum design was achieved. This procedure is very costly. Even now, extrapolating from an existing design may sometimes be more cost effective than a complete top down analysis. But as a general technique of optimization, the experimental method is costly, time consuming, and imprecise.

The advent of the modern powerful digital computer made possible a design optimization process that is different in principle, the major task of which is to specify a description of the system in a mathematically precise way. Once specified, the description is entered into a computer that models the behavior of the system under various conditions defined according to the mission requirements. The impact of the optimization procedure is to reduce the scope of models carried through the test and modification stage. Early in the design phase, a large number of designs can be studied before hardware commitments are made.

**EXPERIMENTAL**                    **MATHEMATICAL MODELLING**
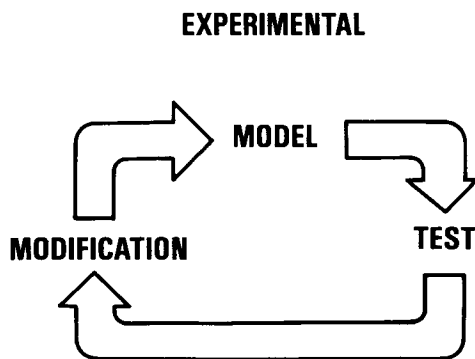


1   TIME CONSUMING

2   COSTLY

3   IMPRECISE
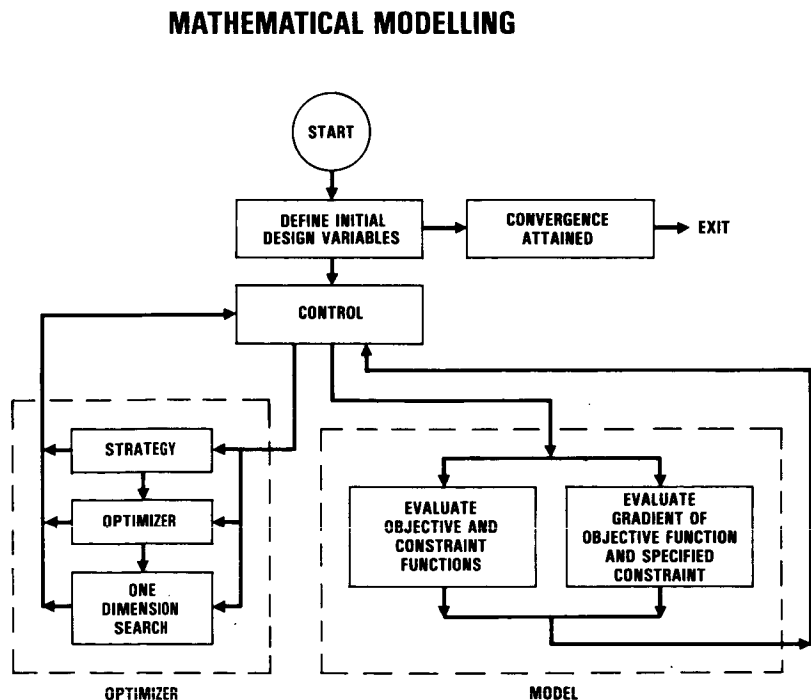
# CONFIGURATION OPTIMIZATION WITH CASH
## (COMPUTER AIDED SIZING OF HELICOPTERS)

In optimizing a helicopter configuration, Hughes Helicopters uses a program called CASH (Computer Aided Sizing of Helicopters), written and updated over the past ten years at HHI, and used as an important part of the preliminary design process of the AH-64. First, Measures of Effectiveness must be supplied to define the mission characteristics of the helicopter to be designed. Then CASH allows the designer to rapidly and automatically develop the basic size of the helicopter (or other rotor-craft) for the given mission. This enables the designer and management to assess the various tradeoffs and to quickly determine the optimum configuration.
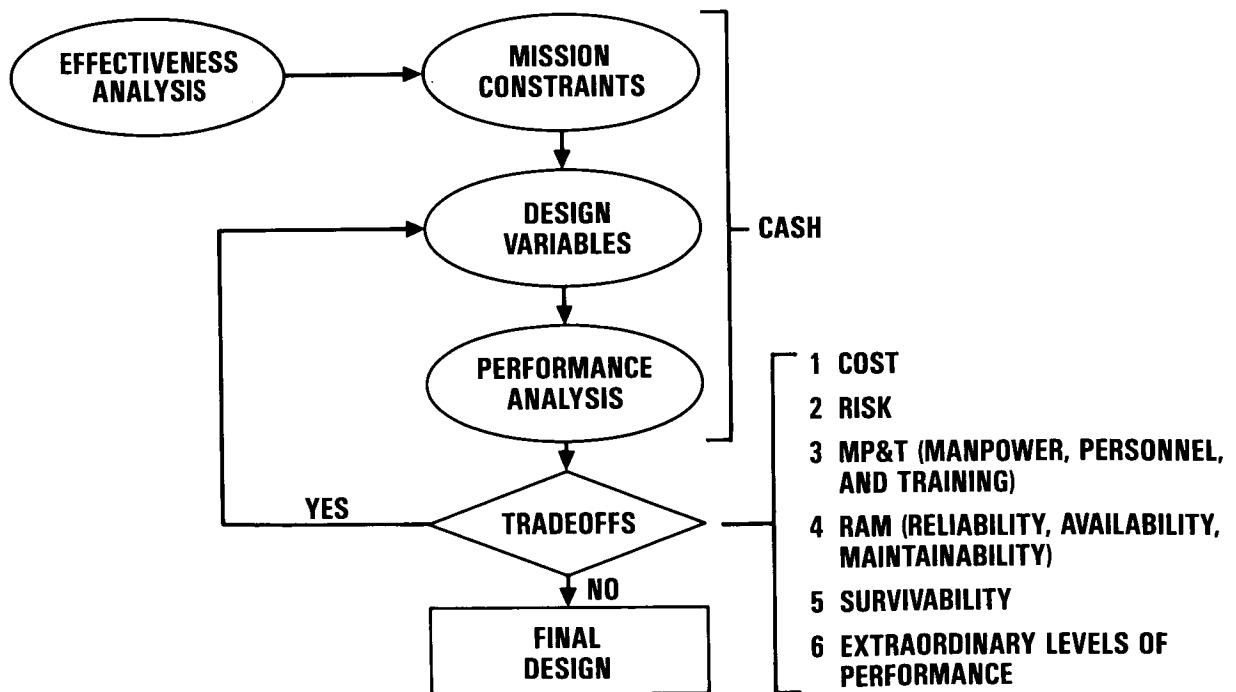
# BASIC DECISION PATH OF THE HHI CASH PROGRAM

The inputs to CASH loosely bound the helicopter design problem by defining required mission characteristics such as payload, range, load factor, maneuver, and gross weight. These items can be defined to any detail or allowed to float and become essentially outputs. Given inputs, the CASH program iterates among the physical design constraints to produce the optimum helicopter (or rotorcraft).

The design constraints include rotor performance, rotor dynamic stability, required rotor blade geometries, and engine characterisitcs. CASH searches for the particular mission segment that dominates the aircraft design. Depending on the mission, this might be hover performance, maneuver, high speed dash capability, or a combination. Once the key design constraints and mission segments are identified, CASH iterates to the optimum geometry to maximize the payload/gross weight fraction.

**INPUT DATA**

| |
|---|
| 1 DESIGN ALTITUDE |
| 2 DESIGN OAT |
| 3 DESIGN GW |
| 4 ROTOR TIP SPEED AND NO. OF BLADES |
| 5 DESIGN VROC |
| 6 MISSION DATA |
| 7 MANEUVERABILITY REQUIREMENTS |

LOAD FACTOR SUBROUTINE

ROTOR SOLIDITY $C_T/\sigma$

HOVERSM SUBROUTINE

M/R RADIUS M/R CHORD IRP REQD FOR VROC

MANUVR SUBROUTINE

ENGINE POWER AND SIZE

ENGINE PERF DATA

SIZE SUBROUTINE

FUSELAGE LENGTH HEIGHT, WIDTH, HORZ AND VERT STAB, T/R OR NOTAR FAN SIZE

PARASITE DRAG SUBROUTINE

EXTERNAL PARASITE DRAG

TOTAL AIRCRAFT PARASITE DRAG

MISSION SUBROUTINE

MISSION FUEL

WEIGHT SUBROUTINE

EMPTY WEIGHT PAYLOAD

COST SUBROUTINE

131

Gross weight and disc loading are CASH parameters that are generally varied to achieve the minimum size helicopter capable of meeting the payload required. With the gross weight and disc loading determined, the rotor diameter is sized, after which the load factor subroutine sizes the solidity to meet the critical maneuverability requirements. In helicopter design, rotor solidity ($\sigma = \frac{bcr}{A_d}$, the blade area divided by the disc area) is a key nondimensional parameter which defines the rotor system performance.

Then, if an existing engine is to be used, the disc loading is adjusted (along with diameter and solidity) to meet the performance requirements. If an arbritrary engine is to be used, it is sized to meet the performance requirements for the input disc loading. The resulting engine characteristics then become the inputs to an engine development program to support the given helicopter design.

GW = CONSTANT
WING LOAD FACTOR = CONSTANT
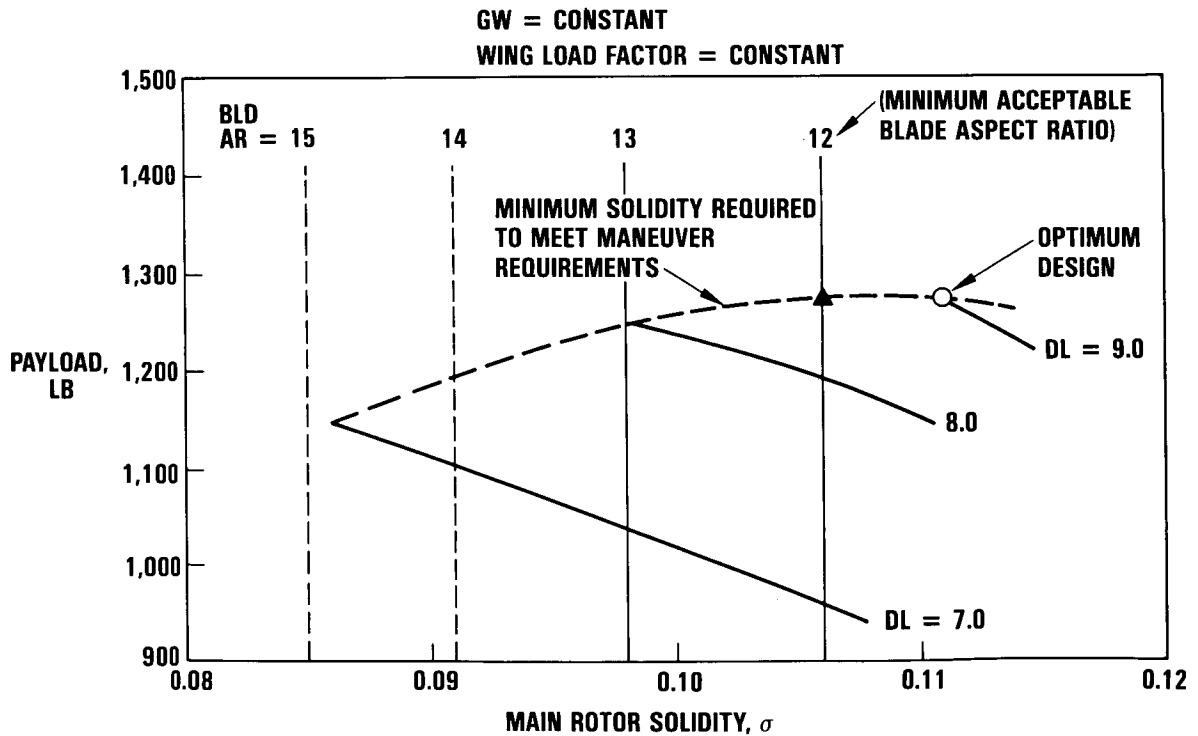
# ROTOR AIRFOIL ENVIRONMENT

Once CASH has defined the configuration, other optimization routines such as OPT, AESOP, and ADS (NASA) can be used to optimize the various components. An example is optimization of rotor blade airfoil profile to achieve a desired performance level. A helicopter rotor airfoil section must satisfy three conflicting goals. First, it must have good low speed lift capability; second, it must have good high Mach number drag characteristics; and third, it must satisfy both the preceding requirements while maintaining a low pitching moment. This requires a balancing of goals and a careful definition of the airfoil contour.
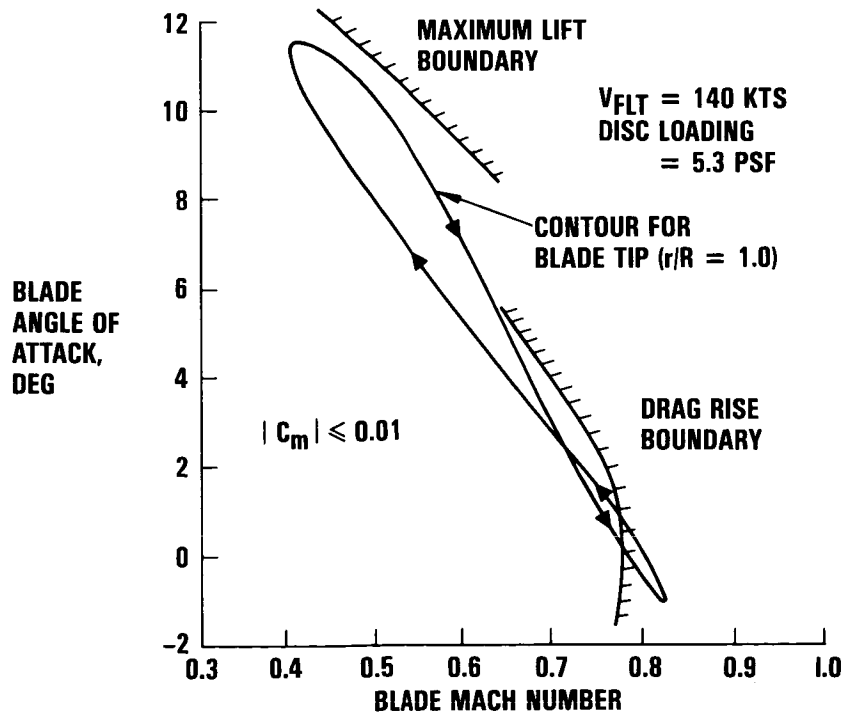
HHI has successfully used an airfoil optimization routine developed at NASA Ames. In using this code, the basic airfoil contour is defined and the code optimally changes that contour to achieve a specified design condition. An example is to maintain lift ($C_l$) and drag ($C_D$) at a certain angle of attack but minimize the section pitching moment ($C_m$). The code develops a series of influence coefficients that represent the impact of geometry changes on the airfoil aerodynamic characteristics. The geometry is then varied locally to meet the requirements.

(COEFFICIENT
OF       CP
PRESSURE)

$C_l$ = CONSTANT (COEFFICIENT OF LIFT)

$C_M$ = PRESCRIBED (COEFFICIENT OF MOMENT)

$C_D$ = MINIMIZED (COEFFICIENT OF DRAG)

BASIC
AIRFOIL
CONTOUR

INFLUENCE
COEFFICIENTS
DETERMINE
SHAPE
IMPACT

134
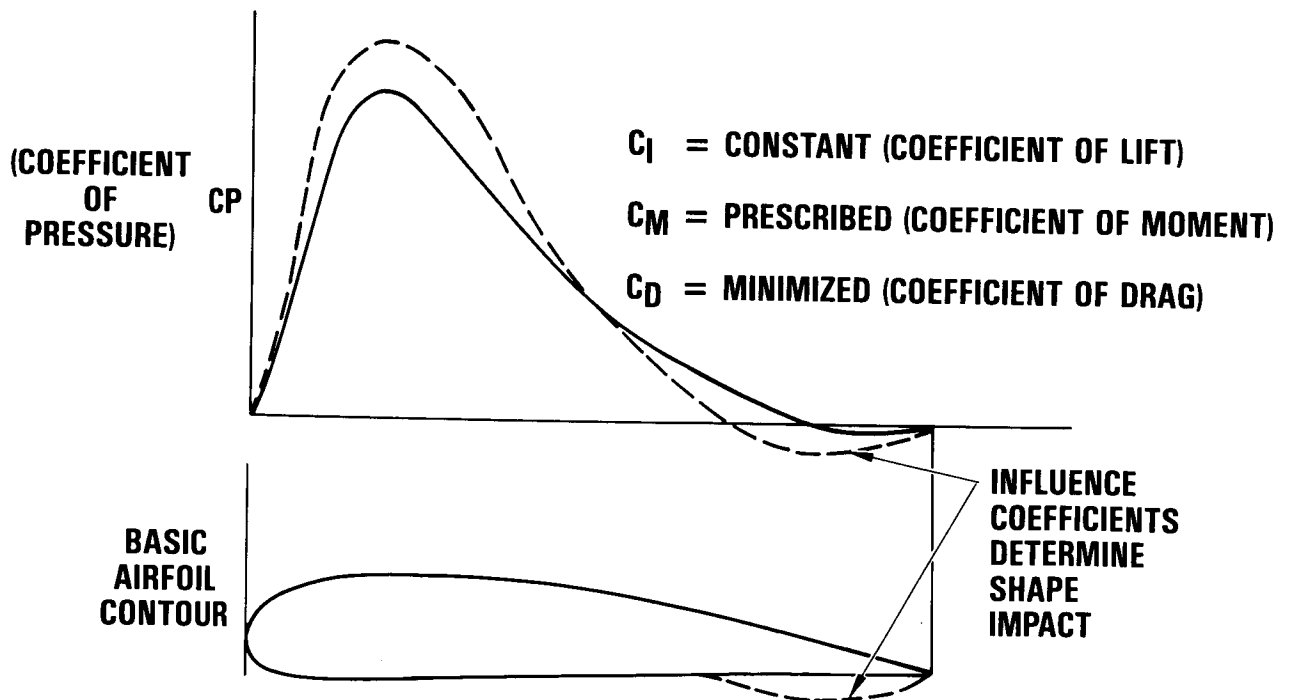
## RESULTS OF AIRFOIL TESTING

After the airfoil optimization was conducted, airfoils were fabricated and tested to verify the results. Tests were conducted at the Lockheed Transonic two-dimensional wind tunnel in August 1983. The test results indicated a significant improvement over the current state-of-the-art boundary. The boundary was defined by plotting the low speed lift coefficient and drag divergence Mach number of all available two-dimensional data after normalization to remove different tunnel effects. (For the purposes of this comparison, the low speed maximum lift coefficient is defined at a Mach number of 0.4, and the drag divergence Mach number is that at which the drag at zero lift increases sharply.)

The results of this optimization application clearly show the potential benefits of optimization techniques.



135
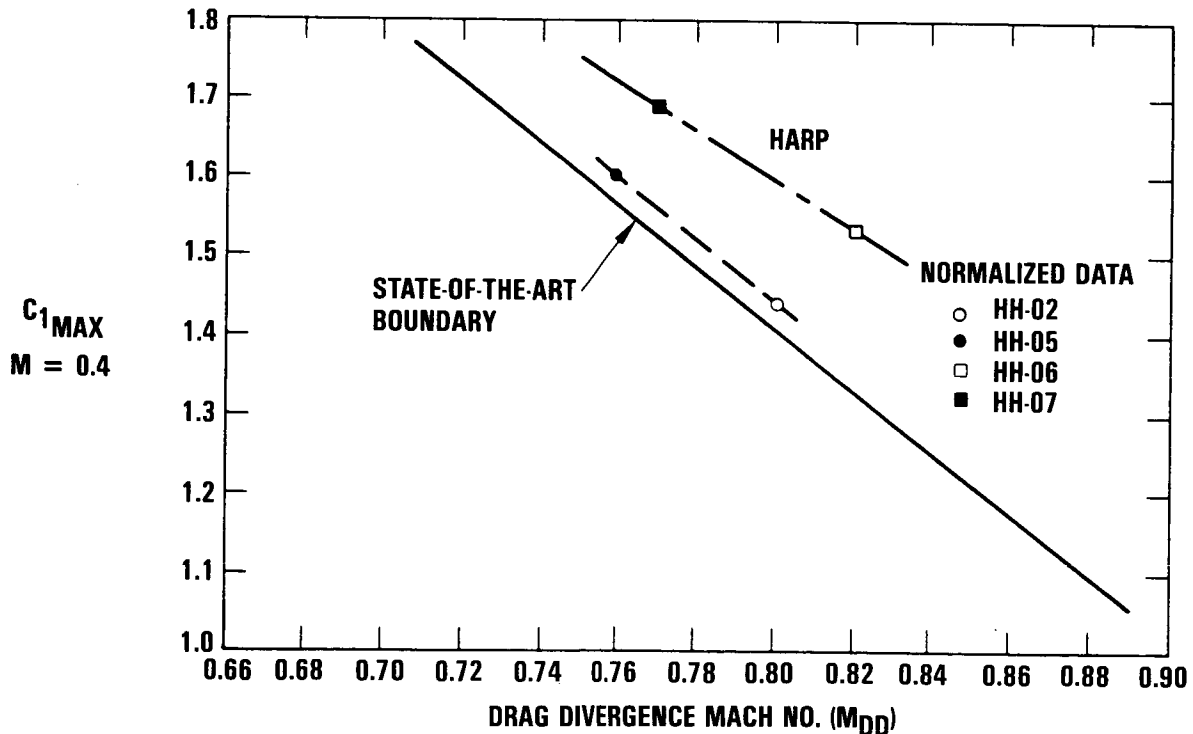
# ROTOR OPTIMIZATION

In another current application, HHI used optimization techniques to define the optimum blade planform and twist for maximum forward flight efficiency. The optimized parameter was the rotor lift-to-drag ratio. A suitable forward flight performance model was incorporated into the ADS optimization procedure, and the baseline rotor was the HH 500D (five rectangular planform blades with a linear 8 degrees of twist). The optimized rotor shows a nonlinear twist increased to 12 degrees and a nonlinear blade planform taper 5:1 over the outer 25 percent of the rotor. This blade is predicted to have a 20 percent increase in L/D when compared to the baseline blade. Independent of the optimization development, HHI designed an advanced rotor blade using more conventional techniques. That optimal design matches very closely this optimized design, which was generated in a fraction of the design time. This indicates the design schedule impact that optimization techniques have. The experimental verification of these predictions will take place in late 1984 when a rotor designed using this information will be flight tested.
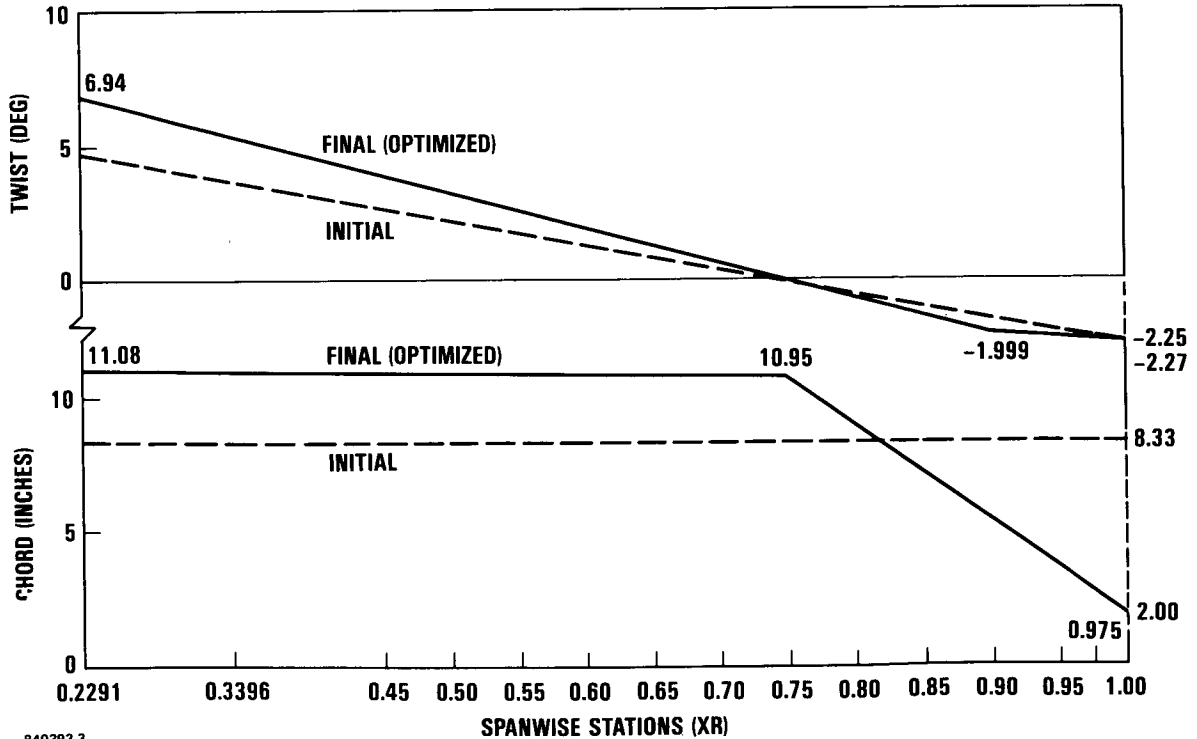
SUMMARY

Based on the applications to date, the prospects for optimizing the design of a helicopter to a given mission faster, more efficiently, less expensively, and with greater precision grow ever brighter. Perhaps the entire helicopter - configuration and components together - may be optimized in one process, with significant synergistic benefits, sometime in the future.

Hughes Helicopters, Inc. recognizes these prospects and has taken tested and proven steps toward them in its CASH program, and in its development and use of various component optimization programs. The plans for the future include the application of these optimization techniques to the structural optimization of rotor blades with the anticipated benefits of improved performance and reduced vibration/load. Less vibration will reduce crew fatigue, increase structural life, and improve weapons systems accuracy.
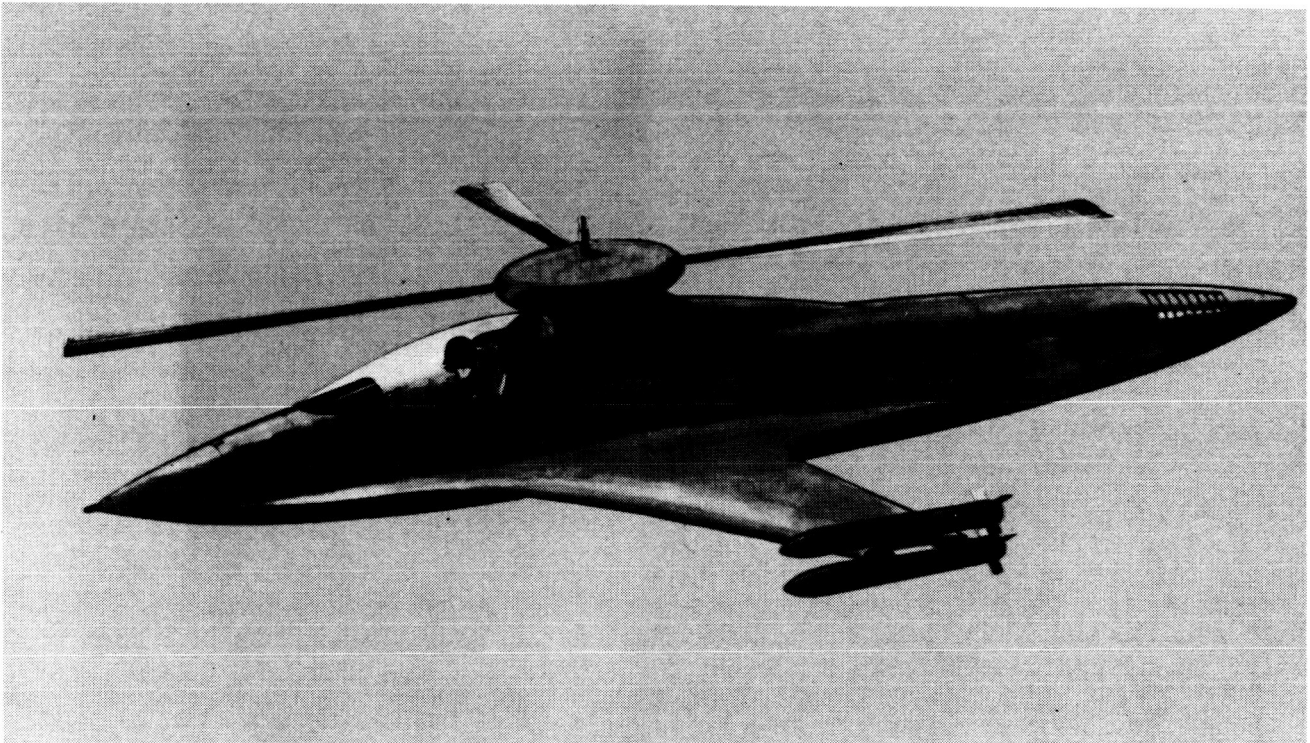
HHI Concept of U.S. Army LHX

137

# ROLE OF OPTIMIZATION IN INTERDISCIPLINARY ANALYSES
## OF NAVAL STRUCTURES

S.K. Dhir and M.M. Hurwitz

David W. Taylor Naval Ship Research and Development Center
Bethesda, Maryland   20084

# ABSTRACT

This paper discusses the need for numerical design optimization of naval structures and illustrates the complexity of problems that arise due to the significant roles played by three major disciplines, i.e., structural mechanics, acoustics, and hydrodynamics. A major computer software effort that has recently begun at the David W. Taylor Naval Ship R&D Center to accommodate large multidisciplinary analyses is also described. In addition to primarily facilitating, via the use of data bases, interdisciplinary analyses for predicting the response of the Navy's ships and related structures, this software effort is expected to provide the analyst with a convenient numerical workbench for performing large numbers of analyses that may be necessary for optimizing the design performance. Finally, an example is included that investigates several aspects of optimizing a typical naval structure from the viewpoints of strength, hydrodynamic form, and acoustic characteristics.

# INTRODUCTION

The past two decades have witnessed an unprecedented growth and activity in the field of computer-based numerical solutions to problems of physics. Amongst these, perhaps the most promising and certainly the most popular solution procedure developed and utilized by scientists and engineers has been the method of finite elements. This method, although originally developed for analysis of structural engineering problems, has found applications in several other disciplines of computational physics. The usual objective when analyzing a typical problem in computational physics is to evaluate the performance of a given system or a design, e.g., a specific structural configuration, when subjected to certain service conditions. With the aid of today's large computer programs such as NASTRAN,[1] prediction of stresses, displacements, and frequencies for a large integral structure such as a destroyer with all its discontinuities has become more or less a routine matter. Even though having such computational tools available in the hands of a designer is a substantial step forward, these are often not the most efficient ways of converging to a good design. It appears that some kind of design optimization procedure would be the key to developing an effective design tool. The considerable activity in this field in the past decade is very gratifying and is in fact a clear indication that effective design optimization procedures are no longer relegated to the distant

future. The general message that emerges from the current literature on structural design optimization is that the basic technology now exists to efficiently design relatively small structures defined by several hundred design variables under multiple loading conditions and subject to sizing, stress, displacement, buckling, frequency, and flutter constraints.[2,3] This may still be a far cry from designing the structure of a complete ship, but nevertheless it is a definite and encouraging beginning. Another message that comes across from the literature is the absence of an effective technique for shape optimization of large structures, which is of course a very important issue.

A large number of discipines play an important role in ship design, viz. structural mechanics, hydrodynamics, acoustics, and electromagnetics. Thus an efficient ship would be simultaneously lightest and strongest, fastest, quietest, and invisible to electromagnetic sensors. Aside from the optimization problem, which would involve multiple objective functions, even some straight-forward analysis problems become nontrivial when multiple disciplines have to be considered. Often it is necessary to resort to numerical iteration procedures when an efficient coupled procedure is not available. Despite all those complexities, we have made a very modest beginning toward developing computer-based design tools with limited optimization capability. One of these design tools, ASSET (Advanced Surface Ship Evaluation Tool)[4] is an interactive computer program for use in the exploratory and feasibility design phases of monohull surface ships such as frigates, cruisers, and destroyers. ASSET addresses virtually all major technological domains of design that are relevant to such ships, including geometric definition of hull and superstructure, resistance, propulsion, machinery, weight, hydrostatics, seakeeping, cost, and manning. The program features design synthesis capability, database management of design data, and extensive input/output options including interactive graphics. The other design tool, SUBSET, is a similar tool which is being developed for submerged structures. Both ASSET and SUBSET are interactive computer tools which do not, however, address the optimization of detailed ship design. With the rapid advances in individual analysis procedures, computing hardware, and sophisticated software technology, DTNSRDC is becoming greatly interested in developing and/or acquiring an optimization capability for detailed design.

The following sections will discuss the presently ongoing work at DTNSRDC in the area of optimization of detailed design as well as in analysis procedures.


RECENT ACTIVITY IN OPTIMIZATION


The recent level of activity in detailed optimization at DTNSRDC has been low. In the area of preliminary and conceptual design of ship hulls, the ASSET program previously mentioned is used. Currently, however, the majority of the optimization effort at DTNSRDC is being performed with the COPES/CONMIN[5] computer program in the areas of hydrodynamics and structures. For example, one application involves the minimum surface area design of ship appendages subject to maneuvering constraints. The authors have been using COPES/CONMIN in propeller-related design work, the experiences of which will now be described in some detail.

The purpose of our first experience with COPES/CONMIN was to demonstrate its capability for propeller design. Specifically, our test problem was to minimize the strain energy of a finite element model of a composite propeller subjected to a pressure load. The five design variables were material properties, the purpose of which was to design the effective properties of the composite material. The four constraints involved relationships among the design variables as well as a constraint on the deflection of the propeller tip. The finite element analysis of each new COPES/CONMIN design was to be performed with COSMIC/NASTRAN, hereafter

known as NASTRAN. This demonstration was intended to be completed within two weeks.

The problems with our proposed test began early. COPES/CONMIN works most conveniently when the routines needed to analyze a new design can be made part of the COPES/CONMIN program. When that is not possible, as is the case with NASTRAN, two options are available. (1) The first option uses approximate optimization, in which trial designs, with their respective objective and constraint values, must be supplied, after which COPES/CONMIN performs curve-fitting to calculate a new design. Each new design then becomes an additional trial design at the next iteration. Also, since NASTRAN cannot be loaded into the computer's central memory simultaneously with COPES/CONMIN, pre- and post-processors must be developed to transfer information. For example, once a new design is created, a NASTRAN pre-processor must be written to access the COPES/CONMIN design (which is written to a scratch file in our modified version of COPES/CONMIN) and develop the new NASTRAN finite element data. After NASTRAN is run with the new design, a post-processor accesses needed results, computes values of objective and constraints, and modifies the COPES/CONMIN data, after which COPES/CONMIN creates another new design. This looping process through COPES/CONMIN, pre-processor, NASTRAN, and post-processor is set up automatically within the computer's job control language and continues until the pre-processor has determined that convergence has taken place or until a pre-defined number of loops have been executed. (2) The second option uses the standard optimization techniques of CONMIN and sets up the data in such a way that CONMIN can be restarted after NASTRAN has run. The problem with (2) is that gradients of the objective function, design variables, and violated constraints are required for each design. These gradients are computed using finite difference techniques and multiple executions of the analysis routine (NASTRAN). Because such differencing can be very expensive ($6.00 per analysis for our case), we chose (1).

In order to gain confidence in using COPES/CONMIN, we first ran a sample problem from the program's users manual. The problem was to minimize the volume of a cantilevered beam subject to an end load. The design variables were the width B and height H of the beam cross section, with various constraints on stresses and deflection. The correct result is B = 1.818, H = 18.179. The users manual used approximate optimization with the following four trial designs:

|   | TRIAL | | | |
|---|---|---|---|---|
|   | 1 | 2 | 3 | 4 |
| B | 1. | 2. | 4. | 3. |
| H | 15. | 20. | 10. | 12. |

COPES/CONMIN gave B = 1.818, H = 18.168 after eight iterations. We ran the same problem with the following ten trial designs:

|   | TRIAL | | | | | | | | | |
|---|---|---|---|---|---|---|---|---|---|---|
|   | 1 | 2 | 3 | 4 | 5 | 6 | 7 | 8 | 9 | 10 |
| B | 2. | 1. | 3. | 4. | 5. | 15. | 5. | 4. | 3. | 2. |
| H | 5. | 3. | 20. | 11. | 8. | 1. | 6. | 9. | 13. | 7.5 |

After 24 iterations, B = 3.161, H = 18.713. Changing the tenth H value from 7.5 to 18. resulted in B = 1.853, H = 18.219 after 6 iterations, and B = 1.824, H = 18.187 after 24 iterations. At least two conclusions can be drawn from this test. (1) It

helps to know the answer before beginning the problem. (2) Too much scattered information may not be useful for approximate optimization, although the program developer has suggested using a random number generator to create the trial designs.

With this information in hand, we proceeded with our composite propeller. With our two-week time limit fast approaching, we used ten trial designs and 50 iterations, which took 12 minutes of CPU time on a CDC CYBER 170/750 computer. While convergence was slow, there was steady improvement in the objective function which gave us some encouragement for future work.

Approximately a year after this demonstration, we were asked to assist DTNSRDC's Ship Performance Department in the optimization of a propeller/shaft system. Since the various design aspects of the propeller, such as weight, thrust, torque, etc., affected the shaft, but the design aspects of the shaft, such as cross-sectional area, bearing locations, etc., did not affect the propeller, we decided to perform two separate optimizations within the same computer run.

The first optimization was for the propeller. The hydrodynamic analysis routine for the propeller was small enough to include as part of COPES/CONMIN and therefore standard optimization was used. Various objective functions used were weight, efficiency, tip speed, and weighted normalized sums of these functions. Design variables included propeller diameter, angular velocity, and others. Constraints included hub diameter, thrust, weight, efficiency, tip speed (these latter three when not used as objective functions), and others. COPES/CONMIN gave good, reasonable results in all cases. The number of times that the hydrodynamic analysis routine was executed varied between 50 and 150, depending on the case run. However, since the analysis routine used less than 0.5 CPU seconds on a CDC CYBER 176 computer, costs were small.

The second part of the task was to minimize the shaft weight using various outputs of the propeller optimization, including propeller weight, torque, and steady and unsteady thrusts. The design variables were the inner and outer diameters of the shaft. The constraints included various combinations of static stresses (one NASTRAN run), factor of safety, natural frequencies corresponding to axial and vertical modes (a second NASTRAN run), and acoustic levels computed by another program which uses NASTRAN forced response output (a third NASTRAN run). Because of the NASTRAN analyses required, approximate optimization was used with five trial designs. The computer job control language loop for this second task began with COPES/CONMIN and continued through three separate NASTRAN analyses and an acoustic analysis interspersed with five pre- and post-processors. Ten iterations were performed (@$25.00 per iteration) with good volume reductions and an apparent trend towards a convergent solution. We then decided to remove from these 15 designs (the initial 5 trial designs plus the 10 computed ones) the first 5 trials and continue the iterations. The subsequent designs were significantly lower in volume than any of the first 10 computed designs and still remained feasible.

While our results for the propeller/shaft system were very good, a number of questions remain. What are the true trade-offs between standard optimization and approximate optimization in COPES/CONMIN? Were we saving money initially with approximate optimization by avoiding the finite differencing required to compute gradients, but paying later by not arriving at a better design more quickly? Is the apparent local minimum initially computed more likely to occur with approximate optimization than with standard optimization? Will the cost for such a multi-disciplinary design process become prohibitive for a relatively small number of design variables? How does one convince a sponsor who is not versed in numerical optimization that a significantly better design is worth the funds expended even if it is not the theoretically optimum design?

Finally, we need to mention the development of the pre- and post-processors. While the development of these processors is quite straightforward given a fixed

geometry with a known set of design variables, that is not usually the situation in the preliminary ship design process. It takes some time (and iterations) to decide on the design variables (inner and outer diameters of the shaft, bearing locations, bearing stiffness, a combinaton of all these), design parameters (one-section or two-section shaft, shaft length, sand in the shaft or not), and applicable engineering theory (which acoustic analysis, added mass due to fluid effects, etc.). Each time a new approach was considered, the pre- and post-processors were changed (often considerably) to reflect new data and analysis programs. Such code changes can hopefully be minimized with an integrated, database-managed software system. Such systems are currently under development at a number of agencies. In particular, Wright-Patterson Air Force Base is developing an integrated software system for optimization, while DTNSRDC is developing IDEAS (Interdisciplinary Engineering Analysis for Ships), which will be discussed in the next section of the paper.

## INTERDISCIPLINARY ENGINEERING ANALYSIS FOR SHIPS

The IDEAS (Interdisciplinary Engineering Analysis for Ships) system being developed at DTNSRDC is intended to be an integrated database-managed software system which can significantly smooth the transitions between analyses in different disciplines. For example, suppose that a propeller is to be analyzed for its hydrodynamic, structural, and acoustic characteristics. The hydrodynamic analysis, using finite difference techniques, computes and saves loads. The structural analysis, using finite element techniques, can be performed only after accessing the hydrodynamic loads (the storage scheme for which will differ from program to program), interpolating the loads from the finite difference model to the finite element model, and formatting the loads into those required for the structural analysis program. Similar considerations are required to access the structural deformations for input to an acoustic analysis. In addition to these transformations of data, the development of the two numerical models, finite difference and finite element, usually emanates from drawings shared by the hydrodynamicists and structural analysts, each group separately digitizing the drawings. With an integrated software system such as IDEAS, the data transitions between programs in the system should be very easy. All analysts who need to numerically model a structure will be able to access a common geometrical/mathematical description of the structure without having to locate and digitize drawings. Such a system will allow easy access to the performance characteristics of previous designs, as is often the need in ship and propeller design.

We are planning to use as the basic architecture of IDEAS the Integrated Analysis Capability (IAC)[6] recently developed by NASA's Goddard Space Flight Center. The architecture of the IAC was designed to support an integrated, database-managed system of engineering software and data. It was also designed to allow easy "plug-in" of new analysis programs. Therefore, it is our intention to use the IAC to build an integrated system of DTNSRDC engineering software, including analysis programs such as NASTRAN, and ABAQUS, as well as automatic numerical model generators and other pre- and post-processors usually associated with such analyses. The initial effort for IDEAS was begun in FY84.

## OPTIMIZATION OF ANALYSIS PROCEDURES

In addition to the design optimization, DTNSRDC has also been involved in other related optimization efforts which have proven to be very useful.

Since the finite element method is essentially an approximate numerical technique for solving practical differential equations of physics, it has some inherent

error associated with it. Knowledge and control of this error are obviously critical to the analysts. A few years ago we began a new effort to evaluate FEARS,[7] a finite element computer program developed by Professor Ivo Babuska at the University of Maryland and based on adaptive meshing and a posteriori error estimation concepts. After each successive iteration this program computes the strain energies in various elements and, based on certain error criteria, makes a decision with regard to further subdivision of individual elements. The computation continues until a certain specified error bound is reached. After initial installation and debugging, the FEARS computer program has been enhanced in several ways. A post-processor has since been developed which computes the stresses more accurately. This post-processor is based on fitting the data to some appropriate analytical expressions that are then used to obtain the desired stresses which are proportional to derivatives of the original data.[8] The program was also modified so that it can now solve some limited plate bending problems.[9] It is now planned to develop a similar error capability without adaptive meshing which would initially be used to compute the error in any given NASTRAN run.

Another effort of DTNSRDC's interest has been to maintain a current version of a post-processor, BANDIT,[10] which is used to resequence the finite element models for minimizing the bandwidth of their stiffness matrices. This program is kept up to date by continuously evaluating and using the newer resequencing algorithms which from time to time keep appearing in the literature. We also maintain a set of test problems which are used to evaluate the effectiveness of these resequencing algorithms. In the near future we are planning to develop a similar resequencing capability for ABAQUS.

At DTNSRDC, we recently developed a NASTRAN-based finite element capability to predict the magnetostatic fields associated with ships and submerged structures. An interactive tool was then developed that can be used to compute the distribution of degaussing coil currents that would minimize the magnetostatic anomaly due to the ship in the Earth's magnetic field. This procedure was based on a simple least squares fit. There are now plans to enhance this capability to include a constrained optimization on the coil currents, taking into account cost, weight, power, capacity, and so forth.


## SUMMARY AND CONCLUSIONS

From the foregoing description of various types of activities in the general area of optimization, it is quite evident that DTNSRDC has a positive interest and an urgent need for an effective computer-based capability that would contribute toward improvements in ship design. The problem of optimizing a complete ship from the viewpoints of all the relevant disciplines is clearly a monumental task; nevertheless, a definite beginning has been made in the shape of capabilities for optimizing the exploratory and feasibility designs of ships. Progress is also being made in evaluating and developing and/or modifying existing optimization programs for detailed designs.

# REFERENCES

1.  "The NASTRAN Users' Manual (Level 17.5)", NASA SP-222(05), Dec. 1978.

2.  Rozvany, G.I.N. and Z. Mroz, "Analytical Methods in Structural Optimization." Applied Mechanics Reviews, Vol. 30, No. 11, Nov. 1977, pp. 1461-1470.

3.  Vanderplaats, G. N., "Structural Optimization - Past, Present, and Future," AIAA 1981 Annual Meeting and Technical Display, May 12-14, 1981, AIAA Paper 81-0897.

4.  Beyer, C.F., M.D. Devine, and S.K. Tsao, "ASSET - Advanced Surface Ship Evaluation Tool," Boeing Computer Services Company Report, BCS 40372, May 1982.

5.  Madsen, L.E., and G. N. Vanderplaats, "COPES - A FORTRAN Control Program for Engineering Synthesis," Naval Postgraduate School, Monterey, CA, Report NPS69-81-003, March 1982.

6.  Young, J.P., et al., "Integrated Analysis Capability (IAC) Activity," Second Chautauqua on Productivity in Engineering and Design - The CAD Revolution, Schaeffer Analysis, Mont Vernon, NH, 1982.

7.  Gignac, D.A. and I. Babuska, "NASTRAN and FEARS Analyses of Two Problems of Plane Elasticity," David W. Taylor Naval Ship R&D Center Report DTNSRDC/CMLD-82/17, July 1982.

8.  Brooks, E.W. and I. Babuska, "A Post-Processing Approach to Precise Data Extraction from a NASTRAN Solution," Twelfth NASTRAN Users' Colloquium, Orlando, Fla., 10-11 May 1984.

9.  Gignac, D.A. and I. Babuska, "Feasibility of Applying the FEARS Program to the Plate Bending Problem," David W. Taylor Naval Ship R&D Center Report, DTNSRDC/CMLD-83/11, May 1983.

10. Everstine, G.C., "The BANDIT Computer Program for the Reduction of Matrix Bandwidth for NASTRAN," David W. Taylor Naval Ship R&D Center Report 3827, March 1972.

# APPLICATION OF OPTIMIZATION TECHNIQUES
## TO VEHICLE DESIGN - A REVIEW

B. Prasad and C. L. Magee

Ford Motor Company
Dearborn, Michigan

ABSTRACT


This paper reviews the work that has been done in the last decade or so in the application of optimization techniques to vehicle design. Much of the work reviewed here deals with the design of body or suspension (chassis) components for reduced weight. Other papers dealing with system optimization problems for improved functional performance, such as ride or handling, are also reviewed. The paper is organized according to the types of application rather than constraints imposed or the objective function chosen for an optimization process.

In reviewing the work on the use of optimization techniques, one notes the transition from the rare mention of the methods in the 70's to an increased effort in the early 80's. Efficient and convenient optimization and analysis tools still need to be developed so that they can be regularly applied in the early design stage of the vehicle development cycle to be most effective. Based on the reported applications, the paper attempts to assess the potential for automotive application of optimization techniques. The major issue involved remains the creation of quantifiable means of analysis to be used in vehicle design. The conventional process of vehicle design still contains much experience-based input because it has not yet proven possible to quantify all important constraints. This restraint on the part of the analysis will continue to be a major limiting factor in application of optimization to vehicle design.

1. INTRODUCTION

In the past several years, significant mass reductions in the automotive fleet have resulted from downsizing, better design of structural components, improved configuration, and use of alternate materials. The role of optimization techniques in aiding in one or more of the above tasks and during proper estimation or selection of optimum parameters in vehicles can be seen to be slowly increasing. This is reflected in the number of papers now being published or submitted for publication in the SAE or other automotive journals.

The use of the computer as a possible design tool was well understood as early as 1965 by Dunseth (ref. 1) as a means of reducing problem-solving time. At that time, the use of optimization techniques was at its very infancy. Only a very few application papers employing this technique existed. The first few such potential applications in the automotive field were in the design of suspension and vibration isolaters. Bender (refs. 2 and 3) was one of the first who proposed the use of the techniques for vehicle suspension design, and Wolkovitch (ref. 4) did the same for optimization of the mechanical system response under shock and vibration environments. However, it took several years for the optimization technique to make any significant debut in the structural areas relating to automotive design (refs. 5 and 6). During the early 1970's applications began to increase as the techniques were applied to a number of automotive structural components. Some of the suspension components were again the first to be studied due to previous familiarity with them (refs. 7 and 8). Significant growth in the use of the techniques for structures has only been found in the late 1970's and the early 1980's when quite a few general purpose finite element analysis and design programs were made publicly available. References 9 to 23 outline some of the design-oriented computer programs currently in use for structural design optimization.

Although the topic of optimization is still new to many workers in the auto-
motive field, there are also expert users among the vehicle analysts and designers.
In the last few years, a number of good general review papers have surfaced but none
dealing specifically with automotive design. Past reviews on optimization have
concentrated on such aspects as optimization techniques (refs. 24 to 28), con-
straints (refs. 25 to 32), elements used such as plates or beams (ref. 31) or design
approaches (refs. 4, 26, 27, and 32). Most of the applications referred to either
were standard benchmark problems (such as transmission towers) or were character-
istic mainly of aerospace structures.

## 2. REVIEW OF CURRENT AUTOMOTIVE APPLICATIONS

In this section, various vehicle applications of optimization technology that
are reported in the literature are reviewed. The topics are covered in five
separate subheadings, namely, "Primary Structures," "Chassis and Suspension,"
"Engine and Powertrain," "Body Panels and Mechanisms," and "Vehicle Systems." The
last topic covers those areas which deal with the vehicle as a whole or in which
more than one vehicle subsystem is involved. The primary structures, which include
most of the thin walled beams, the body joints, and some panels and bars, form the
"skeleton" of the vehicle body structure and function as the main load-carrying
structures to satisfy the "global load" requirements. The structural components
included in this subset are the upper and lower front rails, all pillars, rockers,
the roof rails and header, the floor tunnel, etc. (see fig. 1). The other sub-
systems such as "Chassis and Suspensions" or "Body Panels" and the corresponding
reinforcements do not contribute significantly to meeting global load require-
ments. The design criteria for the body panels are generally governed by local or
regional structural requirements such as strength, oil canning, denting, etc.

Fig. 2 shows a breakup for mass distribution of a typical vehicle curb weight
(VCW = 2020 lb) in terms of the chosen subsystems. The total mass of the primary
structures is about 400 lb (20% of VCW). The miscellaneous items such as fuel,
battery, seats, etc. make up the total curb weight.

## 2.1 Primary Structures

The primary structure or skeleton frame is that portion of the body which is
composed of beam-like members carrying the major loads. Most of the work on PS
deals with the car body as a whole and has attempted to retain its significant
(basic) characteristics (refs. 5, 6, and 33 to 35). Some have oversimplified the
design problem by not considering the component's interactions or not including all
the important design criteria such as frequencies, stresses, displacements, and
buckling or side constraints which result from packaging or manufacturing. A few
have estimated the total mass reduction potential for alternate materials based on
the "equal stiffness" substitution rule (refs. 36 and 37). The latter approach
ignores the fact that critical design criteria may change as new materials are
introduced and that the interaction of components may alter the expected mass
reduction.

Others who have attempted a more advanced approach have either considered multiple design criteria including stiffness, strength and frequency or have included several important service loads (refs. 5, 33, and 35). The scope of model fidelity and design variables in these studies was, however, limited. In particular, simplified beam models (see fig. 3) have been used which only approximately describe the complex real vehicle structures. In addition, in all the studies reported in references 34 and 38 only the beam gauges were varied; the heights, widths and section shapes of the beams were fixed. The sectional dimensions were relaxed in reference 5, but the locations of the joints and their stiffnesses were fixed. In reference 35, a more detailed beam and plate model (see fig. 3) was used for better stiffness and mass distributions, but only the gauges of beams and plate elements were employed as design variables. The local design constraints for the panels (plates) such as buckling, denting, etc. were ignored. This resulted in a design in which most of the panels were driven to minimum gage; the gauges of the beams remained the potent sizing variables.

## 2.2 Body Panels and Mechanisms

Double-layered panels are used in many car components, such as the deck lid, hood, floor pan, fender, and quarter panel. Finite element simulation for their analysis is not difficult since most of the outer panels can be idealized by an area element (a plate or shell element), and the inner panels can be idealized by line elements. However, the use of optimization for panel design is still very rare (refs. 39 to 48). Initial optimization attempts either did not consider all the important design constraints or simplified the problems. For example, reference 39 only considered the weight reduction potential by material substitution or design changes based on "equal" structural characteristics. Reference 40 used CONMIN for optimization but limited the constraints to overall bending and torsion and design variables to three parameters ($t_o$, $t_i$, and b). (See fig. 4(a).)

Another study (ref. 41) of alternate materials considered eight design variables (see fig. 4) and three stiffness criteria (including edge bending) (see fig. 5). A more complete set of design variables (13 to 16) based on inner reinforcements independence was considered in reference 44. (See fig. 6.) A more practical set of constraints (dent resistance, stiffness, buckling and springback) were considered in references 43 and 46; however, the equations used were mostly empirical and were difficult to extrapolate. Another alternate material study similar to that of reference 39 was reported in reference 47 for metal-to-composite substitution. Besides the dimensions of the inner and outer panels, the locations of the inner panels were chosen as design variables (ref. 48). (See fig. 7.) In reference 45 the shape parameters of sheet metal structures were considered for design against crush.

## 2.3 Chassis and Suspension

The design of a vehicle's suspension is generally a compromise among competing design requirements aimed at satisfying comfortable passenger ride and good vehicle road handling performance. Numerous optimization studies have been conducted on suspension design (refs. 3, 7, and 49 to 64), shock and vibration isolation (refs. 4 and 65 to 73), impact absorption (refs. 72 and 74), and wheels (refs. 75 and 76). In most studies, the main concern was that of selecting quantifiable measures of vibration which directly affect ride or handling performance. Examples of these measures of vibration include rms values of displacement, acceleration, rate of

change of acceleration (jerk), and absorbed power. Other measures, such as movement within the rattle space (without contacting bump stops (ref. 62)), low dynamic load between tire and road surface for good directional control and limitations on the allowable rolling angle (ref. 53), and tire life, have also been of some concern. In the time domain analysis (or experiment) the rms values, for example, can be obtained by

$$
\text{rms (a)} = \left[ \int_o^t a^p (t) \, dt \right]^{1/p}
$$

where "a" stands for any of the vibration parameters: displacement, velocity, acceleration or jerk. Several such criteria have been used (refs. 60 to 63, 72, 73, and 76) but the simulation models were often simplified for estimating "a" or like parameters.

Most investigators have considered the suspension design problem as an idealized lumped spring-mass and damper system (see figs. 8 and 9 for two such idealizations) and used multi-criterion optimization, nonlinear programming formulation or an optimal control theory, often with feedback capabilities. Bender (refs. 2 and 3) and several others used a weighted sum of the quantities describing ride comfort and subsequently minimized this single quantity. A few employed an approach where these performance criteria were treated as independent functionals of a multi-objective system (refs. 49 to 51). Optimal control theory was used in the synthesis of an active suspension by Bender and others (refs. 3, 8, 53, 55 to 57, 60, and 64) and for vehicle suspension models by Haug and others (refs. 61 and 71). Two recent publications are discussed here. Thompson (ref. 63) used a frequency locus method to develop formulas for the optimum spring and damper rates in conventional car suspensions. The analysis is based on a linear four-degree-of-freedom model shown in fig. 8. The front and rear spring and damper rates (with a constraint on overall static stiffness) are obtained using the conjugate direction method to minimize the weighted sum of the mean-squared tire forces on random roads.

Haug (ref. 61) used an adjoint variable method to minimize the driver-absorbed power on a nominal road, subject to bounds on absorbed power on a rough road, driver peak acceleration over a discrete obstacle, suspension jounce and rebound travel, wheel hop, and limits on design parameters. The analysis is based on a linear five-degree-of-freedom model shown in fig. 9. Spring stiffness and damping coefficients were chosen as design variables and optimal control theory was employed for numerical optimization. There are also some structural optimization studies on chassis components, as opposed to the suspension system optimization discussed above (refs. 75 and 76). Automobile wheels (refs. 75 and 76) and a rear suspension torque arms (ref. 77) are some of the new applications wherein the importance of shape optimization is explored for potential weight savings.

## 2.4  Engine and Powertrain

On the engine and powertrain side, the use of optimization started somewhat late (1975). Engine control optimization, fuel economy and emissions received the initial attention (refs. 78 to 84). Applications now exist in quite a few areas of engine control and components design. A number of papers have considered determining the necessary engine mount parameters (mount locations, rates and mount rate ratios) required to achieve a number of performance objectives (refs. 85 to 87). Reference 85 considered the ride improvement and reference 86 considered the limits

on vertical, pitch and fore/aft mode frequencies plus the decoupling of the modes of vibration as their performance objectives for engine mounts. Other engine applications include design for low noise (ref. 88), unbalances (ref. 89) and engine controls (ref. 90). The use of finite element analysis in component optimization is considered in reference 91 for gasoline engines, in reference 92 for diesel engines and in reference 93 for IC engine pistons. In reference 94 a continuously variable transmission was designed to control emission for a given fuel, whereas in reference 95 the emission efficiency and power of five automotive fuels were compared in one engine with standard transmission. Engine applications for fuel economy performance and emission optimization can be envisioned as useful but none have been reported in the literature.

## 2.5  Vehicle Systems

In this section we consider cases where the entire car is simulated using some sort of mathematical model for use in optimization. In reference 96 a computer simulation program, PROMETHEUS, developed by the National Highway Traffic Safety Administration (NHTSA), was used. A pedestrian hazard index, which is estimated as a function of forces and accelerations to which the pedestrian is exposed (called EPIC), is minimized. The design variables were selected from the hood/grille/bumper assembly, which was characterized using a skewed hyper ellipse

$$\left(\frac{x + y \tan\theta}{HL}\right)^N + \left(\frac{y}{HH \cos\theta}\right)^N = 1$$

where HL, HH, $\theta$, and N were chosen as design variables.

In reference 97, some important design constraints dictated by specifications were used; namely, the steering column displacement during crash was not to exceed five inches (ref. 98) and the occupant injury index was kept below the specified value (ref. 99). The weighted residual of the unsatisfied constraints was minimized by varying sheet metal thicknesses and geometry. Occupant injury, or the vehicle crash severity index (VCSI), was simulated as a simple function of the passenger compartment deceleration. In reference 100, vehicles were regarded as rigid bodies and model equations of impact were derived from impulse/momentum balances, equivalent coefficient of friction, and moment of restitution. The least-squares-fit approach (ref. 100) was employed to fit experimentally determined velocity components to the analytically derived equations of the vehicle collision model.

In reference 101, a methodology for optimizing design parameters for vehicle safety is described. The methodology, which is based upon a limiting performance design philosophy, characterizes changes in the structure and the restraint system of an image vehicle which lead to progressive improvements in vehicle crashworthiness.

Reference 102 proposes a preliminary design of front and rear body structures by analytical and experimental evaluation of the impact strength and crash energy capacity, followed by resizing of related members. Though the analysis may be reasonable and the result may appear mathematically accurate, often the "design criteria" used for the components in most of the studies (refs. 96, 97, and 100 to 102) fall short of practicality. References 103 and 104 are some of the earlier (1970) uses of optimization to the design of front end and restraint systems, respectively.

## 2.6 Other Components

In recent years, there has been noticeable interest in developing capability or methods to attack new or more difficult problems in automotive design, especially those relating to structural areas. References 77 and 105 to 108 outline some typical but diverse developments. They include shape optimization (ref. 77), general capability to obtain design sensitivity for any calculable response function (ref. 105), procedures to optimize solid components (ref. 106) and the capability to address multi-objective systems (those in which more than one design objective may be present at one time) (ref. 107). Naturally, only a few typical examples of automotive components, namely, rear suspension torque arm (ref. 77), composite wheel (ref. 105), engine bearing cap (ref. 106) and connecting rod (ref. 107), are included with each.

## 3. COMPLEXITY IN THE VEHICLE DESIGN PROCESS

The automotive design process is complex since it involves a number of constraints and design criteria which need to be considered for the design trade-off to be meaningful. The constraints on vehicle design are many and some have not received a quantitative underpinning (ref. 102). Cost is one of these and it is an important attribute because it often involves elements such as alternate materials fabrication, manufacturability (forming, welding, machining, casting), and assembly procedures, none of which is easily quantifiable but may lead to significant changes in the way the automobiles are currently built. In a second category, several important vehicle attributes such as ride, noise, handling, vibration, etc., can be included which do carry some analysis basis along with a vast experimental data base. Nonetheless, most of these attributes have subjective elements (human response is essential) and thus their design criteria are often questionable and also appear difficult to extrapolate. A third class of vehicle attributes--- appearance, style and interior arrangement, etc.---contain irreducible subjective elements, which can only be quantified if accurate mathematical models for human behavior are developed. This is a long-term proposal at best. In addition, some areas relating to system behavior, such as occupant simulation in frontal and side impact, have not yielded to reliable analysis. In these areas optimization will remain underutilized.

On the structural side, however, there exist quite a few areas which have yielded to sound and reasonable analytical bases (either numerical or closed form). For such applications the design problem becomes a straightforward direct linking process with an optimization counterpart. Many problems (such as static and dynamic analysis for strength, stiffness, frequency and compliance) can easily be handled through this process since they can be modeled using finite elements, for which optimization linking may have been "generically" established. There are several FEM-based programs which have established design optimization capability on a general basis (refs. 11 to 13 and 18 to 20). Crashworthiness for automobiles is, however, an exception because it has not yet received an established viable and economical base for behavior characterization. The existing finite element theory of shells and plates does not prove to be economical. Some authors have used simplified system (rigid-body lumped mass) models for the simulation of a problem such as frontal crush or side impact. They have, in many instances, coupled their analysis models with the optimization programs for the purpose of obtaining their new design parameters (refs. 96 and 97). The question of validity for their so-called "optima," however, remains an issue. From the above discussion, it is

apparent that it may not be possible to come up with a reasonable set of constraints (all quantifiable) and a good set of criteria for problems such as vehicle crush which can lead to a meaningful optimal design at the end. Developments in these areas will be a key determinant in further progress in the utilization of optimization in vehicle design.

# 4. STATUS/TREND IN OPTIMIZATION TECHNOLOGY

## 4.1 Design Variables

Optimization studies in the automated design of structures can be classified into four groups of design variables:

a. Size variables, which define the sizes (excluding lengths) of the structural members

b. Geometrical variables, which are typically the spatial coordinates of the intersections of the structural members

c. Materials variables, such as Young's modulus, density, etc.

d. Topological variables, which define the configuration---e.g., which members are to be included in the structure and which ones are not

The overwhelming majority of the work in structural synthesis has involved only sizing types of variables, and several extensive programs have been developed to handle this general class of problem. Materials and geometrical variables have received less attention, although a number of programs which include these variables (refs. 13, 15, and 18 to 20) do exist. The difficulties with geometric variables arise due to the inherent problems associated with changing geometry and the need for looping the model generation algorithm within an optimization system. The latter difficulties also appear common or even more pronounced with topological variables but the topological variables differ with the rest of the above three in one important way.

Topological variables by nature are discrete variables and, unlike continuous variables, cannot be used with finite differencing. Therefore, one encounters mathematical barriers while attempting to use a well-developed technique or an optimization program based on a gradient technique with the rest of the variables. Some nongradient techniques may prove useful. However, the literature on topological optimization within the finite element framework is sparse, and for automotive-related problems it is almost nonexistent. Most of the topological optimization in real practice is performed using intuition and judgment, with computer analyses and engineering/graphics often acting as helpful tools.

## 4.2 Generic Modeling

A recent technique called "generic modeling" (ref. 75) has been found to be quite useful and suitable for this type of application. It lends itself to incorporation as an integral part of an automated system, which is most critical for the efficient use of optimization and design programs. The generic modeling approach not only relieves the user of the burden of recreating the model, but also cuts down model modification time (topology, geometry, etc.) substantially.

154

Initially, generic modeling is slightly more expensive than the conventional graphics system approach. However, the cumulative cost of conventional modeling increases at a much faster rate as the number of modeling changes increases during the design process (fig. 10). Specific modeling cost comparisons for a wheel and vehicle body structure are provided in reference 75. For example, after the body structure model had been modified about ten times, the total cost of conventional modeling was about 100% more than the corresponding cost of generic modeling. (See fig. 10.) Although the generic modeling procedure has been applied to wheel and simple body models, the fuel potential will only be realized by applying it to the development of larger size models. Such a versatile generic modeling procedure will not be easy to develop because substantial efforts are necessary to model complex body parts with lengthy logic and procedures. Attainment of such a procedure promises a large potential payoff, not only in reduced cost and efficient structure, but also in providing a timely input to the vehicle design cycle.

## 4.3  Computer Programs

Most of the current general purpose computer programs (GPCP) either are based on mathematical programming techniques (ref. 25) or use recursive design methods obtained from optimality criteria (ref. 24). These methods enable the designer to arrive directly at a solution that satisfies the provisions for strength, stiffness, vibration, ride, handling, harshness, noise, safety and/or serviceability (as the case may be) while making the most efficient use of materials. Much progress has been made during the past quarter century since the direct methods of mathematical programming were first applied to optimization problems of structural design (refs. 1 and 24 to 32). The effort has led to the appearance of several textbooks and useful developments (refs. 9 to 23) which provide a unified treatment of the topic. These references are not complete, merely indicative. Most programs are now equipped with schemes which may be approximate but minimize the number of calls to the required analysis system in order to reduce the overall cost of total optimization.

## 4.4  Constraint Approximations

The constraint approximation concept is one such popular scheme which is commonly found in most present GPCP. The programs ODYSSEY (ref. 15), ACCESS (ref. 10), PROSSS (refs. 11 and 12) and PARS (refs. 18 to 22) use a Taylor series expansion, linear or reciprocal, in design variables (whenever appropriate) for the constraints. A more general power form of constraint approximation is used in EAL/PARS (ref. 22). This facilitates simulation of a number of constraints and structural types, if present. Reference 22 also includes a new method for collapsing a number of active constraints into a few representative equivalent constraints without losing the essential nature of the original problem. The major advantage of this approach is that design sensitivity vectors and constraint approximations need to be calculated for only a reduced number of equivalent constraints. For large problems, this often results in significant computational savings (ref. 21).

## 4.5  Optimization Algorithms

Optimization algorithms in most of the efficient computer codes are often derived from first order methods, which require gradient information for the

155

constraints and objective function. A number of programs (ODYSSEY (ref. 15), OPUS (ref. 13), PARS (refs. 18 to 20), and PROSSS (refs. 11 and 12)) use CONMIN, which is a feasible directions algorithm (ref. 9), as an optimizer. EAL/PARS (refs. 18 to 20) has two optimizers, CONMIN and a second one based on a variable penalty method (VPM) which uses SUMT (Sequence of Unconstrained Minimization Technique) with a modified Newton method. The required information of the second derivatives in Newton's method is supplied approximately but explicitly as a function of first derivatives and their initial values (ref. 21). The method, therefore, is designed to provide a second-order convergence rate at a cost no higher than what is usually required for the first-order methods.

## 4.6  Design Sensitivity

Design sensitivity computations are probably the most expensive ventures of any optimization technique. Most GPCP, therefore, tend to include this capability in one form or the other. The efficiency, of course, depends upon their mode of linking and the sensitivity technique used (ref. 105). It is now widely believed that the cost of gradient computations through analytical means is the most economical, though the procedure differs with the number of active constraints and design variable ratios. (See ref. 105.) Finite differencing is considered to be the most expensive method for calculating sensitivity.

## 5.  POTENTIAL FUTURE AND PROSPECTS

From the foregoing discussion, it is indicative that progress in optimization and sensitivity capability (especially in structural areas) has improved significantly. With the ability to handle any design variable, as specified by "generic modelling" (ref. 75) and increased efficiency (ref. 21), the cost of optimization is becoming a "less serious" barrier to application. Adequate "quantification" of the associated constraints and "clear-cut" definition of the design criteria remain major stumbling blocks for the widespread use of optimization. Until it is possible to quantify (at least crudely) most of the important constraints that we encounter today in automotive design, the prospects for optimization as an integral part of the design process appear uncertain and may remain so for the foreseeable future.

Design sensitivity will perhaps remain a major mode of design iteration, with "analysts" serving as a major input source to decision making (refs. 105 and 108). This is because most of the important constraints are experience based (often subjective), and adequate quantification has not been well enough established to seek automation. An important near-term outgrowth of recent developments in optimization technology is that this process (i.e., sensitivity calculation) can now be accomplished much more efficiently. Thus, the input of analysis to design is becoming more timely and valuable. The capability to apply optimization to various systems will grow at a steady pace and the CAD/CAM interfaces to design will become more popular and automated. The availability of more efficient optimization systems and programs will grow commercially. In addition, with the exploding computer technology and cost of hardware declining, the computational cost for design and optimization will continue to be a less severe barrier to medium or moderately large size applications. Thus, we might expect more utilization of optimization with graphics and "man-in-the-loop" modes of operation.

Design with topological variables (such as configuration or appearance) will
continue to be done on a "one-at-a-time" basis. A topology is first selected based
on the understanding of the design requirements and packaging, and its shape,
geometry or sectional parameters are then optimized. This may not be as efficient
as one would find in a "simultaneous" design mode, but the process is likely to stay
at least until the stage arrives when, through advances in the field of artificial
intelligence, the designer will be able to put his thoughts into a computer
language.


## 6. CONCLUSIONS

It has not proved possible to quantify all the important constraints, such as
ride, NVH (noise, vibration, and harshness), and manufacturability, that need to be
considered in the design of automotive vehicles for overall system goals. This
limitation on the part of the analytical basis will apparently continue to set the
pace for the use of optimization.

On the structural side, the trend in the use of advanced techniques in vehicle
design is away from methods tailored to specific components and shapes and toward
methods that can handle material and shape changes in design for a number of com-
ponents. For modeling, this trend manifests itself with the use of generic modeling
or similar methods which reduce the time requirement or eliminate user interfaces.
For the analysis part, the trend is toward the use of finite element or similar
discretization techniques. For the design part, the trend is away from costly trial
and error modes of approach and more toward the use of design sensitivity and/or
general numerical optimization algorithms.


## REFERENCES

1.  Dunseth, J. H., "The Use of a Computer as a Design Tool," SAE Paper 65-986A,
    Int. Automotive Engineering Congress, Detroit, Jan. 1965.

2.  Bender, E. K., Karnopp, D. C., and Paul, I. L., "On the Optimization of Vehicle
    Suspensions Using Random Process Theory," ASME-67-TRANS-12, Mech. Eng.,
    Vol. 89, 1967.

3.  Bender, E., "Optimum Linear Preview Control with Application to Vehicle
    Suspension," ASME J. Basic Engineering, Vol. 90, 1968, pp. 213-221.

4.  Wolkovitch, J. "Techniques for Optimizing the Response of Mechanical Systems to
    Shock and Vibration," SAE Transactions, Vol. 77, 1969. (Also SAE Paper
    No. 680748, 1968.)

5.  Bennett, J. A. and Nelson, M. F., "An Optimization Capability for Automotive
    Structures," SAE Paper No. 790972, 1979.

6.  Hasselgren, A. and Svanberg, K., "Using Finite Element Methods and Optimization
    Techniques in Lightweight Car Design," presented at the International
    Conference on Modern Vehicle Design Analysis, England, June 22-24, 1983.

7.  Thompson, A. G., "A Simple Formula for Optimum Damping in Suspensions,"
    Automotive Engineering, 1972, Vol. 3, No. 4, Inst. of Mechanical Engineers,
    p. 20.

8.  Hullender, D. A., "Minimum Vehicle-Guideway Clearances Based on a Contact Frequency Criterion," ASME Journal of Dynamic System, Measurement and Control, Vol. 96, 1974, pp. 213-217.

9.  Vanderplaats, G. N., "CONMIN - A Fortran Program for Constrained Function Minimization," NASA TM X-62282, 1973.

10. Schmit, L. A. and Fleury, C., "An Improved Analysis Synthesis Capability Based on Dual Methods - ACCESS 3," AIAA/ASME/ASCE/AHS 20th Structures, Structural Dynamics and Materials Conference, St. Louis, Mo., April 1979, AIAA Paper No. 79-0721.

11. Sobieszczanski-Sobieski, J. and Bhat, R. B., "Adaptable Structural Synthesis Using Advanced Analysis and Optimization Coupled by a Computer Operating System," AIAA/ASME/ASCE/AHS 20th Structures, Structural Dynamics and Materials Conference, St. Louis, Mo., April 1979, pp. 20-71, AIAA Paper No. 79-0723.

12. Rogers, J. L., Sobieszczanski-Sobieski, J. and Bhat, R. B., "An Implementation of the Programming Structural Synthesis System (PROSSS)," NASA TM-83180, Dec. 1981.

13. Adelberg, M. L. and DeVries, R. I., "OPUS - A Programming System Approach to Structural Optimization," SAE Paper No. 811316, 4th Int. Conference on Vehicle Structural Mechanics, Nov. 18-20, 1981, pp. 151-160.

14. McCormick, C. W. (ed.), "MSC/NASTRAN User's Manual, MSC/NASTRAN Version 62," The MacNeal-Schwendler Corporation, Los Angeles, 1981.

15. Bennett, J. A. and Botkin, M. E., "Automated Design for Automotive Structures," ASME Paper No. 81-DET-91, presented at the Design Engineering Technical Conference, Hartford, CT, Sept. 1981.

16. Kecman, D., "Program WEST for Optimization of Rectangular and Square Section Tubes from the Safety Point of View," SAE Paper No. 811312, Proc. of 4th Int. Conference on Vehicle Structural Mechanics, 1981, pp. 99-112.

17. Osborn, J. and Thiel, L., "Optimal Design of Minimum Weight Structures," SAE Paper No. 810686, presented at the Earthmoving Industry Conference, Peoria, Illinois, April 1981.

18. Haftka, R. T. and Prasad, B., "Programs for Analysis and Resizing of Complex Structures - PARS," Computers and Structures, Vol. 10, Nos. 1-2, pp. 323-330, 1979.

19. Haftka, R. T., Prasad, B., and Tsach, U., "PARS: Programs for Analysis and Resizing of Structures - User Manual," NASA CR-159007, 1979.

20. Prasad, B. and Haftka, R. T., "Organization of PARS - A Structural Resizing System," Advances in Engineering Software Journal, Vol. 4, No. 1, 1982, pp. 9-19.

21. Prasad, B., "Approximation, Adaptation and Automation Concepts for Large-Scale Structural Optimization," Engineering Optimization, Vol. 6, 1983, pp. 129-140.

22. Prasad, B., "An Integrated System Approach to Structural Synthesis," Eighth Conference on Electronic Computations, James K. Nelson, Editor, American Society of Civil Engineers, New York, NY, Feb. 1983, pp. 155-171.

23. Whetstone, W. D., "EISI-EAL: Engineering Analysis Language," Proc. of the Second Conference on Computing in Civil Engineering, ASCE, 1980, pp. 276-285. (Also as "Reference Manual Vol. 2: Structural Analysis Primary Processors," System Level 209I, Engineering Information Systems, Inc., CA, July 1983.)

24. Khot, N. S., Venkayya, V. B. and Berke, L., "Experiences with Minimum Weight Design of Structures Using Optimality Criteria Methods," SAE Paper No. 770607, 1977.

25. Vanderplaats, G. N., "Automated Design Using Numerical Optimization," SAE Paper No. 791061, 1979.

26. Ragsdell, K. M., "Optimization as a Tool for Automotive Design," SAE Paper No. 800432, 1980.

27. Dill, J. C. and Bliss, F. W., "Computer Graphics - Assessment of State-of-the-Art, Parts I and II," SAE Paper No. 800010, 1980.

28. Kamal, M. M., "Impact of Computer Developments on Engineering Applications - Past, Present and Future," SAE Paper No. 800011, 1980.

29. Mayne, R. W., "Optimization Techniques for Shock and Vibration Isolator Development," The Shock and Vibration Digest, Vol. 8, No. 1, 1976, pp. 87-94.

30. Rao, S. S., "Structural Optimization Under Shock and Vibration Environment," Shock and Vibration Digest, Feb. 1979, Vol. 11, pp. 3-12.

31. Haftka, R. T. and Prasad, B. "Optimum Structural Design with Plate Bending Elements - A Survey," AIAA J., Vol. 19, No. 4, April 1981, pp. 517-522.

32. Barone, M. R., "Modeling and Computational Techniques in Automotive Structures," AMD Vol. 50, Computational Methods in Ground Transportation Vehicles, edited by M. M. Kamal and J. A. Wolf, 1982.

33. Haftka, R. T. and Prasad, B., "Lightweight Design of the Sides of a Typical 100 Ton High Side Gondola Car," SAE Paper No. 790973, 3rd Int. Conference on Vehicle Structural Mechanics, Oct. 1979, Troy, MI, pp. 11-18.

34. Fenyes, P. A., "Structural Optimization with Alternate Materials - Minimum Mass Design of the Primary Structure," SAE Paper No. 810228, 1981.

35. Miura, H., Lust, R. V., and Bennett, J. A., "Integrated Panel and Skeleton Automotive Structural Optimization," SAE Paper No. 811317, 4th International Conference on Vehicle Structural Mechanics, pp. 161-169, 1981.

36. Hsia, H. and Kidd, J. A., "Weight Reduction Potential of Passenger Cars and Light Trucks by Material Substitution," SAE Passenger Car Meeting, Dearborn, MI, SAE Paper No. 800803, June 1980.

37. Reid, D. and Stevenson, P., "Optimal Substitution of Lightweight Materials in Automobiles," SAE Paper No. 800828, 1980.

38. Bennett, J. A., "Minimum Weight Design of a Body-Beam Structure Made of Continuous Fiber Composites," Proceedings of XVIII FISITA Congress, Hamburg, Germany, May 1980.

39. Chang, D. C., and Justusson, J. W., "Structural Requirements in Material Substitution for Car-Weight Reduction," SAE Paper No. 760023, 1976.

40. Chang, D. C. and Barone, M. R., "Structural Optimization in Panel Design," SAE Paper No. 770610, 1977.

41. Chang, D. C., "Optimal Designs with Alternate Materials Suitable for High-Volume Production," SAE Paper No. 790975, 1979.

42. Rolf, R. L., Sharp, M. L. and Herbein, W. C., "Minimizing the Weight of Aluminum Body Panels," SAE Paper No. 790164, 1979.

43. Vadhavkar, A. V., Fecek, M. G., Shah, V. C. and Swenson, W. E., "Panel Optimization Program (POP)," SAE Paper No. 810230, 1981.

44. Prasad, B., "Some Considerations in Efficient Design of Lightweight Structures," SAE Paper No. 811315, 4th International Conference on Vehicle Structural Mechanics, Detroit, Michigan, Nov. 1981, pp. 141-149.

45. Akerstrom, T., Jernstrom, C. and Wierzbicki, T., "Shape Optimization of Sheet Metal Structures Against Crash," SAE Paper No. 811314, 1981.

46. Herbein, W. C., Wolf, N. P. and Bockhold, J. J., "Minimizing the Weight and Cost of an Aluminum Deck Lid," SAE Paper No. 810783, 1981.

47. Chang, D. C., Wu, K-M and Vella, J. R., "Potential Mass Reduction and Material Cost Penalties of Body Panels with Alternate Materials," SAE Paper No. 810229, 1981.

48. Du, H. A. and Tang, S. C., "Minimum Weight Design of a Car Trunk Deck-Lid Subject to Overall Stiffness Constraints," Journal of Mechanical Design, Vol. 104, pp. 831-836, 1982.

49. Esmailzadeh, E., "Design Synthesis of a Vehicle Suspension System Using Multi-Parameter Optimization," Vehicle System Dynamics, 7, 1972, pp. 83-96.

50. Metwalli, S. M., Afimiwala, K. A. and Mayne, R. W., "Optimum Design of Vehicle Suspension," ASME Paper No. 73-ICT-58, 1973.

51. Potter, R. A., and Willmert, K. D., "Optimum Design of a Vehicle Suspension System," ASME 73-DET-46, 1973.

52. Hedrick, J. K. "Some Optimal Control Techniques Applicable to Suspension System Design," ASME Paper No. 73-ICT-55, 1973.

53. Young, J. W., and Wormley, D. N., "Optimization of Linear Vehicle Suspensions Subjected to Simultaneous Guideway and External Force Disturbances," ASME Journal of Dynamic Systems, Measurement and Control, Series G, Vol. 95, No. 2, 1973, pp. 213-219.

54. Thompson, A. G., "Quadratic Performance Indices and Optimum Suspension Design," Proc. Inst. of Mechanical Engineers, 1973, Vol. 187, No. 9/73, pp. 129-139.

55. Thompson, A. G., "Design of Active Suspensions," Proc. Inst. of Mechanical Engineers, Vol. 185, No. 36, pp. 553-563, 1971.

56. Thompson, A. G., Davis, B. R. and Pearce, C. E. M., "Optimal Linear Active Suspension with Finite Road Preview, SAE Paper No. 800520, 1980.

57. Blazer, L. A., "Optimal Control with Partial Preview of Disturbances and Rate Penalties and its Application to Vehicle Suspension," International Journal of Control, Vol. 33, No. 2, 1981, pp. 323-345.

58. Johnson, R. N. and Fine, D. S., "Suspension Optimization for Better Vehicle Handling," Developments in Mechanics, Proc. of 17th Midwestern Mechanics Conference, Ann Arbor, Michigan, May 1981, pp. 135-136.

59. Egbert D. E. and Linlecki, A., "Computer Optimization of Trailer Suspensions," Mechanism and Machine Theory, Vol. 16, 1981, pp. 369-384.

60. Hrovat, D. and Hubbard, M., "Optimum Vehicle Suspensions: Minimizing RMS Rattlespace, Spring-Mass Acceleration, and Jerk," Trans. ASME, Journal of Dynamic Systems, Measurement and Control, Vol. 103, No. 3, 1981, pp. 228-236.

61. Haug, E. J., "Vehicle Suspension Dynamic Optimization," presented at the International Conference on Modern Vehicle Design Analysis, London, England, June 22-24, 1983.

62. Lu, X-P, Li, H-L and Papalambros, P., "A Design Procedure for Optimization of Vehicle Suspensions," paper presented at the International Conference on Modern Vehicle Suspensions," London, England, June 22-24, 1983.

63. Thompson, A. G., "Suspension Design for Optimum Road-Holding," SAE Paper No. 830663, 1983.

64. Ghoneim, H. and Metwalli, S. M., "Optimum Vehicle Suspension with a Damped Absorber," ASME Paper No. 83-DET-42, presented at the Design and Production Engineering Technical Conference, Dearborn, Mi., Sept. 11-14, 1983.

65. Karnopp, D. C., and Trikha, A. K., "Comparative Study of Optimization Techniques for Shock and Vibration Isolation," Journal of Eng. for Industry, Trans. ASME, Vol. 91, No. 4, 1969, pp. 1128-1132.

66. Van Deusen, B. D., "Truck Suspension System Optimization," SAE Paper No. 710222, 1971.

67. Sevin, E. and Pilkey, W. D., "Optimum Shock and Vibration Isolation," Monograph No. 6, The Shock and Vibration Information Center, Naval Research, U.S. Dept. of Defense, Washington, D.C., 1971.

68. Wilmert, K. D. and Fox, R. L., "Optimum Design of a Linear Multi-Degree-of-Freedom Shock Isolation System," Journal of Engineering for Industry, Vol. 94, May 1972, pp. 465-471.

69. Esmailzadeh, E., "Optimization of Pneumatic Vibration Isolation System for Vehicle Suspension," Trans. ASME, Journal of Mech. Design, 1977.

70. Hedrick, J. K., Billington, G. F. and Dreesbach, D. A., "Analysis, Design and Optimization of High Speed Vehicle Suspension Using State Variable Techniques," ASME Journal of Dynamic System, Measurement and Control, Vol. 96, 1974, pp. 193-203.

71. Hsiao, M. H., Haug, E. J. and Arora, J. S., "A State Space Method for Optimal Design of Vibration Isolators," Journal of Mechanical Design, Vol. 100, 1978.

72. Soom, A. and Lee, Ming-San, "Optimal Design of Linear and Nonlinear Vibration Absorbers for Damped Systems," Journal of Vibration, Acoustics, Stress and Reliability in Design," ASME, Vol. 105, Jan. 1983, pp. 112-119.

73. Hati, S. K. and Rao, S. S., "Cooperative Solutions in the Synthesis of Multi-Degree-of-Freedom Shock Isolation Systems," Journal of Vibration, Acoustics, Stress and Reliability in Design, ASME, Vol. 105, Jan. 1983, pp. 101-103.

74. Afimiwala, K. A. and Mayne, R. W., "Optimum Design of an Impact Absorber," Journal of Engineering for Industry, Vol. 96, Feb. 1974, pp. 124-130.

75. Kulkarni, H. T., Prasad, B. and Emerson, J. F., "Generic Modeling Procedure for Complex Component Design," SAE Paper No. 811320, 4th International Conference on Vehicle Structural Mechanics, Detroit, Michigan, 1981.

76. Riesner, M. and DeVries, R. I., "Finite Element Analysis and Structural Optimization of Vehicle Wheels," SAE Paper No. 830133, 1983.

77. Botkin, M. E., "Shape Optimization of Plate and Shell Structures," AIAA Paper No. 8100553, AIAA/ASME/ASCE, 22nd Structures, Structural Dynamics and Materials Conference, Atlanta, GA, April 1981.

78. Auiler, J. E., Zbrozek, J. D. and Blumberg, P. N., "Optimization of Automotive Engine Calibration for Better Fuel Economy - Methods and Applications," SAE Paper No. 770076, 1977.

79. Rishavy, E. A., Hamilton, S. C., Ayers, J. A. and Keane, M. A., "Engine Control Optimization for Best Fuel Economy with Emission Constraints," SAE Paper No. 77075, 1977.

80. Cassidy, J. F., "A Computerized On-Line Approach to Calculating Optimum Engine Calibrations," SAE Paper No. 770078, 1977.

81. Dohner, A. R., "Transient System Optimization of an Experimental Engine Control System Over the Federal Emissions Driving Schedule," SAE Paper No. 780286, 1978.

82. Matsumoto, K. et al., "Engine Control Optimization for Smaller Passenger Cars," SAE Paper No. 780590, 1978.

83. Prabhakar, R., Citron, S. J. and Goodson, R. E., "Optimization of Automotive Engine Fuel Economy and Emissions," ASME Publications 75 WA/Aut-19, 1975.

84. Rao, H. S., Cohen, A. I., Tennant, J. A. and VanVoorhies, K. L., "Engine Control Optimization Via Nonlinear Programming," SAE Paper No. 790177, 1979.

85. Baum, J, H., Bennett, J. A. and Crane, T. G., "Truck Ride Improvement Using Analytical and Optimization Methods," SAE Paper No. 770609, 1977.

86. Johnson, S. R. and Subhedar, J. W., "Computer Optimization of Engine Mounting Systems," SAE Paper No. 790974, 1979.

87. Bernard, J. E. and Starkey, J. M., "Engine Mount Optimization," SAE Paper No. 830257, 1983.

88. Lalor, N., "Computer Optimized Design of Engine Structures for Low Noise," SAE Paper No. 790364, 1979.

89. Nivi, H., Seth, B. B. and Field, N. L., "Optimum Phaser Tolerances for Machines with Designed Unbalance," Journal of Mechanisms, Transmissions and Automation in Design, ASME Paper No. 83-DET-36, presented at the Design and Production Engineering Technical Conference, Dearborn, Mi., Sept. 11-14, 1983.

90. Tennant, J. A., Cohen, A. I., Rao, H. S. and Powell, J. D., "Computer Aided Procedures for Optimization of Engine Controls," International Journal of Vehicle Design, Vol. 4, No. 3, 1983, pp. 258-269.

91. Fukuda, M., "Engine Component Design Through the NISSAN Structural Analysis System," SAE Paper No. 800320, 1980.

92. Lalor, N., "Finite Element Optimization Techniques of Diesel Engine Structures," SAE Paper No. 820437, 1982.

93. Rao, S. S. and Srinivasa Rao, S. S., "Optimum Design of I.C. Engine Pistons," ASME Paper No. 83-DET-31, presented at the Design and Production Engineering Conference, Dearborn, Mi., Sept. 11-14, 1983.

94. Radtke, R. R., Unnewehr, L. E. and Freedman, R. J., "Optimization of a Continuously Variable Transmission with Emission Constraints," SAE Paper No. 810107, 1981.

95. Watson, H. C. and Milkins, E. E., "Comparison and Optimization of Emission Efficiency and Power of Five Automotive Fuels in One Engine," International Journal of Vehicle Design, Vol. 3, No. 4, 1982, pp. 463-476.

96. Twigg, D. W., Tocher, J, L. and Eppinger, R. H., "Optimal Design of Automobiles for Pedestrian Protection," SAE Paper No. 770094, 1977.

97. Bennett, J. A., Lin, K. H. and Nelson, M. F., "The Application of Optimization Techniques to Problems of Automotive Crashworthiness," SAE Paper No. 770608, 1977.

98. Steering Control Rearward Displacement. Code of Federal Regulations, Title 49, Part 571, Section 204, Federal Motor Vehicle Safety Standard, Transportation Dept., 1977.

99.  Occupant Crash Protection in Passenger Cars, Multipurpose Passenger Vehicles, Trucks, and Buses.  Code of Federal Regulations, Title 49, Part 571, Section 208, Federal Motor Vehicle Safety Standard, Transportation Dept., 1972.

100.  Brach, R., "Identification of Vehicle and Collision Impact Parameters from Crash Tests," ASME Paper No. 83-DET-13, presented at the Design and Production Engineering Technical Conference, Dearborn, Mi., Sept. 11-14, 1983.

101.  White, K. P., Pilkey, W. D., Gabler, H. C. and Hollowell, T., "Optimizing Design Parameters for Highway Vehicle Safety," International Journal of Vehicle Design, Vol. 4, No. 6, 1983, pp. 618-632.

102.  Augustitus, J. A., Kamal, M. M. and Howell, L. J.  "Design Through Analysis of an Experimental Automobile Structure," SAE Paper No. 770597, 1978.

103.  Moore, D. F., "Minimization of Occupant Injury by Optimum Front-End Design," SAE Paper No. 700416, International Automobile Safety Conference Compendium, Detroit, Michigan, May 13-15, 1970.

104.  Searle, J., "Optimum Occupant Restraints," SAE Paper No. 700422, International Automobile Safety Conference Compendium, Detroit, Michigan, May 13-15, 1970.

105.  Prasad, B. and Emerson, J. F., "A General Capability of Design Sensitivity for Finite Element Systems," AIAA Paper No. 82-0680-CP, pp. 175-186, AIAA/ASME/ASCE/AHS  23rd Structures, Structural Dynamics and Materials Conference, Atlanta, GA, May 1982.

106.  Imam, M. H., "Minimum Weight Design of a 3-D Solid Components," Computers in Engineering, 1982, Vol. III, Edited by Hulbert, L. E., et al., ASME, New York, NY, pp. 119-126, 1982.

107.  Prasad, B. and Emerson, J. F., "Optimal Structural Remodeling of Multi-Objective Systems," Computers in Engineering, 1982, Vol. III, Edited by Hulbert, L. E., et al., ASME, New York, NY, pp. 99-108, 1982.  (Also in Computers and Structures, Vol. 18, No. 4, 1984, pp. 619-628.)

108.  Chon, C. T. and Du, H. A., "An Alternative Approach to Design Sensitivity Analyses for Large-Scale Structures," Computers in Engineering, 1983, Vol. III, Edited by Dietrich, D. E., et al., ASME, New York, NY, pp. 233-237, 1983.
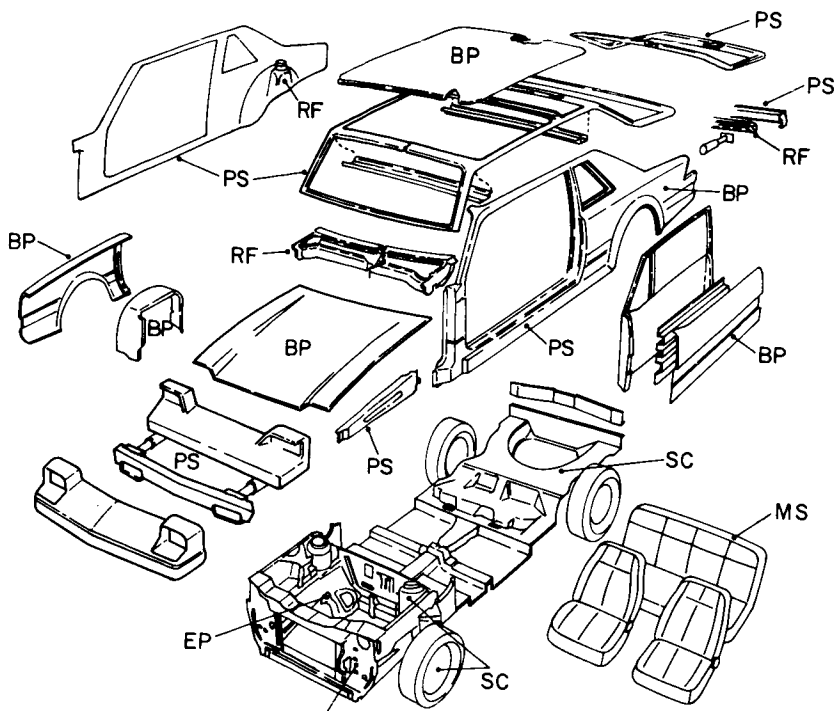
Figure 1. Division of vehicles into six subsystems: primary structures (PS), body panels (BP), engine and powertrain (EP), suspension and chasis (SC), reinforcement and fixtures (RF), and miscellaneous (fuels, seats, battery, etc.) (MS).
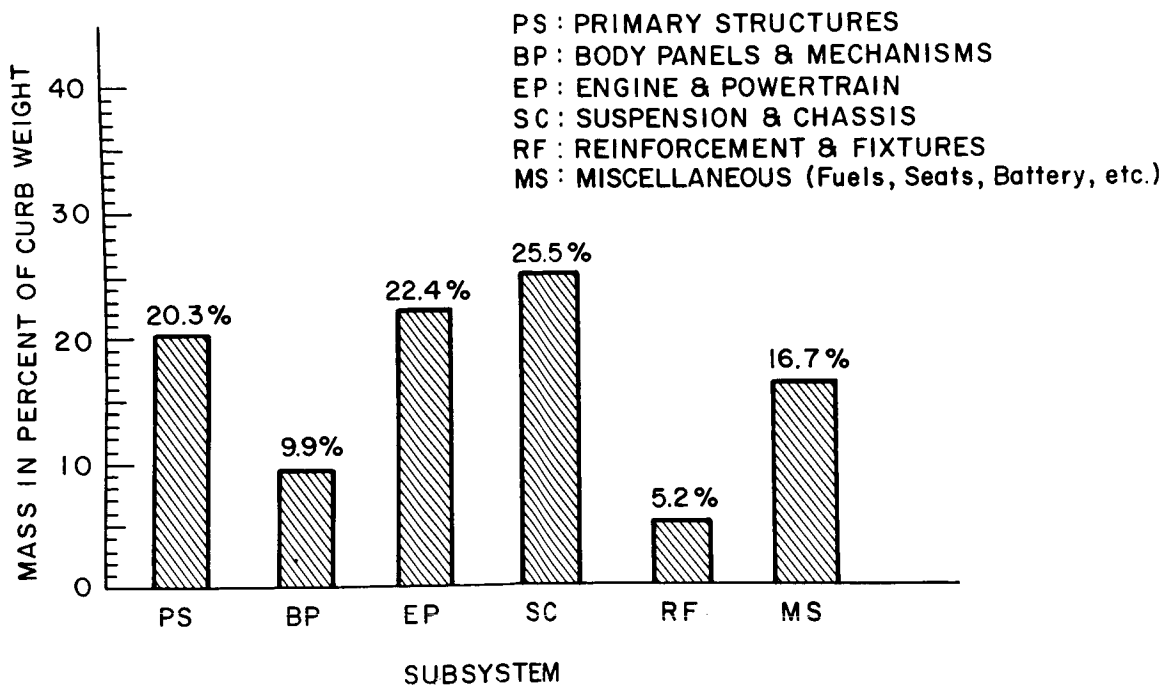


PS : PRIMARY STRUCTURES
BP : BODY PANELS & MECHANISMS
EP : ENGINE & POWERTRAIN
SC : SUSPENSION & CHASSIS
RF : REINFORCEMENT & FIXTURES
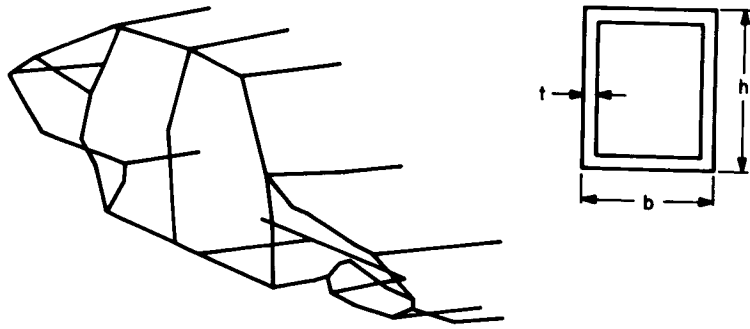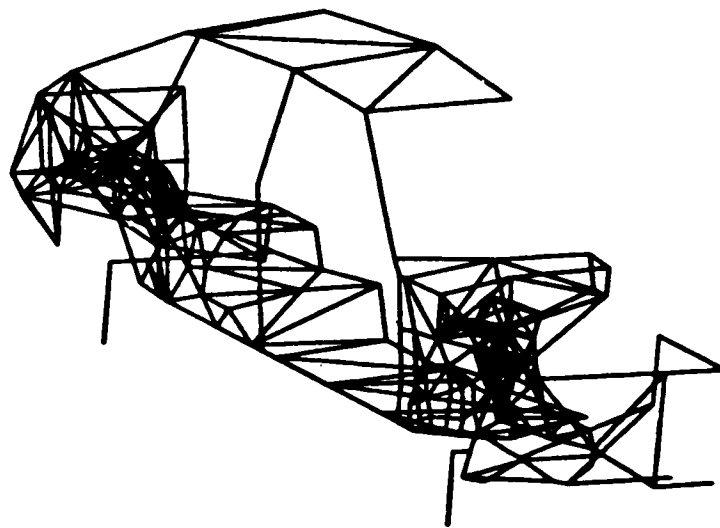MS : MISCELLANEOUS (Fuels, Seats, Battery, etc.)

Figure 2. Mass distribution of subsystems in a typical car (curb weight = 2020 lb).
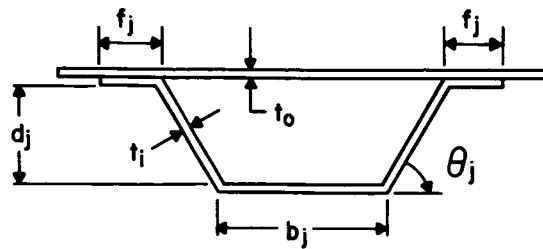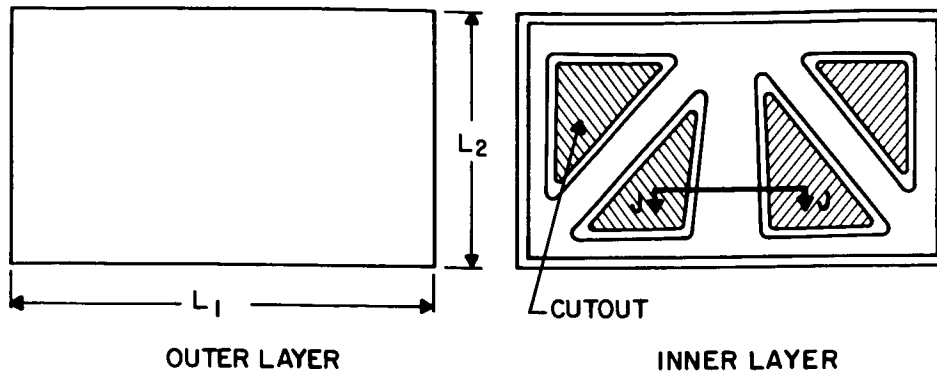
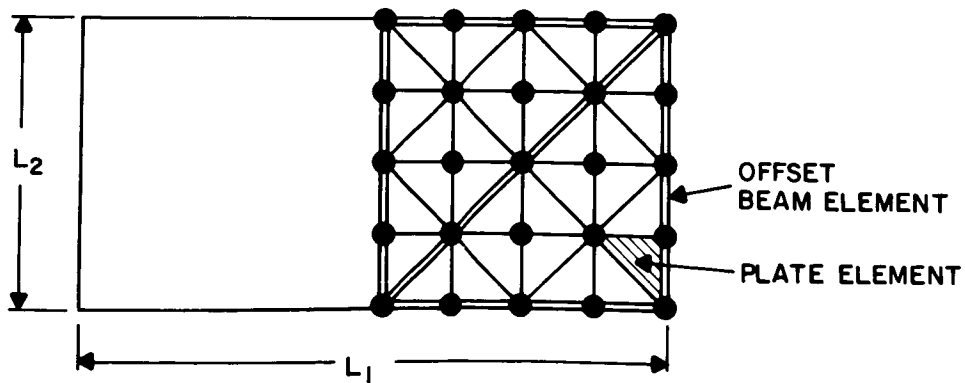(a) Typical simplified beam model.  (Adapted from refs. 5 and 15.)



(b) Typical beam/plate model.  (Adapted from ref. 35.)

Figure 3.  Beam models for optimization.

(a) Double-layer panel.



(b) Finite element model (32 plate elements, 20 offset beam elements, no. of design
variables = 8) (ref. 41).

Figure 4. Mathematical models for optimization with alternate materials.
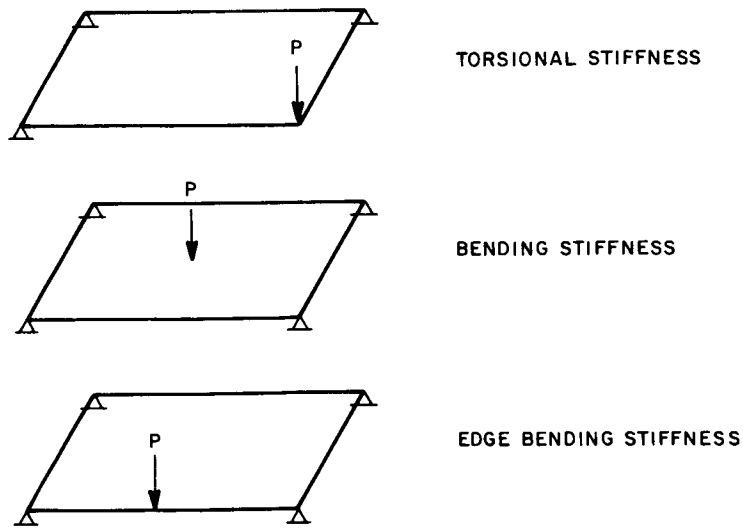
Figure 5. Frequently used stiffness design criteria for double panel.



(a) ORIGINAL OFFSET
BEAM SECTIONS

(b) SIMPLIFIED
EQUIVALENT
SECTION
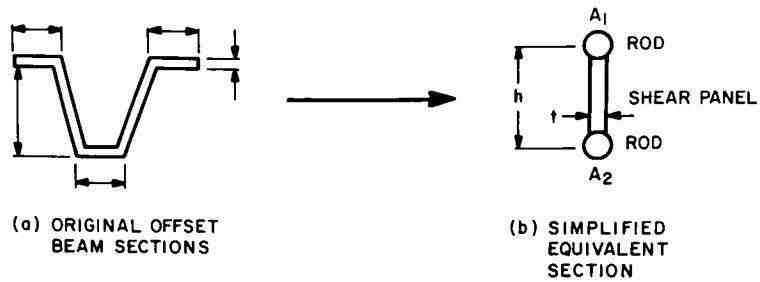
(a) Cross sectional idealizations. (A maximum of 4 design variables per stiffener is allowed.)
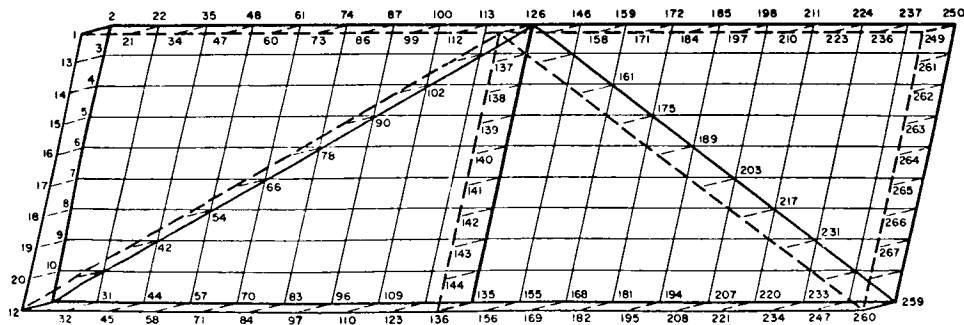


(b) Detailed finite element model (number of design variables = 16.) (Adapted from ref. 44.)

Figure 6. Finite element model.

168
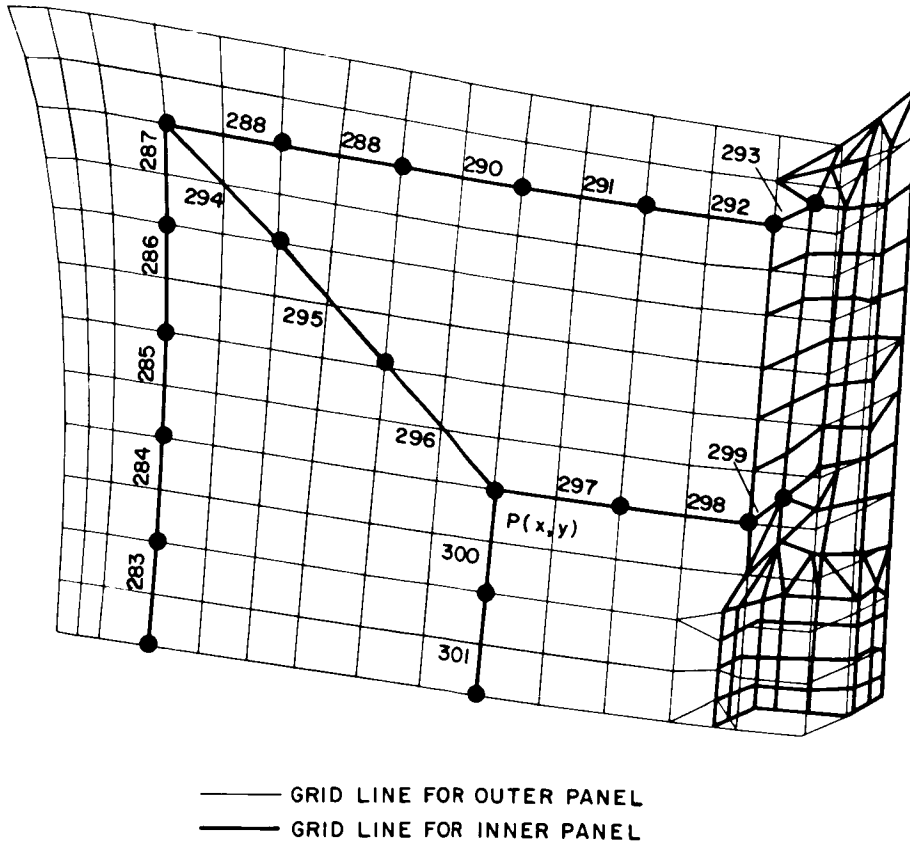
Figure 7. Half model of truck decklid (38 beams, 196 plates, number of design variables = 4) (ref. 48).
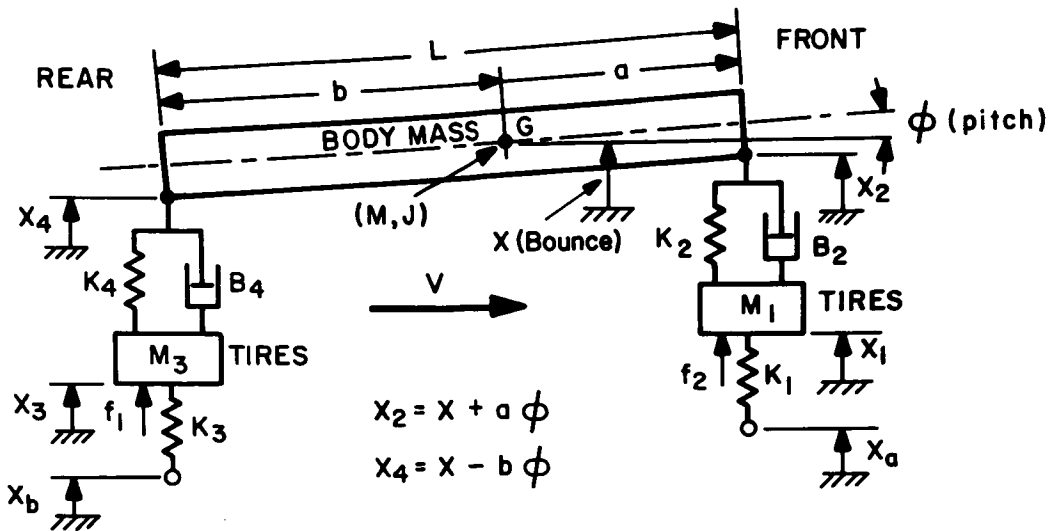


Figure 8. Linear half vehicle model (four degrees of freedom) (ref. 63).
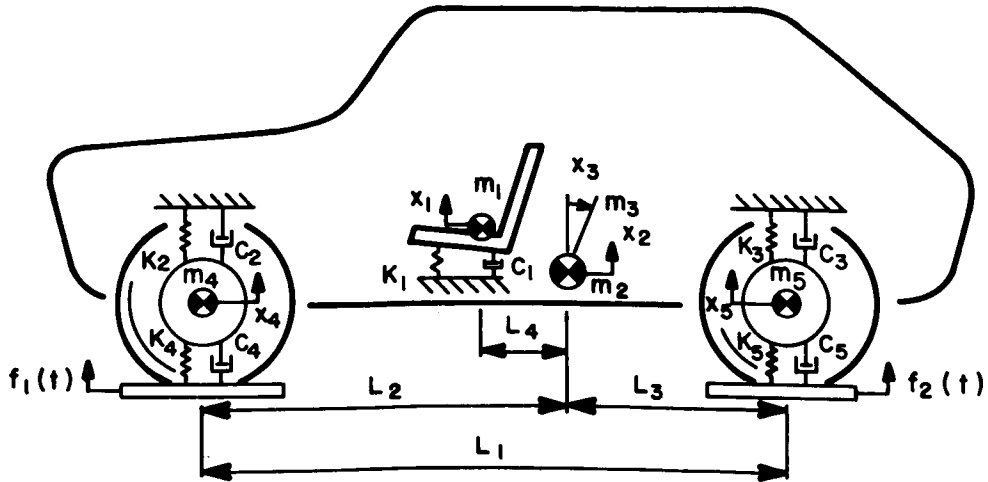
Figure 9.  Linear half vehicle model (five degrees of freedom) (ref. 61).
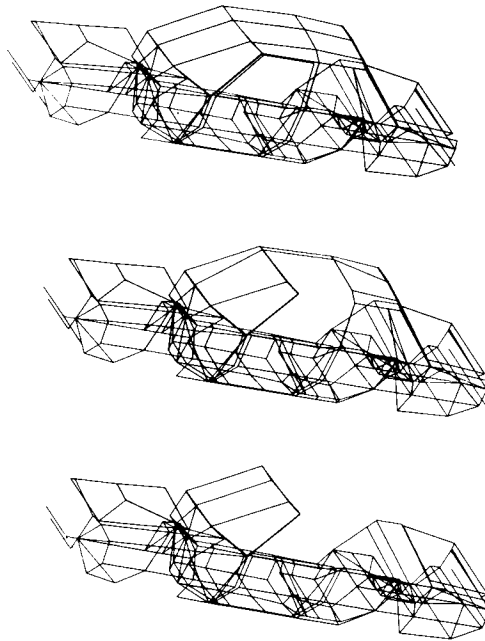


(a) Vehicle body models derived using generic approach.

Figure 10.  Generic modelling approach.

$$\text{PAYOFF} : \left[ \dfrac{\text{Conventional} - \text{Generic}}{\text{Generic Cost}} \right] \times 100$$
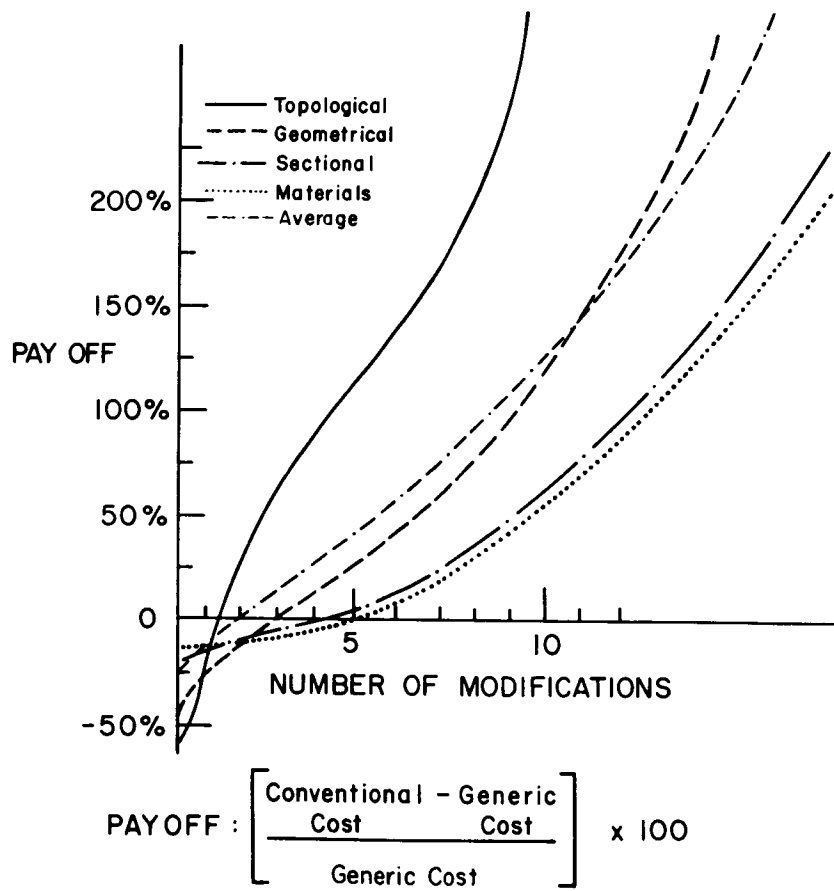
(b) Payoff from using generic modelling approach.

Figure 10. Concluded.

# STRUCTURAL OPTIMIZATION IN AUTOMOTIVE DESIGN

J. A. Bennett and M. E. Botkin
General Motors Research Laboratories
Warren, MI   48090

# TYPICAL ENGINEERING DESIGN ORGANIZATION

Although mathematical structural optimization has been an active research area for twenty years, there has been relatively little penetration into the design process. Experience indicates that often this is due to the traditional layout-analysis design process. In many cases, optimization efforts have been outgrowths of analysis groups which are themselves appendages to the traditional design process. As a result, optimization is often introduced into the design process too late to have a significant effect because many potential design variables have already been fixed. A series of examples (Ref. 1-6) will be given to indicate how structural optimization has been effectively integrated into the design process (Fig. 1).
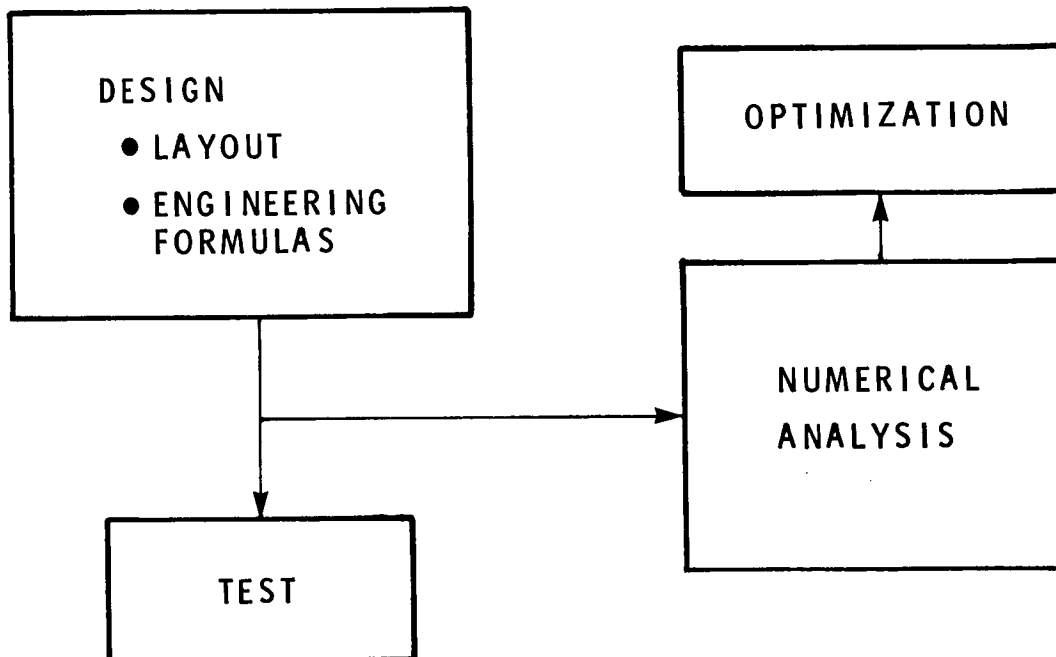
Figure 1

## TYPICAL BEAM SECTIONS AVAILABLE IN OPTIMIZATION

The examples in this paper have been obtained with a general purpose structural optimization code developed at the General Motors Research Laboratories which allows both constraint approximation methods and full mathematical programming methods with exact constraint evaluation to be used as required. A feasible directions algorithm is used as the optimizer in both cases. A design library of thin-walled beam elements (Fig. 2) and triangular plate elements (bending and membrane) is available. Multiple load conditions and multiple boundary conditions may be applied and frequency, displacement, and stress constraints may be used.
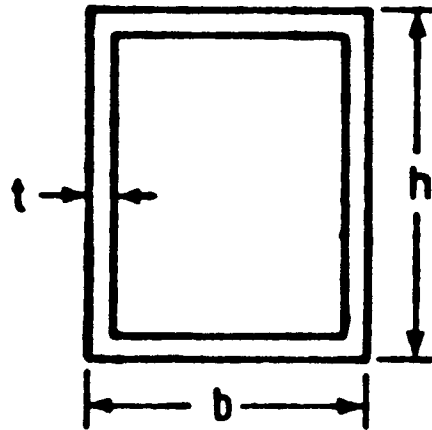
**BOX BEAM**
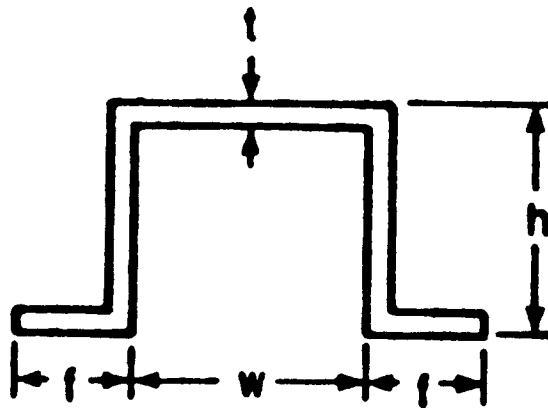
**HAT SECTION**

Figure 2

# EARLY CONFIGURATION DECISIONS

There are often several competing structural configurations for a major portion of the structure. Rarely are these competing configurations examined on a rational basis. This example examines an optimization study of three configurations proposed for a front structure. The structures were split into upper and lower configurations. Front structure I may be characterized by an upper structure securely attached to the cowl bar and a lower structure comprised of a mid-rail and triangulated lower rail. Structures II and III each have an irregular slanted shear wall for the upper structure and a mid-rail and engine cradle comprising the lower structure, with structure III having an additional under-car longitudinal rail. Each of these front structures was modeled on a common rear structure as shown in Fig. 3. The remaining front structures are shown in Figs. 4 and 5. All structures were subjected to the same set of force load conditions and frequency constraints. In the optimization, all beam cross section dimensions, including widths and heights, were taken as design variables. In addition, beams throughout the structure, not just in the front structure, were allowed to vary. It has been found that relatively simple beam models with truss elements representing the stiffness of critical panels have been sufficient for preliminary design.



———————  Beam Element

·············  Truss Element
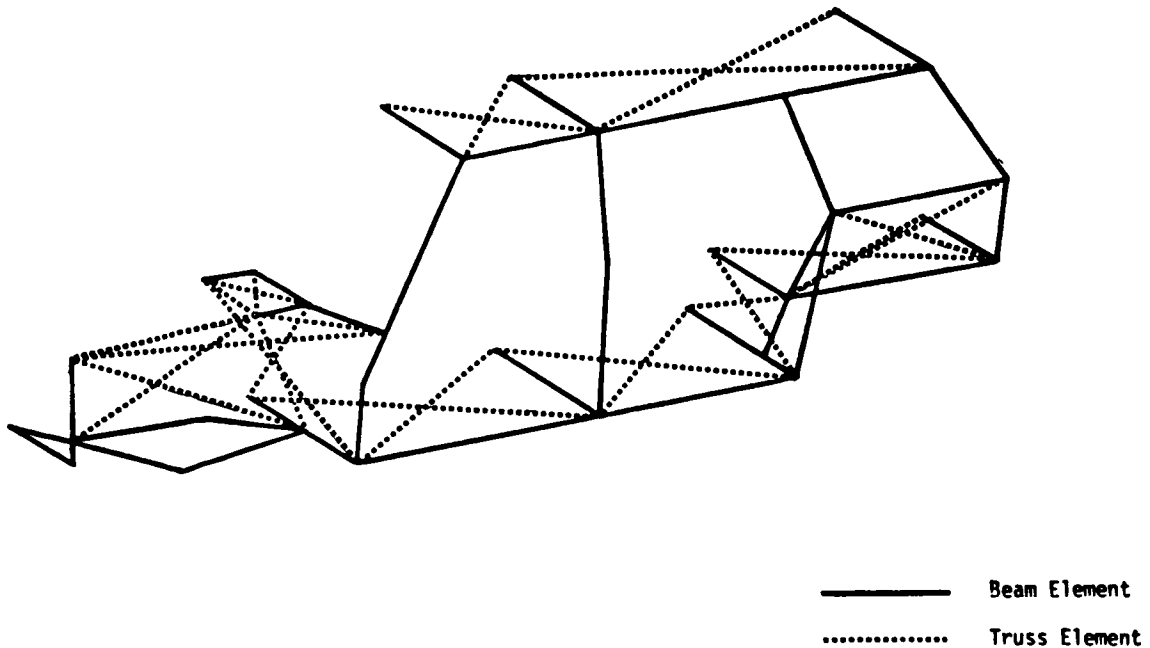
STRUCTURE I
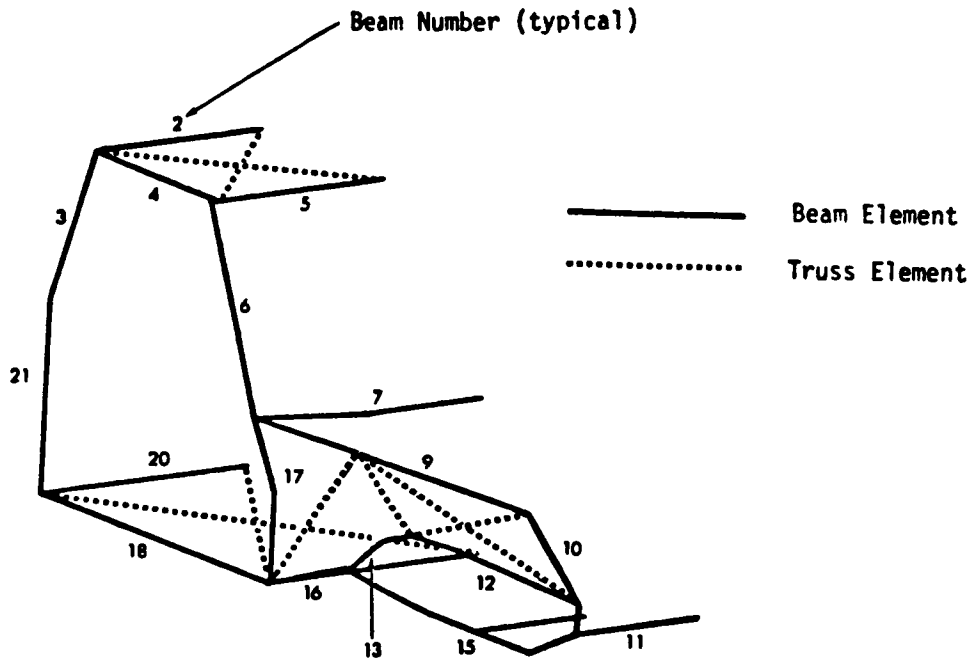
Figure 3

FRONT STRUCTURE II
(Rear structure common with Structure I)

Figure 4
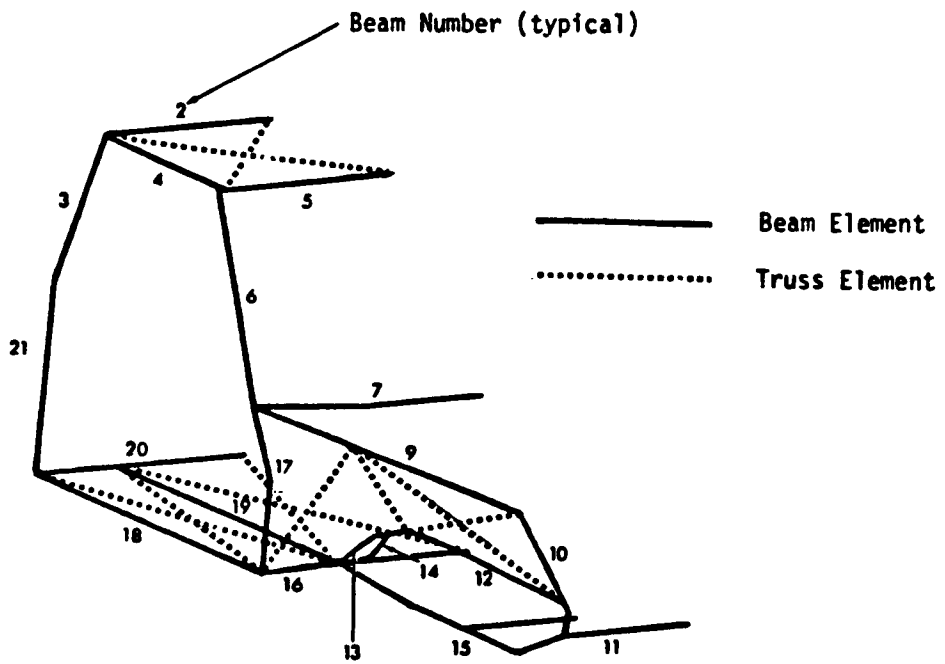


FRONT STRUCTURE III
(Rear structure common with Structure I)

Figure 5

# LOAD CONDITIONS AND CONSTRAINTS

It is necessary to include an extensive set of load conditions so that all possible critical load conditions are covered (Fig. 6). Typically, 10-15 loads, including static, inertia relief, and frequency conditions, are used.

## Symmetric Load Conditions

- Jacking (statics)
- 4 g bump both front wheels (inertia relief)
- 4 g bump both rear wheels (inertia relief)
- 1 g brake (inertia relief)
- Front bumper (inertia relief)
- Rear bumper (inertia relief)
- Roof crush (statics)
- Cowl crush (statics)
- Roof bow (statics)

## Asymmetric Load Conditions

- 4 g bump one front wheel (inertia relief)
- 4 g bump one rear wheel (inertia relief)
- Torsional jacking (statics)

## Frequency Constraints

- Symmetric - first mode > 18 Hz
- Asymmetric - first mode > 21 Hz

Figure 6

## OPTIMUM MASS SUMMARY

The total structural masses for the front end configurations considered are shown in Fig. 7. The lower III/upper I configuration, with a mass of 127.4 kg, was the lightest of the structures. It is interesting to note here that the difference in total mass between the lightest and heaviest of the acceptable designs is only 8.2 kg, approximately 6.5%. Given the apparent differences in the load-carrying capabilities and stiffness characteristics of the various front structures, it would seem that the structure, as a whole, must have been able to compensate for the inherent differences in load-carrying capacity of a particular configuration, resulting in a series of designs having virtually the same total mass but different mass distributions. This indicated that nonstructural reasons could be used to make the final selection. The important consideration here is that all designs met the same load criteria since they were all treated as constraints in the optimization. Thus, by entering the early phase of the design process, important design direction was given by optimization.

| Front Structure Configuration | Total Mass (kg) |
| --- | --- |
| 1. Lower III / Upper I | 127.4 |
| 2. Lower III / Upper II | 132.7 |
| 3. Lower II / Upper II | 135.2 |
| 4. Lower II / Upper I | 135.6 |

Figure 7

# ROCKER SECTION STUDY

As the design progresses, nonstructural decisions begin to dictate the shapes of various structural members. While the shapes of these members should be influenced by the earlier optimization study, often the nonstructural influences prevail. This effect can be evaluated as shown in Fig. 8. In this case, the proposed rocker section was replaced in the model and only the thickness was allowed to vary in this section. In addition, the rest of the design variables in the remainder of the structure were also allowed to change. The proposed irregular section produced a mass penalty of 4.51 g. This was deemed severe enough to attempt a redesign of this component. Again, this information is difficult to obtain without an optimization capability.
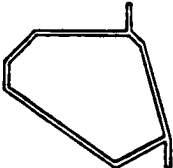
**Configuration**                                                    **Optimized Mass(kg)**

Baseline Model - Rectangular Rocker Section
(7.62cm x 11.23cm)                                                        112.0



Revised Rocker Section - Irregular Shape                                    116.5



Figure 8

# HOOD STRUCTURE OPTIMIZATION MODEL

As a final example, we will take the design of a secondary structural component of a typical construction in which the inner structure is primarily a beam structure and the outer is a plate structure (Fig. 9). This detailed model clearly would occur later in the design process, as opposed to the simpler models shown in the other two examples.

For this particular study, the outer structure was assumed to be of constant thickness. Each of the inner beams was assumed to be a channel section of constant thickness and size. The heights of all beams were set at 2.5 cm.

Two load conditions were used for this study. The first assumed the hood was supported on three of its four support points, and a deflection constraint of 2.0 cm was placed on the fourth point under a dead weight load. This load was the estimated final mass of the hood uniformly distributed on all nodes. The second load condition was the hood in its fully supported condition with a 75 kg load distributed over the center portion. Each load condition required a separate boundary condition set.

OUTER
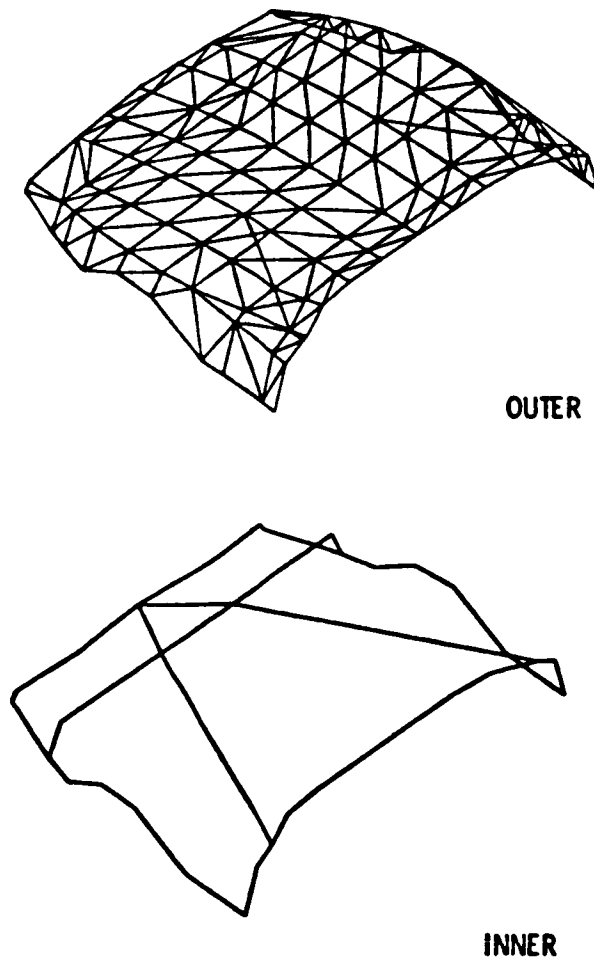
INNER

Figure 9

# HOOD STRUCTURE INNER CONFIGURATION

Three different stiffener patterns were optimized as shown in Fig. 10. As might be expected, the more triangulated structure required the lowest mass. In this design, the minimum width of the beam section was allowed to be a very small number (0.15 cm). As the width of the channel section approaches this number, the section approaches a blade type of stiffener, typical of molded SMC structures or a hem flange or turned edge in steel. As can be seen from Fig. 11, beams 3 and 4 reached this condition. Since beam 3 is on an edge, this suggests a turned edge would be sufficient. In this example, more detailed information about the final structure is being obtained.

Total Mass

28.9 kg

Mass = 22.6 kg

| Beam | t | width | flange | height |
|------|------|-------|--------|--------|
| 1 | .076 | 1.14 | .05 | 2.5 |
| 2 | .076 | 1.21 | .05 | 2.5 |
| 3 | .076 | .36 | .05 | 2.5 |
| 4 | .076 | .33 | .05 | 2.5 |
| 5 | .076 | 1.31 | .05 | 2.5 |
| skin | .076 | | | |

28.2 kg

skin mass = 17.3 kg
Beam mass = 5.3 kg

Dimensions in cm

22.6 kg
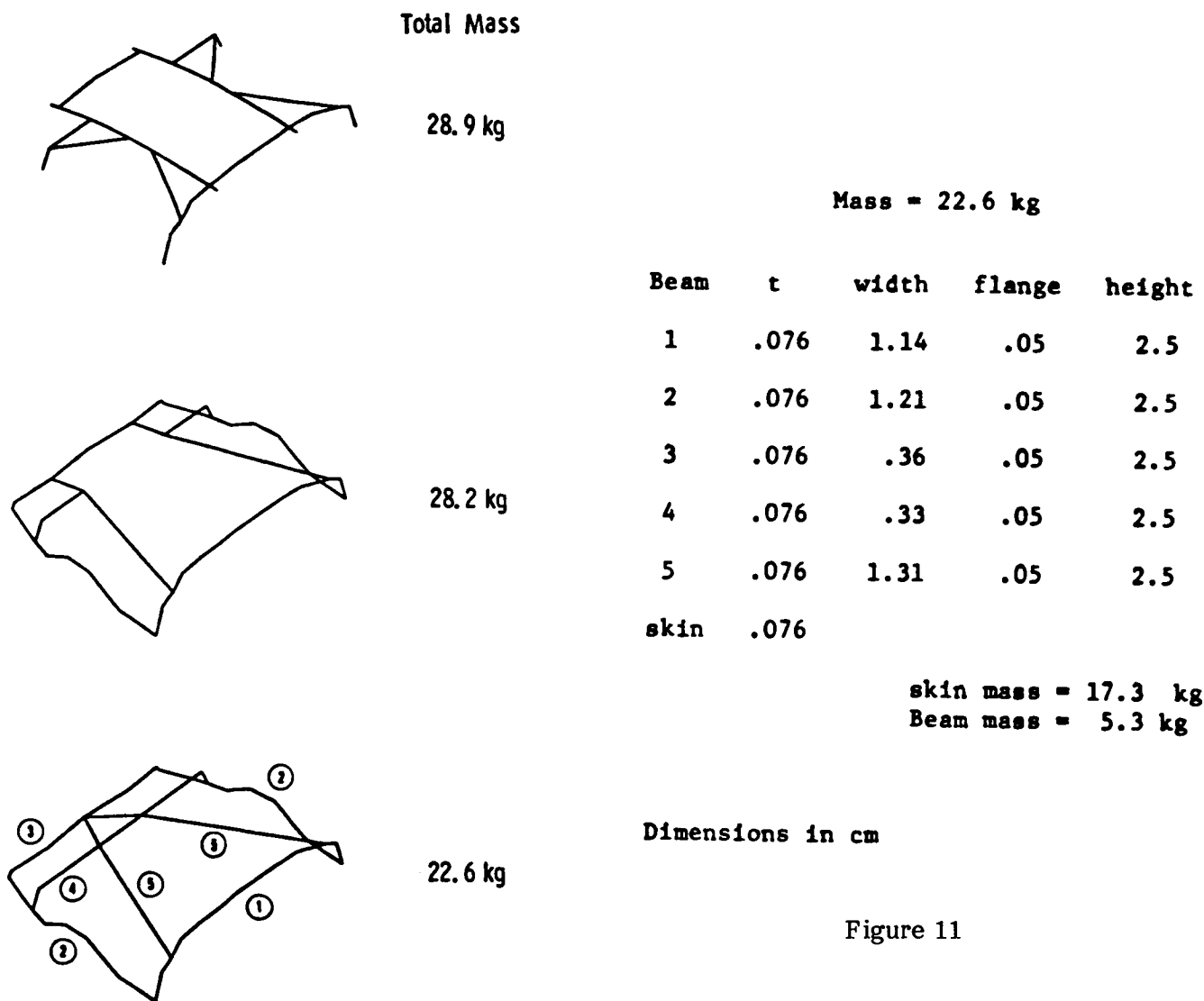
Figure 11

Figure 10

# BOUNDARY ELEMENTS

Ultimately one would like to merely describe the function and limitations of the structure in some conceptually convenient terms and then allow the computer to automatically make adjustments in some way to produce a best design. This process will require the implementation of a boundary-based description of the problem as opposed to a nodal description as used in typical finite element analysis programs. Since the design process will be under the control of an optimization program, the analysis mesh must continually be generated as the design changes. In addition, it is necessary to guarantee the continuing accuracy of the analysis as the design changes. These considerations suggest the integration of a boundary-based automatic mesh generation scheme with adaptive mesh refinement techniques and structural optimization to produce an effective shape optimization program.

A mesh generator for multi-connected, two-dimensional regions which requires only boundary information was chosen. This information is initially a continuous description which is then discretized. The algorithm then distributes points uniformly throughout the region and connects them to form triangles. An averaging form of smoothing is applied to produce triangles of roughly uniform shape. The problem can then be described in terms of a set of boundary design elements, each of which has associated with it a set of design variables (Fig. 12). As the design changes, the new mesh can be generated from the new boundary description.



i  Key Node

ⓘ  Boundary Element

$d_j$  Design Variable (typical)
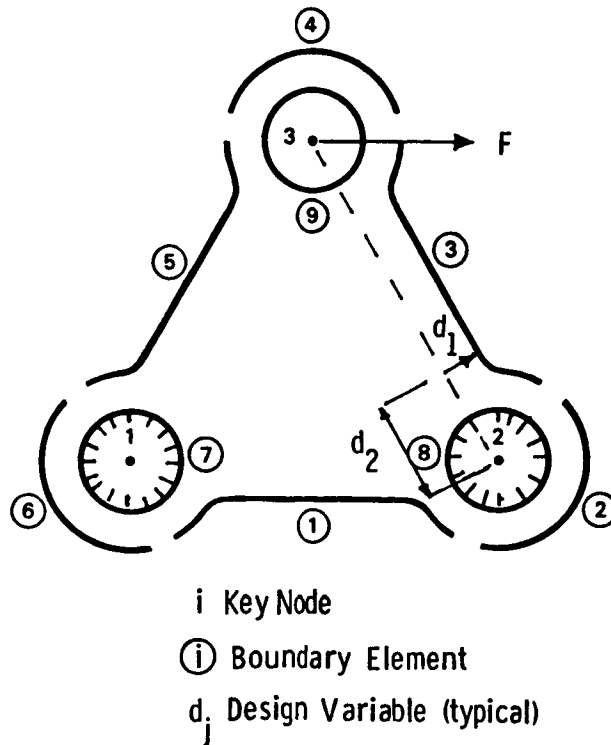
Figure 12

C - 3

# MESH REFINEMENT

When finite element analysis is used for a fixed configuration optimization, the integrity of the model is assured at the start of the optimization and is assumed to remain acceptable throughout the design process. However, when the design process is changing the shape of the part and the shape and location of cutouts, this assumption is no longer valid. One way of handling this problem is to use the concept of adaptive mesh refinement. In this concept, information from one analysis is used to identify regions of the finite element mesh which need further refinement. This refinement can take the form either of adding additional elements in the area to be refined or of increasing the order of the existing finite elements. The mesh refinement approach has been chosen since it can be used with existing elements and does not require the formulation of new finite elements. In addition, it can be effectively integrated with the mesh generation scheme described earlier since it merely involves the addition of more points to be triangulated. Regions of refinement are based on strain energy density (SED) gradient contours. Typical contours and a refined area are shown in Fig. 13.

UNREFINED

REFINEMENT AREAS

REFINED
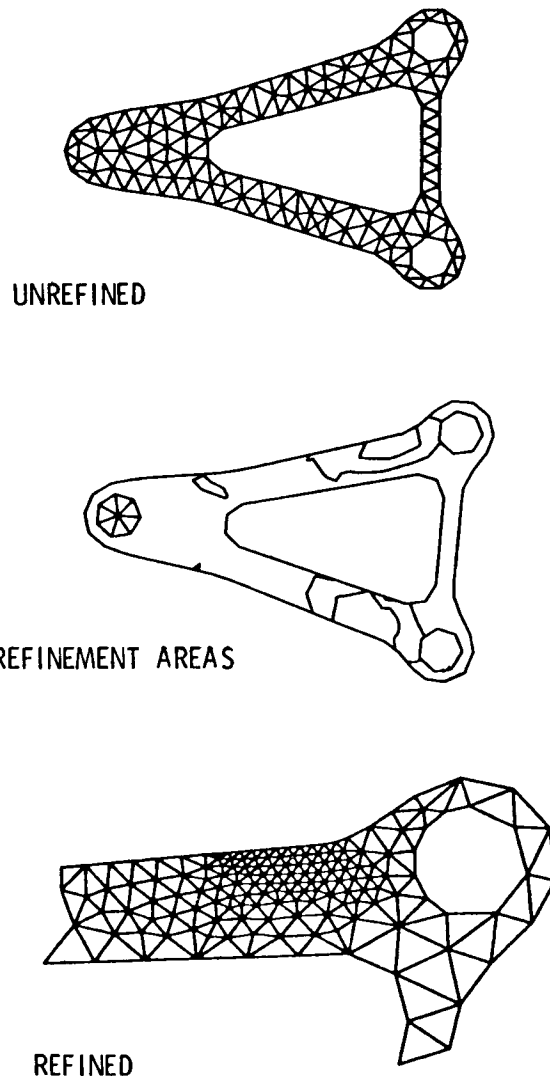
Figure 13

# NONPLANAR STRUCTURES

It is convenient to think of three distinct forms of nonplanar thin structures. The first of these structures, for example, can be described by a mathematical transformation from a simple flat surface into a cylindrical surface. Secondly, the surface may take the form of a general shallow shell which may not be obtained from a simple mapping relationship but can be obtained by projection. Thirdly, the structure may be made up of several segments which may be either planar or one of the two previously mentioned forms (Fig. 14). In each of these forms, the ideas discussed in Ref. 5 can be used in the planar form to describe the segments, generate the mesh, and carry out the refinement.

(a) Transformation

$$z = R \cos \theta$$

(b) Projection

$$z = Q(x,y)$$

Q = Interpolation Description of Surfaces

(c) Assembly of Segments
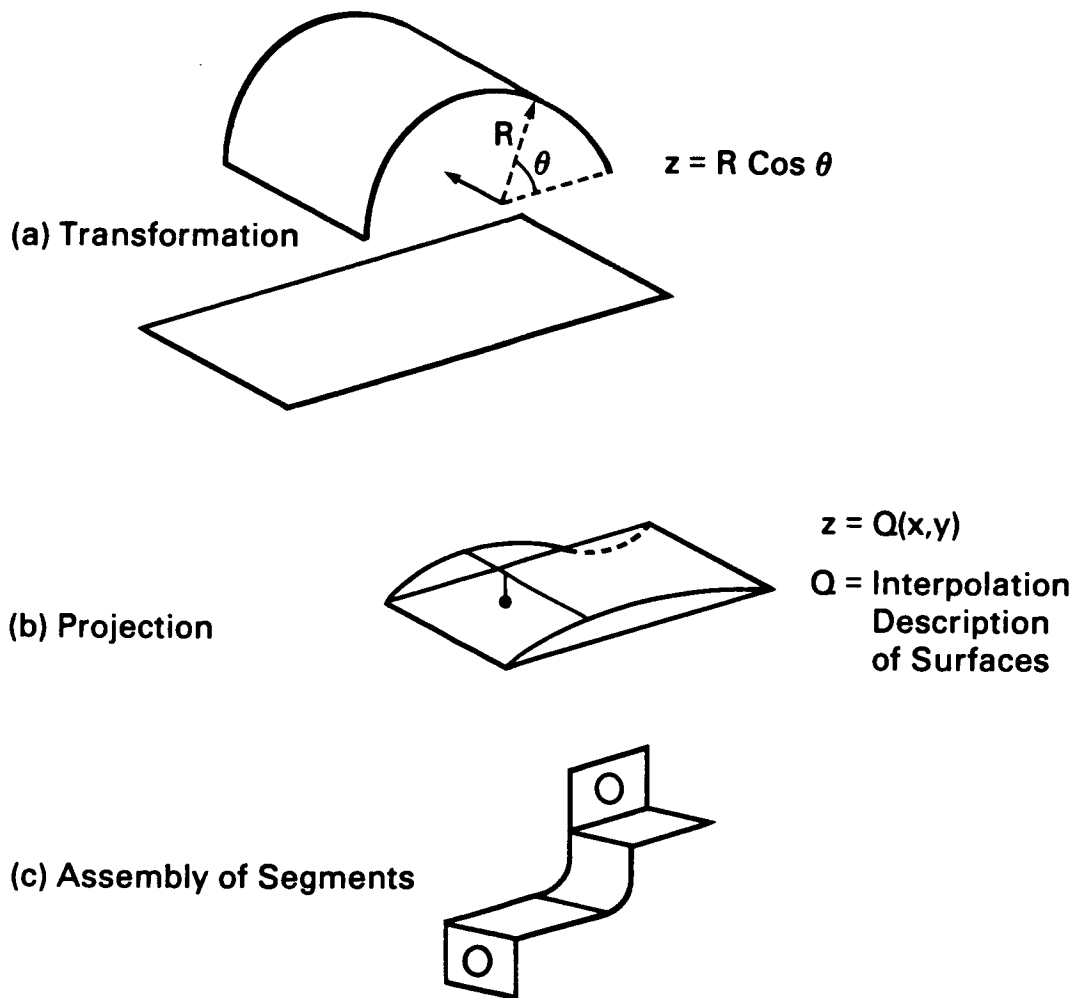
Figure 14

# FOLDED PLATE EXAMPLE

An example of a plate folded through a 90° angle is shown in Fig. 15. A static loading of 400 N is applied to point A normal to the plane of the triangular segment, thus causing bending moments in the plate. After the structure has been triangulated, it is rotated as required.

Eleven design variables control the shape of the plate. The outer edge of the lower segment is the double cubic shape design element type with four design variables. Each of the sloping outer edges of the upper segment is a double cubic but with only two design variables each. The size of the triangular interior cutout is controlled by the location of the key nodes. The z-coordinates of all the nodes and the x-coordinates of the two bottom nodes are variables. The variables are appropriately linked to yield a symmetric design. The material thickness was also allowed to vary but remained at minimum gage throughout the design.

The stress in the structure was constrained to be everywhere less than the yield stress. In addition, geometric behavior constraints were imposed to limit the minimum distance between boundary segments to be less than 0.29 cm.

A plot of mass versus optimization step number is shown in Fig. 16. Plots of the initial and final designs are shown in Figs. 15 and 17 with the strain energy difference contours showing the areas which were refined in the design. The size of the triangular cutout was limited by stress constraints. The boundaries along the folded edge, however, were controlled by the geometric behavior constraint which limits how close two edges may be to each other.
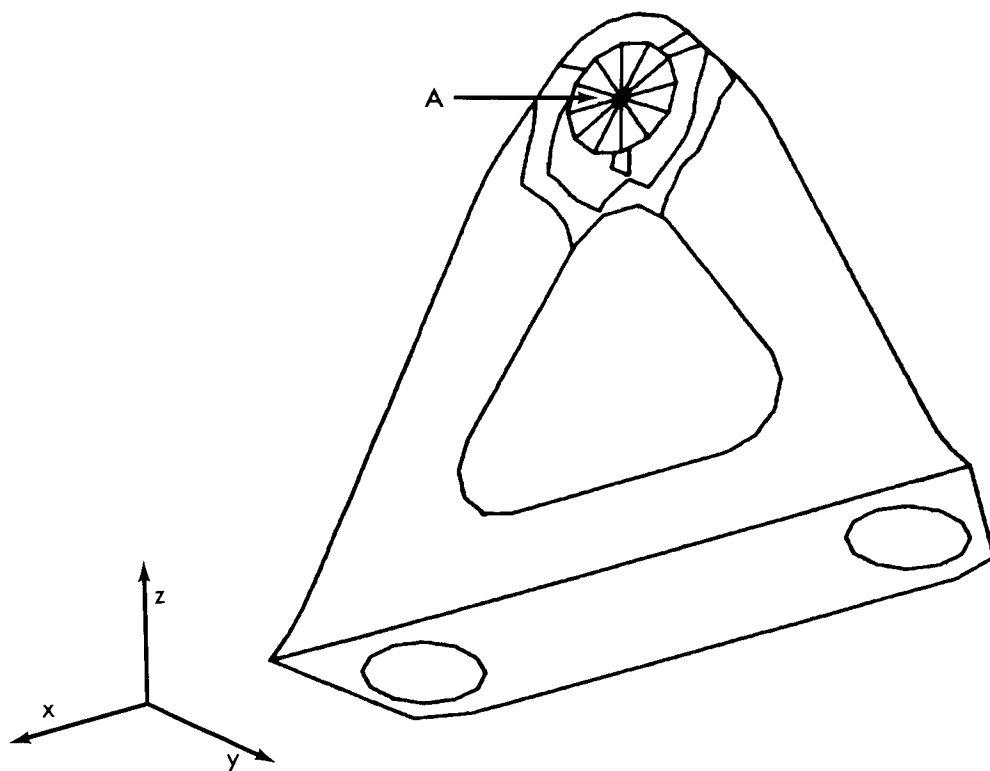


INITIAL DESIGN

Figure 15
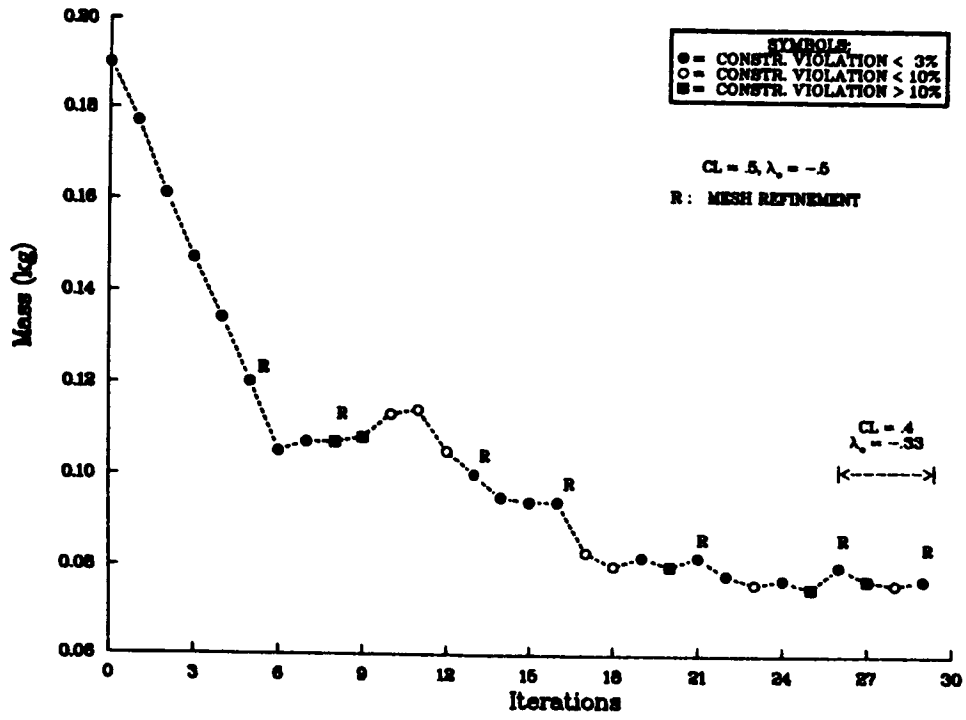
Figure 16
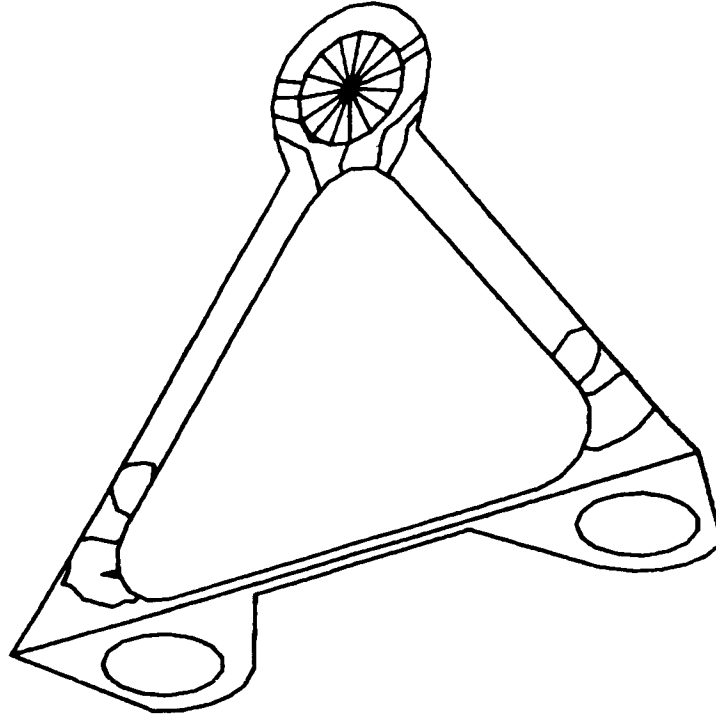


FINAL DESIGN

Figure 17

## OBSERVATIONS

1. The mathematical tools exist to develop an effective structural optimization program. These tools may have to be developed for a particular industrial situation.

2. Optimization can be most effective if it is initiated in the preliminary design phase with simple models when the critical parameters of the design can be most affected. This requires an easily used optimization program.

3. An organization arrangement where optimization is introduced through an analysis group which is appended to the traditional design and test organization will probably not be successful because by the time optimization is applied, few design freedoms will be available.

4. The finite element model used must be accurate and the load conditions and constraints must be carefully chosen. Therefore, the user must possess the same universality of view required of the traditional engineering designer with the appreciation of the numerical aspects required of the finite element analyst. This combination of skills is not evident in either distinct group, and it will be necessary to provide a thoughtful learning environment to produce engineers who can effectively use these new tools.

5. The approach taken in the shape optimization in which the finite element model is generated from a design description of the part suggests a direction which will resolve some of the concerns described above.

## REFERENCES

1. Bennett, J. A., and Botkin, M. E., "Automated Design for Automotive Structures," Journal of Mechanical Design, ASME Transactions, Vol. 104, October 1982, pp. 799-805.

2. Lust, R. V., and Bennett, J. A., "Structural Optimization in the Design Environment," Proceedings of the 4th SAE International Vehicle Structural Mechanics Conference, SAE Paper No. 811318, Detroit, MI, November 18-20, 1981.

3. Miura, H., Lust, R. V., and Bennett, J. A., "Integrated Panel and Skeleton Automotive Structural Optimization," Proceedings of the 4th SAE International Vehicle Structural Mechanics Conference, SAE Paper No. 811317, Detroit, MI, November 18-20, 1981.

4. Bennett, J. A., "Application of Linear Constraint Approximations of Frame Structures," Proceedings of the International Symposium of Optimum Structural Design, University of Arizona, Tucson, AZ, October 19-22, 1981.

5. Bennett, J. A., and Botkin, M. E., "Shape Optimization of Two-Dimensional Structures with Geometric Problem Description and Adaptive Mesh Refinement," Proceedings of the 24th AIAA Structures, Structural Dynamics, and Materials Conference, Lake Tahoe, NV, May 2-9, 1983.

6. Botkin, M. E., and Bennett, J. A., "Shape Optimization of Three-Dimensional Folded Plate Structures," 25th AIAA Structures, Structural Dynamics, and Materials Conference, Palm Springs, CA, May 14-16, 1984.

# TRADEOFF METHODS IN MULTIOBJECTIVE INSENSITIVE DESIGN OF AIRPLANE CONTROL SYSTEMS

Albert A. Schy
NASA Langley Research Center
Hampton, Virginia 23665

and

Daniel P. Giesy
Kentron International, Inc.
Hampton, Virginia 23666

This talk presents the latest results of an ongoing study of computer-aided design of airplane control systems, which is based on satisfying requirements on multiple objectives. Constrained minimization algorithms are used, with the design objectives in the constraint vector [1]. We briefly review the concept of Pareto optimality and show how an experienced designer can use it to find designs which are well-balanced in all objectives [2,3]. Then we will discuss the problem of finding designs which are insensitive to uncertainty in system parameters, introducing a probabilistic vector definition of sensitivity which is consistent with the deterministic Pareto optimal problem [4]. Insensitivity is important in any practical design, but it is particularly important in the design of feedback control systems, since it is considered to be the most important distinctive property of feedback control. Methods of tradeoff between deterministic and stochastic-insensitive (SI) design are described, and tradeoff design results are presented for the example of a Shuttle lateral stability augmentation system. This example is used because careful studies have been made of the uncertainty in Shuttle aerodynamics [5]. Finally, since accurate statistics of uncertain parameters are usually not available, the effects of crude statistical models on SI designs are examined.

# OUTLINE

- REVIEW PARETO-OPTIMAL MULTIOBJECTIVE DETERMINISTIC AND STOCHASTIC-INSENSITIVE (SI) DESIGN.

- FORMULATE METHODS OF TRADEOFF BETWEEN DETERMINISTIC AND STOCHASTIC-INSENSITIVE DESIGN.

- DISCUSS TRADEOFF DESIGN RESULTS FOR SHUTTLE LATERAL STABILITY AUGMENTATION SYSTEM EXAMPLE.

- EXAMINE EFFECTS OF INACCURATE STATISTICAL MODELS ON STOCHASTIC-INSENSITIVE DESIGN.

# MULTIOBJECTIVE DESIGN BY CONSTRAINED MINIMIZATION

The Pareto-optimal formulation of multiobjective design is not an optimization method in the usual sense, since it does not determine a unique solution. Pareto-optimal solutions comprise that portion of the boundary of the achievable domain which is noninferior to all others in the sense that every other solution must be worse in at least one objective. In the literature on multiobjective optimization it is generally assumed that some higher-level "decision maker's" logic exists which can lead to an optimal solution. We assume, to the contrary, that no optimal solution exists for practical multiobjective design problems. Our Pareto-optimal algorithm is a valuable tool for the designer, since it enables the computer to calculate example Pareto-optimal solutions using a constrained minimization algorithm. However, the quality of the design depends on critical decisions made by the designer, who must choose the objective functions and values of associated scaling parameters which lead to solutions which are well-balanced in the disparate objectives, control the tradeoff iterations, and choose the final design. Rather than seeking some undefinable optimization index for complex systems, the design process is based on whatever computable objectives the designer considers important, with consideration of computational cost subordinated to the designer's judgment.

- **PARETO-OPTIMAL FORMULATION**

- **THERE IS NO OPTIMAL SOLUTION**

- **COMPUTER CALCULATES EXAMPLE PARETO-OPTIMAL SOLUTIONS USING CONSTRAINED MINIMIZATION ALGORITHM**

- **DESIGNER INTERACTION IS ESSENTIAL**
  - **CHOOSES AND SCALES OBJECTIVES**
  - **CONTROLS TRADEOFF ITERATIONS**
  - **CHOOSES FINAL DESIGN**

191

In this figure we present the constrained minimization formulation which leads to the example Pareto-optimal designs. Let $z$ be the vector of design variables, $\eta$ a scalar dummy variable, and $f(z)$ the vector of objective functions, and let $g(z) \leq 0$ represent a vector of auxilliary constraints. Then for arbitrary vectors $a$ and $b$ (with $b_j > 0$), solution of the constrained minimization problem on the first line leads to a design on the boundary of the achievable domain which is at least locally Pareto optimal. It is well known that this minimization problem is equivalent to the min-max problem on the second line. The particular solution obtained depends on the choice of $a$ and $b$. Suppose the designer chooses for $a_j$ values of the objectives which he considers marginally acceptable, and another set of very desirable objectives, $a_{D_j}$. Then defining $b = a - a_D$ should yield a solution well balanced in the objectives, since $a$ and $a_D$ have been so chosen. This method, known as the "Goal Attainment Method" [6], is illustrated in the sketch. The cross-hatched curve indicates the boundary of the achievable domain in objective space, and the part between the cross-hatched bars is the Pareto domain. At any iteration the constraints on $f$ are at $(a + \eta b)$. As $\eta$ is minimized the constraints move toward the boundary, and the solution is forced to the deterministic optimal, $f_D^*$, corresponding to the minimum $\eta_D^*$. The line joining $f_D^*$ and $a$ plays an important role in the tradeoff formulations.
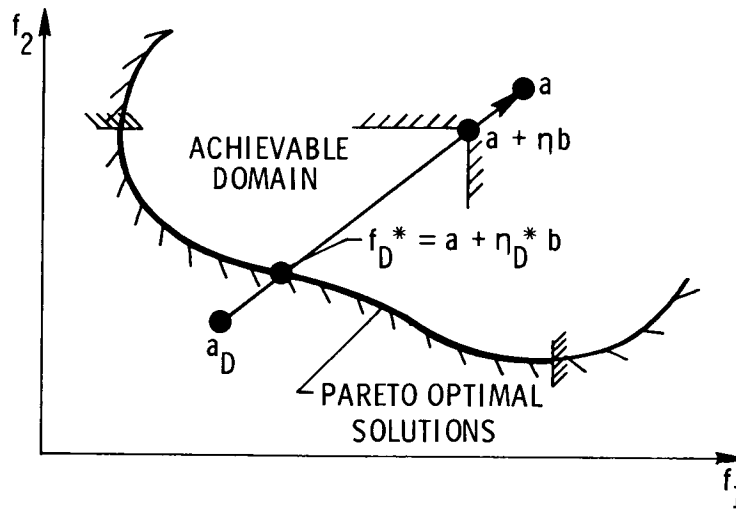


$$\text{MIN } \eta \quad \text{s.t. } f(z) \leq a + \eta b \text{ AND } g(z) \leq 0$$
$$z, \eta$$

$$\text{EQUIVALENT TO:} \quad \text{MIN MAX}_{z \quad j} \left[ \frac{f_j(z) - a_j}{b_j} \right], \quad b_j > 0$$

$$\text{GOAL ATTAINMENT:} \quad b = a - a_D$$

We now formulate the SI design algorithm and two tradeoff methods. The designer must specify a vector, y, of parameters with significant uncertainties and their probability distributions. Then the objective functions are f(z,y), and the stochastic sensitivity vector, s(z), is defined by the probabilities that specified requirements will be violated; i.e., that $f_j(z,y) > \hat{f}_j$, where $\hat{f}$ is a vector of requirement values.

Since this definition is only useful when $\hat{f}_j > f_{D_j}^*$ , it is desirable to solve the deterministic problem first. Defining the Pareto-optimal SI design as that which minimizes the maximum sensitivity, the constrained minimization algorithm takes the form shown. Computational problems will be discussed later, but it is worth noting that insensitive design does not require accurate calculation of the probabilities.

Both tradeoff methods use a scalar parameter to vary a vector inequality along the line of varying constraints shown on the sketch for the deterministic design. For $\hat{f} \approx f_D^*$, the SI designs must be very like the deterministic. Introducing a scalar parameter, $\hat{\tau}$, and defining $\hat{f}(\hat{\tau})$ as in Method 1, $\hat{\tau} \approx 1$ gives deterministic-like solutions, and decreasing $\hat{\tau}$ provides a sort of tradeoff procedure, with increasing emphasis on insensitive design. Method 2 is a more precise tradeoff. Here $\hat{f}$ is fixed at a value giving insensitive design, and constraints on nominal objectives, $\bar{f}$, are varied in a similar manner giving a tradeoff between sensitivity and nominal values of objectives.

# PARETO-OPTIMAL STOCHASTIC-INSENSITIVE DESIGN (SI)

### DEFINE: $s(z) \triangleq \underset{y}{PROB} [f(z,y) > \hat{f}]$, $\hat{f} > f_d^* = a + \eta_d^* b$

$$MIN \; \eta \; S.T. \; s(z) \leq \eta, \; g(z) \leq 0$$
$$z, \eta$$

# TRADEOFF METHODS IN SI DESIGN

## 1. VARY $\hat{f}$ WITH SCALAR $\hat{\tau}$.

$$\hat{f}(\hat{\tau}) = a + \hat{\tau} \; \eta_d^* b$$

## 2. VARY CONSTRAINTS ON NOMINAL f-VALUES

### FIX $\hat{f}$ AND CONSTRAIN $f(z,\bar{y}) \triangleq \bar{f}(z) \leq a + \bar{\tau} \; \eta_d^* b$

# DESCRIPTION OF EXAMPLE CASE

The example case is design of a lateral stability augmentation system (SAS) for Shuttle entry at $M = 2.5$. The linearized lateral response equations are 4th order. System states are sideslip angle ($\beta$), yaw rate (r), roll rate (p) and bank angle ($\phi$). Controls are aileron and rudder. The control law has 6 feedback gains (SAS design does not require bank angle feedback) and 2 feedforward gains from the pilot's stick input ($\delta_{ap}$) to the controls. The general design objective is to obtain rapid, stable roll response to the stick input, with small sideslip. This example was chosen because statistical uncertainties in Shuttle aerodynamics have been carefully studied, and at $M = 2.5$ these uncertainties have been found to cause unacceptable variation in lateral response using aerodynamic controls [5]. Nevertheless, in the example we use only aerodynamic controls. The design parameter vector z is comprised of the 8 gains. The uncertain parameter vector y contains all 6 aerodynamic control effectiveness coefficients and the 3 sideslip coefficients. (The $\phi$-equation is kinematic and contains no aerodynamic effects.) Uncertainty in control effectiveness will clearly have a strong effect on control system design, and lateral response is sensitive to the sideslip coefficients. In stability axes the standard deviations of the 3 types of coefficients are fairly consistent, and approximate values are shown for sideslip ($A_{i1}$), aileron ($B_{i1}$) and rudder ($B_{i2}$) coefficients. Rudder effectiveness is most uncertain. The y-statistics are considered gaussian and include correlation estimates.

$$\dot{x} = Ax + Bu, \quad x^T = (\beta, r, p, \varphi), \quad u^T = (\delta_a, \delta_r)$$

$$u = Kx + C\,\delta_{ap}, \quad K \triangleq \begin{bmatrix} K_{11} & K_{12} & K_{13} & 0 \\ K_{21} & K_{22} & K_{23} & 0 \end{bmatrix}, \quad C = \begin{bmatrix} C_1 \\ C_2 \end{bmatrix}$$

z-VECTOR: 8 CONTROL SYSTEM GAINS

y-VECTOR: 6 CONTROL EFFECTIVENESS ($B_{ij}$) AND 3 SIDESLIP ($\beta$) DERIVATIVES ($A_{i1}$)

$\sigma_y$-VALUES ($M = 2.5$): $\sigma(A_{i1}) \approx 14\%$, $\sigma(B_{i1}) \approx 12\%$, $\sigma(B_{i2}) \approx 20\%$

## DESIGN OBJECTIVES FOR SHUTTLE LATERAL SAS

In this study, 11 deterministic design objectives are considered. Generally, these are based on military handling-qualities requirements for large transports. Stability is a basic requirement, and the 4 characteristic roots must be considered separately because the requirements in the various modes differ. The bank angle achieved in 6 seconds is the speed of response objective. Decoupling of the rolling motion from yaw-sideslip is achieved by keeping the peak sideslip small and $\left| \omega_\phi^2 / \omega_d^2 \right|$, a ratio of coefficients in the roll transfer function, near unity. For the Shuttle, small sideslip is also a heat-load requirement. It is always desirable to keep control effort small. Since the natural stability of the Shuttle is inadequate, it is clear that saturation in control deflection must be avoided. Rate saturation can lead to violent nonlinear instability. Therefore, the objectives of minimizing the peak control deflections and rates are included. Finally, the sensitivities of the 11 objectives, as previously defined, are also included as objectives. Although the functions $f(z,y)$ are nonlinear in $y$, the stochastic sensitivities were first calculated using a linear-gaussian assumption. These probabilities were checked using a Monte Carlo program, and all but the peak value probabilities were acceptably accurate. Acceptable accuracy was obtained by replacing the probability of violation for the maximum peak by the worst probability for any pair of peaks, using a bivariate gaussian routine. These approximate probabilities are used as the sensitivity functions in the tradeoff studies.

| CATEGORY | OBJECTIVE |
|---|---|

### DETERMINISTIC, $\bar{f}_J(z)$:

| CATEGORY | OBJECTIVE | |
|---|---|---|
| STABILITY | CHARACTERISTIC ROOTS | (4) |
| SPEED OF RESPONSE | BANK ANGLE IN 6 SECONDS | (1) |
| DECOUPLING | PEAK SIDESLIP AND $\left\| \omega_\varphi^2 / \omega_d^2 \right\|$ | (2) |
| CONTROL EFFORT | PEAK MAGNITUDES AND RATES | (4) |

### STOCHASTIC SENSITIVITIES, $s_J(z)$:

| CATEGORY | OBJECTIVE | |
|---|---|---|
| PROBABILITIES OF VIOLATING $\hat{f}$-REQUIREMENTS | $\underset{y}{\mathrm{PROB}} \left[ f_J(z,y) > \hat{f}_J \right]$ | (11) |

195

This figure shows how the sensitivity of the control system varies for the simpler tradeoff method, varying the value of $\hat{f}$. The 4 solid curves give Monte Carlo results for SI designs with $\hat{f}$ values at $\hat{\tau} = 0$, .2, .4 and .6. The Monte Carlo method uses the nonlinear objective functions, so that these probabilities are a more realistic estimate of the sensitivities obtainable using the linear-gaussian approximation in the SI program. Decreasing values of design $\tau$ give designs with more emphasis on insensitivity. The heavy dot on each curve shows the Monte Carlo sensitivity at the design value of $\hat{f}$. Since the probability of violation depends on $\hat{f}$, the curve shows the sensitivity variation with $\hat{f}$, to give a more complete picture of the sensitivity properties. Each curve can be thought of as a sort of vector cumulative distribution function, showing how the worst $P_j$ increases from 0 to 1 as $\hat{\tau}$ increases. The curves are not smooth, because different $P_j$ become worst as $\hat{\tau}$ varies. For comparison, the calculated optimal sensitivities and the Monte Carlo sensitivity values for the deterministic design are also shown. Although the Monte Carlo sensitivities for the 4 SI designs are much larger than the calculated values, comparison with the deterministic results shows that the SI designs are an order of magnitude less likely to have bad values of the objective functions. The usefulness of the probability approximation appears questionable for design $\hat{\tau} < 0.4$. For example, at $\hat{\tau} = 0$ the Monte Carlo sensitivity for the $\hat{\tau} = 0$ design is somewhat larger than those for the $\hat{\tau} = .2$ or .4 designs. Nevertheless, it is clear that the approximation is adequate to yield very significant decreases in sensitivity for SI designs compared to deterministic designs.
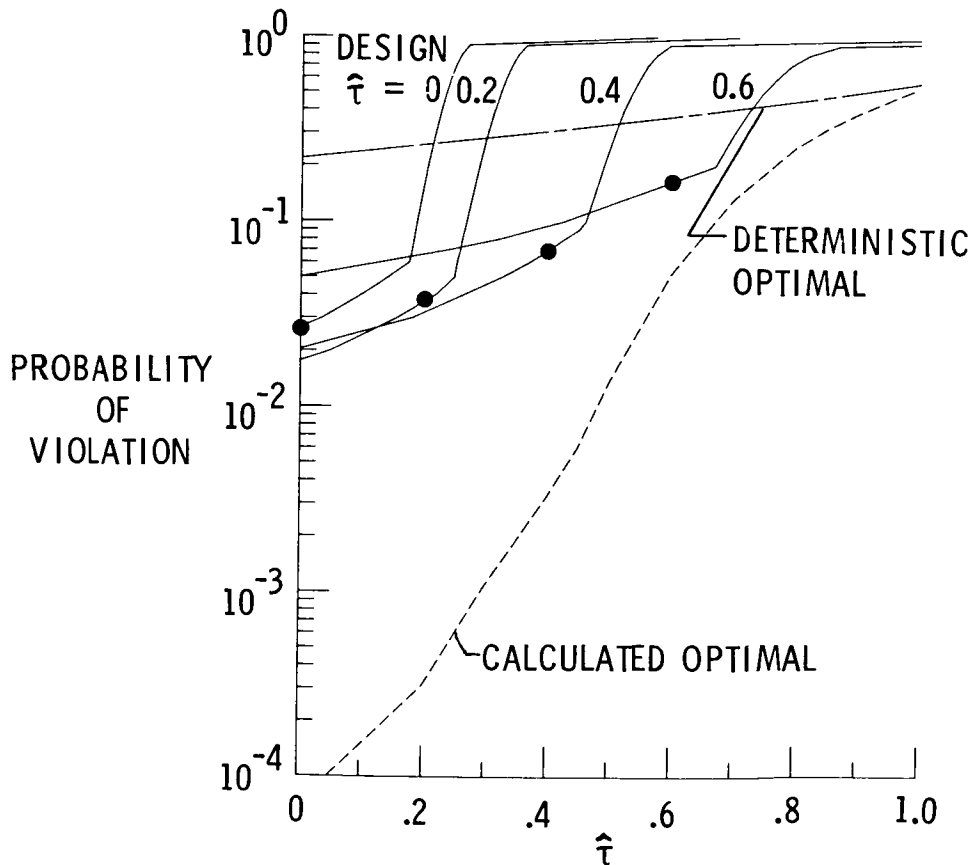
# VARIATION OF SI DESIGNS WITH $\hat{f}(\hat{\tau})$

It is interesting to examine how important properties of the design vary as $\hat{\tau}$ varies from near unity (deterministic-like designs) to lower values, with increasing emphasis on insensitivity. The variation of 4 typical control system gains is shown on the left, and the nominal values of 3 typical objectives and their standard deviations on the right. There are clearly significant changes in design properties in the transition from deterministic designs to those emphasizing low sensitivity. However, as noted in the previous figure, there seems little significant change in gains or other system properties in designs for $\hat{\tau} < 0.4$. As seen on the right, the main tradeoff penalty in nominal objectives for decreased sensitivity is loss of speed of response, as indicated by the bank angle at 6 seconds, $\bar{\phi}(6)$. Typical of the other objectives are the oscillatory damping ratio, $\bar{\zeta}$, which is relatively unchanged, and the damping in roll, $|\bar{\lambda}_R|$, which increases. Note that 2 of the standard deviations decrease for the insensitive designs, but $\sigma_\lambda$ actually increases. This is permitted because of the large increase in $|\bar{\lambda}_R|$. The computer finds gains to meet the varying probability constraints, with freedom to use whatever combinations of $\bar{f}$-values and $\sigma$-values are required.
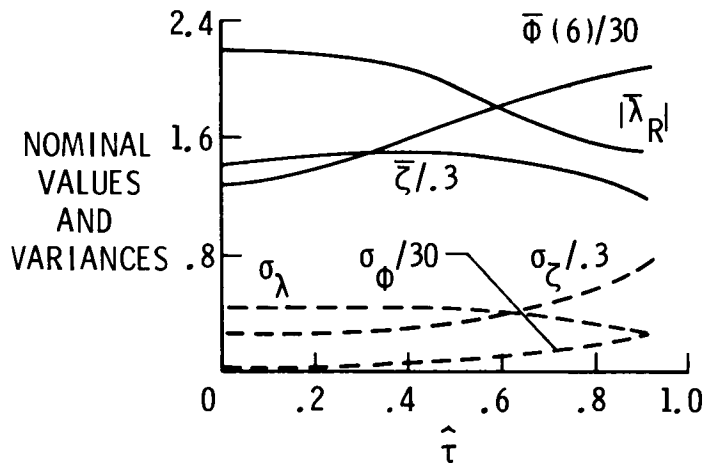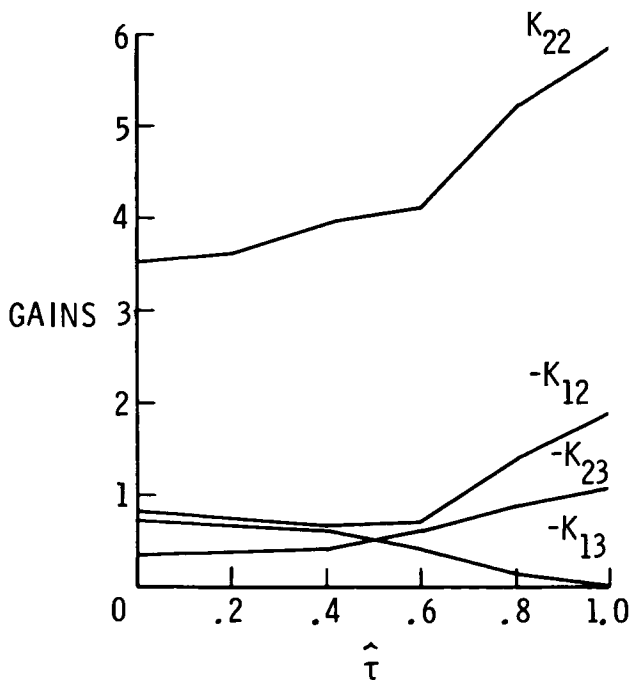
This figure presents Monte Carlo results of the more precise tradeoff between insensitivity and nominal values of objectives. Starting with the SI design at $\hat{\tau} = 0$ as the unconstrained design emphasizing insensitivity, increasingly stringent constraints are imposed on the nominal values by varying $\overline{\tau}$ in $\overline{f}(z) \lesssim a + \overline{\tau}\eta_D*b$. The probability of violation for the constrained designs is shown in the solid curves. Although this method gives more precise control of the values of $\overline{f}_j$ obtained in each SI design, this set of solutions seems similar to the set obtained by simply varying $\hat{\tau}$. In the tradeoff varying $\hat{\tau}$, there was a significant increase in the probability of violations at low $\hat{\tau}$ between designs at $\hat{\tau} \leq .4$ and $\hat{\tau} = .6$. Here the corresponding increase in sensitivity (i.e., the probability of bad objective values) occurs between the designs for $\overline{\tau} = .6$ and $\overline{\tau} = .8$. In problems where the probabilities can be calculated accurately (probabilistic design rather than insensitive design), this more precise method might be preferred, in spite of the added computational burden of adding the hard constraints. Also, there is a certain logical appeal to constraining the nominal objectives to good values while minimizing the probability that the objectives will be worse than marginally acceptable. For our applications, however, accurate statistics are not obtainable, and the simpler method seems preferable.
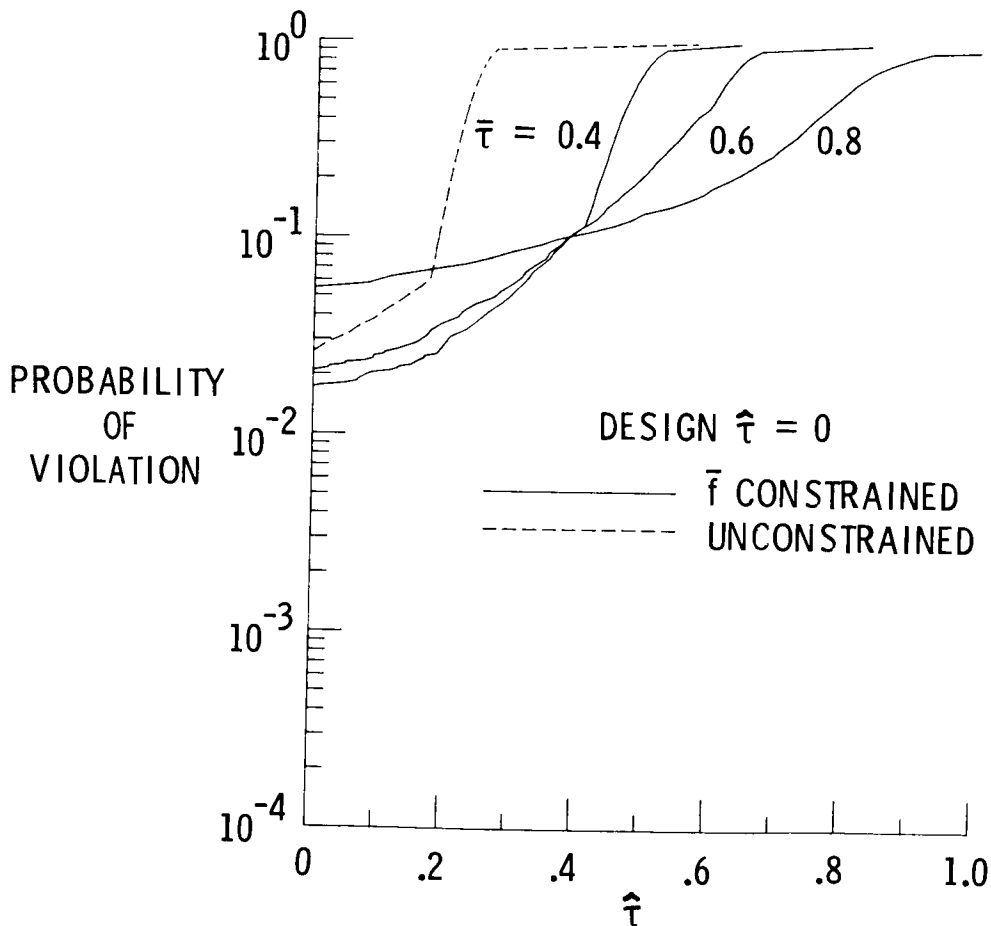
## EFFECTS OF CRUDE STATISTICAL MODEL ON SI DESIGN

In practice, inaccuracy in f-statistics resulting from the linear assumption is likely to be dominated by inaccuracy of the input values of the y-statistics. The statistics for the Shuttle example are more accurate and detailed than would usually be available for control system design. To investigate the effects of using a cruder estimate of the y-statistics on SI design, it was assumed that the sideslip, aileron and rudder coefficients had standard deviations equal to 15%, 15% and 20% of their nominal values, respectively, with no correlations. These crude statistics were used for SI design at $\hat{\tau}$ = 0.4, and this design is compared with the original design at $\hat{\tau}$ = 0.4 and the deterministic design. The figure shows Monte Carlo probabilities based on the Shuttle statistics. The curves are cumulative distribution functions for $\phi(6)$, the objective which always shows a large penalty in expected value in SI designs, and peak $\delta_r$, which is always critical in the calculated probabilities for the SI design. The simplified input statistics give an SI design which has the same basic properties and approximately the same sensitivity as obtained with the more accurate statistics. Although the effectiveness of the SI design does not seem to require an accurate statistical model, accurate calculation of the probabilities does require accuracy of the statistical model. For both SI designs, the simplified statistics predict much larger probabilities of violation than the accurate statistics, and it was found that almost all the discrepancy was caused by neglecting the y-correlations.



DETERMINISTIC
STOCHASTIC, $\hat{\tau}$ = 0.4 ROCKWELL STATS.
STOCHASTIC, $\hat{\tau}$ = 0.4 SIMPLIFIED STATS.

## NO CONTROL LIMITING

Although statistical distribution curves are the best way to compare designs for sensitivity to off-nominal parameters, simulated time histories of off-nominal responses are also useful. The Monte Carlo random set of responses for each control system was ranked using a weighted sum of violations of desired objective values, and time histories of nominal and 5 off-nominal responses at the 99th percentile for 3 SI designs are compared in this figure. The solid curves show the responses of the nominal system and the broken curves are the off-nominal responses. These cases are from the set shown in the tradeoff varying $\hat{f}$, in which it was noted that there is a significant increase in the probability of bad objective values for design at $\hat{\tau} \geq 0.6$. This increased sensitivity is shown here by the increase in scatter of the off-nominal responses for the design at $\hat{\tau} = 0.6$. The tendency for decreased nominal speed of response for the less sensitive designs is evident in the roll rate responses, $p(t)$, and the tendency for large peak values of rudder and rudder rate in the off-nominal responses is evident in the $\delta_r(t)$ responses. In fact, the $\hat{\tau} = 0.6$ off-nominal responses all violate the rudder rate limit of 12°/sec. The next figure includes the control limits in the integration routine to show the destabilizing effect of rate limiting.
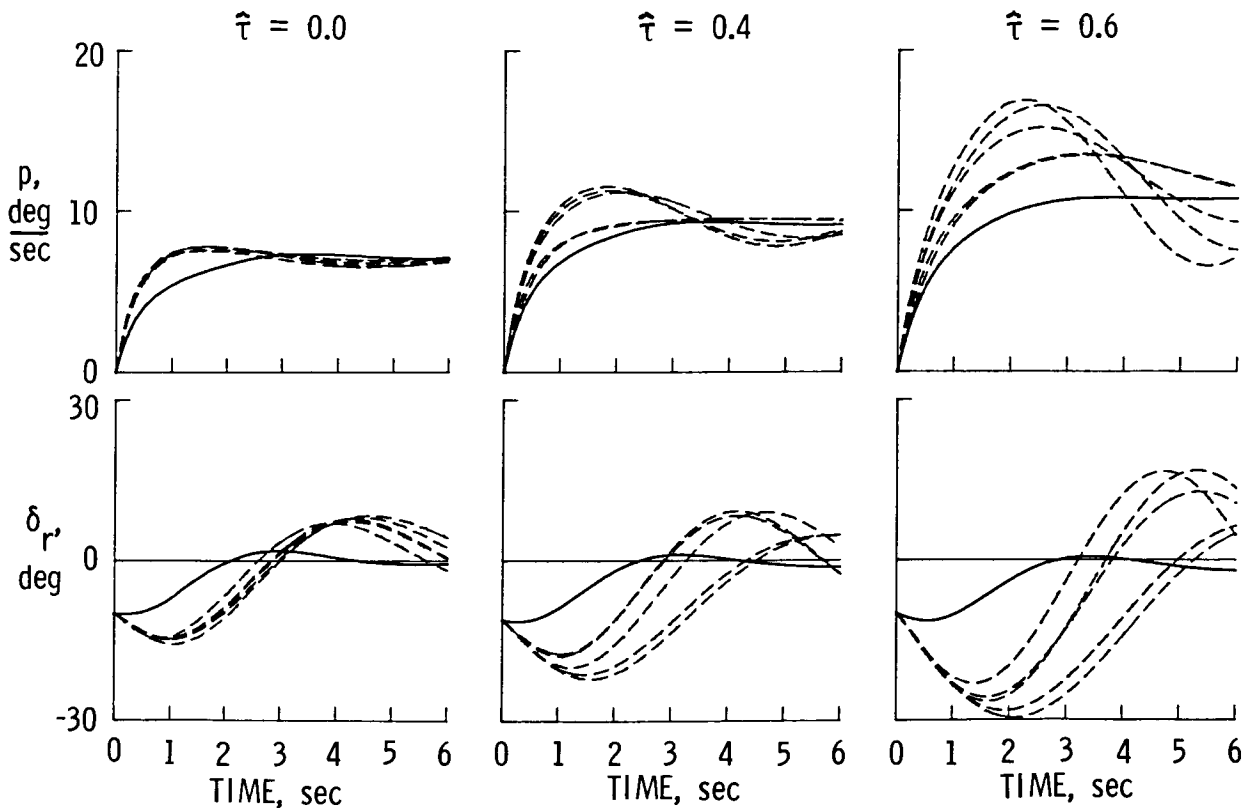
# NOMINAL AND OFF-NOMINAL RESPONSES FOR 3 SI DESIGNS

## INCLUDES CONTROL LIMITING

This figure shows the importance of using peaks in control deflections and rates as design objectives when it is likely that control limiting may occur. Deflection limiting is dangerous when the uncontrolled airplane is unstable, but the nonlinear delays introduced by rate limiting can cause violent instability in an inherently stable system, as shown in these responses for $\hat{\tau} = 0.6$. Although the SI design method calculates only the linear responses, the designer can control the probability that the peaks will violate the control limits, as shown in the results for $\hat{\tau} = 0$ and 0.4. In this case the $a_j$ values for control peaks were chosen at the limiting values and the $a_{D_j}$ values were 20% below the limits. The probabilities at $\hat{\tau} = 0$ are the probabilities that limiting will occur in the linear responses, and keeping these low implies that the probability of control-limiting instability will be low.
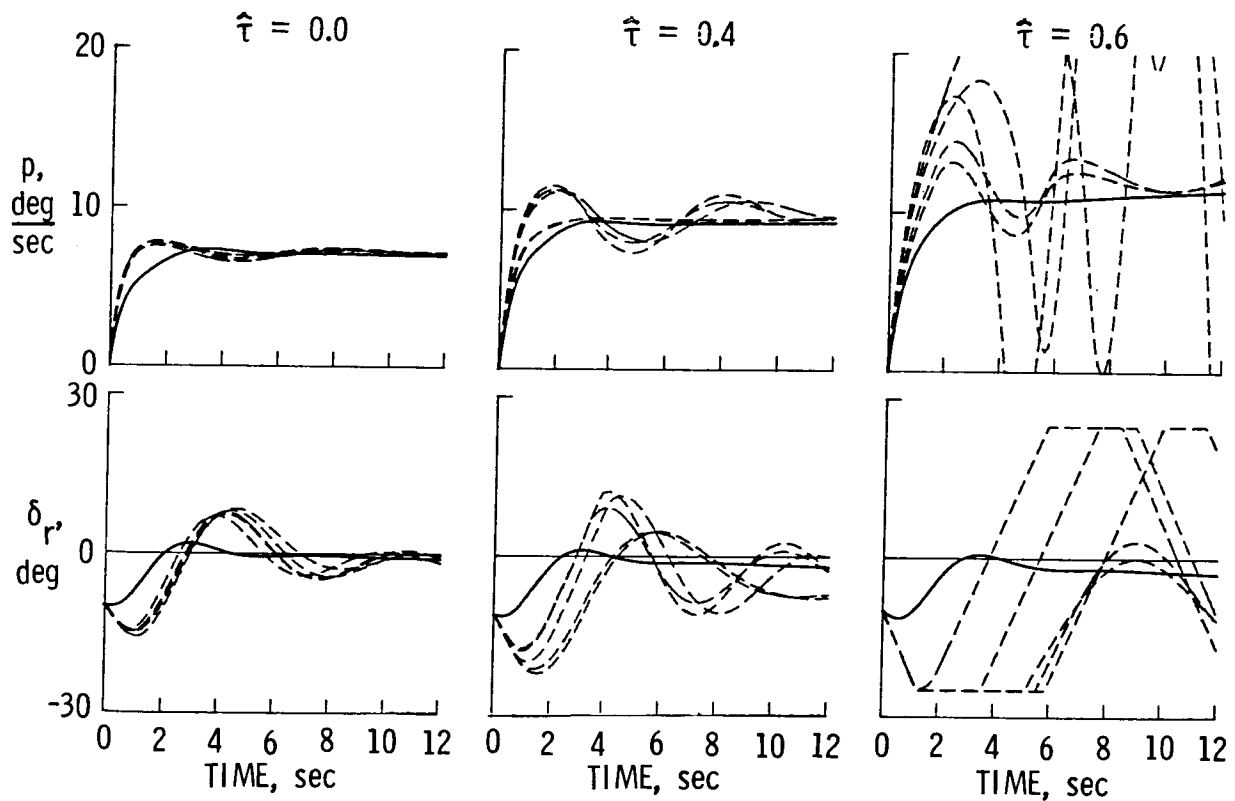
The Pareto-optimal stochastic insensitive design method defines a
vector sensitivity which is related in a very natural way to a set of
objectives chosen by an experienced designer. The designer must also make
important decisions to formulate the constrained minimization algorithm for
obtaining Pareto-optimal insensitive designs which are well balanced in the
objectives and for trading off between insensitivity and nominal values.
The designer, not the computer, makes the critical decisions which deter-
mine the quality of the design. The effectiveness of the method depends on
the designer's judgment, but this makes it easy for him to interact with
the program.

The main conclusions of this study are listed on the figure. The SI
method yields control system designs with very significant decreases in
sensitivity to parameter uncertainty. The effectiveness of the method does
not depend on having an accurate statistical model. The tradeoff studies
show that there are distinct differences between designs emphasizing insen-
sitivity and deterministic designs. For example, there are large gain
changes as emphasis on insensitivity increases. The two tradeoff methods
are both effective in compromising between insensitivity and nominal values
of objectives. Although the method utilizes only linear response calcula-
tions, it produces designs which are less likely to encounter nonlinear
control-limiting instabilities. Finally, in the example case, the main
penalty for achieving insensitivity was decreased nominal speed of
response. It will be interesting to see if further study shows this
to be a general property of insensitive control system designs.

STOCHASTIC-INSENSITIVE DESIGN GIVES A SIGNIFICANT DECREASE IN
SENSITIVITY TO PARAMETER UNCERTAINTY IN SPITE OF INACCURACY OF
CALCULATED PROBABILITIES.

TRADEOFF STUDIES SHOW THAT SI DESIGNS ARE DISTINCTLY DIFFERENT
FROM DETERMINISTIC DESIGNS.

SEVERAL EFFECTIVE METHODS WERE DEVELOPED FOR OBTAINING DESIGNS
WHICH COMPROMISE BETWEEN INSENSITIVITY AND NOMINAL OBJECTIVE
VALUES.

INSENSITIVE DESIGN CAN BE ESPECIALLY EFFECTIVE WHEN CONTROL
LIMITING IS A PROBLEM.

IN THE SHUTTLE LATERAL SAS EXAMPLE, THE MAIN PENALTY FOR
ACHIEVING INSENSITIVE DESIGNS WAS REDUCED VALUE OF NOMINAL
RESPONSE SPEED.

# REFERENCES

1.  A. A. Schy, W. M. Adams, Jr., and K. G. Johnson:  Computer-Aided Design of Control Systems to Meet Many Requirements.  Proceedings of 17th AGARD Meeting On Advances in Control Systems, Geilo, Norway, 1973.

2.  A. A. Schy, D. P. Giesy, and K. G. Johnson:  Pareto-Optimal Multi-Objective Design of Airplane Control Systems.  Proceedings of 1980 JACC, San Francisco, CA, August 1980.

3.  V. Pareto:  Cours d'Economie Politique Professé à l'Université de Lausanne, Vols. 1 and 2. Lausanne, Switzerland, F. Rouge, 1896.

4.  A. A. Schy and D. P. Giesy:  Multiobjective Insensitive Design of Airplane Control Systems With Uncertain Parameters.  Proceedings of AIAA Guidance and Control Conference, Albuquerque, NM, August 1981.

5.  Anonymous:  Aerodynamic Design Data, Vol. 1 - Orbiter Vehicles.  NASA CR-60686, 1978.

6.  Florian W. Gembicki:  Performance and Sensitivity Optimization:  A Vector Index Approach.  Ph.D. Thesis, Case Western Reserve University, 1974.

STAEBL -- STRUCTURAL TAILORING OF ENGINE BLADES (PHASE II)

M. S. Hirschbein
NASA Lewis Research Center
Cleveland, Ohio


K. W. Brown
Pratt & Whitney Aircraft Company
East Hartford, Connecticut

## Structural Tailoring of Engine Blades (STAEBL)

The STAEBL program was initiated at NASA Lewis Research Center in 1980 to introduce optimal structural tailoring into the design process for aircraft gas turbine engine blades. As indicated in Figure 1, the standard procedure for blade design is highly iterative with the engineer directly providing most of the decisions that control the design process. The goal of the STAEBL program has been to develop an automated approach to generate structurally optimal blade designs.

The program has evolved as a three-phase effort with the developmental work being performed contractually by Pratt & Whitney Aircraft. Phase I was intended as a "proof of concept" in which two fan blades were structurally tailored to meet a full set of structural design constraints while minimizing DOC+I (direct operating cost plus interest) for a representative aircraft. This phase was successfully completed and was reported in references 1 and 2. Phase II has recently been completed and is the basis for this discussion. During this phase, three tasks were accomplished: (1) a nonproprietary structural tailoring computer code was developed; (2) a dedicated approximate finite-element analysis was developed; and (3) an approximate large-deflection analysis was developed to assess local foreign object damage. Phase III is just beginning and is designed to incorporate aerodynamic analyses directly into the structural tailoring system in order to relax current geometric constraints.

### The Goal of STAEBL:  Automated Engine Blade Design

o   Current Design Procedure:

The engineer performs design iterations manually

o   STAEBL Procedure:

Apply mathematical optimization to blade design

### The Evolution of STAEBL

o   Phase I (Completed):   Proof of Concept

Demonstrate the ability to realistically structurally tailor gas turbine engine blades

o   Phase II (Completed):  Develop Software System

Develop a nonproprietary structural tailoring software system with dedicated structural analyses

o   Phase III (Current):   Aerodynamic Analysis

Incorporate  aerodynamic analyses into STAEBL to relax geometric constraints

Figure 1

## STAEBL Procedure

The overall procedure developed for STAEBL during Phase I is shown in Figure 2. The tailoring process was divided into two stages: (1) approximate analysis; and (2) refined analysis. The first stage, outlined by the dotted line, uses approximate analyses for vibration, flutter, stress and FOD (foreign object damage) along with an optimizer to find a candidate optimal design. The COPES/CONMIN optimization code developed by G. N. Vanderplaats was selected as the optimizer for STAEBL [3, 4]. Once a candidate design is found, it is passed to the second stage where refined analyses are performed to evaluate the design against imposed constraints. If all constraints are met, the design is accepted as the optimal design. Otherwise, the constraints imposed during the approximate analyses are modified to reflect the differences between the two levels of analysis, and the structural tailoring procedure is repeated.

During Phase II the approximate analyses and the optimizer were incorporated into a nonproprietary computer code. Also, specialized approximate analyses were developed for basic structural analysis (stress and vibration) and for local FOD analysis.



Figure 2

207
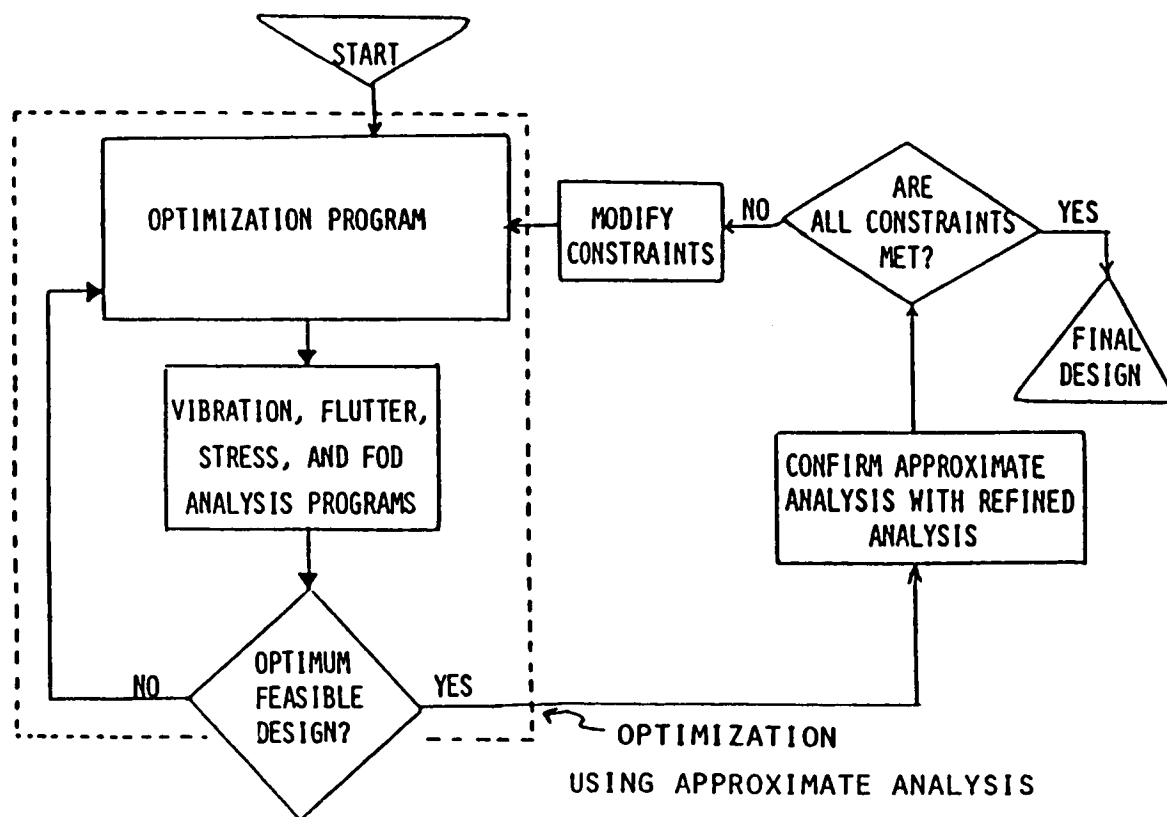
## Demonstration Cases

During Phase I and II, two shroudless fan blade designs were used to demonstrate the effectiveness of STAEBL. These designs are a superhybrid composite fan blade and a hollow titanium fan blade with a composite inlay, shown in Figure 3. The starting point for these designs was a hollow, shroudless titanium fan blade designed by Pratt & Whitney Aircraft as part of the NASA-sponsored Energy Efficient Engine program. Also, during Phase II a solid titanium compressor blade was optimally tailored using STAEBL.

The fan blade cases were selected because of the difficulty in designing an acceptable shroudless blade relative to a shrouded blade. Typically, fan blades are designed with a mid-span shroud that ties neighboring blades together under normal operating conditions. The shroud acts as a connecting ring which greatly stiffens the blade in torsion and bending. Without the shroud the blade can be very susceptible to flutter due to a low torsional natural frequency and may undergo excessively large deflections as a result of a bird strike. However, shrouds add extra weight to the fan stage and result in unwanted aerodynamic blockage.

The independent design variables for the blades included root chord, thickness-to-chord ratio, material thickness, and composite fiber angle. In the case of the hollow blade, the cavity size and location could also be varied. The number of blades was not constant but varied inversely with the blade chord to maintain a fixed solidity.

STAEBL WAS DEMONSTRATED ON TWO FAN BLADES OF ADVANCED CONSTRUCTION



Figure 3

208
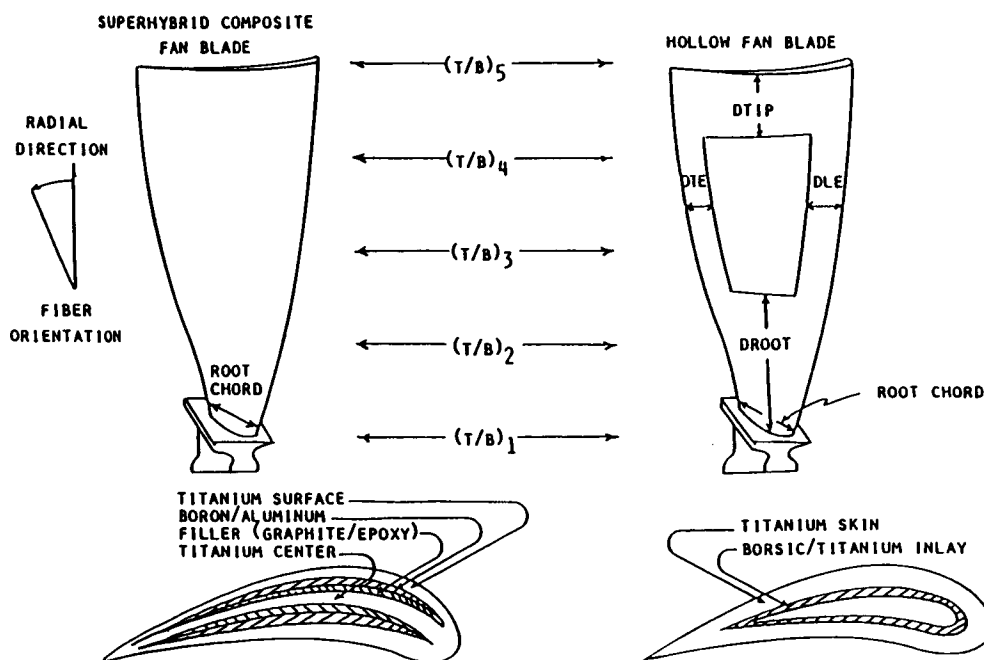
# Design Constraints

In order for the STAEBL procedure to be demonstrated as a useful approach to design engine blades, realistic constraints were imposed on all candidate optional designs, as listed in Figure 4. Geometric constraints consisted of upper limits on thickness-to-chord ratio along the span, and minimum allowable titanium skin thickness and boundaries on the cavity for the hollow fan blade. Engine order resonances were avoided by requiring a frequency margin of 5% for critical engine order/mode combinations. Maintaining this margin over the normal operating range is accepted procedure for avoiding high-cycle fatigue failure. During Phase II an additional option was added to explicitly calculate the forced response of a blade subjected to specified loads of engine order frequencies. Aeroelastic stability was maintained by requiring aerodynamic excitations to be negatively damped in the first three modes (1st and 2nd bending and 1st torsion modes). A critical requirement for fan blades is that they survive a bird strike. During Phase I local damage was based on an empirical factor. This was replaced by an approximate large-deflection analysis during Phase II. A modal response was used in both phases for root bending. The final constraint, stress, was evaluated from a beam analysis during Phase I. During this phase, the beam analysis was also used for the modal analysis. This beam analysis was replaced by an approximate finite-element analysis during Phase II.

Thickness-to-Chord Ratio
Titanium Skin Thickness
Cavity Boundaries

Resonance Margins
    1st Mode    2E (engine order)
    2nd Mode    3E
    2nd Mode    4E
    3rd Mode    4E
    Tip Mode    10 E (compressor)

Flutter-log Decrement
    1st Mode
    2nd Mode
    3rd Mode

F O D    (Bird Ingestion)
    Local Severe Damage
    Root Bending

Stresses
    Steady
    Fatigue
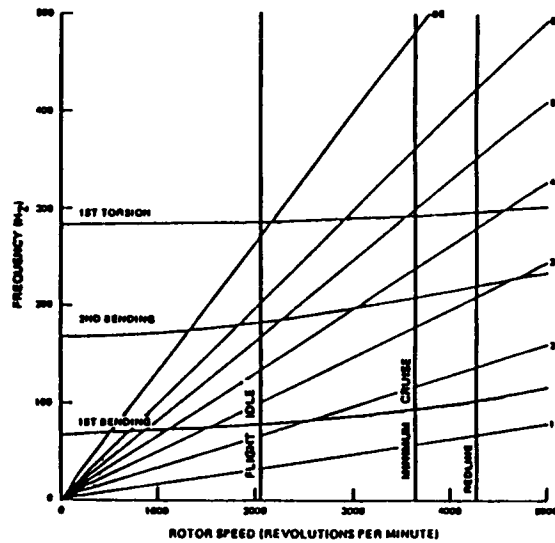


Figure 4

## Structural Tailoring -- Phase I

The two demonstration cases run during Phase I of the STAEBL program were compared to a hollow shroudless titanium blade. In both cases two complete passes through the tailoring system were performed. The final results are shown in Figure 5. The hollow blade converged to an initial optimal blade after 13 iterations. Refined analysis showed stress and resonance constraints to be violated. Correction factors were applied to the constraints to reflect differences between refined and approximate analyses. After the second tailoring, requiring ten iterations, a resonance constraint was still violated. The cause of this violation was traced to incompatibilities between the approximate beam analysis of the blade and the refined finite-element analysis. No further tailoring was attempted. The near-optimal blade weighed 52% less than the reference blade and DOC+I was reduced by .45%. However, due to the 18% reduction in chord, more blades are needed for the stage. As such, the total blade weight per stage decreased by about 40%. The superhybrid blade required 15 iterations to converge to the first optimal candidate design. Refined analysis showed that one resonance and one flutter constraint were not satisfied. Correction factors were applied and a second tailoring requiring 13 iterations was performed. This design satisfied all constraints. The total blade weight for the stage was decreased by about 30% and DOC+I was reduced by .36%. While the reductions in DOC+I are small in absolute terms, engine component improvements which change DOC+I by a few tenths of a percent are considered to be significant.

|  | Reference Blade (Hollow Titanium) | Hollow Titanium Blade With Composite Inlays | Superhybrid Blade |
|---|---|---|---|
| Root Chord (in.) | 9.12 | 7.46 | 8.32 |
| Blade Weight (lb.) | 19.2 | 9.3 | 12.1 |
| $\Delta$(DOC+I) (%) |  |  |  |
|    Engine Wt. | -- | -.33 | -.23 |
|    Engine Cost | -- | -.15 | -.18 |
|    Maintenance | -- | +.03 | +.05 |
|    Total | -- | -.45 | -.36 |
| Active Constraints | 2nd Mode 3E 1st Mode Flutter Local FOD | Min. Blade Thickness Cavity Location 2nd Mode 3E* 2nd Mode Flutter | Min. Blade Thick. 1st Mode Flutter Local FOD |

\* This constraint was not met completely when the tailoring was terminated

Figure 5

# Specialized Finite-Element Analysis

During Phase I of the STAEBL program a beam model was used for approximate structural analyses. During Phase II a specialized coarse mesh finite-element analysis was developed and incorporated into STAEBL. The analysis utilizes variable thickness triangular plate elements to model the blade and Guyan reduction to reduce the size of the assembled mass and stiffness matrices. Lamination theory is used to model the different material layers through the thickness of the blade including the hollow cavity which is considered to be a layer with very small mass and stiffness. Guyan reduction is used to eliminate selected degrees of freedom and to condense the model into three sparse columns of nodes: one near the leading edge of the blade, one near the trailing edge, and one at mid-chord. The accuracy of this analysis was demonstrated on a model of the hollow titanium reference fan blade as shown in Figure 6. The data in the figure compares the natural frequencies of an equivalent beam model used during Phase I and a specialized plate model with a refined plate model. The error between the beam model and the refined model is about 9%, 3%, and 4.5% for the first, second, and third mode, respectively, while the corresponding error for the approximate plate model is uniformly about one-tenth as large. Also, the computer analysis time for the plate analysis, including model generation and reduction, is about the same as the solution time for the simpler beam analysis and only about 6% of the solution time for the refined analysis.

$E^3$ FAN BLADE NATURAL FREQUENCIES (CPS)

|  | APPROXIMATE BEAM MODE 66 DOF | SPECIALIZED PLATE MODEL 24 DOF.* | NASTRAN PLATE MODEL 1260 DOF |
|---|---|---|---|
| 1ST MODE | 101.0 | 92.9 | 93.0 |
| 2ND MODE | 216.3 | 209.8 | 209.2 |
| 3RD MODE | 288.7 | 274.6 | 276.1 |
| COMPUTER TIME (CPU SEC) | 6.0 | 6.2** | 109 |

*. REDUCED FROM 330 DOF
** INCLUDES MODEL GENERATION AND DOF REDUCTION

Figure 6

## Approximate Severe FOD Analysis

One of the fundamental constraints imposed on turbine engine fan blades is the ability to survive a bird strike. This takes the form of surviving strong bending moments at the blade root and resisting severe local damage in the impact zone. Modal analysis of the blade with an impulsive impact load can be used adequately to estimate root bending. However, local damage analysis typically requires a fully nonlinear large-deflection analysis with an interacting impactor model. This involves too much computational effort to be useful for design iterations and, as such, empirical parameters are usually used as was done during Phase I of the STAEBL program. During Phase II an approximate large-deflection finite-element analysis was developed with an interactive representative loading model, depicted in Figure 7. The finite-element analysis models the impact region by retaining standard linear elastic bending in the chordwise direction but uses fully yielded large-deflection membrane action in the spanwise direction. This results in a model with linear mass and stiffness matrices which can be analyzed by conventional means. The bird is modeled by a representative loading profile which interacts with the blade to determine relative impact velocity and angle of impact which is used to identify the loaded nodes, peak pressure, and load duration. The approach taken is to use the first 10 natural modes to expand the deflections and loads in the impact region. The equations are then integrated numerically to determine structural response.



Figure 7

212
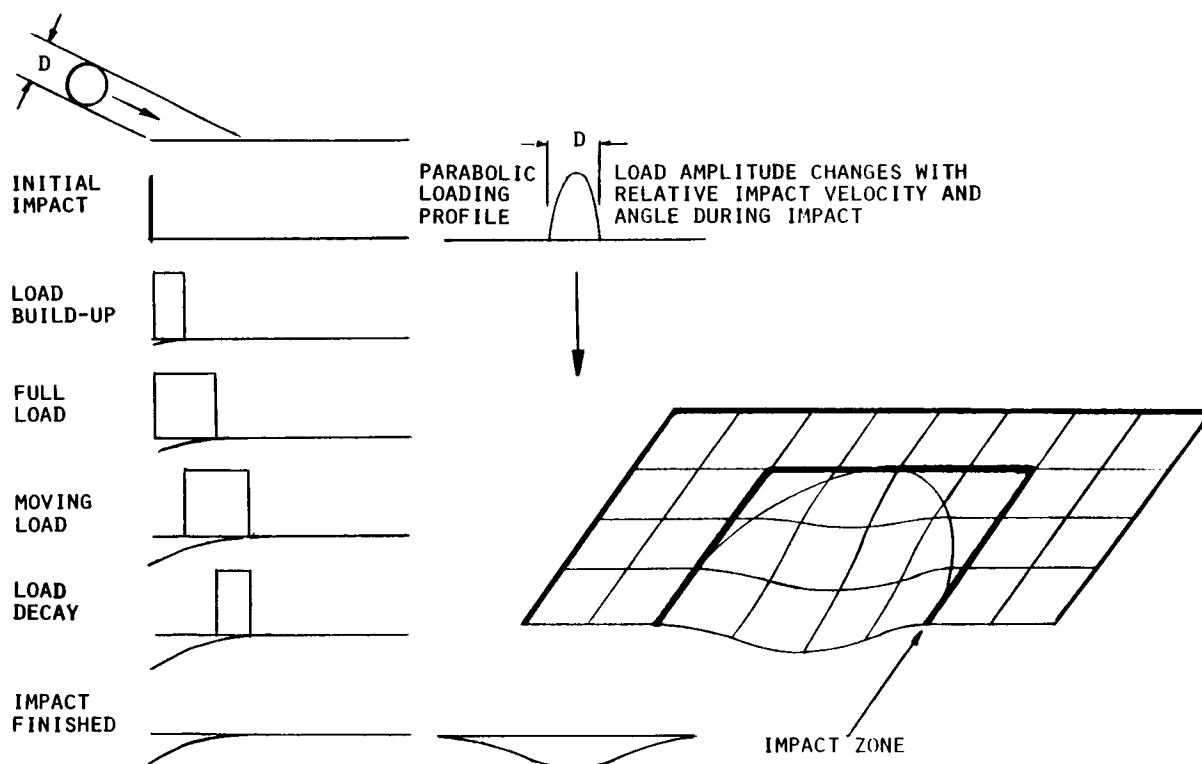
## Impact Analysis Demonstration Cases

The accuracy of the approximate severe FOD analysis was demonstrated by comparison with a refined, fully nonlinear, large-deflection finite-element analysis using a nonlinear interacting fluid impactor model. The refined analysis was calibrated against experimental data in which a 1" diameter gelatin ball was fired at a thin titanium plate clamped on three sides [5]. Two experimental cases were run: a "light" impact with an impact velocity of 12,400 in/sec. and a "severe" impact with a velocity of 19,000 in/sec. In both cases the angle of impact was 30°. The plate was 6" x 3" x .067" for the light impact and was tapered from mid-chord toward the free edge. For the severe impact, the maximum plate thickness was .126". The results from the approximate and refined analyses are shown in Figure 8. Note that in both impact cases the average strains for the two levels of analysis agree very well and the overall final deflection shapes are in good agreement. Differences between the peak strains for the two analyses are large. However, the approximate average strains can be scaled uniformly to agree with the refined analysis peak strains for the two cases shown. Finally, the computer time for the approximate analysis was only about .6% of the time required for the refined analysis. As such, the approximate severe FOD analysis can provide a good estimate of the degree of local damage, or possible failure, resulting from a bird strike at the expense of very little computer time.

EXAMPLE -- IMPACT OF A SPHERE ONTO TITANIUM PLATE
(APPROXIMATED BIRD STRIKE)

LIGHT IMPACT · · · SEVERE IMPACT

ANALYTICAL COMPARISON

| | AVG. STRAIN (%) | | MAX. STRAIN (%) | | | COMPUTER TIME (SEC) | |
| | STAEBL | FULL N. L. | STAEBL | SCALED STABEL* | FULL N. L. | STAEBL | FULL N.L. |
|---|---|---|---|---|---|---|---|
| LIGHT | 1.02 | 1.00 | 4.7 | 5.1 | 5.8 | 1.8 | 300 |
| SEVERE | 4.0 | 4.0 | 11.0 | 20.0 | 19.5 | 1.8 | 300 |

* AVG. STAEBL x 5.0
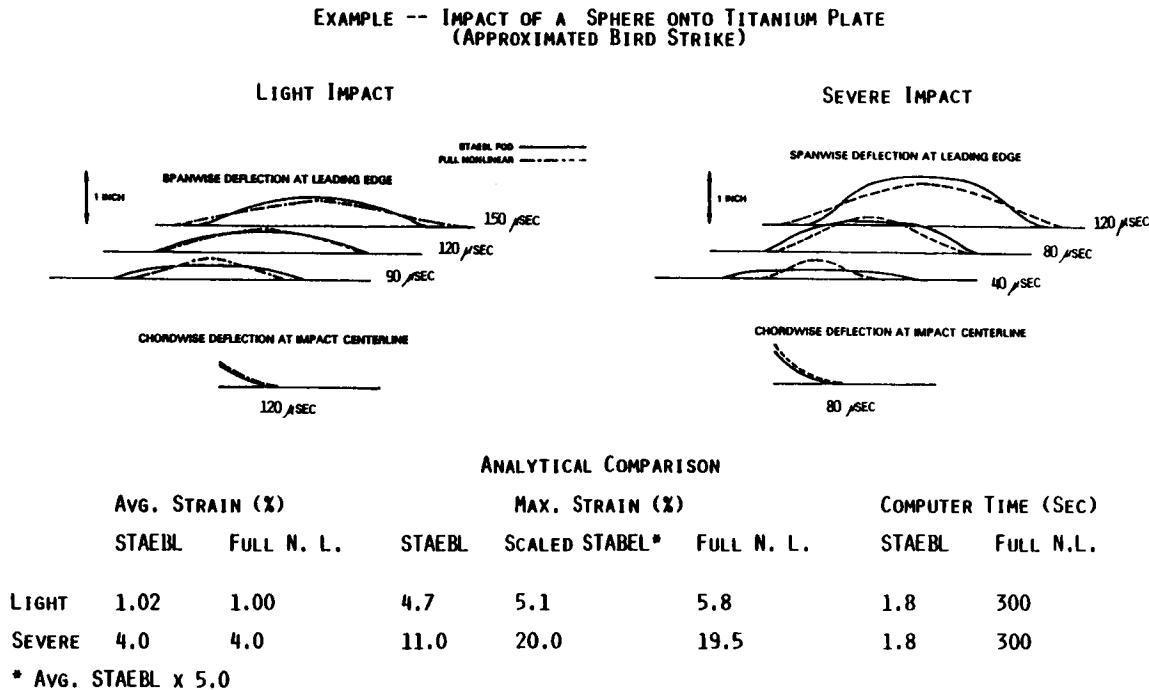
Figure 8

## Structural Tailoring - Phase II - Fan Blades

During Phase II of the STAEBL program, a hollow shroudless titanium fan blade with composite inlays and a superhybrid fan blade were structurally tailored, as was done during Phase I. The results are shown in Figure 9. Again, the reference blade was the hollow shroudless titanium Energy Efficient Engine fan blade designed by Pratt & Whitney Aircraft for NASA.

The initial design for the hollow blade was very similar to the reference blade. However, no appreciable improvement could be made after three optimization iterations. A new initial design was selected similar to the optimal hollow blade found during Phase I. A new optimal design was then found after ten iterations. Refined analysis showed no constraints were violated but that the design could be further improved. New calibration factors were calculated and the blade was re-optimized. The second tailoring converged after seven iterations. After the first pass through STAEBL, DOC+I was reduced by .53%. The second pass resulted in a further improvement to .61%.

The initial design for the superhybrid blade was the same initial design used during Phase I. After 15 iterations, STAEBL converged to an optimal design which was shown by refined analysis to violate a resonance and a flutter constraint. New approximate analysis calibration factors were calculated and a second tailoring was performed. This design converged in 19 iterations. It did not violate any constraints and reduced DOC+I by .48%.

| | Reference Blade (Hollow Titanium) | Hollow Titanium Blade with Composite Inlays | Superhybrid Blade |
|---|---|---|---|
| Root Chord (in) | 9.12 | 7.81 | 7.89 |
| Blade Weight (lb) | 19.2 | 8.86 | 9.73 |
| Stage Weight (lb) | 460.8 | 248.3 | 269.9 |
| $\Delta$(DOC+I) (%) | | | |
| Engine Wt. | -- | -.16 | -.35 |
| Engine Cost | -- | -.38 | -.19 |
| Maintenance Cost | -- | -.07 | +.06 |
| TOTAL | - | -.61 | -.48 |
| Active Constraints | 2nd Mode 3E 1st Mode Flutter Local FOD | 1st Mode Flutter Max.Blade Thickness Cavity Location | Min.& Max.Blade Thickness 1st Mode Flutter Local FOD |

Figure 9

## Structural Tailoring - Phase II - Compressor Blade

During Phase II, a solid titanium sixth-stage compressor blade from the Energy Efficient Engine was also optimally tailored. This blade had an added constraint that the "tip" mode must avoid resonance with the 10th engine order excitation. This mode was identified by STAEBL during the tailoring procedure by comparing the tip deflection of leading and trailing edges of the blade with the tip mid-chord deflection for all modes calculated. Also, for this case the objective was changed to minimizing stage weight. A candidate optimal design was found by STAEBL after nine iterations. Refined analysis showed that no constraints were violated. The results are summarized in Figure 10. The individual blade weight was reduced by 56% and total stage weight was reduced by 28%. While the initial design had no active constraints, a resonance constraint was active for the tailored blade.

|  | Reference Blade | Tailored Blade |
|---|---|---|
| Root Chord (in.) | 2.807 | 1.710 |
| Blade Weight (lb.) | .431 | .191 |
| Stage Weight (lb.) | 11.2 | 8.02 |
| Active Constraints | None | 1st Mode 2E |

Figure 10

## STAEBL Computer Code

STAEBL has been prepared as a nonproprietary computer code which includes a central executive, an optimizer, and all approximate analyses. The code has been delivered to NASA and is being prepared for public release. The general program architecture is shown in Figure 11. The code was designed in a modular form with separate modules for all key functions. The interfacing module functions as the executive and provides the communication links between the optimizer and the approximate analyses. Currently, the optimizer in STAEBL is COPES/CONMIN. However, during Phase III of the STAEBL program, the structural tailoring procedure will be augmented by adding an enhanced optimizer, ADS (Automated Design System) [6]. Since this system allows numerous optimization strategies and techniques to be used, part of the effort will be directed toward finding the most intelligent path for the structural tailoring of engine blades.

Also, during Phase III, the STAEBL procedure will be extended to include an aerodynamic analysis. At the present time, geometric constraints are imposed to maintain an aerodynamic design similar to a specified initial design. By incorporating an aerodynamic analysis capability into STAEBL those constraints can be relaxed and a true structurally optimal blade design can be found.

Due to the success of the STAEBL program, Pratt & Whitney Aircraft considers optimal structural tailoring to be an accepted element of the overall procedure to design new engine blades.

Figure 11

216
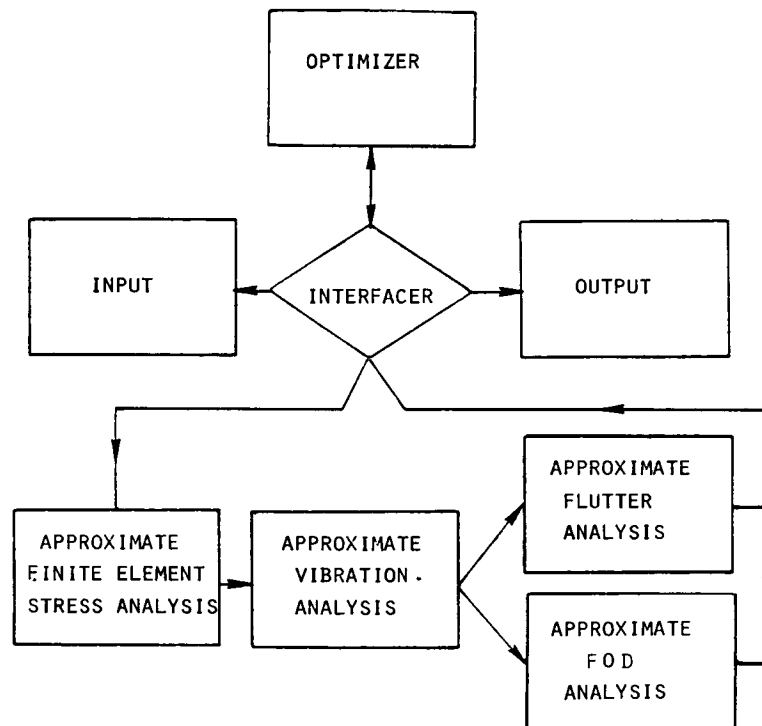
# References

1. C. E. Platt, T. K. Pratt, K. W. Brown, "Structural Tailoring of Engine Blades (STAEBL)", NASA CR-167949, 1982.

2. K. W. Brown, T. K. Pratt, C. C. Chamis, "Structural Tailoring of Engine Blades (STAEBL)", 24th Structures, Structural Dynamics and Materials Conference, Lake Tahoe, Nevada, May 2-4, 1983.

3. G. N. Vanderplaats, "CONMIN - A FORTRAN Program for Constrained Function Minimization: Users Manual", NASA TM X-62282, August 1973.

4. L. E. Madsen, G. N. Vanderplaats, "COPES - A FORTRAN Control Program for Engineering Synthesis" NPS 69-81-003, Naval Postgraduate School, Monterey, California, March 1982.

5. R. S. Bertke, J. P. Barber, "Impact Damage on Titanium Leading Edge from Small, Soft-Body Objects", Air Force Materials Laboratory, AFML-TR-79-4019, , March 1979.

6. G. N. Vanderplaats, "ADS-1: A New General Purpose Optimization Program", 24th Structures, Structural Dynamics and Materials Conference, Lake Tahoe, Nevada, May 2-4, 1983.

OPTIMIZATION OF CASCADE BLADE MISTUNING
UNDER FLUTTER AND FORCED RESPONSE CONSTRAINTS

Durbha V. Murthy and Raphael T. Haftka
Department of Aerospace and Ocean Engineering
Virginia Polytechnic Institute and State University
Blacksburg, Virginia 24061

## INTRODUCTION

In the development of modern turbomachinery, problems of flutter instabilities and excessive forced response of a cascade of blades that were encountered have often turned out to be extremely difficult to eliminate (refs. 1,2). The study of these instabilities and the forced response is complicated by the presence of mistuning; that is, small differences among the individual blades.

The theory of mistuned cascade behavior (refs. 3-8) shows that mistuning can have a beneficial effect on the stability of the rotor. This beneficial effect is produced by the coupling between the more stable and less stable flutter modes introduced by mistuning (ref. 9). The effect of mistuning on the forced response can be either beneficial or adverse. Kaza and Kielb (refs. 5-8) have studied the effects of two types of mistuning on the flutter and forced response: alternate mistuning where alternate blades are identical and random mistuning.

The objective of the present paper is to investigate other patterns of mistuning which maximize the beneficial effects on the flutter and forced response of the cascade. Numerical optimization techniques are employed to obtain optimal mistuning patterns. The optimization program seeks to minimize the amount of mistuning required to satisfy constraints on flutter speed and forced response.
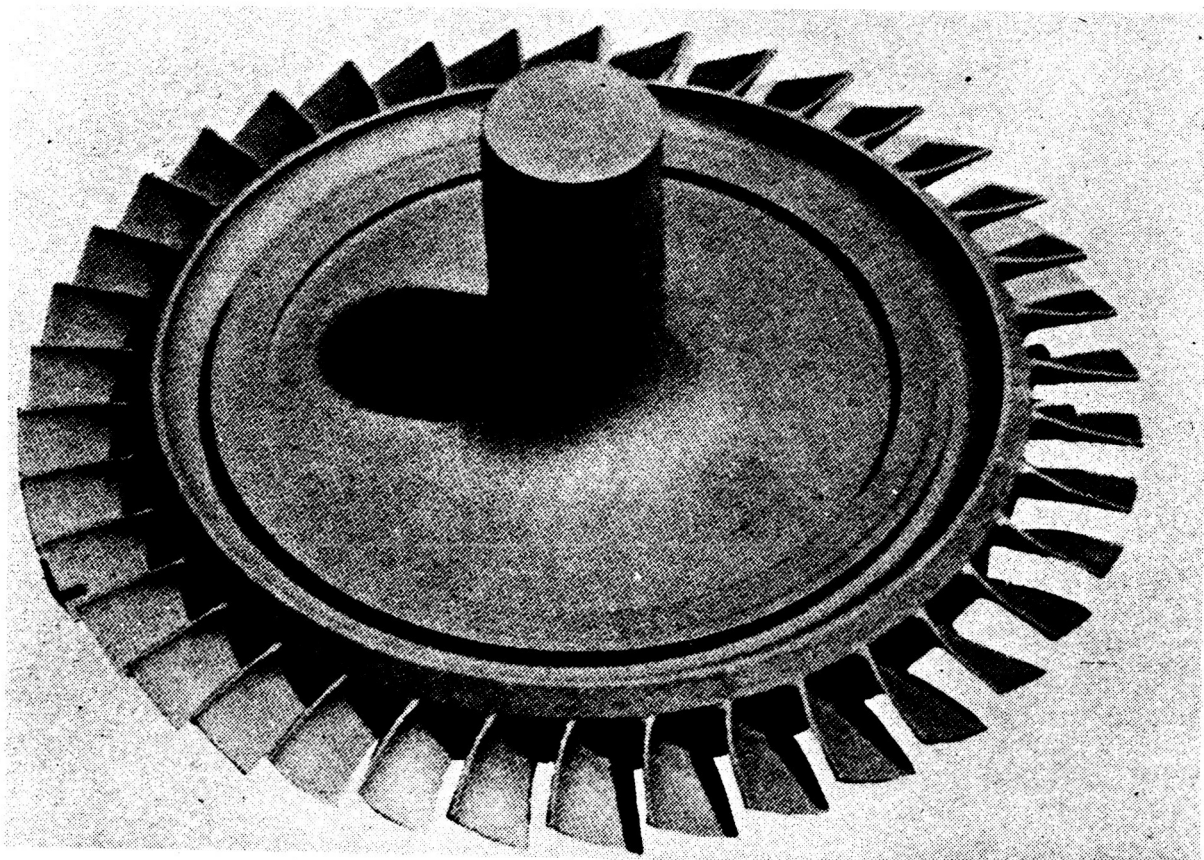
## GEOMETRY OF A TUNED CASCADE

     As shown in the figure, the blades are modeled as an infinite cascade of air-foils in a uniform upstream flow with a velocity V where $\xi$ is the stagger angle. Only two degrees of freedom (bending and torsion) are considered for each blade. For the tuned cascade, the blades are assumed to be in harmonic motion with $h_{ar}$ being the bending amplitude, $\alpha_{ar}$ the torsional amplitude and $\beta_r$ the phase angle between adjacent blades. For an N-blade cascade, that phase angle can take only N discrete values $\beta_r = 2\pi r/N$.
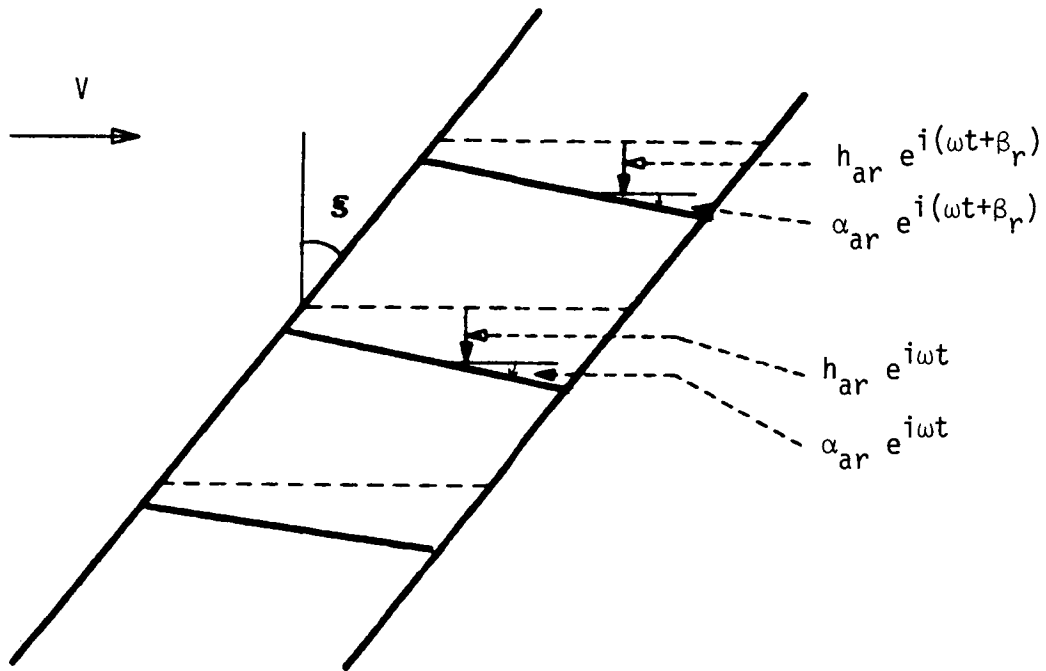
The figure illustrates the structural model of the s-th blade. All the length quantities are non-dimensional with respect to the semichord, b. The blade bending and torsional stiffnesses are modeled through the springs $K_{h_s}$ and $K_{\alpha_s}$ respectively. The effects of centrifugal stiffening due to rotation of the disk are included in the spring constants. The elastic coupling between bending and torsion due to pre-twist, shrouds and rotation is modeled through the offset distance ($x_{\alpha_s}$) of the center of gravity from elastic axis which is located at a distance ba from mid-chord. The chordwise motion of the airfoil is neglected.

The aerodynamic loads on the blade are the lift and moment per unit span $L_s^M$ and $M_s^M$ due to motion and the lift and moment per unit span $L_s^W$ and $M_s^W$ due to wakes. These aerodynamic loads are calculated using Whitehead's extension of Theodorsen's isolated airfoil theory in the incompressible unsteady flow to account for cascade effects (ref. 10).
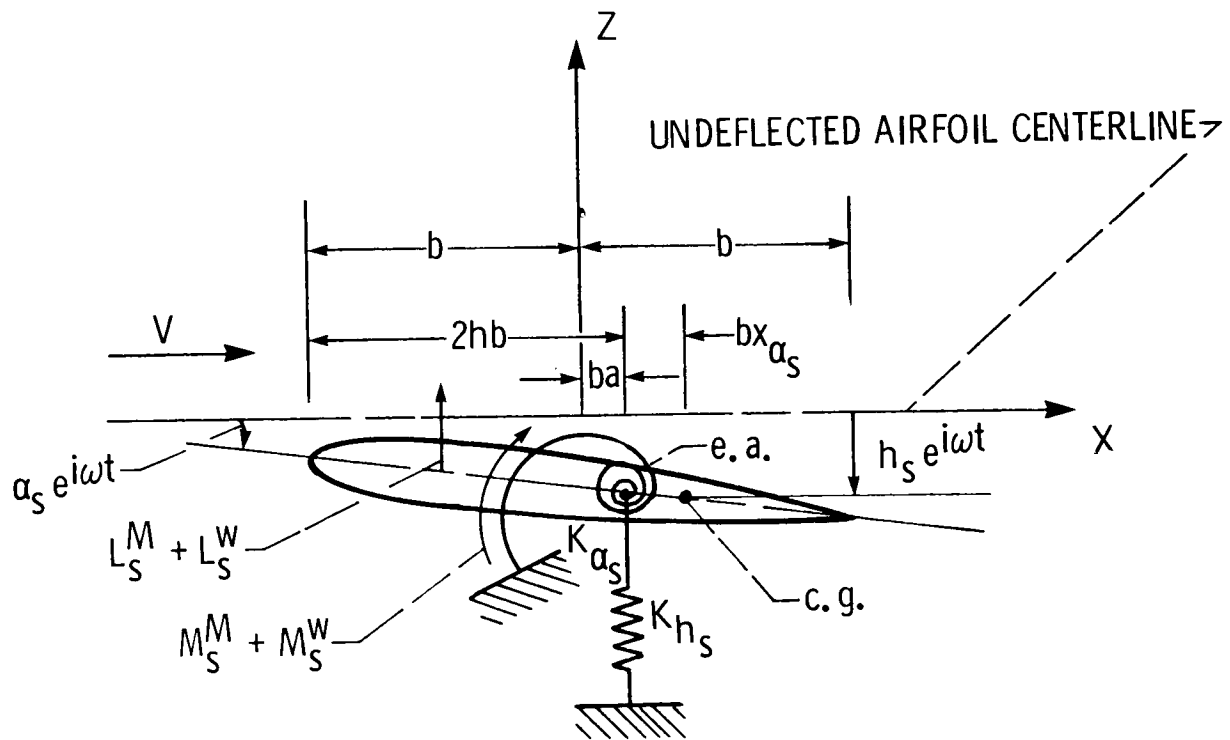
# EQUATIONS OF MOTION

While the motion of a tuned cascade is simple harmonic with a fixed interblade phase angle, the motion of a mistuned cascade is assumed to be a linear combination of the tuned cascade modes. The equation of motion may be written as Eq. (1) where $\{Y\}$ is a vector of complex amplitudes of the tuned cascade modes, $[E]$ is the modal matrix containing all the possible inter-blade phase angle modes, $\{Q\}$ is a forcing vector that depends on the aerodynamic wake forces and $\omega_o$ is a reference frequency.

When no external loads are applied the eigenvalues of the matrix $[P]$ are calculated for a range of reduced frequencies and the flutter speed is found from the condition that the real part of the eigenvalue is zero. For the forced response calculation, the frequency and mode of the excitation has to be assumed. In the present work an entire range of frequencies is scanned for the most critical forced response. The mode of excitation has its only non-zero component in the (N-1)th harmonic.

$$\left[ [P] - [I]\,\gamma \right] \{Y\} = -[E]^{-1} \{Q\} \tag{1}$$

$$\gamma = \left(\frac{\omega_0}{\omega}\right)^2$$

## Stability

$$\left[ [P] - [I]\,\gamma \right] \{Y\} = \{0\} \tag{2}$$

-2N x 2N Eigenvalue problem

$$\frac{i\omega_j}{\omega_0} = \frac{i}{\sqrt{\gamma_j}} = \mu_j \pm i\nu_j$$

## Forced Response

$$\{X\} = -[E] \left[ [P] - \gamma_j [I] \right]^{-1} \{Q\} \tag{3}$$

The figure illustrates the effect of alternate blade mistuning on the flutter speed. The flutter speed increases monotonically with an increase in alternate blade mistuning level. Alternate blade mistuning can have either a beneficial or adverse effect on forced response, depending on the harmonic of excitation.
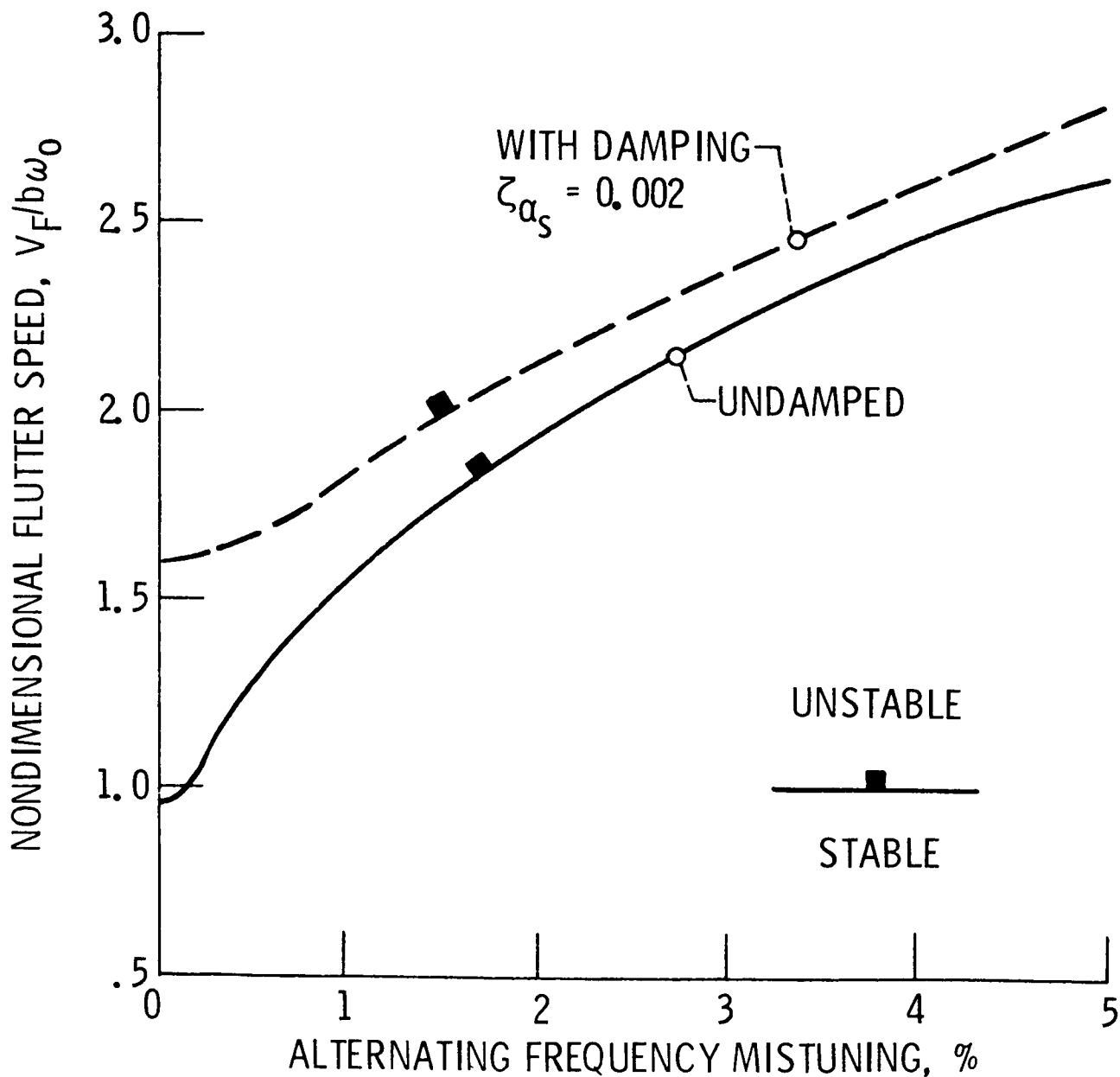
# DESIGN FORMULATION

The objective of the present study is to minimize the amount of mistuning required to satisfy given constraints on the stability and forced response of a cascade. The design variables are the amounts of mistuning in the individual blades $\varepsilon_i$, and the objective function is the sum of the individual mistunings raised to some integer power $p$. A high value of $p$ corresponds to minimizing the maximal blade mistuning while $p=2$ corresponds to minimizing the root mean square mistuning. The flutter constraint is based on the result of ref. 9 which showed that maximum stability is obtained when all eigenvalues have the same real part $\mu$. Therefore, the flutter constraint is a limit on the amount of spread of the real part of the eigenvalues about their average value, $\mu_{av}$, as well as a requirement that all real parts are stable.

Design Variables:

$$\varepsilon_i = \gamma_{\alpha i} - (\gamma_\alpha)_{av} \qquad i = 0, 1, \ldots, N-1$$

Objective Function:

$$F(\{\varepsilon\}) = \sum_{i=0}^{n-1} \varepsilon_i^p$$

Flutter Constraint:

Spread Constraint: $\dfrac{\mu_{cr}}{\mu_{av}} - a_o \geq 0$

Stability Constraint: $\dfrac{\mu_{cr}}{\mu_o} \geq 0$

Forced Response Constraint:

$$1 - \frac{r_i(\omega_j)}{r_{max}} \geq 0, \qquad \omega_j \in \Omega_c$$
$$i = 0, 1, \ldots N-1$$

The constraint on the forced response (Eq. (4) in the figure) requires the calculation of the forced response for a range of frequencies. One way of checking whether any violation occurs in the required range is to evaluate the response at a grid of frequencies dense enough to preclude the possibility of substantial constraint violations between grid points. From the standpoint of the optimization procedure this is very costly because a constraint on the response has to be applied at each grid frequency. For the cases reported here a grid of 101 frequencies had to be used in the range $0.95 \leq \omega/\omega_o \leq 1.05$.

Two alternative techniques were used to reduce the cost of calculating the response constraints and their derivatives. The first is identifying local peaks of the response (as a function of $\omega$) and enforcing the constraints only at these peaks. The main savings of this technique is in terms of derivative calculations. The second technique is based on the assumption that the response is most critical at the eigenfrequencies of the stability problem. This technique results in even larger savings. The results in terms of number of constraints and computer time for a full optimization are shown in the table for a seven-blade cascade.

RESPONSE AT 0.5 PERCENT ALTERNATE DESIGN (K=0.66)



| Method | No. of Constraints | CPU Time IBM 3081 |
|---|---|---|
| Dense Grid | 707 | 30.8 min. |
| Critical Point | 18-21 | 8.25 min. |
| Eigen-Frequencies | 14 | 3.67 min. |

LEGEND: $l$ ┼─┼─┼ BLADE 1 ◆─◆─◆ BLADE 2 ───── BLADE 3 ───── BLADE 4
───── BLADE 5 ┼─┼─┼ BLADE 6 ─⊟─⊟─⊟ BLADE 7
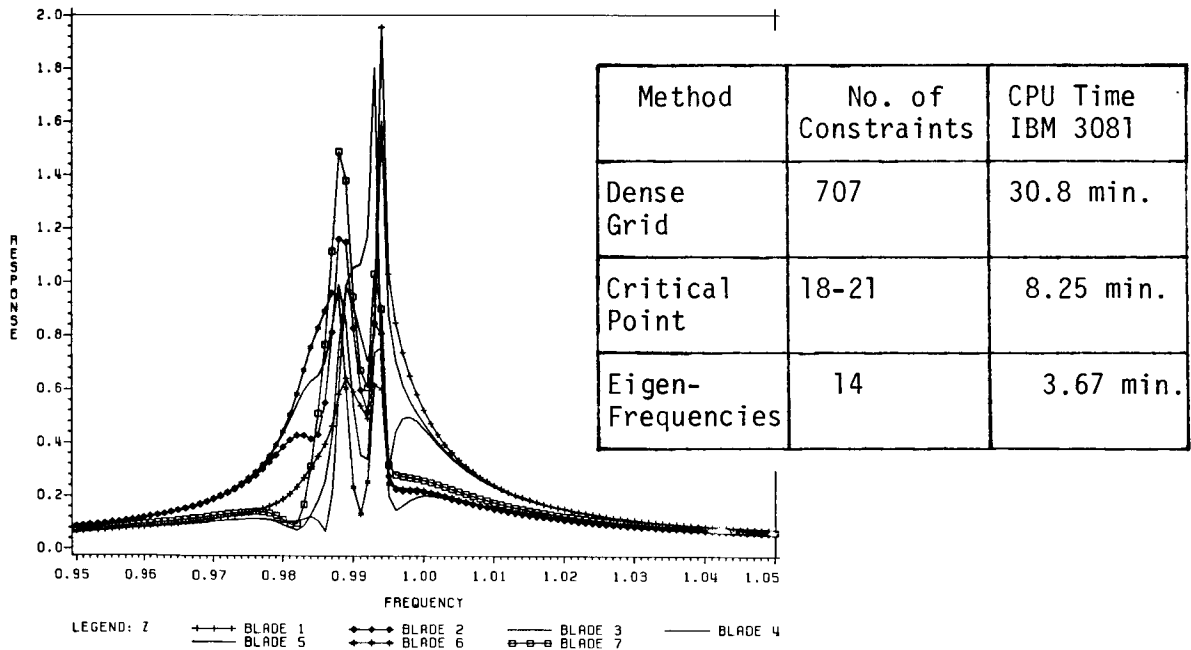
Forced Response Constraint

$$1 - \frac{r_i(\omega_j)}{r_{max}} \geq 0$$

# NEWSUMT OPTIMIZER

The optimization program used to obtain numerical results is the NEWSUMT program (ref. 11). It uses the sequence of Unconstrained Minimization Technique (SUMT) with an extended interior penalty function (ref. 12) to represent the constraints. Each unconstrained minimization is performed by using Newton's method with approximate derivatives (ref. 12). The optimization procedure is particularly efficient when the complexity of a problem is in the constraint and the objective function is fairly simple. For this reason the amount of mistuning is optimized subject to a constraint on the response, rather than optimizing the response subject to a constraint on the amount of mistuning.

Minimize $F(\vec{X})$

subject to $g_j(\vec{X}) \geq 0,$    $j = 1, 2, \ldots, m$

- SUMT - Sequential Unconstrained Minimization Technique

- Extended Interior Penalty Function

- Newton's Method with Approximate Second Derivatives

# OPTIMIZATION SUBJECT TO FLUTTER CONSTRAINT

The first set of results were obtained for a twelve blade cascade subject to a flutter constraint of the form

$$\frac{\mu_{cr}}{\mu_{av}} - 0.584 \geq 0$$

where $\mu_{cr}$ is the real part of the least stable eigenvalue and $\mu_{av}$ the average real part. The results are summarized in the table. They show that the optimized mistuning pattern is about 78.52% better than the alternate mistuning design which satisfies the same constraint. The maximum individual blade mistuning is 0.91% versus 1.4% for the alternate mistuning, and the optimized pattern is still alternating in sign.

TABLE 1

Results of Optimization with Flutter Constraint (k=0.66)

| | Alternate Mistuning pattern | Optimized Mistuning pattern |
|---|---|---|
| Objective Function | $23.52 \times 10^{-4}$ | $5.053 \times 10^{-4}$ |
| Max. mistuning $\varepsilon_{max}$(percent) | 1.4000 | 0.9097 |
| Least stable eigenvalue | -0.002525 | -0.002526 |
| Mistuning (percentage) | | |
| $\varepsilon_1$ | 1.4000 | 0.7628 |
| $\varepsilon_2$ | -1.4000 | -0.4768 |
| $\varepsilon_3$ | 1.4000 | 0.9018 |
| $\varepsilon_4$ | -1.4000 | -0.6401 |
| $\varepsilon_5$ | 1.4000 | 0.9097 |
| $\varepsilon_6$ | -1.4000 | -0.4683 |
| $\varepsilon_7$ | 1.4000 | 0.6619 |
| $\varepsilon_8$ | -1.4000 | -0.6708 |
| $\varepsilon_9$ | 1.4000 | 0.2620 |
| $\varepsilon_{10}$ | -1.4000 | -0.7796 |
| $\varepsilon_{11}$ | 1.4000 | 0.1575 |
| $\varepsilon_{12}$ | -1.4000 | -0.6201 |

# EFFECT OF OBJECTIVE FUNCTION FORM

The use of the sum of the squares of the individual blade mistunings as the objective function is equivalent to minimizing the root mean square of the mistuning pattern. Another possible objective function is the maximum individual blade mistuning. This objective function has the disadvantage of having discontinuous derivatives with respect to the design variables, $\varepsilon_i$. To avoid this problem the maximum-individual-blade objective function can be approximated by the sum of a high power of the individual mistunings. To check whether the optimized design is sensitive to the objective function the optimization was repeated with the sum of the sixth powers of the $\varepsilon_i$ being the objective function. The results are summarized in the table and show the effect to be minimal for this case.

TABLE 2

Effects of change in Objective Function (k=0.66)

|  | Optimum I (Exponent = 6) | Optimum II (Exponent = 2) |
|---|---|---|
| Objective Function | $1.698 \times 10^{-4}$ | $5.053 \times 10^{-4}$ |
| Max. mistuning $\varepsilon_{max}$(percent) | 0.8993 | 0.9097 |
| Least stable eigenvalue | -0.002525 | -0.002526 |
| Mistuning (percentage) |  |  |
| $\varepsilon_1$ | 0.7639 | 0.7628 |
| $\varepsilon_2$ | -0.5662 | -0.4768 |
| $\varepsilon_3$ | 0.8927 | 0.9018 |
| $\varepsilon_4$ | -0.5910 | -0.6401 |
| $\varepsilon_5$ | 0.8993 | 0.9097 |
| $\varepsilon_6$ | -0.5352 | -0.4683 |
| $\varepsilon_7$ | 0.6839 | 0.6619 |
| $\varepsilon_8$ | -0.7201 | -0.6708 |
| $\varepsilon_9$ | 0.2476 | 0.2620 |
| $\varepsilon_{10}$ | -0.6621 | -0.7796 |
| $\varepsilon_{11}$ | 0.1709 | 0.1575 |
| $\varepsilon_{12}$ | -0.5837 | -0.6201 |

## OPTIMIZATION SUBJECT TO FORCED RESPONSE CONSTRAINT

The optimization was repeated with a forced response constraint. The constraint stipulated that the maximum response amplitude of the optimized design does not exceed the forced response of a 0.5% mistuning alternate-mistuning design. The two designs are compared in the table. It is shown that the objective function was reduced by 70% which corresponds to 45% reduction in the root mean square of the mistuning.

An attempt to obtain an optimal design subject to both flutter and forced response constraint indicated that the alternate mistuning design cannot be improved upon in both categories. That is, improvements in stability resulted in deterioration in forced response, and vice versa.

TABLE 3

Results of Optimization with Forced Response Constraint
(k=0.8)

|  | Initial Design | Optimized Design |
|---|---|---|
| Objective Function | $3.0 \times 10^{-4}$ | $9.144 \times 10^{-5}$ |
| Max. mistuning $\varepsilon_{max}$ (percent) | 0.5 | 0.4804 |
| Least stable eigenvalue | -0.00138 | -0.00003 |
| Mistuning (percentage) |  |  |
| $\varepsilon_1$ | 0.5 | 0.2457 |
| $\varepsilon_2$ | -0.5 | -0.4804 |
| $\varepsilon_3$ | 0.5 | 0.2677 |
| $\varepsilon_4$ | -0.5 | -0.3049 |
| $\varepsilon_5$ | 0.5 | 0.2299 |
| $\varepsilon_6$ | -0.5 | -0.2620 |
| $\varepsilon_7$ | 0.5 | 0.2463 |
| $\varepsilon_8$ | -0.5 | -0.2024 |
| $\varepsilon_9$ | 0.5 | 0.2419 |
| $\varepsilon_{10}$ | -0.5 | -0.1170 |
| $\varepsilon_{11}$ | 0.5 | 0.2474 |
| $\varepsilon_{12}$ | -0.5 | -0.1123 |

# FORCED RESPONSE COMPARISON

The maximal blade response of the alternate and optimized designs is compared in the figure.

### RESPONSE AT ALTERNATE AND OPTIMUM DESIGNS (K=0.80)
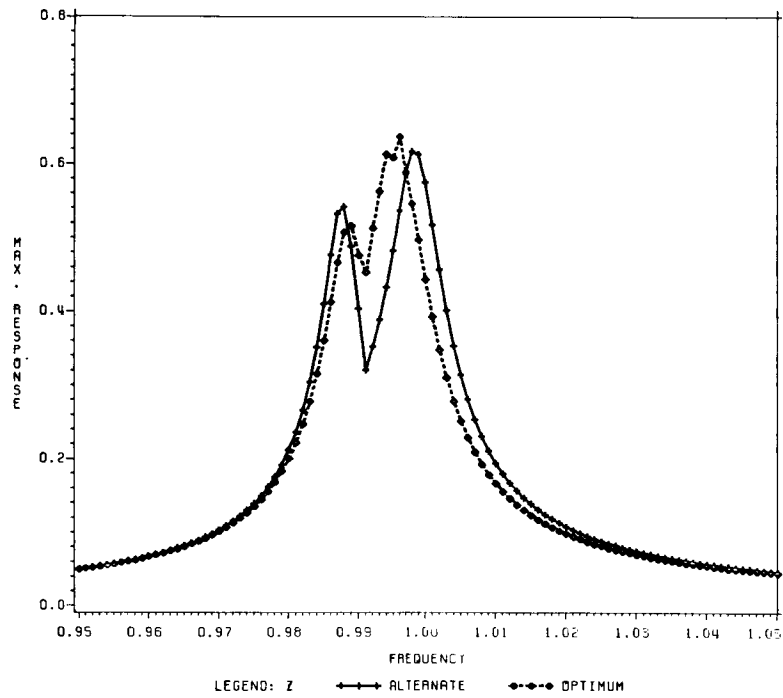
## CONCLUDING REMARKS

An optimization procedure for finding optimal mistuning patterns for cascades subject to flutter and forced response constraints has been developed. The procedure is based on an extended interior penalty function algorithm and seeks to minimize the amount of mistuning required to satisfy the constraints. An efficient form of the forced response constraint which reduces computation costs by an order of magnitude has also been developed.

The optimization procedure has been applied to the design of a 12-blade cascade and the resulting designs compared to alternate mistuning designs. It was found that mistuning amplitudes could be substantially reduced without hurting either the flutter or the forced response characteristics. However, it was not possible for the example problem to improve on the alternate design subject to both constraints.

The designs obtained by the optimization procedure are not practical because they require many different blades. Work is under way to obtain similar results with only 3 or 4 different blade types.

- Optimization Procedure for Design Under Flutter & Forced Response Constraints Developed

- Efficient Forced Response Constraint Resulted in Large Computer Time Savings

- Optimized Designs Superior to Alternate Designs if only Flutter or only Forced Response is Critical

- Number of Different Blades Should be Reduced

# REFERENCES

1. Mikolajczak, A. A., Arnoldi, R. A., Snyder, L. E. and Stargardter, H.: Advances in Fan and Compressor Blade Flutter Analysis and Predictions. Journal of Aircraft, vol. 12, April 1975, pp. 325-332.

2. Gotham, J. I.: Design Considerations for Large Fan Blades. SAE Paper 690387, April 1969.

3. Whitehead, D. S.: Torsional Flutter of Unstalled Cascade Blades at Zero Deflection. R&M 3429, British Aeronautical Research Council, London, 1965.

4. Whitehead, D. S.: Effect of Mistuning on the Vibration of Turbomachine Blades Induced by Wakes. Journal of the Mechanical Engineering Sciences, vol. 8, no. 1, 1966, pp. 15-21.

5. Kaza, K. R. V. and Kielb, R. E.: Effects of Mistuning on Bending-Torsion Flutter and Response of a Cascade in Incompressible Flow. AIAA Paper 81-0532, 1981.

6. Kielb, R. E. and Kaza, K. R. V.: Aeroelastic Characteristics of a Cascade of Mistuned Blades in Subsonic and Supersonic Flows. ASME Paper 81-DET-122, 1981.

7. Kaza, K. R. V. and Kielb, R. E.: Coupled Bending-Bending-Torsional Flutter of Mistuned Cascades with Nonuniform Blades. AIAA Paper 82-0726, 1982.

8. Kaza, K. R. V. and Kielb, R. E.: Vibration Flutter of Mistuned Bladed-Disk Assemblies. AIAA Paper 83-0849, 1983.

9. Nissim, E. and Haftka, R. T.: Optimization of Cascade Blade Mistuning. Report no. VPI-Aero-133, Virginia Polytechnic & State Univ., May 1983.

10. Whitehead, D. S.: Force and Moment Coefficients for Vibrating Airfoils in Cascade. R&M 3254, British Aeronautical Research Council, London, February 1960.

11. Miura, H. and Schmit, L. A.: NEWSUMT-A Fortran Program for Inequality Constrained Function Minimization - Users Guide. NASA CR 159070, 1979.

12. Haftka, R. T. and Starnes, J. H.: Application of a Quadratic Extended Interior Penalty Function for Structural Optimization. AIAA Journal, vol. 14, no. 6, June 1976, pp. 718-724.

SIZING-STIFFENED COMPOSITE PANELS
LOADED IN THE POSTBUCKLING RANGE

S. B. Biggers and J. N. Dickson
Lockheed-Georgia Company
Marietta, Georgia

# THE POSTOP PANEL SIZING CODE

Stiffened panels are widely used in aircraft structures such as wing covers, fuselages, control surfaces, spar webs, bulkheads, and floors. The detailed sizing of minimum-weight stiffened panels involves many considerations. Use of composite materials introduces additional complexities. Many potential modes of failure exist. Analyses for these modes are often not trivial, especially for those involving large out-of-plane displacements. Accurate analyses of all potential failure modes are essential. Numerous practical constraints arise from manufacturing/cost considerations and from damage tolerance, durability, and stiffness requirements. The number of design variables can be large when lamina thicknesses and stacking sequence are being optimized. A significant burden is placed on the sizing code due to the complex analyses, practical constraints, and number of design variables. On the other hand, sizing weight-efficient panels without the aid of an automated procedure is almost out of the question.

The sizing code POSTOP (Postbuckled Open-STiffener Optimum Panels) has been developed (refs. 1 and 2) to aid in the design of minimum-weight panels subject to the considerations mentioned above. Developed for postbuckled composite panels, POSTOP may be used for buckling resistant panels and metallic panels as well. The COPES/CONMIN (refs. 3 and 4) optimizer is used in POSTOP although other options such as those in the ADS (ref. 5) system could be substituted with relative ease. The basic elements of POSTOP are shown in figure 1. Some of these elements and usage of the program are described on the following pages.



Figure 1.

236
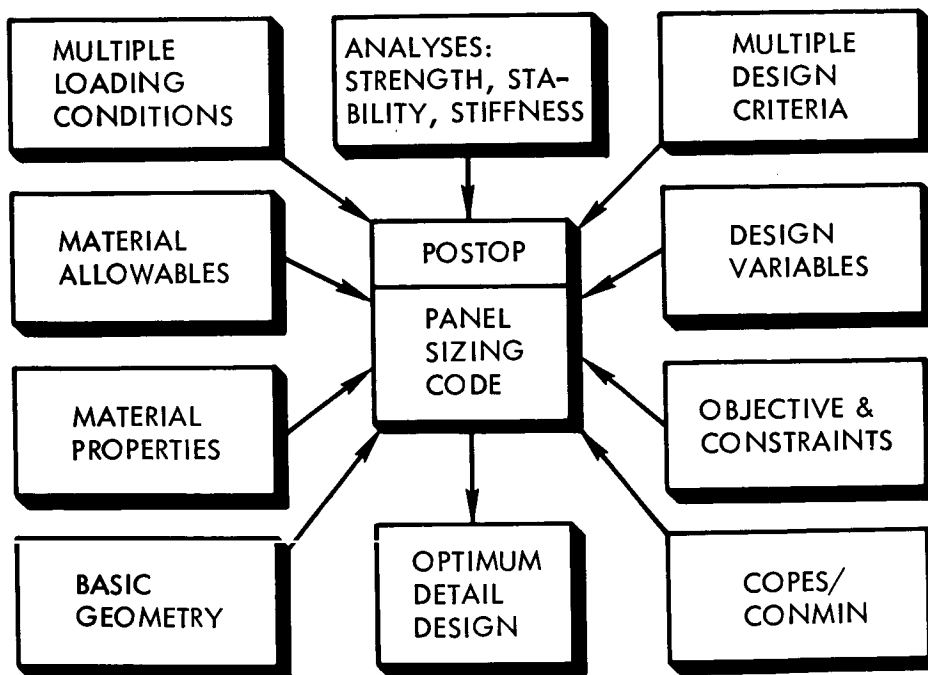
# PANEL GEOMETRY AND LOADS

The basic geometry and types of loads that are considered in POSTOP are shown in figure 2. The stiffener spacing is assumed to be small compared to the panel length. This is normally the case for stiffened panels used in transport aircraft. The stiffeners may have any cross-sectional shape that can be derived from an I-section. The stiffeners may be integral with the skin or separate elements bonded to or cocured with the skin. Examples are shown in the figure.

Combined inplane shear and biaxial loads may be specified. Normal pressure and temperature changes are also considered in the analyses. The bending effects of an initial bow over the panel length and eccentricity of applied loads are included. The interaction of bending due to pressure or eccentricities and inplane loads is accounted for. The effects of stiffness reductions due to postbuckling on this interaction are considered. This interaction can have a significant effect on the panel design and must be considered during sizing.

Aircraft structures are subjected to a large number of independent loading conditions. Often different design criteria are imposed for different load cases. For example, panels may be allowed to operate in the postbuckling regime at certain load levels and be required to be buckling resistant at lower load levels. Conditions associated with high temperature may require different material properties and allowables. Limit and ultimate loading conditions obviously use different material allowables. Nonlinearities require that both limit and ultimate conditions be analyzed. Often many load cases may be eliminated by inspection as being noncritical. However, several load cases usually remain that must be evaluated. The POSTOP code and other available panel sizing codes have this multiple load-cases capability.



PANEL                                    STIFFENERS

Figure 2.

237

# POSTBUCKLING AND STABILITY ANALYSES

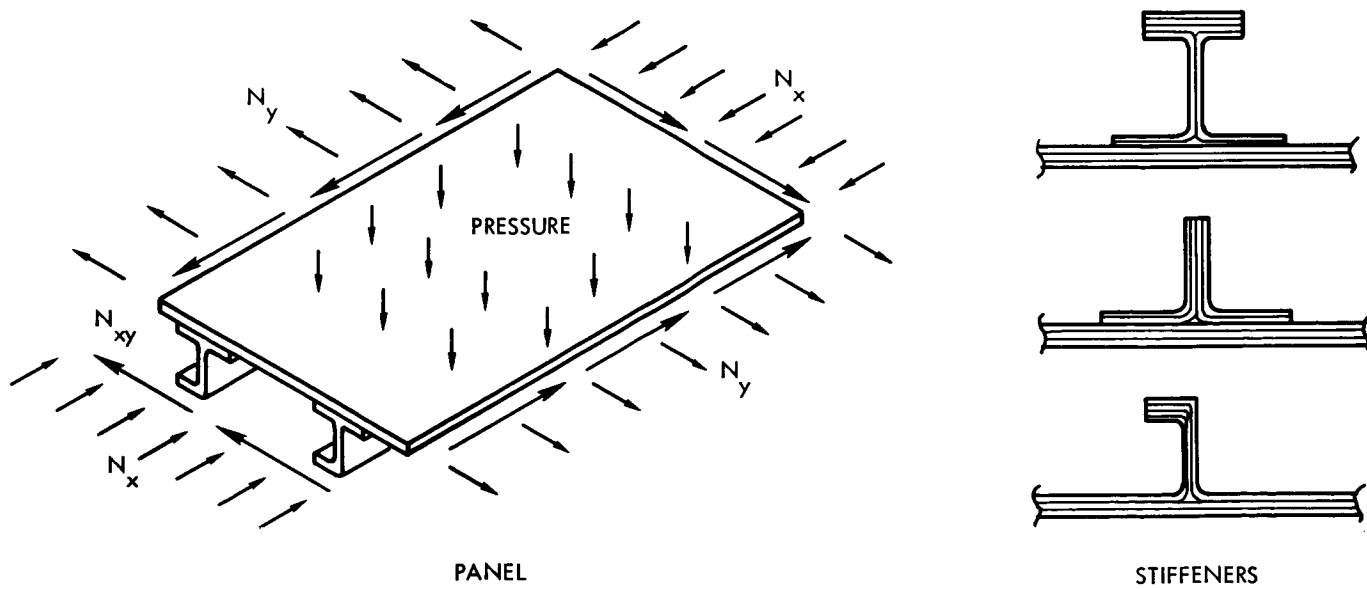Strength and stability analyses performed in POSTOP include initial buckling of the skin and stiffener, postbuckling of the skin, torsional/flexural buckling of the stiffener, and ply-level membrane plus bending strains in the skin and stiffener elements. Various nonlinear effects enter into these analyses.

If the skin is not buckled, the only nonlinearity in the load-deformation relationship results from the interaction of inplane loads and panel bending as mentioned previously. If the skin is buckled, as shown in figure 3, several additional nonlinearities enter into the analysis. After buckling, the compression load in the skin is redistributed, with an increased percentage of the load being carried near the edges, where it is supported by the stiffeners. The secant and tangent stiffnesses of the skin are reduced after buckling. The reduced secant stiffness causes an increased proportion of the panel load to be carried by the stiffener. This increase affects the local and torsional/flexural buckling of the stiffener. The reduced tangent stiffness of the skin also affects the stability of the stiffener since it offers less restraint to incremental deformation. The reduced tangent stiffness increases the interaction of inplane loads and panel bending.

Since the skin and individual stiffener plate elements do not typically buckle at the same load level or in the same wavelengths, the restraint of adjacent elements is considered when computing the skin and stiffener local buckling loads. Likewise, the restraining effects of the skin at the edges of the stiffener attached flanges are included in the torsional/flexural buckling analysis. Local and torsional/flexural buckling analyses are performed for a series of admissible buckling wavelengths and the lowest buckling load level is sought.

Local bending strains are significant in a postbuckled skin. While the membrane strain in the center of the plate may be small, as shown in the figure, the total compressive strain on the concave surface at the buckle crest may exceed the edge strain. On the other hand, the total strain on the convex surface may actually be tensile. Ply-level stresses and strains are computed at critical locations in the skin and stiffener elements and margins of safety are computed based on the maximum strain or the Tsai-Hill criterion.

SKIN BUCKLING, POSTBUCKLING

STIFFENER INITIAL BUCKLING

REDUCED STIFFNESS

LOAD REDISTRIBUTION

STIFFENER TORSIONAL/FLEXURAL BUCKLING
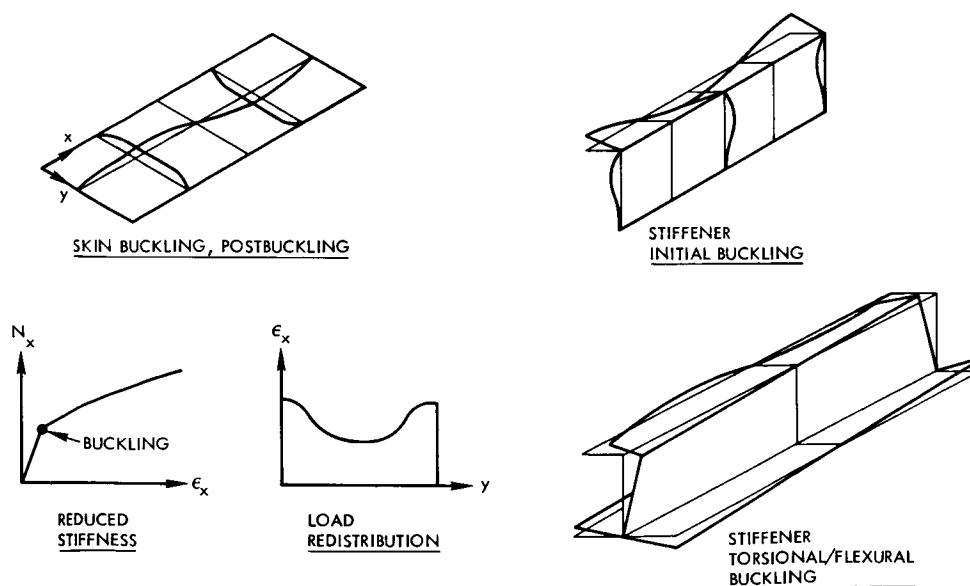
Figure 3.

# SKIN/STIFFENER INTERFACE STRESSES

Separation of the skin and stiffener is one of the most commonly occurring failure modes in postbuckled and pressure-loaded composite panels. A self-contained analysis procedure has been developed and incorporated in POSTOP to evaluate the normal and shear stresses in the interface between the stiffener attachment flange and the skin. Typical deformations and the structural model are shown in figure 4. The flange and skin are modeled as plates connected by an elastic interface layer. The length of the buckling half-wave defines the length of the model. Sinusoidally distributed moments and shears computed from the postbuckled plate analysis are treated as applied loads in the skin plate near the free edge of the attached flange. The effects of the longitudinal compression loads in the plates are included and have been found to be significant. Interface stresses may be computed at any point along the half-wavelength and across the flange width. Normal and short transverse shear stresses are maximum at the buckle wave peak. The long transverse shear stresses are maximum along the buckle node line, where failure involving shear crippling has been observed.

Parametric studies performed with this analysis have shown that the interface stresses may be minimized by proper detail design techniques. For example, the addition of a pad in the skin under the stiffener reduces all interface stresses significantly. The effect of a skin pad on the shear stresses is shown in the figure. Other design variables including flange width and stacking sequence are also available to control the interface stresses. The success or failure of an optimum postbuckled panel design may depend on attention to design details such as these.
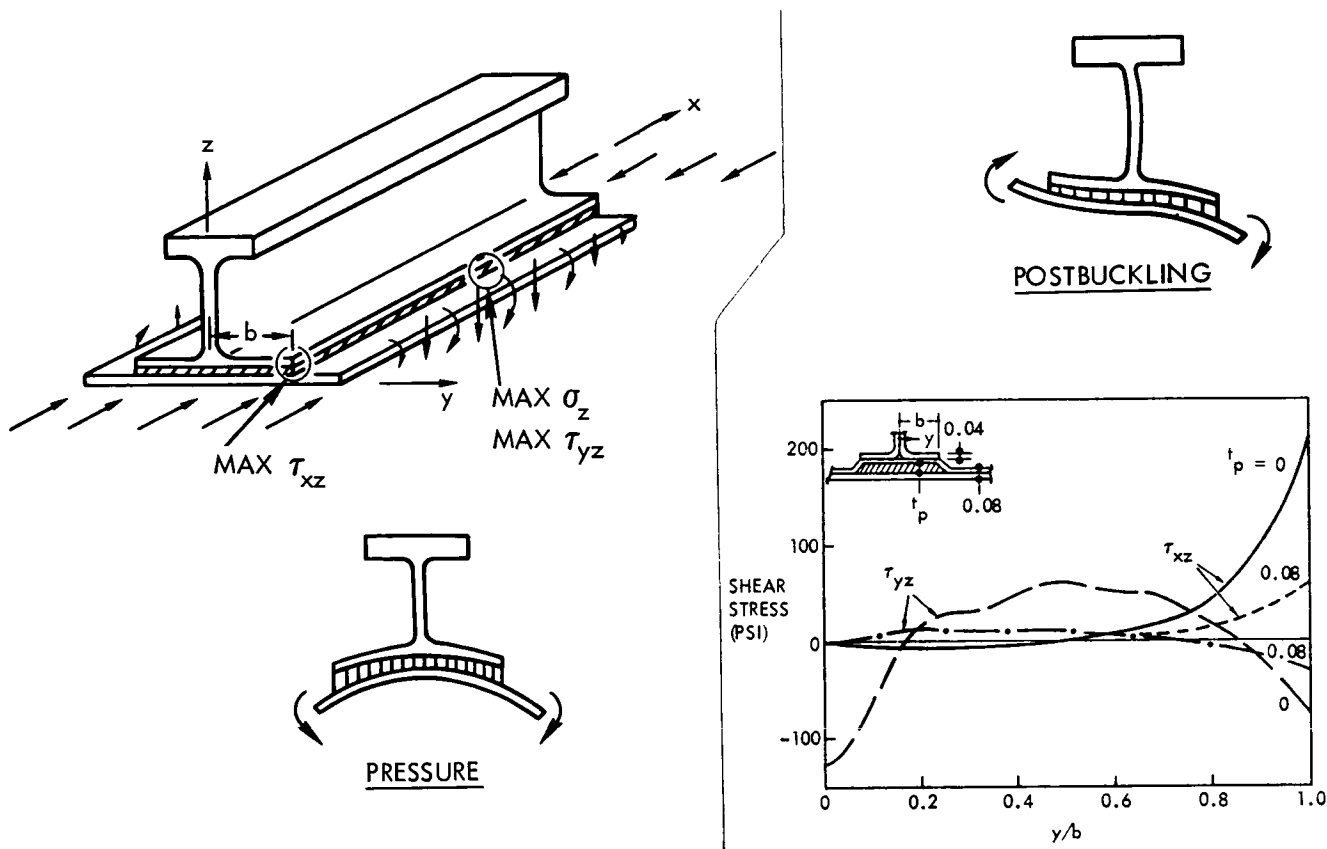


Figure 4.

# OPTIMIZATION PROBLEM FORMULATION

The design variables in POSTOP are shown in figure 5. They are the five element widths of the I-section stiffener, the stiffener spacing and the lamina thicknesses in the skin and the stiffener elements. All design variables are considered to be continuous. Any width except the stiffener height may be set equal to zero to produce stiffeners with cross sections other than the I-shape. Currently up to 20 width and thickness variables may be specified. Any design parameter may be linked to a design variable with a constant multiplier. Using linking to achieve practical designs allows the total number of independent design variables to be in the range of 10 to 15 for most stiffened composite panels. The requirement for lamina thicknesses to be integer multiples of available ply thicknesses and treatment of stacking sequences are discussed later.

The most common objective function in aircraft panel sizing is minimum panel weight. Maximum stiffness or maximum margin of safety in a particular failure mode could be specified as objective functions in certain instances.

Constraints may be placed on the magnitude of the design variables, ratios of selected design variables, panel stiffnesses, and individual margins of safety. When minimum weight is not the objective function, panel weight should be constrained. Proper specification of these constraints allows practical optimum designs to be determined. Added safety may be ensured in certain major failure modes, such as panel instability, by specifying a higher lower bound for the margin of safety in that mode.

The CONMIN program used in POSTOP is a widely used optimizer based on the method of feasible directions. POSTOP uses CONMIN with finite-difference gradients due to the nonlinear nature of the optimization problem and of the structural response.

DESIGN VARIABLES

OBJECTIVE
- MIN. WEIGHT
- MAX. STIFFNESS
- MAX. MARGIN

- LINKING
- STACKING SEQUENCE

CONSTRAINTS
- DESIGN VARIABLES
- DESIGN VAR. RATIOS
- STIFFNESSES
- MARGINS
- WEIGHT

Figure 5.

240

# INTEGER NUMBERS OF PLIES

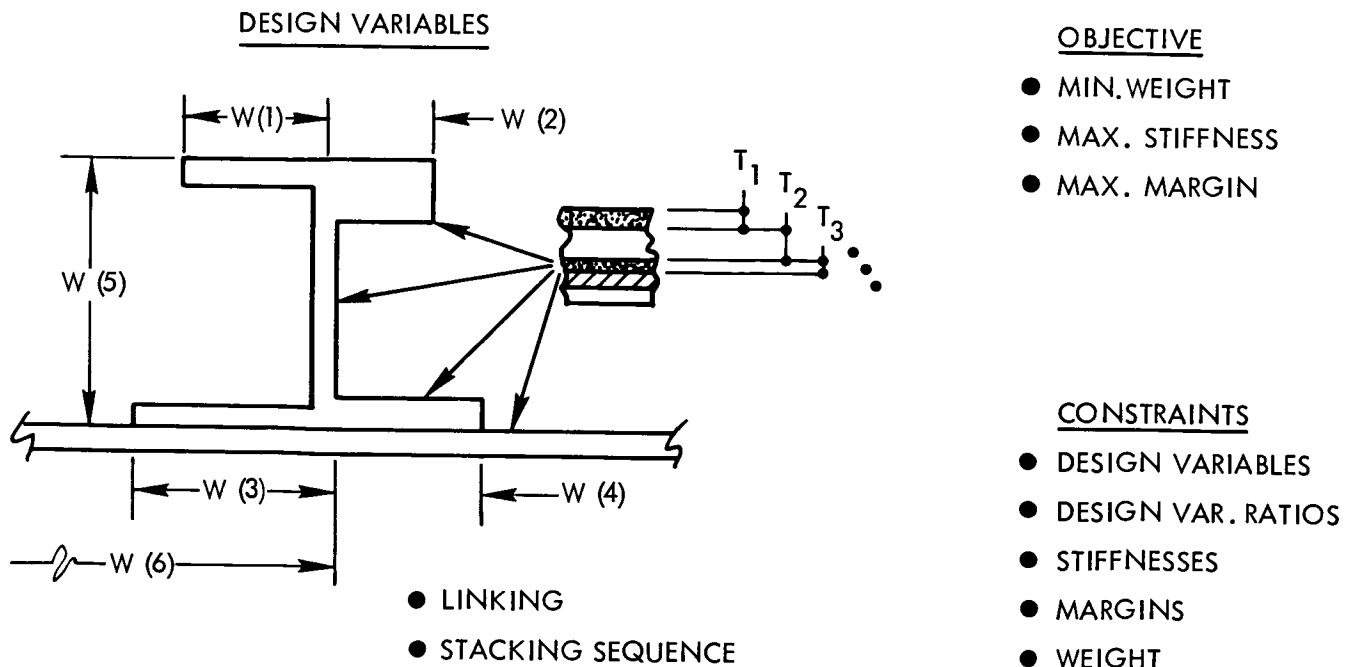Considering lamina thicknesses as continuous variables is a requirement for the CONMIN optimizer used in POSTOP. Optimum designs generally contain laminae having fractional numbers of available plies. In thick laminates, simply rounding the optimum lamina thicknesses up or down to the nearest integer number of plies may have a negligible effect on panel weight. Such rounding of lamina thicknesses becomes more significant when the total laminate thickness is small or when preplied laminae are used to lower fabrication cost. When off-axis material, such as $\pm45$ degree plies, is used it must be supplied in multiples of four to maintain a balanced symmetric laminate. Here the rounding effect is multiplied by four.

The negative aspects of this rounding procedure are generally lessened in importance by several factors. Often if one lamina is rounded up, another can be rounded down, cancelling to some extent the weight penalty. If truly continuous design variables such as spacing and widths are available, a second optimization on only the continuous variables may be performed after lamina thickness rounding. This currently suggested approach to be used with POSTOP is outlined in figure 6. Experience has shown that after rounding and reoptimizing, the weight penalty is usually less than three or four percent compared to absolute optimum fuselage panel designs. This penalty can decrease further when thicknesses vary along the structure length, and plies may be dropped at any point along the length whenever a smaller integer number of plies is required.

There are cases, however, when the current approach leads to the wrong solution. For example, if a $[\pm45_n/0_m/\mp45_n]$ plate is to remain buckling resistant in pure compression, an optimum design might require $n = 1.15$ and $m = 0.0$, since a laminate with only 45-degree plies is optimum for this case. The rounding procedure would require a $[\pm45_2/\mp45_2]$ laminate resulting in a 74-percent penalty. If optimization on integer numbers of plies were used, a $[\pm45/0/\mp45]$ laminate might prove optimum resulting in only a 9-percent penalty. Although this example exaggerates the problem, a method of optimizing on continuous and discrete value design variables simultaneously would be of value in composite panel sizing.



Figure 6.

241
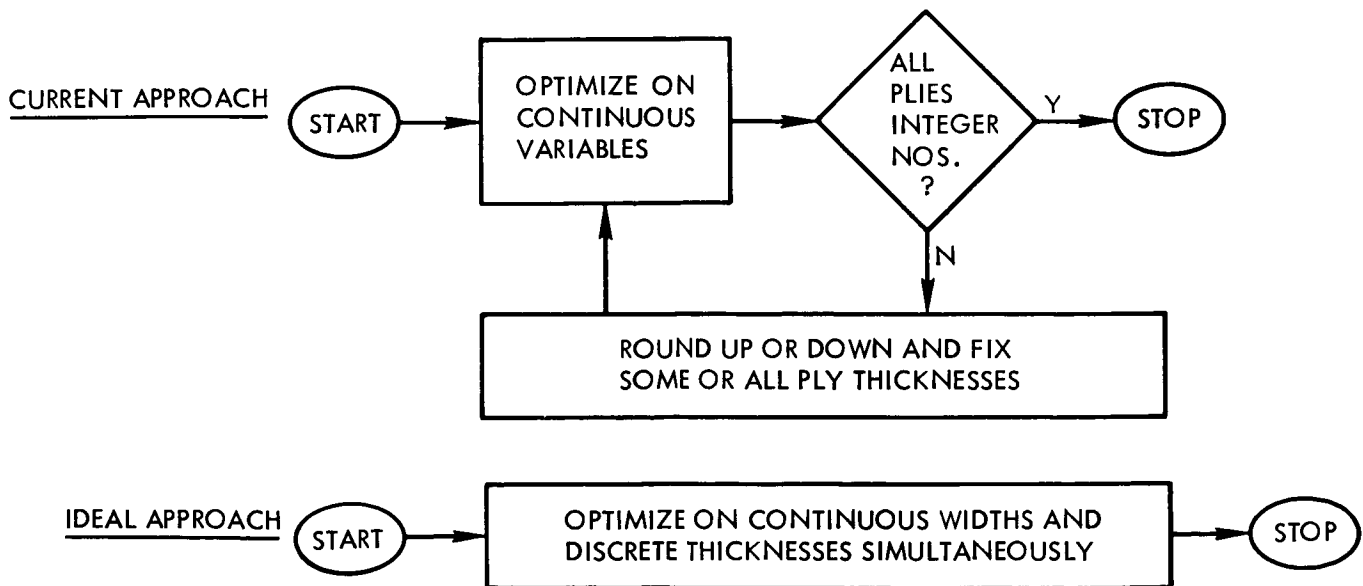
# STACKING SEQUENCE OPTIMIZATION

The stacking sequence of the plies in a laminate can have marked effects on buckling loads, postbuckling response, local bending stresses and stiffnesses, free edge interlaminar stresses, skin/stiffener interface stresses, and delamination growth. Provided an accurate analysis is available to evaluate such effects, optimization on lamina thicknesses can be used directly to determine the optimum stacking sequence as well as the total amount of material required in the various ply orientations.

The approach that can be used in POSTOP to determine optimum stacking sequence is summarized in figure 7. If 0-, 90- and ±45-degree orientations are to be used in a laminate, the laminate specified to start the optimization process should have approximately equal numbers of plies in the three directions. More importantly, material with each orientation should be repeated at least once and the thickness variables should not be linked. Optimization will reduce the thickness of laminae with undesirable orientations to relatively small values, as shown in the figure. These reduced thicknesses are then rounded out of the laminate and the optimum stacking sequence remains. Reoptimization should be performed after rounding.
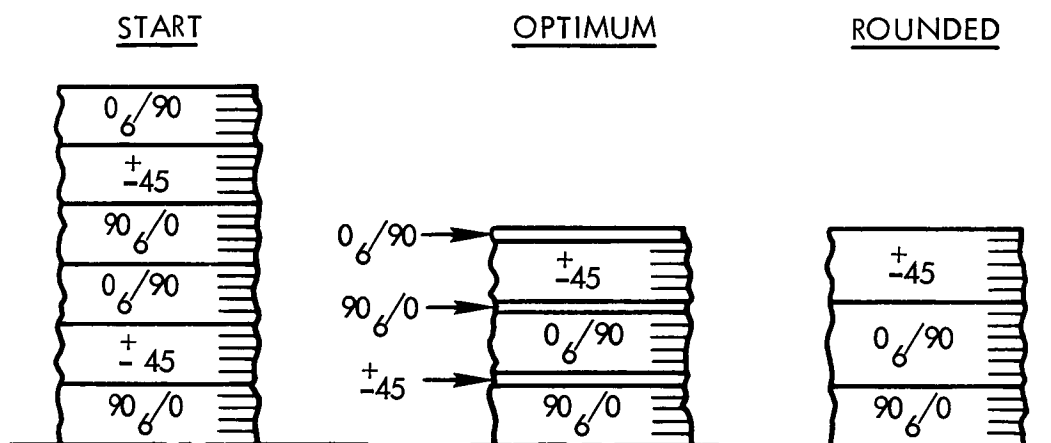


- PROVIDE CHOICE OF LOCATIONS FOR EACH ORIENTATION

- OBSERVE RELATIVE THICKNESS TRENDS

- ELIMINATE LAMINAE WITH RELATIVELY SMALL THICKNESSES

- REOPTIMIZE

Figure 7.

# BENEFITS OF POSTBUCKLED DESIGN

The weight savings of postbuckled panel design relative to buckling resistant design have been recognized in metallic fuselage construction for many years. Reluctance to use postbuckling composite panels exists due to the low out-of-plane strength and stiffness of composites. Recently, design details such as the padded-skin concept and attachment methods such as stitching have been shown to be effective in preventing skin/stiffener separation failures in postbuckled composite panels. Questions still remain as to the durability of such panels in fatigue loading, particularly if interlaminar damage or defects are present. Other failure modes such as shear crippling may become critical when separation is suppressed. Assuming these questions can be answered with new analytical/experimental developments, postbuckling design will become widely used in composite fuselage structures. POSTOP has been used to determine the benefits of postbuckled design for composites as compared to a buckling resistant design approach.

The potential weight savings of postbuckled composite fuselage panels as compared to panels that are required to remain buckling resistant is shown in figure 8(a). Here the mass index (panel weight per unit surface area, W, divided by panel length, L ) is plotted as a function of the load index (compressive stress resultant, $N_x$, divided by panel length) for both buckling resistant and postbuckled designs. Weight savings ranging from 25 percent at the lower load levels to 15 percent at the higher load levels are possible with postbuckled design.

Another advantage of postbuckled design is illustrated in figure 8(b). The effect of stiffener spacing on panel weight is shown for stiffened panels designed for a given load level. Again, postbuckled designs and buckling resistant designs are compared. For the buckling resistant panels, there is a significant weight penalty to increase the stiffener spacing. For the postbuckled panels, on the other hand, there is almost no weight penalty associated with an increase in stiffener spacing. Since increasing the stiffener spacing translates into fewer parts, cost savings may be realized with postbuckled design in addition to weight savings.
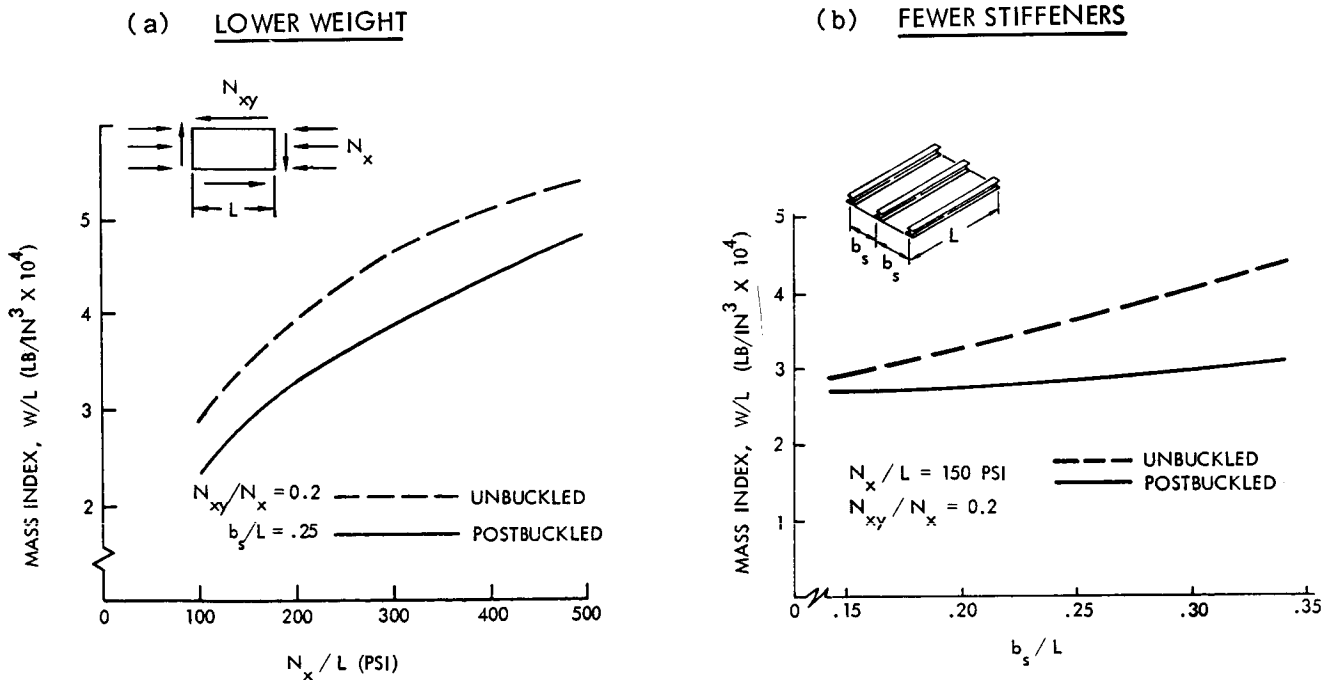
(a)　LOWER WEIGHT　　　　　　　　　(b)　FEWER STIFFENERS



Figure 8.

# MULTI-STATION SIZING PROCEDURE

The feasibility of obtaining optimum designs for stiffened wing, empennage, or fuselage surface panels has, to date, been constrained by the required point-by-point application of most panel sizing codes. Optimum designs obtained at each point satisfy all the design requirements but are not necessarily geometrically compatible with adjacent designs. The panel sizing code, POSTOP, has been extended to allow determination of designs at a number of adjacent stations that are compatible and that minimize the weight of the total surface panel. This improved sizing code increases the structural efficiency, the computational efficiency, and the designer efficiency over that obtained using previous sizing procedures.

Suppose, for example, that a wing surface is to be designed. Point optimum designs may indicate stiffener spacings of 8, 6, 7, and 4 inches at adjacent stations. If a constant stiffener spacing is required, the designer must select an intermediate spacing, weighted in some way to reflect the wider surface dimensions nearer the wing root, and reoptimize the panels. If similar geometric requirements dictate the relationship of stiffener heights, widths, and lamina thicknesses as well as stacking sequences from station to station along the wing, the number of arbitrary decisions required by the designer may soon become overwhelming. Numerous modifications of these decisions and subsequent reoptimizations may be required in attempting to minimize the total weight of the wing surface. A true minimum weight design may never be obtained, even after extensive effort by the designer.

The improved sizing code eliminates the difficulties and inaccuracies described above. Lamina thicknesses, stiffener dimensions, and stiffener spacing are assumed to vary smoothly from station to station. Up to a second-order longitudinal variation of any dimension or thickness is currently allowed, as shown in figure 9. Here $X_{oi}$, $a_i$, and $b_i$ are the design variables for the ith design parameter $X_i(x)$. If optimum values for n design parameters are to be determined at each station on the structure, no more than a total of 3n design variables must be optimized regardless of the number of stations specified. In this way, the size of the optimization problem remains relatively small, the required computer time is decreased, and the likelihood of determining a successful optimum design is increased.



$$X_i(x) = X_{oi} (1 + a_i x + b_i x^2)$$

$$i = 1, \ldots n$$
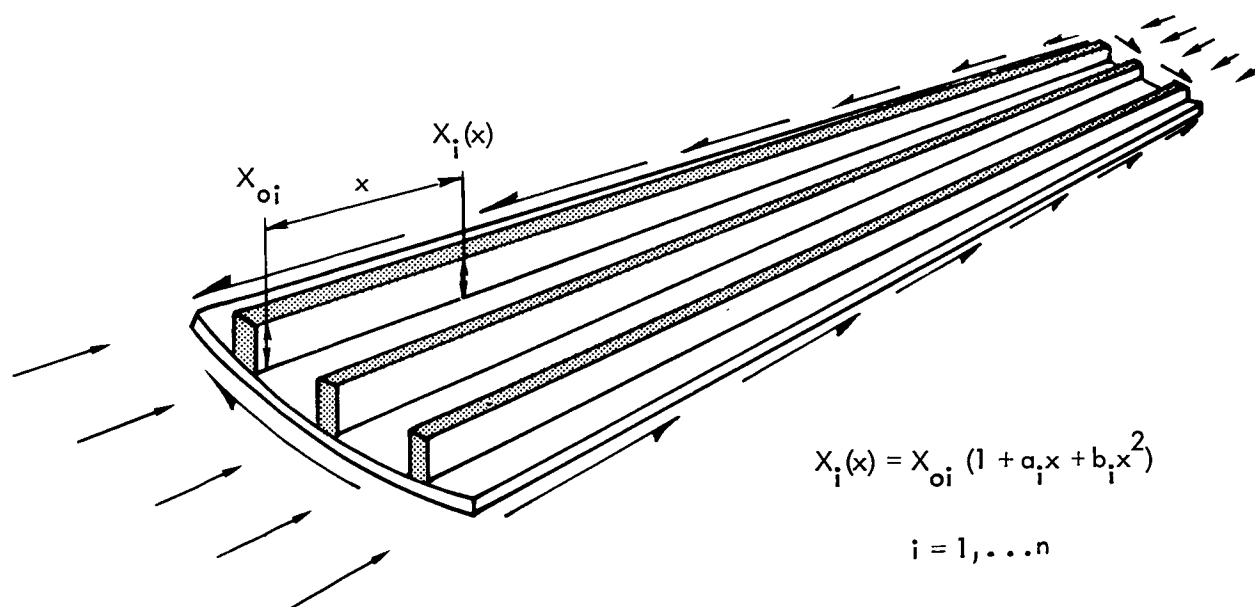
Figure 9.

## EXAMPLE OF MULTI-STATION SIZING

In the optimization procedure, the minimum total weight of the structure is the objective function. The width of the structure may be specified at each station so that the weight of structures with tapering planform, such as wing covers, may be accurately determined. As an example of the application of this procedure, consider a wing surface subject to the ultimate loads listed in figure 10. The wing chord widths and minimum shear stiffness requirements are also shown in the figure. For simplicity, assume that the surface panel is to be aluminum with integral stiffeners, as shown in the figure. The allowable effective stress is 53 ksi. Local buckling is not allowed. The station-to-station geometric constraints are (1) constant stiffener spacing; (2) linearly varying stiffener height, flange width, and web thickness; and (3) second-order variations in the skin and flange thicknesses. The six design parameters and the 13 associated design variables are listed in figure 10.

| STATION (IN) | SPANWISE LOAD (LB/IN) | SHEAR LOAD (LB/IN) | CHORD WIDTH (IN) | SHEAR STIFF. REQ'D. (LB/IN X $10^6$) |
|---|---|---|---|---|
| 79 | 20,850 | 2850 | 144 | 1.05 |
| 142 | 17,890 | 2880 | 139 | 0.94 |
| 260 | 13,070 | 2280 | 129 | 0.75 |
| 368 | 8,990 | 1940 | 120 | 0.65 |
| 522 | 4,400 | 1450 | 107 | 0.51 |
| 673 | 1,220 | 660 | 95 | 0.36 |



| PARAM. / VARIABLE | w | h | b | $t_f$ | $t_w$ | $t_s$ |
|---|---|---|---|---|---|---|
| $X_{oi}$ | $X_{o1}$ | $X_{o2}$ | $X_{o3}$ | $X_{o4}$ | $X_{o5}$ | $X_{o6}$ |
| $a_i$ | $a_1$ | $a_2$ | | $a_4$ | $a_5$ | $a_6$ |
| $b_i$ | | | | $b_4$ | | $b_6$ |
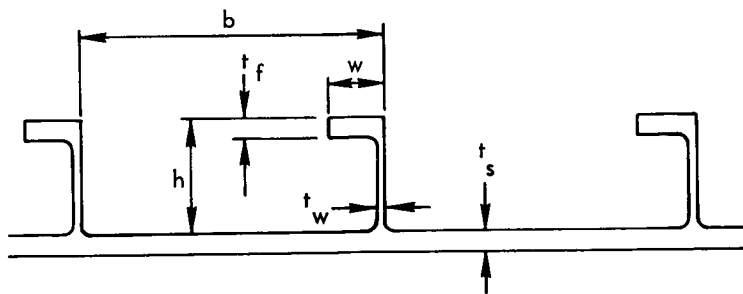
Figure 10.

# COMPARISON OF RESULTS

The results of the sequential application of the point-by-point optimization procedure to the same wing surface panel are shown in figures 11(a) through (g). In each design cycle, optimum designs were obtained at each of the six stations with six independent computer runs. In Cycle 1, all six design parameters were allowed to vary freely. The resulting designs, shown in figure 11(a), violate all of the station-to-station constraints. Using the optimum stiffener spacings from Cycle 1, a constant spacing of 6.22 inches was computed with the panel weight per unit length at each station as weighting factors. Using this constant value for stiffener spacing, a second optimization cycle was performed with the remaining five parameters as design variables. The resulting designs are presented in figure 11(b) with the constrained stiffener spacing shown as a short dash line. Next, the stiffener height constraint was applied. A third optimization cycle was performed using the remaining four parameters as design variables. The resulting designs are presented in figure 11(c) with the newly constrained parameter, h, shown as a short dash line and the previously constrained parameter, b, shown as a long dash line. This process was continued until all station-to-station constraints were imposed. The resulting final design is shown in figure 11(g). The total weight of the optimum surface panel is 1912 pounds, only 2 percent heavier than the multi-station optimum. However, 42 separate computer runs were required by the point-by-point procedure, and 1400 computing units were used.

The dimensions of the optimum design obtained with the new sizing code are shown in figure 11(h). The total weight of this surface panel is 1881 pounds. This design was obtained in one computer run that used 1000 computing time units.

This simple example shows the benefits of multi-station optimization. Compared with point-by-point optimization, a small reduction in structural weight and a 30 percent reduction in computer time were achieved. The designer time was greatly reduced by eliminating the cycle-to-cycle decision concerning practical constraint should be applied next and how it should be applied. Reduction of the number of data setups and computer runs from 42 to 1 results in the most dramatic improvements in efficiency. Improvements in structural, computational, and designer efficiencies increase as the number of design variables increases.
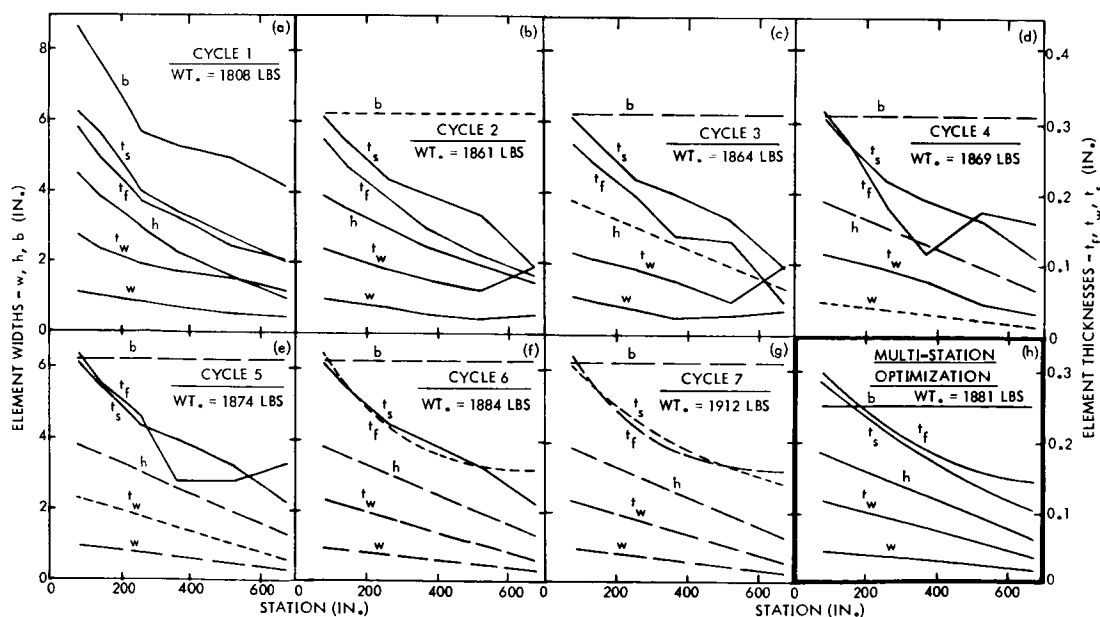


Figure 11.

# POSTBUCKLED FUSELAGE INTERNAL LOAD REDISTRIBUTION

A fuselage subjected to multi-axis bending, shear, and torsion will experience panel-to-panel as well as skin-to-stiffener load redistribution after skin buckling. This circumferential redistribution is due to the effect of reduced skin stiffnesses on the overall bending and torsional stiffness of the fuselage. An iterative procedure has been developed to compute this redistribution and the reduced global bending and torsional stiffnesses associated with skin buckling. Reduced global stiffnesses may, in turn, affect the computation of external loads on the fuselage.

As an example of the internal load redistribution, consider a circular fuselage subject to a vertical shear $V_z$, a torsion $M_z$, and a bending moment $M_y$. Figure 12 shows the shear flow and axial load distribution as a function of load level. The neutral-axis shift toward the upper tension-loaded portion of the fuselage is clear. As a result, the tension loads increase at an increasing rate after buckling. Likewise, an increasing proportion of the compression loads is carried by the panels close to the sides of the fuselage after buckling. In this single-cell example, no redistribution of shear load occurs as it does in the case of a multi-cell fuselage. However, even in this example, consideration of combined shear and biaxial loads is important due to their interactive effect on postbuckled plate stiffnesses.

$$\text{APPLIED LOADS} \Bigg\} \begin{cases} M_x = 100 \ V_z \\ M_y = 1000 \ V_z \end{cases} \qquad F = \frac{\text{ACTUAL LOAD APPLIED}}{\text{LOAD AT INITIAL BUCKLING}}$$



SHEAR FLOW, $N_{xy}$        AXIAL LOAD, $N_x$

Figure 12.

# MULTI-LEVEL STRUCTURAL DESIGN INTERACTION

Aircraft structural design is carried out on several levels of detail. Optimization at any level causes interaction with the others. Nonlinearities due to postbuckling stiffness reductions cause external and internal load redistribution and additional interaction between design levels. Figure 13 illustrates potential interaction between five levels of analysis and design detail. Dashed lines between major components and subcomponents, and between stiffened panels and laminates indicate that the two adjacent items are sometimes not treated separately.

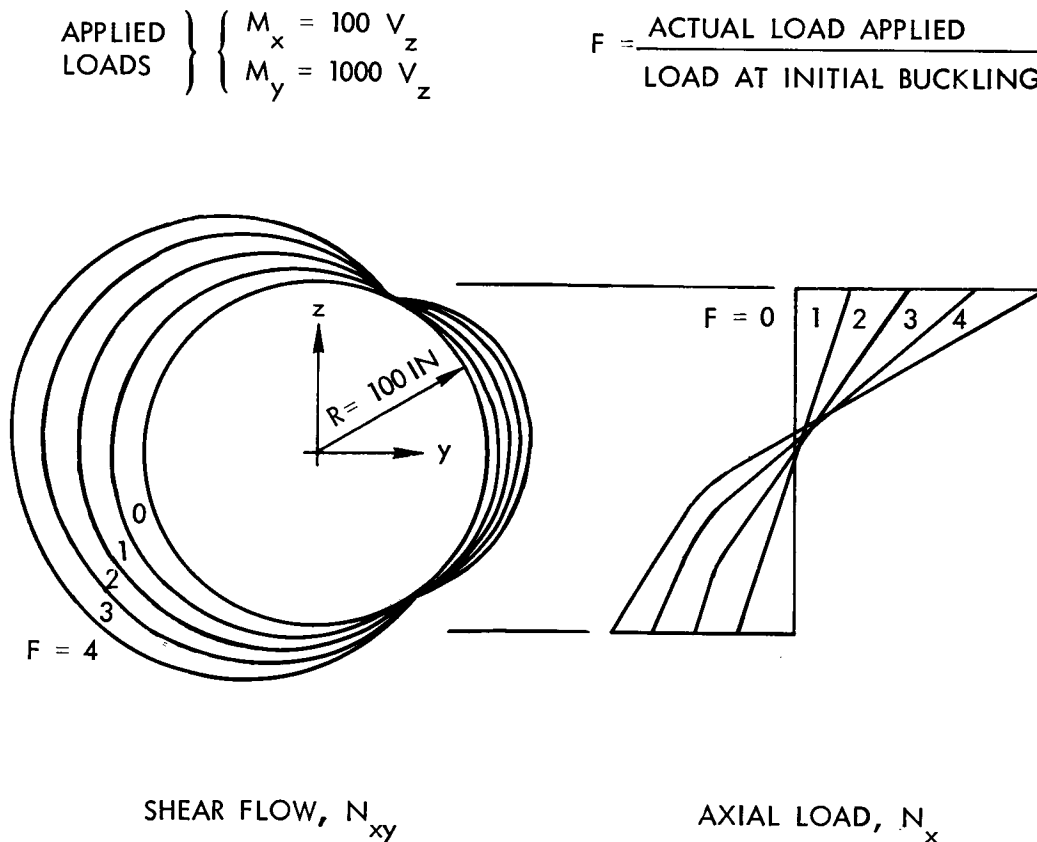For a fixed aircraft configuration, approximate external loads (rigid loads) are computed. Based on these loads, initial component designs are determined. Refined external loads (flexible loads) are determined iteratively, accounting for the effects of structural deformations. Optimization to minimize undesirable deformations may be performed. If significant response changes ($\Delta$) occur, the flexible loads must be re-computed. Otherwise, refined analyses at the subcomponent level begins. Internal loads on panels are computed. If any panels are buckled, stiffness reductions occur and the loads must be redistributed in an iterative procedure such as the fuselage load redistribution described previously. If postbuckling stiffness reductions cause significant overall stiffness changes ($\Delta$: buckle), it is necessary to return to the major component analysis to recompute the flexible external loads. If optimization at the subcomponent level (e.g., the multi-station approach discussed previously) causes significant changes ($\Delta$: opt.), it may be necessary to recompute the flexible external loads and/or to restart the subcomponent analysis.

Once interaction at the three upper levels is complete, panel loads are defined and detail panel sizing begins (e.g., with POSTOP or equivalent). Postbuckling requires an iterative redistribution analysis for the skin and stiffener loads. Detailed stress, stiffness, and stability analyses are then performed. If panel sizing causes significant panel stiffness changes, it may again be necessary to return to the subcomponent or major component level. This multi-level interaction, along with complex analyses and iterative nonlinear procedures required at each level, provides a challenging problem. Interaction with nonstructural disciplines provides additional challenges. Multi-level optimization approaches (refs. 6 and 7) appear to be promising solutions to the problem.
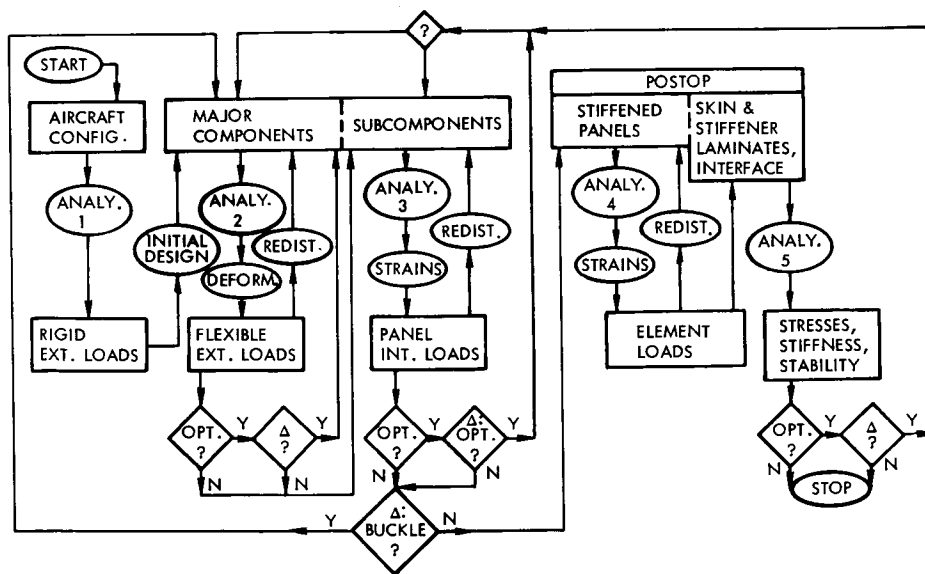


Figure 13.

# REFERENCES

1. Dickson, J. N., and Biggers, S. B.: POSTOP: Postbuckled Open-STiffener Optimum Panels - Theory and Capability. NASA CR-172259, December 1983.

2. Biggers, S. B. and Dickson, J. N.: POSTOP: Postbuckled Open-STiffener Optimum Panels - User's Manual. NASA CR-172260, December 1983.

3. Vanderplaats, G. N.; Sugimoto, H.; and Sprague, C. M.: ADS-1: A New General-Purpose Optimization Program. 24th Structures, Structural Dynamics, and Materials Conference, Part 1, pp. 117-123, Lake Tahoe, Nevada, 1983.

4. Madsen, L. E. and Vanderplaats, G. N.: COPES - A Fortran Control Program for Engineering Synthesis. Report No. NPS69-81-003, Naval Postgraduate School, Monterey, Calif., March 1982.

5. Vanderplaats, G. N.: CONMIN - A Fortran Program for CONstrained Function MINimization - User's Manual. NASA TM X-62282, 1973.

6. Sobieski, J.: A Linear Decomposition Method for Large Optimization Problems - Blueprint for Development. NASA TM-83248, February 1982.

7. Schmit, L. A., and Mehrinfar, M.: Multilevel Optimum Design of Structures with Fiber-Composite Stiffened-Panel Components. AIAA Journal, Vol. 20, No. 1, January 1982.

OPTIMAL REDESIGN STUDY OF THE HARM WING

S. C. McIntosh, Jr.
McIntosh Structural Dynamics, Inc.
Palo Alto, California

M. E. Weynand
Texas Instruments Inc.
Lewisville, Texas

# PROJECT TASKS

The purpose of this project was to investigate the use of optimization techniques to improve the flutter margins of the HARM AGM-88A wing. The missile has four cruciform wings, located near mid-fuselage, that are actuated in pairs symmetrically and antisymmetrically to provide pitch, yaw, and roll control. The wings have a solid stainless steel forward section and a stainless steel crushed-honeycomb aft section. The wing restraint stiffness is dependent upon wing pitch amplitude and varies from a low value near neutral pitch attitude to a much higher value at off-neutral pitch attitudes, where aerodynamic loads lock out any free play in the control system. The most critical condition for flutter is the low-stiffness condition in which the wings are moved symmetrically. Although a tendency toward limit-cycle flutter is controlled in the current design by controller logic, wing redesign to improve this situation is attractive because it can be accomplished as a retrofit.

Project tasks are listed in figure 1. In view of the exploratory nature of the study, it was decided to apply the optimization to a wing-only model, validated by comparison with results obtained by Texas Instruments (TI). Any wing designs that looked promising were to be evaluated at TI with more complicated models, including body modes. The optimization work was performed by McIntosh Structural Dynamics, Inc. (MSD) under a contract from TI.

1. Develop simplified wing-only models and match TI frequencies and mode shapes for four root restraints--symmetric low and high stiffness, antisymmetric low and high stiffness.

2. Perform flutter analyses at M = 0.8, 1.2, 1.5, 2.5. Compare results with those computed by TI.

3. Optimize for improved flutter margins; concentrate on critical configuration (symmetric, low stiffness).

4. Assess optimized wing designs in cooperation with TI; perform additional analyses, optimizations, and assessments as time, funding permit.

5. Submit a Final Report.

Figure 1

# FLOW DIAGRAM OF ANALYSIS AND OPTIMIZATION TASKS

The various computer codes used in this project and their functions are illustrated in figure 2. The tasks on the left side of the figure represent the traditional flutter-analysis cycle, with the exception of the design-variable linking capability in DVLINK. This code permits arbitrary combinations of design variables to be linked together, or slaved, so that a number of different optimization models can be created from a single output file of the finite-element code SAMGEN. DVLINK also includes a scaling capability, so that discrete finite-element models of any new design can be created without recourse to SAMGEN. Design variables for either bending or in-plane elements can be used.

Program PARMAT makes use of the system's natural modes from VIBE and the discrete mass and stiffness matrices from DVLINK associated with each design variable to create the corresponding generalized mass and stiffness matrices. Program WEIGHT makes use of the input data for SAMGEN to compute weight coefficients for each design variable to be used in determining the objective function (weight). All this information is passed to the optimization executive routine FLTOPT, which is coupled to the general-purpose optimization code CONMIN (ref. 1). The development of the original versions of the analysis codes is described in refs. 2 and 3.

All of the MSD computations were performed on a DEC VAX 11/780 minicomputer.

| Program | Purpose |
|---------|---------|
| SAMGEN | Generate finite-element model, discrete derivative matrices |
| DVLINK | Generate linked, scaled finite-element model |
| COLAPS | Collapse mass, stiffness matrices |
| VIBE | Compute natural modes, frequencies |
| AERO | Compute generalized aerodynamic forces--doublet lattice (subsonic), Mach box (supersonic) |
| MAKFIT | Compute polynomial fits of generalized aerodynamic forces in Mach number, reduced frequency |
| FLUTER | Perform flutter analyses |
| WEIGHT | Compute weight coefficients for objective function |
| PARMAT | Compute generalized derivative matrices |
| FLTOPT | Control optimization; evaluate constraints and constraint gradients |
| CONMIN | Optimization driver (feasible directions) |



Figure 2

253

The wing node-point layout and original design-variable numbering are illustrated in figure 3. The node-point layout on the wing and the element thicknesses were identical with those used at TI. The solid forward section was represented by solid triangular bending elements and the sandwich aft section by sandwich triangular bending elements. The TI wing model incorporated quadrilateral elements and sandwich elements with shear flexibility, which the MSD sandwich elements did not have. The MSD wing model was therefore somewhat stiffer than the TI model, and this resulted in MSD-computed natural frequencies that were greater than those computed at TI, particularly for the higher mode numbers. Mode shapes and frequencies for the lower mode numbers (say, the first three) were in very good agreement, however, for both cantilever and free-free test cases.
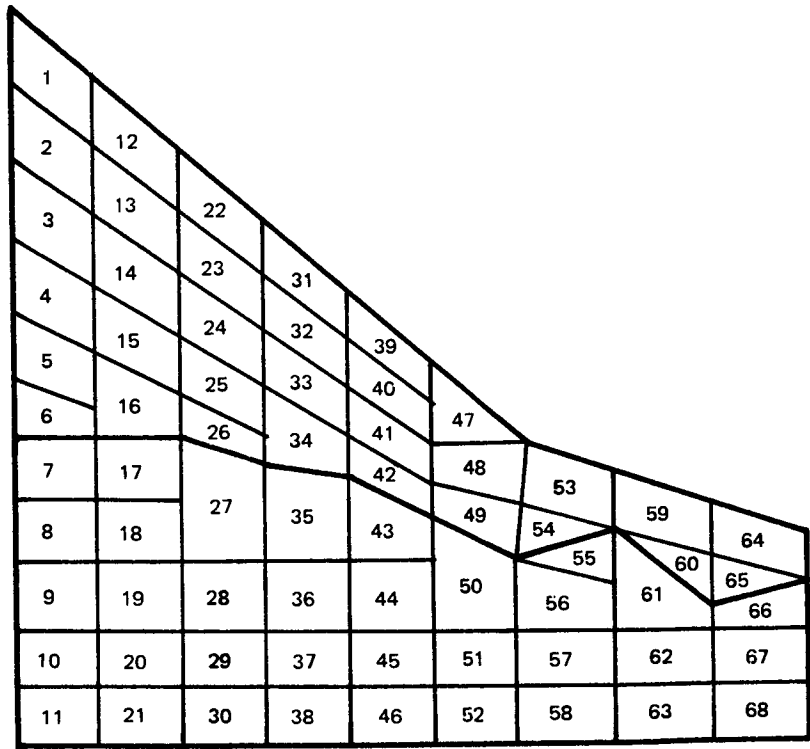


Figure 3

# FREQUENCY COMPARISONS

The wing model to be optimized had linear springs at the root to represent restraint stiffnesses in the pitch (control) and flap (transverse) directions. Four separate configurations had been analyzed by TI--low and high stiffness values for both symmetric and antisymmetric control motions. These four configurations were also analyzed by MSD. Nominal equivalent linear spring rates supplied by TI were used initially for the root restraints and were then varied to provide the best possible match with TI-computed frequencies, where these were available. The results of this matching effort are given in figure 4. For the two low-stiffness configurations, the first two frequencies were matched virtually exactly, with relatively minor variations from the nominal stiffness values. For the one high-stiffness configuration for which TI-computed frequencies were available, it was not possible to match the frequencies very well. In this case, the simple two-spring model was not adequate to represent the root restraint given by the actual hardware. A more representative simplified model was not developed for this configuration, since the two low-stiffness configurations were more critical for flutter.

| | SYMMETRIC | | | | ANTISYMMETRIC | | | |
|---|---|---|---|---|---|---|---|---|
| | $K_\theta$ | $K_f$ | $f_1$ | $f_2$ | $K_\theta$ | $K_f$ | $f_1$ | $f_2$ |
| | Low Stiffness | | | | Low Stiffness | | | |
| TI | 209.0 | 7,880 | 42.78 | 96.00 | 3,279 | 8,640 | 78.29 | 150.8 |
| MSD | 294.6 | 6,458 | 41.53 | 96.72 | 1,679 | 18,550 | 77.84 | 150.9 |
| | High Stiffness | | | | High Stiffness | | | |
| TI | 1,016 | 16,000 | 80.5 | 128 | 2,962 | 28,410 | – | – |
| MSD | 1,930 | 16,000 | 78.8 | 156 | 2,962 | 28,410 | 87.5 | 183 |

$K_\theta$ = pitch stiffness, in-lb/deg
$K_f$ = flap stiffness, in-lb/deg
$f_1$ = first mode frequency, Hz
$f_2$ = second mode frequency, Hz

Figure 4

Flutter analyses of the isolated wing with the four root-restraint conditions discussed previously confirmed that the symmetric low-stiffness condition was the critical one, with the flutter margin in the low supersonic Mach number range most in need of improvement. Redesign to improve the flutter speed at Mach 1.5 was therefore selected as the principal goal. Improvement in the flutter speed was sought by posing the usual optimization problem with weight as the objective function, but with an initial flutter-related constraint that was violated. The flutter constraint was imposed by requiring that the damping parameter g be less than or equal to a critical value of 0.03 (in other words, flutter was defined for 3% structural damping). The altitude, Mach number, and airspeed were fixed. Figure 5 illustrates this concept. An initially infeasible point on the critical flutter branch in V-g space was to be driven to g = 0.03 or less along a constant-V line. The optimization algorithm was thus confronted with two tasks—first, to bring the flutter constraint function g = 0.03 to an acceptable value, and second, to reduce the wing weight, if possible, without violating this constraint.

During constraint evaluation, the value of the reduced frequency was varied to keep the airspeed associated with the critical root equal to the desired airspeed. Generalized coordinates defined by the natural modes of the initial design were retained throughout the optimization.
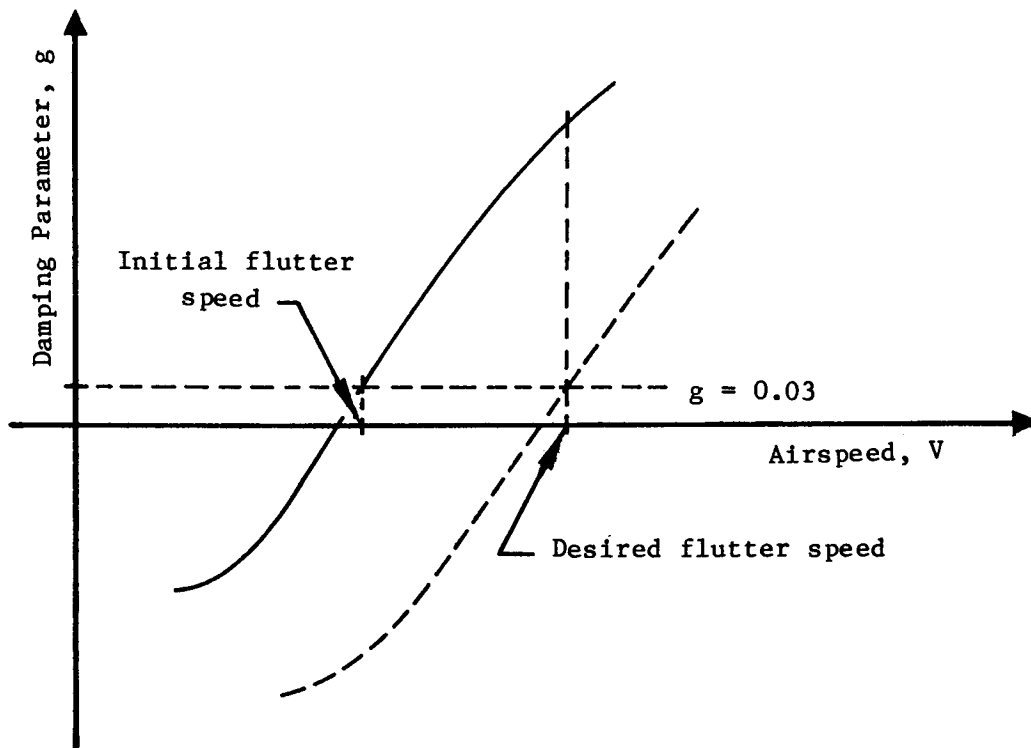


Figure 5

## OPTIMIZATION MODEL NO. 1

In all of the optimization models, the design variables were scale factors on the initial element thicknesses. Hence, the initial values of the design variables were always 1.0. In addition to the primary flutter constraint, upper and lower bounds were also imposed on the design variables.

The first optimization model had six design variables, three in the solid section and three in the sandwich section. An improvement of 300 fps was sought in the flutter speed, with the Mach number and altitude fixed, respectively, at 1.5 and 22,000 ft. Upper and lower bounds of 3.0 and 0.5, respectively, were imposed on the design variables. Convergence was obtained in 14 iterations, and it was found that almost two lb had to be added to achieve the desired increase in flutter speed. Only one design variable--T(1)--was not at an upper or lower bound. Most of the weight increase came from the 30% or so increase in thickness called for by T(1), which governed the inboard leading-edge portion of the wing. These results are illustrated in figure 6.

A complete flutter analysis of the final design with the original generalized coordinates (nine in all) confirmed that the first-mode branch was still the critical flutter branch. It was therefore not necessary to select other points in V-g space to be constrained; this was the case for all the optimization problems considered.
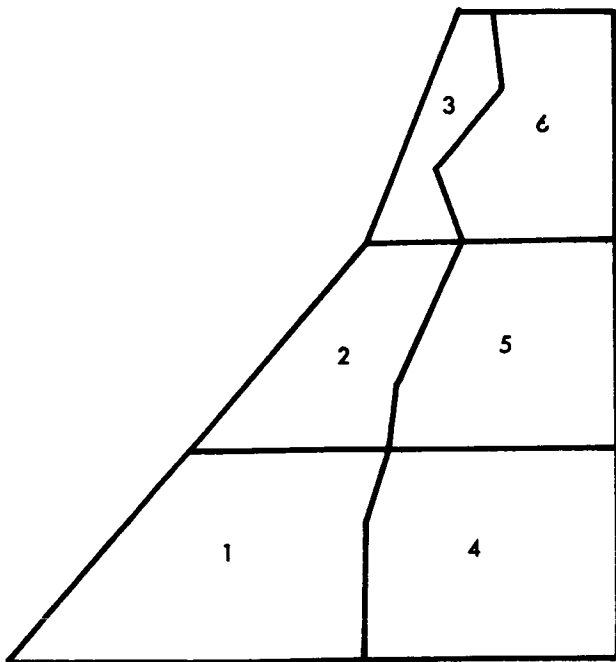


**OPTIMIZATION RESULTS**
Optimization Model No. 1 - 6 DV's

| | | |
|---|---|---|
| Initial Weight: | | 8.707 lb |
| Initial Flutter Speed, M = 1.5: | | 1540 fps |
| Final Weight: | | 10.57 lb |
| Final Flutter Speed, M = 1.5: | | 1842 fps |

Optimal Design:

| I | 1 | 2 | 3 | 4 | 5 | 6 |
|---|---|---|---|---|---|---|
| T(I) | 1.308 | 0.5 | 0.5 | 0.5 | 3.0 | 3.0 |

Figure 6

For the next optimization model, 11 design variables were chosen, as illustrated in figure 7. To allow in a very approximate manner for strength considerations, design variable no. 1 was selected to govern a spanwise portion of the solid section just forward of the juncture between the solid and sandwich sections. Stress analyses at TI has indicated that stresses were highest in this area for the design loading conditions for strength. A more restrictive lower bound, 0.9, was selected for this design variable, and the same 300-fps increase in flutter speed was sought. Convergence was again obtained after 14 iterations, with the desired flutter speed obtained and a weight reduction of over two lb. All design variables except T(6) were at their lower bounds, and T(6) was almost at its upper bound. These results suggest very strongly that much lighter construction--perhaps sandwich--could be used for most of the leading-edge wing portions as well, with a strong spar to carry wing loads into the root. The increase for T(6), which is at the tip, can be interpreted as calling primarily for mass balance, since the increased stiffness there will have little effect.

With such a drastic change in the design, it could be anticipated that the use of fixed modes would result in some inaccuracies. To test this, the optimal design was re-analyzed for flutter with normal modes. The flutter speed calculated for this model was an astonishing 2442 fps--some 600 fps more than the desired flutter speed and 900 fps more than the flutter speed of the initial design. This of course illustrates even more strongly the value of the redesign. In other cases, it is likely that the improvement would not be as great as estimated with fixed modes, and in general it must be expected that the modes would have to be updated and the optimization repeated in order to obtain satisfactory accuracy.



OPTIMIZATION RESULTS
Optimization Model No. 2 - 11 DV's
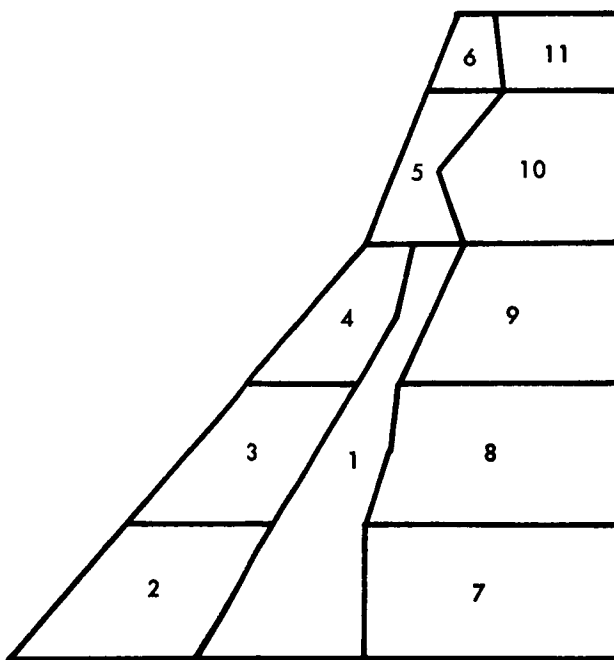
Initial Weight:                     8.707 lb
Initial Flutter Speed, M = 1.5:     1540 fps

Final Weight:                       6.430 lb
Final Flutter Speed, M = 1.5:       1842 fps

Optimal Design:

| I    | 1   | 2   | 3   | 4   | 5   | 6     |
|------|-----|-----|-----|-----|-----|-------|
| T(I) | 0.9 | 0.5 | 0.5 | 0.5 | 0.5 | 2.796 |

| I    | 7   | 8   | 9   | 10  | 11  |
|------|-----|-----|-----|-----|-----|
| T(I) | 0.5 | 0.5 | 0.5 | 0.5 | 3.0 |

Flutter speed, M = 1.5, optimal design with normal modes - 2442 fps!

Figure 7

258

# OPTIMIZATION MODEL NO. 3

    This model resembled model no. 2, but more chordwise divisions were chosen, and the number of design variables was increased to 15. The optimal design was obtained in 13 iterations and is almost the same as that found for the 11-DV case, as can be seen in figure 8.

OPTIMIZATION RESULTS
Optimization Model No. 3 - 15 DV's

| | | |
|---|---|---|
| Initial Weight: | | 8.707 lb |
| Initial Flutter Speed, M = 1.5: | | 1540 fps |
| Final Weight: | | 6.466 lb |
| Final Flutter Speed, M = 1.5: | | 1842 fps |

Optimal Design:

| I | 1 | 2 | 3 | 4 | 5 | 6 |
|---|---|---|---|---|---|---|
| T(I) | 0.9 | 0.9 | 0.9 | 0.5 | 0.5 | 0.5 |

| I | 7 | 8 | 9 | 10 | 11 | 12 |
|---|---|---|---|---|---|---|
| T(I) | 0.5 | 0.5 | 2.754 | 0.5 | 0.5 | 0.5 |

| I | 13 | 14 | 15 |
|---|---|---|---|
| T(I) | 0.5 | 0.8260 | 3.0 |

Figure 8

For this model, additional spanwise cuts were selected in order to see if more design flexibility in the chordwise direction would produce different results. However, the optimal design for this 14-DV case was not substantially different from the two previous optimal designs; see figure 9 for details.


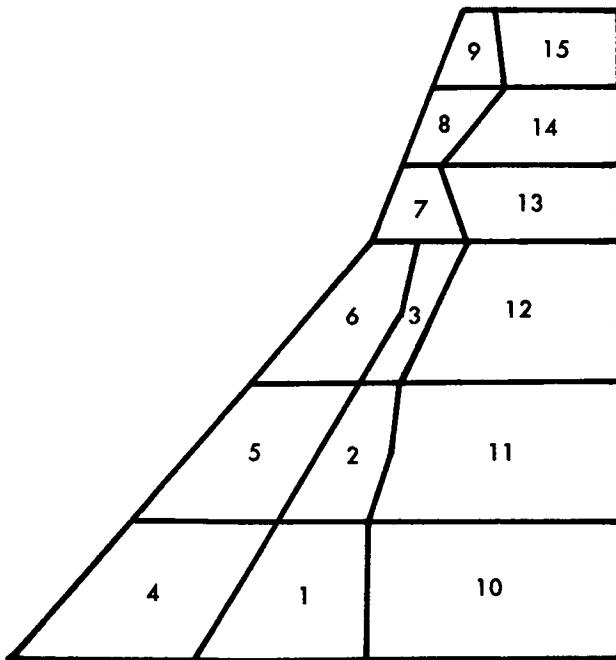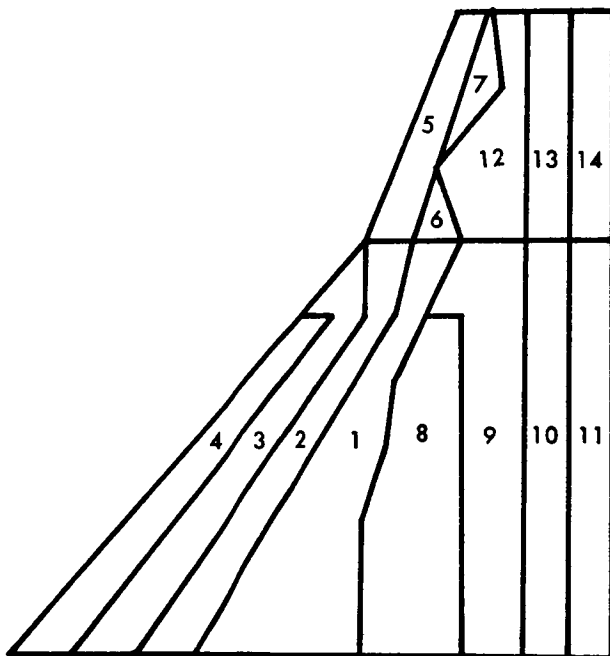
OPTIMIZATION RESULTS
Optimization Model No. 4 - 14 DV's

Initial Weight:                           8.707 lb
Initial Flutter Speed, M = 1.5:   1540 fps

Final Weight:                             6.755 lb
Final Flutter Speed, M = 1.5:     1842 fps

Optimal Design:

| I | 1 | 2 | 3 | 4 | 5 | 6 |
|---|---|---|---|---|---|---|
| T(I) | 0.9 | 0.5 | 0.5 | 0.5 | 0.5 | 0.5 |

| I | 7 | 8 | 9 | 10 | 11 | 12 |
|---|---|---|---|---|---|---|
| T(I) | 3.0 | 0.5 | 0.5 | 0.5 | 0.5 | 0.8066 |

| I | 13 | 14 |
|---|---|---|
| T(I) | 3.0 | 3.0 |

Figure 9

## COMPARISON OF NATURAL FREQUENCIES

The optimal wing-only design from optimization model no. 2 was modelled at TI and incorporated in a model of the complete missile which includes wings, tail fins, missile body, and shafts, actuators, and linkage. Figure 10 presents comparisons of the isolated-wing natural frequencies, the optimized complete-model natural frequencies, and those for the baseline complete model. Frequencies computed at TI for the wing model are in excellent agreement with those computed at MSD. When this wing model was coupled with the rest of the missile, only the first wing bending mode was affected. The interaction of the optimized wing with the internal structure and the missile body has resulted in a much lower frequency.

| | Frequency (HZ) | | | |
|---|---|---|---|---|
| Mode Description | Optimized Wing Model | | Complete Model | |
| | MSD | TI | Optimized | Baseline |
| Damper (pitch) | – | – | 9.0 | 8.7 |
| Actuator (pitch) | 40.3 | 39.6 | 40.5 | 42.4 |
| First Body Bending | – | – | 45.8 | 45.5 |
| First Wing Bending | 92.9 | 89.1 | 73.6 | 96.3 |
| Second Body Bending | – | – | 141 | 141 |
| Second Wing Bending | 175 | 170 | 171 | 204 |

Figure 10

## FLUTTER BOUNDARY OF COMPLETE MODEL

The optimized complete model was then analyzed for flutter at TI, at Mach numbers of 1.2, 1.5, and 2.0. These flutter points are compared with the flutter boundary of the baseline model in figure 11. Although the improvement in the flutter boundary at Mach 1.5 is not as great as is indicated by the wing-only analysis, it is nevertheless very significant. This improvement carried over to Mach 2.0, but there was virtually no change in the flutter boundary at Mach 1.2. This indicates that a somewhat different flutter mechanism was involved at Mach 1.2, and an additional flutter constraint at that Mach number would have to be included to obtain improvement there.
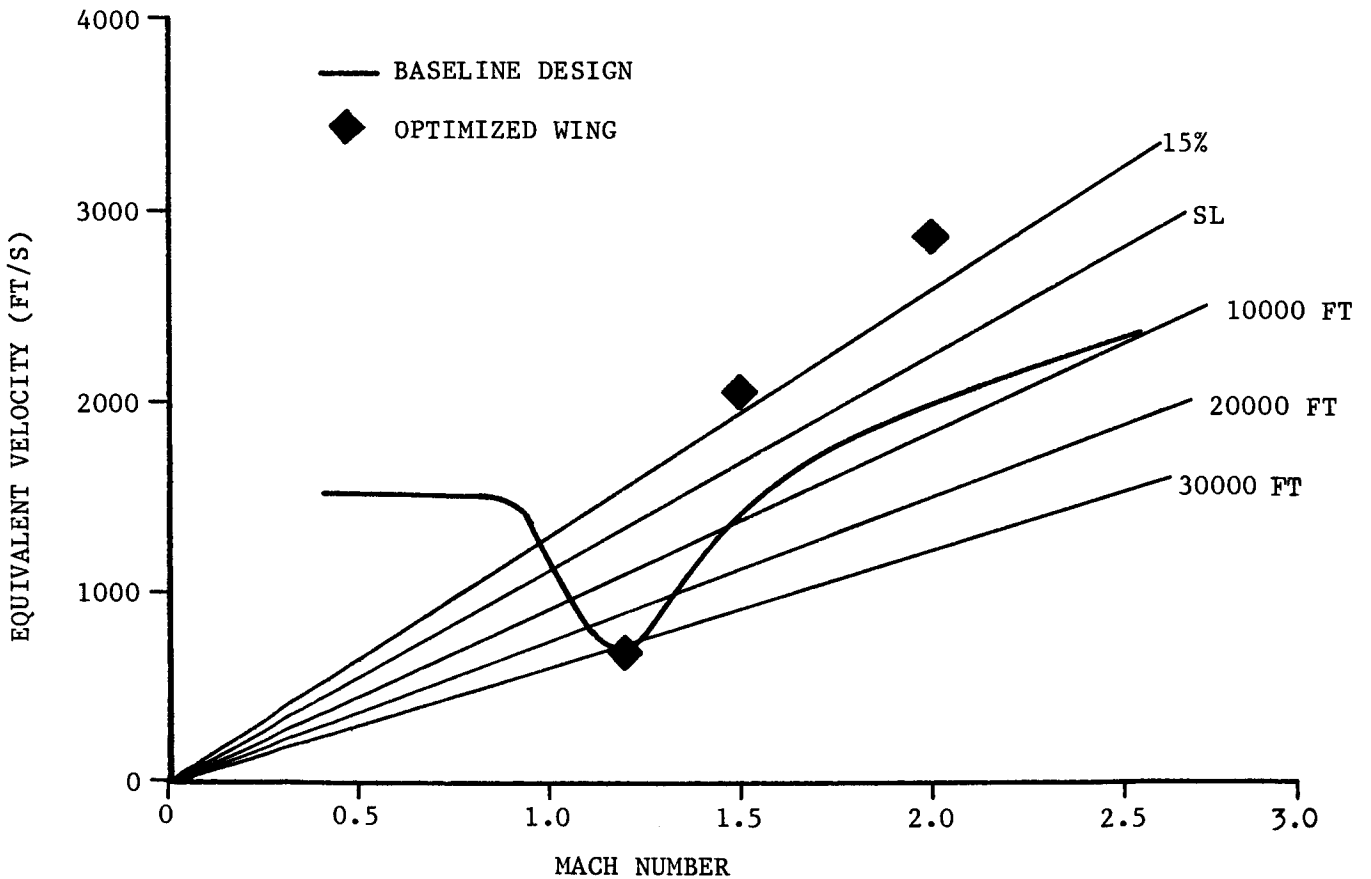


Figure 11

# CONCLUDING REMARKS

Although the results obtained here cannot be translated directly to a new design, they do indicate strongly how a redesign could proceed, with both reduced weight and substantially improved flutter margins. It is also worth noting that sensitivity studies from the initial design would not necessarily suggest modifications such as were finally determined by optimization. For example, the weight histories in all of the cases studied above showed an initial increase in weight, sometimes of three lb or more, just to satisfy the constraint before any weight reduction was attempted. Optimization can thus be viewed as an organized and effective way of arriving at an often counterintuitive result.

# REFERENCES

1. Vanderplaats, G. N.: CONMIN--A Fortran Program for Constrained Function Minimization. User's Manual. NASA TM X-62282, Aug. 1973; Addendum, May 1978.

2. Gwin, L. B. and S. C. McIntosh, Jr.: A Method of Minimum-Weight Synthesis for Flutter Requirements, Part I--Analytical Investigation, Part II--Program Documentation. AFFDL-TR-72-22, Pts. I and II, June 1972.

3. Gwin, L. B. and S. C. McIntosh, Jr.: Large Scale Flutter Optimization of Lifting Surfaces, Part I--Analytical Investigation, Part II--Program Documentation. AFFDL-TR-73-91, Pts. I and II, Jan. 1974.

COMPOSITE MATERIAL DESIGN, ANALYSIS, AND PROCESSING
OF SPACE MOTOR NOZZLE COMPONENTS*

Edward L. Stanton
PDA Engineering
Santa Ana, California

# A NONLINEAR PROGRAMMING METHOD FOR SYSTEM DESIGN
## WITH RESULTS THAT HAVE BEEN IMPLEMENTED

Frank Hauser
Boeing Aerospace Co.
Seattle, Washington

# OPTIMIZATION THEORY

The field of optimization is as broad and interrelated as the problems it attempts to solve. However, there appear to be two general categories:

(1) The indirect or classical methods, based on the calculus of variations, which are often said to involve "parachuting" to the optimum

(2) The direct or programming methods, which involve searching or climbing to the optimum

To list individual methods in the categories is difficult because many that involve indirect methods actually "search for places to parachute". For example, two Lagrangian methods that involve searching are: (1) the Sequential Gradient Restoration Algorithm (ref. 1); and (2) the Projected Lagrangian. The NICO program (Nonlinear Inequality Constrained Optimization) is definitely a Gradient Search Method.

- Indirect or classical, based on calculus of variations (parachuting)
  - Lagrangian methods
  - Optimal control e.g. LQR
  - Etc.

- Direct or programming (searching or climbing)
  - Simplex algorithm
  - Dynamic programming
  - Integer programming
  - Etc.
  - Gradient methods
    - Projected gradient algorithm
    - Method of constrained derivatives
    - NICO
    - Etc.

# NICO - GENERAL NONLINEAR PROGRAMMING ALGORITHM

Nonlinear Programming is perhaps the most powerful category in the field of optimization. With it, engineering problems can be solved directly; i.e., the problem does not have to be fit into a canonical form, wherein it can lose some of its features. The general nonlinear programming problem is to determine values for n variables, which satisfy m nonlinear constraints:

$$G_i(X_1, \ldots, X_n)[<, =, >]B_i \qquad\qquad i = 1, \ldots, m$$

and, in addition, maximize (or minimize) a nonlinear objective function

$$Z = f(X_1, \ldots, X_n)$$

All engineering problems fit this formulation, though many times the G's and f are only in the engineer's mind as he solves the problem by trial and error. The field of nonlinear programming contains systematic ways to solve the problem if it can be quantified. In most cases, it can be.

NICO can be further classified as a Parameter Optimization method; i.e., it finds the best values for variables whose "first guess" values are input by the user.

Determine $X_n$ values that satisfy nonlinear constraints

$$G_i(X_1, \ldots, X_n) \left\{ \begin{array}{c} < \\ = \\ > \end{array} \right\} B_i \qquad\qquad i = 1, \ldots, m$$

and maximize (minimize) nonlinear objective function

$$Z = F(X_1, \ldots, X_n)$$

Note: n not related to m

# NICO ITERATIVELY FORMS AND SOLVES
## THE FOLLOWING PROBLEM

The fundamental principle in NICO is to iterate to the final solution by solving a succession of linear programming problems.

NICO has two distinctive features: (1) the "first guess" does not have to satisfy any of the constraints (in most real engineering problems, the "first guess" is seldom feasible); and (2) it can converge to local interior as well as exterior optima.

In NICO, the objective is not as important as the constraints. But in most, if not all, engineering problems, the solution is dominated by the constraints. In fact, the optimum is constrained; i.e., constraints literally define the best values of the objective.

- Matrix of constraint equations

$$G_i(\overline{X_o + \Delta X}) = G_{io} + \sum_{j=1}^{n} \left(\frac{\partial G_i}{\partial X_j}\right)_o \Delta X_j \left\{ \begin{array}{c} < \\ = \\ > \end{array} \right\} B_i$$

Where $\Delta X_j = X_j - X_{jo}$ and $\left(\dfrac{\partial G_i}{\partial X_j}\right)_o$ is computed via finite difference

- Objective function to be maximized

$$Z(\overline{X_o + \Delta X}) = Z_o + \sum_{j=1}^{n} \left(\frac{\partial Z}{\partial X_j}\right)_o \Delta X_j$$

- Variable constraints

$$X_{jL} \leq X_j \leq X_{ju}$$

270

## ACADEMIC OPTIMIZATION EXAMPLE

This figure shows the application of NICO to an academic problem.  It shows how NICO iterated to the solution from three different nonfeasible "first guesses". It also shows another distinctive feature of NICO; i.e., it concentrates on the constraints.  Run 2 shows how the objective function decreases during the first few iterations in order to reach a feasible solution.  NICO moves in a "deflected gradient" direction; i.e., the objective function gradient is deflected by the constraints.  Often this is exactly what the engineer does as he optimizes, since most real engineering problems are dominated by the constraints, with the objective function providing only a general direction.



Academic Optimization Example
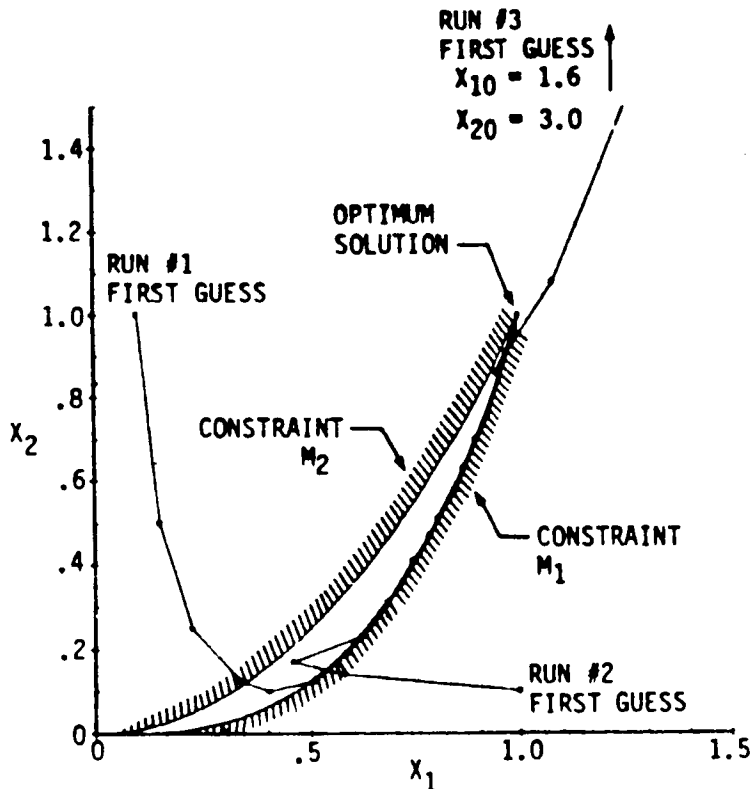
$$\max \quad Z = X_1$$

$$\text{Subject to :} \quad M_1 = X_2 - X_1^3 \geq 0.$$

$$M_2 = X_1^2 - X_2 \geq 0.$$

The academic example of the previous figure has an unusual situation at the point $X_1 = X_2 = 0$. As shown on this figure, the two "feasible regions" of this example are connected by this single point. NICO had no difficulty passing through this point, because it uses a "hunting" technique and operates much like an engineer as he iterates via a succession of trail points.



Academic Optimization Example
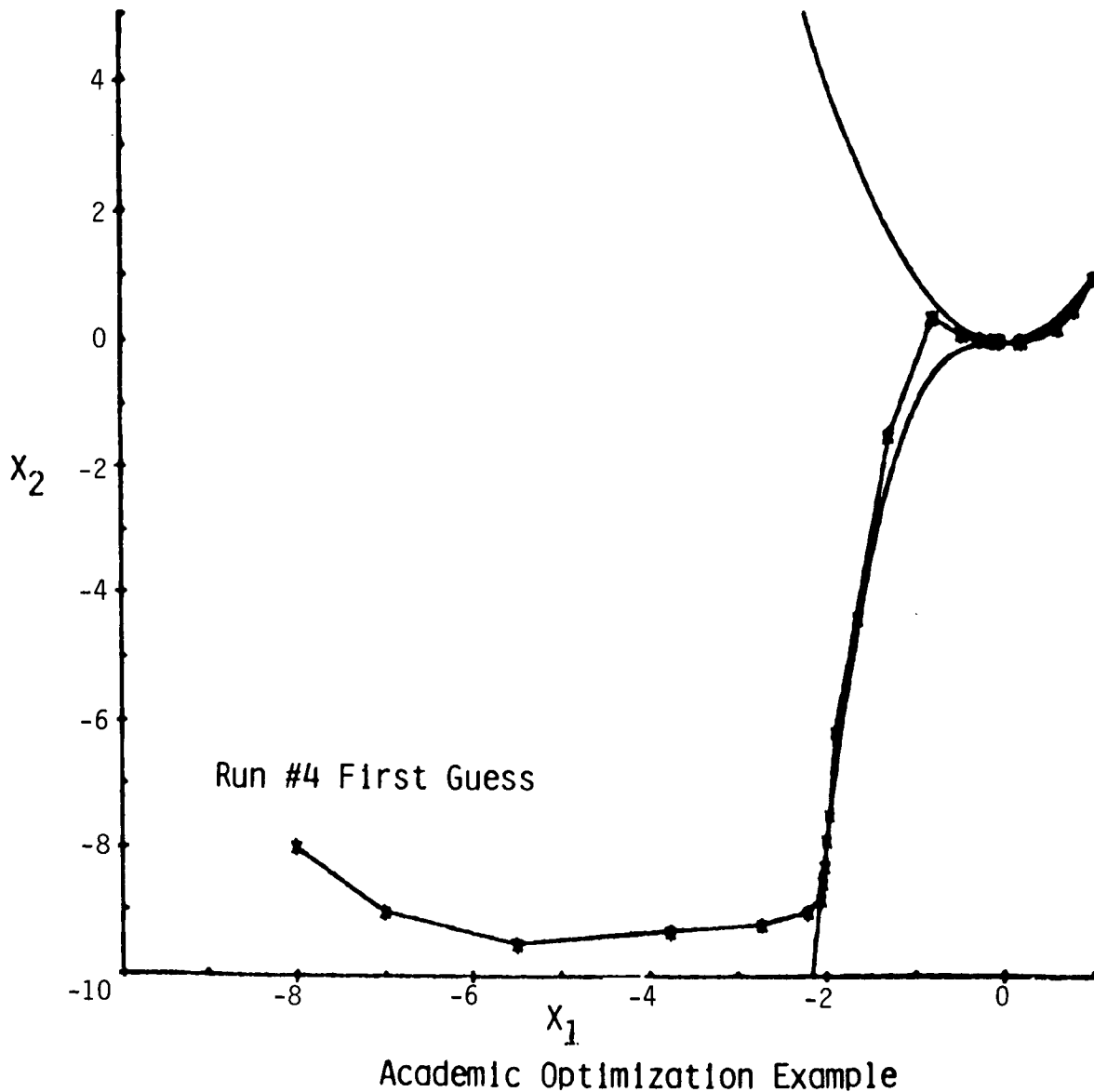
# NICO APPLICATIONS

(1) NICO was first applied to launch vehicle autopilot design and produced gains and filters for several (at least two) vehicles that flew. It has also been applied to a so-called Variable Payload Vehicle where it also produced results that were installed in software that actually flew. The latest successful application is on a Variable Trajectory Vehicle, where its design of the roll-yaw autopilot falls in the category of multivariable design.

(2) NICO was also applied to the control effector "trim" or static moment balance problem on an early space shuttle proposal.

(3) Another application included handling quality transient response criteria in the design of a reentry vehicle control system.

(4) Waterjet propulsion and lift system components were "sized" on a large Surface Effect Ship.

(5) NICO was used in an iceberg transportation study to select candidate icebergs, propulsion system size, and the best route.

| | |
|---|---|
| • Launch vehicle autopilot design | • Frequency response |
| | • Transient response |
| • Launch vehicle autopilot command mixer design | • Static moment balance |
| • Reentry vehicle autopilot design | • Handling qualities |
| • Surface Effect Ship Sizing | • Propulsion and lift system for payload/range |
| • Iceberg transportation | • Candidate icebergs, propulsion system, route |

# NICO LINKED TO LINEAR ANALYSIS PROGRAM

NICO is currently linked as a subroutine to a program that computes frequency responses. Previously, the engineer ran the linear analysis program iteratively, by trial and error selection of control system gains and filters, until the desired stability margins were achieved. NICO replaces the engineer, who now only inputs a "first guess". The engineer can now concentrate on the most important job; i.e., math modelling. NICO does the technically unchallenging job of iterating.

The interface program searches the system response and passes to NICO the array of current values of each of the constraints. It also passes the value of the objective function. NICO passes back new values for the variables that are to be used in computing the next frequency response.

```
┌──────────────────────────────────────────────────────────────────────┐
│                            Engineer                                    │
│                        Problem Definition                              │
└──────────────────────────────────────────────────────────────────────┘
   Math Model              Objective              • First guess variables
   + Data                  Function (z)             ($X_{no}$)
                                                   • Constraint requirements
                                                     ($B_j$)
┌──────────────────┐                  ┌──────────┐            ┌──────────────┐
│ Simulation Program│  Variables      │          │ Variables  │              │
│ (e.g. MDELTA      │                 │          │            │     NICO      │
│ Linear Analysis   │  Response (e.g.  │ Interface│ Constraints ($G_i$) │ "The Gopher"  │
│ Program)          │                 │          │            │              │
│                   │  Frequency      │          │ Objective (z) │          │
│                   │  Response)      │          │            │              │
└──────────────────┘                  └──────────┘            └──────────────┘
                                                                  $X_n$, $G_i$
```
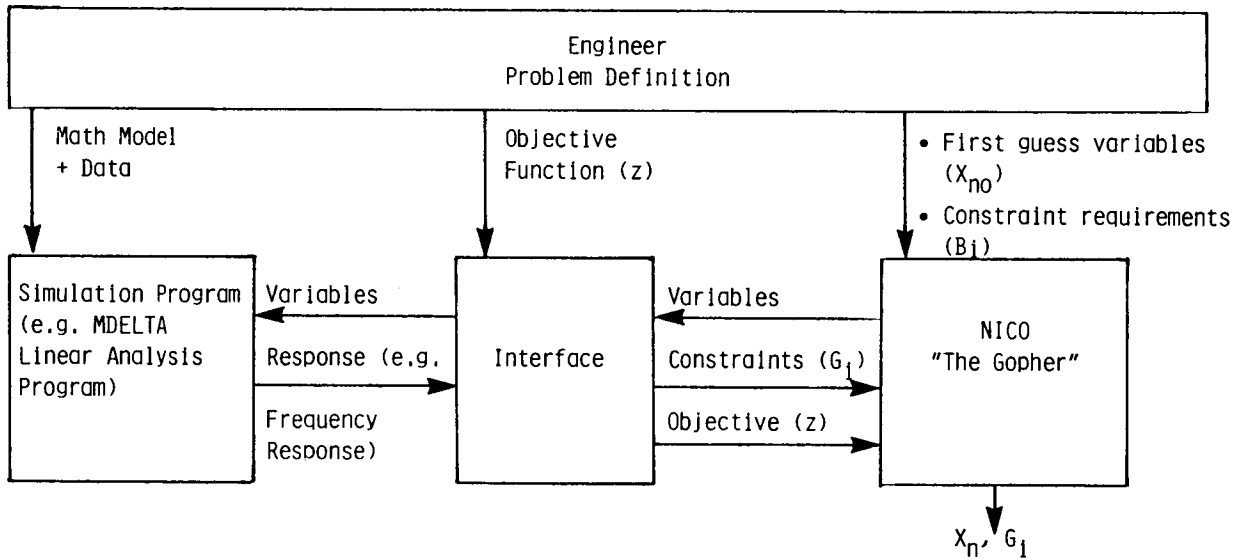
# NICO RESULTS THAT HAVE BEEN IMPLEMENTED

NICO was used to design an autopilot for a "so-called" variable payload vehicle. The gains and filters that were computed by NICO were programmed in the software of this vehicle on a mission that actually flew. The top figure shows that the initial user defined (first guess) values for the gains and filters resulted in an unstable bending mode. After six iterations, NICO produced values that stabilized this mode and exceeded all required stability margins. The final iteration resulted in a better system than had been previously designed by manual techniques, and it is felt that NICO required less engineering and computer time.
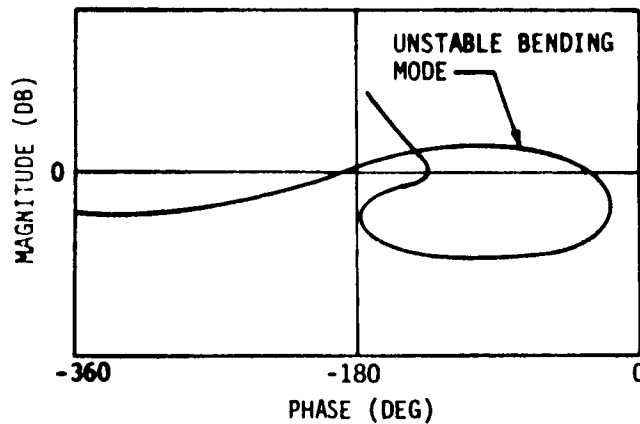


● FIRST GUESS RESULTED IN
  UNSTABLE BENDING MODE
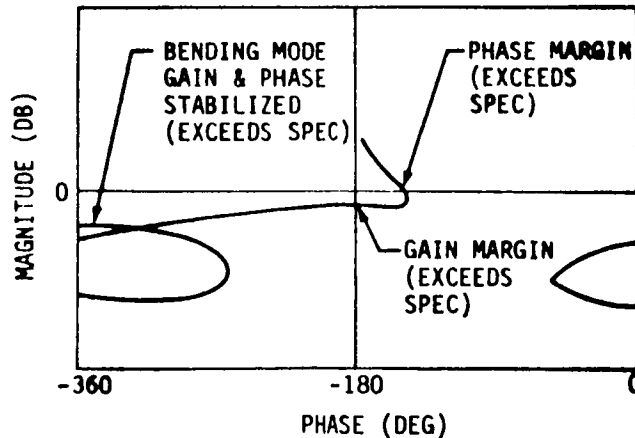


● 6 ITERATIONS LATER, STABILIZED
  WITH ALL MARGINS MET

# NICO MULTI-INPUT MULTI-OUTPUT CONTROL SYSTEM DESIGN

There have always been discussions about the shortcomings of classical frequency response design methods when dealing with multi-input multi-output (MIMO) control system design. The difficulties with MIMO systems arise from interactive effects; i.e., the action of one feedback loop affects the actions of the others. The standard practice used successfully by the "classical" engineer is simply to design all loops simultaneously. This iterative design approach includes an extensive tolerance analysis and yields optimum systems. NICO automates this classical approach.

This figure is a remarkable example of NICO applied to MIMO. This was the design of a roll-yaw autopilot on a variable trajectory vehicle. On every step, NICO simultaneously considered:

(1) Stability margins of the roll loop with the yaw loop closed
(2) Stability margins of the yaw loop with the roll loop closed
(3) Shape of the frequency response of roll due to command with all loops closed
(4) Shape of the frequency response of sideslip due to command with all loops closed

Disturbance rejection could also have been simultaneously considered by reducing the peak value of the frequency response of roll, sideslip, and all fin angles due to a disturbance like the wind.



ROLL DUE TO COMMAND, TIME RESPONSE, ALL LOOPS CLOSED



SIDESLIP DUE TO COMMAND, TIME RESPONSE, ALL LOOPS CLOSED
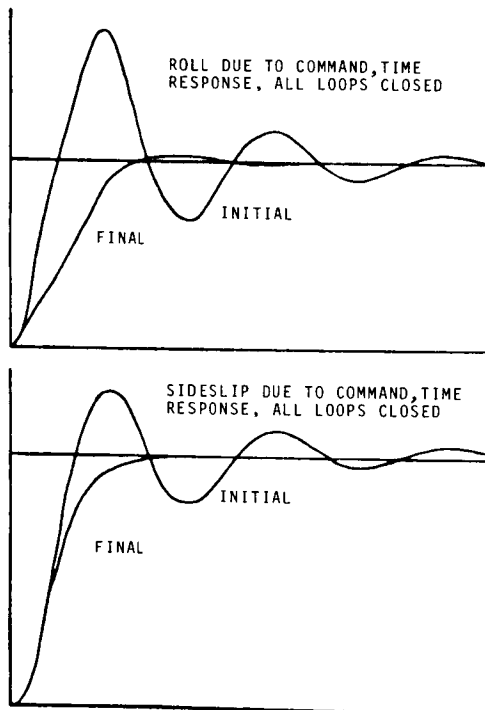
| PHASE MARGIN (DEGREES) | | |
|---|---|---|
| | INITIAL | FINAL |
| ROLL OPEN, YAW CLOSED | 22. | 60. |

| FREQUENCY RESPONSE, PEAK RESONANCE (dB), ALL LOOPS CLOSED | | |
|---|---|---|
| | INITIAL | FINAL |
| ROLL DUE TO COMMAND | 9. | 0. |
| SIDESLIP DUE TO COMMAND | 5. | 0. |

# SURFACE EFFECT SHIP SIZING

At one point in its development, NICO was linked to a program that computed the range/speed/payload performance of a Surface Effect Ship. NICO was used to establish: (1) the pump diameter, inlet area, and nozzle area of the waterjet propulsion system; (2) the lift system air flow rate; and (3) the vehicle speed that would maximize the payload for a given range. The constraints were: (1) maximum pump diameter, inlet area, nozzle area, horsepower, and air flow rate; (2) minimum speed; and (3) maximum speed possible while avoiding pump cavitation.

## RESULTS

|  | Engineer | NICO | Change |
|---|---|---|---|
| • Payload (short tons) | 3760 | 4000 | +6.4% |
| • Cruise Speed (knots) | 43 (cavitating) | 46 (No cavit.) | +6.5% |
| • Travel Time (hours) | 60 | 56.7 | +5.4% |

## ADVANTAGES

|  | Engineer | NICO |
|---|---|---|
| • Faster Response | Over two weeks of engineering manhours | 1 day |
| • Lower Cost | Over 40 runs varying major parameters (>$100) | 1 run (< $20) |
| • Improved Results | Feasible ship found, but not true optimum | True Optimum |

## REFERENCE

1. Miele, A.; Calastro, A.; Rossi, F.; and Wu, A. K.: A Modification of the Sequential Gradient Restoration Algorithm for Mathematical Programming Problems with Inequality Constraints, Aero-Astronautics Report No. 124, Rice Univ., 1975.

APPLICATION OF OPTIMIZATION TECHNIQUES TO THE DESIGN OF A
FLUTTER SUPPRESSION CONTROL LAW
FOR THE DAST ARW-2

William M. Adams, Jr., and Sherwood H. Tiffany
NASA Langley Research Center
Hampton, Virginia

OUTLINE

This paper describes the design of a candidate flutter suppression (FS) control law for the symmetric degrees of freedom for the DAST ARW-2 aircraft. The results shown here illustrate the application of several currently employed control law design techniques. Subsequent designs, obtained as the mathematical model of the ARW-2 is updated, are expected to employ similar methods and to provide a control law whose performance will be flight tested. This study represents one of the steps necessary to provide an assessment of the validity of applying current control law synthesis and analysis techniques in the design of actively controlled aircraft. Mathematical models employed in the control law design and evaluation phases are described. The control problem is specified by presenting the flutter boundary predicted for the uncontrolled aircraft and by defining objectives and constraints that the controller should satisfy. A full-order controller is obtained by using Linear Quadratic Gaussian (LQG) techniques (Refs. 1-4). The process of obtaining an implementable reduced-order controller is described (Refs. 5,6). One example is also shown in which constrained optimization techniques (Refs. 7-11) are utilized to explicitly include robustness criteria within the design algorithm.


● MATHEMATICAL MODELING

● ARW-2 FLUTTER CHARACTERISTICS

● CONTROLLER DESIGN OBJECTIVES AND CONSTRAINTS

● FULL-ORDER CONTROLLER DESIGN

● REDUCED-ORDER CONTROLLER DEFINITION

● MAXIMIZATION OF ROBUSTNESS OF REDUCED-ORDER CONTROLLER

C-4

# SENSOR SIGNAL INPUTS TO SYMMETRIC FLUTTER SUPPRESSION CONTROL LAW

The symmetric FS control law described here receives a feedback signal obtained by differencing the output of two vertical accelerometers located as shown on the outboard portion of the wing. Antisymmetric contributions are removed by summing signals from each wing semispan. The signal, properly compensated, is fed to each outboard aileron actuator. The objective of the FS design is to determine the compensation required to suppress flutter while satisfying other design criteria such as control power and robustness constraints.

Note that the control law is single-input/single-output (SISO). Furthermore, the sensor signal accentuates the observability of predominantly torsional modes at the expense of predominantly bending modes. It is planned, in a subsequent study, to investigate the benefit of including the sum of the accelerometer outputs as an additional feedback signal.
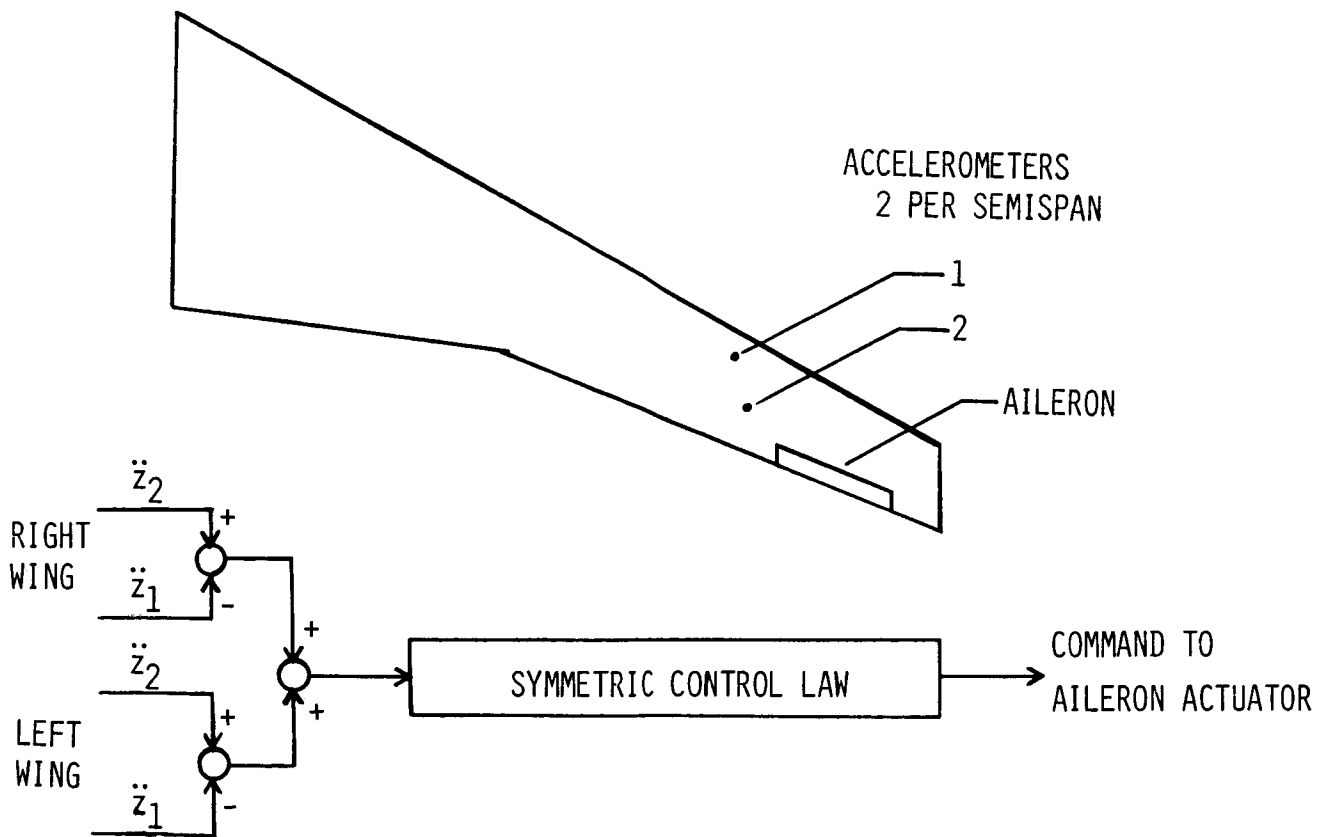
Mathematical models were developed using the ISAC (Interaction of Structures, Aerodynamics and Controls, Ref. 12) program. A modal characterization of the aircraft was employed which resulted from performing a free-free vibration analysis with symmetric constraints. Twelve symmetric modes were retained for the modeling: mean-body vertical translation and pitch plus 10 symmetric elastic modes.

Unsteady aerodynamic forces were computed for oscillatory motion by using a doublet lattice technique (Refs. 13,14) for several Mach numbers (M) and, at each Mach number, for a range of reduced frequencies (k). Reduced frequency satisfies the relationship $k = \omega b/U$ where b is a reference length (chosen here to be one half the mean aerodynamic chord of the wing), U is airspeed and $\omega$ is frequency in rad/sec.

A third-order transfer function representation of the actuator was employed which provided a good fit to its experimentally determined frequency response below a frequency of 300 rad/sec.

Approximate unsteady aerodynamic forces for arbitrary motion were generated in order to obtain a linear, time invariant (LTI) state space model. A least squares curve fit was made, at each Mach number, of the complex matrix of frequency dependent aerodynamic force coefficients, using a matrix function (Refs. 15-19). Constraints were imposed upon the rigid body and gust columns of $A_0$, $A_1$ and the $C_I$ matrices which required that the curve fit match the tabular data and its slope at k=0 (Ref. 20). In addition, the column of $A_2$, corresponding to forces due to gust inputs, was constrained to be zero.

The resulting LTI state space evaluation model was 77th order. (Four lag terms were employed in the s-plane fit and a second-order Dryden representation (Ref. 21) of the gust spectrum was used.)

o  MODAL CHARACTERIZATION OF STRUCTURE (2 RIGID BODY AND 10 FREE-FREE ELASTIC MODES)

o  DOUBLET LATTICE COMPUTATION OF UNSTEADY AERODYNAMIC FORCES

o  3RD ORDER REPRESENTATION OF ACTUATOR

o  S-PLANE APPROXIMATION OF UNSTEADY AERODYNAMICS (4 LAG TERMS)

$$Q = A_0 + A_1 S + A_2 S^2 + \sum_{I=1}^{4} \frac{S C_I}{(S + B_I)}$$

o  77 STATE EVALUATION MODEL

# DESIGN MODEL

A reduced-order model of the plant was developed in order to lower the cost of the control law design. Only two lag terms were used in the s-plane approximation. Modes with natural frequencies below or near the open-loop flutter frequency which were observed to have little effect upon the flutter characteristics were truncated. Modal residualization (Refs. 3,10,22,23) was employed to retain the static effects of the highest frequency modes. Five modes were retained in the design model, which had a 25th order state space representation (10 vehicle, 10 aerodynamic, 3 actuator, 2 gust).

- TRUNCATE NONCRITICAL MODES IN FLUTTER FREQUENCY RANGE OR BELOW

- REMOVE HIGH-FREQUENCY MODES BY MODAL RESIDUALIZATION

- TWO LAG S-PLANE AERODYNAMIC FORCE APPROXIMATION

- 25 STATE DESIGN MODEL

Bode plots of the symmetric signal sent to the controller per unit commanded control input were generated for the analysis and design models. The design model sensor signal amplitude is in good agreement with that of the full-order evaluation model. Phase angle comparisons, not shown, also exhibit excellent agreement at frequencies below 500 rad/sec.

The evaluation model Bode plot was actually generated using the second-order form of the equations of motion. The unsteady aerodynamic forces computed using the doublet lattice technique are in the proper form for this frequency domain analysis. Therefore, no s-plane approximation is needed.
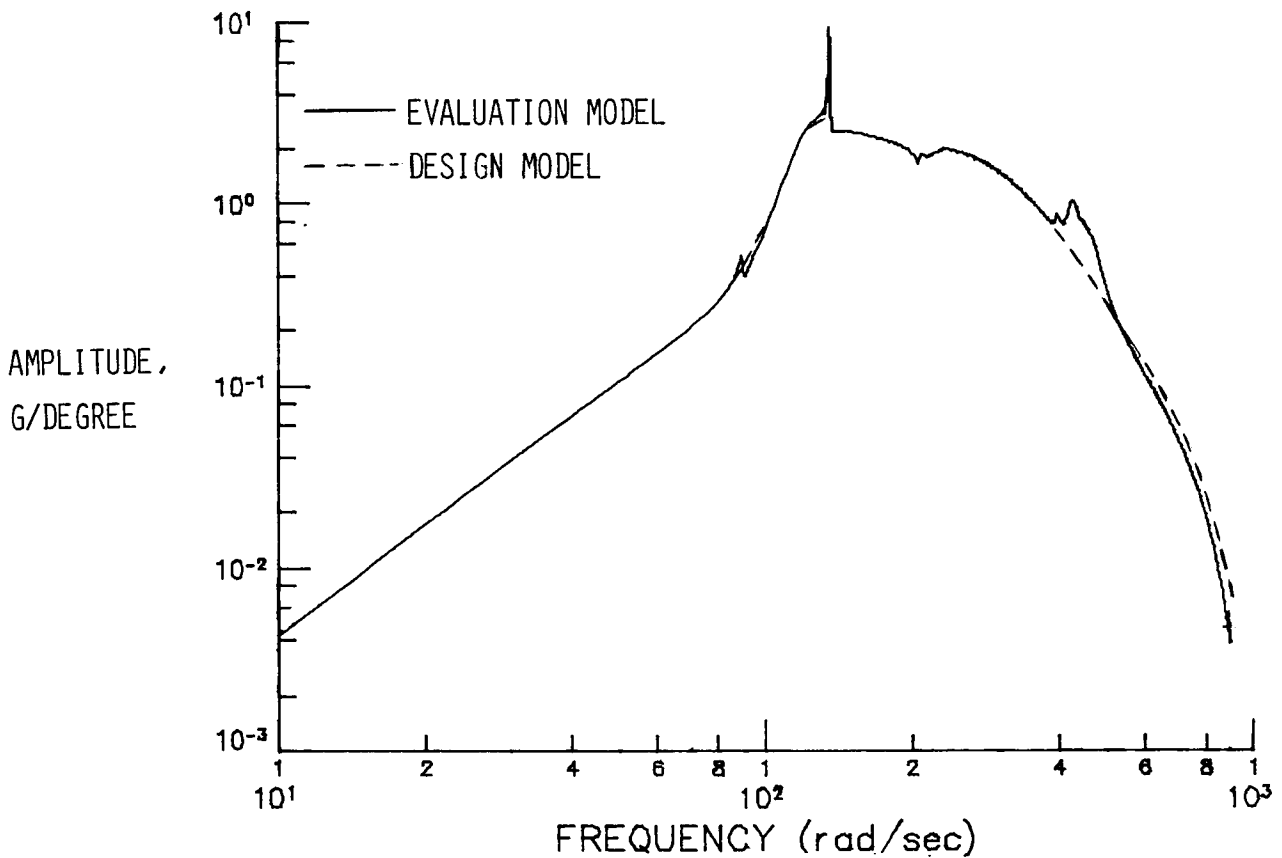
# FLUTTER BOUNDARY, FS-OFF; NOMINAL STABILITY MARGIN BOUNDARY
## AND FLUTTER BOUNDARY, FS-ON

The predicted flutter boundary (FS-off) is shown as the solid line. Flutter occurs, for the uncontrolled aircraft, to the right of this line. The dashed line identifies a boundary to the left of which the FS control law should provide stability with ± 6 dB gain margins and ± 45° phase margins. In addition, to the left of this dashed boundary, the root mean square (rms) control deflection should be less than 15° and the rms control rate should be less than 740°/sec in the presence of random turbulence (Dryden spectrum with rms velocity of 12 ft/sec). The remaining curve defines a boundary to the left of which the FS control law should provide stability.

This paper presents results that show control law performance at the two points noted. Reference 24 gives more details about the FS design discussed here and also defines the performance over a range of flight conditions of a control law for which the overall gain is scheduled as a function of dynamic pressure.

The nominal design point, identified with a square, is at M=0.86 and an altitude of 15,000 ft. Note that the uncontrolled plant is unstable at this condition, which is at a dynamic pressure 16.5 percent above the open loop flutter point.

The point identified with a circle defines the flight condition at which constrained minimization techniques are employed to maximize control law robustness.
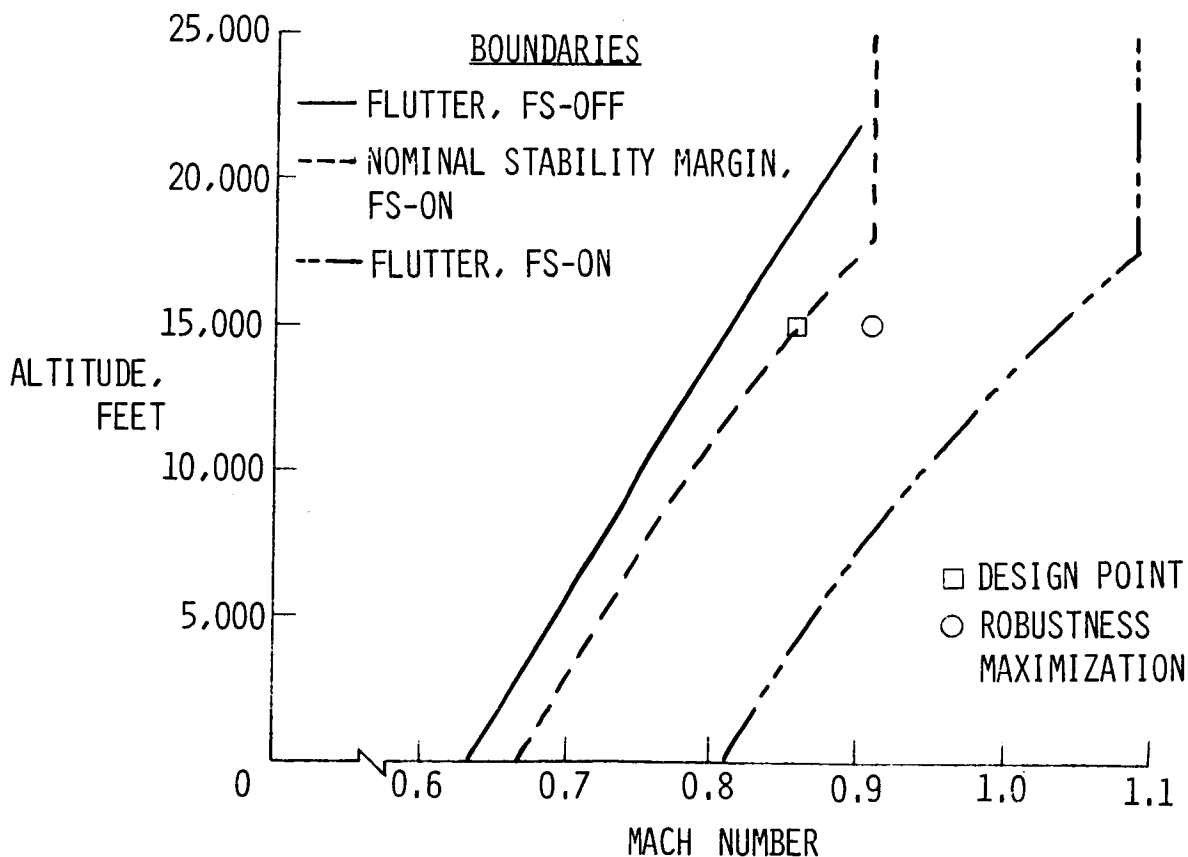
Two control law design approaches were employed. In the first of these, optimal regulator theory was employed to determine a full-state feedback gain matrix. In this phase of the design the state weighting matrix was set to zero and the control weighting matrix was set to the identity. This choice of weighting matrices, plus the constraint that the closed-loop system be stable, results in the minimum control effort solution which stabilizes the system (Ref. 5). The controller also reflects unstable poles about the imaginary axis while leaving stable poles fixed. The next step in the design was to construct a steady-state Kalman estimator based upon the 12 ft/sec rms gust input and a nominal set of measurement error statistics. The robustness of the resulting LQG design was then improved by using the robustness recovery technique of adding fictitious noise at the input (Ref. 4). The ORACLS (Ref. 1) software was utilized to obtain the LQG designs. The 25th order controllers found were reduced to implementable sizes. The order reduction was accomplished by transforming the controller state space representation to block diagonal form and examining the poles, zeros, and residues of the full-order controller. Modal truncation was performed in the transformed domain to obtain candidate reduced-order controllers. It was found (Ref. 24) that the controller could be reduced from 25th order to 9th order with minimal degradation in controller performance.

The second design approach, which will be discussed after some specific LQG results are presented, made use of a nongradient-based, nonlinear programming algorithm (Refs. 25,26) to maximize robustness properties.

- **MINIMUM CONTROL EFFORT LQ SOLUTION (ZERO STATE WEIGHTING)**

- **STEADY-STATE KALMAN ESTIMATOR**

- **DOYLE-STEIN ROBUSTNESS RECOVERY**

- **SELECTION OF REDUCED-ORDER CONTROLLER (9TH ORDER CHOSEN)**

- **ROBUSTNESS MAXIMIZATION**

# CLOSED-LOOP BLOCK DIAGRAM

This block diagram defines parameters that will be shown in subsequent figures to demonstrate controller performance. The output, y, is the FS sensor signal. G is the uncontrolled plant transfer function, y/u. The full model in frequency domain form (no s-plane approximation) was employed to perform a "one time" computation of G (iω) at a discrete set of frequencies. H, here and in the results to follow, is a reduced-order controller. The white-noise inputs included in the design process are gust ($W_G$), measurement ($W_M$) and control ($W_U$). Controllers were designed for a range of controller input noise intensities in order to determine an acceptable trade-off between robustness recovery, control power requirements and controller band-width. Results will be shown for two input noise intensity levels; zero and a "nominal" level selected as resulting in an acceptable design. The controller performance results are presented in terms of Nyquist plots which are polar plots of HG with the loop broken as indicated and with frequency as the independent variable.
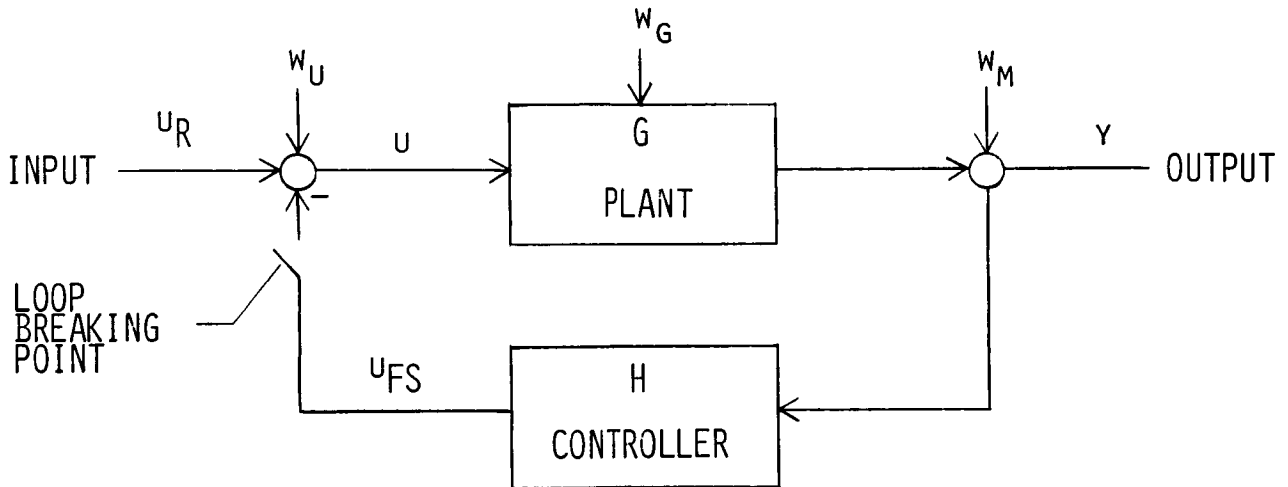
# NYQUIST PLOT OF HG TRANSFER FUNCTION
## (ZERO INPUT NOISE DESIGN)

This Nyquist plot is for a controller designed by applying LQG techniques with zero process noise intensity at the control input followed by controller order reduction (from 25th to 9th order). Since the uncontrolled plant is unstable with a complex conjugate pair of unstable poles, the Nyquist plot must, for closed—loop stability, encircle the −1 point once in a counterclockwise direction as ω varies from 0 to ∞. The arrow indicates the direction of increasing frequency. Gain margins of ± 6 dB are achieved. However, the 45° phase margin constraint is violated. Reference 24 contains additional data, such as the control power requirements and the frequencies corresponding to the gain margin and phase margin points.

# NYOUIST PLOT OF HG TRANFER FUNCTION
## (NOMINAL INPUT NOISE DESIGN)

Additional full-order LQG controller designs were obtained with process noise intensity as a variable. Nyquist plots and controller Bode plots were examined for each of the resulting full-order controllers. A "nominal input noise" design was chosen which met the performance specifications, and order reduction techniques were employed to obtain an implementable controller (9th order). The Nyquist plot shown here, which is constructed by using the frequency domain evaluation model and the "nominal noise intensity" reduced-order controller, meets the gain margin and phase margin specifications. Both gain margins and phase margins are better than those achieved by using the "zero input noise intensity" controller of the previous figure. The rms control deflection and rate requirements of both controllers were within the constraints.
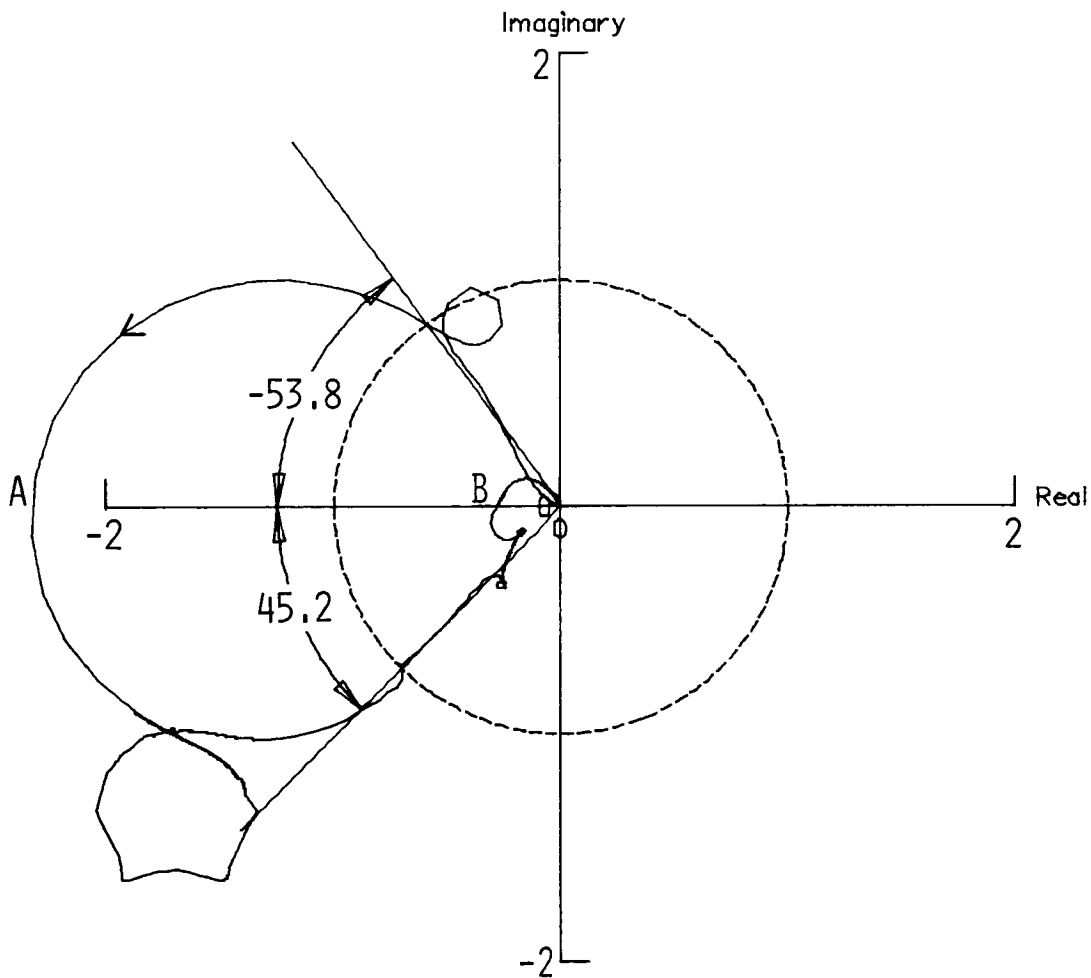
The phase margin and gain margin improvements that were obtained by increasing process noise at the input were not achieved without cost. A Bode plot of the "zero" and "nominal" input process noise controllers reveals that increasing the noise has degraded the controller high-frequency rolloff characteristics.
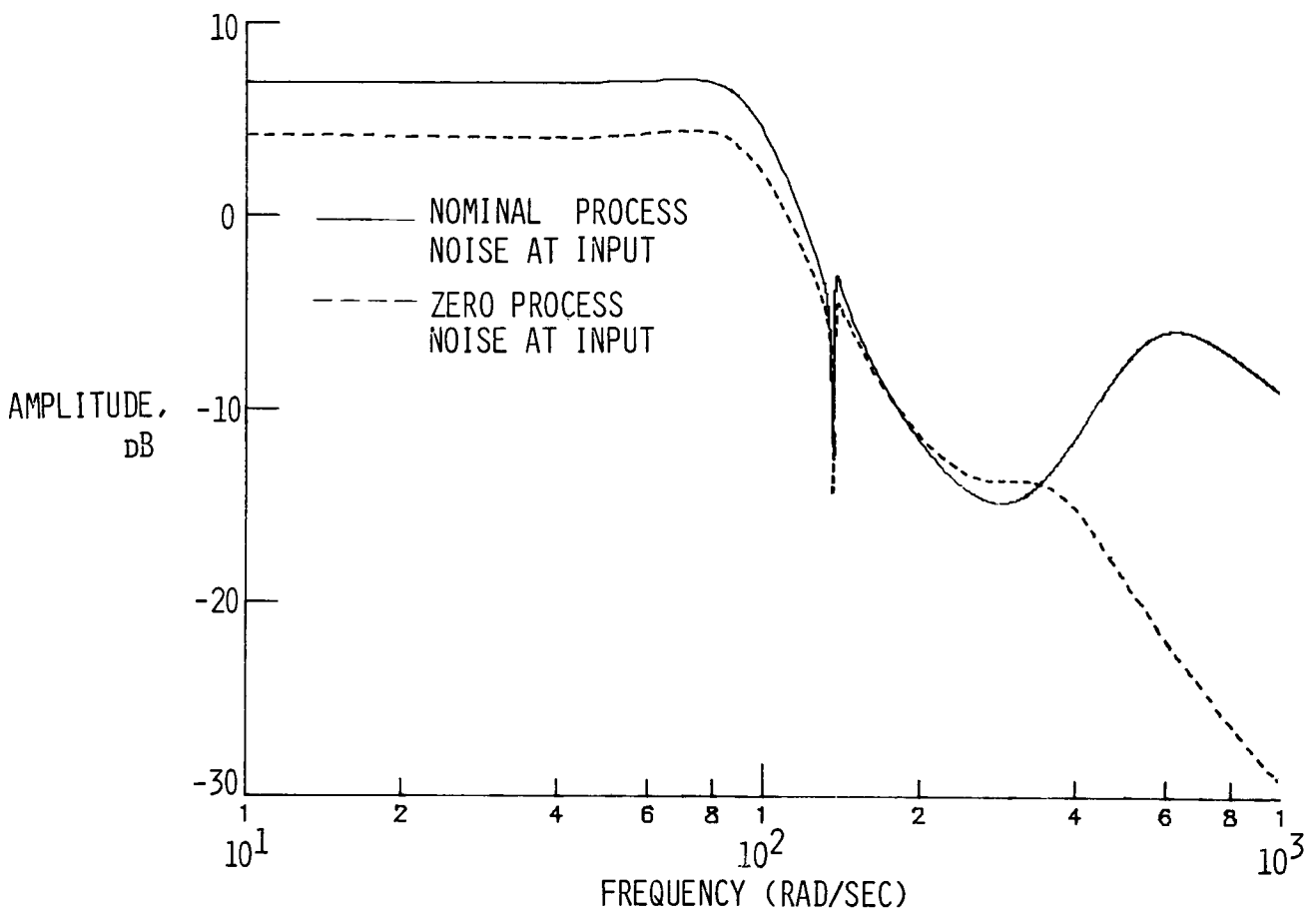
An alternate design approach which allows explicit consideration of design criteria will now be described. The approach, which requires that the form of the control law be specified, is particularly applicable in modifying an existing control law when small changes occur in the plant or in satisfying criteria not fully considered in a previous design. Nongradient-based constrained minimization techniques are employed to maximize the minimum singular value of the return difference transfer function subject to explicit constraints on stability, gain margins, phase margins and control power requirements. A similar approach (Ref. 11), which employs a gradient-based optimizer, has been applied to improve the robustness of a lateral stability augmentation control law.

The method is applied to determine a controller for a flight condition having a Mach number of 0.91 and an altitude of 15,000 feet. The reduced-order controller found for the M = 0.86, 15,000-foot altitude flight condition was chosen to define the control law form and the initial values for the design variables. Nine of the controller coefficients were selected as design variables. Fixed-controller elements were lumped into a filter T(s). Stability was determined by computing the number of counterclockwise encirclements of the −1 point as ω varied from 0 to ∞. The phase margin requirements for this condition were relaxed to ± 40°.

In performing the constrained optimization, it was observed that control power requirements never reached their available limits. Control power constraints were, therefore, removed from the computations. This allowed the remaining constraints to be evaluated based solely upon the computations required for generation of Nyquist plots.

FIND VALUES FOR THE DESIGN VARIABLES, $D_I$. WHERE

$$(U_{FS}/Y) = D_1 \frac{(s+D_2)(s+D_3)}{(s^2+D_4 s+D_5)} \frac{(s^2+D_6 s+D_7)}{(s^2+D_8 s+D_9)} T(s)$$

AND T(S) IS A FIXED FILTER

SUCH THAT

o   MINIMUM SINGULAR VALUE IS MAXIMIZED
o   CONTROL POWER CONSTRAINTS ARE SATISFIED
o   +6DB $\leq$ GAIN MARGIN $\leq$ -6DB
o   40° $\leq$ PHASE MARGIN $\leq$ -40°

# NYQUIST PLOTS OF HG TRANSFER FUNCTION
## (M = 0.91, H = 15,000 FEET)

The initial controller stabilized the system but gain margin constraints (± 6 dB) and phase margin constraints (± 40°) were violated. The minimum singular value is indicated by the heavy line. The constrained optimization solution has a 26 percent larger minimum singular value; gain margin and phase margin constraints are satisfied to within a 2.5 percent tolerance. Control power requirements (rms requirements) are also reduced with the optimized controller.
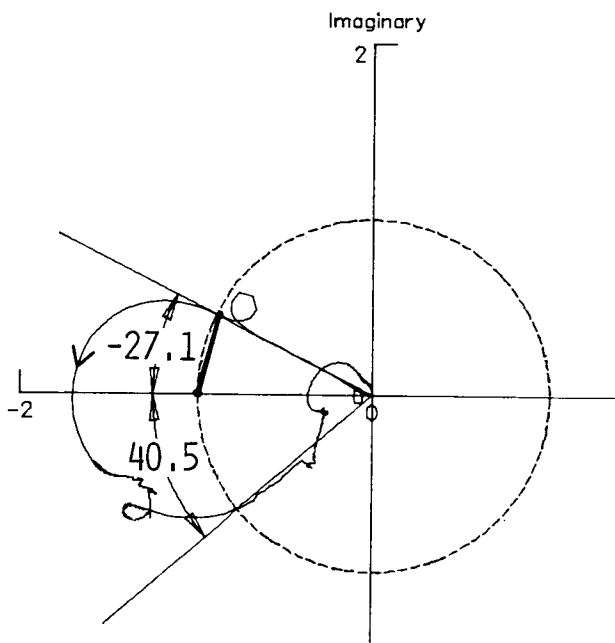
INITIAL CONTROLLER
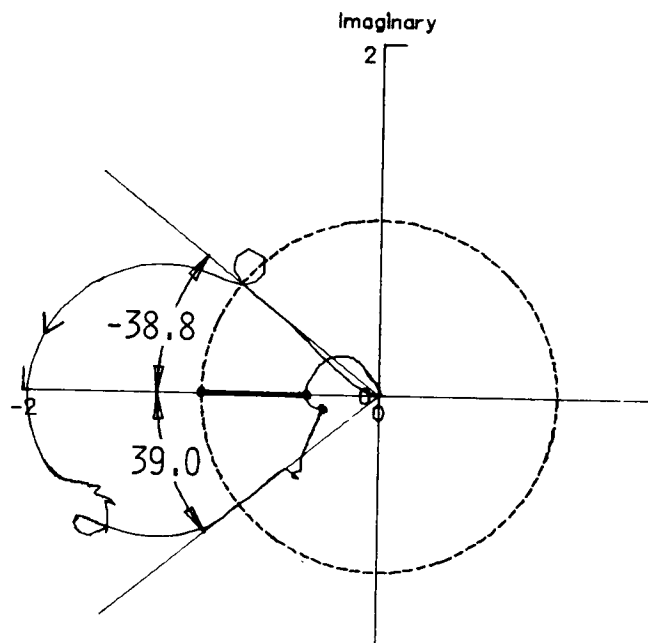
OPTIMIZED CONTROLLER

SUMMARY

Coupling the ISAC program (for definition of plant design and evaluation models) with the ORACLS LQG methodology provided an effective tool for design of full-order controllers. Addition of process noise at the input allowed stability margin criteria to be met. The rms control deflection and rate requirements were also within their constraints. Controller order reduction from 25th to 9th was successfully accomplished with minimal sacrifice in controller performance.

Robustness maximization using nongradient-based constrained optimization techniques substantially increased the minimum singular value of the return difference transfer function for an off-nominal flight condition. Stability was determined at each iteration by computing the number of counterclockwise encirclements of the −1 point as $\omega$ varied from 0 to $\infty$.

New FS control laws will be designed for both symmetric and antisymmetric degrees of freedom when the mathematical model of the ARW-2 is updated.

- 9TH ORDER CONTROLLER DEVELOPED USING LQG TECHNIQUES AND ORDER REDUCTION ACHIEVED DESIGN OBJECTIVES

- ROBUSTNESS MAXIMIZATION USING NONGRADIENT-BASED CONSTRAINED OPTIMIZATION TECHNIQUES INCREASED MINIMUM SINGULAR VALUE SUBSTANTIALLY

- DESIGN WILL BE REPEATED FOR BOTH SYMMETRIC AND ANTISYMMETRIC FLUTTER WHEN UPDATED STRUCTURAL MODEL IS COMPLETED

REFERENCES

1. Armstrong, Ernest S.:   ORACLS - A Design System for Linear Multivariable Control.  Marcel Dekker, Inc., c.1980.

2. Mahesh, J. K.; Stone, C. R.; Garrard, W. L.; and Hausman, P. D.:  Active Flutter Control for Flexible Vehicles.  NASA CR-159160, November 1979.

3. Gangsaas, Dagfin; and Ly, Uy-Loi:  Application of Modified Linear Quadratic Gaussian Design to Active Control of a Transport Airplane.  AIAA Paper No. 79-1746, August 1979.

4. Doyle, J. C.; and Stein, G.:  Robustness with Observers.  IEEE Transactions on Automatic Control, August 1979.

5. Kwakernaak, Huibert; and Sivan, Raphael:  Linear Optimal Control Systems.  Wiley-Interscience, c.1972.

6. Mukhopadhyay, V.; Newsom, J. R.; and Abel, I.:  A Direct Method for Synthesizing Low-Order Optimal Feedback Control Laws with Application to 'Flutter Suppression.  AIAA Paper No. 80-1613, August 1980.

7. Schy, A. A.:  Nonlinear Programing in the Design of Control Systems with Specified Handling Qualities.  Proceedings of 1972 IEEE Conference on Decision and Control, New Orleans, LA, December 1972.

8. Schy, A. A.; Adams, William M., Jr.; and Johnson, K. G.:  Computer-Aided Design of Control Systems to Meet Many Requirements.  NATO AGARD Conference Proceedings No. 137 on Advances in Control Systems, 1973.

9. Knox, J. R.; and McCarty, J. M.:  Algorithms for Computation of Optimal Constrained Output Feedback for Linear Multivariable Systems.  AIAA Paper No. 78-1290, August 1978.

10. Adams, William M., Jr.; and Tiffany, Sherwood H.:  Control Law Design to Meet Constraints Using SYNPAC--Synthesis Package for Active Controls.  NASA TM-83264, January 1982.

11. Newsom, Jerry R.; and Mukhopadhyay, V.:  The Use of Singular Value Gradients and Optimization Techniques to Design Robust Controllers for Multiloop Systems.  AIAA Paper No. 83-2191, August 1983.

12. Peele, Ellwood L.; and Adams, William M., Jr.:  A Digital Program for Calculating the Interaction Between Flexible Structures, Unsteady Aerodynamics, and Active Controls.  NASA TM-80040, January 1979.

13. Albano, E.; and Rodden, W. P.:  A Doublet Lattice Method for Calculating Lift Distributions on Oscillating Surfaces in Subsonic Flows.  AIAA Journal, Vol. 7, No. 2, February 1969, pp. 279-285.

14. Giesing, J. P.; Kalman, T. P.; and Rodden, W. P.:  Subsonic Unsteady Aerodynamics for General Configurations.  AFFDL-TR-71-5, November 1971.

15. Rodger, Kenneth L.:   Airplane Math Modeling Methods for Active Control Design. AGARD CR-228, August 1977.

16. Jones, R. T.:   The Unsteady Lift of a Wing of Finite Aspect Ratio.   NACA Rept. 641, 1940.

17. Vepa, R.:   Finite State Modeling of Aeroelastic Systems.   Ph.D. Dissertation, Department of Applied Mechanics, Stanford University, June 1975.

18. Edwards, John W.:   Unsteady Aerodynamic Modeling and Active Aeroelastic Control.   NASA CR-148019, 1977.

19. Dunn, H. J.:   An Analytical Technique for Approximating Unsteady Aerodynamics in the Time Domain.   NASA TP-1738, November 1980.

20. Boeing Commercial Aircraft Company Staff:   Integrated Application of Active Controls (IAAC) Technology to an Advanced Subsonic Transport Project – Wing Planform Study and Final Configuration Selection.   NASA CR-165630, June 1981.

21. Military Specifications – Flying Qualities of Piloted Airplanes.   MIL-F-8785C, November 5, 1980.   (Superseding MIL-F-8785B, August 7, 1969.)

22. Schwanz, Robert C.:   Consistency in Aircraft Structural and Flight Control Analysis.   AGARD CR-228, August 1977.

23. Newsom, J. R.; Pototsky, Anthony S.; and Abel, I.:   Design of the Flutter Suppression System for DAST ARW-1-1R – A Status Report.   NASA TM-84642, March 1983.

24. Adams, William M.; and Tiffany, Sherwood H.:   Design of a Candidate Flutter Suppression Control Law for DAST ARW-2.   AIAA Paper No. 83-2221, August 15-17, 1983.

25. Olsson, D. M.:   A Sequential Simplex Program for Solving Minimization Problems. Journal of Quality Technology, Vol. 6, No. 1, January 1974, pp. 53-57.

26. Olsson, Donald M.; and Nelson, Lloyd S.:   The Nelder-Mead Simplex Procedure for Function Minimization.   Technometrics, Vol. 17, No. 1, February 1975.

# APPLICATIONS OF CONMIN TO WING DESIGN OPTIMIZATION WITH VORTEX FLOW EFFECT

C. Edward Lan
Department of Aerospace Engineering
The University of Kansas
Lawrence, Kansas

# AERODYNAMIC ANALYSIS OF SLENDER WINGS

Slender wings on supersonic cruise configurations are expected to be thin and highly swept. As a result, edge-separated vortex flow is inevitable and must be accounted for in aerodynamic analysis and design. The present method is based on the method of suction analogy (ref. 1) to calculate the total aerodynamic characteristics. The method requires the solution of the attached flow problem, the latter being solved by a low-order panel method in subsonic and supersonic flow (ref. 2). In essence, the lifting pressure is calculated by using a pressure-doublet distribution satisfying the Prandtl-Glauert equation. From the pressure distribution, the leading-edge suction is calculated. The latter is assumed to be the vortex lift through the method of suction analogy. For a cambered wing, the location of vortex-lift action point is important in predicting the aerodynamic characteristics (ref. 2). It is also seen that the effect of camber shape appears nonlinearly in all aerodynamic expressions. (See fig. 1.)

Prandtl-Glauert Equation: $(1 - M^2) \dfrac{\partial^2 \phi}{\partial x^2} + \dfrac{\partial^2 \phi}{\partial y^2} + \dfrac{\partial^2 \phi}{\partial z^2} = 0$

Boundary Condition: $[A]\{\Delta C_p\} = \left\{ \dfrac{\partial Z_c}{\partial x} \cos \alpha - \sin \alpha \right\}$

Lifting Pressure: $\Delta C_p' = \Delta C_p \cos \alpha - 2 Y_x \sin \alpha \sin \left( \dfrac{\partial Z_c}{\partial y} \right)$

Leading-Edge Suction: $c_s = c_t \dfrac{\sqrt{1 + \left(\dfrac{\partial Z_c}{\partial x}\right)^2 + \left(\dfrac{\partial Z_c}{\partial y}\right)^2} \left| \dfrac{d\vec{r}}{dy} \right|}{\left[ \left( \dfrac{\partial Z_c}{\partial x} \dfrac{dz_\ell}{dy} + 1 \right)^2 + \left( -\dfrac{\partial Z_c}{\partial x} + \dfrac{\partial Z_c}{\partial y} \tan \Lambda \right)^2 \right]^{\frac{1}{2}}}$

$\left| \dfrac{d\vec{r}}{dy} \right| = \sqrt{1 + \tan^2 \Lambda + \left( \dfrac{dz_\ell}{dy} \right)^2}$

Sectional Characteristics: $c_{\ell, p} = \dfrac{1}{c} \int_{x_{\ell e}}^{x_{te}} \Delta C_p' \left( \dfrac{\partial Z_c}{\partial x} \sin \alpha + \cos \alpha \right) \Big/ \sqrt{1 + \left(\dfrac{\partial Z_c}{\partial x}\right)^2 + \left(\dfrac{\partial Z_c}{\partial y}\right)^2} \, dx$

$c_{d, p} = \dfrac{1}{c} \int_{x_{\ell e}}^{x_{te}} \Delta C_p' \left( -\dfrac{\partial Z_c}{\partial x} \cos \alpha + \sin \alpha \right) \Big/ \sqrt{1 + \left(\dfrac{\partial Z_c}{\partial x}\right)^2 + \left(\dfrac{\partial Z_c}{\partial y}\right)^2} \, dx$

$c_{\ell, v\ell e} = c_s \left( \dfrac{\partial Z_c}{\partial x} \sin \alpha + \cos \alpha \right) \Big/ \sqrt{1 + \left(\dfrac{\partial Z_c}{\partial x}\right)^2 + \left(\dfrac{\partial Z_c}{\partial y}\right)^2}$

$c_{d, v\ell e} = c_s \left( -\dfrac{\partial Z_c}{\partial x} \cos \alpha + \sin \alpha \right) \Big/ \sqrt{1 + \left(\dfrac{\partial Z_c}{\partial x}\right)^2 + \left(\dfrac{\partial Z_c}{\partial y}\right)^2}$

Action Point of Vortex Lift: $r = c_s c$

To design the camber shape, the camber slope is represented by a cosine Fourier series at each of several spanwise stations. The Fourier coefficients are the design variables. To design a leading-edge flap in the vortex flow (i.e. a vortex flap), the coordinates of corner points and the deflection angle are the design variables. The process of wing design is to determine the camber shape and twist distribution such that an objective function, typically the drag, is minimized, subject to various constraints (fig. 2). The latter may include the lift, the magnitude of maximum geometric twist and the magnitude of vortex lift. Other types of constraint are possible (ref. 3). The design of a vortex flap can be described in a similar manner.

## Camber Representation for Each Spanwise Station:

$$\left(\frac{\partial Z_c}{\partial x}\right)_k = \sum_{j=1}^{N} a_j \cos (j-1) \theta_k$$

$$\theta_k = \frac{(2k-1)\pi}{2N}$$

## Design Variables: $a_j$

## Optimization Problem:

Minimize $F = -\dfrac{C_L}{C_{D_o} + C_{D_i}}$

Subject to Constraints ($G_j$) of

    (1) A Given Lift Coefficient

    (2) A Given Ratio of Vortex Lift to Total Lift

    (3) Magnitude of Local Angles of Attack (Twist)

Figure 2

# WING DESIGN OPTIMIZATION BY "CONMIN"

To achieve the wing design optimization, the aerodynamic analysis method
is coupled with CONMIN - Constrained Function Minimization Program (refs. 4 and 5).
In a typical wing design problem, as many as 70 design variables may be employed.
The solution is determined iteratively.

The process starts with the calculation of values of objective and constraint
functions for the input design variables. Gradients of these functions are then
calculated and CONMIN will determine the best way of changing the design variables
to achieve the minimum drag design without violating constraints. (See fig. 3.)
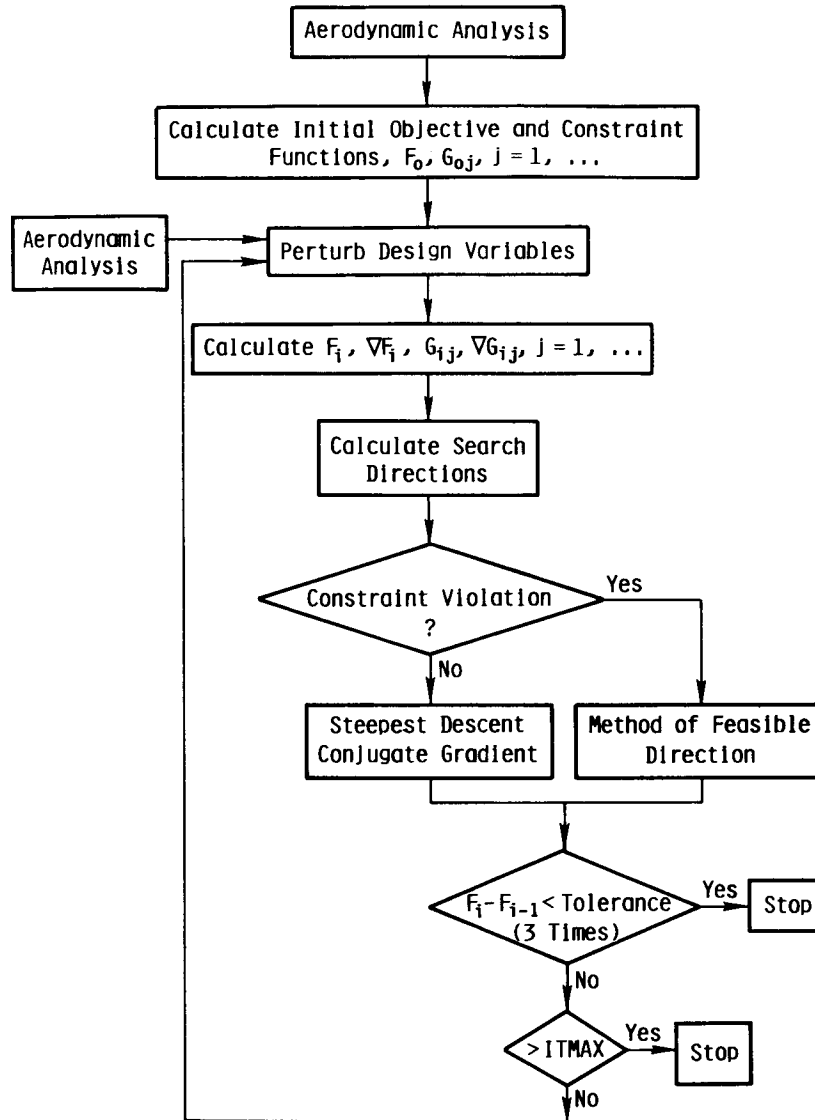
Figure 3

# RESULTS OF VORTEX FLOW AND ATTACHED-FLOW DESIGN FROM AN INITIAL FLAT SURFACE

$$C_{L_{des}} = 0.3, \quad M = 0, \quad TWIST \leq 8 \; DEG$$

Design results very much depend on the imposed constraints. For simplicity, only the constraint of having the lift coefficient, twist and vortex lift be greater than 5% of total lift in the case of the vortex flow design will be imposed in the present study. Results show that starting from an initial flat surface, the final camber shape designed with the vortex flow concept (called the VF design) is similar to that designed with the attached-flow concept (called the AF design) except near the root and the tip. In the mid-semispan region, the surface has large aft camber. Note that if the effect of $\partial z_e/\partial y$ is ignored and the twist constraint is not imposed, as is usually done in a conventional method, the resulting shapes would involve larger forward camber and unrealistically large twist (ref. 3 and 6). (See fig. 4.)
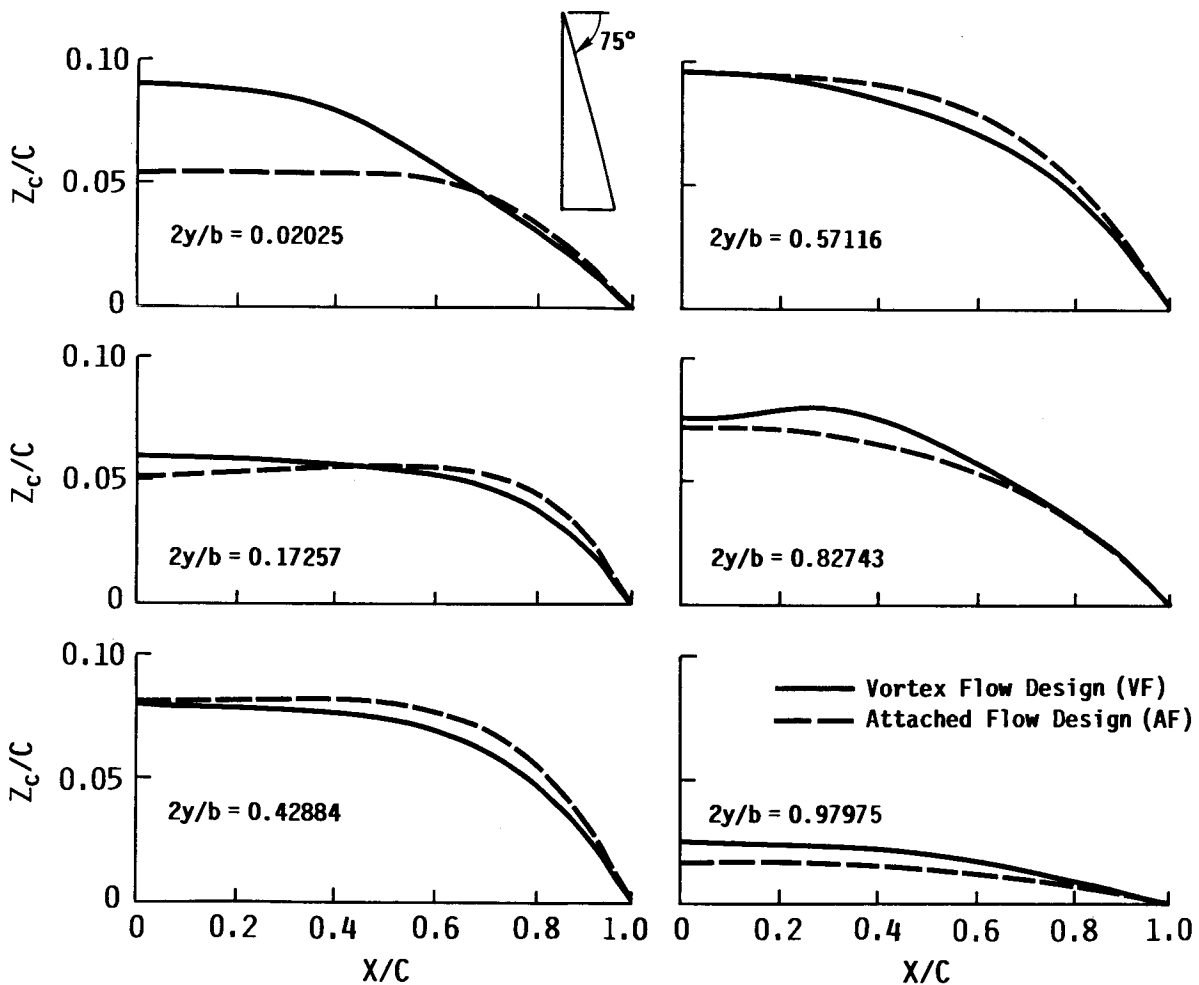


Figure 4

## VORTEX FLOW DESIGN FROM DIFFERENT STARTING SHAPES
### $C_{L_{des}} = 0.3$, $M = 0$, TWIST $\leq$ 8 DEG

In the present nonlinear optimization problem with a large number of design variables, the final solution depends on the initial input. In other words, there are many relative minima in the design space. To show this, the vortex flow design with the same constraints is calculated from three input shapes – a flat surface, the camber shape of the attached-flow design in figure 4 reduced by 10%, and the original camber shape of the attached-flow design. As shown in figure 5, the results are all different. To determine a solution close to a global minimum, Vanderplaats et al. (ref. 7) suggested beginning the optimization from several different initial designs.
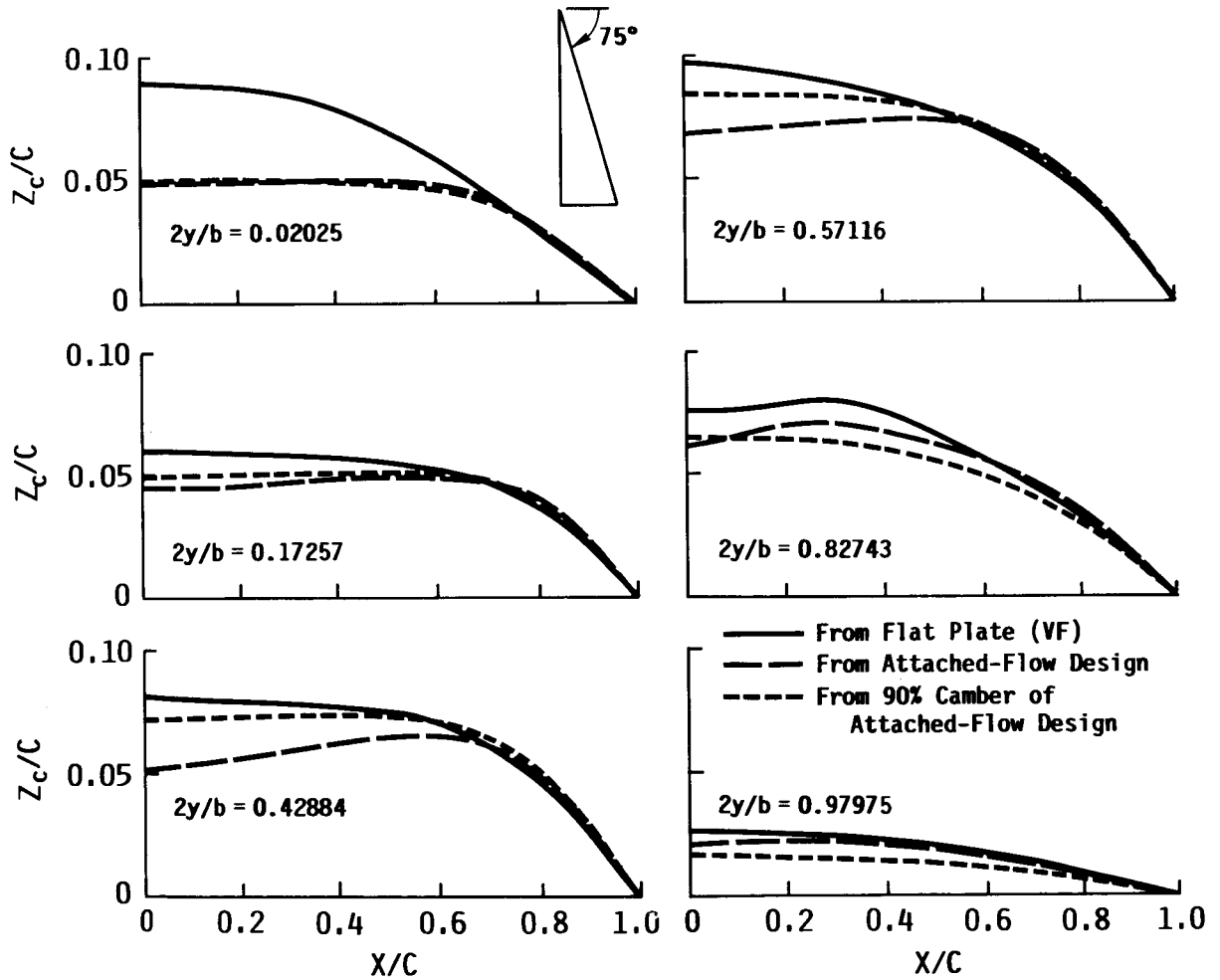


Figure 5

## DESIGN FROM A FLAT SURFACE FOR A DESIGN LIFT
## COEFFICIENT OF 0.6, M = 0, and TWIST ≤ 8 DEG

By increasing the design lift coefficient to 0.6, the attached-flow concept did not produce a feasible design under the specified twist constraint. However, a converged feasible design was easily obtained under the vortex flow concept. It is seen from figure 6 that at high lift forward camber is needed to provide more forward-facing surface to produce a thrust force.
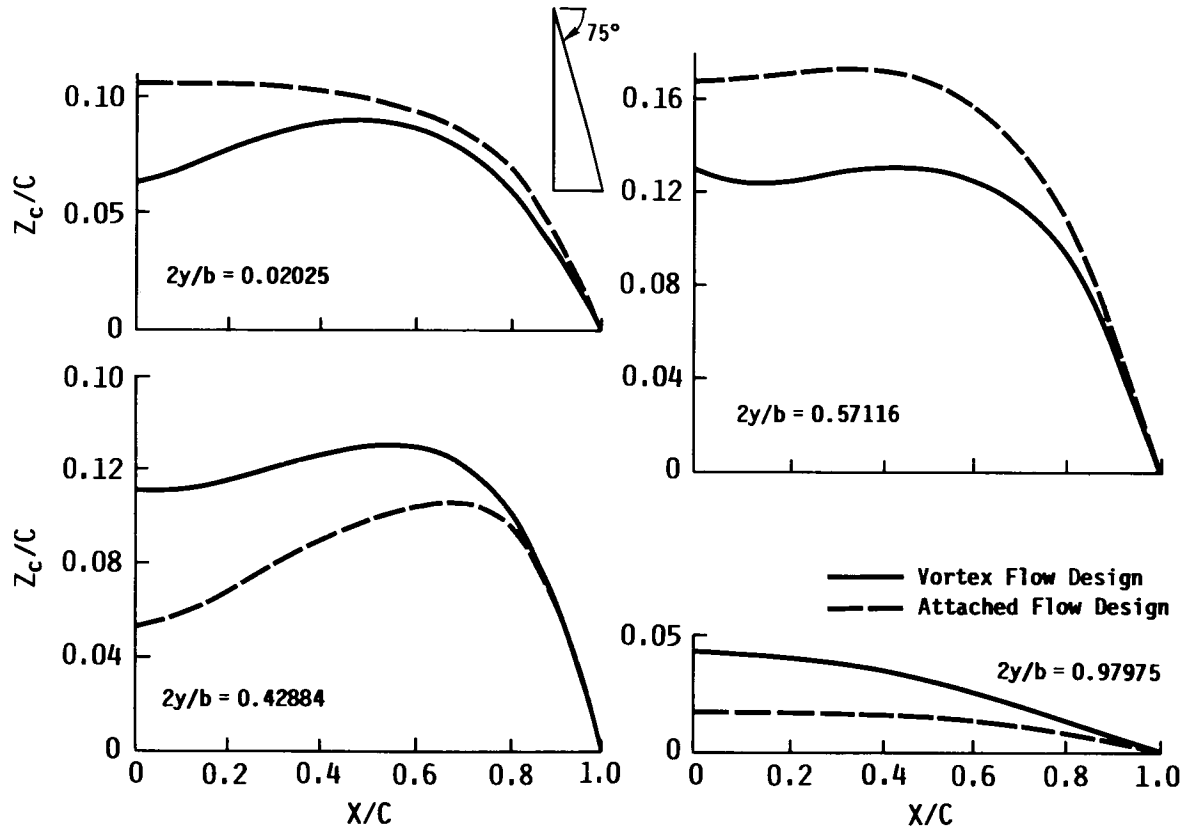


Figure 6

PARTIAL VORTEX FLOW DESIGN
$$C_{L_{des}} = 0.3, \text{ TWIST} \leq 8 \text{ DEG}$$

In applications, there are always some other practical constraints, such as some inboard portion being specified. The present method allows a certain portion of the planform to be unchanged during the optimization process. For example, in figure 7 three types of vortex flow design are presented, one started from a flat surface, the other from the attached-flow design, and the last one (called the VPA design) also from the attached-flow design, but with the inboard one-third fixed. The results show that in the VPA design more forward-facing surface exists in the outboard portion to take advantage of the vortex-induced thrust.
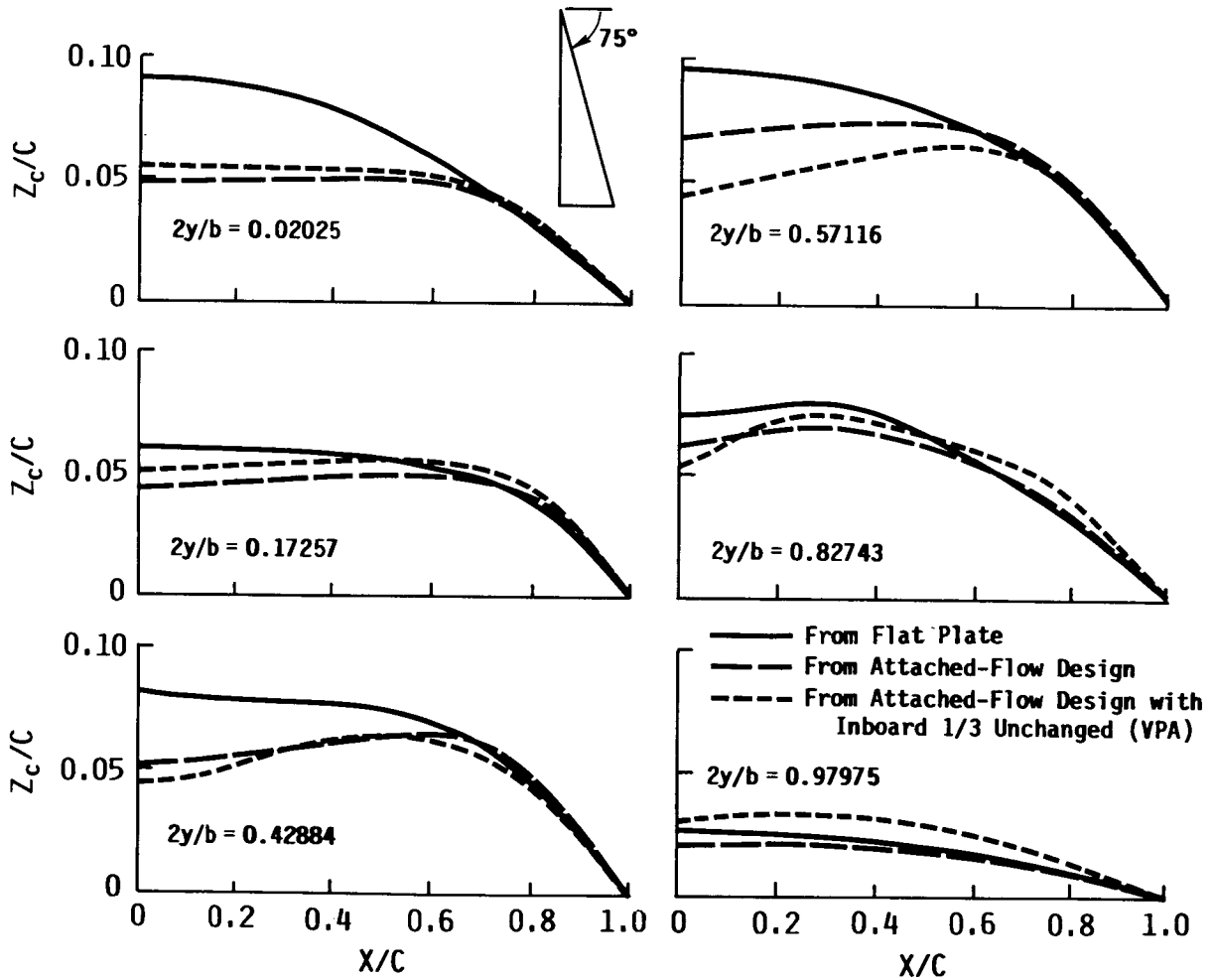


Figure 7

## PERFORMANCE COMPARISON OF DIFFERENT DESIGN CONCEPTS
$$C_{L_{des}} = 0.3, \quad M = 0, \quad TWIST \leq 8 \ DEG$$

At the design lift coefficient of 0.3, all three design configurations have about the same $C_{D_i}$, reaching the planar minimum value of $C_L^2/\pi A$. At off-design conditions, the attached-flow design (AF) would be superior if the flow could remain attached. When the flow is separated, the AF design (not shown) will have approximately the same performance as the VF design. On the other hand, the partial vortex flow design (VPA) seems to be superior throughout the off-design $C_L$. (See fig. 8.)
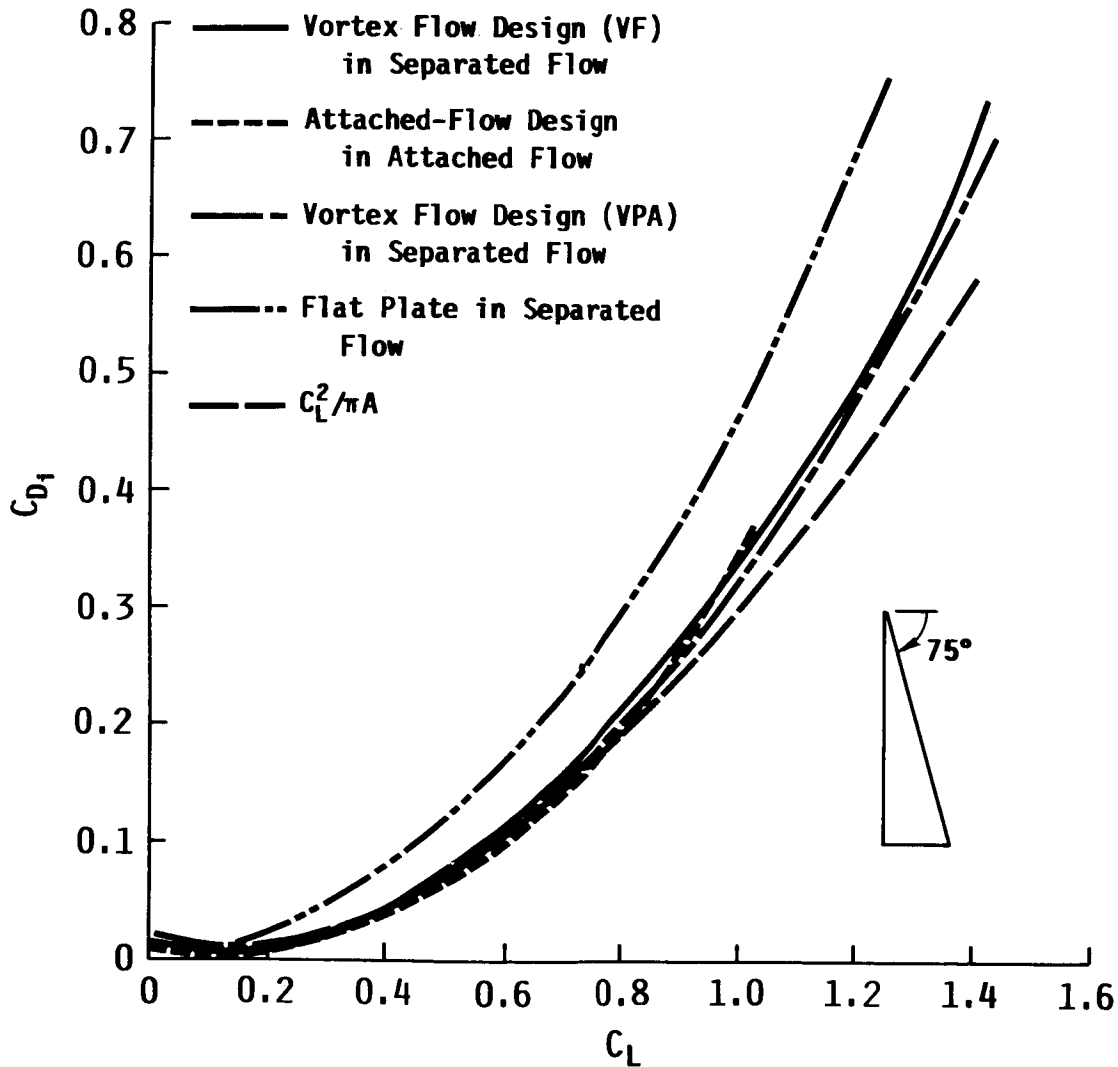


Figure 8

# VORTEX FLAP DESIGN
$$C_{L_{des}} = 0.3, \quad M = 0$$

   A vortex flap is a leading-edge flap which takes advantage of vortex-induced thrust to reduce the drag. The present method is capable of determining the size and deflection angle of the flap in such a way that the drag is minimized, subject to the lift constraint. As presented in figure 9, by assuming an initial $\alpha$ of 5 deg. and $\delta_n = 0$ deg., an optimum size of the flap is determined with a final $\alpha$ of 7.7 deg. and $\delta_n = -15.1$ deg.

Input: $\alpha = 5°$

$\delta_n = 0°$

Final: $\alpha = 7.7°$

$\delta_n = -15.1°$

Input Shape

Final Shape
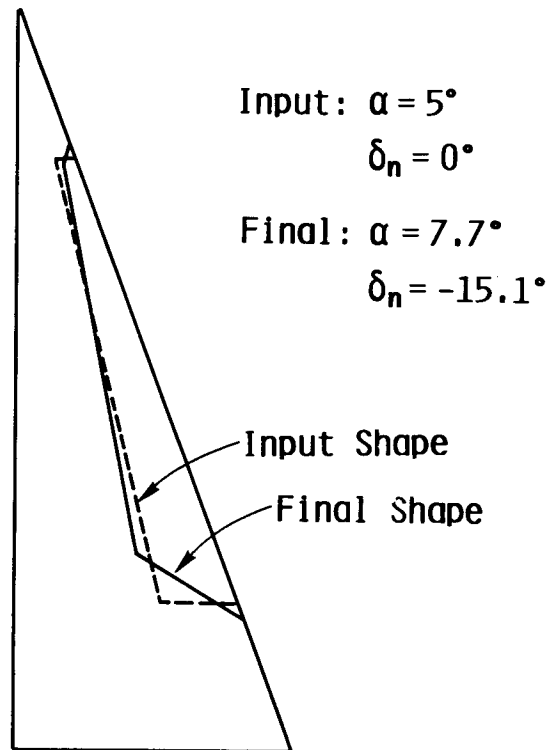
Figure 9

## SYMBOLS AND ABBREVIATIONS

| | |
|---|---|
| $A$ | aspect ratio |
| $[A]$ | aerodynamic influence coefficient matrix |
| AF | attached-flow design with a flat surface as the starting solution |
| $a_j$ | Fourier coefficients for the camber slope |
| $b$ | wing span |
| $c$ | local chord |
| $C_{D_i}$ | induced drag coefficient |
| $C_{D_o}$ | minimum drag coefficient |
| $C_L$ | lift coefficient |
| $C_{L_{des}}$ | design lift coefficient |
| $\Delta C_p$ | lifting pressure coefficient |
| $c_s$ | sectional suction coefficient |
| $c_t$ | sectional thrust coefficient |
| $F$ | objective function |
| $G$ | constraint function |
| $M$ | Mach number |
| VF | vortex flow design with a flat surface as the starting solution |
| VPA | vortex flow design with the attached-flow design as the starting solution and inboard one-third portion remaining unchanged |
| $x,y,z$ | a rectangular coordinate system |
| $z_c$ | camber ordinate |
| $z_\ell$ | camber ordinate along the leading edge |
| $\alpha$ | angle of attack |
| $\delta_n$ | leading-edge flap angle measured normal to hinge line, negative downward |
| $\gamma_x$ | streamwise vortex density |
| $\Lambda$ | leading-edge sweep angle |
| $\phi$ | perturbation velocity potential |

# REFERENCES

1. Polhamus, E.C.: Prediction of Vortex-Lift Characteristics by a Leading-Edge Suction Analogy. Journal of Aircraft, Vol. 8, April 1971, pp. 193-199.

2. Lan, C.E. and Chang, J.-F.: Calculation of Vortex Lift Effect for Cambered Wings by the Suction Analogy. NASA CR-3449, July 1981.

3. Chang, J.-F. and Lan, C.E.: Design of Wings with Vortex Separated Flow. NASA CR-172198, September 1983.

4. Vanderplaats, G.N.: CONMIN - A Fortran Program for Constrained Function Minimization - User's Manual. NASA TM X-62282, 1981.

5. Riley, K.M.: FRANOPP - FRamework for ANalysis and OPtimization Problems - User's Guide. NASA CR-165653, January 1981.

6. Lamar, J.E.: Subsonic Vortex-Flow Design Study for Slender Wings. Journal of Aircraft, Vol. 15, September 1978, pp. 611-617.

7. Vanderplaats, G.N., Hicks, R.N. and Murman, E.M.: Applications of Numerical Optimization Techniques to Airfoil Design. NASA SP-347, Part II, Paper No. 25, p. 749, 1975.

# CALCULATED EFFECTS OF VARYING REYNOLDS NUMBER AND DYNAMIC PRESSURE ON FLEXIBLE WINGS AT TRANSONIC SPEEDS

Richard L. Campbell
NASA Langley Research Center
Hampton, Virginia

# INTRODUCTION

The recent dedication of the National Transonic Facility (NTF) marked the beginning of a new era of research in transonic wind tunnels. Soon tests will be performed on models of complete aircraft configurations at full-scale Reynolds and Mach numbers. This capability will also provide an excellent opportunity to evaluate the transonic aerodynamic computer codes that utilize boundary layer theory to model viscous effects. While the cryogenic operating temperatures of the NTF are responsible for some of the increased Reynolds number range, it will be necessary to utilize high tunnel pressures to fully exploit the high Reynolds number capability of this facility (see ref. 1). Because of the range of dynamic pressures to which a model may be subjected (up to about 7000 psf), it is highly desirable to account for model aeroelastic deformation when making calculations using the transonic computer codes.

This report describes a computational method which has been developed that includes the effects of static aeroelastic wing deflections in steady transonic aerodynamic calculations. This method, known as the Transonic Aeroelastic Program System (TAPS), interacts a 3D transonic computer code with boundary layer and a linear finite element structural analysis code to calculate wing pressures and deflections. The nonlinear nature of the transonic flow makes it necessary to couple the aerodynamic and structures codes in an iterative manner.

TAPS has been arranged in a modular fashion so that different aerodynamic or structures programs may be used with a minimum of coding changes required. A complete description of the development of TAPS is given in reference 2; this paper will present results obtained using two different aerodynamic codes in TAPS and correlate those results with experimental data.

# DESCRIPTION OF TRANSONIC AEROELASTIC PROGRAM SYSTEM (TAPS)

A flow chart illustrating the method of analysis used in TAPS is shown in figure 1. An aerodynamic model and a structural wing model are first developed for the test configuration. The structural wing model is then run through the structures code to obtain an influence coefficient matrix, which is saved for later use in calculating wing deflections. An initial, unconverged run is made with the aerodynamics code to obtain wing pressures; these pressures are then interpolated from the aerodynamic grid to the structural grid and converted to the input format of the structures code by the first translator module. The structures code then solves for the wing deflections using the influence coefficient matrix and nodal forces determined from the calculated wing pressures. These deflections are interpolated back to the aerodynamics grid and arranged as an input file to update the configuration shape in the next aerodynamic calculation. This aerodynamic/structural cycle is automated and may be continued until both the wing pressures and deflections have converged to the satisfaction of the user. The convergence criteria used in this study were negligible shock movement or change in pressure levels between successive iteration cycles based on comparison of pressure distribution plots and wing tip deflection changes of less than 2 percent.

TAPS has been arranged in a modular fashion so that it would be relatively easy to use different aerodynamic or structural codes. For this study, two aerodynamic codes were used: WIBCO, an extended small-disturbance wing/body code with a 2D strip boundary layer (ref. 3); and TAWFIVE, a full-potential wing/body code coupled with a 3D integral boundary layer (ref. 4). The SPAR structural analysis program (ref. 5) was used to make the wing deflection calculations for all cases.

Including the aeroelastic deflections did not appear to have any adverse effect on the convergence of the aerodynamic calculations; no underrelaxation of the deflections was required. The boundary layer effects seemed to be a more important factor affecting the rate of convergence. The calculation of wing deflections was also relatively inexpensive, being less than 10 percent of the cost of an aerodynamic/structural cycle (which includes 30-50 aerodynamic iterations) and less than the cost of the boundary layer calculations.
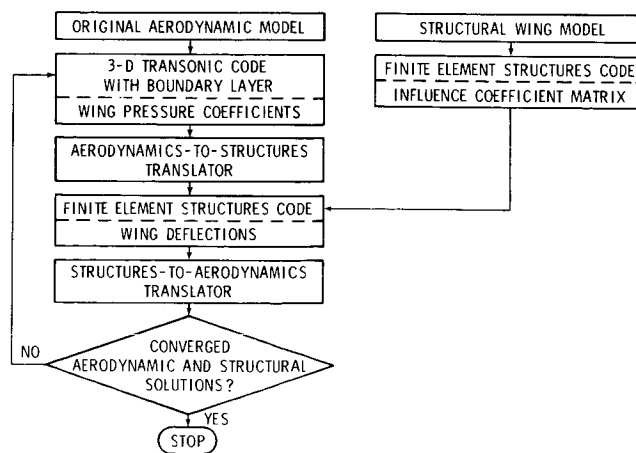


Figure 1

# ADVANCED TECHNOLOGY TRANSPORT (ATT) MODEL DESCRIPTION

The first configuration used to evaluate TAPS was the Advanced Technology Transport (ATT) model (refs. 6 and 7). A top view of the right wing panel is shown in figure 2. The wing had a span of 45.0 in., a quarter-chord sweep of 33°, an aspect ratio of 7.498, and a taper ratio of 0.418. The airfoil sections were NASA supercritical designs with maximum thickness-to-chord ratios of 0.114 near the fuselage and 0.082 near the tip. A highly swept leading-edge glove extended from the fuselage to about $\eta = 0.35$ and there were four trailing-edge control surfaces (three inboard, one outboard). The wing was constructed of solid aluminum with channels for the pressure tubing machined into the upper and lower surfaces. Four main channels were cut into the wing approximately along lines of constant chord with smaller channels branching out to the individual orifice locations.
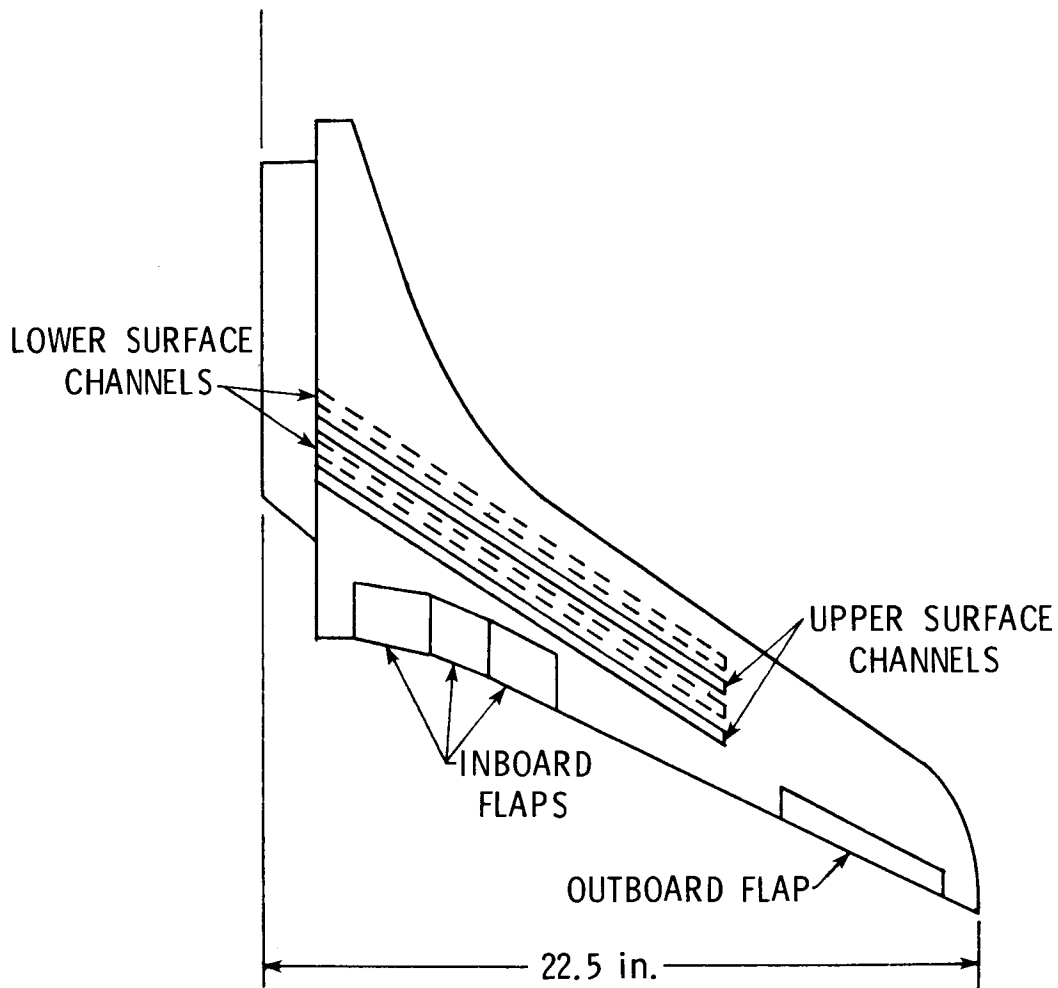


Figure 2

## SPAR MODEL OF ATT WING

The ATT wing was modeled in SPAR using plate elements as shown in figure 3. This element type has been shown to give accurate predictions of deflections for metal wings with small internal or surface channels (see refs. 2, 8, and 9). In addition, using plate elements rather than beam elements permits the calculation of wing camber changes due to aerodynamic loading. The close chordwise spacing of the nodes in the mid-chord region was required in order to define the instrumentation channels. The number of nodes in the spanwise direction was determined from a convergence study in which the number of nodes was increased until there was no change in the calculated deflections. The control surfaces were modeled using unconnected coincident points at the sides of the segments to allow them to deform independently of the other segments and the main wing. The flap attachment tab was represented by short, thin elements. A cantilever constraint was applied at the outboard edge of the first row of elements, corresponding to the side of the fuselage.
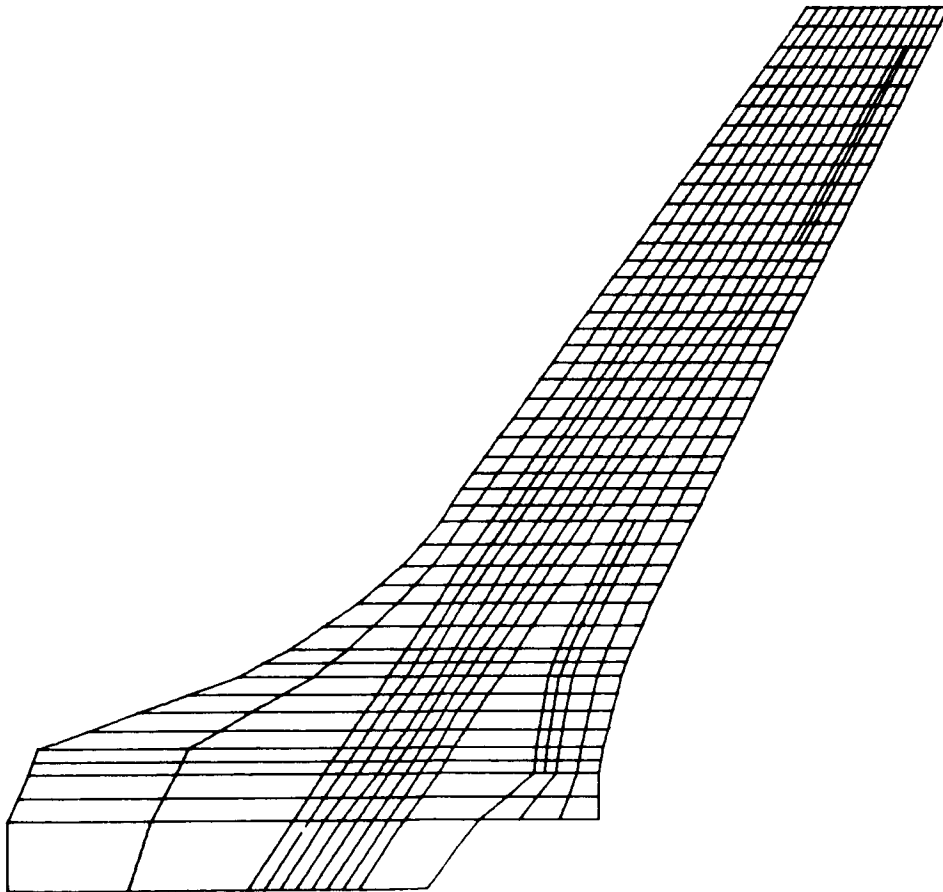


Figure 3

## CROSS SECTION OF ATT WING AS MODELED IN SPAR

A representative cross section of the finite-element model, along with the actual cross section of the wing, is illustrated in figure 4. As can be seen, the four main channels remove a substantial amount of metal in an area that is important to the bending stiffness of the wing. The plate thicknesses were determined by averaging the thicknesses at the four nodes defining the plate. The thickness at a node at the leading edge was increased from zero to one-third the thickness at the next streamwise node to give a more accurate representation of that region of the wing. The vertical location of a node was midway between the upper and lower surface of the wing (or the bottom of a channel) at that location. The flap attachment tab was not offset vertically but was set to the actual tab thickness. No attempt was made to model the small channels leading from the main channels to the orifice locations.



LEADING EDGE

FLAP ATTACHMENT TAB
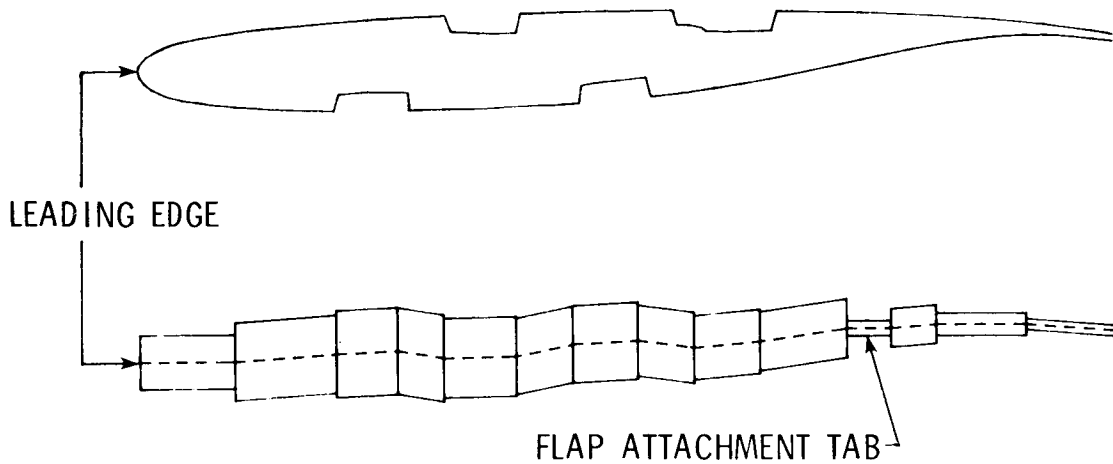
Figure 4

# ATT MID-SEMISPAN WING PRESSURE DISTRIBUTIONS CALCULATED USING WIBCO

In the wind tunnel tests of the ATT model (ref. 6), several runs were made at a Mach number of 0.90 but at different total pressures in an attempt to examine Reynolds number effects. The wing pressure distributions from these runs indicated that the anticipated rearward shock movement with increasing Reynolds number did not occur; instead, the shock moved forward and weakened. This is what would happen if the increase in dynamic pressure (resulting from the increase in total pressure to obtain the higher Reynolds number) caused a significant increase in the aeroelastic washout of the wing. Two of the test conditions were run in TAPS to see if these changes could be accurately predicted.

The tunnel Mach number of 0.90, Reynolds numbers (based on mean aerodynamic chord) of 1.58 and 4.87 million, and dynamic pressures of 536 and 1613 psf were used as input for TAPS. When comparing pressure distributions calculated with transonic potential flow codes it is often necessary to analyze the configuration at an angle of attack that differs from the experimental angle to improve the correlation between theory and experiment. Since the primary interest in this example was predicting pressure changes due to aeroelastic and Reynolds number effects, the angle of attack was increased by 1.14 degrees in the calculations to give better agreement with the experimental upper surface pressures at the lower dynamic pressure condition. This increment was then maintained in the calculations for the higher dynamic pressure case. The change in angle of attack is larger than normally required, but this would be expected since previous correlations did not account for the reduction in wing loading caused by model deformations.

The axisymmetric fuselage option in WIBCO was used for these calculations. The computational wing plane was originally located to match the low wing of the wind tunnel model, but this resulted in instabilities in the calulations, so the wing plane was shifted toward mid-fuselage. Boundary layer transition locations were set to correspond to the transition strip locations given in reference 7.

The calculated pressure distributions at $\eta$ = 0.54 for the two cases are shown in figure 5 along with the corresponding experimental results. The changes in pressure levels between the two cases caused by changing Reynolds number and dynamic pressure were predicted reasonably accurately on the upper surface ahead of the shock, but the shock locations and the pressure changes aft of the shock did not correlate well at all. This is probably related to the non-conservative finite-difference scheme used in WIBCO, which tends to calculate shock locations that are too far forward. The lower surface pressure increments were predicted fairly well.

|  | | α | η | q, psf | R x $10^{-6}$ |
|---|---|---|---|---|---|
| —————— | THEORY | 4.00 | 0.54 | 536 | 1.58 |
| — — — | THEORY | 3.77 | 0.54 | 1613 | 4.87 |
| ○ | EXPERIMENT | 2.86 | 0.55 | 536 | 1.58 |
| □ | EXPERIMENT | 2.63 | 0.55 | 1613 | 4.87 |
|  | (FLAGGED SYMBOLS DENOTE LOWER SURFACE) | | | | |

M = 0.90
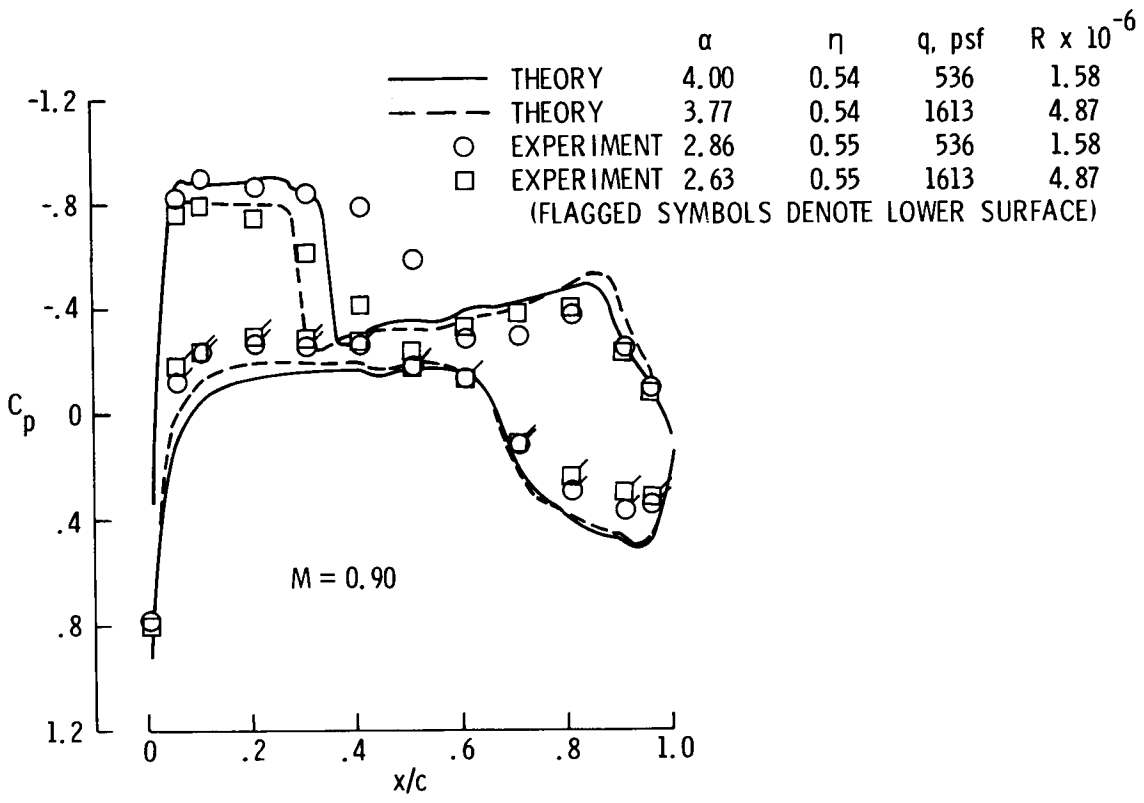
Figure 5

# ATT OUTBOARD WING PRESSURE DISTRIBUTIONS CALCULATED USING WIBCO

Figure 6 shows the theoretical and experimental pressure distributions for the ATT at about $\eta$ = 0.72. The pressure changes ahead of the shock are again predicted fairly well, but the shock near mid-chord is calculated to be much too far forward for the lower dynamic pressure case, resulting in poor correlation between theoretical and measured pressure increments over the last half of the airfoil. The good prediction of the upper surface pressure distribution for the higher pressure case with its weaker, more forward shock can be attributed to the aeroelastic twist reducing the angle of attack and thus presenting an easier case for the aerodynamic code to solve. The calculated aeroelastic twist increments at this wing station were about -0.9° and -2.5° for the low and high dynamic pressure cases, respectively.

Even with the poor correlation between theory and experiment in some areas, it is obvious that the large changes in the experimental pressure distribution were at least qualitatively predicted using TAPS, emphasizing the importance of including aeroelastic effects in transonic calculations. The correlation should improve as more accurate aerodynamic codes are incorporated into TAPS.



|  | | $\alpha$ | $\eta$ | q, psf | $R \times 10^{-6}$ |
|---|---|---|---|---|---|
| —— | THEORY | 4.00 | 0.73 | 536 | 1.58 |
| — — | THEORY | 3.77 | 0.73 | 1613 | 4.87 |
| O | EXPERIMENT | 2.86 | 0.71 | 536 | 1.58 |
| □ | EXPERIMENT | 2.63 | 0.71 | 1613 | 4.87 |

(FLAGGED SYMBOLS DENOTE LOWER SURFACE)

M = 0.90
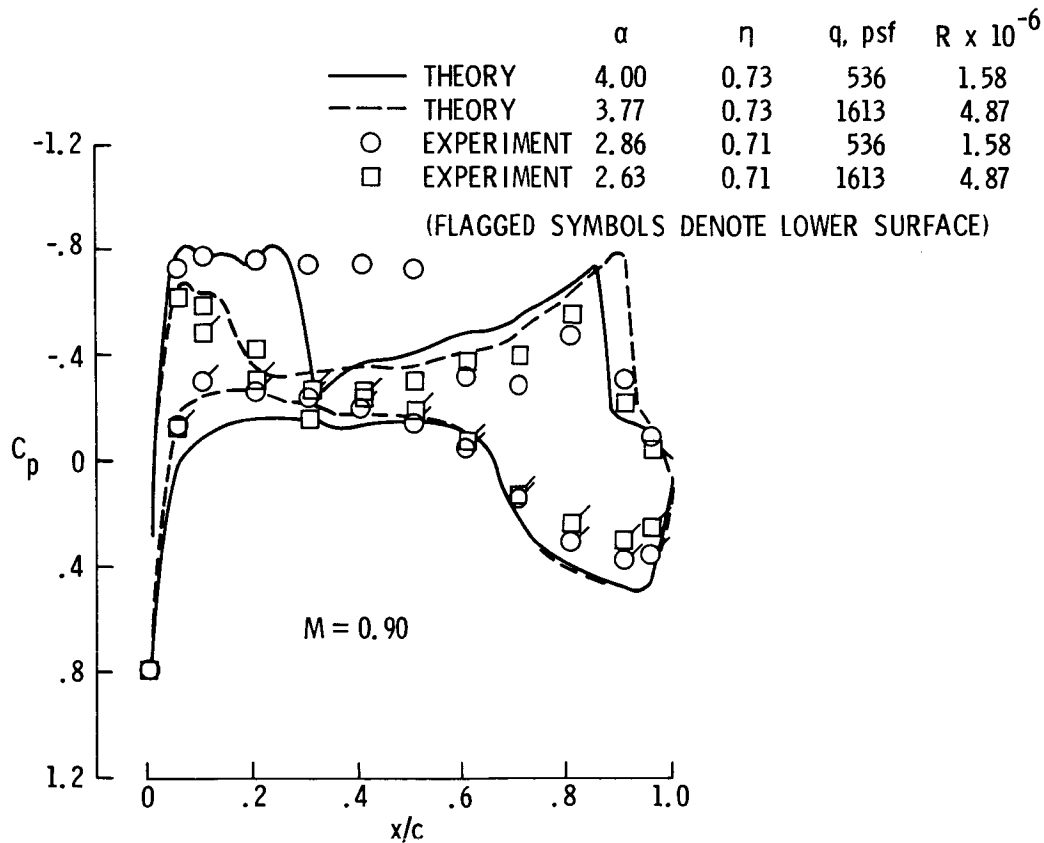
Figure 6

## CALCULATED EFFECTS OF INDEPENDENT VARIATION OF REYNOLDS NUMBER AND DYNAMIC PRESSURE

The TAPS analysis method can be used to predict what changes would have been seen in the ATT pressure distributions if the Reynolds number could have been increased without changing the dynamic pressure. This is shown in figure 7 along with the effects of changing dynamic pressure while maintaining a constant Reynolds number. As can be seen, there is not much of an effect on the pressure distribution caused by increasing just Reynolds number. The thinner boundary layer at the higher Reynolds number does not reduce the effective trailing edge camber as much, causing the second shock to be slightly farther aft than in the lower Reynolds number case. Changing the dynamic pressure had a much greater effect at these conditions for this configuation. The shock near mid-chord moved forward and weakened considerably while the second shock moved slightly aft in the higher dynamic pressure case. The lower surface pressure coefficients became more negative, as expected, from the aeroelastic washout.
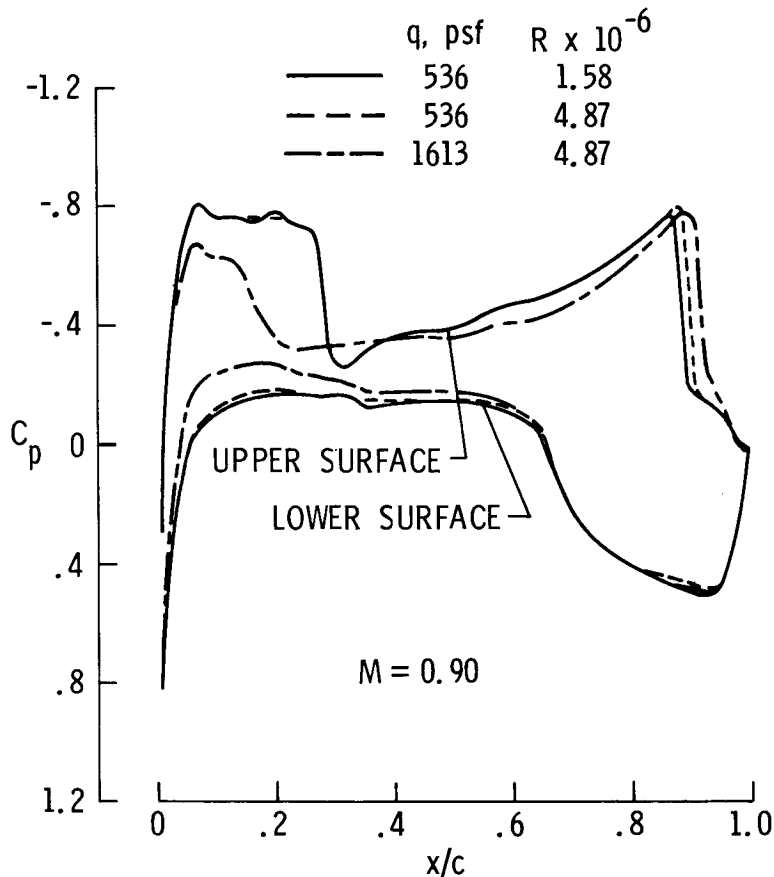


Figure 7

# ATT MID-SEMISPAN PRESSURE DISTRIBUTIONS CALCULATED USING TAWFIVE

Recently, the fully conservative full-potential TAWFIVE code was substituted
for WIBCO as the aerodynamic module in TAPS. The two test conditions for the
ATT configuration were run in this new version of TAPS to see if the predicted
pressure distributions could be improved, especially with regard to shock
location. The TAWFIVE code was somewhat more difficult to run than WIBCO
in that both the inviscid and boundary layer components showed some instabi-
lities initially. The aerodynamic model had to be changed to a mid-wing
configuration and the sweep of the leading-edge glove had to be reduced near
the side of the fuselage in order to eliminate these instabilities. The input
flow conditions were the same as those used for the WIBCO runs, including the
angle-of-attack increment of 1.14° added to the experimental angles.

Figure 8 shows the resulting pressure distributions for the ATT cases at
about $\eta$ = 0.55. Overall, the correlation is very good. The shock location is
predicted very well for the low dynamic pressure case, but is slightly too far
aft in the high dynamic pressure calculations. The upper surface pressure
coefficient level for the latter case is also slightly too negative, indi-
cating that the angle of attack for this wing station is too high. The
predicted lower surface pressure coefficients are too positive, but are in
closer agreement with the data than were the WIBCO predictions (see figure
5). In general, the pressure increments and shock movement calculated using
TAPS with TAWFIVE correlated reasonably well with the experimental results at
this wing station.

| | $\alpha$ | $\eta$ | q, psf | R x $10^{-6}$ |
|---|---|---|---|---|
| —————— THEORY | 4.00 | 0.56 | 536 | 1.58 |
| — — — THEORY | 3.77 | 0.56 | 1613 | 4.87 |
| O EXPERIMENT | 2.86 | 0.55 | 536 | 1.58 |
| □ EXPERIMENT | 2.63 | 0.55 | 1613 | 4.87 |

(FLAGGED SYMBOLS DENOTE LOWER SURFACE)



M = 0.90
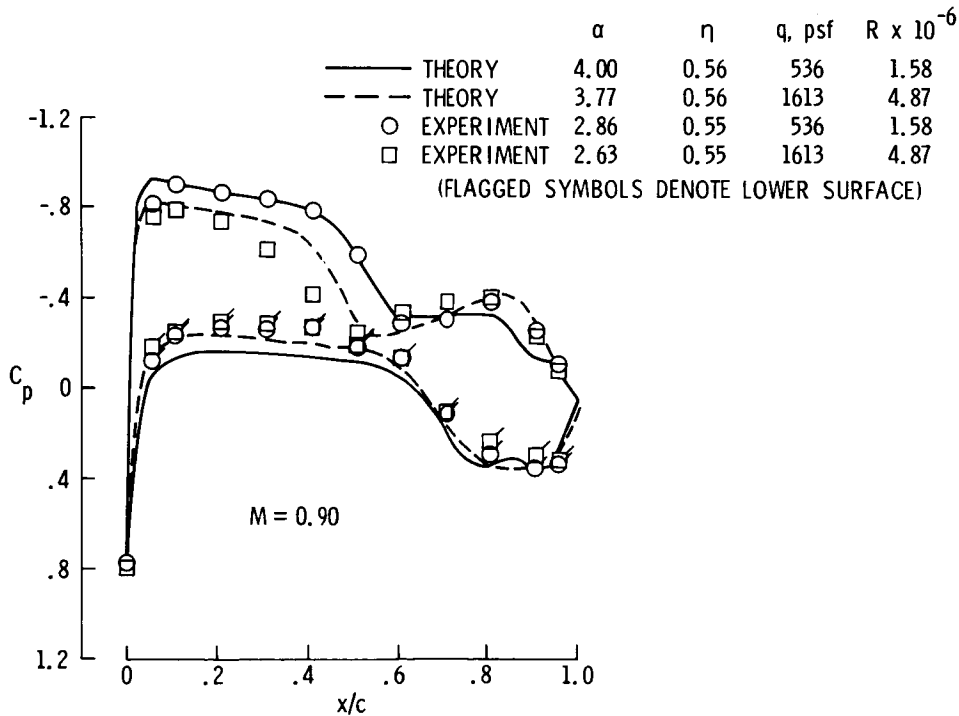
# ATT OUTBOARD PRESSURE DISTRIBUTIONS CALCULATED USING TAWFIVE

Figure 9 shows the calculated and experimental pressure distributions for the ATT configuration at about η = 0.72. As at the mid-semispan station, the correlation between theoretical and experimental shock location and pressure levels is good for the low dynamic pressure case. For the high dynamic pressure condition, the upper surface pressure coefficients ahead of the shock are too negative, again indicating that the local angle of attack is too high. This would also cause the calculated shock location to be too far aft, since the supercritical airfoil section used is very sensitive to angle of attack. It appears that the theoretical model of the wing may be too stiff, possibly because it does not account for the effects of the small channels to the pressure orifice locations. It is interesting to note, however, that the twist increments calculated using TAWFIVE were within two percent of the values predicted using WIBCO, and the pressures calculated by WIBCO showed good agreement with the experimental pressures for the high dynamic pressure case. It is also possible that the pressures near the wing tip, which have a large effect on the wing deflections, may not be calculated correctly, but no data were available for comparison outboard of η = 0.71. A third possible source of the discrepancy is that the theory-to-experiment angle increment of 1.14° determined using WIBCO is larger than that required for TAWFIVE. The pressure increments due to changing dynamic pressure and Reynolds number were predicted qualitatively on the lower surface, with the predicted increment being slightly too large.



| | α | η | q, psf | R x 10$^{-6}$ |
|---|---|---|---|---|
| —— THEORY | 4.00 | 0.74 | 536 | 1.58 |
| — — THEORY | 3.77 | 0.74 | 1613 | 4.87 |
| O EXPERIMENT | 2.86 | 0.71 | 536 | 1.58 |
| □ EXPERIMENT | 2.63 | 0.71 | 1613 | 4.87 |

(FLAGGED SYMBOLS DENOTE LOWER SURFACE)

M = 0.90
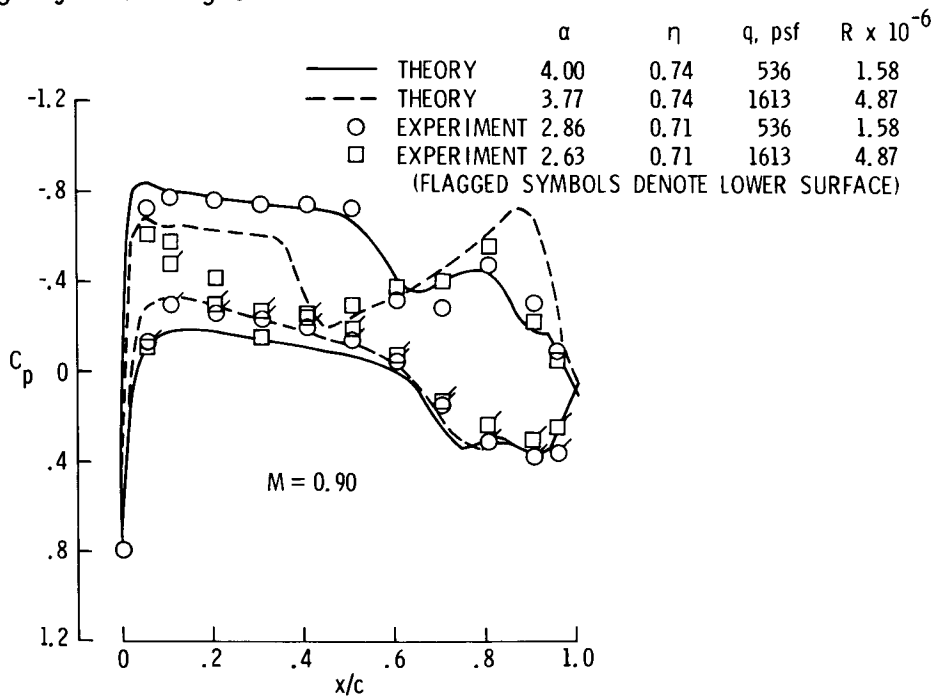
Figure 9

## TF-8A GEOMETRY AND SPAR MODEL DESCRIPTION

The second configuration used as a test case in TAPS was the TF-8A model described in reference 10. A top view of the SPAR model of the wing is shown in figure 10. The wing had a span of 32.34 in., a quarter-chord sweep of 42.24°, an aspect ratio of 6.8, and a taper ratio of 0.36. The NASA super-critical airfoil sections varied in maximum thickness-to-chord ratio from 0.114 near the fuselage to 0.071 near the tip. This configuration also had a highly swept leading-edge glove that extended to approximately $\eta = 0.35$.

The TF-8A wing was fabricated from solid aluminum with surface channels for the pressure instrumentation. No attempt was made to include these channels in the SPAR model since their geometry was not defined in the available refer-ences. A 12 x 50 node grid was generated, extending from the wing symmetry plane to the tip. Plate element thicknesses and the vertical location of the nodes were determined as described for the ATT model. A cantilever constraint condition was enforced at the wing symmetry plane.
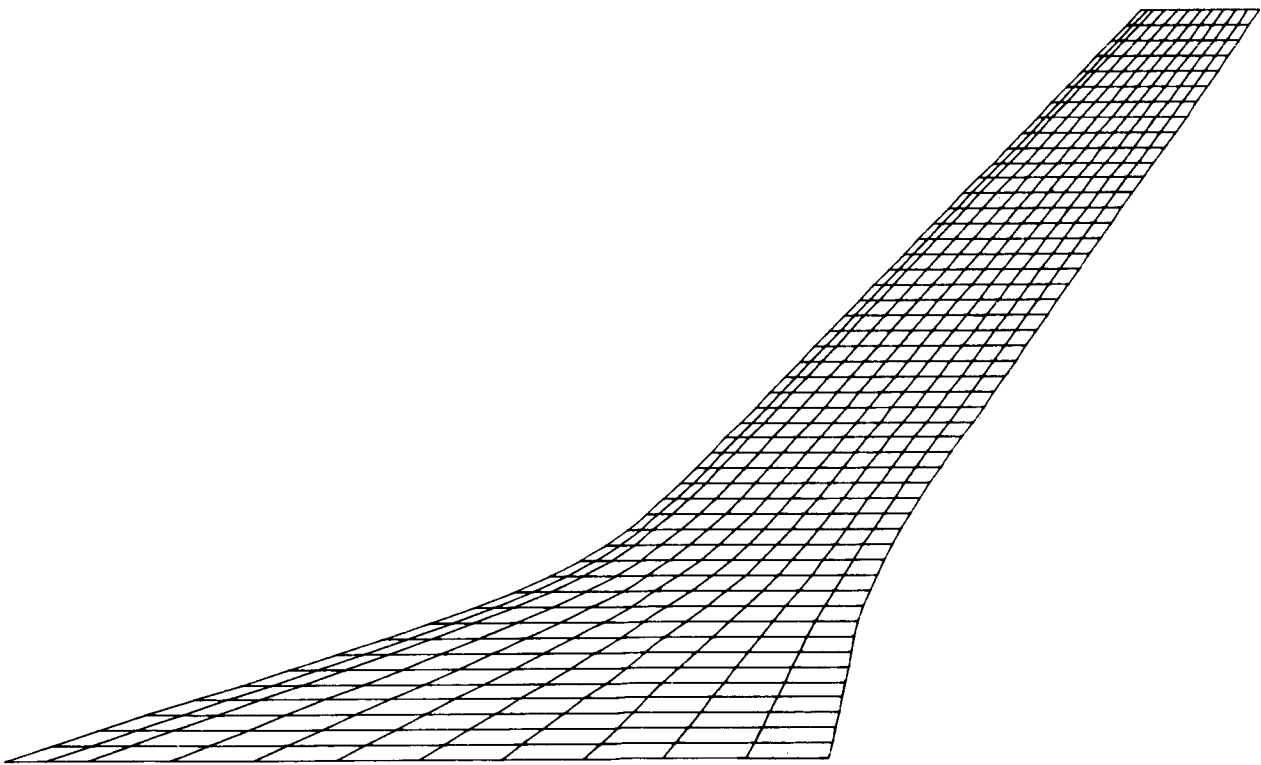


Figure 10

# TF-8A MID-SEMISPAN WING PRESSURE DISTRIBUTIONS CALCULATED USING WIBCO

Two test conditions for the TF-8A were run in TAPS using the tunnel Mach number of 0.95, dynamic pressures of 425 and 850 psf, and Reynolds numbers (based on the mean aerodynamic chord) of about 1.0 and 2.0 million. The experimental angle of attack was increased from 4.0° to 4.6° to try to improve the theory-experiment correlation at the lower dynamic pressure condition. A mid-wing location on an axisymmetric fuselage was used in WIBCO. The theoretical boundary layer transition locations were matched to the transition strip locations on the wind tunnel model.

The resulting pressure distributions are presented along with the experimental results in figures 11 and 12. As can be seen in figure 11, the correlation between theory (with the angle-of-attack adjustment) and experiment is good at about the mid-semispan station. The shock which occurs experimentally around x/c = 0.3 on the upper surface is not predicted by the theory, which instead calculates an isentropic compression of about the same pressure increase in that region. Also, the predicted lower surface pressure coefficients are somewhat more positive than the experimental values. Except for a small region near the leading edge and the area just aft of the shock, the increments in the experimental pressures caused by changing Reynolds number and dynamic pressure, though small, were predicted reasonably well.



|  | α | η | q, psf | R x 10$^{-6}$ |
|---|---|---|---|---|
| —— THEORY | 4.6° | 0.49 | 425 | 0.98 |
| — — — THEORY | 4.6° | 0.49 | 850 | 1.96 |
| O EXPERIMENT | 4.0° | 0.48 | 425 | 0.98 |
| □ EXPERIMENT | 4.0° | 0.48 | 850 | 1.96 |

(FLAGGED SYMBOLS DENOTE LOWER SURFACE)

M = 0.95

Figure 11

322
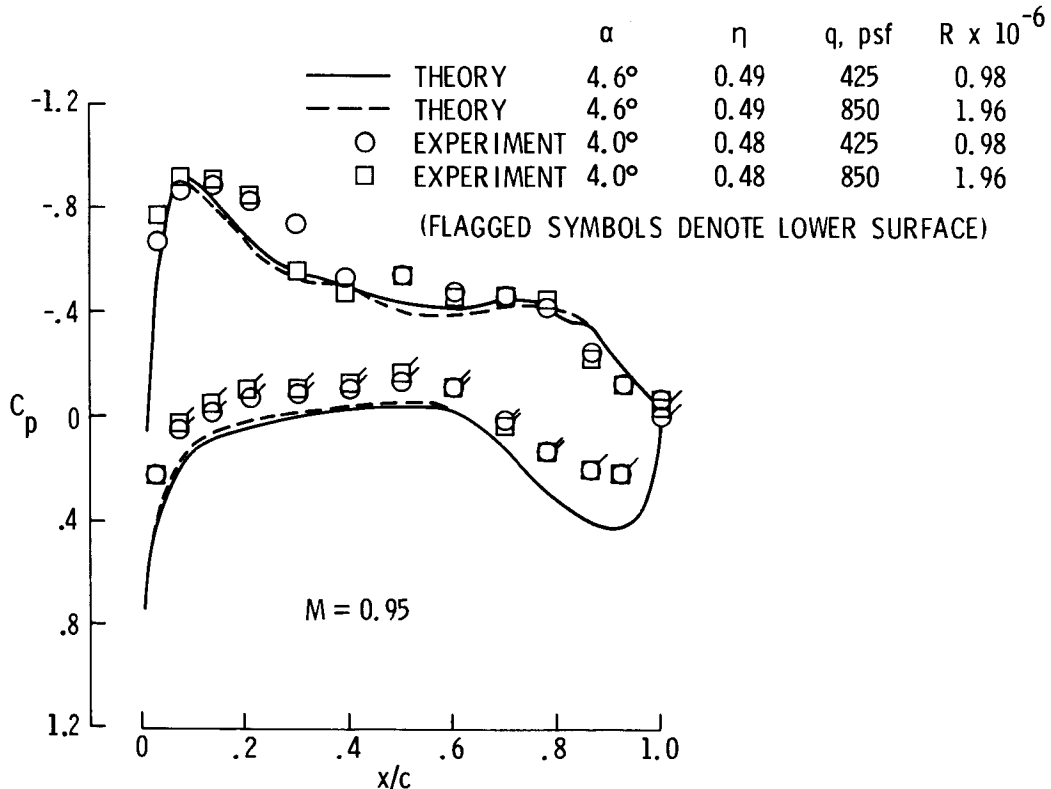
# TF-8A OUTBOARD WING PRESSURE DISTRIBUTIONS CALCULATED USING WIBCO

The correlation between theoretical and experimental pressure distributions for the TF-8A deteriorates at η = 0.80 (figure 12). The predicted shock location is much too far forward and is followed by a re-expansion of the flow and a second shock that is not present in the data. Pressure coefficients on the upper surface near the leading edge were calculated to be more negative than the experimental values and lower surface pressure levels did not correlate well anywhere. The poor correlation in shock location and leading-edge pressures can probably be attributed to the non-conservative differencing and the small-disturbance approximation, respectively, used in WIBCO. It is likely that the correlation for this case could also be improved by using the TAWFIVE version of TAPS. It should be noted that the changes in pressure levels at this wing station resulting from the change in Reynolds number and dynamic pressure were predicted fairly accurately except near the shock. This would indicate that the integrated effect of the loads on the wing resulted in approximately the correct change in wing shape.



| | | $\alpha$ | $\eta$ | q, psf | $R \times 10^{-6}$ |
|---|---|---|---|---|---|
| —————— | THEORY | 4.6° | 0.80 | 425 | 0.98 |
| — — — | THEORY | 4.6° | 0.80 | 850 | 1.96 |
| O | EXPERIMENT | 4.0° | 0.80 | 425 | 0.98 |
| □ | EXPERIMENT | 4.0° | 0.80 | 850 | 1.96 |

(FLAGGED SYMBOLS DENOTE LOWER SURFACE)

M = 0.95
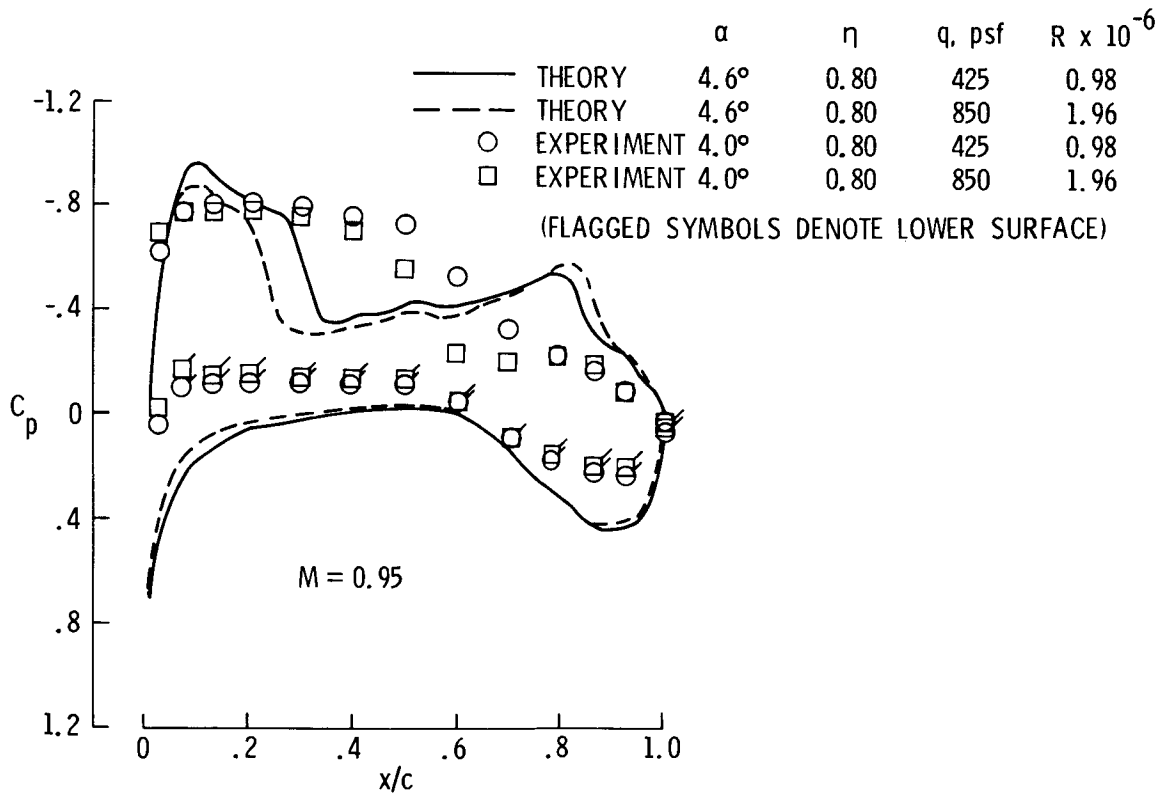
Figure 12

# STATIC AEROELASTIC TWIST DISTRIBUTIONS FOR THE TF-8A MODEL

The spanwise distributions of aeroelastic twist corresponding to the pressure distributions shown in figures 11 and 12 are given in figure 13. The experimental values were obtained during the wind tunnel test of the model using stereophotogrammetry as described in reference 10. The calculated values agree very well with the experimental data for both the low and high dynamic pressure cases; the twist increment at the tip for the high dynamic pressure case is overpredicted by about 0.2° which according to reference 9 is within the accuracy of the data. While the agreement is good, it should be noted that this is partly due to the offsetting effect of some errors. The pressure distributions shown in figures 11 and 12 indicate that the calculated lift is greater and the pitching moment more negative than the experimental values, which would result in the predicted twist being too large. However, since the wing channels were not modeled, the theoretical model is stiffer than the actual wing, thereby compensating to some extent for the higher calculated loads.

| | | $\alpha$ | q, psf |
|---|---|---|---|
| —— | THEORY | 4.6° | 425 |
| - - - | THEORY | 4.6° | 850 |
| O | EXPERIMENT | 4.0° | 425 |
| □ | EXPERIMENT | 4.0° | 850 |

Figure 13

## CONCLUSIONS

A simple method of including aeroelastic effects in 3D transonic calculations has been developed. Known as the Transonic Aeroelastic Program System, or TAPS, the method couples a transonic computer code with a finite element structural analysis program in an iterative fashion. The calculations for this study were made using the SPAR structural analysis code with either the small-disturbance WIBCO code or the full-potential TAWFIVE code a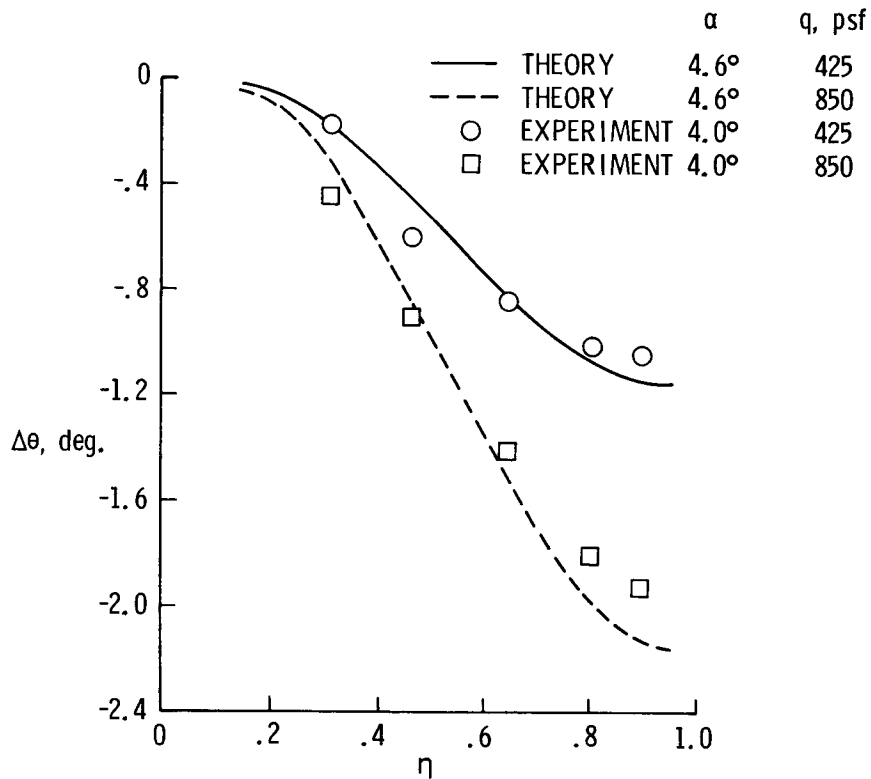s the aerodynamic module. Both aerodynamic codes used interactive boundary layer calculations to model viscous effects. Calculated results from TAPS were compared with data for two test cases. The following conclusions were drawn from this study (see figure 14):

1.  TAPS gave fairly good predictions of pressure increments due to changes in Reynolds number and dynamic pressure, except near shocks.

2.  The TAWFIVE version of TAPS generally gave more accurate predictions of the pressure distributions (especially shock locations) than did the WIBCO version for the configuration and conditions used in this study. WIBCO did give better correlation at the outboard station for the high dynamic pressure case.

3.  Wing deflections calculated using TAPS correlated well with deflections optically measured in a wind tunnel.

- ● TAPS PROVIDES A SIMPLE METHOD OF INCLUDING AEROELASTIC EFFECTS IN TRANSONIC CALCULATIONS.

- ● TAPS GAVE FAIRLY GOOD PREDICTIONS OF PRESSURE INCREMENTS DUE TO CHANGES IN REYNOLDS NUMBER AND DYNAMIC PRESSURE, EXCEPT NEAR SHOCKS.

- ● TAPS/TAWFIVE GENERALLY GAVE MORE ACCURATE PREDICTIONS OF PRESSURE DISTRIBUTIONS (ESPECIALLY SHOCK LOCATIONS) THAN TAPS/WIBCO.

- ● WING DEFLECTIONS CALCULATED USING TAPS CORRELATED WELL WITH DEFLECTIONS OPTICALLY MEASURED IN A WIND TUNNEL.

Figure 14

325

# SYMBOLS

| | |
|---|---|
| $C_p$ | pressure coefficient |
| $M$ | free-stream Mach number |
| $q$ | dynamic perssure, psf |
| $R$ | Reynolds number based on mean aerodynamic chord |
| $x/c$ | chordwise station |
| $\alpha$ | angle of attack, degrees |
| $\Delta\theta$ | static aeroelastic twist increment, degrees |
| $\eta$ | semispan station |

326

# REFERENCES

1. Fuller, Dennis E.: Guide for Users of the National Transonic Facility. NASA TM-83124, July 1981.

2. Campbell, Richard L.:  A Computational Method for Predicting the Effects of Varying Reynolds Number and Dynamic Pressure on Flexible Wings at Transonic Speeds.  Masters Thesis, George Washington University, February 1984.

3. Boppe, Charles W.: Transonic Flow Field Analysis for Wing-Fuselage Configurations.  NASA CR-3243, 1980.

4. Melson, N. Duane; and Streett, Craig L.:  TAWFIVE - A Users' Guide.  NASA TM-84619, September 1983.

5. Whetstone, W. D.:  SPAR Structural Analysis System - Reference Manual, Vol. I, NASA CR-145098-1, February 1977.

6. Struzynski, N. A.:  Transonic Wind Tunnel Tests of a Model of the Advanced Technology Transport.  Calspan No. T18-073, November 1973.

7. Mann, Michael J.; and Langhans, Richard A.:  Transonic Aerodynamic Characteristics of a Supercritical-Wing Transport Model With Trailing-Edge Controls.  NASA TM X-3431, October 1977.

8. Mehrotra, S. C.; and Gloss, B. B.:  Computation of Wind Tunnel Model Deflections.  AIAA-81-0482-CP, Atlanta, Georgia, April 1981.

9. Mehrotra, S. C.; and Robinson, J. C.:  Structural Modeling of High Reynolds Number Wind Tunnel Models.  AIAA-82-0602-CP, Williamsburg, Virginia, March 1982.

10. Brooks, Joseph D.; and Beamish, Jerry K.:  Measurement of Model Aeroelastic Deformations in the Wind Tunnel at Transonic Speeds Using Stereophotogrammetry.  NASA TP-1010, October 1977.

# INFLUENCE OF ANALYSIS AND DESIGN MODELS
## ON MINIMUM WEIGHT DESIGN

M. Salama
Jet Propulsion Laboratory
Pasadena, California


R. K. Ramanathan
Northrop Aircraft
Hawthorne, California


L. A. Schmit and I. S. Sarma
University of California
Los Angeles, California

Many practical structural design problems that can truly benefit from a formal optimization procedure typically involve very large number of degrees of freedom, design variables, and behavioral constraints which are computationally burdensome. While this large dimensionality of the analysis-design models presents no significant computational difficulties from the point of view of achieving an optimum design, it places real limitations on the economic advantages of using optimization methods as routine design tools.

As a means of accommodating the minimum weight design of large problems within reasonable costs, it has been an accepted practice in most structural optimization computer programs to employ a number of approximations that lead to reducing the problem dimensions during various phases in the optimization process. Thus, in addition to reductions in the number of degrees of freedom implied in selecting a particular finite element analysis model, dimensionality during the design phase may be reduced further by imposing certain preselected relationships between the design variables (linking and/or basis reduction), and by temporary deletion of constraints that are not potentially critical.

In this paper, we examine the results of numerical experiments designed to illustrate how the minimum weight design, accuracy, and cost can be influenced by (a) refinement of the finite element analysis model and associated load path problems and (b) refinement of the design variable linking model. The numerical experiments range from simple structures where the modelling decisions are relatively obvious and less costly to the more complex structures where such decisions are less obvious and more costly. All numerical experiments used in this paper employ the dual formulation in ACCESS-3 computer program (1,2).

Guidelines are suggested for creating analysis and design models that predict a minimum weight structure with greater accuracy and less cost. These guidelines can be useful in an interactive optimization environment and in the design of heuristic rules for the development of knowledge-based expert optimization systems.

330

# EXPERIMENT 1

## UNIFORMLY LOADED CANTILEVER BEAM

In the first numerical experiment, we consider the optimum weight dependence on the number of design variables (D.V.) and degrees of freedom (D.O.F.) for the cantilever beam of figure 1. The properties are: elastic modulus = $10 \times 10^6$ lb/in$^2$, Poissons's ratio = 0.3, and weight density 0.1 lb/in$^3$. In the successively refined design and analysis models shown, the design variables are taken as the bar areas and shear panel thicknesses.

The design constraints are:
Displacement upper/lower bound = ± 0.3 in. at the free end
Upper and lower bound on the conbined Von Mises stresses = ± 25000 lb/in$^2$
Minimum gage = 0.1 in$^2$ for bar area, and 0.01 in. for panel thickness
The bottom model shows the 24-D.V. and 48-D.O.F. combination
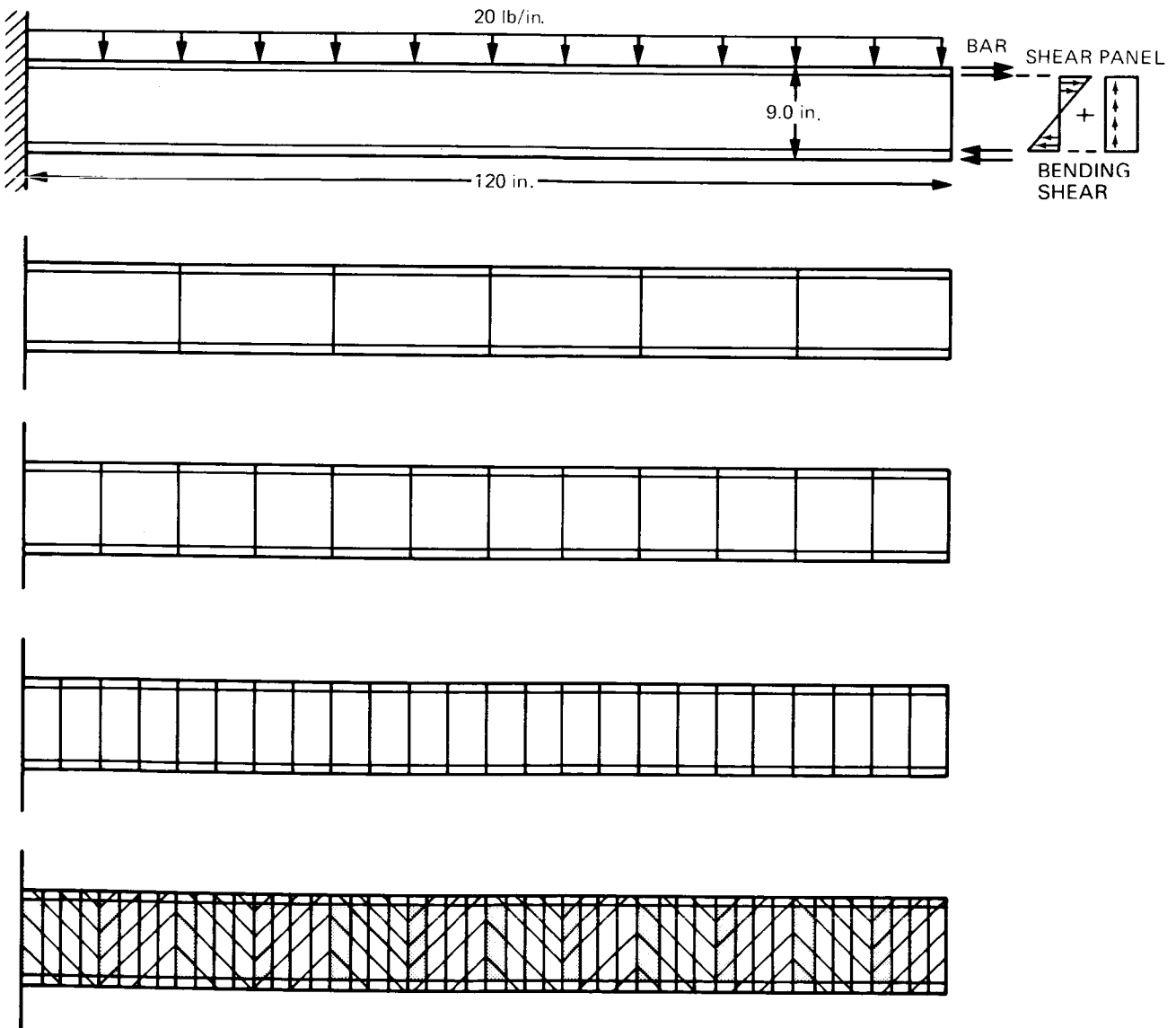


Figure 1

In figure 2 below, the optimum weight ($W_{opt.}$) is displayed in figure 2a against changes in the number of D.V., with the number of D.O.F. held constant, and against changes in the number of D.O.F. in figure 2b while holding the D.V. constant.

These results suggest the following observations.

1. A segment of the bar elements of length $\alpha$ from the free end was designed by minimum gage. The distance $\alpha$ increased with refined D.V. and D.O.F. models. Stresses were well below their limits throughout.

2. A greater number of D.O.F. results in higher optimum weight (more flexible structure), while a greater number of D.V. results in lower optimum weight.

3. In an evolving optimization process, it is expedient to start with the practically most crude design and analysis models, then refine both models simultaneously along the dotted line paths (figure 2b), limited by manufacturability constraints and computational cost. This is much less expensive than the analysis-driven alternative of starting with a highly refined analysis model and a crude D.V. model that may be successively refined.
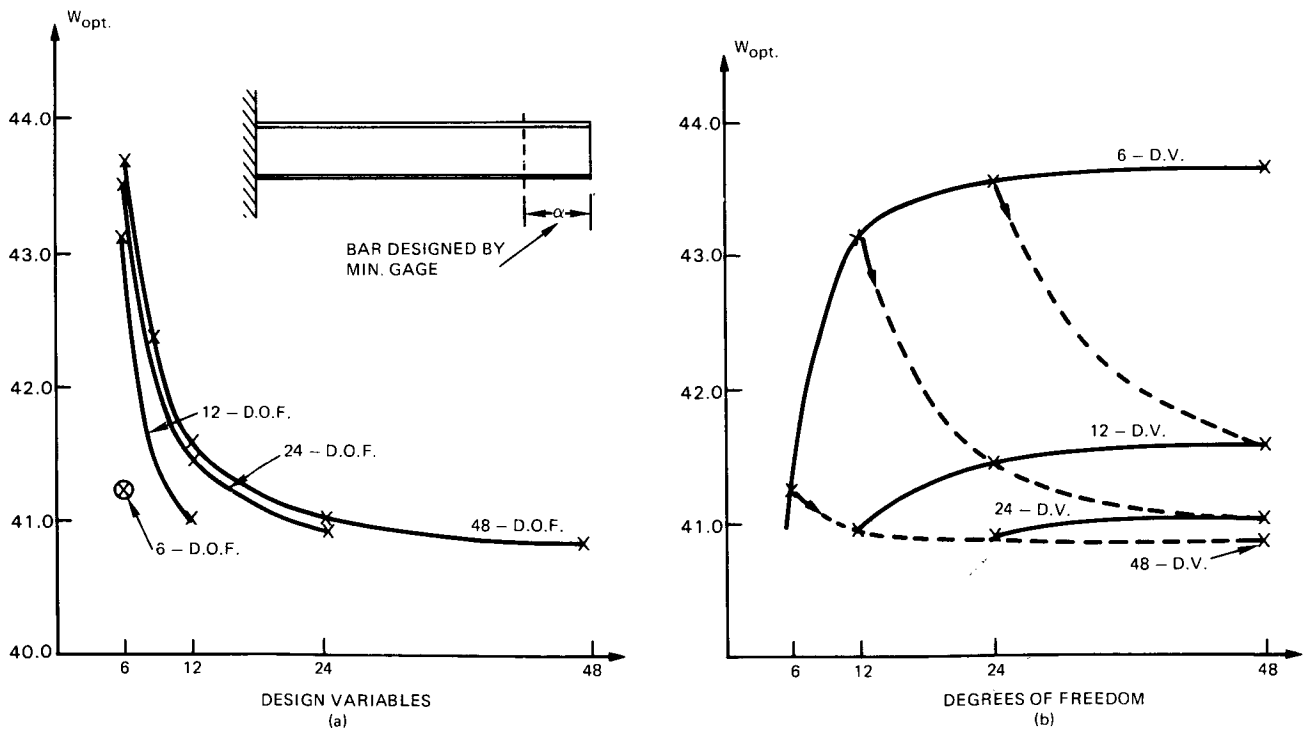


Figure 2

## STRESS-CRITICAL CANTILEVER BEAM

Stress criticality was enforced by removing the bound on the free end deformation. From figure 3 below, only the shaded shear panel region of length $\beta$ was stress-critical, with the bar in that region stressed up to $\sim 88\%$ of its capacity. The portion $\alpha$ from free end was designed by minimum gage. The sizes of the regions designated by $\alpha$ and $\beta$ were D.V. and D.O.F. dependent. Of course, had the panel been able to carry only shear, the bar would have been stressed to its fullest.

The same observations (2) and (3) made for the deformation-critical design apply as well in the stress-critical case to a greater extent. Comparison of figures 2 and 3 reveals greater sensitivity of the stress-critical design (over the deformation-critical design) to variations in D.V. and D.O.F. model refinements. This is because stress constraints must be satisfied locally by the linked group, while tip deformation is satisfied globally by contributions of all D.V. groups.
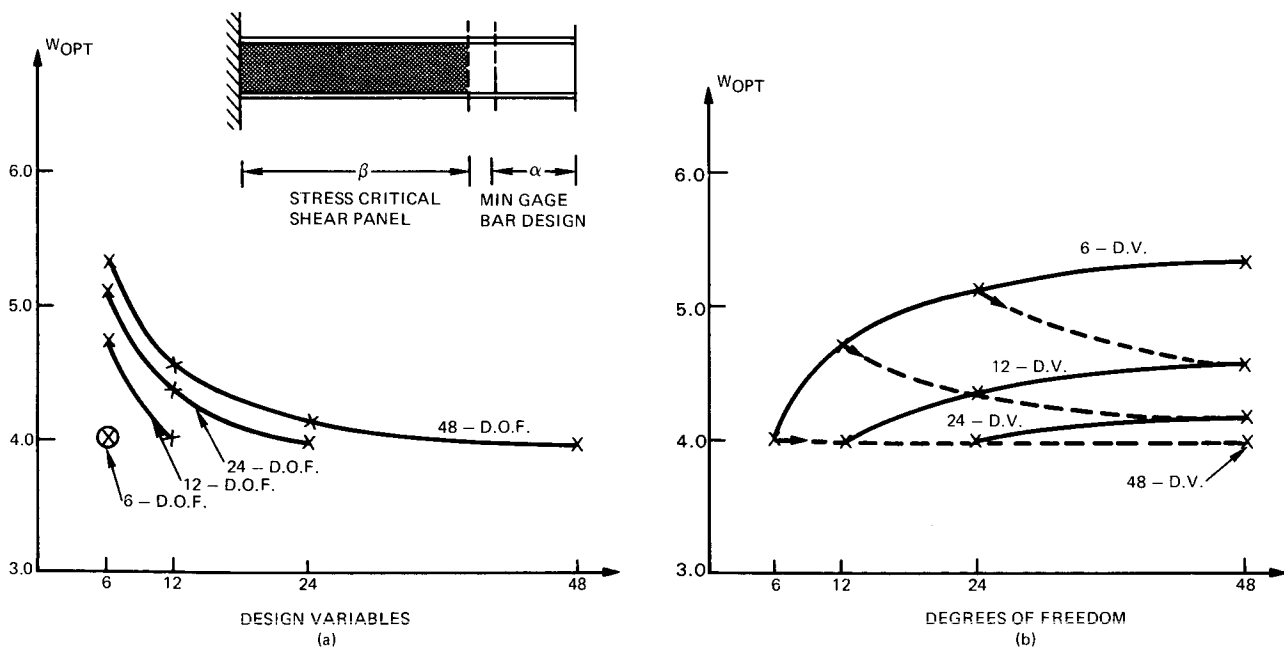


Figure 3

OPTIMIZATION COST FOR STRESS-CRITICAL CANTILEVER

The two figures below display the relative cost of optimizing the cantilever beam as a function of the number of D.V. while holding the number of D.O.F. constant (figure 4a) and as a function of D.O.F. while holding the number of D.V. constant (figure 4b). The cost values are normalized to the smallest (2.2 CPU seconds used for 6 D.O.F. 6 D.V.), and include both analysis and optimization costs. All curves are for 10 analysis/optimization stages that start with the same initial uniform design. Thus figure 4 does not reflect any convergence related costs. The following comments can be made.

1.  The relative costs below confirm observation (3) made in connection with figure 2.

2.  The total optimization cost includes the analysis cost, which depends upon the number of D.O.F. in the model, and the optimization cost, which depends on the number of potentially active constraints and D.V. Gradient computations, in the present case by the pseudo load method, constitute a large percentage of the optimization costs. This explains the relative insensitivity of cost for a fixed number of D.V. and variable D.O.F., figure 4b, over the cost of a fixed number of D.O.F. and variable D.V., figure 4a.
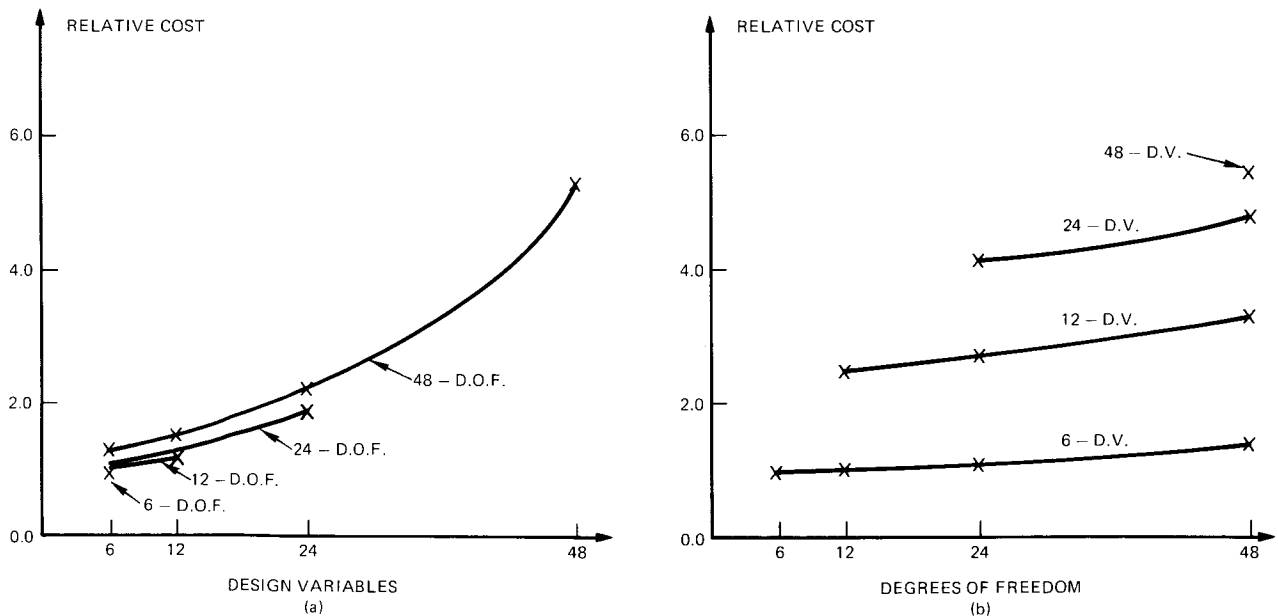


Figure 4

## EXPERIMENT 2

## LOAD INTRODUCTION IN A FIXED-FIXED BEAM

In complex geometries it is not always possible nor desirable to use spatially uniform analysis and/or design models for optimization. Further, the relative degree of refinement necessary in various regions of the same model is frequently not obvious. Unintended model refinement inaccuracies lead to unbalanced internal loads and incorrect optimum design. This is illustrated here by the symmetric fixed-fixed beam carrying a single load at the center. Thus, the obviously correct symmetric analysis and design models are replaced in the present experiment by the incorrect models of figure 5.

The initially symmetric analysis and design model is successively refined in the number of D.O.F. in the right hand region only, while keeping the design model constant (always with 8-D.V.). The beam properties are the same as in the previous cases.
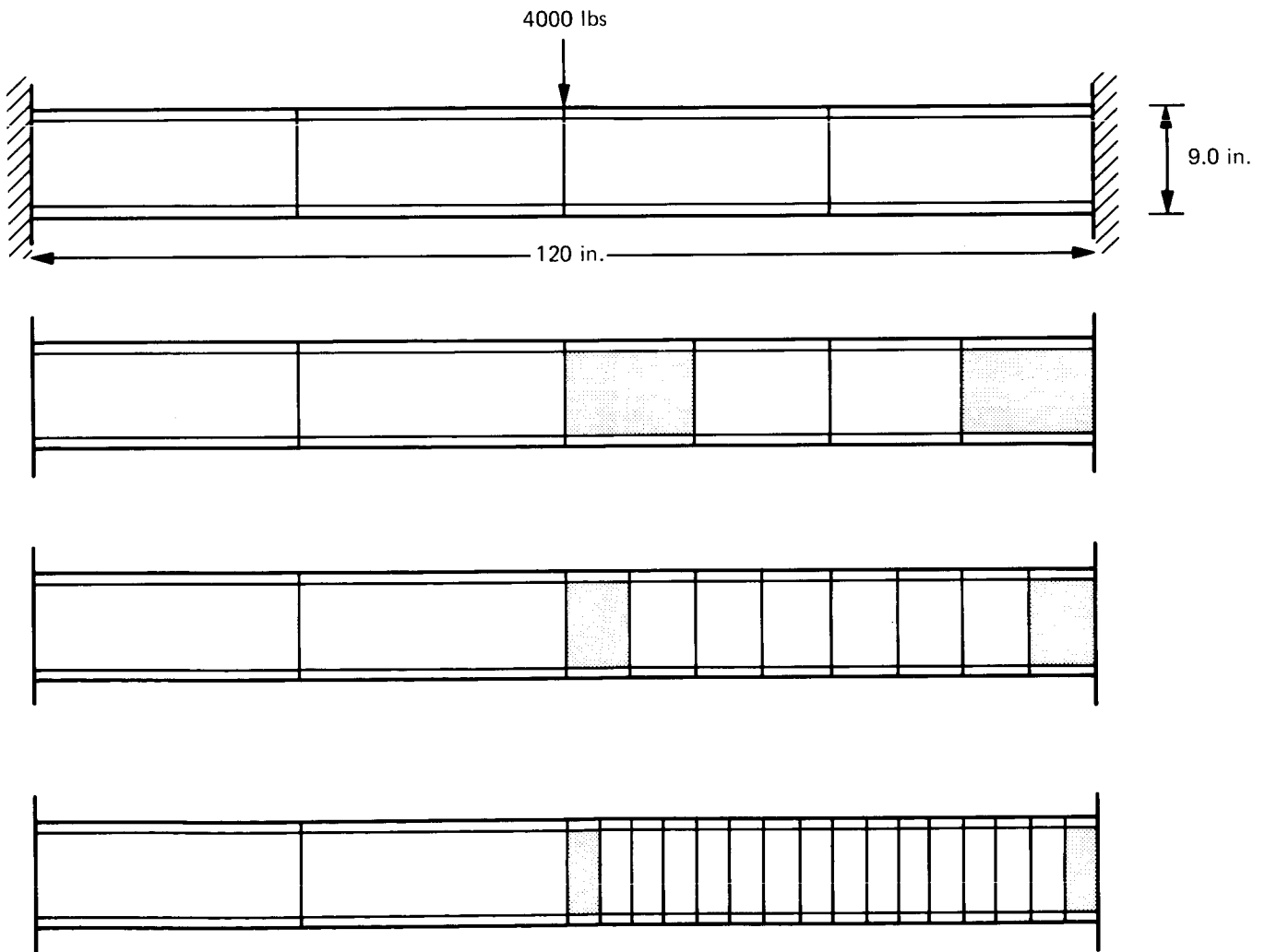


Figure 5

The results of figure 6 show how the optimum weight prediction is influenced by incorrect load distribution borne by unbalanced analysis model refinement. Figure 6 suggests the following conclusions.

1. An unbalanced model causes the load to shift toward the stiffer (less refined) region. Consequently larger model imbalance results in a larger increase in weight of the less refined region over the more refined one. In fact, the displacement-critical design exhibited a weight decrease of the refined region with greater D.O.F. refinements, while the weight of the less refined region continued to increase. Reactions computed for the 34-D.O.F. model were:

   Displacement-critical; left = 2530. lb., right = 1470. lb.
   Stress-critical; left = 2470. lb., right = 1550. lb.

2. As in the previous example, the stress-critical design is more sensitive to D.O.F. refinement than the displacement-critical design.



TOTAL DEGREES OF FREEDOM
(a) DEFORMATION CRITICAL (8 – D.V.)

TOTAL DEGREES OF FREEDOM
(b) STRESS CRITICAL (8 – D.V.)
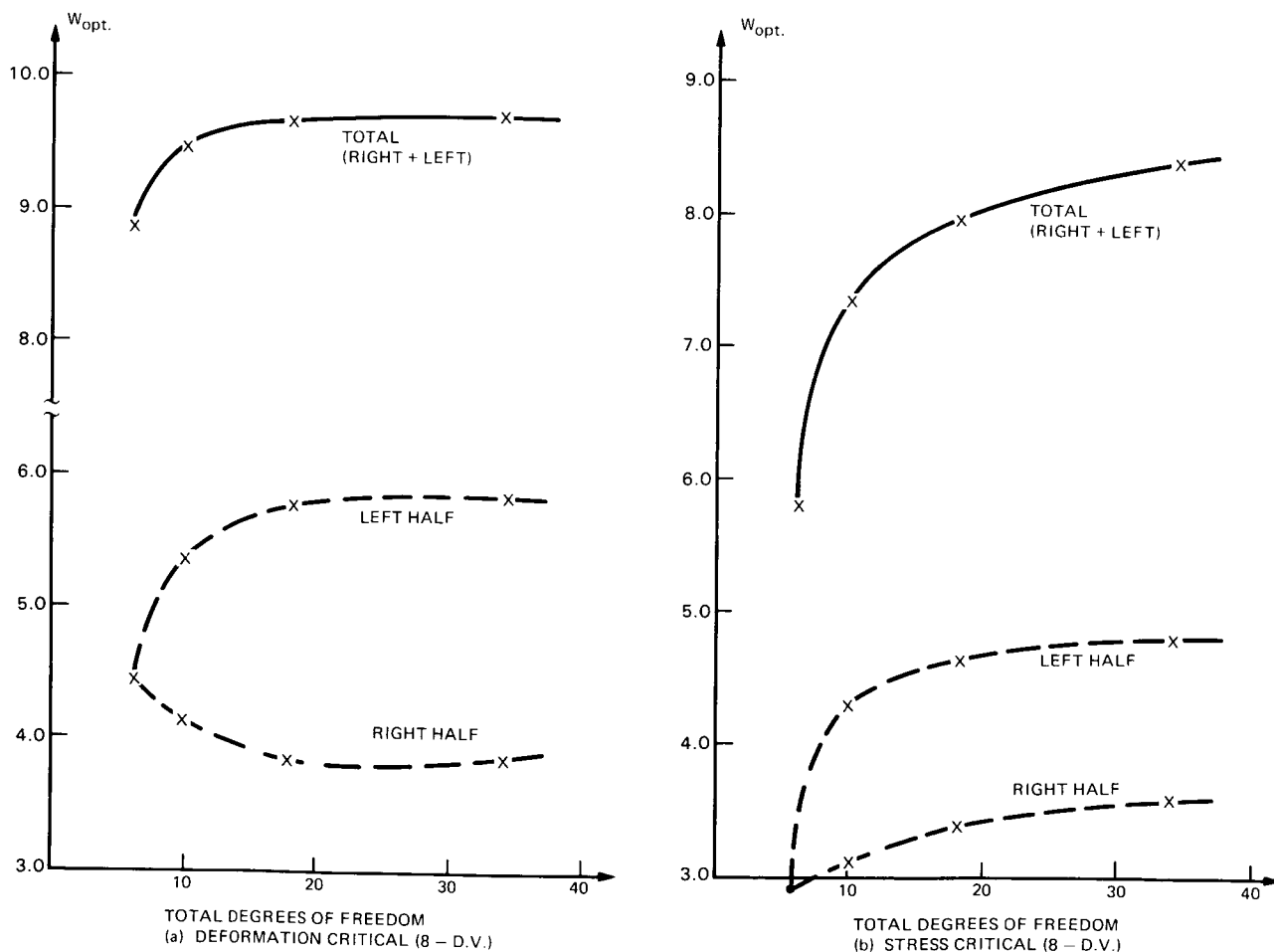
Figure 6

## EXPERIMENT 3

## 4-POINT SUPPORTED RECTANGULAR PLATE

Optimization of the 10 x 12 in., 4-point supported plate of figure 7a is investigated by varying the number of D.O.F. in the model. Some aspects of the same plate problem have been addressed in refs. 2 and 3. The external load and material properties are those of ref. 2. In figure 7b, two models are shown for the symmetric 1/4 plate; a 64-node model (solid lines) with 175 unrestrained D.O.F., and a 225-node model (broken lines) with 644 unrestrained D.O.F. In both cases, the imposed constraints include: minimum plate thickness = .02 in., upper and lower bounds on the out-of-plane displacement = ± .02 in. at the center node and at the exterior corner node, and maximum allowable Von Mises stress $\sigma_v$ = 25,000. psi for all elements. All elements are triangular plate bending elements linked in 32-D.V. groups as indicated by underlined numbers in the table in figure 8.
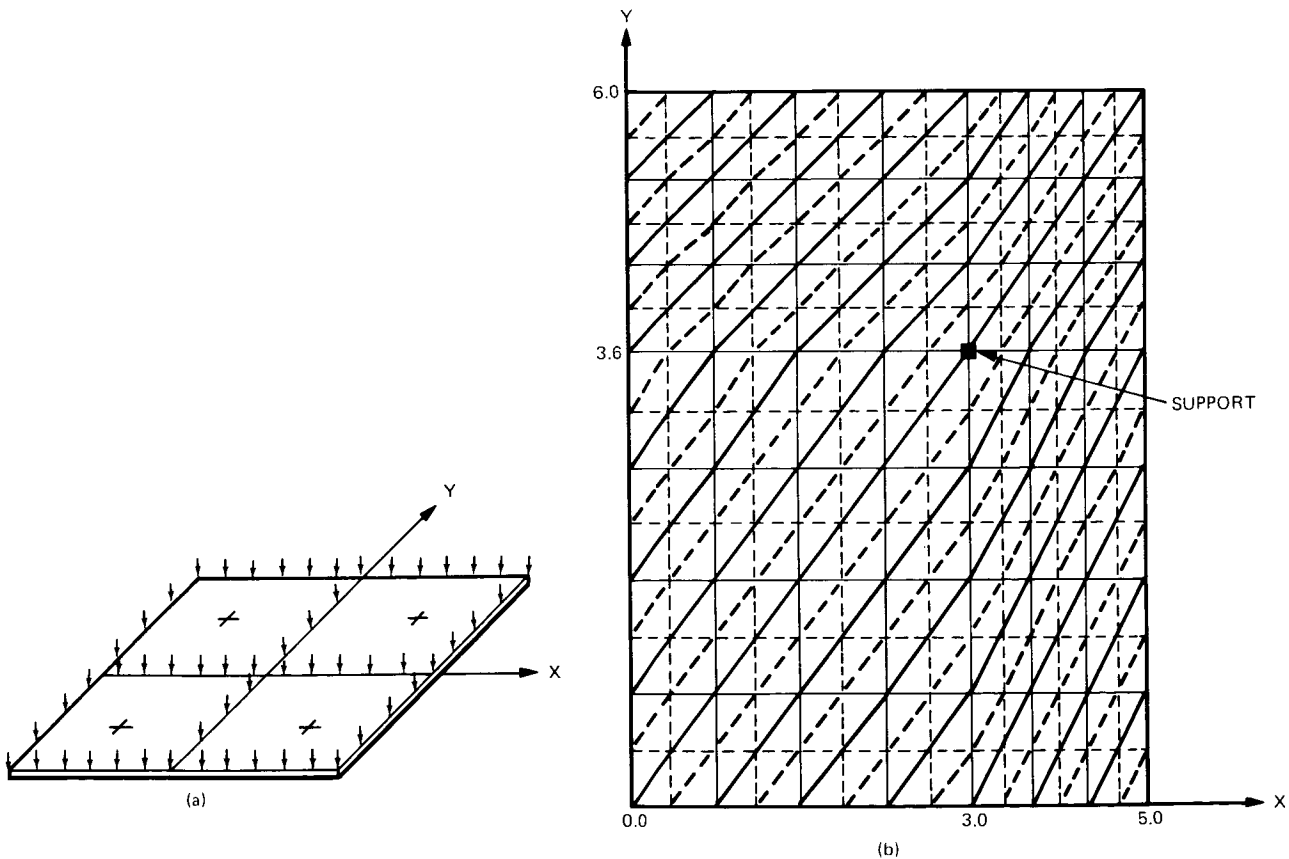


Figure 7

# OPTIMIZATION RESULTS FOR PLATE EXAMPLE

Optimization started with the same initial design of 0.71 in uniform thickness and 5.282 lb weight for both the 64-node and the 225-node models. After 12 analysis/design stages, the 64-node model converged relatively smoothly to 2.386 lb, figure 8a, with the displacement at the exterior corner node about 90% critical and the stresses either below critical or up to 0.3% infeasible in the "starred" groups 3, 28, and 30, figure 8b. Optimization for the refined 225-node model proved to be more difficult. Although the corner node displacement near criticality is reduced to only 60%, all designs produced by stages 3 through 15 oscillated in stress infeasibility from a high of ∿120% to a low of 18.5% at the 15th stage. The move limit used was 100%. Further iteration stages with 10% move limit did not result in reducing the infeasible stresses. This indicates that the infeasibility is more likely to be due to errors in the refined model stress calculations rather than being due to errors in generation of the approximate dual optimization problem. In such cases, it may be desirable to use D.V. values of the least infeasible design after scaling by the infeasibility. In figure 8b, the quantities given in parentheses are the thicknesses produced by the 15th stage (refined model) after scaling by $\sqrt{1.185}$. The corresponding weight is 2.81 lb.
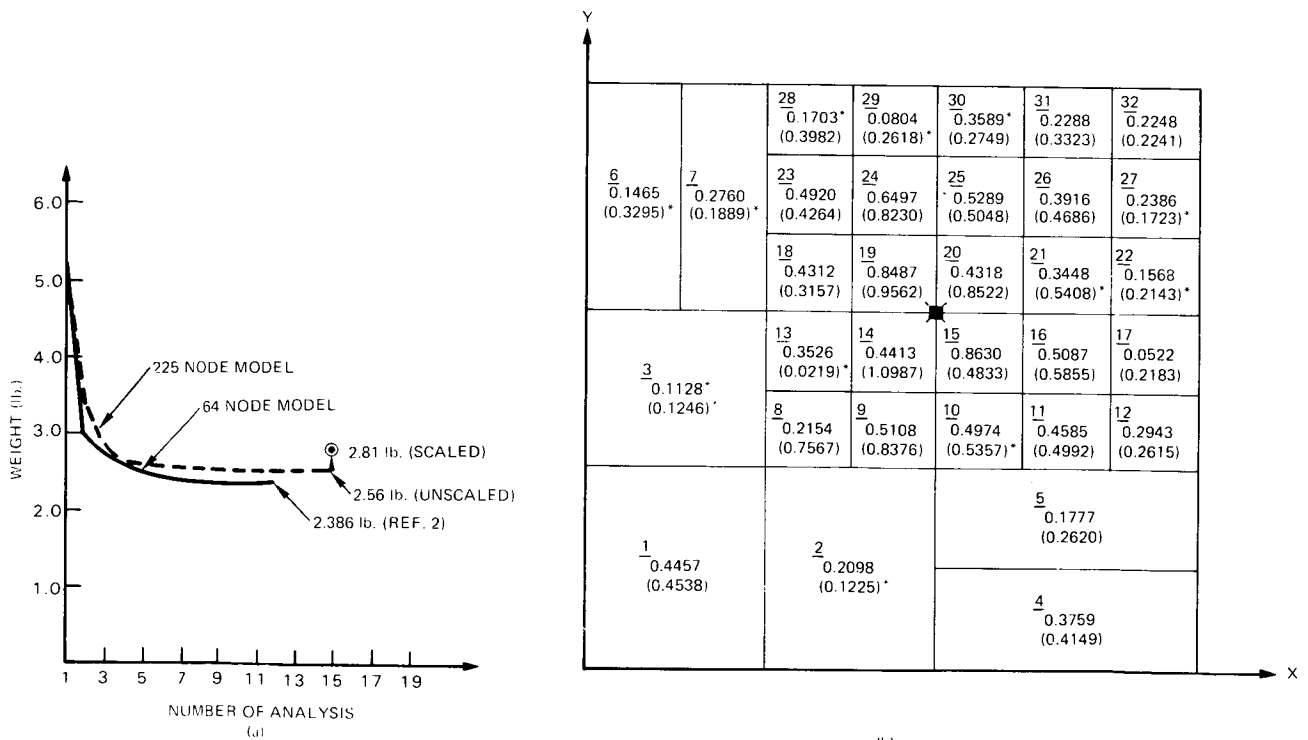


Figure 8

# EXPERIMENT 4

## ANTENNA STRUCTURE

The optimization of the antenna structure of figure 9 has been addressed in refs. 2 and 4. However, attention is focused here on exploring design model refinement in an interactive environment. The optimization begins with a 60-D.V. model, then continues with a 90-D.V. model and finally a 125-D.V. model. All three models consist of 340 nodes connected by 1149 axial members for the symmetric half of the antenna under symmetric wind loading of ref. 2. The structures consist of radial rib trusses R1, R2, ..., R4 and interconnecting hoop trusses C0, C1, ..., C9. The design constraints are: 33 displacement constraints limiting the Z-deformation at the outer circumference C9 to ±1.0 in., 18 slope constraints along the rib truss coinciding with the X-axis to limit the slope in the XZ plane to ±.0075, stress constraints on all members (not to exceed ±25,000. psi), and minimum gage = 0.2 in.$^2$ on the area of all D.V. groups.



Figure 9

Several strategies may be used for a systematic D.V. model refinement of a complex problem. For example, one may concentrate on refining only those D.V. with values larger than a certain threshold; i.e., where weight reduction has the highest potential. Alternatively, one may consider refining all D.V. that are near critical with respect to either all behavior and side constraints or only a selected set of these constraints. Of course, any strategy used may have to include other problem-peculiar possibilities, and should be tempered with practical manufacturing varia-bility limitations. In the present antenna example, refinement from the 60-D.V. model to the 90-D.V. model is achieved by breaking down all D.V. not at the minimum gage while keeping the top and bottom members identical. The rib horizontals are excepted. Further refinement from the 90-D.V. model to the 125-D.V. model is accom-plished by breaking the linking between the top and bottom members. Table 1 gives the D.V. values resulting from the three successive optimizations. As can be seen, the refinements allowed for a redistribution of internal loads, and consequently for redistribution of the structural weight. This is also evident from figure 10a which shows that the total weight is reduced from 9250. lb. (at the end of the 60-D.V. opti-mization) to 6614. lb. (at the end of the 125-D.V. optimization). In figure 10b, the cumulative optimization cost is displayed.



Figure 10

## TABLE 1
## OPTIMAL CROSS SECTIONAL AREAS FOR ANTENNA

### Column 1

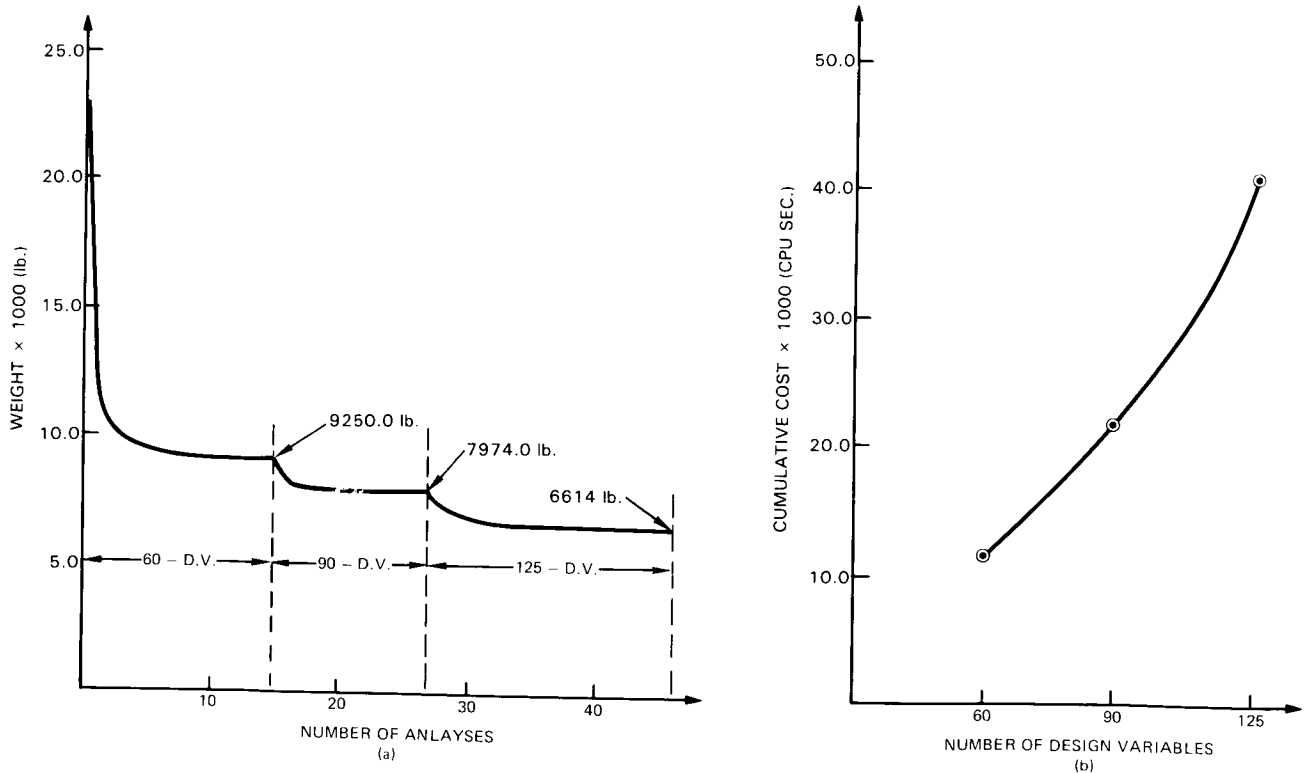| Designation | 60 D.V. | 90 D.V. | 125 D.V. |
|---|---|---|---|
| **Rib Horizontal Type 1** | | | |
| C0-C4 | .200 | .200 | .200 |
| | | | .200 |
| C4-C5 | .636 | .452 | .238 |
| | | | .270 |
| C5-C6 | .552 | .476 | .384 |
| | | | .200 |
| C6-C7 | .774 | .652 | .200 |
| | | | .490 |
| C7-C8 | .542 | .447 | .327 |
| | | | .409 |
| C8-C9 | .396 | .338 | .469 |
| | | | .200 |
| **Rib Horizontals Type 2** | | | |
| C6-C7 | .483 | .483 | .483 |
| C7-C8 | .486 | .485 | .483 |
| C8-C9 | .514 | .500 | .536 |
| **Rib Horizontals Type 3** | | | |
| C3-C4 | .495 | .387 | .200 |
| | | | .200 |
| C4-C5 | .852 | .582 | .200 |
| | | | .240 |
| C5-C6 | .664 | .676 | .325 |
| | | | .231 |
| C6-C7 | .983 | .825 | .204 |
| | | | .863 |
| C7-C8 | .753 | .637 | .515 |
| | | | .484 |
| C8-C9 | .468 | .430 | .560 |
| | | | .200 |
| **Rib Horizontals Type 4** | | | |
| C0-C4 | .532 | .213 | 1.761 |
| | | | .200 |
| | | .389 | 1.892 |
| | | | .200 |
| | | .452 | 1.934 |
| | | | .200 |
| | | .771 | 2.117 |
| | | | .200 |
| C4-C5 | 2.352 | 3.221 | .672 |
| | | | 3.674 |
| C5-C6 | 1.245 | 1.665 | .253 |
| | | | 1.501 |
| C6-C7 | 1.321 | 1.353 | .200 |
| | | | 1.440 |

### Column 2

| Designation | 60 D.V. | 90 D.V. | 125 D.V. |
|---|---|---|---|
| **Rib Horizontals Type 4 (Cont'd)** | | | |
| C7-C8 | .958 | .926 | .534 |
| | | | .823 |
| C8-C9 | .519 | .495 | .567 |
| | | | .200 |
| **Horizontal Diagonals** | | | |
| C3-C4 | .623 | .495 | .200 |
| | | | .200 |
| C5-C6 | .410 | .534 | .359 |
| **Rib Diagonals** | | | |
| C0-C1 | .200 | .200 | .200 |
| | | .200 | .200 |
| C1-C2 | .200 | .200 | .200 |
| | | .252 | .200 |
| C2-C3 | .300 | .200 | .200 |
| | | .498 | .200 |
| C3-C4 | .252 | .200 | .200 |
| | | .200 | .200 |
| | | .548 | .200 |
| C4-C5 | 1.142 | .200 | .377 |
| | | .200 | .200 |
| | | 2.887 | 3.292 |
| C5-C6 | 1.817 | .641 | .859 |
| | | 1.207 | .973 |
| | | 3.473 | 2.735 |
| C6-C7 | .200 | .200 | .200 |
| | | .200 | .200 |
| | | .200 | .200 |
| C7-C8 | .367 | .200 | .200 |
| | | .259 | .330 |
| | | .649 | .609 |
| C8-C9 | .200 | .200 | .200 |
| | | .200 | .200 |
| | | .200 | .200 |
| **Verticals** | | | |
| C0 | .200 | .200 | .200 |
| C1 | .200 | .200 | .200 |
| C2 | .200 | .200 | .200 |
| C3 | .200 | .200 | .200 |
| C4 (R1) | 2.575 | .200 | .200 |
| (R3) | | .200 | .200 |
| (R4) | | 4.112 | 3.578 |
| C5 (R1) | 2.146 | .445 | .354 |
| (R3) | | 1.344 | 1.087 |
| (R4) | | 5.200 | 4.836 |

### Column 3

| Designation | 60 D.V. | 90 D.V. | 125 D.V. |
|---|---|---|---|
| **Verticals (Cont'd)** | | | |
| C6 | .200 | .200 | .200 |
| C7 (R1) | .350 | .200 | .200 |
| (R3) | | .246 | .275 |
| (R4) | | .486 | .432 |
| C8 | .200 | .200 | .200 |
| C9 | .200 | .200 | .200 |
| **Hoop Horizontals** | | | |
| C1 | .200 | .200 | .200 |
| | | | .200 |
| C2 | .200 | .200 | .200 |
| | | | .200 |
| | | .200 | .219 |
| | | | .200 |
| C3 | .500 | .583 | .200 |
| | | | .306 |
| | | .200 | .200 |
| | | | .200 |
| C4 | .507 | .337 | .200 |
| | | | .200 |
| C5 | .200 | .284 | .200 |
| | | | .434 |
| C6 | 3.323 | 2.163 | .200 |
| | | | .334 |
| | | 3.296 | 4.346 |
| | | | 4.417 |
| C7 | .200 | .200 | .200 |
| | | | .200 |
| C8 | .235 | .200 | .481 |
| | | | .200 |
| C9 | 4.348 | 4.306 | 5.268 |
| | | | 5.348 |
| | | 4.047 | .490 |
| | | | .280 |
| **Hoop Diagonals** | | | |
| C1 | .200 | .200 | .200 |
| C2 | .200 | .200 | .200 |
| C3 | .200 | .200 | .200 |
| C4 | 1.256 | .200 | .200 |
| | | .808 | .300 |
| C5 | .326 | .200 | .200 |
| | | .977 | 1.275 |
| C6 | .200 | .200 | .200 |
| C7 | .200 | .200 | .200 |
| C8 | .200 | .200 | .200 |
| C9 | .289 | .283 | .200 |

# CONCLUSIONS

In the optimization of complex structures, selection of the most suitable analysis and design models is frequently not obvious. Accuracy and cost are always limiting and competing factors. Further, design optimization usually is not a one-time process, but is one that evolves with evolution of the design details.

In the preceding pages, results of numerical experiments were discussed to show trends that may be employed in devising cost effective optimization procedures consistent with an evolutionary optimization philosophy, whether it is carried out in the context of a man-machine interactive environment or in the context of an automated expert system. Specifically, the results deal with (1) optimum weight accuracy and associated cost advantages of starting the optimization process with the practically most crude D.V. and D.O.F. models, then simultaneously refining both models in subsequent optimizations; (2) effect of model imbalance on the resulting optimal weight; (3) design infeasibility as a typical difficulty in large problems optimization, and how it may be dealt with; (4) a criterion for selection of successive D.V. model refinements.

# ACKNOWLEDGEMENT

# REFERENCES

1. Fleury, C., and Schmit, L.A., Jr., "Dual Methods and Approximation Concepts in Structural Synthesis", NASA CR-3226, 1980.

2. Fleury, C., Ramanathan, R. K., Salama, M., and Schmit, L.A., Jr., "ACCESS Computer Program for the Synthesis of Large Structural Systems", Chapter 26, New Directions in Optimum Structural Design, Edit., Atrek, E., Gallagher, R. H., Ragsdell, K.M., and Zienkiewicz, O. C., John Wiley & Sons, 1984.

3. Prasad, B., and Haftka, R. T., "Optimal Structural Design with Plate Finite Elements", Proceedings of the ASCE, Journal of the Structural Div., ST 11, November 1979.

4. Levy, R., and Parzynski, W., "Optimality Criteria Solution Strategies in Multiple Constraint Design Optimization", Paper No. 81-0551 presented at the AIAA/ASME/ASCE/AHS 22nd Conf., Seattle, Washington, May 1981.

342

# MULTIDISCIPLINARY SYSTEMS OPTIMIZATION BY LINEAR DECOMPOSITION

J. Sobieski
NASA Langley Research Center
Hampton, Virginia

In a typical design process major decisions are made sequentially. The illustrated example is for an aircraft design in which the aerodynamic shape is usually decided first, then the airframe is sized for strength and so forth. An analogous sequence could be laid out for any other major industrial product, for instance, a ship. The loops in the discipline boxes symbolize iterative design improvements carried out within the confines of a single engineering discipline, or subsystem. The loops spanning several boxes depict multidisciplinary design improvement iterations. Omitted for graphical simplicity is parallelism of the disciplinary subtasks. The parallelism is important in order to develop a broad workfront necessary to shorten the design time.

If all the intradisciplinary and interdisciplinary iterations were carried out to convergence, the process could yield a numerically optimal design. However, it usually stops short of that because of time and money limitations. This is especially true for the interdisciplinary iterations.

# SEQUENTIAL DECISION-MAKING IN DESIGN PROCESS
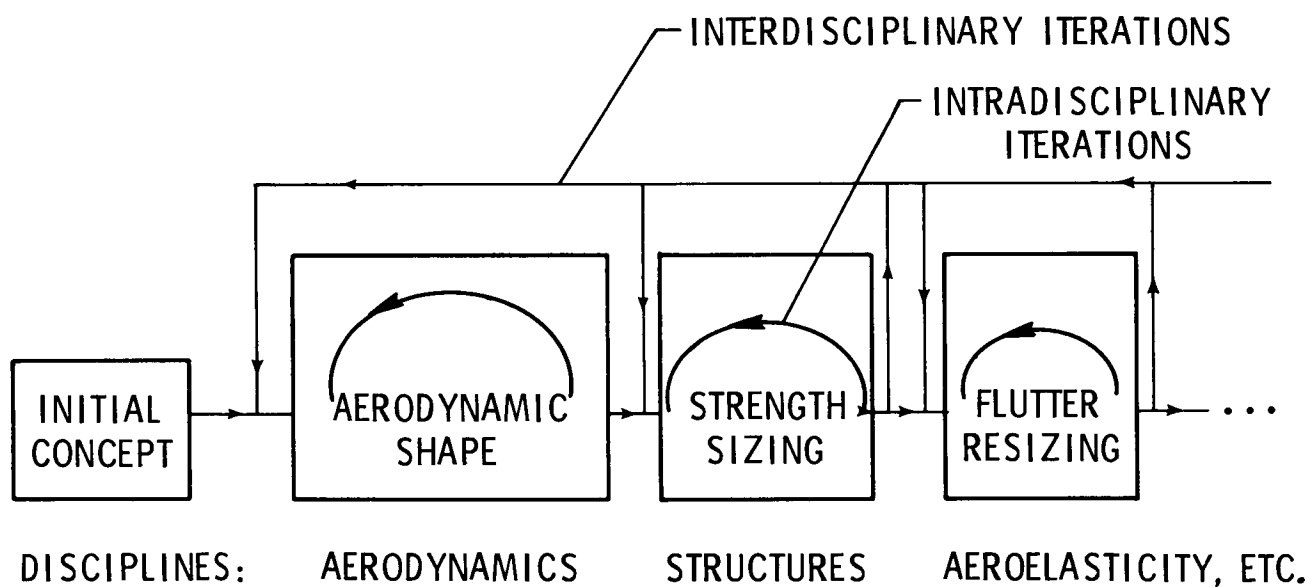
Sequential decision making leads to a paradoxical disparity between the volume of information about the object of the design and the design freedom measured by the number of design variables and options still available to the designers. The former ascends with time because of the analyses and experiments performed, while the latter declines because of casting the decisions "in concrete." The paradox is that we are gaining information but losing freedom to act on it.

## PARADOX OF THE CONVENTIONAL SEQUENTIAL DECISION MAKING IN DESIGN



KNOWLEDGE ABOUT THE OBJECT OF DESIGN

DESIGN FREEDOM

TIME INTO DESIGN PROCESS
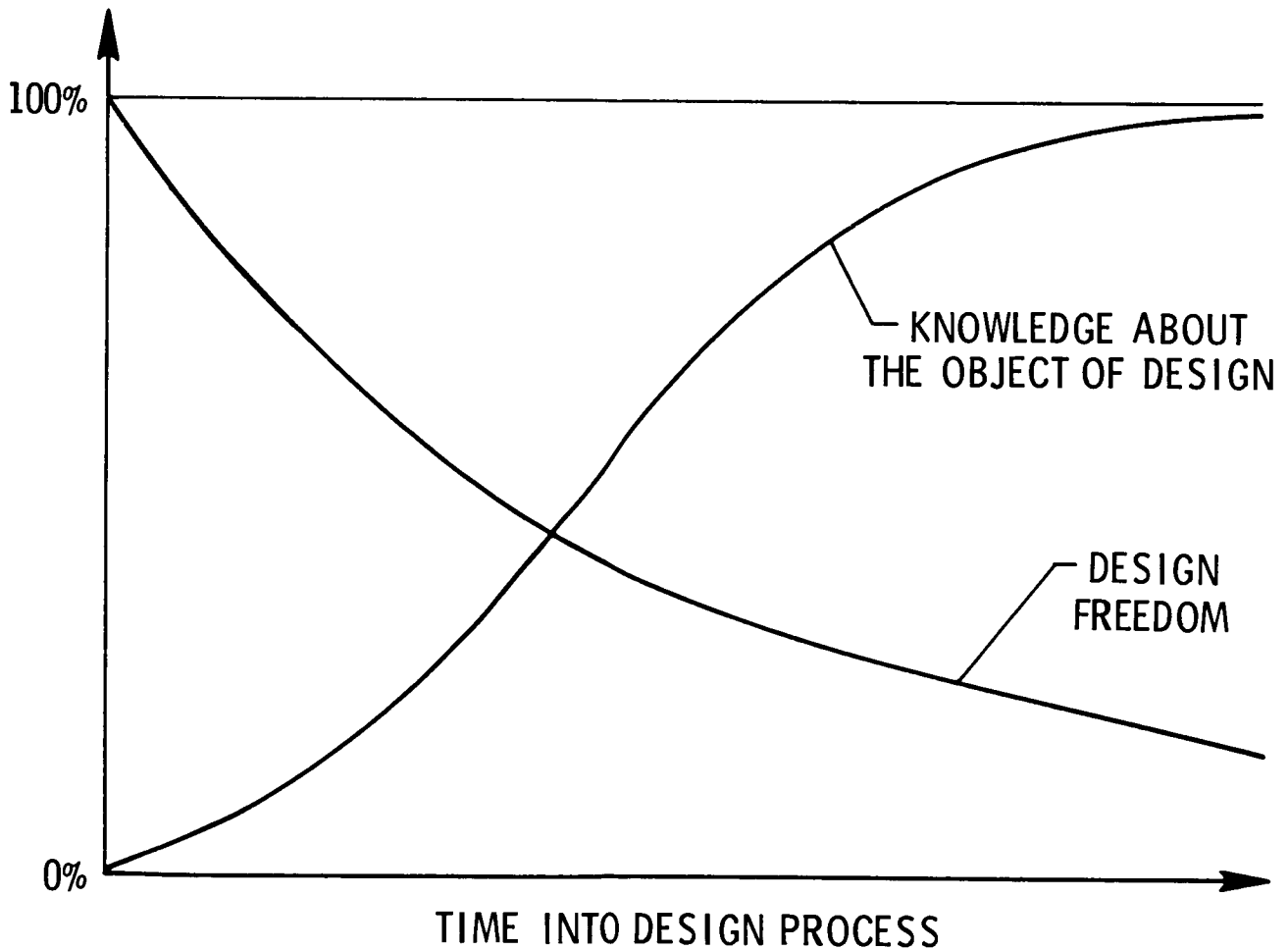
A simple example will reveal that the paradox shown in the previous chart leads to a suboptimal design. For the example, we will look into an aircraft design process at the time when wing planform and structural sizing have already been accomplished to produce a combination of two design variables, the aspect ratio and structural weight, that maximizes a measure of the aircraft performance without violating the constraints. Simplifying the example as much as possible, we can consider a design space formed by the aspect ratio and the structural weight that, we assume, has already been minimized. In that design space, shown in this chart, the aircraft performance can be depicted by a set of contour lines, each line corresponding to a constant value of the performance. Superimposed on the contour lines are the constraint curves, C1 and C2. Each constraint curve divides the design space into the feasible (constraint satisfied ) and infeasible (constraint violated) subspaces (domains). The cross-hatching marks the infeasible side. It is not important for the purposes of this discussion which particular aspect of the aircraft performance was chosen as a measure of goodness (objective function) and what constraints were taken into account in plotting the set of curves, P, C1, and C2. The aircraft range for a given takeoff gross weight and payload and the wing static strength may be thought of as respective examples for P and C2. Inspection of the graphs shows that the design which maximizes P without violating C1 and C2 is at point O1.

## CONSTRAINED MINIMUM
## FOR TWO CONSTRAINTS AND TWO DESIGN VARIABLES



WING MINIMUM STRUCTURAL WEIGHT, $W_{min}$

ASPECT RATIO, $\mathbb{R}$
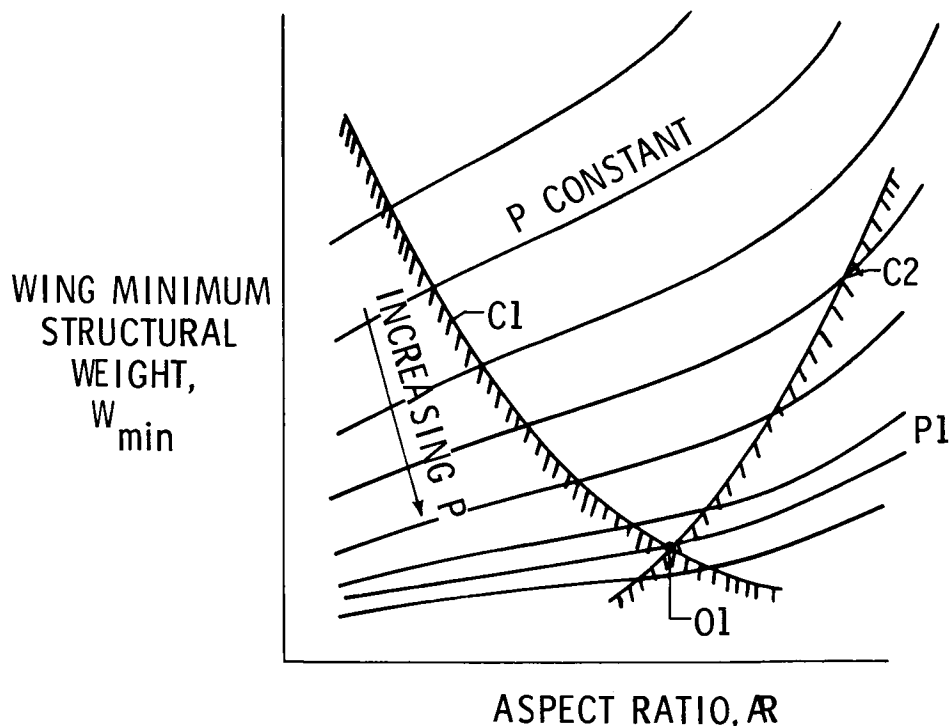
Suppose now that when a flutter speed is subsequently calculated, the design O1 turns out to have too low a flutter speed - in this chart it is shown to be on the infeasible side of the flutter constraint plotted as C3. The design has to be modified to have its flutter speed raised.  If at this point in the design process the configuration - the aspect ratio - is frozen, the increase of the flutter speed can be achieved by stiffening the wing structure at the price of a weight penalty by moving from O1 to O2 at a constant aspect ratio. The weight penalty reduces the performance from P1 to P2.  If the configuration were not frozen, a new optimal design could be located at O3, whose performance P3, although smaller than P1, exceeds P2 (P2 < P3 < P1).  The difference P3 - P2 is a performance penalty for the sequential freezing out of the design options in a sequential design process.  We can say that design O2 is suboptimal relative to the design O3.  Another look at this and the preceding chart, and a little reflection, will show that although the magnitude of the performance penalty, P3 - P2, depends on the shape of the functions involved (P, C1, C2, C3), its existence does not.  Consequently, the example reveals that suboptimal results can be expected in a sequential design process in which each additional stage restricts the number of design variables while bringing in new constraint violations that must be removed.

# A NEW CONSTRAINT ADDED



WING MINIMUM STRUCTURAL WEIGHT, $W_{min}$

ASPECT RATIO, $R$
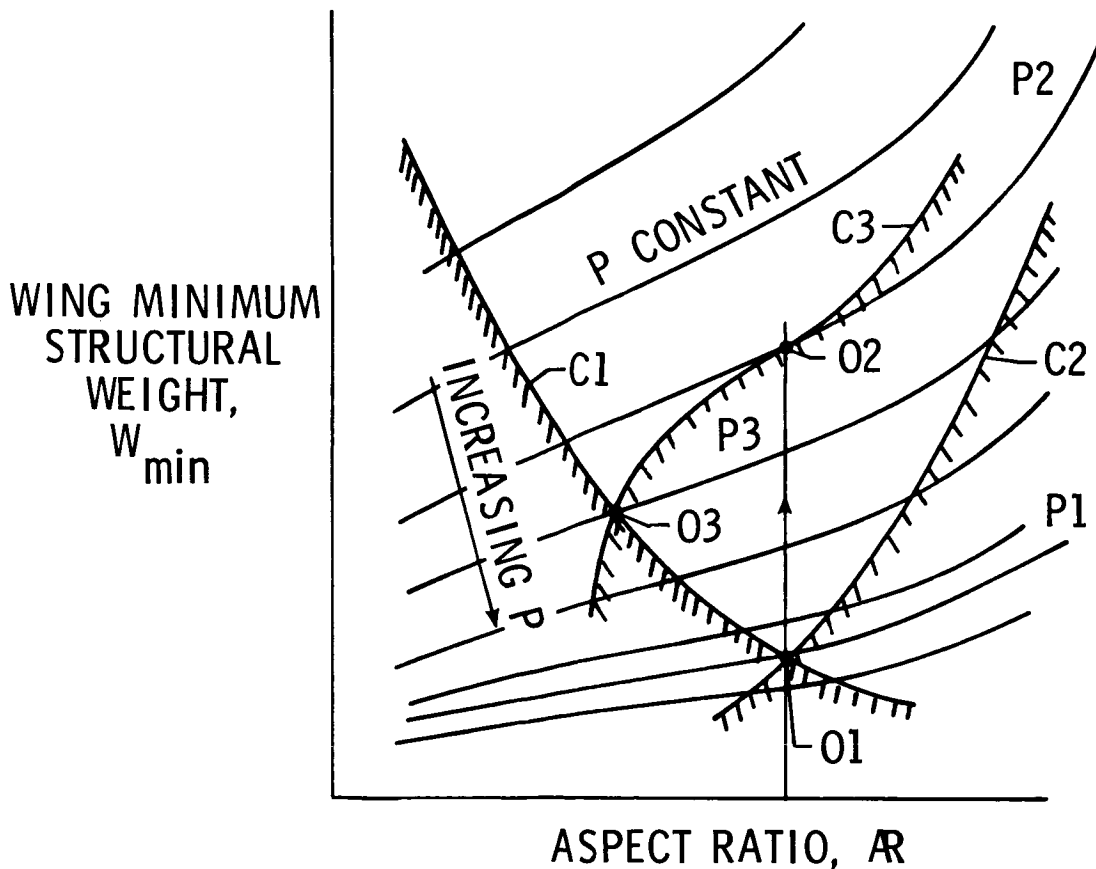
To demonstrate an alternative based on a system approach, reenter the example at the point where the flutter deficiency of the design, labeled 01 in the preceding chart, has been found. The essence of the system approach is decomposition of a large problem into several smaller ones without losing the coupling. Therefore, we recognize in this case that two engineers, or engineering groups, must fix the flutter problem with the least penalty to the performance, P, by cooperating and yet each doing a separate subtask. In this chart the individuals, or groups, are labeled C - for configuration, including aerodynamics and performance, and S - for structures.

The subtask of correcting the flutter problem with a minimum weight penalty $\Delta W_{min}$ is carried out by S for a particular aspect ratio set constant, but only temporarily, by C, and for aerodynamic analysis results (e.g., pressure distribution) and their sensitivity to aspect ratio - all supplied by C. The result produced by S is a flutter-free design at a minimum weight penalty, along with the sensitivity of that design to aspect ratio. That sensitivity is quantified in the form of derivatives of the weight penalty and cross-sectional dimensions with respect to the aspect ratio.

## FINDING NEW CONSTRAINED MINIMUM
## BY ALTERNATING BETWEEN TWO ENGINEERING DISCIPLINES

CONFIGURATION GROUP

C    CHANGE $R$ TO GAIN MAXIMUM PERFORMANCE, $P_{max}$

$R,$   $C_p$(LOCATION),   $\dfrac{\partial C_p}{\partial R}$

$\Delta W_{min},\ \partial(\Delta W_{min})/\partial R$

S

STRUCTURES GROUP

RESIZE CROSS-SECTIONS TO RAISE FLUTTER SPEED WITH A MINIMUM WEIGHT PENALTY, $\Delta W_{min}$
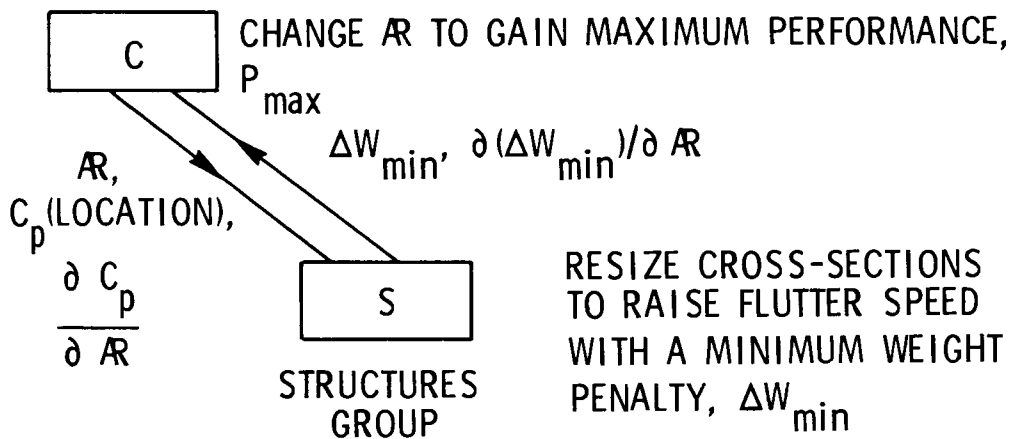
Completion of the above task moves the design from 01 to 02 in this chart, exactly as in the previous discussion. However, group C will now recover a part of the performance penalty by changing the aspect ratio and the weight penalty simultaneously. In this operation, the weight penalty is not an independent variable but is tied to the aspect ratio variation by the sensitivity derivative which tells how much the weight penalty must change per unit of aspect ratio variation to keep the flutter constraint satisfied. Such dependence of weight penalty on aspect ratio is only a linear approximation of a true nonlinear relation and can be depicted by the tangent to C3 at 02 shown in this chart. The configuration improvement produced by C calls now for a move along that tangent toward the increasing performance; that is, toward 03. The move should stop when the tangent veers off too far from C3 in order to let group S repeat its subtask to recover from the linearization error by regenerating the minimum weight penalty and its sensitivity derivative at the new value of the aspect ratio. Thus, by alternating subtasks performed by C and S we can improve the design by moving toward the theoretical optimum at 03 in a staircase fashion: 02 to 02A, to 02B, to 02C, and so on, as long as we see that the performance improvement is worth the effort.

# A PATH TOWARD NEW CONSTRAINED MINIMUM



WING MINIMUM STRUCTURAL WEIGHT, $W_{min}$

ASPECT RATIO, $AR$
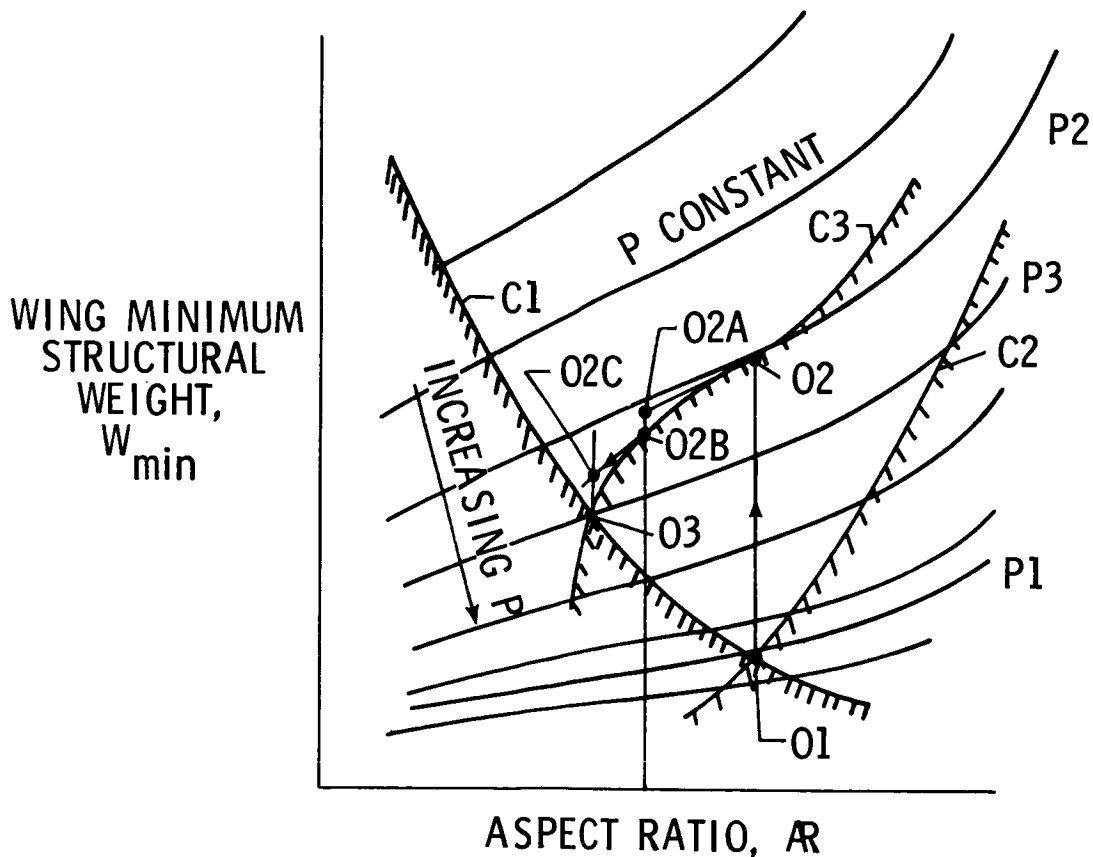
Having introduced the idea of decomposition by means of a simple example we will now generalize the four objectives shown in the chart as guidelines. The first three are self evident. The last one deals with the disparity between the large volume of information that is being processed within a subtask and a relatively small volume of information that couples the subtask (subsystem) to other subtasks (subsystems). For example, contrast the mass of data being manipulated in a finite element analysis of an airframe with the input data of loads, mechanical properties, and geometry, and with the structural weight and critical constraint data which is all that is fed back to the aircraft performance analysis. The decomposition scheme should exploit that disparity. Lack of such disparity indicates that either the decomposition scheme is improper or the problem is not decomposable.

# DECOMPOSITION OBJECTIVES

- BREAK LARGE TASK INTO A NUMBER OF SMALLER ONES

- PRESERVE THE COUPLINGS AMONG THE SUBTASKS

- EXPLOIT PARALLELISM TO DEVELOP A BROAD WORKFRONT OF PEOPLE AND COMPUTERS

- EXPLOIT THE DIFFERENCE OF VOLUME BETWEEN A RELATIVELY LARGE AMOUNT OF INFORMATION PROCESSED INTERNALLY IN A SUBTASK AND A RELATIVELY SMALL VOLUME OF THE COUPLING INFORMATION

There are several decomposition procedures in the literature (ref. 1). However, a literature survey failed to reveal a method that would be capable of accounting for the couplings among the system and subsystems without having to reoptimize the subsystems for every variation of the parent system design variables and that would apply to nonlinear programing problems. Since such repeated reoptimizations would be cost prohibitive in most large-scale engineering applications, a new approach that accounts for the system-subsystem couplings without the repetitive subsystem reoptimizations has been developed at Langley Research Center and is now at a stage of testing and verification. The approach is called "a linear decomposition" for reasons that will become apparent soon.

# SEVERAL WAYS TO HANDLE THE COUPLINGS IN A DECOMPOSED SYSTEM

- BODY OF LITERATURE

- THE PROPOSED APPROACH: A LINEAR DECOMPOSITION

For generality, the chart shows a generic system decomposed into subsystems that form a hierarchical, three-level tree. If the system were a structure, the top level would represent the assembled structure, each subsystem at the middle level would correspond to a substructure, and the bottom level subsystems would simulate individual structural components (e.g., stiffened panels. Thus, three levels is the minimum we need to have each level qualitatively different for generality of the discussion. We assume that the system has been initialized so that physical characteristics are completely defined at each level. It is not necessary for the initialized system to be feasible. The analysis proceeds from top to bottom so that output from analysis of a parent subsystem becomes input for analysis of the subordinated subsystems. For an example, consider a structure assembled of substructures and loaded by forces applied at the substructure boundary nodes. The substructure boundary forces from the assembled structure analysis are fed into the substructure analysis as loads, and the internal forces from substructure analysis enter into the individual structural component analysis.

In many engineering applications, the decomposition must account for the fact that inputs to analysis of a given subsystem may be coming not only from its parent but from any other subsystem at the same or even a different level, including inputs from the subordinated subsystems to their parent. An example of the latter can be drawn from the substructuring analysis in the case where the loads applied to a substructure interior nodes are reduced to the loads applied at the substructure boundary nodes, by performing analysis at the substructure level before commencing the assembled structure analysis. In other words, a system decomposition may lead to a network rather than the "top-down" graph shown in the chart. However, we will limit this discussion to the case depicted in the chart in order to keep it as simple as possible for a clear introduction of the basic approach. Extension of the approach necessary to handle the network systems is presented in ref. 2. It is important that analyses at each level include sensitivity analysis to produce derivatives of the output quantities with respect to the input quantities. These derivatives measure sensitivity of behavior (response). Obviously, if there are several subsystems at a given level, they can be analyzed concurrently.

**ANALYSIS**
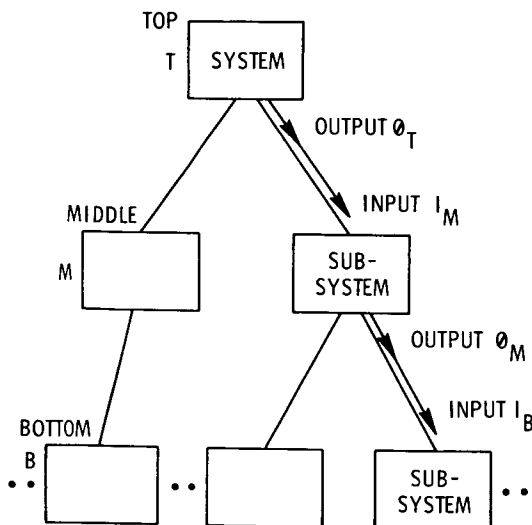


- INITIALIZATION
- TOP-DOWN ANALYSIS
    EACH SUBSYSTEM RECEIVES
    INPUTS FROM ITS PARENT,
    UNDERGOES ANALYSIS AND
    SENDS OUTPUT TO SUB-
    SYSTEMS BELOW

352

This chart introduces a cumulative constraint that will be needed in further discussion. The cumulative constraint is a single number that measures the degree of satisfaction, or violation, of an entire set of constraints. There are several ways to formulate the cumulative constraint as a function of the constraints in the set, for instance, the well known quadratic exterior penalty function is a cumulative constraint. The particular formulation adopted here is a function shown by the equation below and referred to as the Kresselmeier-Steinhauser function. The function is continuous and differentiable, in contrast to the envelope of the constraint functions, which is slope discontinuous at the constraint function intersections, and, as seen in the graph, follows the constraint envelope at a distance that is user-controlled by the factor $\rho$. Increase of the factor draws the function closer to the envelope. The factor ought to be set so that the cumulative constraint function does not loose numerical differentiability by forming sharp "knees" at the constraint intersections.

## CUMULATIVE CONSTRAINT

- A SINGLE NUMBER MEASURE OF THE DEGREE OF SATISFACTION, OR VIOLATION, FOR A SET OF CONSTRAINTS

$$\Omega = f(g_i) \quad i = 1 \longrightarrow m; \quad g_i = \frac{DEMAND}{CAPACITY} - 1 \le 0$$

- AN APPROXIMATE ENVELOPE FUNCTION



$\Omega$; PARTICULARLY THE KRESSELMEIER-STEINHAUSER FUNCTION

$$\Omega = \frac{1}{\rho} \ LN \left( \sum_i \left( e^{\rho g_i} \right) \right)$$

$\rho$ = USER CONTROLLED FACTOR
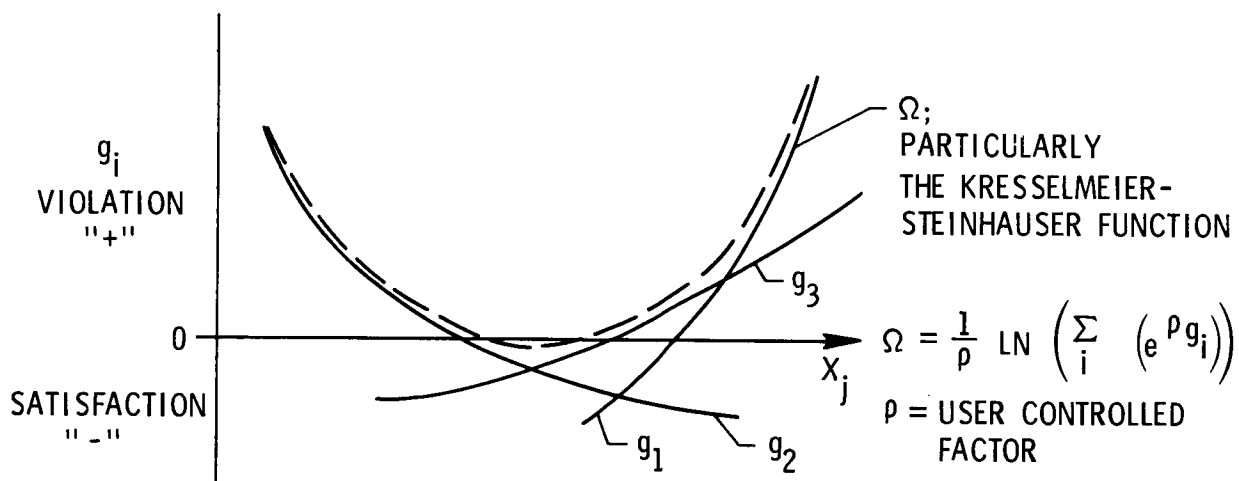
Having completed the analysis and introduced the cumulative constraint, we now begin the optimization which will proceed from the bottom up. Each subsytem optimization at the bottom level is characterized as follows:

1. design variables: physical quantities local to the subsystem, e.g., detailed cross-sectional dimensions of a panel

2. objective function: the cumulative constraint of the subsystem constraints such as local buckling, stress, etc

3. inequality constraints: upper and lower limits on the design variables

4. constant parameters: inputs received from the parent subsystem

5. equality constraints: these constraints may be required in order to preserve the constancy of the parameters (for example, if a parameter is a total cross-sectional area of a panel, an equality constraint on the detailed cross-sectional dimension variables is needed)

The use of a cumulative constraint as the subsystem objective is a logical choice because it is a non-dimensional quantity and therefore comparable among the subsystems regardless of their physical nature, which may vary from one to another. The subsystem optimization is followed by sensitivity analysis of the minimum of the objective with respect to the subsystem input quantities (equal to the output from the parent subsystem). This analysis is called optimum sensitivity analysis to distinguish it from the behavior sensitivity analysis and is carried out not by finite difference but by a special algorithm described in ref. 3. Thus, the results from each subsystem optimization are the minimum of the cumulative constraint and its sensitivity to the output from the parent subsystem. These results are now carried upward to the parent subsystem. If there are several subsystems at a given level, their optimizations can be executed concurrently.

## OPTIMIZATION: BOTTOM LEVEL
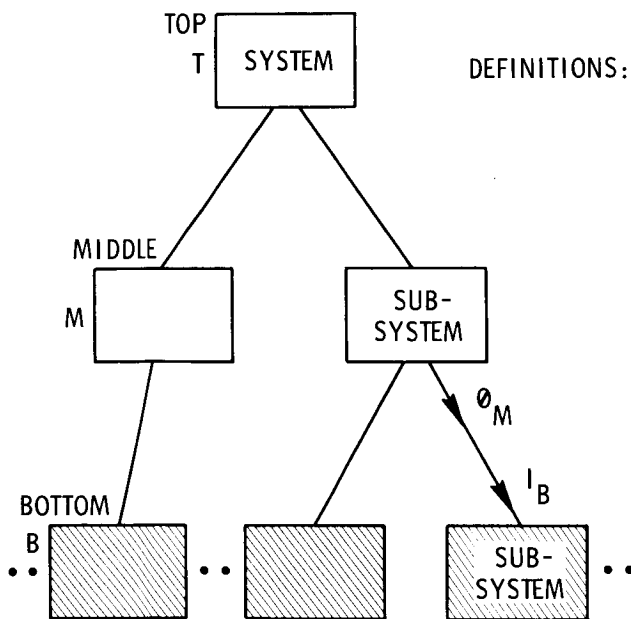


DEFINITIONS: DESIGN VARIABLES $= X_B$

INPUT $= I_B$ RECEIVED FROM ABOVE

$$I_B \equiv \emptyset_M$$

OBJECTIVE FUNCTION:
CUMULATIVE CONSTRAINT
$$\Omega^B$$

OPTIMIZATION PROBLEM:
$$\underset{\{X_B\}}{\text{MIN}} \; \Omega^B (X_B, \emptyset_M)$$
$$L \leq X_B \leq U$$

OPTIMUM SENSITIVITY ANALYSIS:
$$\partial \, \Omega^B_{min} / \partial \emptyset_{Mi}$$

Now, moving up one level to the middle level, we perform a subsystem optimization for each subsystem at that level. The optimization is formulated as follows:

(1) Design variables: physical quantities local to the subsystem, e.g., membrane stiffness of the wing box at several locations over the wing

(2) Objective function: cumulative constraint for a set of constraints that includes the constraints intrinsic to the subsystem itself (e.g., limit on the wing tip deflection) and the minimum values of the cumulative constraints transmitted from the subordinated lower level subsystems (These minimum values are estimated by linear extrapolation (see equation) as a function of the middle level subsystem design variables by means of the optimum sensitivity derivatives taken with respect to the subsystem output quantities which, in turn, are governed by the subsystem design variables. This linear extrapolation eliminates the need to reoptimize the subordinated subsystems for each design variable variation introduced in the parent subsystem and gives the method its name of the linear decomposition.)

(3) Constant parameters

(4) Inequality constraints

(5) Equality constraints are analogous to those defined for the bottom level

The results are a minimum of the cumulative constraint and its derivatives with respect to the system output. They are now carried to the top level.

**OPTIMIZATION: MIDDLE LEVEL**

DEFINITIONS: DESIGN VARIABLES $= X_M$

INPUT $= I_M$ RECEIVED FROM ABOVE

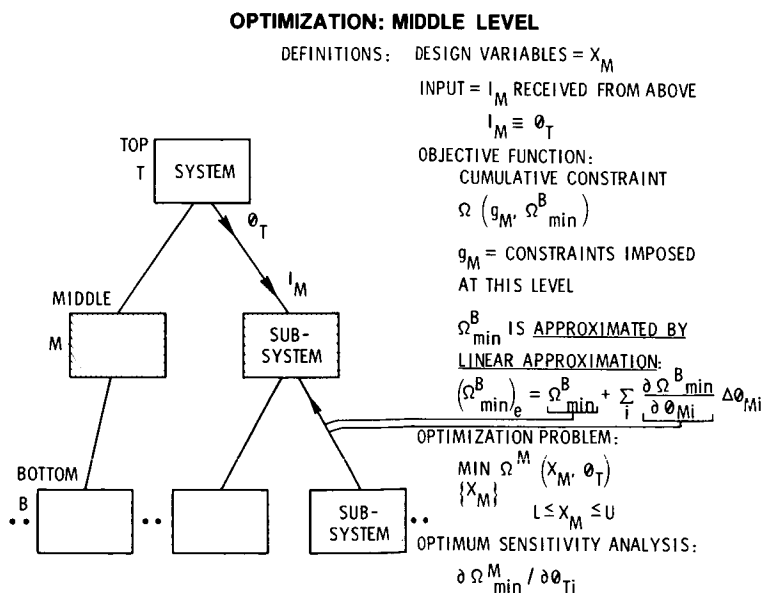$I_M \equiv \Theta_T$

OBJECTIVE FUNCTION:
CUMULATIVE CONSTRAINT

$\Omega\left(g_M, \Omega^B_{min}\right)$

$g_M =$ CONSTRAINTS IMPOSED AT THIS LEVEL

$\Omega^B_{min}$ IS APPROXIMATED BY LINEAR APPROXIMATION:

$\left(\Omega^B_{min}\right)_e = \Omega^B_{min} + \sum_i \frac{\partial \Omega^B_{min}}{\partial \Theta_{Mi}} \Delta\Theta_{Mi}$

OPTIMIZATION PROBLEM:

$\underset{\{X_M\}}{MIN}\ \Omega^M\left(X_M, \Theta_T\right)$

$L \le X_M \le U$

OPTIMUM SENSITIVITY ANALYSIS:

$\partial \Omega^M_{min} / \partial \Theta_{Ti}$



355

Optimization at the top level involves:

1. design variables that govern the entire system, for an aircraft example: configuration geometry, structural weight prescribed for the airframe, etc.

2. objective function as a measure of the system performance, e.g., fuel consumption or Direct Operating Cost

3. inequality constraints on the system performance, e.g., take-off field length, the upper and lower limits on the design variables, and the cumulative constraints from each subsystem linearly extrapolated by means of the optimum sensitivity derivatives (These constraints also include the side constraints and move limits to control the linear extrapolation error.)

Thus, the top level optimization deals with the system performance directly, and has embedded in it the approximation to all the subsystem constraints in the form of the linear extrapolation based on the subsystem optimum sensitivity derivatives. These derivatives quantify the design trade-offs among the subsystem and account for their couplings.

The top-down analysis and the bottom-up optimizations constitute one cycle of the iterative procedure which continues until the extremum of the system objective is found and all the system constraints and the subsystem cumulative constraints are satisfied. For more algorithmic detail, one may consult ref. 2.

## OPTIMIZATION: TOP LEVEL

DEFINITIONS: DESIGN VARIABLES $= X_T$

OBJECTIVE FUNCTION: A MEASURE $F(X_T)$ OF THE SYSTEM PERFORMANCE

CONSTRAINTS:

$g_T =$ SYSTEM PERFORMANCE CONSTRAINTS

$\Omega^M_{min} \leq 0$ FOR EACH M-LEVEL SUBSYSTEM

OPTIMIZATION PROBLEM:

$$\underset{\{X_T\}}{MIN\ F(X_T)}$$

$$g_T \leq 0$$

$$\left(\Omega^M_{min}\right)_e \leq 0$$

$$L \leq X_T \leq U$$

WHERE:

$$\left(\Omega^M_{min}\right)_e = \Omega^M_{min} + \sum_i \frac{\partial \Omega^M_{min}}{\partial \Theta_{Ti}} \Delta\Theta_{Ti}$$



TOP "T" SYSTEM

MIDDLE "M"

SUB-SYSTEM

BOTTOM "B"

SUB-SYSTEM
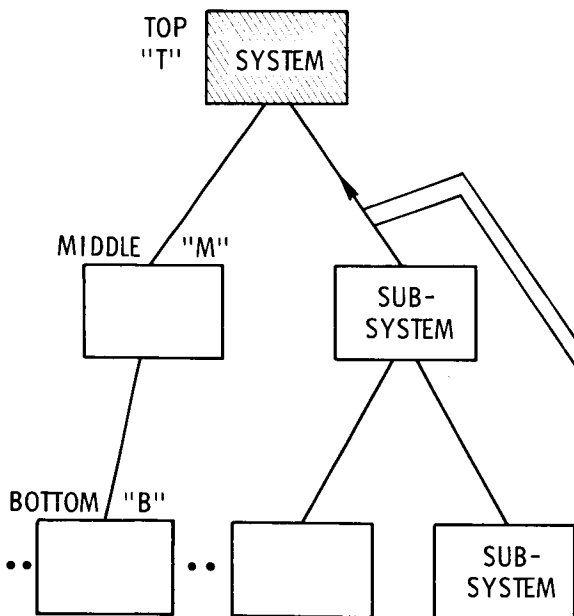
While the procedure described in the previous five charts is generic, the decomposition of the system is problem dependent. It can be done by a common sense inspection and judgment. It can also be done formally by a matrix of the design variables listed along the top and the objective and constraint functions listed vertically. A dot at the row-column intersection means that the variable corresponding to the column appears in the equation corresponding to the row, and a blank means that the variable does not appear in that equation. The three examples show typical patterns.

# MANY WAYS TO DECOMPOSE A SYSTEM

- HEURISTIC: BY EXAMINATION OF THE SYSTEM PHYSICAL MAKE-UP.



- FORMAL: BY INSPECTION OF THE FUNCTIONAL RELATIONS THAT GOVERN THE PROBLEM
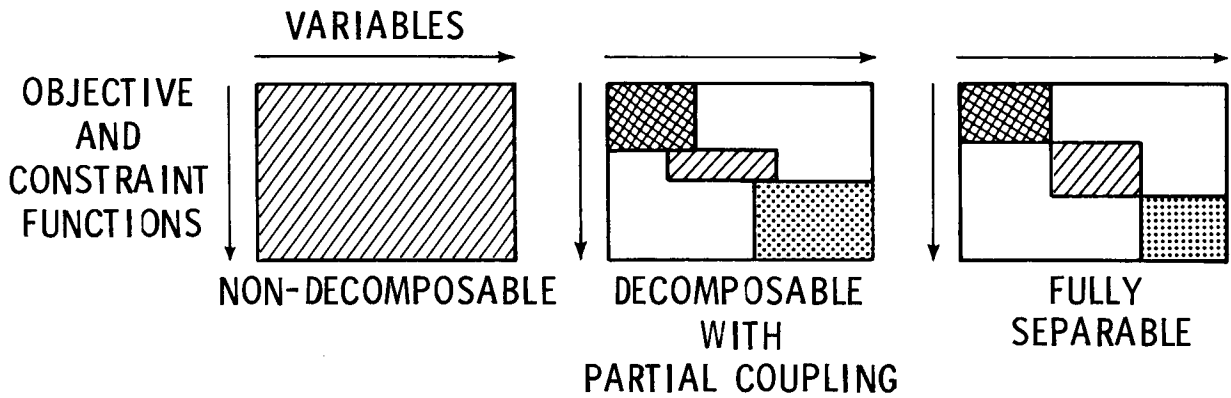
Once the decomposition tree is established, it can be grown with respect to the number of subsystems and the depth and detail of analysis. This adaptability permits maintaining the same overall logic of approach at various stages of design, while changing the modules in that logic - a desirable feature from the standpoint of the process integration.

## DECOMPOSITION ADAPTS TO DESIGN STAGE
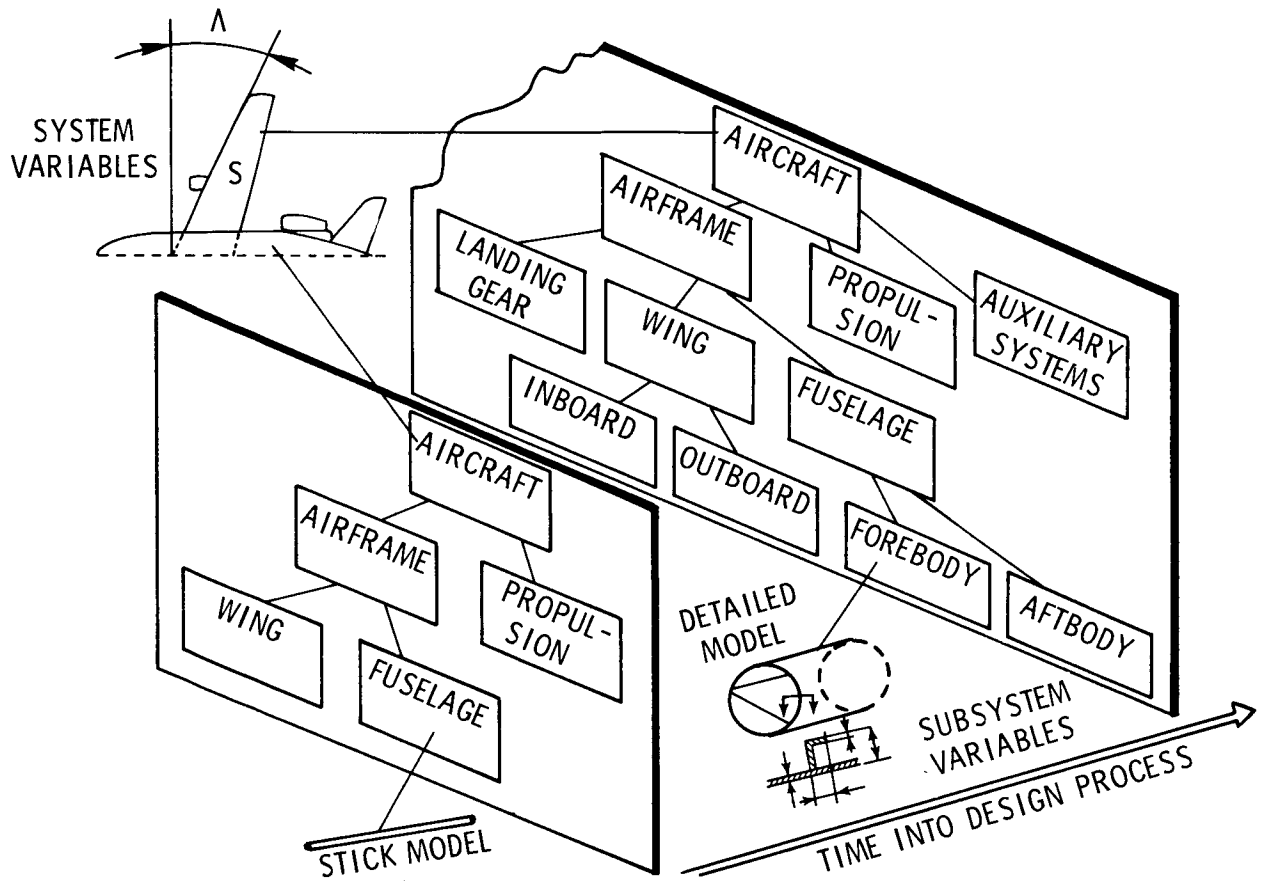
The multilevel procedure described here is still being developed toward a state of maturity required for industrial applications. To achieve that state, research continues to investigate the issues listed below.

# ISSUES TO BE INVESTIGATED

- CONVERGENCE: OVERALL, LOCAL

- COMPUTATIONAL COST

- LATERAL AND REVERSE COUPLINGS

- ACCURACY OF LINEAR EXTRAPOLATIONS BASED ON SENSITIVITY

- SUBTASK SYNCHRONIZATION

- CONSISTENCY OF THE ANALYSIS LEVELS IN VARIOUS SUBTASKS

- JUDGMENTAL DECISIONS, INCLUDING DISCRETE DECISIONS, AND HUMAN CONTROL

The development toward maturity involves a literature survey, numerous tests of several variations of the algorithm using very simple test cases, and a fairly large structural test case. A multidisciplinary test is under way for reconfiguration of a transport aircraft wing treated as a part of an aircraft system and, also, a wing separated from the aircraft. The issues of computational parallelism and synchronization among the subtasks are being explored using a network of microcomputers connected to a central hard disk.

# RESEARCH
# INTO THE MATHEMATICS OF MULTILEVEL DECOMPOSITION

- GOAL: A LEVEL OF MATURITY REQUIRED FOR INDUSTRIAL APPLICATIONS

- LINES OF RESEARCH:

  - SURVEY OF LITERATURE

  - SMALL TEST CASE - A SIMULATOR - TO TEST VARIOUS ALGORITHMS

  - APPLICATION TEST CASES: STRUCTURES
    LOCKHEED PROJECT
    ISOLATED WING CASE
    PARALLEL COMPUTING
    (A NETWORK OF APPLES)

  - GRANT ACTIVITIES TO BE REPORTED IN THIS SESSION

A two-level structural optimization of a framework has been successfully carried out and reported in ref. 4. The decomposition in this case exploits the fact that the end forces acting on each I-beam in the framework can be calculated using A and I for the beams without directly using the beam cross-section design variables. Furthermore, the local constraints in a beam can be calculated using the beam's detailed cross-sectional dimensions and the end forces. Thus, the A's and I's are the system design variables and the detailed dimensions are the subsystem design variables. The beam is optimized by reducing the cumulative constraint to a minimum (maximizing the safety margin). In the process, the beam cross-section is reproportioned while preserving the A and I prescribed for the beam at the system level.

## MULTILEVEL OPTIMIZATION: A FRAMEWORK TEST STRUCTURE (TWO LEVELS)



$M = 20 \times 10^6$ N-cm
$P = 50000$ N

1000 cm
500 cm
1000 cm

ASSEMBLED FRAMEWORK

FIND A's, I's TO MINIMIZE STRUCTURAL WEIGHT SUBJECT TO CONSTRAINTS ON DEFLECTION AND THE BEAM CONSTRAINTS

CUMULATIVE CONTRAINT $\Omega$ AND ITS DERIVATIVES

PARAMETERS: A, I, END FORCES

BEAM

BEAM

BEAM

M  T
N

A - A
NOT TO SCALE

FIND DIMENSIONS OF THE BEAM CROSS-SECTION TO IMPROVE THE CONSTRAINT SATISFACTION AS MUCH AS POSSIBLE WITHIN THE GIVEN PARAMETERS. THE CONSTRAINTS INCLUDE: STRESS, LOCAL BUCKLING, ETC.

The two-level framework structure has been extended to three levels by replacing the I-beams with the box beams made up of stringer-reinforced panels. The panels add the third, bottom level of subsystems. This makes the test more general because it now contains all three level categories: top, middle, and bottom. At the time of this writing the tests are still in progress.

## MULTILEVEL OPTIMIZATION: A FRAMEWORK STRUCTURE (THREE LEVELS)
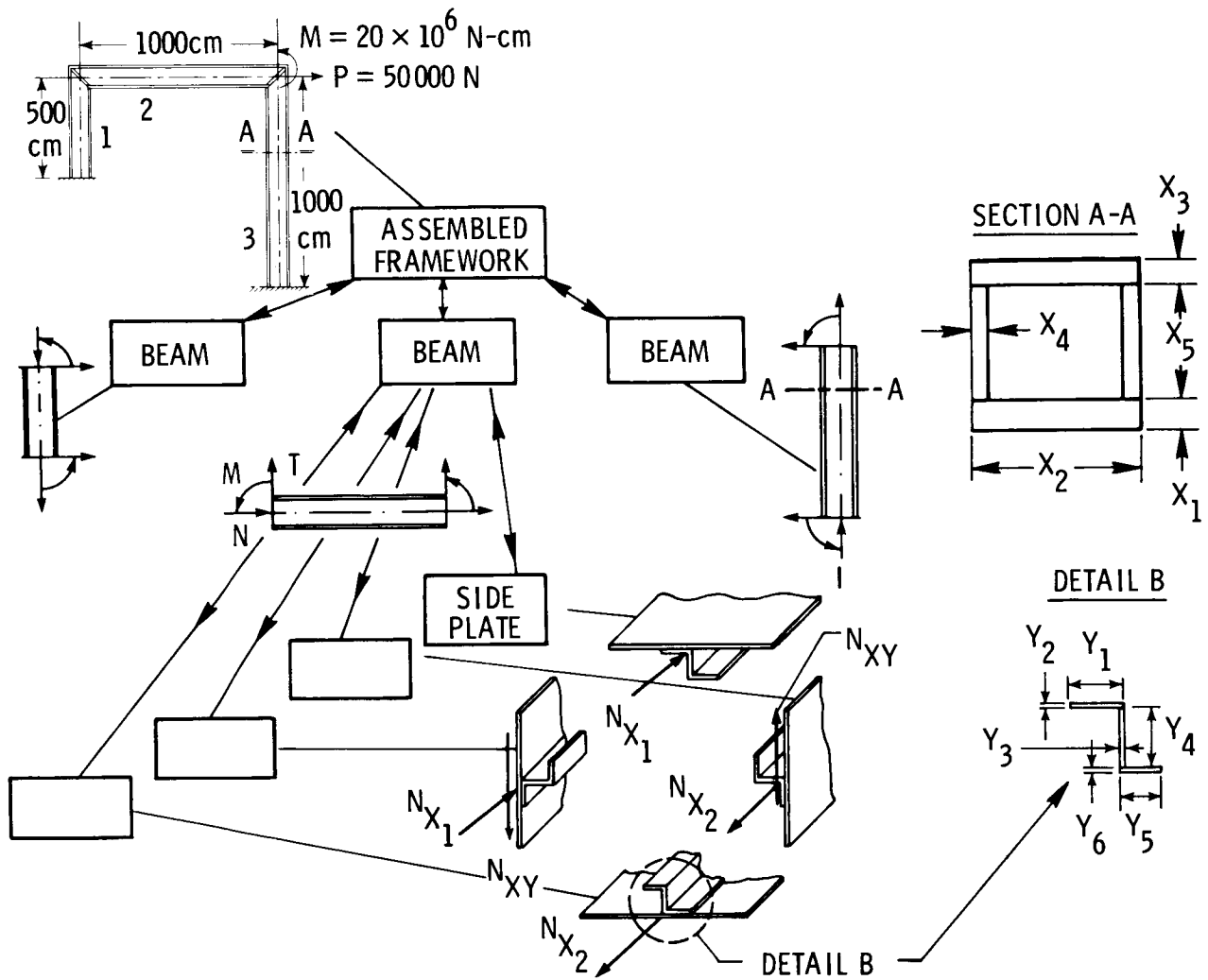
This is a summary of multilevel structural optimization development and testing. The method was also applied in a test case of a high-performance sailplane wing design (ref. 5). The results obtained to date are encouraging.

# TEST APPLICATIONS IN STRUCTURES

TWO LEVELS: GOOD CORRELATION WITH A SINGLE LEVEL TEST CASE

- MINIMUM WEIGHT AGREED WITHIN 2%

- QUITE LARGE DIFFERENCES IN OPTIMUM DESIGN VARIABLES = A "SHALLOW" OPTIMUM

(ref. 4)

SAILPLANE WING (ref. 5)

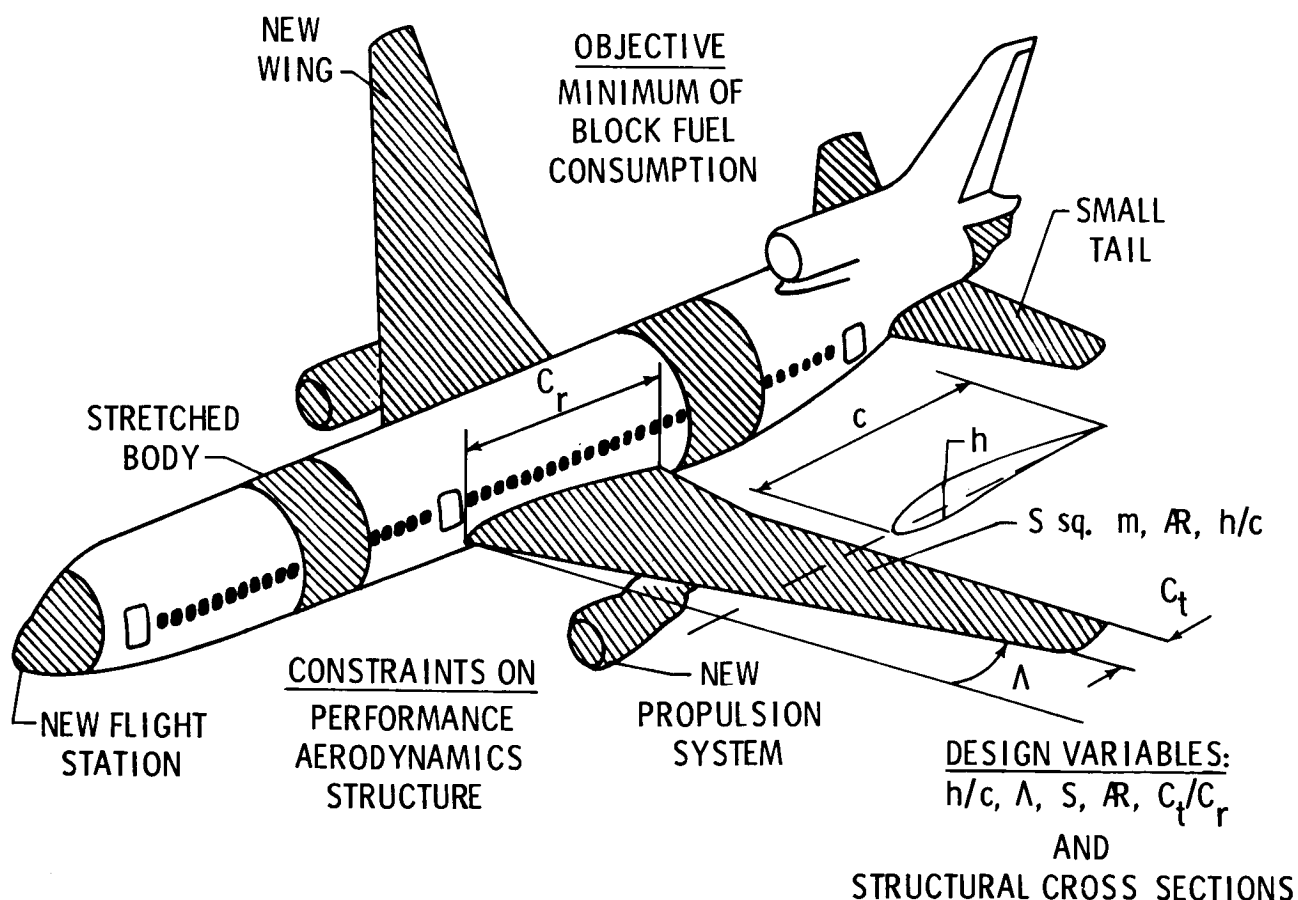THREE LEVELS: REFERENCE SINGLE LEVEL TEST CASE ESTABLISHED

THREE-LEVEL PROCEDURE IMPLEMENTED AND DEBUGGED

RESULTS BEING GENERATED FOR WORK-IN-PROGRESS
(ref. 4)

The wing of a transport aircraft (Lockheed L-1011) is to be reconfigured to minimize fuel consumption for a given mission. The design variables are selected from the geometrical configuration dimensions noted in the drawing and the detailed structural dimensions (not shown) of the wing cover panels reinforced by stringers. A long list of constraints includes the local effects, such as local buckling, and the system performance constraints, such as takeoff field length. The testing is being done jointly with Lockheed-California which supplies the mathematical model (e.g., a finite element model) and the mission and load data, and reconfigures the wing by means of parametric studies using the state-of-the-art tools in each discipline. The Langley team is using the linear decomposition. Comparison of the results will allow assessment of the relative merits of the proposed method. Further details of the test are provided in reference 6.

## MULTILEVEL OPTIMIZATION APPLICATION
## A COOPERATIVE VENTURE WITH LOCKHEED-CALIFORNIA
## (LOCKHEED-GEORGIA INVOLVED)



NEW WING

OBJECTIVE

MINIMUM OF BLOCK FUEL CONSUMPTION

SMALL TAIL

STRETCHED BODY

$C_r$

c

h

S sq. m, AR, h/c

$C_t$

STRETCHED BODY

NEW FLIGHT STATION

CONSTRAINTS ON
PERFORMANCE
AERODYNAMICS
STRUCTURE

NEW PROPULSION SYSTEM

Λ

DESIGN VARIABLES:
h/c, Λ, S, AR, $C_t/C_r$
AND
STRUCTURAL CROSS SECTIONS

Implementation of the proposed multilevel, linear decomposition in design will
fit the existing organization of professionals and will exploit the new
technology of distributed, parallel computing.  It will introduce the new
element of mathematical quantification of the design trade-offs and will
establish a precise definition for information exchange among the specialists
working on their subtasks.  Under the proposed scheme, the decision makers at
each level will know the consequences of their decisions on other coupled
subsystems.  Based on this knowledge, it should be possible to improve the
design integration toward higher performance and lower cost.

## DESIGN OFFICE ORGANIZATION
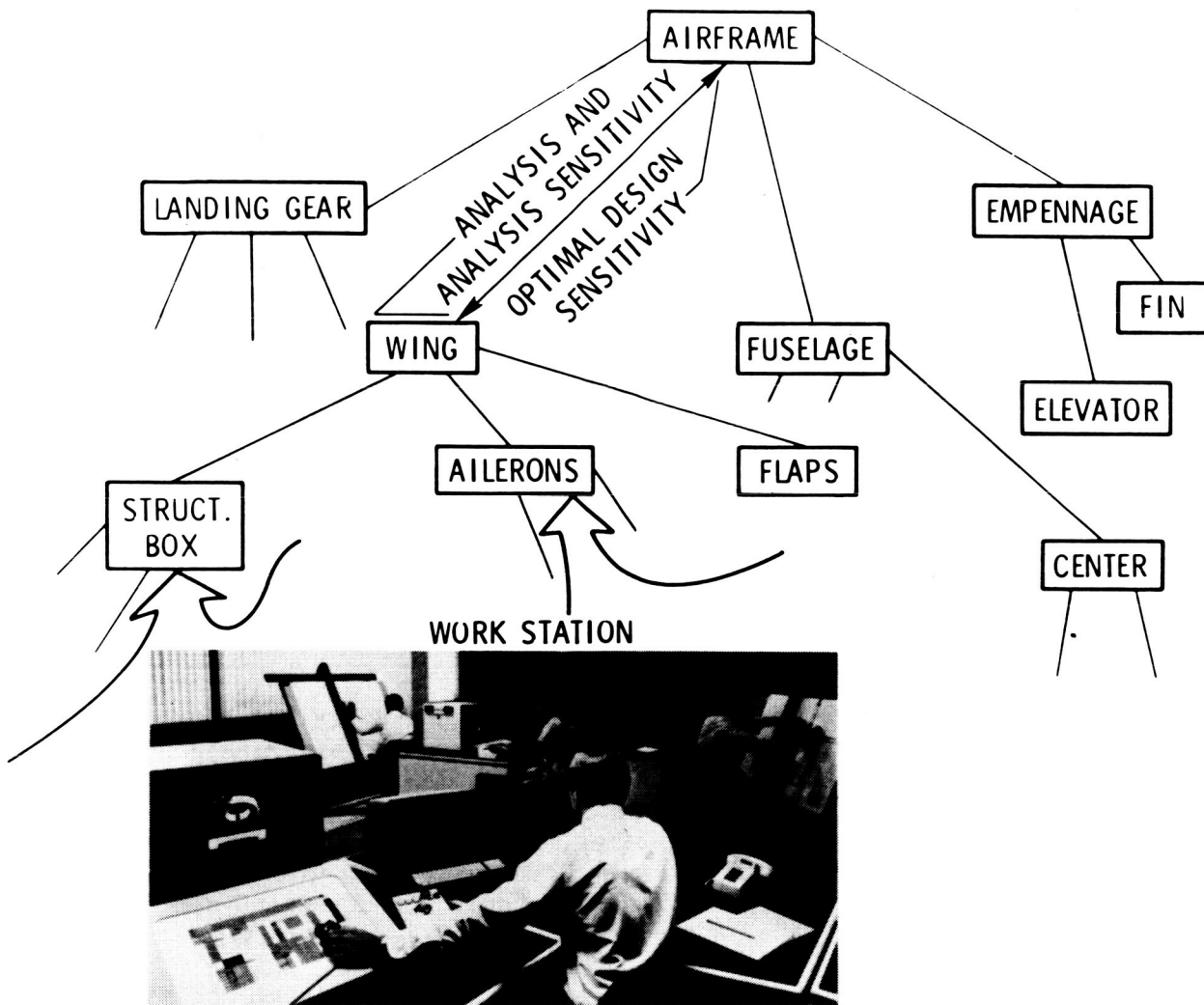
# CONCLUSIONS

- THEORY OF ONE PARTICULAR APPROACH TO DECOMPOSITION DOCUMENTED (ref. 2)

- TESTS ON STRUCTURES: FRAMEWORK, SAILPLANE WING

- TEST ON AN AIRCRAFT CONFIGURATION UNDER WAY

- RESEARCH AND DEVELOPMENT CONTINUE TOWARD MATURITY REQUIRED FOR INDUSTRIAL APPLICATIONS

## REFERENCES

1. Lasdon, L. S.: Optimization Theory for Large Systems. The McMillan Co., New York, 1970.

2. Sobieszczanski-Sobieski, Jaroslaw: A Linear Decomposition Method for Large Optimization Problems - Blueprint for Development. NASA TM-83248, February 1982.

3. Sobieszczanski-Sobieski, J.; Barthelemy, J. F.; and Riley, K. M.: Sensitivity of Optimum Solutions to Problem Parameters. AIAA Paper 81-0548R. AIAA J., Vol. 20, No. 9, September 1982, pp. 1291-1299.

4. Sobieszczanski-Sobieski, Jaroslaw; James, Benjamin; and Dovi, Augustine: Structural Optimization by Multilevel Decomposition. AIAA Paper 83-0832-CP, AIAA/ASME/ASCE/AHS 24th Structures, Structural Dynamics and Materials Conference, Lake Tahoe, Nevada, May 2-4, 1983.

5. Barthelemy, Jean-Francois Marie: Development of a Multilevel Optimization Approach to the Design of Modern Engineering Systems. NASA CR-172184, August 1983.

6. Giles, G. L.; and Wrenn, G. A.: Multidisciplinary Optimization Applied to a Transport Aircraft. Recent Experiences in Multidisciplinary Analysis and Optimization, NASA CP-2327, Part 1, 1984, pp. 439-453.

# STRUCTURAL SENSITIVITY ANALYSIS:
## METHODS, APPLICATIONS, AND NEEDS

Howard M. Adelman
NASA Langley Research Center
Hampton, Virginia

Raphael T. Haftka
Virginia Polytechnic Institute and State University
Blacksburg, Virginia

Charles J. Camarda
NASA Langley Research Center
Hampton, Virginia

Joanne L. Walsh
NASA Langley Research Center
Hampton, Virginia

# INTRODUCTION

The field of sensitivity derivative analysis is emerging as one of the more fruitful areas of engineering research. The reason for this is the recognition of the many practical uses for sensitivity derivatives. Beyond the historical use of derivatives in connection with formal mathematical optimization techniques, recent work has been reported in using sensitivity derivatives in approximate analysis, assessing design trends, analytical model improvement, and determining effects of parameter uncertainties (refs. 1 through 7).

Work supported by the NASA Langley Research Center, under a grant in sensitivity analysis, has been focused on derivatives of thermal response of structures (refs. 8 and 9). Most recently, in-house implementations of generalized structural sensitivity capability in the SPAR and EAL computer programs (refs. 10 and 11) have been completed. Work in the sensitivity area is being expanded, and recent developments both in and outside the structures area have been surveyed to guide the future effort. This paper reviews some innovative techniques applicable to sensitivity analysis of discretized structural systems. These techniques include a finite-difference step-size selection algorithm, a method for derivatives of iterative solutions, a Green's function technique for derivatives of transient response, a simultaneous calculation of temperatures and their derivatives, derivatives with respect to shape, and derivatives of optimum designs with respect to problem parameters. Computerized implementations of sensitivity analysis and applications of sensitivity derivatives are also discussed. Finally, some of the critical needs in the structural sensitivity area are indicated along with Langley plans for dealing with some of these needs.

## DISCIPLINES CONTRIBUTING TO SENSITIVITY ANALYSIS DEVELOPMENT

Sensitivity methodology has been and continues to be an important research area for many disciplines. Appreciation for the uses of sensitivity analysis by a broad spectrum of researchers outside the structures area is very evident. Some of those disciplines are indicated in figure 1. For the most part, the motivation in these other disciplines is the need to quantify the effect of uncertainties in parameters of a system model on the predictions of the model. Examples from physical chemistry are described in references 7 and 12 through 18. A specific use is given in figure 2. Electronics and control theory represented the origin of this type of sensitivity work (refs. 19 and 20) in addition to the use of derivatives to synthesize systems. Recent work in physiology with both human and bacteriological system models is described in reference 21. In the thermodynamics area, reference 22 describes the calculations and use of derivatives of the chemical composition with respect to thermodynamic properties in the mathematical modeling of a coal gasification process. Finally, analytical techniques are beginning to emerge to calculate derivatives of aerodynamic quantities with respect to flow parameters (refs. 23 and 24) as described by Bristow (ref. 25). This paper focuses on contributions to sensitivity methodology originating in or applicable to the structural analysis field.

● CHEMICAL KINETICS

● ELECTRONICS AND CONTROL

● PHYSIOLOGY

● THERMODYNAMICS

● AERODYNAMICS

● STRUCTURAL ANALYSIS

Figure 1

# APPLICATION OF SENSITIVITY DERIVATIVES TO ATMOSPHERIC POLLUTION MODEL

Sensitivity analysis has been used to assess the effects of uncertainties in emission and meteorological parameters on the predictions from a mathematical model for photochemical air pollution (ref. 7). The atmospheric diffusion equation which governs the degree of pollution of a volume of air (an air parcel) contains several parameters: (1) mixing depth - the vertical height of the air parcel containing pollutants; (2) initial concentration of pollutant; (3) photolysis intensity - the rate of photochemical activity; (4) emission rate - the rate at which the pollutant is emitted into the air parcel; and (5) ambient temperature of the air. The calculation of derivatives of concentrations of various pollutants with respect to the aforementioned parameters is described in reference 7. The derivatives were used to rank the importance of the parameters. The calculations were carried out for the example of an "oxidant episode" which occurred in Southern California in 1974. The mathematical simulation of the event began in downtown Los Angeles at 5 a.m. and terminated in San Bernardino County at 8 p.m. The graph in figure 2 shows the sensitivity of the concentration of the pollutant nitric oxide (NO) with respect to each parameter as a function of time. Results indicate that early in the episode the initial concentration and mixing depth are the most important parameters. Midway through, emission rate and ambient temperature were most important, and late in the calculation, ambient temperature and photolysis intensity were most critical. These types of data indicated the need for more exact measurements of the key parameters to improve the air quality mathematical model.



EXAMPLE PROBLEM —
POLLUTION DUE TO OXIDANT EPISODE

SENSITIVITY OF NO CONCENTRATION
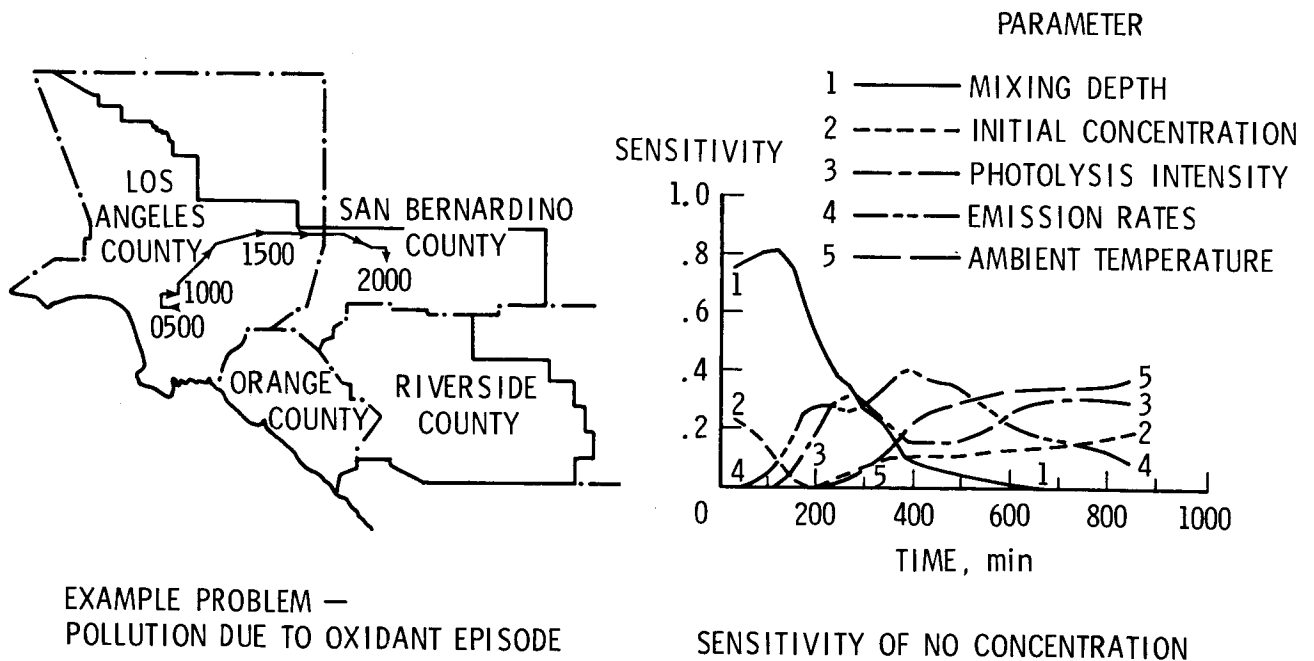
● STUDY RESULTS LED TO RESEARCH FOR MORE
PRECISE MEASUREMENTS OF KEY PARAMETERS

(REF. 7)

Figure 2

The most straightforward method of calculating derivatives is to use a finite-difference approximation. One of the most serious shortcomings of the finite-difference method is the uncertainty in the choice of a perturbation step size. If the step size is too large, truncation errors may occur. These can be thought of as errors due to retention of only the lowest order terms of a Taylor series representation of a perturbed function. If the step size is too small, condition errors may occur (ref. 26). These errors are due to subtraction of nearly equal numbers. In a recent paper (ref. 27), an algorithm was developed to determine the optimum finite-difference step-size, i.e., one that balances the truncation and condition errors. The algorithm is based on approximating the truncation error as a linear function of step size $h$ and the condition error as a linear function of $1/h$. The optimum step size is obtained by equating the condition and truncation errors (fig. 3). This technique has been tested on functions which could be differentiated analytically (ref. 27) and was found to be very effective. A logical extension of this work would be to apply it to matrix equations.

- WANT BEST ESTIMATE OF $\dfrac{\partial f}{\partial v} \approx \dfrac{1}{h}\left(f(v+h) - f(v)\right)$

$$\text{THE PROBLEM} \begin{cases} \text{IF } h \text{ TOO LARGE} - \text{TRUNCATION ERROR} \equiv T(h) \\ \text{IF } h \text{ TOO SMALL} - \text{CONDITION ERROR} \equiv C(h) \end{cases}$$

$$\text{THE SOLUTION} \begin{cases} \text{EXPRESS } T(h) \text{ AND } C(h) \text{ AS SIMPLE COMPUTABLE FUNCTIONS} \\ \text{CHOOSE "OPTIMUM" STEP SIZE } \hat{h} \text{ SO THAT} \end{cases}$$

$$C(\hat{h}) = T(\hat{h})$$

- RESULT — FORMULA FOR $\hat{h}$

- FORMULA VERIFIED BY TESTS ON ANALYTICAL FUNCTIONS

- NEED TO IMPLEMENT FOR MATRIX EQUATIONS
  (REF. 26)

Figure 3

# DERIVATIVES OF ITERATIVE SOLUTIONS

In many structural design problems, the response U is the solution of an algebraic system f(U, v) = 0, where v is a design parameter (fig. 4). When the system is solved iteratively, the iterative process is terminated when the solution error is reduced below a certain tolerance. To obtain the derivative of U with respect to a design parameter by finite differences, the parameter is perturbed and the solution process is repeated to obtain $U_h$. The derivative is then approximated by a finite-difference ratio. The error inherent in this process is due to the termination of the iterative solution process before an exact solution is obtained. Thus $\bar{U}$ and $\bar{U}_h$, obtained by iteration, are only approximations to the corresponding exact solutions U and $U_h$, respectively. Because of noise in the solution process, the difference between $\bar{U}$ and $\bar{U}_h$ can be finite, even for very small values of the perturbation h. In fact, the error is most severe when small values of h are required to avoid large truncation errors in the derivative. A remedy, which is being developed by the second author of this paper, is to define a modified perturbed solution $U_h^*$ which satisfies a modified equation whose right-hand side is not zero but is the residual of the approximate unperturbed equation. By this construction, $U_h^*$ approaches $\bar{U}$ as h approaches zero. Then $U_h^*$ replaces $\bar{U}_h$ in the derivative formula. Finally, $\bar{U}$ serves as the first approximation in the iteration process for $U_h^*$.

- $\bar{U}$ IS SOLUTION TO f(U,v) = 0  $\left.\begin{array}{c} \\ \\ \end{array}\right\}$ APPROXIMATE
- $\bar{U}_h$ IS SOLUTION TO $f\left(U_h, v + h\right) = 0$   $\bar{U}$ AND $\bar{U}_h$
OBTAINED BY ITERATION

$$\partial U / \partial v = 1/h \left(\bar{U}_h - \bar{U}\right)$$

- ERROR MAY BE LARGE DESPITE SMALL h

- SOLUTION — DEFINE $U_h^*$ SUCH THAT

$$f\left(U_h^*, v + h\right) = \underbrace{f(\bar{U}, v)}_{\text{RESIDUAL}} \qquad \text{THEN} \quad \partial U / \partial v = 1/h \left(U_h^* - \bar{U}\right)$$

- WHY IT WORKS   INITIAL GUESS FOR $U_h^*$ IS $\bar{U}$

  $U_h^*$ APPROACHES $\bar{U}$ FOR SMALL h

Figure 4

# GREEN'S FUNCTION METHOD FOR DERIVATIVES OF TRANSIENT RESPONSE

This method, which is well known in applications to solutions of nonhomogeneous differential equations, has been used extensively by physical chemistry researchers (refs. 12 through 18) for calculation of derivatives of response quantities governed by systems of first-order nonlinear ordinary differential equations such as equation (1) shown in figure 5. Numerous applications have been performed for chemical kinetics problems related to air pollution studies. As indicated in this figure, the derivative of the response vector $Y$ with respect to a parameter $\alpha$ satisfies equation (2). The derivative may be represented by an integral expression (eq. 3) involving a kernel $K$ which is the Green's function. The Green's function is the solution to the initial value problem given by equation (4). Comparison of the effort needed to solve equation (2) versus (4) indicates that the Green's function technique is advantageous if the number of design variables $m$ exceeds the number of equations $n$ in the system. One approach to obtaining $K$ is to solve equation (4) directly using an implicit numerical integration technique (ref. 12). An alternate solution for the Green's function is to use the Magnus method (ref. 17) whereby $K$ is expressed as an exponential function of a matrix which is the time integral of the Jacobian matrix $J$. Because the equation of transient heat transfer is a special case of equation (1), the Green's function method is directly applicable to sensitivity of transient temperatures. It is planned to pursue this line of research at Langley as part of our sensitivity development.

● IMPLEMENTED BY PHYSICAL CHEMISTRY RESEARCHERS

● GENERAL PROBLEM

$$\frac{dY}{dt} = f(Y,\alpha,t) \qquad n \text{ EQUATIONS} \qquad (1)$$

$$\frac{dY_\alpha}{dt} = JY_\alpha + f_\alpha \qquad mn \text{ EQUATIONS} \qquad (2)$$

$$J \equiv \partial f/\partial Y \qquad Y_\alpha \equiv \partial Y/\partial \alpha$$

● SOLUTION BY GREEN'S FUNCTION

$$Y_\alpha = \int_0^t K(t,\tau) f_\alpha d\tau \qquad (3)$$

$$\frac{dK}{dt}(t,\tau) - JK(t,\tau) = 0 \qquad n^2 \text{ EQUATIONS} \qquad (4)$$

● APPLICABLE TO TRANSIENT HEAT TRANSFER

Figure 5

# CONCURRENT CALCULATIONS OF TRANSIENT TEMPERATURES AND DERIVATIVES

Derivatives of transient response such as structural displacements and temperatures have been computed following the calculation of the response itself using analytical techniques (refs. 9, 28, 29) and by the Green's function technique (ref. 12). Recently an algorithm for concurrent calculation of transient temperatures and their finite-difference derivatives has been developed (ref. 9). Figure 6 depicts an application to the transient thermal response of an insulated cylindrical shell. Temperatures throughout the shell are computed using an implicit numerical integration technique. Along with temperatures at each time step, finite-difference sensitivity derivatives are calculated with respect to design variables representing insulation thicknesses at 10 locations on the shell surface. The key to the success of the method is that during each time step, when a nonlinear algebraic equation is solved by iteration for the current temperature and the perturbed temperature, the same time step is used for both solutions. Further, the unperturbed temperature serves as the initial guess in the iteration for the perturbed temperature. The numbers in the table are solution times in seconds. The results indicate that the timesaving from the concurrent calculation is substantial, and nearly a factor of 4 advantage is obtained.

| ERROR TOLERANCE ON TEMPERATURE | SEQUENTIAL | | CONCURRENT | |
|---|---|---|---|---|
| | CPU TIME FOR TEMPERATURE CALCULATION | CPU TIME FOR EACH DERIVATIVE | CPU TIME FOR TEMPERATURE PLUS TEN DERIVATIVES | CPU TIME FOR EACH DERIVATIVE |
| .001 | 113 | 113 | 500 | 39 |
| .003 | 78 | 78 | 296 | 22 |
| .010 | 46 | 46 | 168 | 12 |

REGION OF APPLIED HEATING

INSULATED CYLINDER MODEL
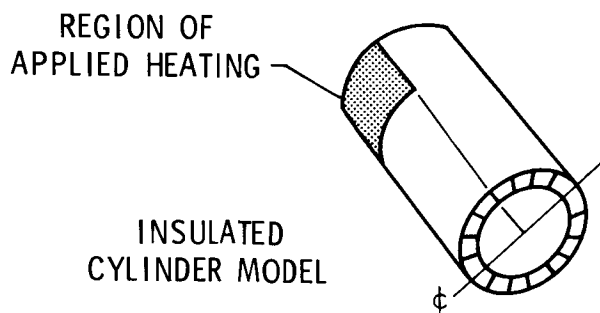
TYPICAL DERIVATIVE

$$\frac{\partial T}{\partial t_{ins}}$$

T = TEMPERATURE

$t_{ins}$ = INSULATION THICKNESS

Figure 6

C-5

## SENSITIVITY DERIVATIVES FOR SHAPE DESIGN VARIABLES

A relatively new topic in structural sensitivity analysis is the calculation of derivatives with respect to shape design variables. Examples are derivatives of displacements or stresses with respect to a beam length or a membrane area (fig. 7). Two approaches have been used. One approach is to differentiate the discretized equations resulting from a finite-element representation. A drawback to this technique is that when shape design variables change, the finite-element mesh is modified. The resulting mesh distortion changes the discretization error and leads to inaccurate derivatives. The second approach, which avoids mesh distortion errors, is to reverse the order of differentiation and discretization (refs. 30 through 32). The procedure is to differentiate the continuum equations of equilibrium and discretize the resulting integral equations. This method uses the concept of a material derivative from continuum mechanics which is composed of two parts: a derivative corresponding to a fixed shape, and a contribution from the change of the boundary. The preferred choice between the two methods is not yet clear. The second approach avoids mesh distortion by its formulation but does not permit shape differentiation of a discretized set of equations. The first method, although suffering from mesh distortion errors, could benefit from a built-in adaptive mesh generation capability which would reduce the mesh distortion.

● EXAMPLES — DERIVATIVE OF

    ● DISPLACEMENTS   WITH   LENGTH OF BEAM

                       RESPECT

    ● STRESSES        TO   AREA OF MEMBRANE

● FIRST METHOD — DISCRETIZE FIRST THEN DIFFERENTIATE

    ● NUMERICAL ERRORS DUE TO MESH DISTORTION

    ● REDUCE ERRORS BY ADAPTIVE MESH GENERATION

● SECOND METHOD — BASED ON MATERIAL DERIVATIVE

    ● DIFFERENTIATE CONTINUUM EQUATIONS THEN DISCRETIZE

    ● AVOIDS MESH DISTORTION ERRORS

Figure 7

The problem addressed by this technique (refs. 33, 34) is to obtain derivatives of an objective function  F  and design variables  V  from an optimized solution with respect to parameters  P  which were held constant during the optimization. The most obvious and thus most useful application of the technique is extrapolation of an optimum design for variations of a problem parameter.  For example, the effect of varying the height  H  of the truss in figure 8 is assessed by using optimum sensitivity derivatives.  Extrapolated values of the mass  F  and one of the cross-sectional areas  $A_1$, based on derivative with respect to  H, are compared with those obtained by reoptimization with different values of  H.  As shown in the lower right portion of figure 8, the results agree very closely for up to a 20-percent change in  H.  Other applications of these types of derivatives include optimization for multiple-objective functions, assessing the effects of adding or deleting constraints, and most recently using the derivatives as links between subsystems during multilevel optimization (ref. 35).
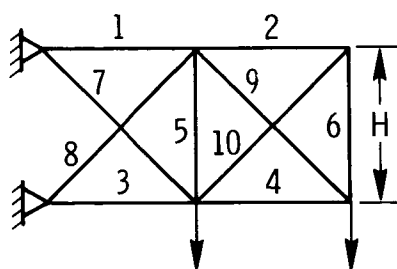
GIVEN AN OPTIMUM DESIGN:
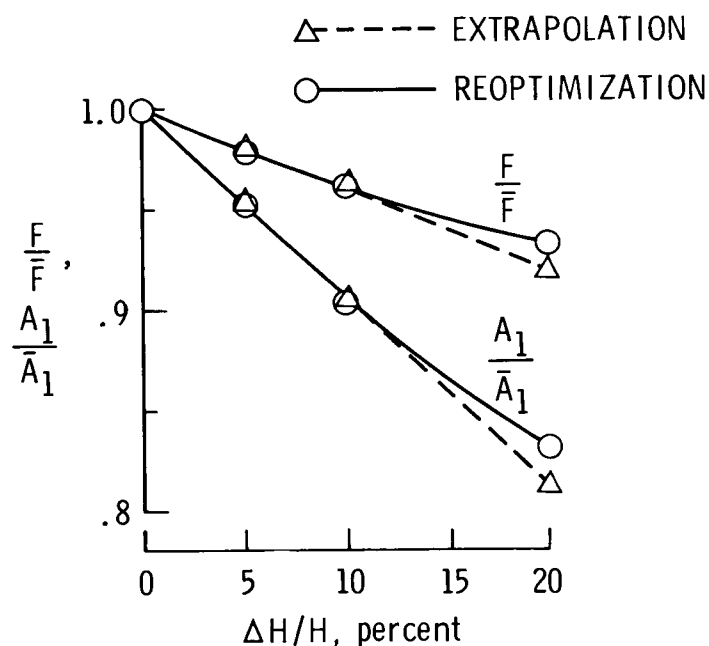
F = OBJECTIVE FUNCTION    V = DESIGN VARIABLES

P = PROBLEM PARAMETERS

ANALYSIS GIVES  $\frac{\partial F}{\partial P}$  AND  $\frac{\partial V}{\partial P}$



● EXAMPLE — EFFECT OF TRUSS HEIGHT ON OPTIMUM DESIGN

(REF. 33)

Figure 8

376

# COMPUTER IMPLEMENTATION

Some progress has occurred in providing general-purpose software for sensitivity analysis (fig. 9). The Green's function technique described earlier has been implemented in a computer program denoted AIM (ref. 18). Use of this program requires supplying subroutines to define the system of equations - specifically, the vector f and the matrix J in figure 5. The capability for computing derivatives of static displacements, stresses, and vibration and buckling eigenvalues and eigenvectors has been implemented in the SPAR finite-element program (ref. 10) and EAL (refs. 11, 36). The EAL (Engineering Analysis Language) system contains the SPAR finite-element modules, but additionally EAL provides FORTRAN-like commands which permit branching, testing data, looping, and calling the SPAR modules (similar to calling FORTRAN subroutines). A recent level of a proprietary version of the NASTRAN computer program also has capability for static displacement, stress, and eigenvalue derivatives (ref. 37).

●AIM (GREEN'S FUNCTION TECHNIQUE)

  ●GENERAL FIRST-ORDER EQUATIONS

  ●DERIVATIVES WRT PARAMETERS IN EQUATIONS

●SPAR (COSMIC) AND EAL (PROPRIETARY)

  ●DERIVATIVES OF —
        ●DISPLACEMENTS
        ●STRESSES
        ●EIGENVALUES
        ●EIGENVECTORS

●NASTRAN (PROPRIETARY)

  ●DERIVATIVES OF —
        ●DISPLACEMENTS
        ●STRESSES
        ●EIGENVALUES

Figure 9

# APPLICATION OF STRUCTURAL SENSITIVITY ANALYSIS TO SPACE ANTENNA

An application of sensitivity analysis to reveal structural design trends is illustrated in figure 10. The structure is an Earth-orbiting antenna reflector subjected to nonuniform heating leading to thermal distortions which can degrade antenna performance (ref. 11). The structure is modeled using only rod elements. There are three design variables representing, respectively, the cross-sectional areas of the elements in the upper surface ($A_1$), the elements joining the upper and lower surfaces ($A_2$), and the elements in the lower surface ($A_3$). Derivatives of the center deflection with respect to each design variable were calculated and are shown in the figure. A positive derivative indicates that increasing the design variable increases the response. A negative derivative indicates that increasing the design variable decreases the response. The seemingly contradictory result that increasing a design variable can increase a response stems from the fact that the thermal loads are proportional to the rod cross-sectional areas. From the table in figure 10, we see that increasing $A_1$ has the largest effect on reducing deflection but at the cost of a weight increase. On the other hand, decreasing either $A_2$ or $A_3$ would reduce the deflection and at the same time reduce weight. It is at the discretion of the designer as to which of the alternatives is a better choice. The sensitivity derivatives provide the data for that judgment.
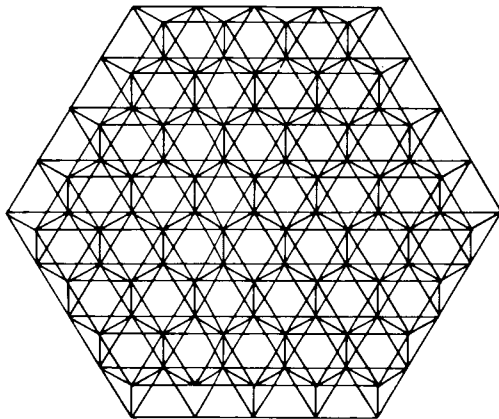


ANTENNA MODEL

$w_0$ = CENTER DEFLECTION

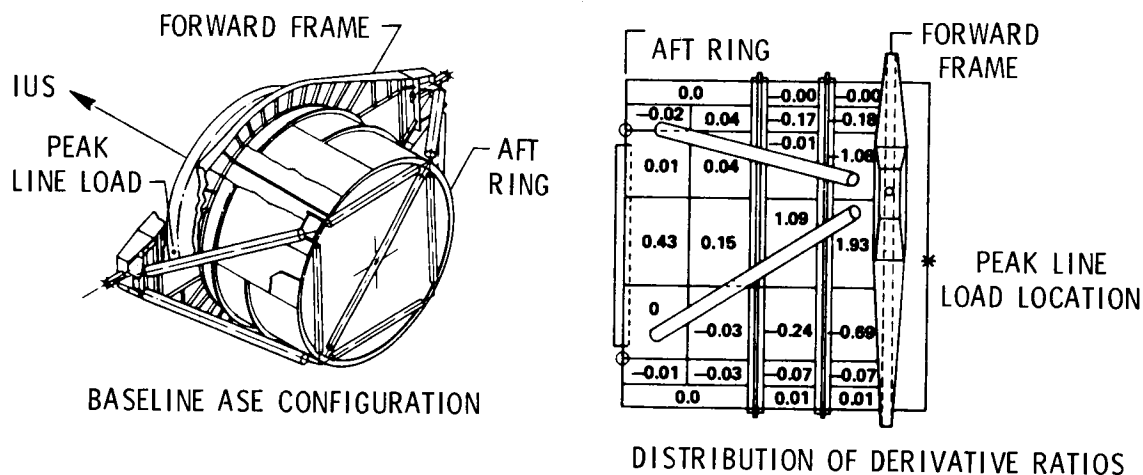| DESIGN VARIABLE — ELEMENT AREA, $A_i$ | $\partial w_0 / \partial A_i$ |
|---|---|
| UPPER SURFACE | $-2.4 \times 10^{-4}$ |
| DIAGONALS | $8.3 \times 10^{-5}$ |
| LOWER SURFACE | $1.8 \times 10^{-4}$ |

DERIVATIVES OF CENTER DEFLECTION

Figure 10

378

## APPLICATION OF SENSITIVITY ANALYSIS TO SHUTTLE PAYLOAD

Sensitivity analysis has been used to redesign the Airborne Support Equipment (ASE) assembly on the Space Shuttle orbiter (ref. 5). The ASE supports the inertial upper stage (IUS) vehicle in the payload bay. The purpose of the IUS vehicle is to transport payloads further into space once the orbiter has established low-Earth orbit. The shell of the ASE is subjected to large launch loads and is designed for an ultimate load of 3000 lb/in. An initial sculptured skin design met the design load but was too heavy. A sensitivity analysis was performed to determine which skin gages had the largest effect on loads and to determine which type of modified construction would give the largest weight reduction (among isogrid, waffle, and stiffened skin). The structure was modeled and divided into zones as shown on the right side of figure 11. Derivatives of compressive loads and weight with respect to longitudinal, circumferential, and shear stiffening were computed for each zone. As an example, consider derivatives with respect to the longitudinal stiffness design variable $t_a$. The numbers in the zones are ratios of derivatives of load to derivatives of weight for the sculptured skin design. Negative values indicate that increasing a design variable decreases the load, and positive values indicate that increasing a design variable increases the load. The analysis revealed that derivatives with respect to longitudinal and shear stiffness were the largest, derivatives with respect to circumferential stiffness were negligible, and derivatives with respect to shear stiffness were nearly all positive. Based on these results, the shell was redesigned as a longitudinally stiffened machined skin. (The isogrid was rejected because of high shear stiffness; the waffle construction was rejected due to unneeded high circumferential stiffness.) The resulting design satisfies the ultimate load constraint with a large margin of safety and an acceptably low weight.



BASELINE ASE CONFIGURATION

DISTRIBUTION OF DERIVATIVE RATIOS

$$\frac{\partial N / \partial t_a}{\partial W / \partial t_a}$$

$t_a$ = LONGITUDINAL STIFFNESS

- STUDY RESULTS
  - LARGE DERIVATIVES WRT LONGITUDINAL AND SHEAR STIFFNESS
  - SMALL DERIVATIVES WRT CIRCUMFERENTIAL STIFFNESS

- OUTCOME — REDESIGNED SHELL AS LONGITUDINALLY STIFFENED MACHINED PANEL

SATISFIED DESIGN REQUIREMENTS WITH LOW WEIGHT

(REF. 5)

Figure 11

As a result of surveying methods applicable to computing structural sensitivity derivatives, a list of needs has emerged (fig. 12).  First, continued development of methods for derivatives of transient response and derivatives with respect to shape design variables and material properties should have high priority. Further, techniques developed for sensitivity derivatives in nonstructural disciplines such as physical chemistry have much to offer and should be evaluated for their adaptability to structural areas.  It appears that structural designers have made insufficient use of the power and utility of sensitivity derivatives to guide design modifications and to assess uncertainties in their models.  Their use can be accelerated by demonstrations of practical applications of sensitivity analysis and careful documentation (by optimization and sensitivity specialists) to guide structural analysts and designers not experienced in formal optimization and sensitivity analysis. Finally, sensitivity analysis needs to be routinely included as a standard feature in general-purpose structural analysis software packages.  Near-term plans at Langley include evaluation of the Green's function method for derivatives of transient thermal response, methods for derivatives of spacecraft thermal response with respect to material properties, and implementation of the optimum finite-difference step-size technique for finite-element sensitivity analysis.  Concurrent with this effort, demonstration problems will be selected and solved.

- ● TRANSIENT RESPONSE

- ● MATERIAL PROPERTIES AND SHAPE

- ● PRACTICAL APPLICATIONS

- ● ROUTINE INCLUSION IN GENERAL-PURPOSE COMPUTER PROGRAMS

LANGLEY PLANS

- ● EVALUATE GREEN'S FUNCTION METHOD FOR TRANSIENT TEMPERATURES

- ● DERIVATIVES WRT MATERIAL PROPERTIES

- ● IMPLEMENT FINITE-DIFFERENCE STEP-SIZE ALGORITHM

- ● SENSITIVITY DEMONSTRATION PROBLEMS

Figure 12

## SUMMARY

This paper was based on a recently conducted survey of methods for sensitivity analysis of structural response (fig. 13). The survey was not limited to research in the structural area alone and revealed that a broad range of disciplines are using sensitivity analysis and contributing to the methodology. In almost every instance, methods from the nonstructural disciplines are directly applicable to the structures area. An example application from chemical kinetics was described in which sensitivity analysis was used to assess the impact of parameter uncertainties in a mathematical model used in air pollution studies.

The bulk of the paper has focused on a selected set of innovative methods applicable to sensitivity analysis of structural systems. The analysis techniques include a finite-difference step-size selection algorithm, a method for derivatives of iterative solutions, a Green's function technique for derivatives of transient response, concurrent calculation of temperatures and their derivatives, derivatives with respect to shape, and derivatives of optimum designs with respect to problem parameters. Two applications were described wherein derivatives were used to guide structural design changes to improve an engineering design without recourse to formal mathematical optimization. Plans at Langley for contributing to identified critical needs were cited. Among the needs were implementation of methods for derivatives of transient response, derivatives with respect to shape and material properties, solution and documentation of sensitivity analysis demonstration problems, and routine inclusion of sensitivity analysis as a feature in general-purpose structural analysis computer programs. Langley near-term plans in the sensitivity area include evaluating the Green's function method for derivatives of transient thermal response, developing methods for derivatives with respect to material properties, implementation of the finite-difference step-size algorithm, and solution of sensitivity demonstration problems.

- LANGLEY CONDUCTING SURVEY OF METHODS FOR SENSITIVITY DERIVATIVES

- PAPER REVIEWED RECENTLY DEVELOPED TECHNIQUES

  - OPTIMUM FINITE-DIFFERENCE STEP-SIZE ALGORITHM

  - METHOD FOR DERIVATIVES OF ITERATIVE SOLUTIONS

  - GREEN'S FUNCTION METHOD FOR TRANSIENT RESPONSE

  - SIMULTANEOUS CALCULATION OF TEMPERATURES AND DERIVATIVES

  - DERIVATIVES WITH RESPECT TO SHAPE

  - DERIVATIVES OF OPTIMUM DESIGNS WITH RESPECT TO PROBLEM PARAMETERS

- REVIEWED USES OF DERIVATIVES AND CITED APPLICATIONS

- CITED NEEDS AND OUTLINED LANGLEY PLANS

Figure 13

REFERENCES

1. Schmit, L. A., Jr.; and Farshi, B.: Some Approximation Concepts for Structural Synthesis. AIAA J., vol. 12, no. 5, May 1974, pp. 692-699.

2. Storaasli, O.; and Sobieszczanski, J.: On the Accuracy of the Taylor Approximation for Structure Resizing. AIAA J., vol. 12, no. 2, Feb. 1974, pp. 231-233.

3. Noor, K.; and Lowder, E.: Structural Reanalysis Via a Mixed Method. Comput. and Struct., vol. 5, no. 1, Apr. 1975, pp. 9-12.

4. Robinson, J. C.: Application of a Systematic Finite-Element Model Modification Technique to Dynamic Analysis of Structures. NASA TM-83292, 1983.

5. Musgrove, M. D.; Reed, J. M.; and Hauser, C. C.: Optimization Using Sensitivity Analysis. J. Spacecraft & Rockets, vol. 20, no. 1, Jan.-Feb. 1983, pp. 3-4.

6. Cukier, R. I.; Fortuin, C. M.; Shuler, K. E.; Petschek, A. G.; and Schaibly, J. H.: Study of the Sensitivity of Coupled Reaction Systems to Uncertainties in Rate Coefficients. I. Theory, J. Chem. Phys., vol. 59, 1973, pp. 3873-3878.

7. Tilden, J. W.; and Seinfeld, J. H.: Sensitivity Analysis of a Mathematical Model for Photochemical Air Pollution. Atmospheric Environment, vol. 16, no. 6, 1982, pp. 1357-1364.

8. Haftka, R. T.: Techniques for Thermal Sensitivity Analysis. Int. J., Numerical Meth. in Engineering, vol. 17, 1981, pp. 71-80.

9. Haftka, R. T.; and Malkus, D. S.: Calculation of Sensitivity Derivatives in Thermal Problems by Finite Differences. Int. J. Numerical Meth. in Engineering, vol. 17, 1981, pp. 1811-1821.

10. Giles, G. L.; and Rogers, J. L., Jr.: Implementation of Structural Response Sensitivity Calculations in a Large-Scale Finite-Element Analysis System. Proc. 23rd Structures, Structural Dynamics and Materials Conference, May 10-12, 1982, New Orleans, LA., pp. 348-359.

11. Camarda, C. J.; and Adelman, H. M.: Implementation of Static and Dynamic Structural Sensitivity Derivative Calculations in the Finite-Element-Based Engineering Analysis Language System (EAL). NASA TM-85743, 1984.

12. Hwang, J. T.; Dougherty, E. P.; Rabitz, S.; and Rabitz, H.: The Green's Function Method of Sensitivity Analysis in Chemical Kinetics. J. Chem. Phys., vol. 69, Dec. 1978, pp. 5180-5191.

13. Dougherty, E. P.; and Rabitz, H.: Computational Kinetics and Sensitivity Analysis of Hydrogen-Oxygen Combustion. J. Chem. Phys., vol. 72, no. 12, June 15, 1980, pp. 6571-6586.

14. Eslava, L. A.; Eno, L.; and Rabitz, H.: Further Developments and Applications of Sensitivity Analysis to Collisional Energy Transfer. J. Chem. Phys., vol. 73, no. 10, Nov. 1980, pp. 4998-5012.

15. Demiralp, M.; and Rabitz, H.: Chemical Kinetic Functional Sensitivity Analysis: Derived Sensitivities and General Applications. J. Chem. Phys., vol. 75, no. 4, Aug. 1981, pp. 1810-1819.

16. Edelson, D.: Computer Simulation in Chemical Kinetics. Science, vol. 214, no. 27, Nov. 1981, pp. 981-986.

17. Kramer, M. A.; and Calo, J. M.: An Improved Computational Method for Sensitivity Analysis: Green's Function Method with "AIM". Appl. Math. Modeling, vol. 5, Dec. 1981, pp. 432-441.

18. Kramer, M. A.; Calo, J. M.; Rabitz, H.; and Kee, R. J.: AIM: The Analytically Integrated Magnus Method for Linear and Second-Order Sensitivity Coefficients. Sandia National Laboratories Report SAND-82-8231, Aug. 1982.

19. Goddard, P. J.; Vilalaz, P. A.; and Spence, R.: Method for the Efficient Computation of the Large Change Sensitivity of Linear Nonreciprocal Networks. Electronics Letters, vol. 7, Feb. 1971, pp. 112-113..

20. Radanovic, L., ed.: Sensitivity Methods in Control Theory. Pergamon Press Ltd., 1966.

21. Leonard, J. I.: The Application of Sensitivity Analysis to Models of Large Scale Physiological Systems. NASA CR-160228, Oct. 1974.

22. Irwin, C. L.; and O'Brien, T. J.: Sensitivity Analysis of Thermodynamic Calculations. U.S. Dept. of Energy Report DOE/METC/82-53, 1982.

23. Dwyer, H. A.; Peterson, T.; and Brewer, J.: Sensitivity Analysis Applied to Boundary Layer Flow. Proc. 5th International Conference on Numerical Methods in Fluid Dynamics, A. I. van de Vooren and P. J. Zandbergen, eds., Springer-Verlag (Berlin), 1976, pp. 179-184.

24. Bristow, D. R.; and Hawk, J. D.: Subsonic Panel Method for Designing Wing Surfaces from Pressure Distributions. NASA CR-3713, July 1983.

25. Bristow, D. R.: Sensitivity Analysis in Computational Aerodynamics. Recent Experiences in Multidisciplinary Analysis and Optimization, NASA CP-2327, Part 1, 1984, pp. 385-394.

26. Gill, P. E.; Murray, W.; Saunders, M. A.; and Wright, M. H.: Computing the Finite-Difference Approximations to Derivatives for Numerical Optimization. U.S. Army Research Office, Report No. DAAG29-79-C-0110, May 1980.

27. Gill, P. E.; Murray, W.; Saunders, M. A.; and Wright, M. H.: Computing Forward Difference Intervals for Numerical Optimization. SIAM J. Sci. Stat. Comput., vol. 4, June 1983, pp. 310-321.

28. Haug, E. J.; Arora, J. S.; and Feng, T. T.: Sensitivity Analysis and Optimization of Structures for Dynamic Response. J. Mech. Des., vol. 100, Apr. 1978, pp. 311-318.

29. Haug, E. J.; and Feng, T. T.: Optimal Design of Dynamically Loaded Continuous Structures. Int. J. Numerical Meth. in Engineering, vol. 12, 1978, pp. 299-317.

30. Rousselet, B.; and Haug, E. J.: Design Sensitivity Analysis in Structural Mechanics. III. Effects of Shape Variation. J. Struct. Mech., vol. 10, no. 3, 1983, pp. 273-310.

31. Dems, K.; and Mroz, Z.: Variational Approach By Means of Adjoint Systems to Structural Optimization and Sensitivity Analysis - II: Structure Shape Variation. Int. J. Solids and Structures, vol. 20, no. 6, 1984, pp. 527-552.

32. Choi, K. K.; and Haug, E. J.: Shape Design Sensitivity Analysis of Elastic Structures. J. Struct. Mech., vol. 11, 1983, pp. 231-269.

33. Sobieszczanski-Sobieski, J.; Barthelemy, J. F.; and Riley, K. M.: Sensitivity of Optimum Solutions to Problem Parameters. AIAA J., vol. 20, Sept. 1982, pp. 1291-1299.

34. Barthelemy, J. F. M.; and Sobieszczanski-Sobieski, J.: Optimum Sensitivity Derivatives of Objective Functions in Nonlinear Programing. AIAA J., vol. 21, no. 6, pp. 913-915.

35. Sobieszczanski-Sobieski, J.: Structural Optimization: Challenges and Opportunities. NASA TM-85741, 1984.

36. Prasad, B.; and Emerson, J. F.: A General Capability of Design Sensitivity for Finite-Element Systems. Proc. 23rd Structures, Structural Dynamics and Materials Conference, May 10-17, 1982, pp. 175-186.

37. Joseph, J. A., ed: MSC/NASTRAN Application Manual, Version 63A, MacNeal-Schwendler Corp., April 1983.

# SENSITIVITY ANALYSIS IN COMPUTATIONAL AERODYNAMICS

Dean R. Bristow
McDonnell Aircraft Company
St. Louis, MO

## SUBSONIC INVISCID PANEL METHOD
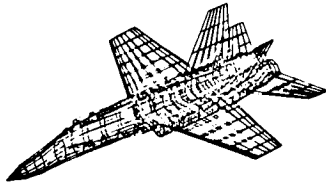


### MCAERO

INPUT:  GEOMETRY

OUTPUT:  PRESSURE

### DMCAERO

INPUT:  GEOMETRY

OUTPUT:  $\dfrac{\partial\ \text{PRESSURE}}{\partial\ \text{GEOMETRY}}$

## INTERACTING VISCOUS AND INVISCID THEORIES FOR HIGH $\alpha$
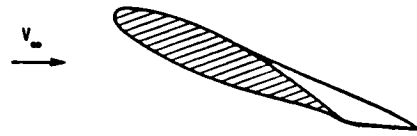


INVISCID THEORY $\longrightarrow$ $\dfrac{\partial\ \text{PRESSURE}}{\partial\ \text{GEOMETRY}}$

VISCOUS THEORY $\longrightarrow$ $\dfrac{\partial\ \text{GEOMETRY}}{\partial\ \text{PRESSURE}}$

$$\left[ P + \frac{\partial P}{\partial G}\,\Delta G \right]_{\text{INVISCID}} = \left[ P + \left(\frac{\partial G}{\partial P}\right)^{-1}\Delta G \right]_{\text{VISCOUS}}$$

## PREDICTION ACCURACY OF MCAERO

### CONVENTIONAL ANALYSIS MODE

#### 6.4° ANGLE-OF-ATTACK      MACH 0.50



**YAV-8B Surface Panel Modeling**

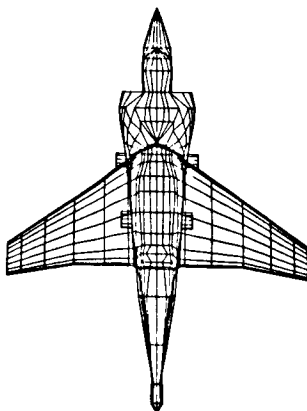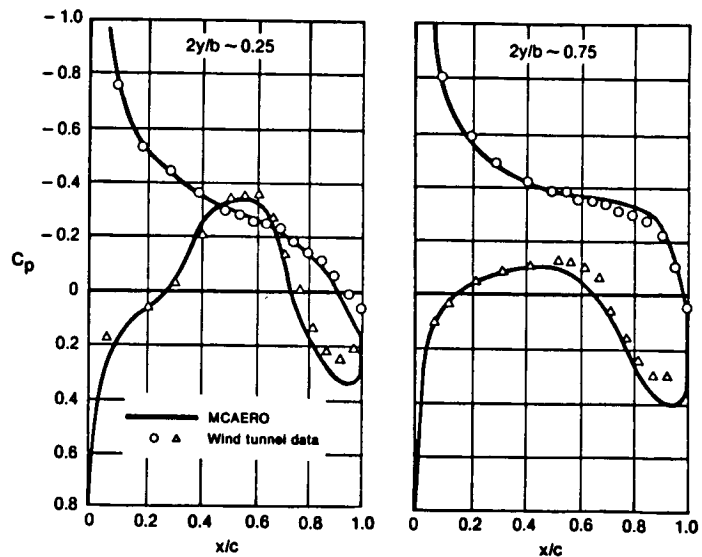# PERTURBATION ANALYSIS METHOD

Perturbed Geometry
$(x, y, z)_j + (\Delta x, \Delta y, \Delta z)_j$

Baseline Geometry $(x, y, z)_j$

$V_\infty$
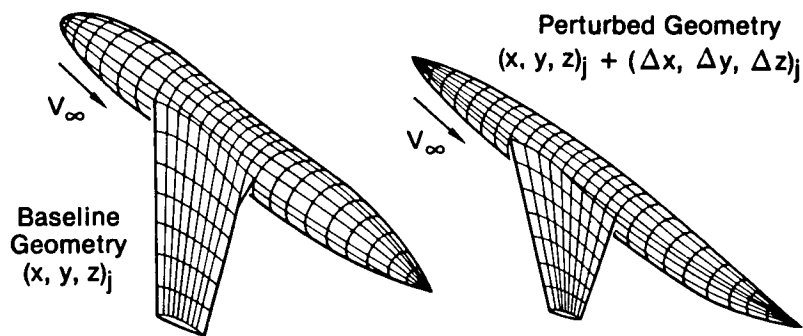
### Objective

- Subsonic Inviscid Analysis of Multiple Geometry Perturbations at Small Additional Cost

### Approach

- Precalculated Baseline Matrix of Potential

  Derivatives $\left\{\dfrac{\partial \phi i}{\partial x_j}, \dfrac{\partial \phi i}{\partial y_j}, \dfrac{\partial \phi i}{\partial z_j}\right\}$

- Linear Extrapolation

$$(\phi_i + \Delta \phi_i) = \phi_i + \sum_j \left\{\frac{\partial \phi i}{\partial x_j} \Delta x_j + \frac{\partial \phi i}{\partial y_j} \Delta y_j + \frac{\partial \phi i}{\partial z_j} \Delta z_j\right\}$$

## SIMPLE DEMONSTRATION OF PERTURBATION ANALYSIS METHOD
### 2-D INCOMPRESSIBLE FLOW

$V_\infty$

Baseline Geometry

Geometry Perturbation (NACA-0012 to Circle)

—— Exact potential flow solution    O Perturbation analysis method

Circular Cylinder

Baseline

$C_P$

x/c

GP23-0206-3

387
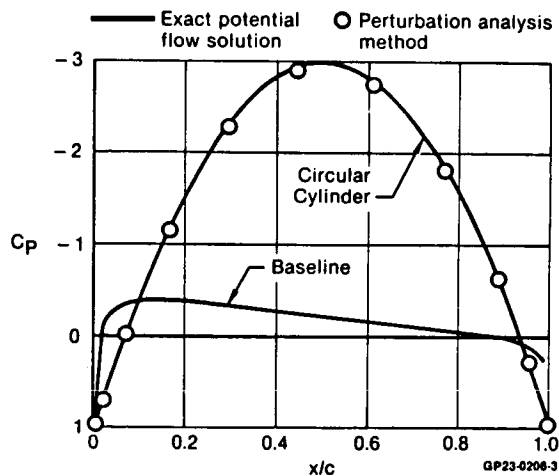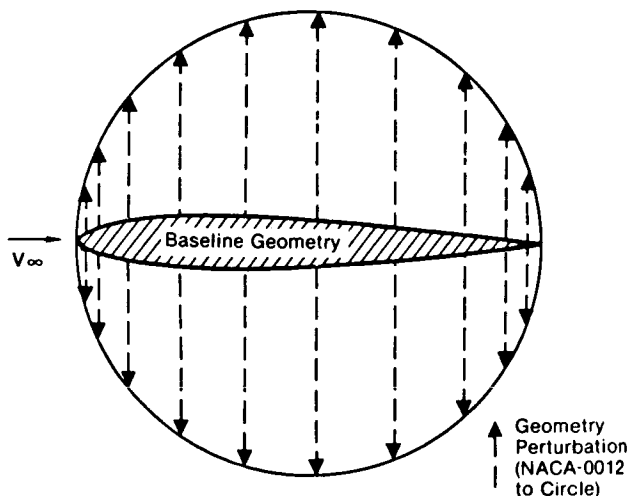
## VARIATION OF FLOW PROPERTIES WITH THICKNESS
### ELLIPTICAL CYLINDER AT 0° INCIDENCE
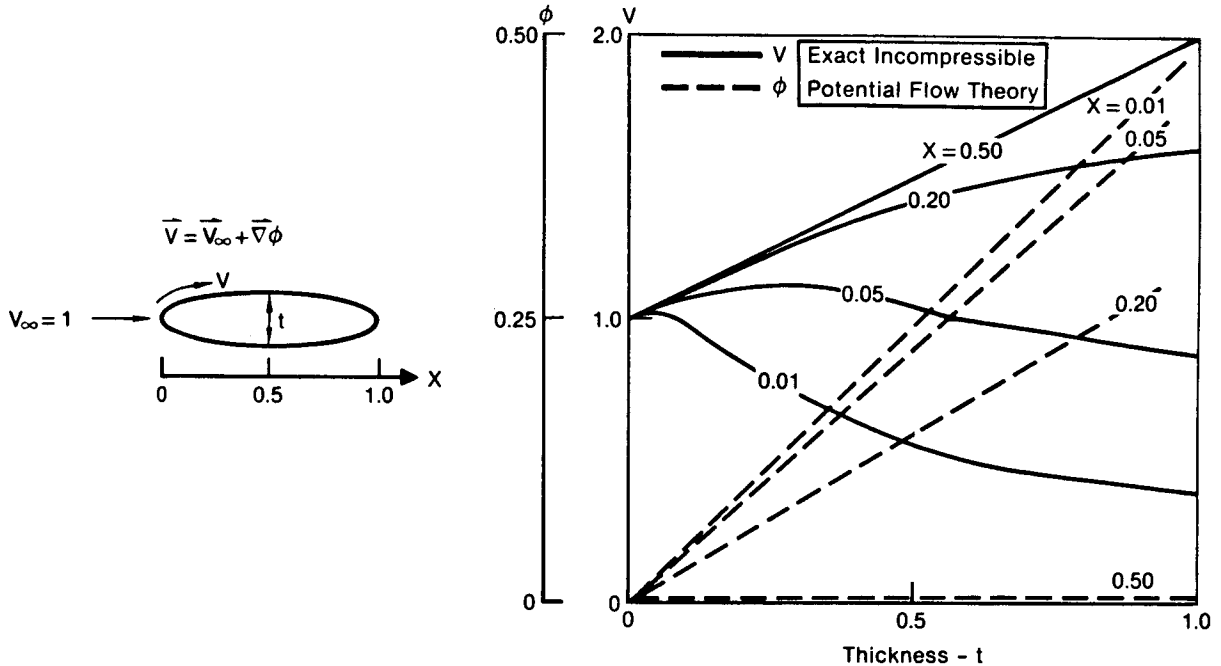


# Procedure for Calculating Perturbation Matrix

### 1. Conventional Panel Method Calculations

$$[A_{ij}] \cdot \phi_j = BC_i \quad \longrightarrow \quad \phi_i = [A_{ij}]^{-1} \cdot BC_j$$

### 2. First-Order Expansion

$$[A_{ij}] \cdot \frac{\partial \phi_j}{\partial z_k} + \phi_j \cdot \left[ \frac{\partial A_{ij}}{\partial z_k} \right] = \frac{\partial BC_i}{\partial z_k}$$

$$\frac{\partial \phi_i}{\partial z_k} = [A_{ij}]^{-1} \cdot \left\{ \frac{\partial BC_j}{\partial z_k} - \phi_\ell \cdot \left[ \frac{\partial A_{j\ell}}{\partial z_k} \right] \right\}$$

388

**BASELINE WING PANELING
FOR PERTURBATION
ANALYSIS TEST CASES**
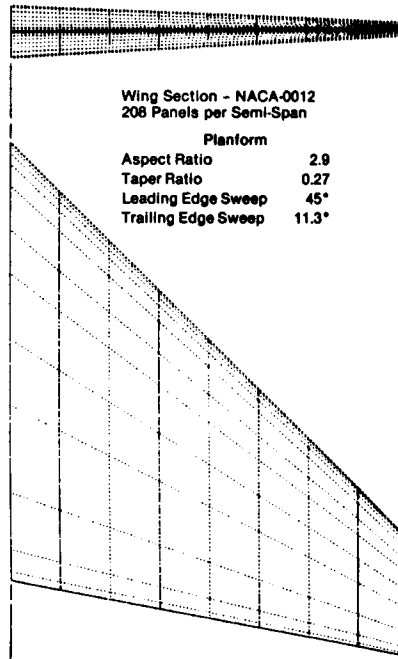
Wing Section - NACA-0012
208 Panels per Semi-Span

Planform
Aspect Ratio          2.9
Taper Ratio           0.27
Leading Edge Sweep    45°
Trailing Edge Sweep   11.3°

**FIGHTER WING
AT 5° ANGLE OF ATTACK**

COMPUTING TIME

——— CONVENTIONAL
"EXACT" ANALYSIS          245 SECS

o    PERTURBATION
ANALYSIS METHOD          7SECS

| BASELINE | PERTURBED |
|----------|-----------|
| ROOT | ROOT |
| TIP | TIP |

20% SEMI-SPAN

80% SEMI-SPAN

389
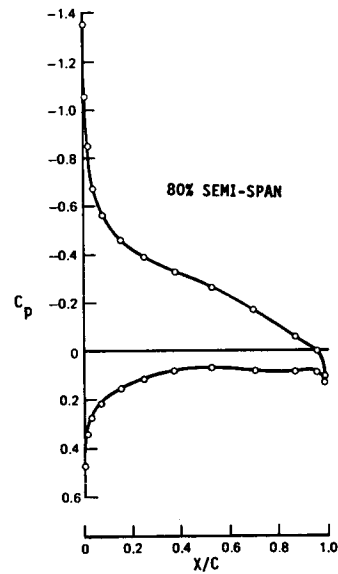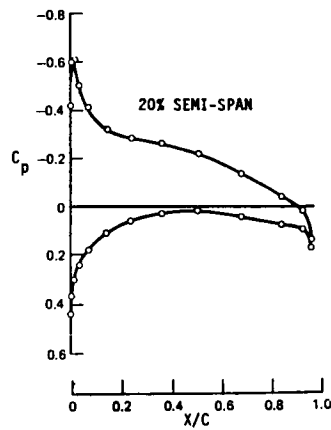
## APPLICATIONS OF INVISCID SENSITIVITY MATRIX

- EFFICIENT ANALYSIS OF MULTIPLE GEOMETRY PERTURBATIONS

- PRESCRIBED PRESSURE WING DESIGN

- UNSTEADY AERODYNAMICS

- AERODYNAMIC-STRUCTURAL DESIGN OPTIMIZATION

- STRONG VISCOUS-INVISCID INTERACTIONS

## TWO-DIMENSIONAL AIRFOIL VISCOUS AERODYNAMICS
### (LOW SPEED)

### GIVEN
- **SOLID GEOMETRY**
- **REYNOLDS NUMBER**
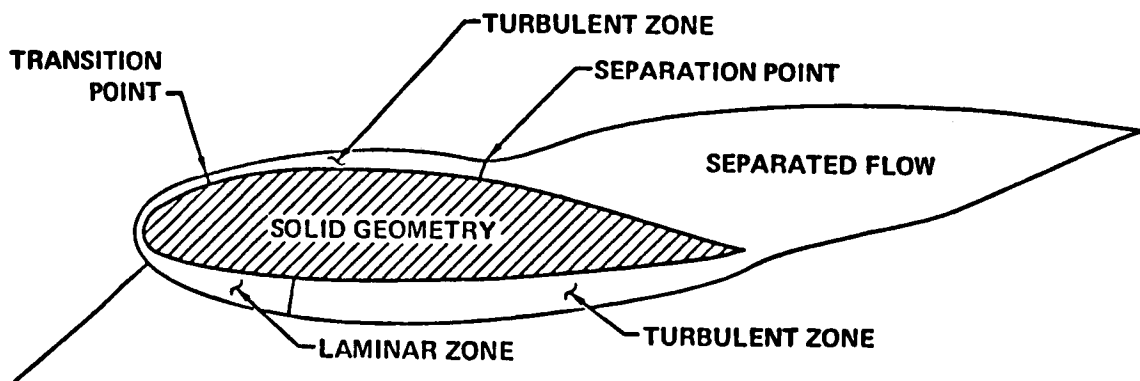


### SOLUTION - GENERAL CASE
- **PRESSURE DISTRIBUTION**
- **LIFT, DRAG, AND PITCHING MOMENT**
- **SEPARATION POINT**
- **TRANSITION POINT**

# CALCULATED INVISCID PRESSURE GEOMETRY SENSITIVITY MATRIX

PERTURBATION TO y AT POINT j

RESULTING PERTURBATION TO $C_p$ DISTRIBUTION

CALCULATED MATRIX

- APPROACH: ANALYTICAL EXPANSION
  TO MCAIR PANEL METHOD

# CALCULATED VISCOUS DISPLACEMENT-PRESSURE SENSITIVITY MATRIX

PERTURBATION TO $C_p$ AT POINT j

RESULTING PERTURBATION TO DISPLACEMENT
DISTRIBUTION

CALCULATED MATRIX

- APPROACH: ANALYTICAL EXPANSION TO
  BOUNDARY LAYER METHOD

$$Y_i + \Delta Y_i = \delta_i^* + \sum_j \left( \frac{\partial \delta_i^*}{\partial C_{P_j}} \cdot \Delta C_{P_j} \right)$$

$$C_{P_i} + \sum_j \left( \frac{\partial C_{P_i}}{\partial Y_j} \cdot \Delta Y_j \right) = C_{P_i} + \Delta C_{P_i}$$

## PREDICTION ACCURACY AT HIGH ANGLE-OF-ATTACK (16°$\alpha$)
### GA(W)-1 AIRFOIL
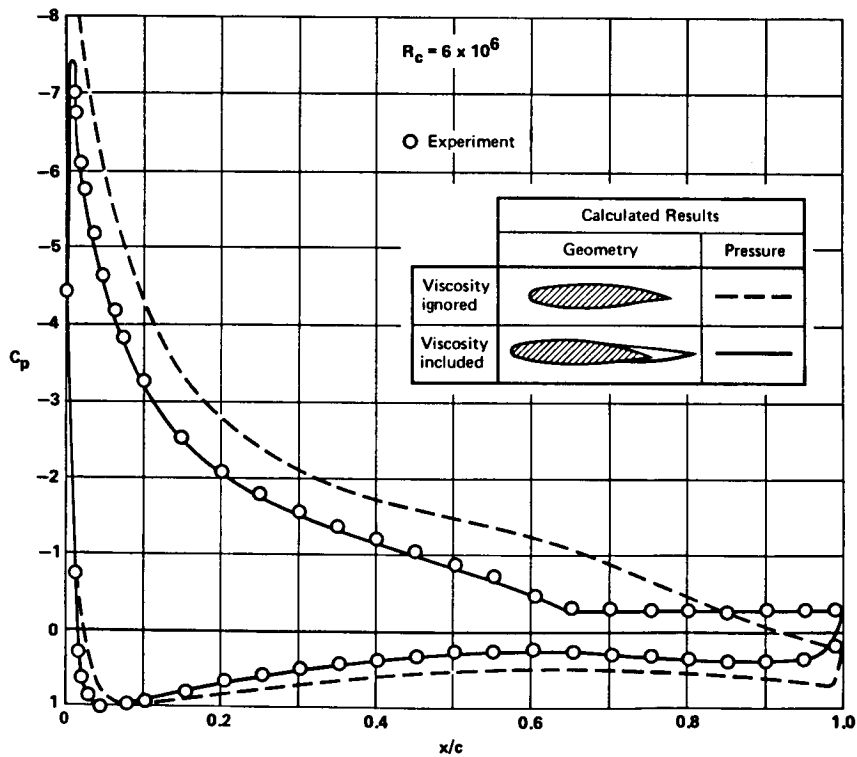
# TYPICAL CHANGE BETWEEN SUCCESSIVE ANGLES OF ATTACK



**EFFECTIVE SHAPE**

- – – Solution geometry from $16^\circ$ $\alpha$
- —— Solution at $18^\circ$ $\alpha$ (converged in one iteration)

$\alpha = 18^\circ$

$R_c = 6 \times 10^6$
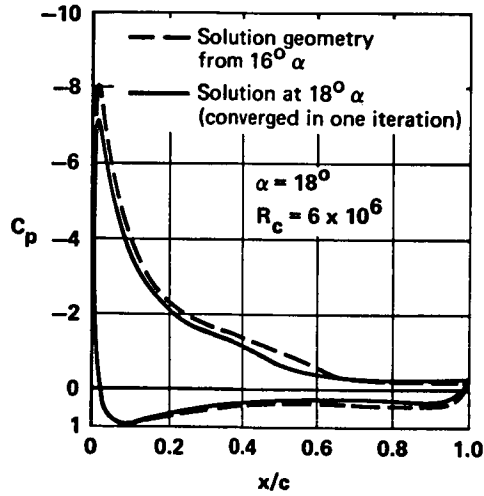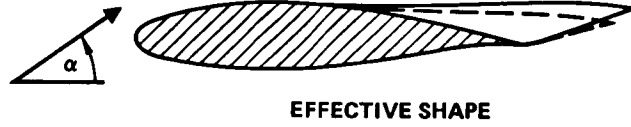
# ACCURACY OF FORCE AND MOMENT PREDICTIONS
## NASA GA(W)-1

$R_c = 6 \times 10^6$

—— Present Method
○ Experiment
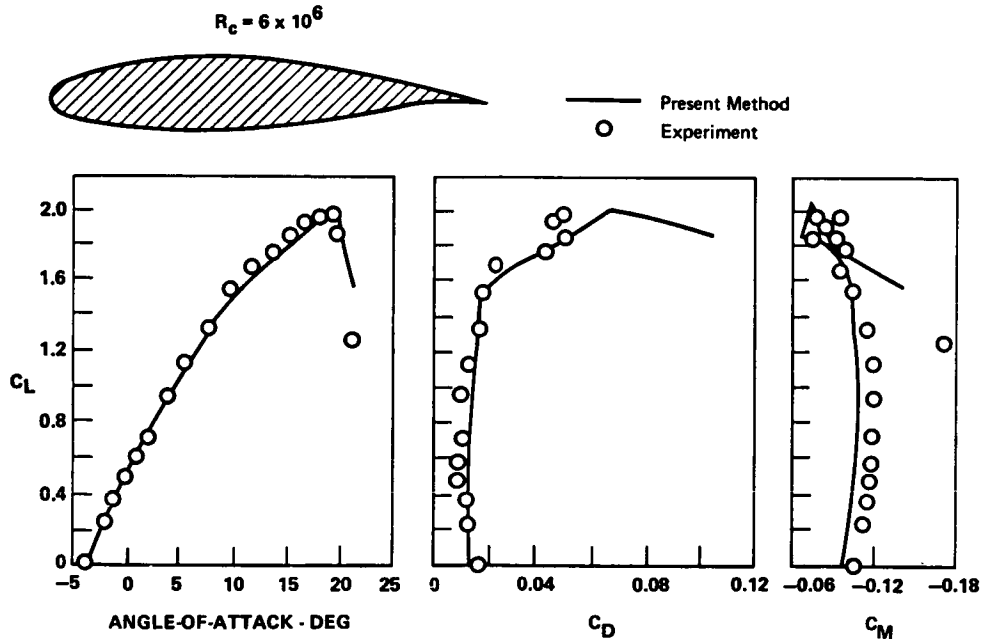
# EFFECT OF REYNOLDS NUMBER ON AIRFOIL PERFORMANCE



MS$_1$- 0313 AIRFOIL

| | STALLED AIRFOIL ANALYSIS PROGRAM | EXPERIMENT | REYNOLDS NUMBER |
|---|---|---|---|
| | – – – | □ | $2 \times 10^6$ |
| | —— | ○ | $6 \times 10^6$ |
| | ········ | △ | $9 \times 10^6$ |

ANGLE OF ATTACK ~ DEG

$C_D$

$C_M$
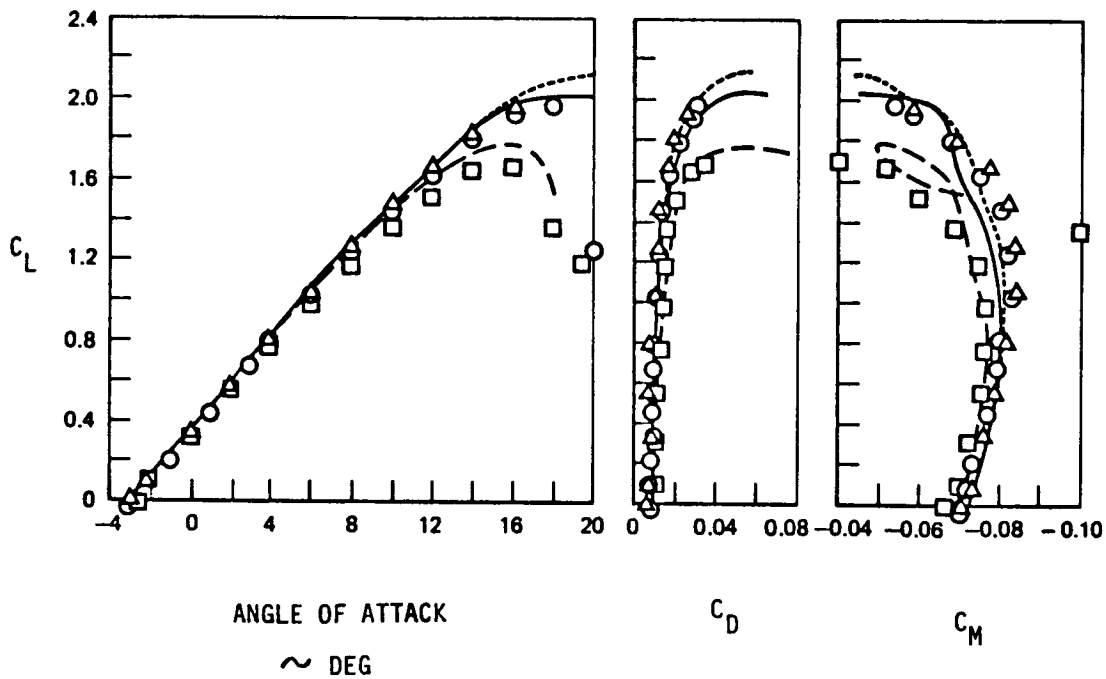
## CONCLUSIONS REGARDING SENSITIVITY ANALYSIS APPROACH

● POWERFUL EXTRAPOLATION TOOL

● APPROPRIATE FOR STRONG INTERACTION BETWEEN DISTINCT THEORIES

394

AIRCRAFT CONFIGURATION OPTIMIZATION
INCLUDING
OPTIMIZED FLIGHT PROFILES

L. A. McCullers
Kentron International, Inc.
Hampton, Virginia

# FLIGHT OPTIMIZATION SYSTEM

The Flight Optimization System (FLOPS) is an aircraft configuration optimization program developed for use in conceptual design of new aircraft and in the assessment of the impact of advanced technology. Figure 1 shows the modular makeup of the program. It contains modules for preliminary weights estimation, preliminary aerodynamics, detailed mission performance, takeoff and landing, and execution control. An optimization module is used to drive the overall design and in defining optimized flight profiles in the mission performance. Propulsion data, usually received from engine manufacturers, are used in both the mission performance and the takeoff and landing analyses. Although executed as a single in-core program, the modules are stored separately so that the user may select the appropriate modules (e.g., fighter weights versus transport weights) or leave out modules that are not needed.
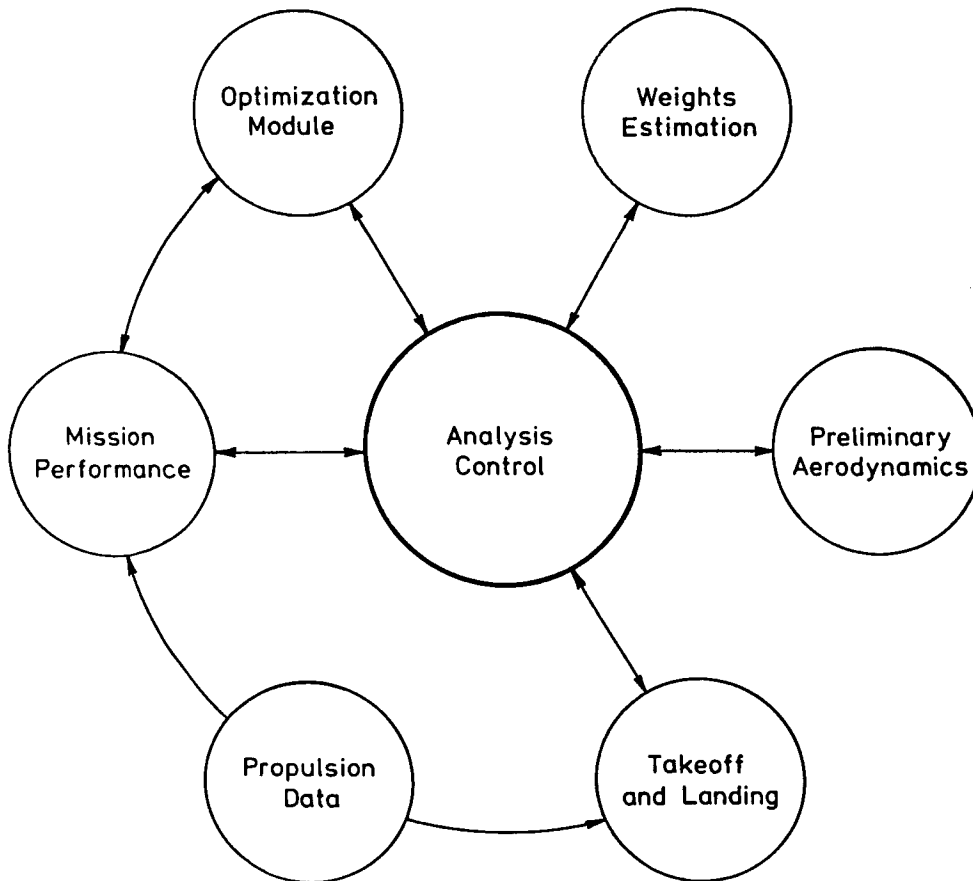


Figure 1

# WEIGHT EQUATION DEVELOPMENT

The weight equations in the preliminary weights estimation modules were developed by curve fitting statistical data from existing aircraft using an optimization program. A form which made sense physically was selected for each equation and all constants (coefficients, exponents, factors, etc.) were optimized using nonlinear programming techniques. The objective was to minimize the sum of the squares of the percentage errors between the actual and predicted weights. A nonlinear programming technique is superior to traditional curve fitting techniques in that the form of the equation and the variables are arbitrary. Fighter weight equations were developed using a data base of 22 recent fighter and attack aircraft. The transport data base included aircraft from the T-39 Sabreliner to the Boeing 747. Figure 2 shows the correlation for the fighter fuselage weight equation.

$$W_{fus} = 13.068 \, (GW/1000)^{.898} (Q/100)^{.635} (FL/FD)^{.502} (1 + .034 \, \Lambda_{VAR})$$
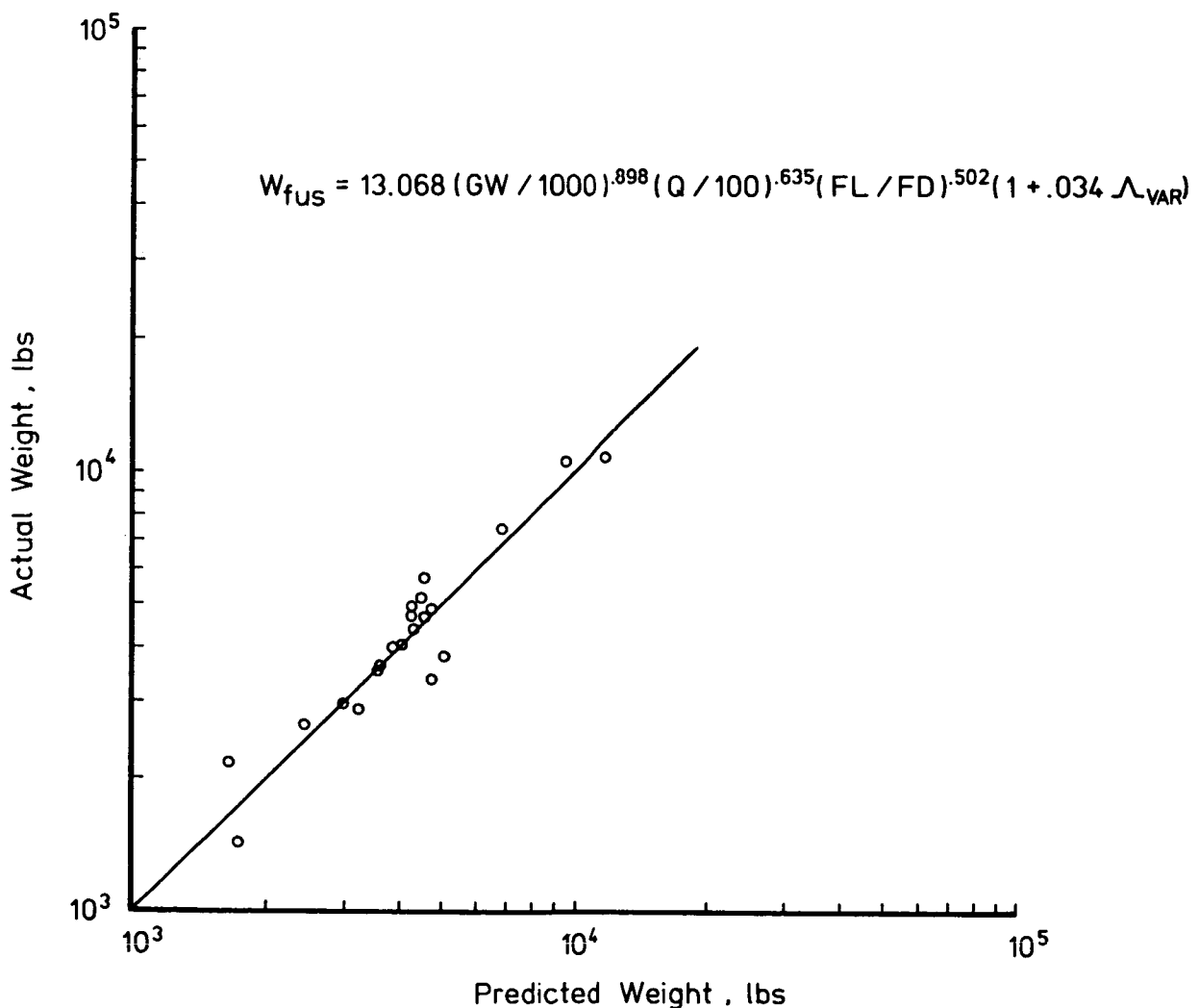


Figure 2

# WING WEIGHT EQUATION DATA

The FLOPS program was developed for the evaluation and optimization of advanced aircraft concepts which usually have unconventional wings. Insufficient statistical data existed to accurately predict the effects on wing weight of composite aeroelastic tailoring, forward sweep, and strut bracing and the relationship between sweep angle and flutter and divergence weight penalties for very high aspect ratio wings. The Aeroelastic Tailoring and Structural Optimization program (ATSO, ref. 1) was used to generate a series of optimum wing designs to predict these effects. Trend data from these studies, some of which are shown in figure 3, were used with data from existing aircraft to generate a multi-term equation that accurately predicts weights for existing wings and provides reasonable trend data for unconventional wings.
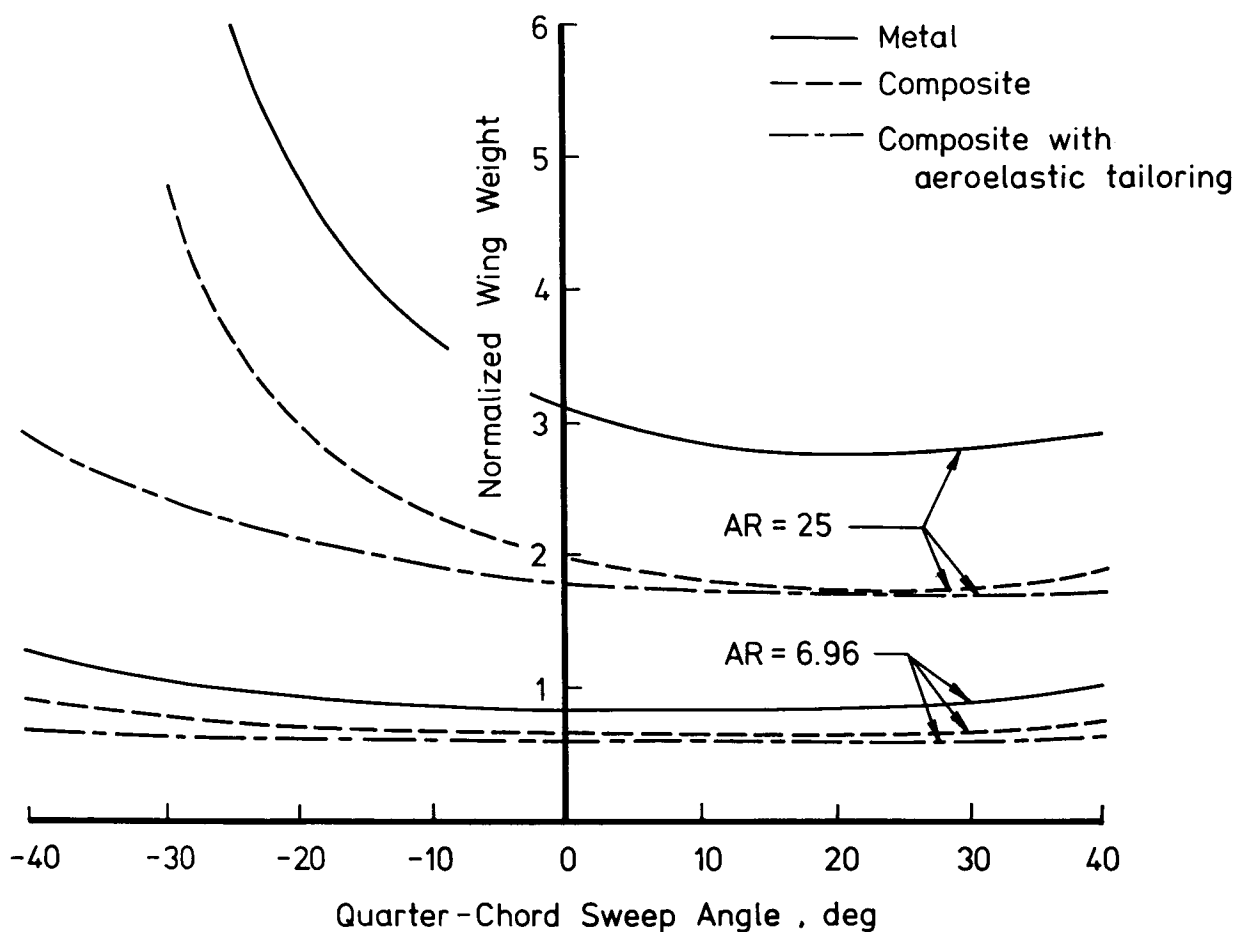


Figure 3

AERODYNAMICS MODULE

Preliminary aerodynamics data are generated using the Empirical Drag
Estimation Technique (EDET, ref. 2). Modifications have been made to improve
the accuracy of the calculations, such as implementation of the Sommer and
Short T' Method for skin friction drag (ref. 3). In addition, modifications
have been made to extend the range of the program to forward swept wings and
higher aspect ratios, as indicated in figure 4, and to more accurately account
for taper ratio. FLOPS also has the capability to use input aerodynamic data
and scale it with changes in wing area and engine size. Typically, this op-
tion is used for supersonic cruise aircraft concepts, and EDET is used for
subsonic aircraft.


o   EDET - Empirical Drag Estimation Technique

o   Modifications :

   ●   Forward Swept Wings

   ●   Sommer and Short T' Method

   ●   Efficiency Variation with Aspect Ratio
       and Taper Ratio

o   All or Part of Aerodynamics Data May Be
    Input and Scaled


Figure 4

# TAKEOFF AND LANDING ANALYSIS

FLOPS has the capability to perform detailed takeoff and landing analyses, as shown in figure 5, including evaluation of constraints on approach speed, missed approach climb gradient, second segment climb gradient, landing field length, and takeoff field length (or balanced field length for multi-engine aircraft) including ground effects. FLOPS also has a series of handbook-type formulas which predict these quantities. These formulas have been correlated against the detailed analyses and are normally used during optimization with the detailed analysis used for a point design evaluation.

TAKEOFF

Gear up

Climb

Obstacle

Start

Rotate

Liftoff

Start

Approach

LANDING

Obstacle

Flare

Touchdown

Brake

Stop
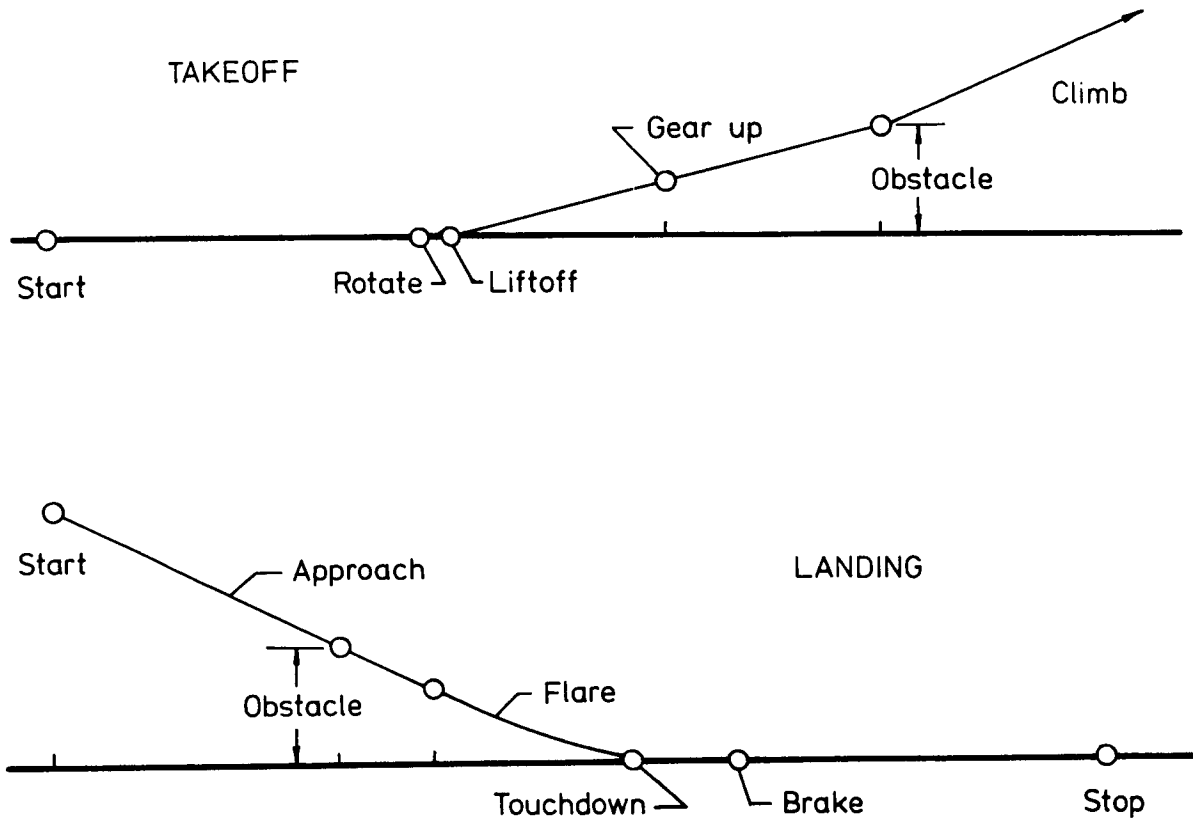
Figure 5

# MAIN MISSION ANALYSIS

Mission performance is calculated for all segments using a step integration technique to provide precise values for fuel burned, elapsed time, distance covered, and changes in speed and altitude. The primary mission can be composed of any reasonable combination of climbs, cruises, refuelings, payload releases, accelerations, turns, holds, and descents. A typical military attack mission is shown in figure 6. Speed and altitude continuity may be maintained or ignored at the analyst's option.
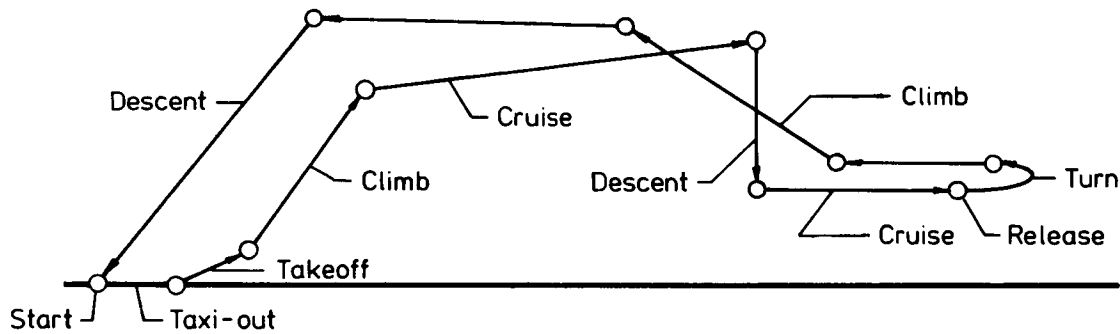


Figure 6

# RESERVE MISSION ANALYSIS

The reserves may be specified as a percentage of the total fuel or as the fuel required to fly an alternate mission or as a combination of the two. A typical reserve mission is shown in figure 7 consisting of fuel for a missed approach, flight to an alternate airport, and a specified hold. Each type of segment for the main and reserve missions is specified independently and the segments are linked together to fly the mission.
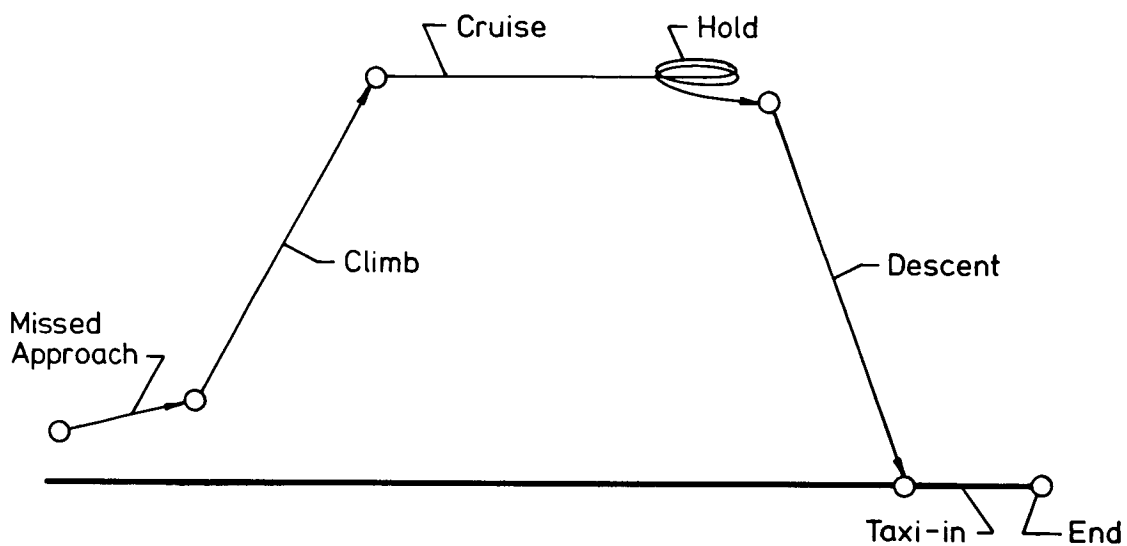


Figure 7

# CLIMB PROFILE OPTIMIZATION

The climb profiles may be specified by the user or they may be optimized by the program. For optimization, the climb is divided into a series of energy steps, and the combination of speed and altitude that maximizes the objective is determined for each energy level. The objective may be minimum time to climb, minimum fuel to climb, minimum time to distance (interceptor mission), or minimum fuel to distance (the most economical). Figure 8 shows a minimum fuel to climb profile superimposed on a contour plot of the objective function used for this case.
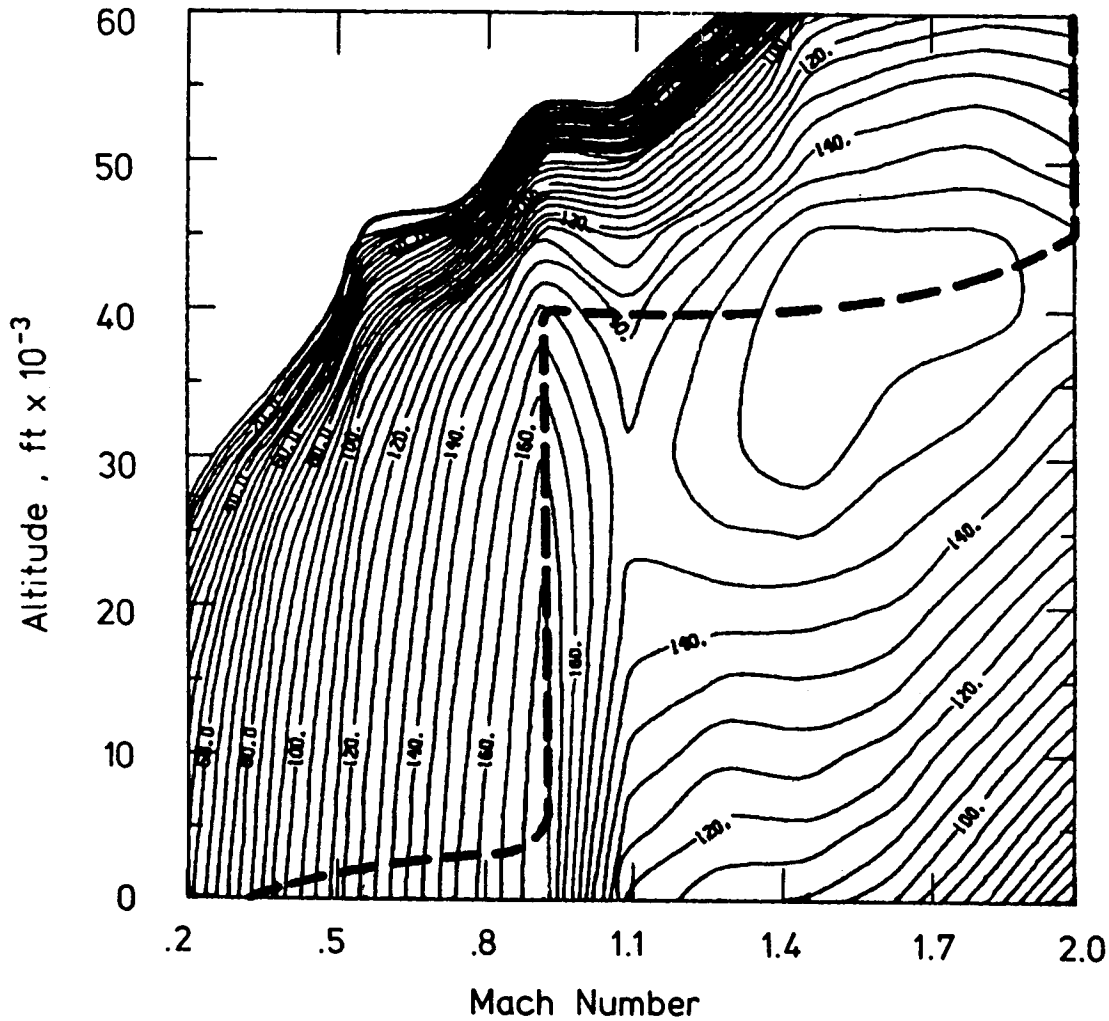


Figure 8

# MINIMUM TIME TO CLIMB PROFILE

A minimum time to climb profile is shown on figure 9 superimposed on contours of its objective function, specific excess power. The program tracks the maximum rate of climb until it reaches the specified cruise conditions. These plots were for a small, high thrust-weight ratio fighter. A variety of constraints, such as obeying FAA rules or not diving through Mach 1, may be placed on the climb segment. In addition, a suboptimization may be performed on engine power setting for minimum fuel options. This is normally used for engines with afterburners.
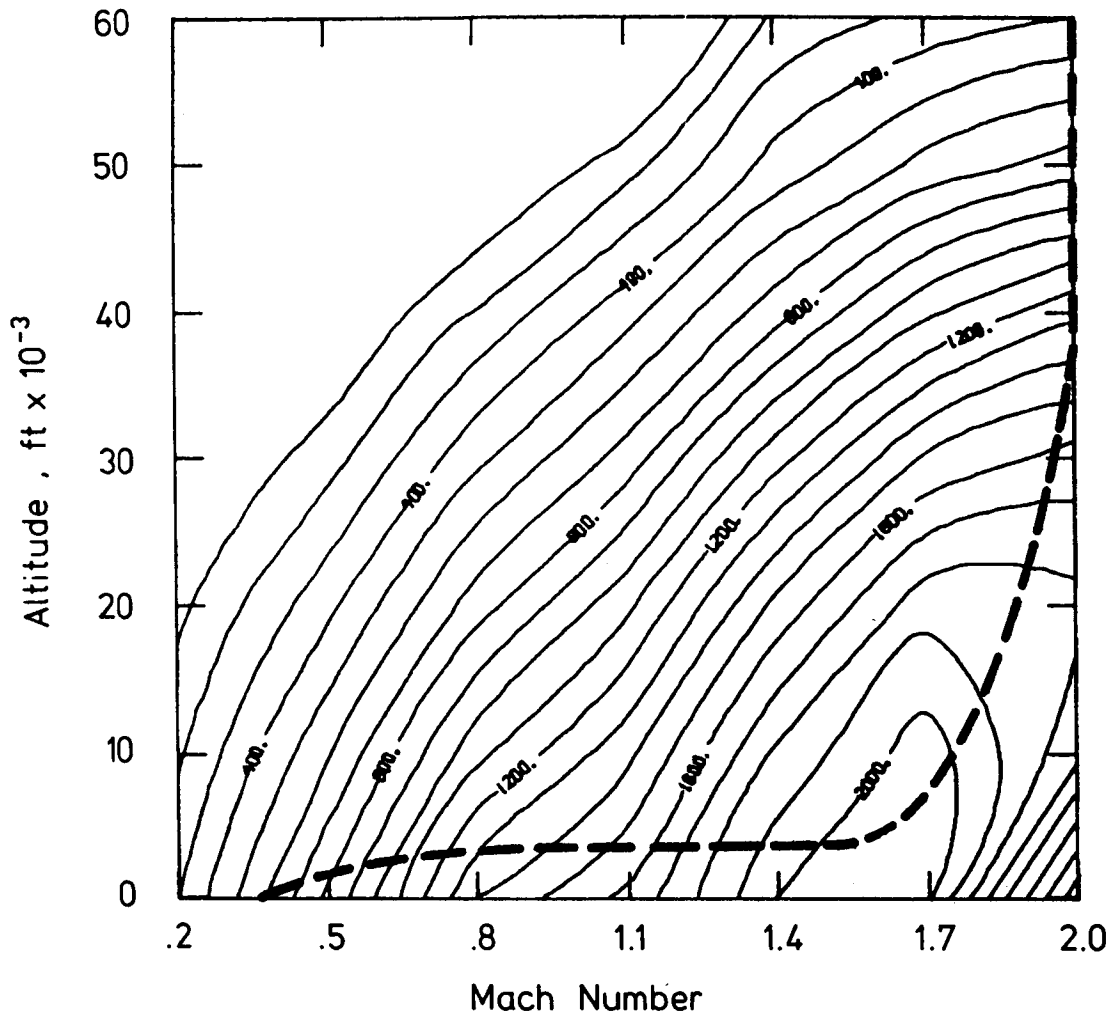


Figure 9

# IMPACT OF CRUISE OBJECTIVE

There are ten options for specifying each cruise segment: optimum altitude, optimum Mach number, or both for either maximum specific range or minimum fuel flow (endurance segment); fixed Mach number and altitude; fixed altitude and constant lift coefficient; and maximum Mach number for either fixed altitude or optimum altitude. In addition, a suboptimization may be performed on feathering engines. This is particularly useful in endurance missions. Figure 10 shows the differences in altitude and speed for a very long range turboprop transport flown to achieve maximum range and maximum endurance.
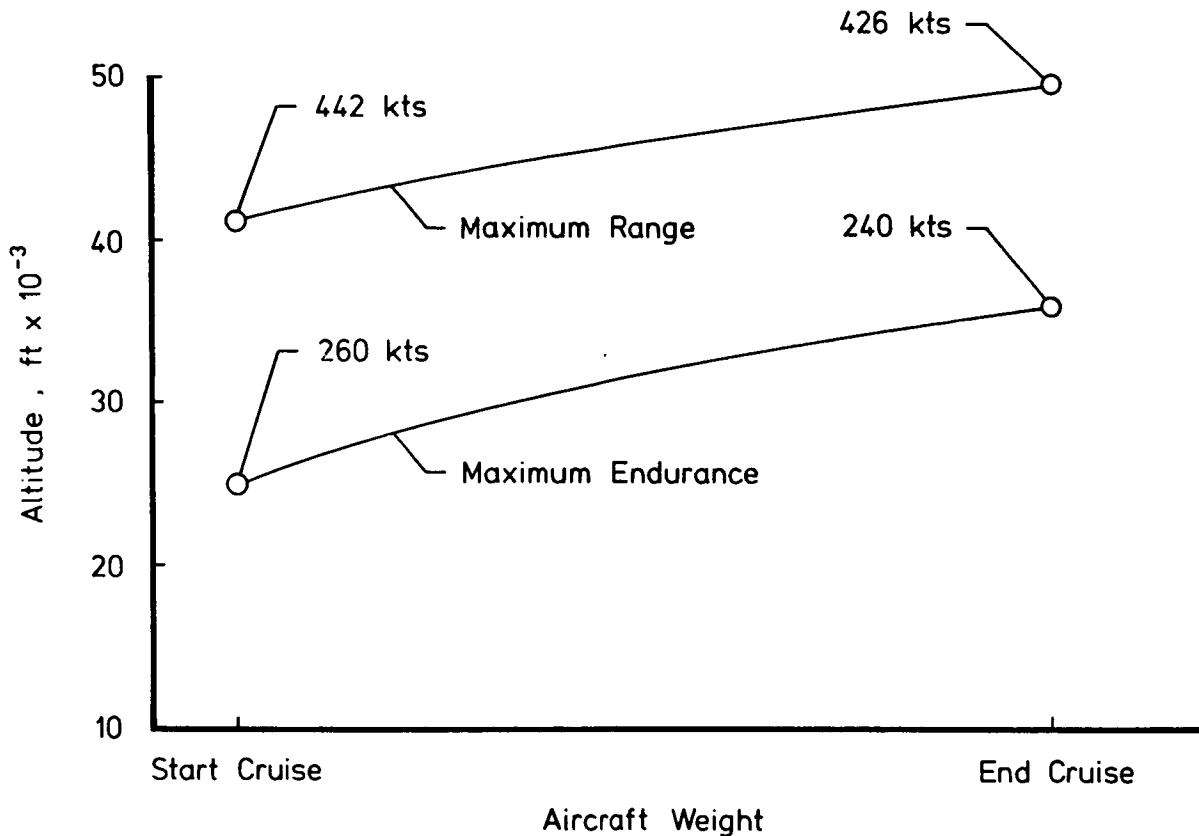
Figure 10

# DESCENT PROFILE

The descent segment may be flown along a specified profile, at a constant lift coefficient, or at the maximum lift-drag ratio. An optimized profile is shown in figure 11 superimposed on a contour plot of an objective function based on lift-drag ratio.
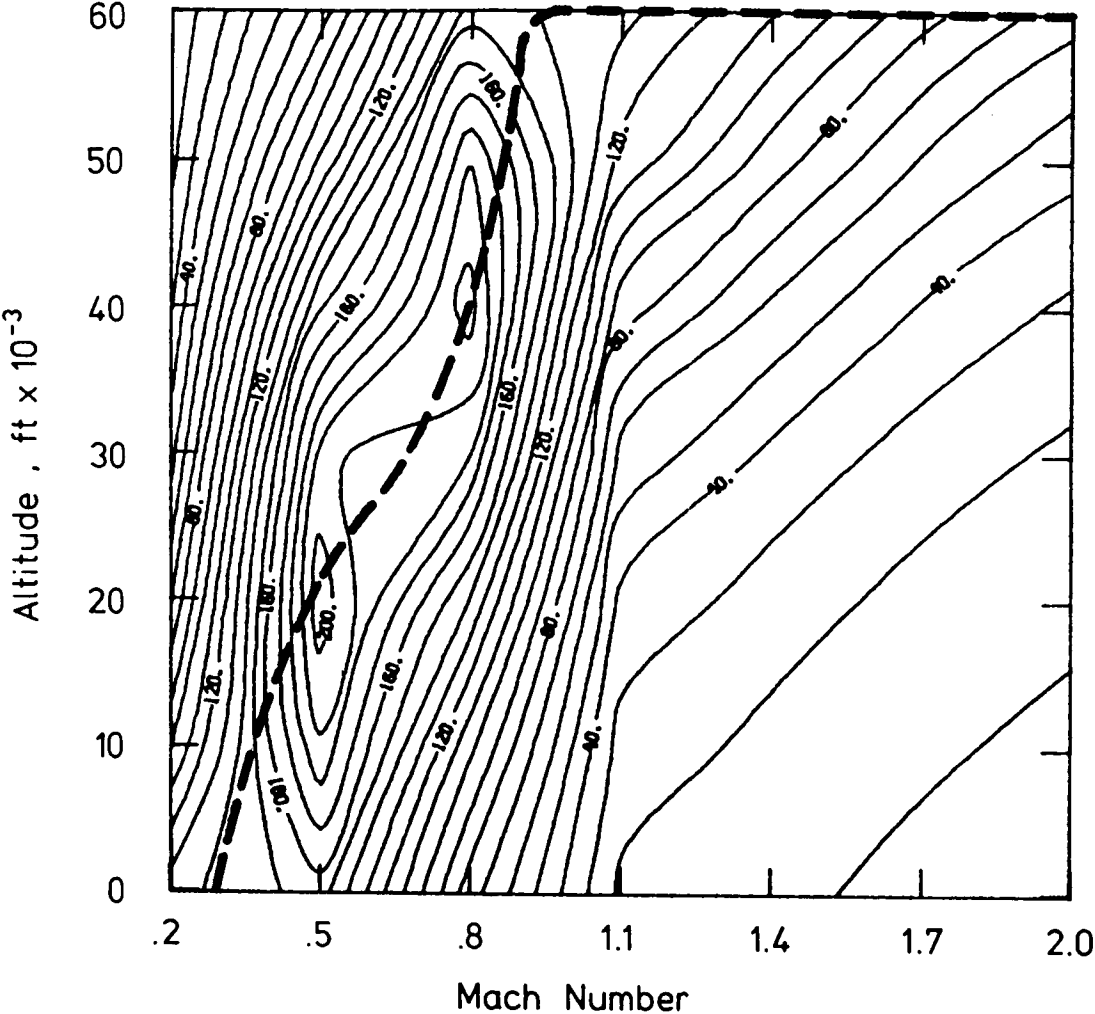


Figure 11

## DESIGN VARIABLES AND CONSTRAINTS

The nine available design variables for parametric variation or optimization as well as the six available constraints are shown in figure 12. Usually the altitude and Mach number are determined during flight profile optimization and are not used as design variables. Also, there are two modes of operation of the program. If the gross weight is specified (or an active design variable), the range (or endurance time) is calculated and should be a constraint in an optimization. A more effective way to use the program is to fix the range and iterate to find the gross weight. In this way the range constraint is always satisfied and the gross weight is a fall out, not a variable, leaving only six active design variables and five constraints for a normal problem.

# DESIGN VARIABLES            CONSTRAINTS

| DESIGN VARIABLES | CONSTRAINTS |
|---|---|
| o  Wing Area | o  Range |
| o  Wing Aspect Ratio | o  Takeoff Field Length |
| o  Wing Thickness – Chord Ratio | o  Landing Field Length |
| o  Wing Taper Ratio | o  Approach Speed |
| o  Wing Sweep Angle | o  Second Segment Climb Gradient |
| o  Thrust (Engine Size) | |
| o  Gross Weight | o  Missed Approach Climb Gradient |
| o  Maximum Altitude | |
| o  Maximum Mach Number | |

Figure 12

# PARAMETRIC VARIATION

A matrix of point designs may be created by parametrically varying one or more design variables. If two variables are used, contour plots such as the one shown in figure 13 can be obtained. Contours of supersonic cruise range are plotted for variations in wing loading (which can be used instead of wing area) and thrust-weight ratio (instead of thrust). Using this option, sensitivities to the design variables can be determined.

**Contours of Range**
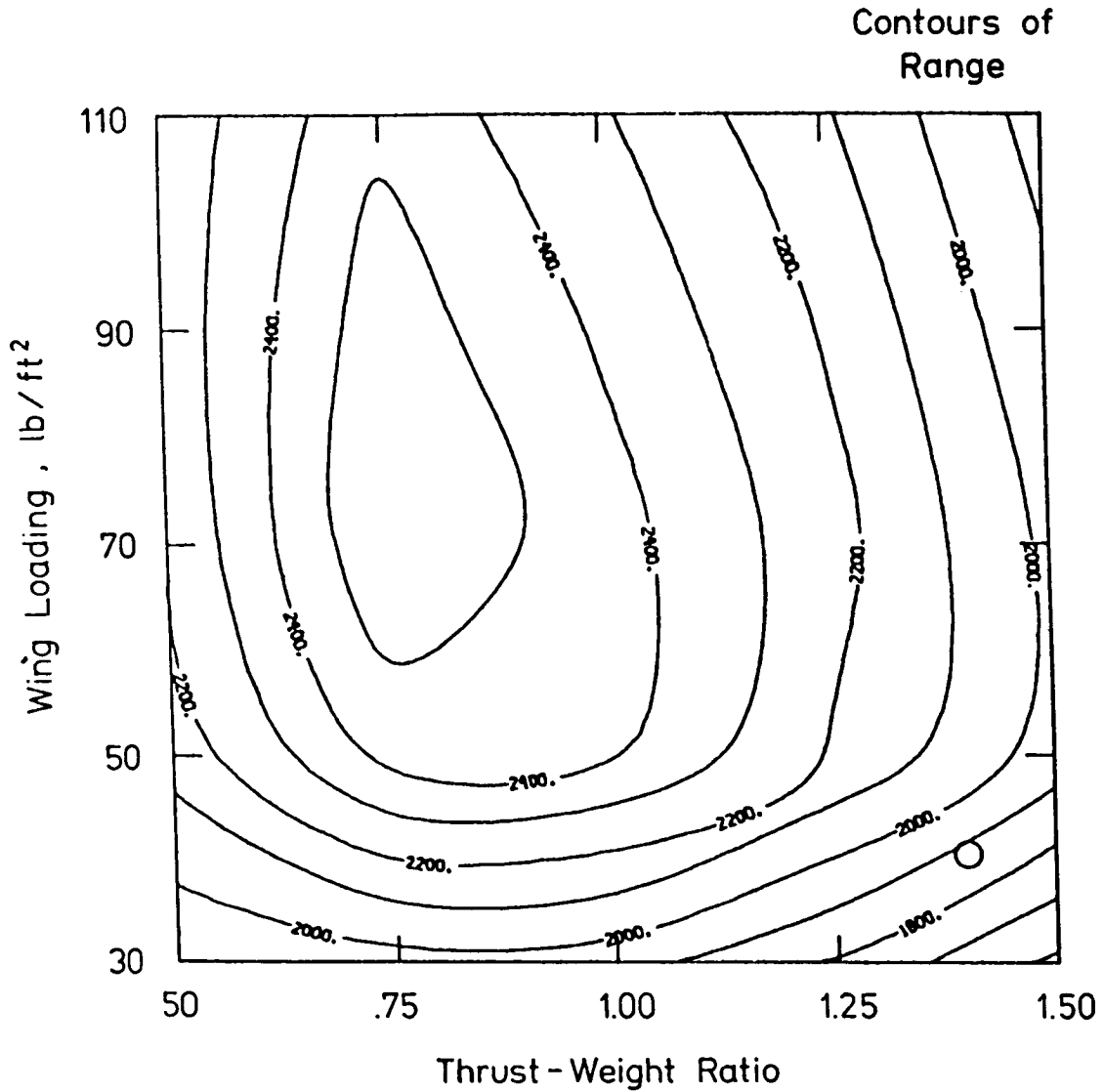


Figure 13

## OPTIMIZATION

As shown in figure 14, the objective function for the configuration optimization is a function of gross weight, total fuel, and range. This provides the capability to minimize the gross weight or fuel for a specified range or to maximize the range for a given gross weight. Figure 14 also indicates some of the optimization techniques used. Programs containing simplex and feasible directions algorithms were also used for optimization. The results, however, were inferior to those obtained using the DFP and BFGS algorithms.

o   Objective = $F_1 \cdot$ Weight + $F_2 \cdot$ Fuel + $F_3 \cdot$ Range

o   Davidon – Fletcher – Powell ( DFP ) or

   Broyden – Fletcher – Goldfarb – Shano ( BFGS ) Algorithm

o   Quadratic Extended Interior Penalty Function

o   One – Dimensional Search Uses Quadratic
   Interpolation to a Minimum

Figure 14

Figure 15 shows the path taken by the program for the unconstrained optimization of range on a fixed gross weight supersonic cruise fighter. The starting point thrust-weight ratio was 1.4 for high maneuverability, and the wing loading was 40 psf for a low approach speed. The figure shows that if both of these constraints are relaxed, the range may be increased by over 35 percent. All contour plots shown in this presentation were made using the FLOPS contour plot options.
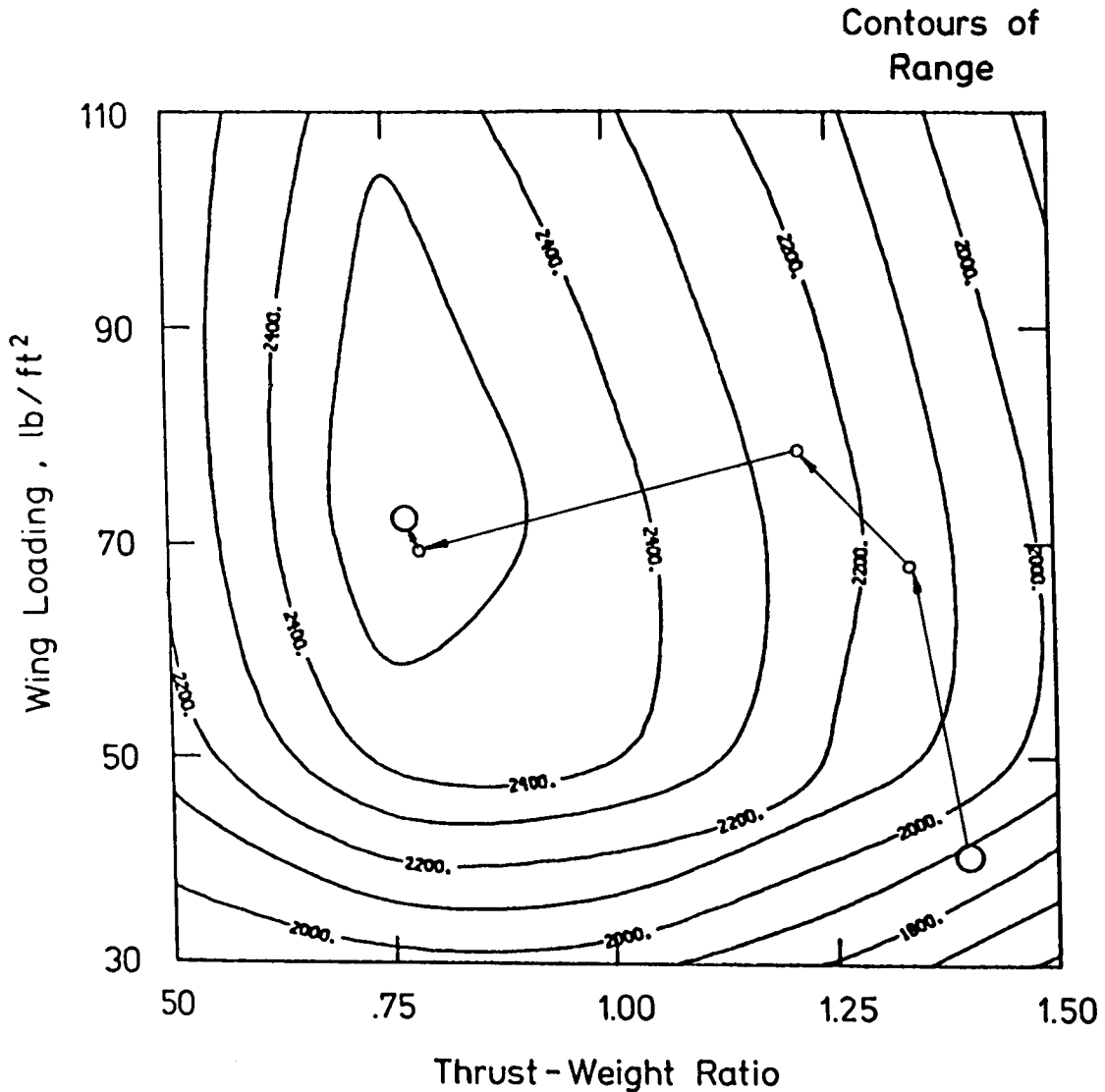


Figure 15

# WEIGHT VARIATION WITH OBJECTIVE FUNCTION

Figure 16 shows the variation of operating weight empty (OWE), gross weight, and mission fuel with aspect ratio for a series of optimum designs. Wing sweep, thickness-chord ratio, and wing area were also active design variables. Delta weights shown are from values for the minimum gross weight design at an aspect ratio of 9.3. The minimum OWE design at an aspect ratio of less than six saves about 12,000 pounds in OWE but uses over 40,000 pounds more fuel. The minimum fuel design at an aspect ratio of about 17 saves nearly 20,000 pounds of fuel but has an OWE penalty of nearly 100,000 pounds which is off the scale in the figure.
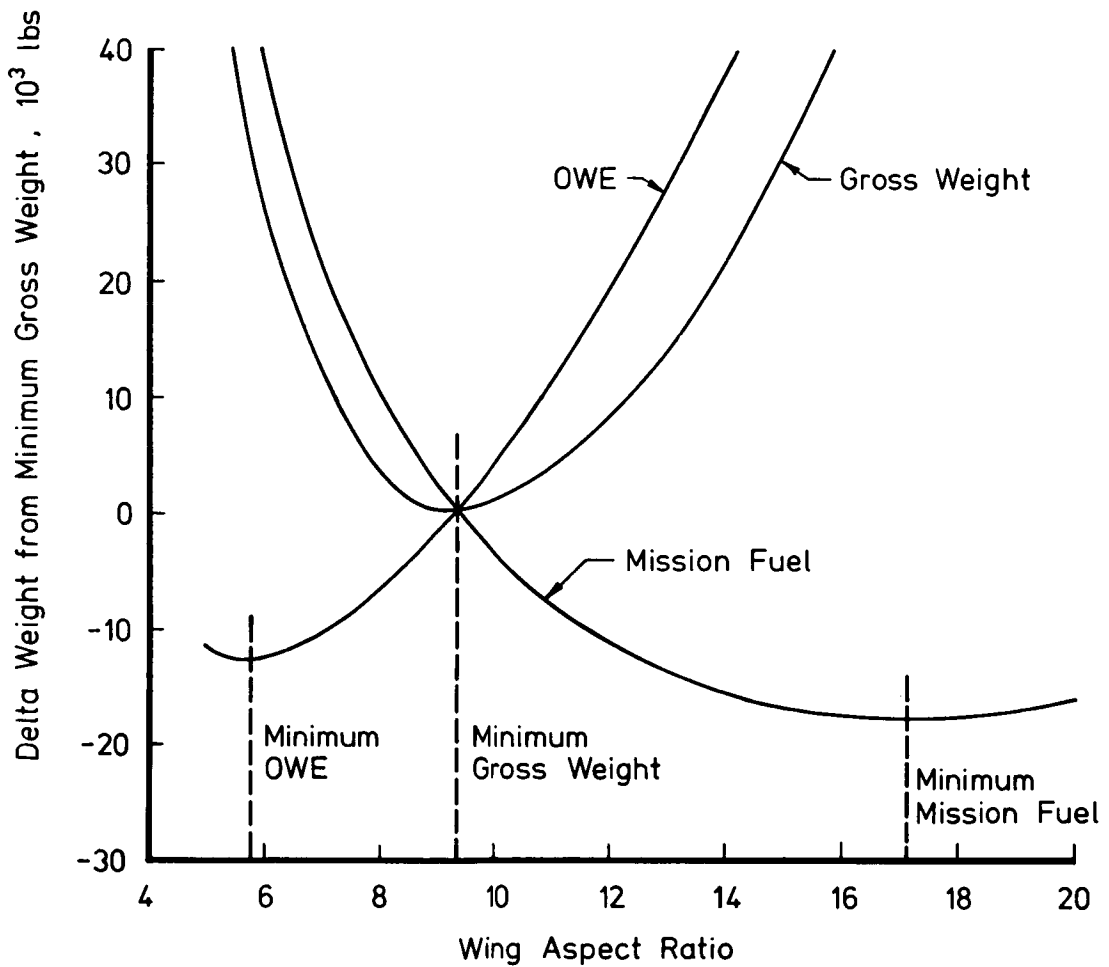


Figure 16

## PROBLEM AREAS

There are several problem areas, as shown in figure 17, which can make convergence to an optimum design more difficult. The degree of design variable interdependence necessitates the use of at least an approximate second order algorithm. For example, in order to increase the thickness-chord ratio, it is usually necessary to increase the wing sweep or decrease the Mach number. Design variable scaling, when dealing with variables several orders of magnitude apart, is as important as the optimization algorithm. The initial value to the two-thirds power seems to work well as a scaling factor. In a program with multiple nested iterations, analytical convergence is crucial to accurate gradients and smooth convergence of the optimization process. In addition, the objective function is not always well defined.

In conclusion, optimization techniques and programs exist which can be used routinely to help solve engineering problems. They should be used not necessarily to define the optimum piece of hardware to be built, but as essential tools in the design process.

o   Design Variable Interdependence

o   Design Variable Scaling   [ VALUE$^{2/3}$ ]

o   Analytical Convergence

o   What is the Objective ?

Figure 17

## REFERENCES

1. McCullers, L. A.; and Lynch, R. W.: Dynamic Characteristics of Advanced Filamentary Composite Structures, Volume II - Aeroelastic Synthesis Procedure Development. AFFDL-TR-73-111, 1974.

2. Feagin, Richard C.; and Morrison, William D., Jr.: Delta Method, An Empirical Drag Buildup Technique. NASA CR-15171, 1978.

3. Sommer, Simon C.; and Short, Barbara J.: Free-Flight Measurements of Turbulent-Boundary-Layer Skin Friction in the Presence of Severe Aerodynamic Heating at Mach Numbers From 2.8 to 7.0. NACA TN-3391, 1955.

# THE ADS GENERAL-PURPOSE OPTIMIZATION PROGRAM

G. N. Vanderplaats
Naval Postgraduate School
Monterey, California 93943

## THE GENERAL OPTIMIZATION TASK

The mathematical statement of the general nonlinear optimization problem is given in Figure 1. The vector of design variables, $X$, includes all those variables which may be changed by the ADS program in order to arrive at the optimum design. The objective function $F(X)$ to be minimized may be weight, cost or some other performance measure. If the objective is to be maximized, this is accomplished by minimizing $-F(X)$. The inequality constraints $g_j(X)$ include limits on stress, deformation, aeroelastic response or controllability, as examples, and may be nonlinear implicit functions of the design variables, $X$. The equality constraints $h_k(X)$ represent conditions that must be satisfied precisely for the design to be acceptable. Equality constraints are not fully operational in version 1.0 of the ADS program (ref. 1) although they are available in the Augmented Lagrange Multiplier method. The side constraints given by the last equation are used to directly limit the region of search for the optimum. The ADS program will never consider a design which is not within these limits.

The ADS program was developed under NASA Research Grant 57910.

FIND THE VECTOR OF DESIGN VARIABLES, $\underline{X}$, THAT WILL

MINIMIZE $\qquad F(\underline{X})$

SUBJECT TO

$$G_J(X) \leq 0 \qquad J=1,M$$

$$H_K(\underline{X}) = 0 \qquad K=1,L$$

$$X_I^L \leq X_I \leq X_I^U \qquad I=1,N$$

Figure 1

Figure 2 shows the overall design program structure with the particular structure of the ADS program on the right. The main program is provided by the user, as well as the routines to evaluate the objective and constraint functions (analysis) and their gradients (if available). If gradient information cannot be supplied by the user, an option is included in ADS to calculate this information by finite difference. The ADS program is itself a subroutine which controls the flow of the optimization process. When function or gradient evaluations are required, control is returned to the calling program. After the information is evaluated, ADS is called again and the optimization proceeds. This program organization provides the flexibility for the user to terminate the program any time control is returned to the main program and then re-start from this point at a later time. This also provides a convenient means of performing multi-level and multi-discipline optimization where several modules in the main program call ADS independently. Also, if during analysis a sub-optimization task is performed, this may call ADS, even though the results become input to a higher level in the overall optimization process. Within the ADS program a three level structure exists, with the control routine directing the flow of information. The Strategy level is used if the problem is to be solved by conversion to a sequence of unconstrained minimizations, sequential linear programming, or other technique whereby the optimization task is converted to a sequence of problems. The Optimizer performs the actual optimization task either directly, as in the method of feasible directions, or as a sub-problem within a Strategy. Finally, the One-Dimensional Search portion performs a line search to minimize the objective in a direction specified by the Optimizer. The particular techniques used at each of these three levels are described in the figures to follow.
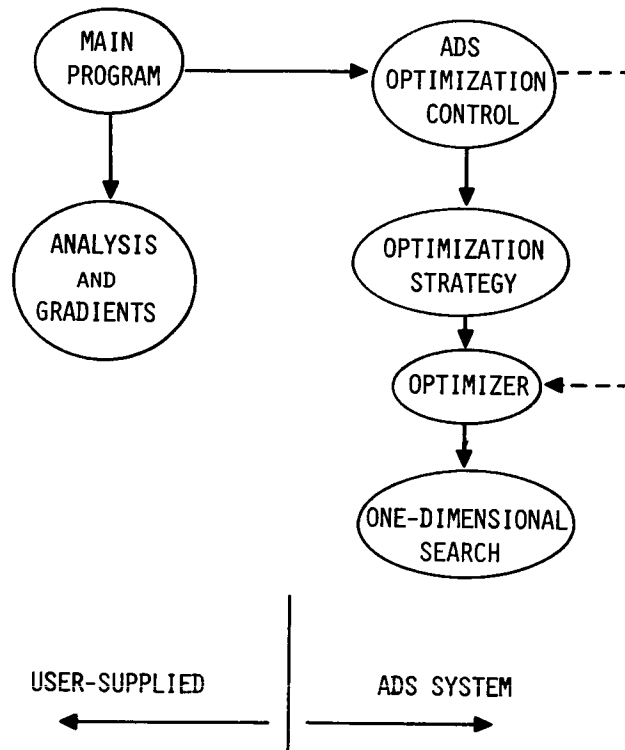


Figure 2

Figure 3 lists the Strategies available in version 1.0 of the ADS program. The parameter ISTRAT is used to designate the strategy to be used. ISTRAT=0 would be used if optimization is to be performed by a direct method such as the method of feasible directions or if the problem is unconstrained. Options 1-5 are various forms of Sequential Unconstrained Minimization Techniques. Option 6 is classical Sequential Linear Programming with move limits to insure stability. Option 7 is also a form of sequential linear programming, but instead of producing a sequence of infeasible designs as the optimum is approached, this method produces a sequence of improving feasible designs. Option 8 is a relatively new algorithm whereby the Lagrangian function is approximated as a quadratic and the constraints are linearized. This approach retains the essential nonlinearity of the problem, even for linear objective functions. Theoretically, a Quadratic Programming sub-problem is solved in this method. However, by using a direct method for optimization as opposed to a special purpose QP optimizer, some of the theoretical difficulties with the method are overcome. Early experience with the ADS program has shown that Sequential Linear Programming is more effective than is usually thought and that Sequential Quadratic Programming as coded here is a particularly powerful strategy.

| ISTRAT | METHOD |
|--------|--------|
| 0 | NONE. GO DIRECTLY TO OPTIMIZER |
| 1 | EXTERIOR PENALTY FUNCTION METHOD |
| 2 | LINEAR EXTENDED INTERIOR PENALTY FUNCTION METHOD |
| 3 | QUADRATIC EXTENDED INTERIOR PENALTY FUNCTION METHOD |
| 4 | CUBIC EXTENDED INTERIOR PENALTY FUNCTION METHOD |
| 5 | AUGMENTED LAGRANGE MULTIPLIER METHOD |
| 6 | SEQUENTIAL LINEAR PROGRAMMING |
| 7 | METHOD OF INSCRIBED HYPERSPHERES (METHOD OF CENTERS) |
| 8 | SEQUENTIAL QUADRATIC PROGRAMMING |

Figure 3

The optimization algorithms available in the ADS program are listed in Figure 4. The parameter IOPT is used to indicate the optimizer to be used. Options 2, 4 and 5 are used for solving unconstrained problems or for the unconstrained minimization sub-problem in a Sequential Unconstrained Minimization strategy. When an unconstrained optimization method is used, the design is still limited by the side constraints. This insures that, for example, minimum gage constraints are never violated, even when using a Sequential Unconstrained Minimization Technique at the Strategy level. Two feasible directions algorithms are available for constrained optimization. These are used for direct optimization of constrained problems as well as for solving the linear or quadratic programming sub-problem of strategies 6-8. The Method of Feasible Directions algorithm is essentially the same as that contained in the earlier program, CONMIN (ref. 2). The Modified Method of Feasible Directions (ref. 3) is similar to the Generalized Reduced Gradient Method, but is more storage efficient. Also, in the one-dimensional search, this method uses a least squares technique rather than Newton's method for maintaining feasibility.

## UNCONSTRAINED

| IOPT | METHOD |
|------|--------|
| 2 | FLETCHER-REEVES CONJUGATE DIRECTION METHOD |
| 4 | DAVIDON-FLETCHER-POWELL VARIABLE METRIC METHOD |
| 5 | BROYDON-FLETCHER-GOLDFARB-SHANNO VARIABLE METRIC METHOD |

## CONSTRAINED

| IOPT | METHOD |
|------|--------|
| 1 | METHOD OF FEASIBLE DIRECTIONS |
| 3 | MODIFIED METHOD OF FEASIBLE DIRECTIONS |

Figure 4

Figure 5 lists the One-Dimensional Search routines available in ADS. Five algorithms are available for both constrained and unconstrained problems. The parameter IONED is used to identify the algorithm to be used. Options 1 and 6 are usually not useful except for special purpose applications. The remaining methods are different combinations of the Golden Section method and Polynomial Interpolation. The Golden Section method is normally only useful if function evaluations are very cheap and if high precision of the one-dimensional search is desired. While this method is usually applied only to unconstrained problems, it has been modified to find the constrained minimum for use in ADS. Normally options 4 and 9 are the most efficient and reliable, where the solution is first bounded and then refined by polynomial interpolation. One unique feature of the ADS program is that, if no feasible solution can be found, a design is sought which minimizes the constraint violations. Thus, on termination, the constraints which must be relaxed to produce a realistic design are easily identified.

## UNCONSTRAINED

| IONED | METHOD |
|-------|--------|
| 1 | BOUNDS ONLY |
| 2 | GOLDEN SECTION METHOD |
| 3 | GOLDEN SECTION + POLYNOMIAL INTERPOLATION |
| 4 | BOUNDS + POLYNOMIAL INTERPOLATION |
| 5 | POLYNOMIAL INTERPOLATION/EXTRAPOLATION WITHOUT FIRST GETTING BOUNDS |

## CONSTRAINED

| IONED | METHOD |
|-------|--------|
| 6 | BOUNDS ONLY |
| 7 | GOLDEN SECTION METHOD |
| 8 | GOLDEN SECTION + POLYNOMIAL INTERPOLATION |
| 9 | BOUNDS + POLYNOMIAL INTERPOLATION |
| 10 | POLYNOMIAL INTERPOLATION/EXTRAPOLATION WITHOUT FIRST GETTING BOUNDS |

Figure 5

ADS PROGRAM OPTIONS

Not all combinations of Strategy, Optimizer and One-Dimensional search are appropriate. For example, an unconstrained minimization method would not be a valid optimization technique for use with Sequential Linear Programming. Figure 6 shows the acceptable combinations of modules, where the numbers correspond to the control parameters ISTRAT, IOPT and IONED. In this table, an X is used to denote a valid combination of methods. First, a Strategy is chosen appropriate to the problem at hand. Next, moving across the row, the Optimizer is chosen from among the valid options, and finally, moving down the column, the One-Dimensional search routine to be used is chosen. An example is shown by the solid line beginning at Strategy number 5 (the Augmented Lagrange Multiplier Method). The Broydon-Fletcher-Goldfarb-Shanno optimizer (IOPT=5) is used to solve the unconstrained minimization sub-problem and the One-Dimensional search is to be performed using polynomial interpolation after first bounding the solution (IONED=4). It is clear from this table that a large number of independent combinations of methods are available. It may be expected that, as experience is gained with the program, many of the options will prove not to be useful for practical design and that a few will survive as preferred options. One of the unique features of the program organization is that one-to-one comparisons may be made between methods by changing only four input parameters to ADS. No other coding modifications are needed.

| STRATEGY | OPTIMIZER | | | | |
|---|---|---|---|---|---|
| | 1 | 2 | 3 | 4 | 5 |
| 0 | X | X | X | X | X |
| 1 | 0 | X | 0 | X | X |
| 2 | 0 | X | 0 | X | X |
| 3 | 0 | X | 0 | X | X |
| 4 | 0 | X | 0 | X | X |
| ⑤ | 0 | X | 0 | X | Ⓧ |
| 6 | X | 0 | X | 0 | 0 |
| 7 | X | 0 | X | 0 | 0 |
| 8 | X | 0 | X | 0 | 0 |
| ONE-DIM. SEARCH | | | | | |
| 1 | 0 | 0 | 0 | 0 | 0 |
| 2 | 0 | X | 0 | X | X |
| 3 | 0 | X | 0 | X | X |
| 4 | 0 | X | 0 | X | Ⓧ |
| 5 | 0 | X | 0 | X | X |
| 6 | 0 | 0 | 0 | 0 | 0 |
| 7 | X | 0 | X | 0 | 0 |
| 8 | X | 0 | X | 0 | 0 |
| 9 | X | 0 | X | 0 | 0 |
| 10 | X | 0 | X | 0 | 0 |

Figure 6

Figure 7 shows the program organization for using ADS. The user must begin by allocating array storage for the vector of design variables, constraints, and design variable bounds, as well as work arrays for use in ADS. Also at this point the basic control parameters such as the number of design variables, the options ISTRAT, IOPT and IONED and similar parameters are defined. The basic program flow control parameter INFO is initialized here to -2. Then the ADS subroutine is called to initialize all internal parameters to their default values. These include convergence criteria, finite difference steps and the like. Control is then returned to the calling program and the user is free to over-ride the default values of the internal parameters if desired. ADS is then called again and the optimization process proceeds from here. Whenever function or gradient information is needed, control is returned to the calling program with INFO=1 or 2 respectively. The user evaluates the needed information and calls ADS again. This iterative process continues until the optimization task is complete, at which point ADS returns a value of INFO=0. All information is transferred to and from ADS via a single parameter list. No additional common blocks or data transfer mechanisms are required. Any time that control is returned to the calling program, the user may store the contents of the parameter list on mass storage and terminate the program. The program may be restarted from here by reading the information back and continuing the program flow. In the event that the user wishes to use all default options in ADS, the first call to ADS may be omitted. In this case INFO is initialized to zero and the optimization proceeds without the first initialization step.

BEGIN

ALLOCATE ARRAY STORAGE

DEFINE BASIC VARIABLES

INFO ← -2

CALL ADS (INFO,ISTRAT,IOPT,IONED, . . )

OVER-RIDE DEFAULT PARAMETERS
WHICH ARE NOW CONTAINED IN
ARRAYS WK AND IWK IF DESIRED

CALL ADS (INFO,ISTRAT,IOPT,IONED, . . )

INFO = 0 — YES → EXIT
OPTIMIZATION
IS COMPLETE

NO

YES — INFO = 1 — NO

EVALUATE
OBJECTIVE
AND
CONSTRAINT
FUNCTIONS

EVALUATE
GRADIENT OF
OBJECTIVE
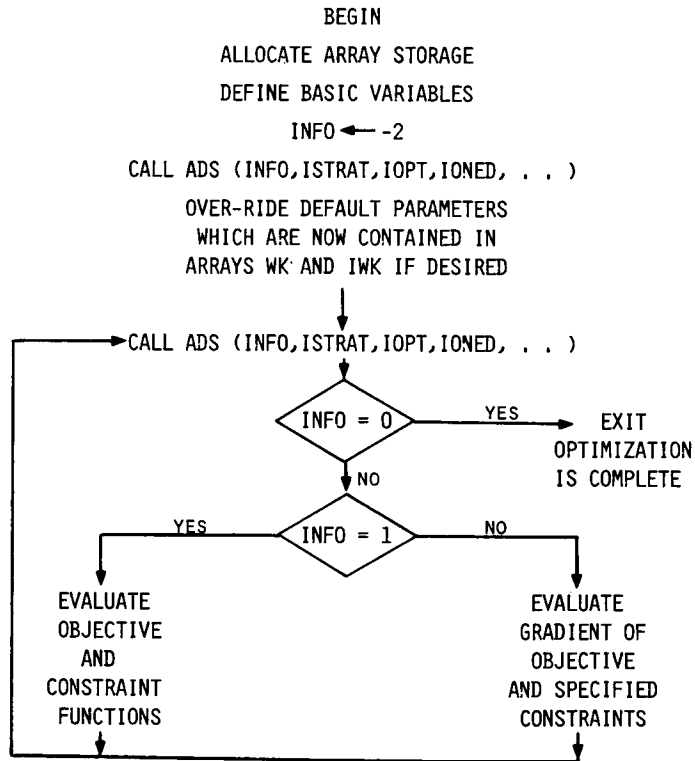AND SPECIFIED
CONSTRAINTS

Figure 7

## DESIGN EXAMPLE

Figure 8 gives an example of the ADS program for solution of the 10-bar truss commonly found in the literature. Here no special effort has been made to formulate the problem for efficient optimization. The design variables are the member cross-sectional areas (as opposed to reciprocal variables which would be much more efficient). The structure is stress constrained, subject to the single loading case shown. The table gives the optimization results for various combinations of ISTRAT, IOPT and IONED. The number of function and gradient evaluations is also given. In this example, all default parameters in ADS are used and no attempt was made to "fine tune" the program to this problem. Also, it should be noted that as experience is gained with the program, these defaults will be modified to improve efficiency of the general design task. As may be expected, Sequential Unconstrained Minimization methods required a relatively high number of function and gradient evalutions. Also, the use of the Golden Section algorithm in the One-Dimensional search dramatically increases the number of function evaluations without noticable improvement in the result. Direct methods appear to be relatively efficient and the Sequential Quadratic Programming method is seen to be a particularly powerful Strategy. Assuming early experience with this method is indicative of its efficiency for general design problems, this appears to offer an impressive capability for engineering design. As experience is gained with the program, further refinements can be expected. The over-all motivation in the development of the ADS program has been to provide a user-friendly, general, and efficient tool for a wide variety of engineering design problems of practical interest.

DESIGN EXAMPLE: THE 10-BAR TRUSS
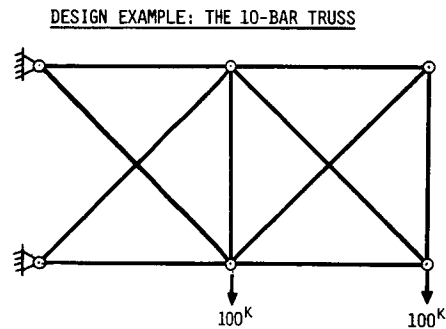


| ISTRAT | IOPT | IONED | OPTIMUM | ANALYSES | GRADIENTS |
|--------|------|-------|---------|----------|-----------|
| 0 | 1 | 7 | 1516.8 | 305 | 39 |
| 0 | 1 | 9 | 1519.7 | 120 | 30 |
| 0 | 3 | 8 | 1497.8 | 489 | 8 |
| 0 | 3 | 9 | 1497.3 | 114 | 6 |
| 1 | 2 | 4 | 1648.4 | 114 | 27 |
| 1 | 4 | 2 | 1534.2 | 384 | 37 |
| 1 | 4 | 5 | 1549.4 | 109 | 33 |
| 2 | 4 | 5 | 1522.7 | 133 | 41 |
| 2 | 5 | 2 | 1505.2 | 528 | 51 |
| 3 | 4 | 4 | 1511.3 | 211 | 51 |
| 4 | 5 | 4 | 1500.8 | 209 | 52 |
| 5 | 4 | 4 | 1504.0 | 210 | 47 |
| 5 | 5 | 4 | 1496.3 | 235 | 54 |
| 6 | 3 | 9 | 1510.3 | 20 | 20 |
| 7 | 3 | 10 | 1509.5 | 47 | 47 |
| 8 | 1 | 9 | 1498.0 | 28 | 6 |
| | CONMIN | | 1500.9 | 104 | 31 |

Figure 8

## REFERENCES

1. Vanderplaats, G. N., Sugimoto, H. and Sprague, C. M., "ADS-1: A New General-Purpose Optimization Program," Proc. AIAA/ASME/ASCE/AHS 24th Structures, Structural Dynamics and Materials Conference, Lake Tahoe, NV, May 1983, AIAA Paper No. 83-0831-CP.

2. Vanderplaats, G. N., "CONMIN - A FORTRAN Program for Constrained Function Minimization, User's Manual," NASA TM X-62282, Aug. 1973.

3. Vanderplaats, G. N., "A Robust Feasible Directions Algorithm for Design Synthesis," Proc. AIAA/ASME/ASCE/AHS 24th Structures, Structural Dynamics and Materials Conference, Lake Tahoe, NV, May 1983.

# SHAPE DESIGN SENSITIVITY ANALYSIS
## OF BUILT-UP STRUCTURES

Kyung K. Choi
Center for Computer Aided Design
The University of Iowa
Iowa City, Iowa

# SHAPE DESIGN OF A FILLET

Selection of the best shape of a fillet in a tension bar such that no yielding occurs has long attracted the attention of engineers. Dimensions and notations for the bar and fillet are shown in figure 1. With symmetry, only the upper half of the bar is considered. The boundary segment $\Gamma^1$ is to be varied, but with fixed points at A and B. The segment $\Gamma^3$ is the central line of the fillet and $\Gamma^4$ and $\Gamma^2$ are uniformly loaded edges.

The optimal design problem is to find a boundary shape $\Gamma^1$ to minimize the total area of the fillet such that no yielding occurs. Constraints are placed on von Mises yield stress, averaged over small regions or finite elements $\Omega_k$ on which $m_k$ is a characteristic function with value 1/(area of $\Omega_k$) and $\phi(\sigma(z))^k$ is normalized von Mises yield stress.

The classical boundary value problem is reduced to a variational or energy related problem which not only has excellent properties of existence and uniqueness but also provides the mathematical foundation for finite element analysis. The variational formulation may be viewed as the principle of virtual work and the finite element method as an application of the Galerkin method to the variational equation for approximate solution of the boundary value problem.
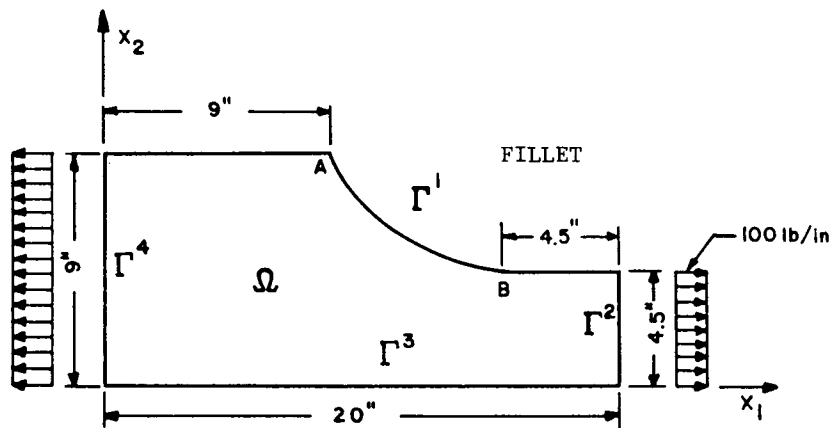


Design Variable: Shape of $\Gamma^1$

Cost: $\psi_0 = \iint_\Omega d\Omega$

Constraint: $\psi_k = \iint_\Omega \phi(\sigma(z))m_k \, d\Omega \leqslant 0$, $\qquad k = 1,2,\ldots,NE$

Virtual Work Equation:

$$a(z,\bar{z}) \equiv \iint_\Omega \sum_{i,j=1}^{2} [\sigma^{ij}(z)\epsilon^{ij}(\bar{z})]d\Omega = \int_{\Gamma^2} \sum_{i=1}^{2} T_i \bar{z}_i \, d\Gamma \quad,$$

for all kinematically admissible virtual displacements $\bar{z}$

Figure 1

# MATERIAL DERIVATIVE AND ADJOINT VARIABLE METHOD

Since shape of the domain is treated as the design variable, it is convenient to think of $\Omega$ as a continuous medium and utilize the material derivative idea from continuum mechanics. The process of deforming $\Omega$ to a new domain $\Omega_\tau$ may be viewed as a dynamic process as shown in figure 2. One can define a transformation as $x_\tau = x + \tau V(x)$ where $\tau$ plays the role of time and x is a point in initial domain $\Omega$ that moves to point $x_\tau$ in the deformed domain $\Omega_\tau$. Note that the "shape design velocity" $V(x)$ of point x can be considered as a perturbation of design variable. A detailed discussion of this method can be found in references 1 and 2.

The adjoint variable method of design sensitivity analysis (refs. 1, 2, and 3) is applied by defining an adjoint equation for an adjoint displacement field $\lambda^k$ to obtain the variation $\psi_k'$ where $\Omega_k$ is the small region or the finite element considered, $m_k$ is a characteristic function for the corresponding $\Omega_k$, and $\phi$ is the normalized von Mises yield stress.

Note that only boundary integrals appear in the expression for $\psi_k'$. The normal movement $(V^T n)$ plays the role of shape design perturbation and can be expressed in terms of shape design parameters.



$$x_\tau = x + \tau V(x)$$

$$V(x) = \frac{dx_\tau}{d\tau}$$
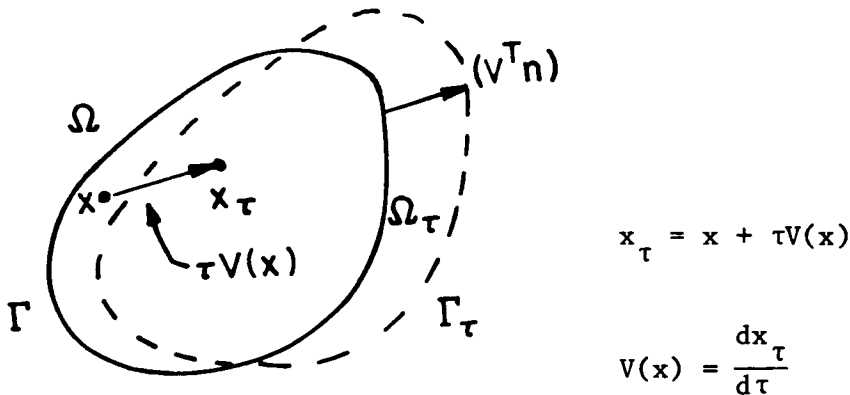
Material derivative of cost: $\psi_0' = \int_\Gamma (V^T n) d\Gamma$

Material derivative of constraint $\implies$ Adjoint equation

$$a(\lambda^k, \bar{\lambda}) = \iint_\Omega \sum_{i,j=1}^{2} [\frac{\partial \phi}{\partial \sigma^{ij}} (z) \sigma^{ij}(\bar{\lambda})] m_k \, d\Omega$$

$$\psi_k' = - \int_{\Gamma 1} [\sum_{i,j=1}^{2} \sigma^{ij}(z) \varepsilon^{ij}(\lambda^k)] (V^T n) d\Gamma - \int_{\Gamma_k} m_k (\psi_k - \phi)(V^T n) d\Gamma$$

Figure 2

# PARAMETRIZATION OF BOUNDARY $\Gamma$

In order to compute design sensitivity $\psi_k'$, the variable boundary should be parameterized in terms of a design variable vector b (refs. 2 and 3). Presume that points on the boundary $\Gamma_\tau$ are specified by a vector $x_\tau(\alpha;b)$ from the origin of the coordinate system to the point S on the boundary, as shown in figure 3, where $\alpha$ is a parameter vector.

When the vector b of design variables, $b = [b_1,\ldots,b_m]^T$, has been defined, the domain optimization problem reduces to selection of the finite dimensional vector b to minimize a cost function, subject to the constraints. By defining $x_\tau(\alpha;b) \equiv x(\alpha;b + \tau\delta b)$, one can define the velocity field at the boundary by taking the derivative of $x_\tau$ with respect to $\tau$. Taking the scalar product of V with the unit outward normal to the boundary $\Gamma$ and substituting the result into the analytical expressions for $\psi_0'$ and $\psi_k'$ yields numerically computable sensitivity formulas.
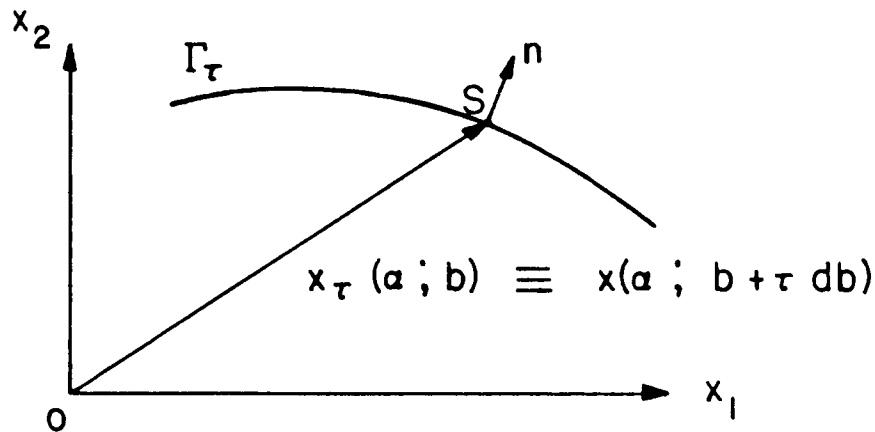


$$V = \frac{d}{d\tau}[x(\alpha;b + \tau\delta b)] = \frac{\partial x}{\partial b}\delta b$$

$$(V^T n) = \left[n^T \frac{\partial x(\alpha;b)}{\partial b}\right]\delta b$$

$$\psi_0' = \left[\int_\Gamma n^T \frac{\partial x}{\partial b} d\Gamma\right]\delta b$$

$$\psi_k' = \left[\int_\Gamma G(z,\lambda^k)\left(n^T \frac{\partial x}{\partial n}\right)d\Gamma\right]\delta b$$

Figure 3

# COMPARISON OF FINITE ELEMENT METHODS

Since shape design sensitivity information is given as a boundary integral, one has to check the accuracy of the numerical analysis results on the boundary. For comparison of accuracy, constant stress triangular (CST), linear stress triangular (LST), and 8-noded isoparametric (ISP) elements with optimal stress (refs. 4 and 5) are used to calculate design sensitivity. That is, stress values are evaluated at Gauss points and linearly extrapolated to obtain boundary stresses and strains.

For boundary parameterization, piecewise linear and cubic spline representations are used. In order to compare accuracy of results obtained with different finite elements, the same small region should be used to average stress. The small regions selected are shown in figure 4, located next to the variable boundary where it is most difficult to obtain accurate design sensitivity results (ref. 2).

Define $\Delta\psi_k \equiv \psi_k(b + \delta b) - \psi_k(b)$. The ratio of $\psi'$ and $\Delta\psi$ times 100 is used as a measure of accuracy; i.e., 100% means that the predicted change $\psi'$ is exactly the same as actual change. Numerical results with $\delta b = 0.001b$ are shown in figure 4.
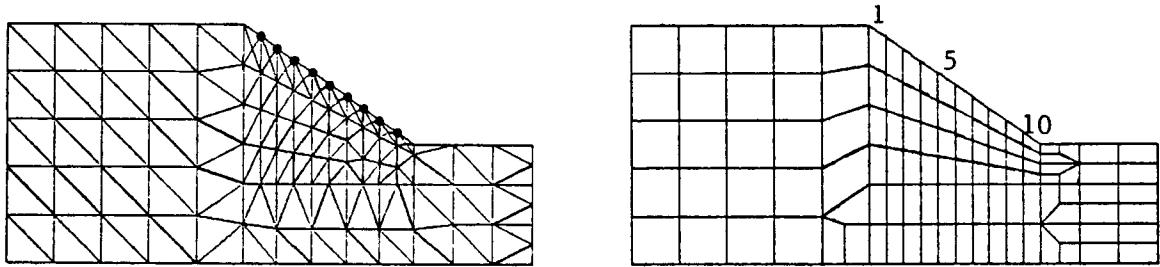


Sensitivity Check ($\psi'/\Delta\psi \times 100$)%

| Region No. | Piecewise Linear | | | Cubic Spline |
|---|---|---|---|---|
| | CST | LST | ISP | ISP |
| 5 | 67.5 | 99.2 | 102.8 | 102.6 |
| 6 | 68.6 | 99.2 | 101.8 | 101.7 |
| 7 | 68.3 | 99.1 | 100.0 | 100.4 |
| 8 | 70.1 | 99.1 | 98.4 | 97.4 |
| 9 | 79.3 | 98.3 | 105.2 | 104.9 |
| 10 | 183.6 | 87.0 | 102.8 | 104.1 |

Figure 4

The cubic spline function, which has two continuous derivatives everywhere and possesses minimum mean curvature, is employed here to define the moving boundary and 8-noded isoparametric finite elements shown in figure 5 are used for analysis. The finite element model contains 131 elements, 458 nodal points, and 846 degrees of freedom.

Heights of nodes that define the varied boundary are chosen as the design variables, as shown in figure 5. The fillet is optimized using the Linearization Method (ref. 6). Convergence criteria require the L-2 norm of direction vector p to be zero at the optimum point, where p is obtained by solving a quadratic programming problem. For numerical data, Young's modulus, Poisson's ratio, and allowable yield stresses are $30 \times 10^6$ psi, 0.293, and 120 psi respectively.

The initial design is b = [5.55, 5.1, 4.65, 4.2, 3.75, 3.3, 2.85, 2.4, 1.95]$^T$. Initially, cost, maximum stress violation, and $||p||$ are 145.1 in$^2$, $2.1 \times 10^{-1}$, and 2.0 respectively. After optimization, they are reduced to 133.4 in$^2$, $6.0 \times 10^{-4}$, and $8.8 \times 10^{-4}$, respectively. The final design is shown in figure 5 with design variable b = [2.64, 2.13, 1.90, 1.74, 1.61, 1.55, 1.5, 1.5, 1.5].
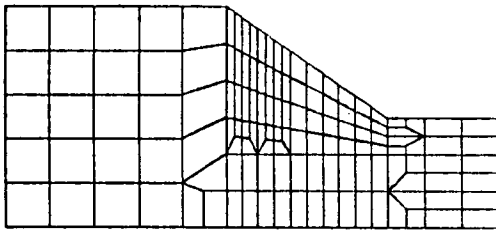


(a)  initial design

(b)  final design

$\psi_0 = 145.1$ in.$^2 \rightarrow 133.4$ in.$^2$
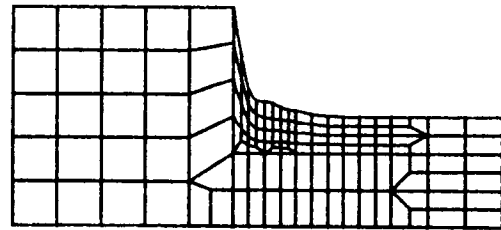
$\max \psi_k = 2.1 \times 10^{-1} \rightarrow 6.0 \times 10^{-4}$

Figure 5

# DESIGN OF AN ENGINE CONNECTING ROD

An engine connecting rod connects the crankshaft and piston pin of an engine, transmitting axial compressive load during firing and axial tensile load during the suction cycle of the exhaust stroke. The geometry of the connecting rod considered is shown in figure 6. Considering that the loads acting on the rod are in a plane and that the rod is nearly symmetric about this plane, one can reasonably assume that the rod is in a plane stress state. With the main interest in the shank and neck regions, the shape of the shank and neck regions of the rod are to be determined through the optimization process. The optimum thickness distribution, which varies independently from the domain variation, is to be determined in the optimization process. To satisfy the condition that the distance between the piston pin and the crankshaft is prescribed, it is required that the length of the rod not be changed.
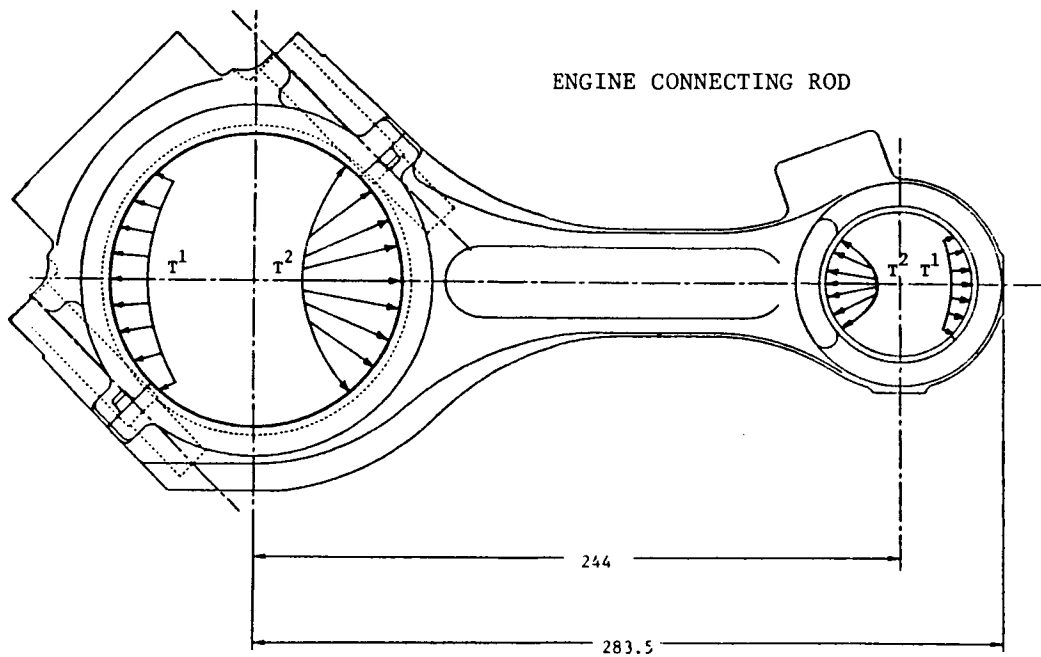


Design variables: Thickness h and shape of shank area

Figure 6

# DESIGN SENSITIVITY ANALYSIS OF CONNECTING ROD

The optimal design problem is to find a boundary shape and shank thickness to minimize total volume of the rod, with stress constraints. For stress constraints, lower and upper bounds are imposed on averaged principal stresses of inertia and firing loads.

As in the fillet design problem, one can use the principle of virtual work to derive a variational equation of elasticity. One can then employ the material derivative idea from continuum mechanics and an adjoint variable technique to calculate the shape design sensitivity formulas (ref. 7). The sensitivity expression resulting from thickness variation can also be found using the same adjoint variable method (ref. 2).

To use the sensitivity formulas computationally, the thickness function h is selected to be piecewise constant over strips of finite elements that run along the shank. Also, a cubic spline function is used to parameterize the boundary. (See fig. 7.)

Cost:

$$\psi_0 = \iint_\Omega h \, d\Omega$$

Constraint:

$$\psi_k = \iint \phi(\sigma(z)) m_k \, d\Omega \le 0 \quad , \qquad k = 1, 2, \cdots, 2NE$$

$$\psi_0' = \int_\Gamma h(v^T n) d\Gamma + \iint_\Omega \delta h \, d\Omega$$

$$\psi_k' = \iint_\Omega F_1(z, \lambda^k) \delta h \, d\Omega + \int_\Gamma F_2(z, \lambda^k)(v^T n) d\Gamma$$

Figure 7

# OPTIMIZATION OF CONNECTING ROD

With the sensitivity coefficient obtained, one can apply the Linearization Method (ref. 6) to obtain the optimum shape and thickness distribution. An 8-noded isoparametric element is used for analysis. A finite element model including 422 elements, 1493 nodal points, and 2983 degrees of freedom is employed. For numerical data, Young's modulus and Poisson's ratio are $2.07 \times 10^5$ MPa and 0.298 respectively. Upper and lower bounds of principal stresses of inertia are 136 MPa and −80 MPa, whereas they are 37 MPa and −279 MPa for the firing case.

The manufacturer's design is taken as an initial design, where the cost functional, maximum constraint violation, and $||p||$ were initially 726050 $mm^3$, $2.7 \times 10^{-1}$, and 5.9, respectively, and two constraints were active or violated around the neck area (near section a-a). After optimization, they are reduced to 697182 $mm^3$, $1.0 \times 10^{-3}$, and $6.5 \times 10^{-1}$, respectively, with 50 stress constraints active. The shape of the initial and final designs and several cross sections are illustrated in figure 8.



—— initial design

- - - - final design

Section a-a   Section b-b   Section c-c   Section d-d
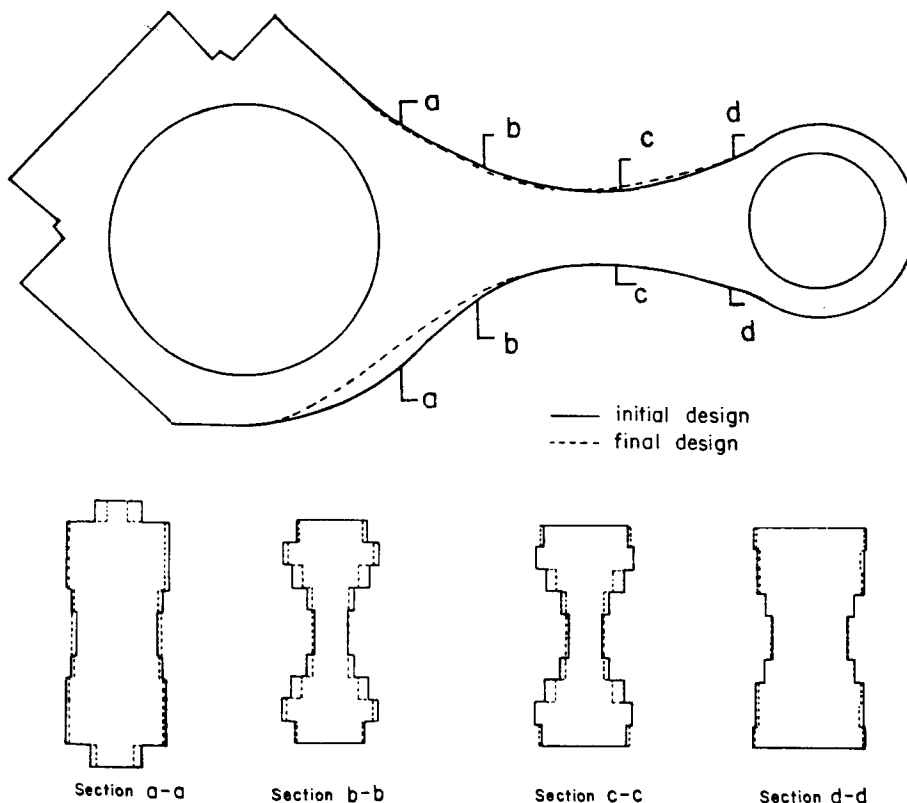
$$\psi_0 = 726050 \ mm^3 \rightarrow 697182 \ mm^3, \qquad max \ \psi_k = 2.7 \times 10^{-1} \rightarrow 1.0 \times 10^{-3}$$

Figure 8

Figure 9 shows a truss-beam-plate built-up structure in which thin flat plates, stiffened by longitudinal and transverse beams, are supported by four 4-bar trusses. A uniformly distributed load is applied to the plates. The points supported by trusses are at the intersection of two crossing beams nearest the free edges of the structure. The plates and beams are assumed to be welded together. The design variable in this problem is the combination of plate thickness, width and height of the rectangular cross sections of beams, and positions of beams. The design problem is to minimize the volume of the built-up structure, subject to constraints on displacement, stress, natural frequency, and bounds on design variables.

The state variable for this built-up structure consists of the plate displacements, beam displacements and torsion angles, and nodal displacements of the trusses, which satisfy kinematic interface conditions (kinematically admissible displacement fields). Hamilton's principle results in a variational formulation of the governing structural equilibrium and eigenvalue (free vibration) equations.
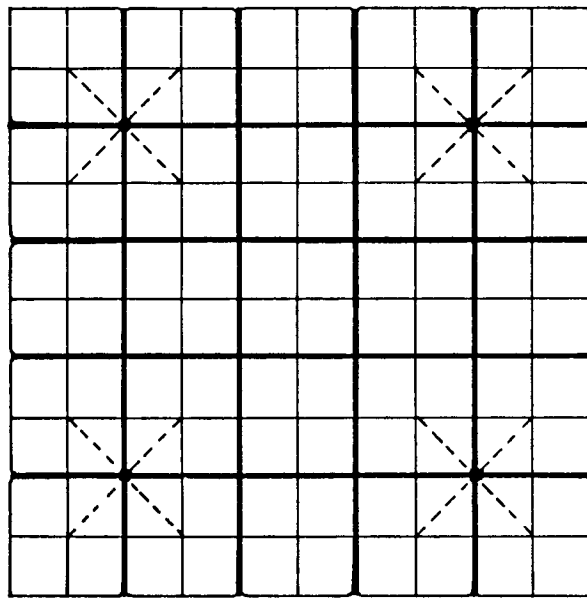


(a) Top View
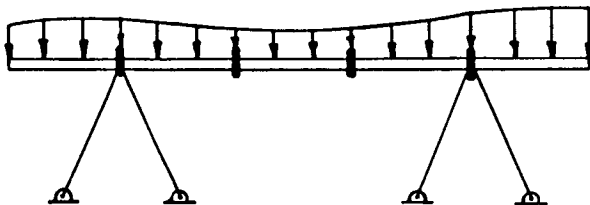
(b) Side View

BEAM-PLATE-TRUSS

Design Variables:

    Beam cross-sectional area

    Plate thickness

    Positions of Beams

Constraints:

    Displacement

    Compliance

    Eigenvalue

    Stress on beams and plates

Figure 9

# DESIGN SENSITIVITY ANALYSIS OF BEAM-PLATE-TRUSS

Design sensitivity analysis with respect to conventional design variable and shape using material derivative and adjoint variable method may be extended directly to the built-up structure problems. For conventional design variation, the general sensitivity formula contains contributions from each structural component directly. For shape variation, contributions from each component appear as integrals over common boundaries, using interface conditions on the common boundaries.

In figure 10, comparison between actual changes and predictions for constraints with 5% changes in all conventional design variable are presented. A finite element model of 100 plate elements, 80 beam elements, and 16 truss elements is used, with 363 degrees of freedom for total structure. For numerical data, Young's modulus, Poisson's ratio, and material density are $3.0 \times 10^7$ psi, 0.3, and 0.1 lb/in$^3$ respectively. Results shown in figure 10 indicate that sensitivity accuracy is very good for conventional design.

$$\psi_k' = \sum_{i,j} \iint_{\Omega^{ij}} F_1(z,\lambda^k) dh \, d\Omega + \sum_{i,j} \int_{\Gamma^{ij}} F_2(z,\lambda^k)(V^T n) d\Gamma$$

## SENSITIVITY CHECK FOR CONVENTIONAL DESIGN

| Constraint | El. No. | $\psi'/\Delta\psi \times 100$ | Constraint | El. No. | $\psi'/\Delta\psi \times 100$ |
|---|---|---|---|---|---|
| Displace- ment | C | 112.7 | | 1 | 95.1 |
| | | | | 3 | 111.3 |
| Stress on beam element | 1 | 108.8 | stress on plate element | 5 | 109.5 |
| | 3 | 109.7 | | 12 | 109.7 |
| | 5 | 109.6 | | 14 | 109.5 |
| | 11 | 106.8 | | 23 | 109.1 |
| | 13 | 110.0 | | 25 | 109.8 |
| | 15 | 109.2 | | 35 | 115.1 |
| | | | | 45 | 113.9 |
| Eigenvalue | | 91.3 | | | |

Figure 10

## SHAPE DESIGN SENSITIVITY CHECK FOR BEAM-TRUSS-PLATE

It is well known (ref. 8) that finite element results on interface boundaries, where abrupt changes in the boundary conditions occur (interface conditions), are far from being satisfactory. Based on this fact, a finer grid is used for shape design sensitivity calculations. Only one quarter of the entire structure is used for calculation, due to symmetry. A nonconforming 12 degrees-of-freedom finite element is used for plates. A finite element model of 400 rectangular plate elements, 80 beam elements, and 4 truss element is used, with total of 1281 degrees of freedom. The same numerical data that are used in conventional design sensitivity calculations are used.

In figure 11, sensitivity accuracy results are given for 5% uniform changes in all shape design variables (positions of beams). Results in figure 11 show reasonably good agreement between sensitivity predictions $\psi_k'$ and actual changes $\Delta\psi_k$ for all except some stress constraints on plate elements. That is, the sensitivity results for the stress constraints on plate elements adjacent to the interface (marked by *) are poor, even with finer grid.

| Constraint | El. No. | $\psi'/\Delta\psi \times 100$ | Constraint | El. No. | $\psi'/\Delta\psi \times 100$ |
|---|---|---|---|---|---|
| Displace- ment | C | 97.5 | | 1 | 100.7 |
| | | | | 19 | 103.6 |
| | | | | 44 | 109.9* |
| Compliance | | 92.3 | | 58 | 98.7 |
| | | | Stress on plate element | 85 | 188.3* |
| | | | | 128 | 97.8 |
| Eigenvalue | | 95.5 | | 149 | 98.7 |
| | 1 | 99.6 | | 175 | 91.8 |
| Stress on beam element | 21 | 99.7 | | 198 | 109.6 |
| | 30 | 100.0 | | 237 | 449.0* |
| | 45 | 98.3 | | 259 | 138.8* |
| | 55 | 103.1 | | 296 | 95.9* |
| | 77 | 103.9 | | 317 | 87.8 |
| | | | | 358 | 105.3 |
| | | | | 400 | 111.3 |

Figure 11

# DESIGN OF A SIMPLE BOX BUILT-UP STRUCTURE

A simple box built-up structure, in which five plane elastic solid plates are welded together, attached to a wall is shown in figure 12. A uniformly distributed line load is applied on top of the two side plates and the end plate. The shape design variable in this problem is the length d, width b, and height h of the box.

As in the beam-plate-truss case, the principle of virtual work results in a variational formulation of the governing structural equations. Then, one can use the material derivative idea and an adjoint variable method to obtain the shape sensitivity formula.

In view of beam-plate-truss shape sensitivity results, an equivalent but alternate form of shape sensitivity formula is used for this problem. Since finite element results are accurate on the domain and not on the boundary, the shape sensitivity formula is expressed in terms of domain integral (refs. 1 and 2). Hence, instead of $(V^T n)$, one has terms V and (div V) in the sensitivity formula.
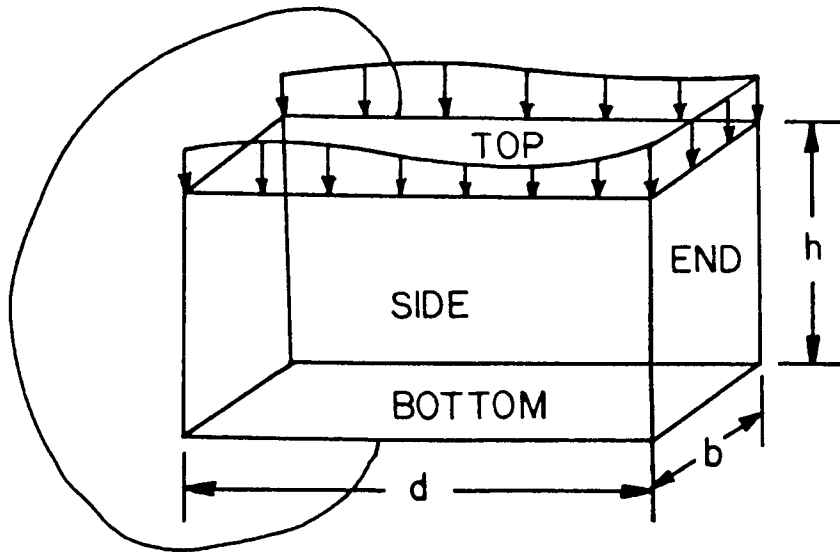


Design Variables:  d, b, and h

Constraints:  $$\psi_k = \iint_\Omega \phi(\sigma(z)) m_k \, d\Omega \leqslant 0 \quad , \quad k = 1,2,\cdots,NE$$

$$\psi_k' = \sum_i \iint_{\Omega^i} \left[ g(\lambda,z)^T V + F(\lambda,z) \text{div } V \right] d\Omega$$

Figure 12

435

# SHAPE DESIGN SENSITIVITY FOR SIMPLE BOX

Since shape design variables are given as d, b, and h, one can assume the velocity field to be linear on each plate and thus (div V) is constant. An 8-noded isoparametric element is used for analysis. A finite element model of 320 elements, 993 nodes, and 1886 degrees of freedom is used. For numerical data, Young's modulus and Poisson's ratio are $1.0 \times 10^7$ psi and 0.316 respectively. The dimension of the structure is b = d = h = 8 in. and the thickness of the plates is 0.1 in. Uniform external load is 4.77 lb/in.

In figure 13, the sensitivity accuracy result is given separately for 3% change in d and h. Results given in figure 13 show excellent agreement between predictions $\psi_k'$ and actual changes $\Delta\psi_k$. The boundary method that is applied to the beam-plate-truss built-up structure is tested to the same box problem with unacceptable results. The domain method of shape design sensitivity for built-up structure has a promising future. Work continues in evaluating the method on larger scale examples.

| Region | El. No. | $\psi'/\Delta\psi \times 100$ $\delta d = 0.03d$ | $\psi'/\Delta\psi \times 100$ $\delta h = 0.03h$ | Region | El. No. | $\psi'/\Delta\psi \times 100$ $\delta d = 0.03d$ | $\psi'/\Delta\psi \times 100$ $\delta h = 0.03h$ |
|---|---|---|---|---|---|---|---|
| Top | 1 | 97.6 | 103.6 | Side | 129 | 96.2 | 103.4 |
| | 15 | 98.2 | 103.6 | | 143 | 98.1 | 103.0 |
| | 29 | 98.8 | 103.5 | | 157 | 98.0 | 102.6 |
| | 43 | 100.4 | 103.6 | | 171 | 95.6 | 103.0 |
| | 57 | 110.1 | 103.5 | | 184 | 100.4 | 103.2 |
| Bottom | 72 | 97.9 | 103.3 | End | 264 | 99.9 | 103.7 |
| | 86 | 98.5 | 103.2 | | 278 | 114.1 | 103.9 |
| | 100 | 98.5 | 103.1 | | 291 | 95.1 | 101.1 |
| | 114 | 100.9 | 103.3 | | 307 | 120.3 | 103.5 |
| | 128 | 100.9 | 103.2 | | 320 | 99.9 | 103.7 |

Figure 13

## REFERENCES

1. Choi, K. K. and Haug, E. J., "Shape Design Sensitivity Analysis of Elastic Structures," Journal of Structural Mechanics 11(2), 231-269, 1983.

2. Haug, E. J., Choi, K. K., and Komkov, V., Design Sensitivity Analysis of Structural Systems, Academic Press, in press, 1984.

3. Haug, E. J., Choi, K. K., Hou, J. W., and Yoo, Y. M., "A Variational Method for Shape Optimal Design of Elastic Structures," New Directions in Optimum Structural Design (Ed. E. Atrek, G. H. Gallagher, K. M. Ragsdell, and O. C. Zienkiewicz), John Wiley & Sons Ltd., 1984.

4. Francavilla, A., Ramakrishnan, C. V., Zienkiewicz, O. C., "Optimization of Shape to Minimize Stress Concentration," Journal of Strain Analysis, Vol. 10, No. 2, 63-70, 1975.

5. Cook, R. D., Concepts and Application of Finite Element Analysis, John Wiley & Sons, 1981.

6. Choi, K. K., Haug, E.J., Hou, J. W., and Sohoni, V. N., "Pshenichny's Linearization Method for Mechanical System Optimization," Journal of Mechanisms, Transmissions, and Automation in Design, Transactions of the ASME, Vol. 105, 97-103, 1983.

7. Yoo, Y. M., Haug, E. J., and Choi, K. K., "Shape Optimal Design of an Engine Connecting Rod," ASME J. of Mechanical Design, in press, 1984.

8. Babuska, I. and Aziz, A. K., "Survey Lectures on Mathematical Foundations of the Finite Element Method," The Mathematical Foundations of the Finite Element Method with Applications to Partial Differential Equations, (Ed. A. K. Aziz), Academic Press, 1972, pp. 1-359.

# MULTIDISCIPLINARY OPTIMIZATION APPLIED TO A TRANSPORT AIRCRAFT

Gary L. Giles
NASA Langley Research Center
Hampton, Virginia

and

G. A. Wrenn
Kentron International, Inc.
Hampton, Virginia

# INTRODUCTION

Decomposition of a large optimization problem into several smaller subproblems has been proposed as an approach to making large-scale optimization problems tractable. To date, the characteristics of this approach have been tested on problems of limited complexity (e.g., reference 1). The objective of the effort described in this paper is to demonstrate the application of this multilevel optimization method on a large-scale design study using analytical models comparable to those currently being used in the aircraft industry. The purpose of the design study which is underway to provide this demonstration is to generate a wing design for a transport aircraft which will perform a specified mission with minimum block fuel. This paper includes (1) a definition of the problem, (2) a discussion of the multilevel decomposition which is used for an aircraft wing, (3) descriptions of analysis and optimization procedures used at each level, and (4) numerical results obtained to date. Computational times required to perform various steps in the process are also given. Finally, a summary of the current status and plans for continuation of this development effort are given (fig. 1).

OBJECTIVE: TO DEMONSTRATE THE APPLICATION OF MULTILEVEL OPTIMIZATION METHOD IN A LARGE SCALE DESIGN STUDY.

APPLICATION: TO GENERATE A WING DESIGN FOR A TRANSPORT AIRCRAFT TO PERFORM A SPECIFIED MISSION WITH MINIMUM BLOCK FUEL.

PRESENTATION
OUTLINE:
- PROBLEM DEFINITION
- MULTILEVEL DECOMPOSITION
- ANALYSIS AND OPTIMIZATION PROCEDURES
- NUMERICAL RESULTS
- OBSERVATIONS

Figure 1

# MULTILEVEL OPTIMIZATION APPLICATION

The multilevel optimization procedure is being applied to an L-1011 derivative
transport aircraft which is being studied by the Lockheed-California Company
as discussed in reference 2. The focus of this particular study is to design
a new wing to give minimum fuel consumption for a specified flight profile.
Design variables include overall wing geometric shape defined by aspect ratio,
sweep, total area, taper ratio and thickness ratio. In addition, variables
describing the wing structure within that shape are determined down to the
level of cross-sectional dimensions of stiffened-skin wing cover panels. As
overall wing geometry changes are made, the structure is reoptimized and the
static aeroelastic effects on aerodynamics are calculated but no aerodynamic
optimization of wing airfoil shape is performed. (See fig. 2.)
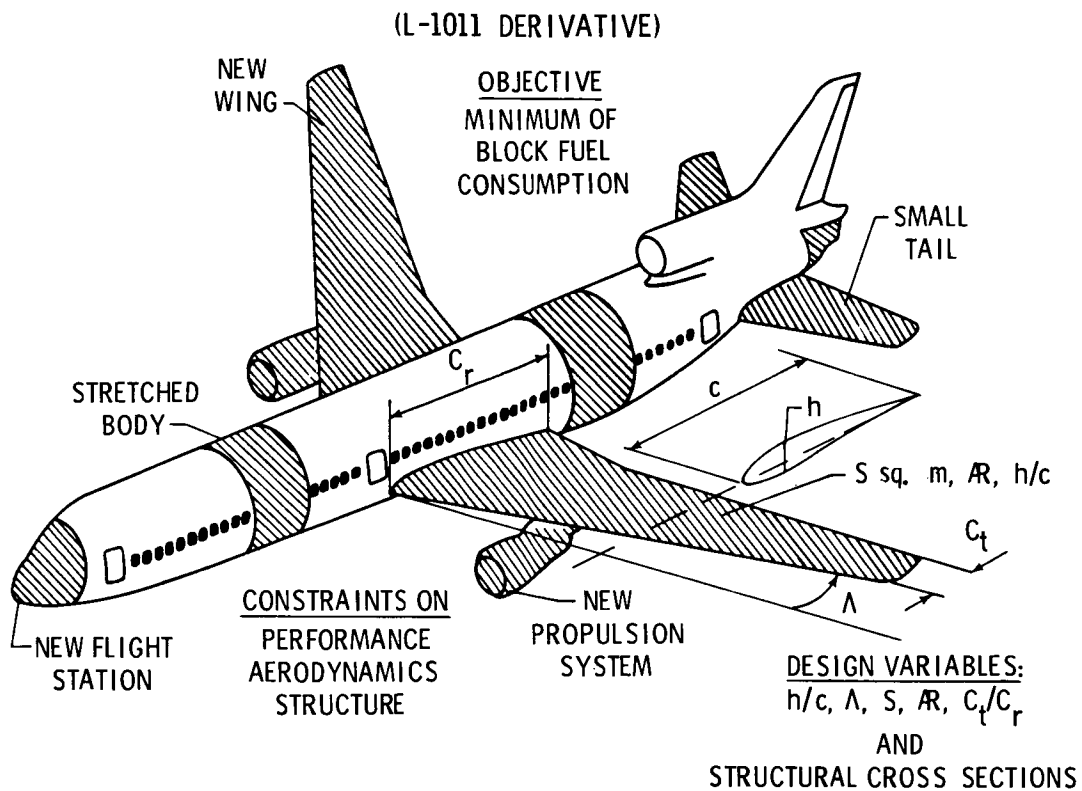


Figure 2

## COOPERATIVE VENTURE WITH LOCKHEED

The study of the transport aircraft wing is being performed as a joint venture
with the Lockheed-California Company. Lockheed is using their integrated
structural design system which computerizes their conventional design methods
to perform such studies (reference 2). Parametric studies are used to
calibrate weight equations to perform overall configuration trade studies.
Structural sizing for this calibration is based on fully stressed design with
stiffened wing cover panels selected from design charts representing
predesigned cross sections. Aeroelastic considerations such as flutter and
gust are included in the Lockheed procedures. Multilevel optimization is
being applied at NASA Langley, initially to get the procedure implemented at
all levels for strength design and subsequently to include aeroelastic
considerations. Lockheed is under contract to provide sufficient design data
from their studies to allow NASA personnel to study the same configuration at
the same level of detail. (See fig. 3.)

LOCKHEED - CALIF.

CONVENTIONAL PARAMETRIC
   STUDIES

- STRUCTURES:

  INTEGRATED ANALYSIS

  FULLY STRESSED DESIGN

  PREDESIGNED CROSS SECTIONS

- AEROELASTIC CONSIDERATIONS

NASA   LANGLEY

SYSTEMATIC MATHEMATICAL
   OPTIMIZATION

- MULTILEVEL APPROACH FROM
  CONFIGURATION LEVEL DOWN
  TO STRUCTURAL SIZING
  LEVEL

- DISCIPLINARY ANALYSES
  COMPARABLE TO LOCKHEED'S
  AS TO THEIR DEGREE OF
  DETAIL

Figure 3

# FINITE-ELEMENT STRUCTURAL MODEL

The finite-element representation of the structure was developed by Lockheed
personnel for analysis by the NASTRAN program used in their PADS system
(reference 3). Since the focus was on wing design, a fairly detailed model is
used for the wing structure and the regions of the fuselage necessary to get
proper representation of the wing-body intersection. The wing and wing-body
intersection structure is modeled primarily with rod and membrane panel
elements. The remainder of the structure (fore and aft fuselage, empennage,
engine, and landing gear) is modeled using beam elements. This NASTRAN model
was converted to be compatible with the Engineering Analysis Language (EAL)
system (reference 4) for analysis at NASA Langley. The resulting model has
641 joints for a symmetric half model. During design studies, only the cover
panels in the upper and lower surfaces of the main wing box (216 elements)
were resized (fig. 4).



641 JOINTS
1539 ELEMENTS (216 RESIZED)
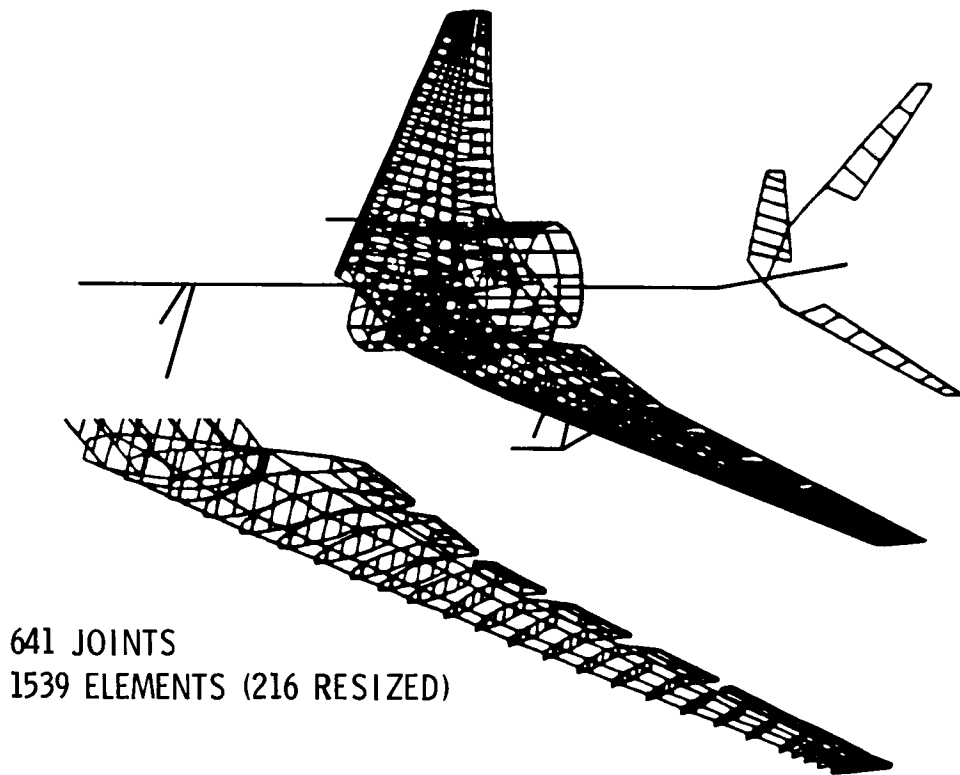
Figure 4

The decomposition for wing design is a particular case of the general multilevel decomposition methodology described in reference 5. The wing design process is decomposed into three separate optimization problems, as shown in figure 5. At the top level, design variables such as wing structural weight, aspect ratio, and sweep are used to minimize fuel consumption subject to performance constraints. The optimum values of these variables are then passed to the middle level as fixed parameters where the distribution of wing box cover skin material is determined which will give a minimum measure of constraint violation. Next, these optimum distributions are passed to the bottom level where the optimum cross-sectional dimensions of each of the stiffened panels are calculated. The optimization procedures at the middle and bottom levels are used to minimize a single cumulative constraint violation associated with that level. This cumulative constraint is a differentiable envelope function of all individual constraints. The particular envelope function used is the Kresselmeir-Steinhauser function (reference 6). The cumulative constraints and their derivatives are passed upward between levels. Iteration between the three levels is performed until all constraints are satisfied. Analysis and optimization procedures used at each level are discussed next.

| AIRCRAFT PERFORMANCE | MINIMIZE FUEL CONSUMPTION SUBJECT TO PERFORMANCE CONSTRAINTS |

$W_s$, AR, $\Lambda$, ...  $\Omega^m$, $\partial \Omega^m / \partial W_s$

| WING BOX COVER SKIN | MINIMIZE CONSTRAINT VIOLATION FOR WING STRUCTURE |

$t_1$, $t_2$ ...  $\Omega^B$, $\partial \Omega^B / \partial t_1$

| STIFFENED PANEL 1 | STIFFENED PANEL 2 | $\bullet \bullet \bullet$ | MINIMIZE CONSTRAINT VIOLATION FOR EACH PANEL |
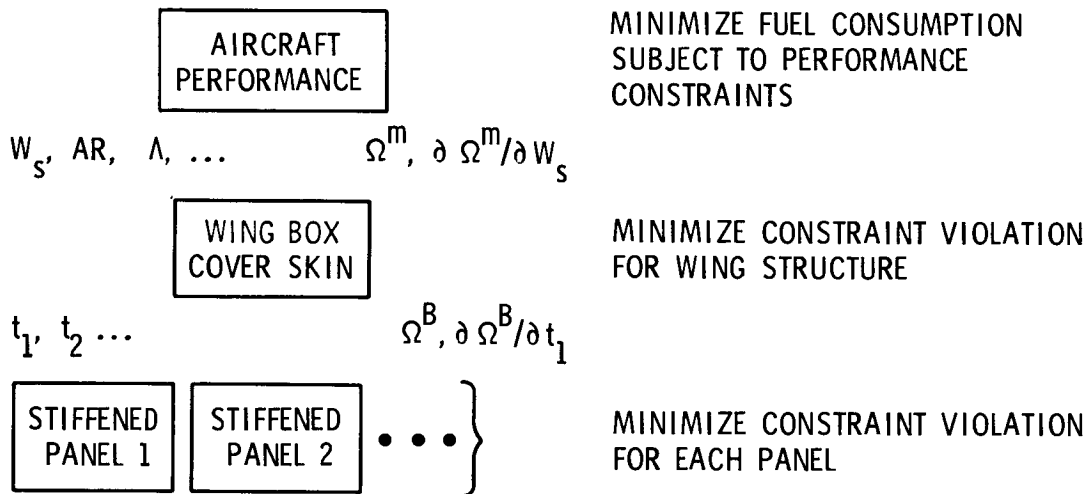
$\Omega$ - CUMULATIVE CONSTRAINT,
KRESSELMEIR-STEINHAUSER FUNCTION USED

Figure 5

444

# TOP LEVEL PROCEDURES

The Flight Optimization System (FLOPS) (reference 7) is used to perform overall optimization at the top level. The objective is to determine the aircraft wing configuration which minimizes block fuel consumption for a specified mission. Performance constraints include limits on approach speed, field length, and climb gradient thrust. Cumulative constraints from the lower levels must also be satisfied. The standard version of FLOPS uses statistical equations to calculate wing weight as a function of wing geometry. Modifications have been made so that the program can be implemented in the multilevel optimization procedure by including wing structural weight as a design variable and adding the cumulative constraint from the lower levels. (See fig. 6.)

- FLOPS MISSION PERFORMANCE PROGRAM USED (REF 7)

- MODIFICATIONS TO FLOPS NECESSARY FOR MULTILEVEL IMPLEMENTATION
    - WEIGHT OF WING STRUCTURE INCLUDED AS A DESIGN VARIABLE
    - ADD A CONSTRAINT: CUMULATIVE CONSTRAINT FROM BOTTOM AND MIDDLE LEVELS

Figure 6

## MIDDLE LEVEL PROCEDURES

The optimum distribution of material in the wing box cover skins is calculated by the middle-level procedures. Displacements and stresses are calculated using the model in figure 4 as input to the EAL system. Analytical derivatives of these quantities are calculated using the procedures described in reference 8 which are implemented as sequences of input statements to EAL. The design variables used in optimization are coefficients in a polynomial expression for the cover thickness distribution. The distribution currently being used is illustrated in figure 7. As indicated on figure 5, the objective function is a cumulative constraint from the middle and bottom levels with a fixed weight of the wing box covers from the top level specified as a constraint. Optimization is performed using CONMIN (reference 9) in a sequence of steps in which the results from the structural analysis are approximated by linear extrapolation.

- EAL USED FOR STATIC ANALYSIS AND DERIVATIVES

    - ANALYTICAL DERIVATIVES USED FOR THICKNESS VARIABLES

- DESIGN VARIABLES    =    COEFFICIENTS IN EXPRESSION FOR COVER THICKNESS DISTRIBUTION

    $$\text{TSKIN} = C_0 + C_1 (1 - \beta) + C_2 (1 - \beta)^2$$

- OBJECTIVE FUNCTION    =    MINIMUM CUMULATIVE CONSTRAINT FROM:

    MIDDLE LEVEL - WING TIP DISPLACEMENT
    BOTTOM LEVEL - PANEL CUMULATIVE CONSTRAINTS

- CONSTRAINT    =    FIXED WEIGHT OF WING BOX COVERS

- PIECEWISE LINEAR OPTIMIZATION PROCEDURE USING CONMIN

Figure 7

# INITIAL SKIN PANEL DESIGN VARIABLE LINKING

The thickness properties of the finite elements representing the wing box cover skins are described in the spanwise direction by the quadratic expression in terms of the nondimensional parameter "$\beta$" ($\beta=0$ at the wing root and $\beta=1$ at the tip) shown on figure 8. Two quadratic segments are used, one inboard of the engine pylon and the other outboard. A constant thickness is specified in the chordwise direction. The upper and lower wing box cover skin properties are taken to be symmetric with respect to the wing middle surface. The six coefficients of the two quadratic expressions are the design variables used during optimization. This linking scheme is used to reduce the number of design variables during initial testing of the multilevel optimization procedure. It is recognized that this simplified linking restricts the possible distributions available for optimization and these restrictions will have to be removed after the initial testing phase.

$$TSKIN = C_0 + C_1 (1 - \beta) + C_2 (1 - \beta)^2$$

CONSTANT

- SYMMETRIC UPPER AND LOWER WING BOX COVER SKINS

Figure 8
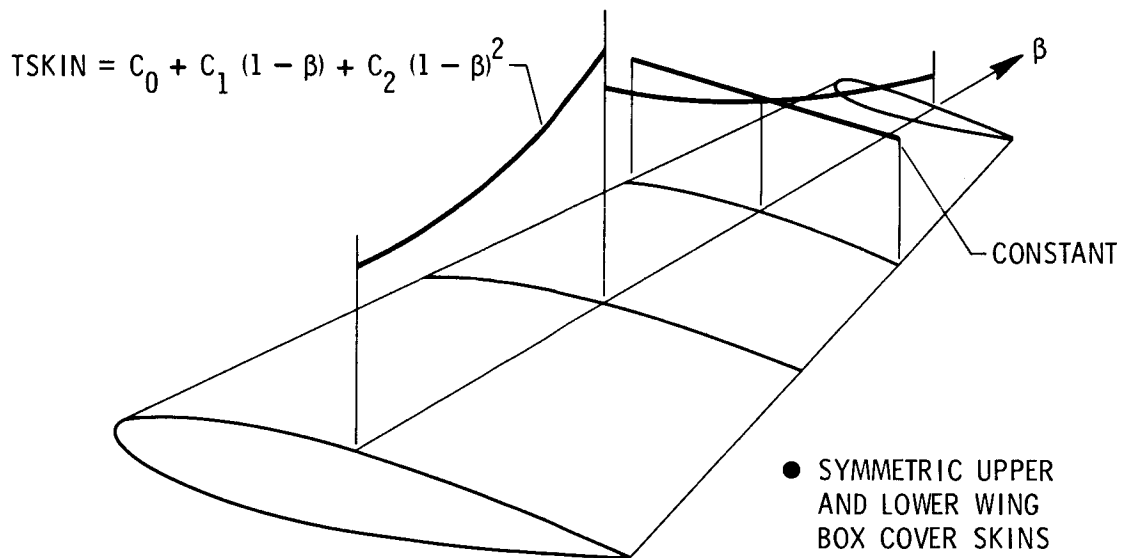
Each of the 216 wing box cover panels is optimized by the bottom level procedures. Although properties of corresponding panels on the upper and lower surfaces are taken to be the same, the panel loads are not the same. Therefore, each pair of panels is optimized in order to assure consideration of the panels with the critical loadings. The design variables are the cross-sectional dimensions of a stiffened panel, as shown in figure 9. The objective function is a cumulative constraint composed of contributions from five stress constraints and eight buckling constraints that are considered. The CONMIN program is used for optimization. After each panel is optimized, an optimum sensitivity analysis is performed to get derivatives of the cumulative constraint with respect to parameters such as panel length, width and stress resultants which are passed down from the middle level. The algorithm described in reference 10 is used for these calculations. Finally, these optimum sensitivity derivatives are combined wih structural response derivatives from the middle level to form cumulative constraint derivatives which are subsequently used in the middle-level optimization process.

PANEL OPTIMIZATION                    OPTIMUM SENSITIVITY ANALYSIS

● DESIGN VARIABLES                    ● PARAMETERS



● FAILURE MODES                       $\dfrac{\partial \Omega}{\partial N_x},\ \dfrac{\partial \Omega}{\partial N_y}\ \cdots$
   STRESS   (5)
   BUCKLING (8)

● CONMIN USED                         CUMULATIVE  CONSTRAINT  CALCULATION

$$\frac{\partial \Omega^B}{\partial t_1} = \frac{\partial \Omega}{\partial N_x} \frac{\partial N_x}{\partial t_1} + \ldots$$

Figure 9

448

# MULTILEVEL OPTIMIZATION IMPLEMENTATION FOR L-1011 DERIVATIVE WING

The general characteristics of the computer programs used in each of the three levels have been described in the previous discussions of the levels. The original intent was to tran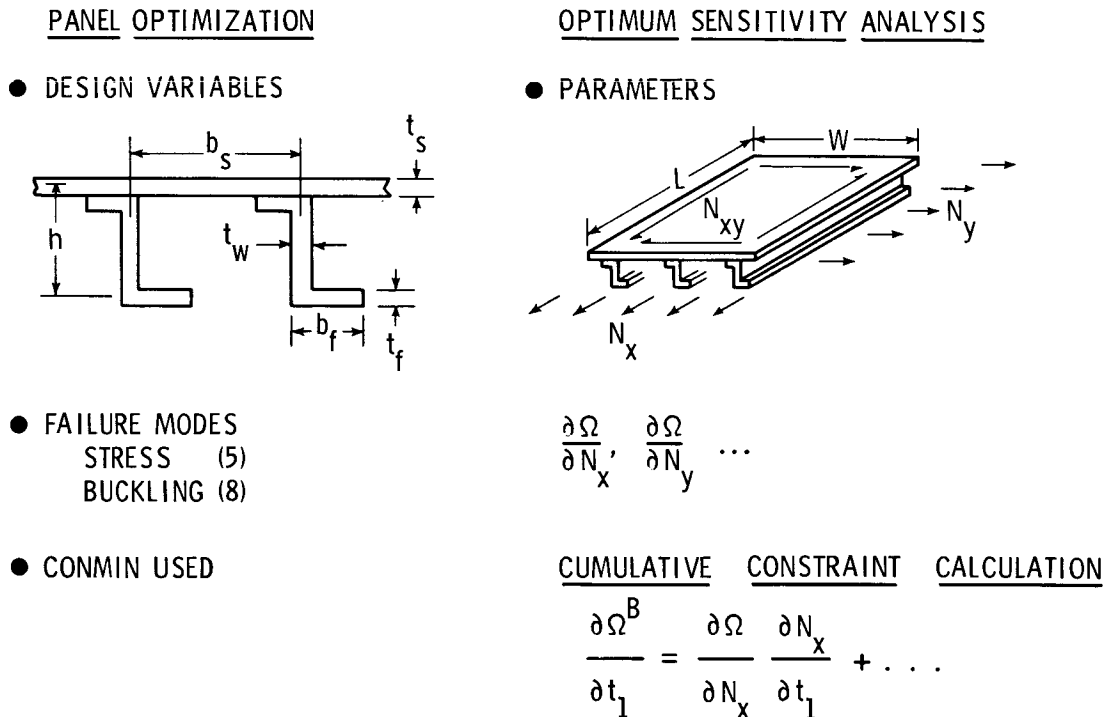sfer all data between levels via the Relational Information Management (RIM) system (reference 11). Since the procedures in the middle level are all related to the EAL structural analysis system, its data base was used for all data communication within the middle level. It was found that the bottom level was tightly coupled to the middle level in terms of types and quantities of data that had to be shared. Consequently, the bottom level was implemented as an EAL processor and utilities described in reference 12 were used to provide data communication to the EAL data base. The relatively small amount of data communication required between the middle level and top level is handled using the RIM system. (See fig. 10.)

LEVEL

```
TOP       ┌──────────────────┐
          │ MISSION          │
          │ PERFORMANCE      │
          └──────────────────┘

          ┌───────────────────────────┐
          │ ┌──────────────────────┐  │
          │ │ LOADS CALCULATION    │  │
          │ └──────────────────────┘  │
          │                           │   E
          │ ┌──────────────────────┐  │   A        R
MIDDLE    │ │ STRUCTURAL ANALYSIS  │  │   L
          │ │ AND RESPONSE         │  │   D        I
          │ │ DERIVATIVES          │  │   A
          │ └──────────────────────┘  │   T        M
          │                           │   A
          │ ┌──────────────────────┐  │   B
          │ │ STRUCTURAL SIZING    │  │   A
          │ └──────────────────────┘  │   S
          └───────────────────────────┘   E

          ┌───────────────────────────┐
BOTTOM    │ STIFFENED PANEL           │
          │ OPTIMIZATION              │
          └───────────────────────────┘
```
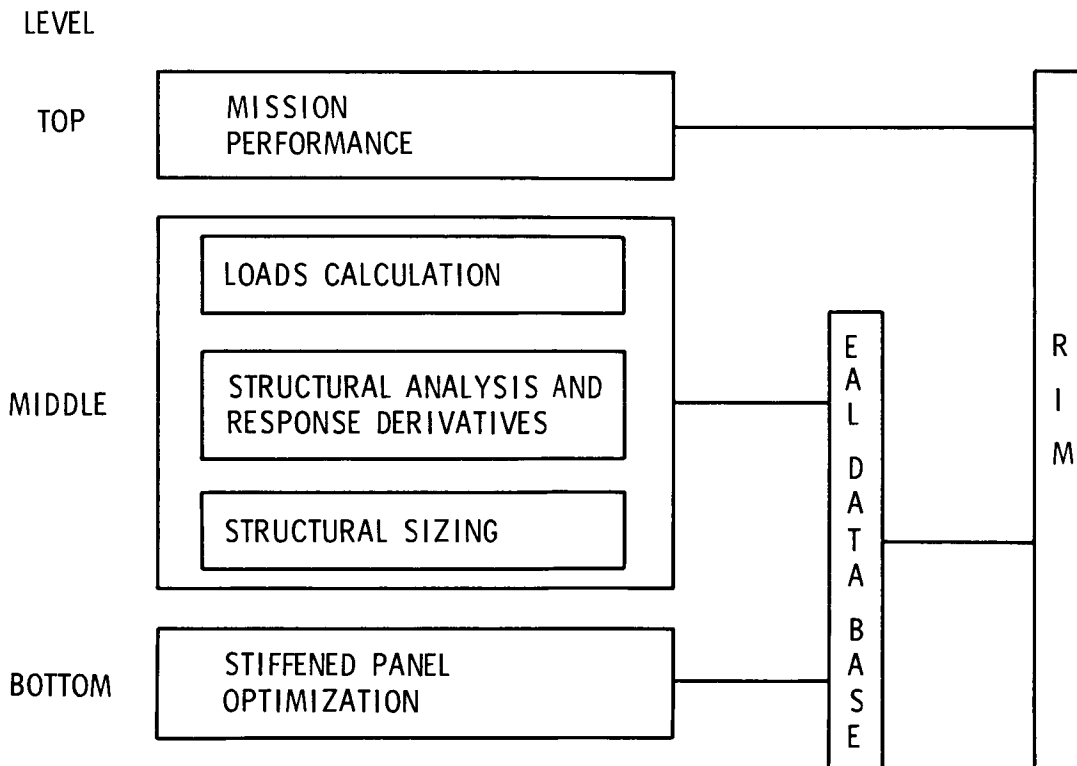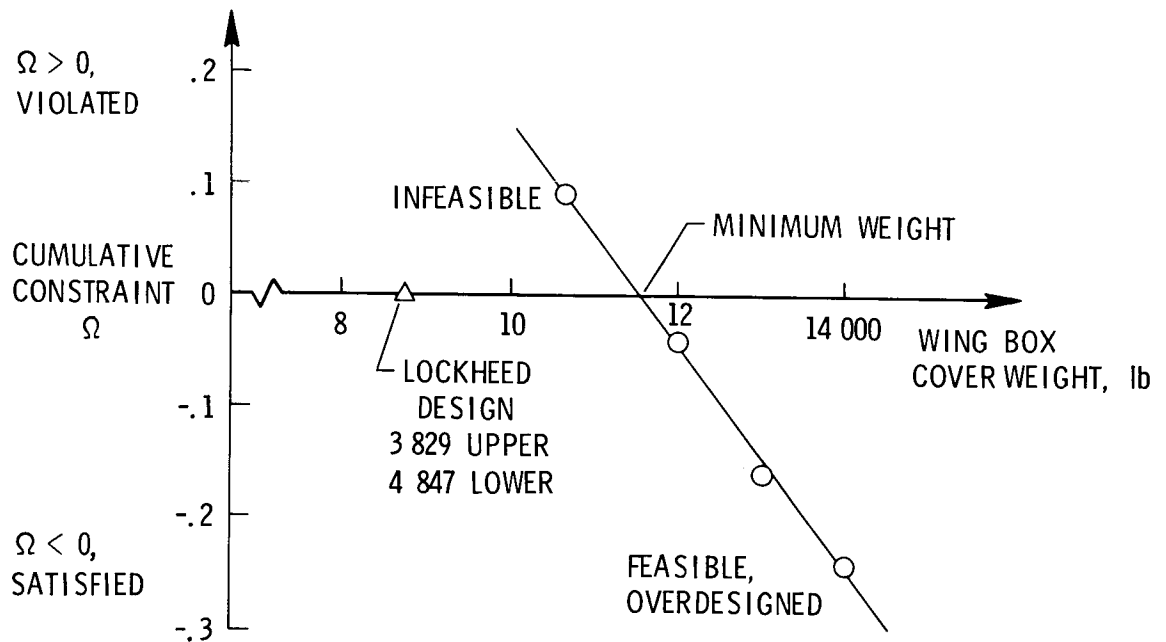
Figure 10

449

# MINIMUM WEIGHT SIZING BY INDIRECT METHOD

To assess the results being produced by the bottom two levels, an indirect method of calculating a minimum weight design was employed. The middle and bottom levels were used to calculate minimum values of the middle-level cumulative constraint for four values of wing box cover weight. These optimized designs are indicated by the circular symbols on figure 11. The point above the horizontal axis is infeasible since the cumulative constraint has a positive value and the three points below the axis satisfy all constraints but are overdesigned. The minimum weight design is located where a line through these points intersects the horizontal axis as shown on the figure. This design is heavier than the minimum weight design produced in the Lockheed studies. The difference is attributed to the restrictions imposed by the initial design variable linking scheme, figure 8, that is being used for testing purposes.

Figure 11

# TYPICAL SUMMARY OF COMPUTATIONAL ACTIVITY

A summary of the computational activity for the major tasks involved in the
operation of the middle and bottom levels is shown in figure 12. Both
normalized CPU time and I/O count are given. Performing a static structural
analysis and calculating derivatives of the response quantities involve
considerable computational activity. A large portion of CPU time is required
for panel optimization at the bottom level where 216 separate optimization
runs are made. Only a small amount of I/O activity is required in these
calculations. The CPU time required for optimization at the middle level is
an order of magnitude less than that required for the structural analysis and
derivatives that are used for linear approximation during optimization. Total
CPU time, I/O count, and cost are shown at the bottom of the figure for five
piecewise linear optimization cycles on a CDC Cyber 175 computer.

| TASK | NORMALIZED CPU TIME | NORMALIZED I/O COUNT | |
|---|---|---|---|
| INITIALIZE | .052 | .134 | |
| STATIC STRUCTURAL ANALYSIS | .174 | .277 | |
| STATIC DERIVATIVES | .137 | .243 | |
| PANEL OPTIMIZATION & SENSITIVITY ANALYSIS ($\approx 35$ ITERATIONS/PANEL) | .613 | .025 | ←216 PANELS |
| LINEAR OPTIMIZATION CYCLE FOR $\Omega$ (10 ITERATIONS) | .024 | .321 | |
| | 1.000 | 1.000 | |

FOR 5 PIECEWISE     CPU TIME     650 sec
LINEAR CYCLES     I/O COUNT     34 000
ON CYBER 175     COST     $350

Figure 12

## CONCLUDING REMARKS

The current status of the implementation of the multilevel optimization procedure is summarized on figure 13. The aircraft wing design process has been decomposed into three levels. The bottom two levels have been implemented using the EAL system and have been successfully tested. This initial testing resulted in the demonstration of an indirect method for minimum weight design which may prove to be an attractive alternative to conventional methods that have been used in the past. The three-level system can be tested when the FLOPS program is incorporated at the top level and efforts to demonstrate the application of the multilevel optimization method on a large-scale design study are continuing.

- AIRCRAFT WING DESIGN DECOMPOSED INTO THREE LEVELS

- INTEGRATION AND TESTING OF BOTTOM TWO LEVELS SUCCESSFULLY COMPLETED

- MINIMUM WEIGHT SIZING BY INDIRECT METHOD DEMONSTRATED

- FLOPS PROGRAM TO BE INCORPORATED AT TOP LEVEL

- STUDY CONTINUING

Figure 13

# REFERENCES

1. Sobieszczanski-Sobieski, Jaroslaw; James, Benjamin; and Dovi, Augustine:
   Structural Optimization by Multilevel Decomposition. AIAA Paper
   83-0832-CP, AIAA/ASME/ASCE/AHS 24th Structures, Structural Dynamics,
   and Materials Conference, Lake Tahoe, Nevada, May 2-4, 1983.

2. Radovcich, N. A.:  Some Experiences in Aircraft Aeroelastic Design Using
   Preliminary Aeroelastic Design of Structures (PADS). Recent Experiences
   in Multidisciplinary Analysis and Optimization, NASA CP-2327, Part 1,
   1984, pp. 455-503.

3. Radovcich, N. A.:  Preliminary Aeroelastic Design of Structures (PADS)
   Methods Development and Application. Presented at the AGARD 56th
   Structures and Materials Panel Meeting, London, United Kingdom, April
   1983.

4. Whetstone, W. D.:  EISI-EAL:  Engineering Analysis Language. Proceedings
   of the Second Conference on Computing in Civil Engineering, American
   Soc. Civil Eng., 1980, pp.276-285.

5. Sobieski, J.:  Multidisciplinary Systems Optimization by Linear Decompo-
   sition. Recent Experiences in Multidisciplinary Analysis and Optimi-
   zation, NASA CP-2327, Part 1, 1984, pp. 343-366.

6. Kresselmeir, G.; and Steinhauser, G.:  Systematic Control Design by
   Optimizing a Vector Performance Index. Proceedings of IFAC Symposium on
   Computer-Aided Design of Control Systems, Zurich, Switzerland, 1971.

7. McCullers, L. A.:  Aircraft Configuration Optimization Including Optimized
   Flight Profiles. Recent Experiences in Multidisciplinary Analysis and
   Optimization, NASA CP-2327, Part 1, 1984, pp. 395-412.

8. Giles, Gary L.; and Rogers, James L., Jr.:  Implementation of Structural
   Response Sensitivity Calculations in a Large-Scale, Finite-Element
   Analysis System. AIAA Paper 82-0714, presented at the 23rd
   AIAA/ASME/ASCE/AHS Structures, Structural Dynamics, and Materials
   Conference, New Orleans, Louisiana, May 10-12, 1982.

9. Vanderplaats, G.:  CONMIN - A FORTRAN Program for Constrained Function
   Minimization, User's Manual. NASA TM X-62282, August  1973.

10. Sobieszczanski-Sobieski, J.; Barthelemy, J.-F.; and Riley, K. M.:
    Sensitivity of Optimum Solutions to Problem Parameters. AIAA Paper
    81-0548R. AIAA Journal, Vol. 20, No. 9, September 1982, pp. 1291-1299.

11. RIM - Relational Information Management System Version 6. Report No.
    70101-03-017, Boeing Computer Services, Seattle, Washington, May 1983.

12. Giles, Gary L.; and Haftka, Raphael T.:  SPAR Data Handling Utilities.
    NASA TM-78701, September 1978.

SOME EXPERIENCES IN AIRCRAFT AEROELASTIC
DESIGN USING PRELIMINARY AEROELASTIC
DESIGN OF STRUCTURES [PADS]

Nick A. Radovcich
Lockheed-California Company
Burbank, California

ABSTRACT

Preliminary design for an optimal aircraft configuration requires the integration of aeroelastic analysis into the configuration selection process. Configurations of aircraft in the early design stage are usually based on analytical and statistical weight methods from past experience, and approximate loads and stress analyses. This often leads to the freezing of external geometry before strength and flutter analyses are complete, thereby decoupling the powerful but time-consuming process of structural design to minimum weight from the configuration optimization process. If the lengths of time could be shortened to perform accurate loads, structural design, and flutter optimization analyses, then structural optimization could proceed in concert with the overall configuration optimization. Better aircraft of advanced types could then be designed.

A methodology was developed to upgrade current capabilities in ASSET (Automated System Synthesis and Evaluation Technique) for including results from aeroelastic considerations. ASSET provides the traditional rapid and cost-effective solution to configuration selection for any aircraft mission, within the limitation that the structural weight is based on statistical data. PADS (Preliminary Aeroelastic Design of Structures) is being developed to generate structural weight data that include aeroelastic considerations which in turn could be used to update ASSET's data base during configuration trade-off studies. Aeroelastic inputs to ASSET will lead to significant improvements in the configuration selection process especially when advanced designs combine composite structures with unusual planform geometry and operating conditions.

The paper discusses the design experience associated with a benchmark aeroelastic design of an out of production transport aircraft, and reports on current work being performed on a high aspect ratio wing design. The PADS system will be briefly summarized and some operational aspects of generating the design in an automated aeroelastic design environment will be discussed.

456

# INTRODUCTION

Preliminary design for an optimal aircraft configuration may require the integration of aeroelastic considerations into the configuration selection and design process. Aeroelastic design incorporates the effects of aircraft structural flexibility on static and dynamic loads, control effectiveness, and aeroelastic stability into the sizing of the structure. Configurations of aircraft in the early design stage are usually based on statistical and analytical weight methods computed from approximate loads and stress analyses. This often leads to the freezing of external geometry before strength and flutter analyses are sufficiently advanced, thereby decoupling the powerful but time-consuming process of structural design to minimum weight from the configuration optimization process. If the elapsed time to perform more accurate loads, structural design, and flutter optimization analyses is shortened, then structural optimization can proceed in concert with the overall configuration optimization, and more efficient advanced types of aircraft can be designed.

# ACRONYMS & DEFINITIONS

| | |
|---|---|
| ACS | - active control system |
| ASSET | - Advanced Systems Synthesis and Evaluation Technique |
| CADAM° | - Lockheed's computer aided design system |
| CBUS | - Continuous Batch User Specification |
| CPP | - command processor program in CBUS |
| DBM | - data base management |
| DMS | - data base management system |
| DOF | - degree of freedom |
| FAMAS | - Lockheed's matrix data based computing system for aeroelastic analysis |
| FINDEX | - Lockheed's DMS for matrices and NASTRAN tables |
| FSD | - fully stressed design algorithm |
| Lockheed | - Lockheed-California Company |
| MLC | - maneuver load control |
| NASA | - National Aeronautics and Space Administration |
| NASTRAN | - structural finite element program developed by NASA |
| PADS | - Preliminary Aeroelastic Design of Structures |
| PSASA | - panel sizing and stress allowables |
| RAP | - resource allocator program in CBUS |
| RDMS | - run data management system |
| SIC | - structural influence coefficients |
| SMG | - structural model generator, a finite element model generator which represents a family of aircraft designs. |

° Registered trademark of CADAM, Inc.

Aeroelastic analysis of an aircraft structure is a substantial undertaking involving many disciplines and complex data paths. A short time ago, preliminary aeroelastic analysis was reserved for projects on the verge of achieving go-ahead status while preliminary aeroelastic design was not even attempted.

In the past, the level of effort required for an accurate aeroelastic design was not justifiable relative to the answers provided by statistical methods which were supported by historical data bases. Today, however, there are many combinations of advanced technologies and configurations, such as supercritical airfoils, high aspect ratio wings, forward swept wings, active controls, aeroelastic tailoring, and new materials, that have no historical data base from which to derive the statistical or parametric weight equations. Two questions (Figure 1) regarding the role of aeroelastic design in preliminary design are:

1) How to integrate aeroelastic design in P.D.?

2) How to make aeroelastic design timely?


- ## HOW TO INTEGRATE AEROELASTIC DESIGN PROCESS INTO AIRCRAFT CONFIGURATION SELECTION?


- ## HOW TO REDUCE ELAPSED TIME FOR AEROELASTIC DESIGN?

Figure 1

APPROACH

There are two options available for acquiring a rapid aeroelastic analysis and design capability:  generate or acquire special programs tailored to rapid analysis procedures; or adapt existing engineering methodology and the associated computer tools to requirements of rapid analyses.  Software maintenance is a major part of any proposed computer-aided design system.  Lockheed-California Company (Lockheed) has an extensive library of computer programs which support airplane design through final and production design phases.  It would be convenient to extend the application of that software into the preliminary design phase instead of creating specialized software and to update statistical based weight equations used in the design process (Figure 2).

Airplane design involves complex interactions between the conceptual designer, the customer with design specifications, and the engineers with final design and manufacturing requirements.  Since many facets of the engineering process defy quantification, the computer methodology used to improve the flow of design information must be:  1) flexible  and 2) highly modular.  Flexibility will permit inputs into the design process from many sources, and modularity will deter obsolescence when new engineering design processes become available.

Against the background of existing data management systems, existing computing systems of great sophistication, and high-level languages oriented to the user-friendly atmosphere, the company decided to use the production design computing tools and to attack directly their known deficiencies with respect to preliminary design applications.  A computer system was postulated which would act as a bare tree from which existing computer programs could be hung as needed in a user-friendly and highly modular environment.

## ● UPDATE STATISTICAL BASED WEIGHT EQUATION USED IN CONFIGURATION SELECTION PROCESS

## ● USE EXISTING DESIGN AND ANALYSIS PROGRAMS
### — STATIC AND DYNAMICS LOADS
### — FINITE ELEMENT METHODS FOR STRUCTURE
### — FULL STRESS REPRESENTATION
### — WEIGHT DISTRIBUTION
### — STRUCTURAL SIZING FOR LOADS
### — FLUTTER
### — STRUCTURAL SIZING FOR FLUTTER AND DEFLECTION
### — ACTIVE CONTROLS

## ● AGGRESSIVE USE OF PRE- AND POSTPROCESSORS

## ● UNINTERRUPTED COMPUTING CAPABILITY

Figure 2

The goal of Preliminary Aeroelastic Design of Structures (PADS) is to develop computer operating system architecture and design methodology to be used to generate an accurate aeroelastic design within the conceptual and early preliminary design phases. This aeroelastic design data base will permit more accurate weights to be established during the configuration trade-off studies. The long term goal is to define an accurate aeroelastic design within an elapsed time which is measured in weeks and to perform a design perturbation within elapsed time which is measured in days (Figure 3). Design perturbations include changes to any variable which does not require significant data preparation. For the wing, these variables will include sweep, planform definition, taper, airfoil sections, t/c, and aspect ratio.

The work to achieve these goals is in progress. PADS capabilities currently include a structural finite element model generator, weight distribution, grid transformations, steady maneuver loads for symmetric conditions, dynamic gust loads, landing loads, brake loads, flutter analysis, and structural sizing.

This paper will address four areas:

1.  The formulation of computer operating system technology and data management techniques which will permit the definition and execution of engineering processes in a continuous, user-friendly computing environment

2.  The definition of engineering processes for preliminary aeroelastic design of structures which may be used to derive an accurate structural weight for a wing in the elapsed time normally available for a conceptual design phase

3.  The presentation of results from the PADS validation effort, computer software as well as engineering processes, using a known airplane design data base

4.  The presentation of results from a high aspect ratio wing design

## AEROELASTIC CONSIDERATIONS
## FOR ADVANCED DESIGN

|  | BEFORE PADS | AFTER PADS (GOAL) |
|---|---|---|
| • ELAPSED TIME | 2 TO 6 MONTHS | • 5 DAYS SETUP |
|  |  | • 1 DAY DESIGN PERTURBATIONS |
| • COSTS | MODEL COMPLEXITY MUST COVER ALL POSSIBLE ANALYSIS REQUIREMENTS — NO QUICK LOOK CAPABILITY | MODEL COMPLEXITY MATCHES ANALYSIS REQUIREMENTS — |
|  | 4 TO 10 MAN MONTHS | 2 MAN WEEKS |

Figure 3

# PADS/ASSET INTERFACE

Lockheed's Advanced Systems Synthesis and Evaluation Technique (ASSET) computer program provides a rapid and cost-effective solution to configuration selection for any aircraft mission, but only within the limitation that the structural weight must be based on semianalytical and statistical data. An ASSET study usually requires that a baseline aircraft model be created and exercised in ASSET to represent an actual known aircraft data base. This model then is modified through adjustments to parametric coefficients to simulate changes to baseline aircraft systems, structural arrangement, material usage, design parameters, and mission requirements. Once complete, the model is passed into the ASSET design cycle for sizing, configuration trade-off analysis, and performance evaluation.

The PADS goal is to update the weight data base during configuration trade-off studies as well as to perform general aeroelastic analysis and design in a highly computerized environment. Figure 4 shows the interaction between PADS and ASSET during a typical configuration trade-off study. Aeroelastic inputs to ASSET will lead to significant improvements in the configuration selection process, especially when advanced designs combine advanced structural materials, such as composites, with unusual geometry.

PADS development consists of two distinct efforts:

● The development of the computer operating system which will permit continuous computing capability in a user-friendly and engineering-defined environment.

● The definition and mechanization of basic engineering processes for use in aeroelastic design and analysis.

The computer operating system will have applications outside of PADS whenever a requirement exists to integrate diverse computing programs under one operating system.
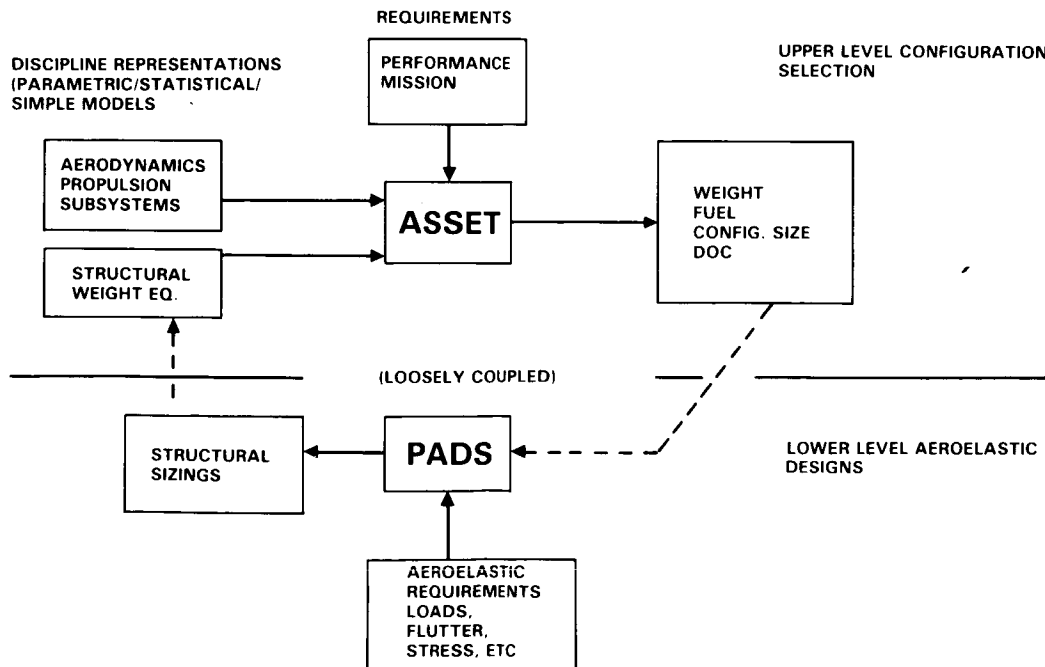


Figure 4

The design specifications of the operating system for PADS mirror the specifications of a computer hardware bus. The specifications of the computer hardware bus define an interfacing system for use in interconnecting data processing, data storage, and peripheral data control devices in a closely coupled configuration. Two objectives of a hardware bus are 1) to provide communication between two devices on the bus without disturbing the internal activities of the other devices interfaced to the bus, 2) to specify protocols that precisely define the interaction between the bus and devices interfaced to it.

If the word "devices" is replaced by "load modules/programs", the above specifications for a hardware bus come close to defining the specifications for a computer operating system in terms of a software bus. One of the reasons the operating system was named Continous Batch User Specification was to carry over the bus concept into the operating system acronym, namely CBUS.

The user normally accesses the computer through areas designated as "TARGET PROGRAMS" and Data Bases as shown in the Figure 5. While this level gives the user most of the flexibility, the user usually must address a lot of detailed work just to execute a simple task. CBUS provides the interface between target programs and data bases and commands that define a computing function or process. The user under this architecture executes processes which may contain hundreds of target programs executions and data base references.
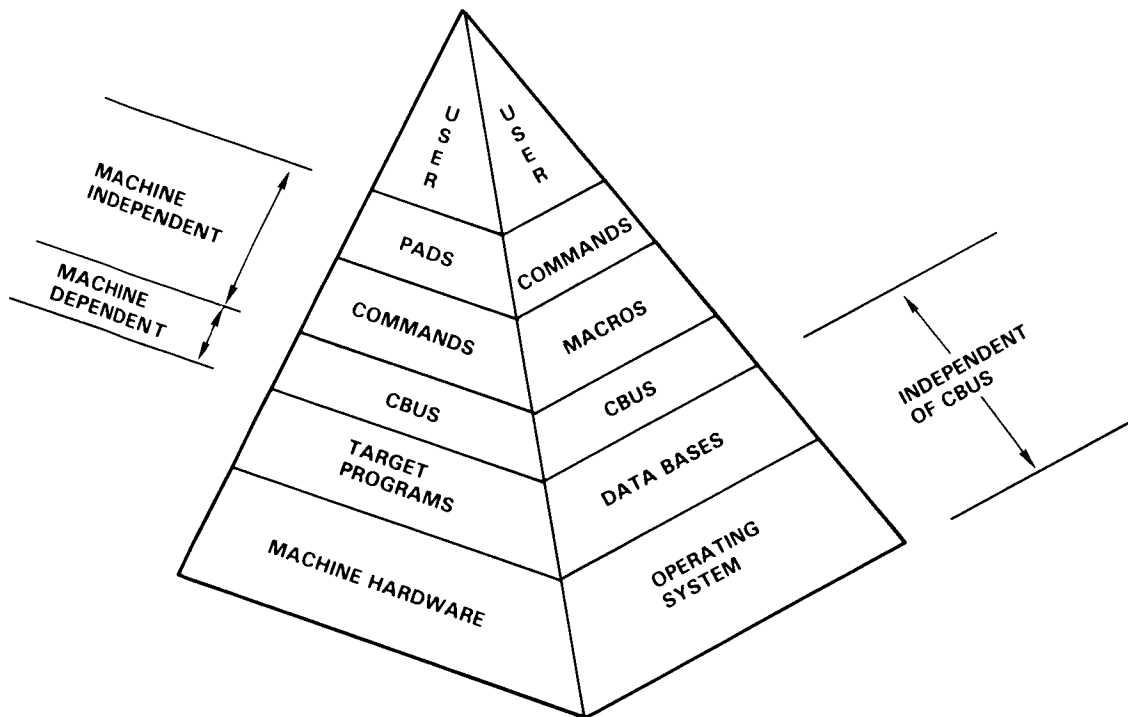


Figure 5

## CBUS OPERATING SYSTEM SPECIFICATIONS

The CBUS operating system (Figure 6) will 1) access and make use of any existing data base, 2) be able to use any existing or independently developed program, 3) impose no requirements on programs to be integrated into the operating system, 4) interface with the user with high-level, user-friendly language, 5) allow the command language names/keywords and computing processes to be definable outside of the operating system, 6) use existing data base management systems for storage of permanent data, 7) enable the computing process to be uninterrupted, and 8) permit the execution of an unlimited number of equivalent batch jobs in one computer run, in one uninterrupted computing segment.

- **ACCESS AND USE ANY EXISTING DATABASE SYSTEM**

- **IMPOSE NO REQUIREMENTS ON EXISTING PROGRAMS FOR INTEGRATION**

- **INTERFACE WITH HIGH-LEVEL, USER-FRIENDLY LANGUAGE**

- **ALLOW USER DEFINED NAMES AND KEYWORDS**

- **USE EXISTING DBMS FOR STORAGE OF PERMANENT DATA**

- **ALLOW THE COMPUTING PROCESS TO BE UNINTERRUPTED**

- **PERMIT THE EXECUTION OF UNLIMITED NUMBER OF EQUIVALENT BATCH JOBS**

Figure 6

# CBUS GENERAL CHARACTERISTICS

The CBUS operating system consists of four players:  1) the monitor, 2) the resource allocator, 3) the command processor, and 4) the target (Figure 7).  Each player is a separate executable load module in its own right, with the monitor, command processor, and resource allocator having a special interrelationship.

The monitor is the upper level program which loads other executable load modules into core for execution.  The resource allocator is a program which allocates and redefines computer resources as required by the next target.  The target is any executable load module (program) which the monitor will attach and execute during the continuous computing sequence.

The command processor program (CPP) interprets user supplied information and builds a stream of data which instructs the resource allocator on how to arrange the resources of the computer to satisfy the needs of the next program to be executed, while under the umbrella of the monitor.  The command processor data source is a library of macros/commands, including the names of the macros/commands, which are user-generated.  Figure 7 illustrates the essential features of the operating system.
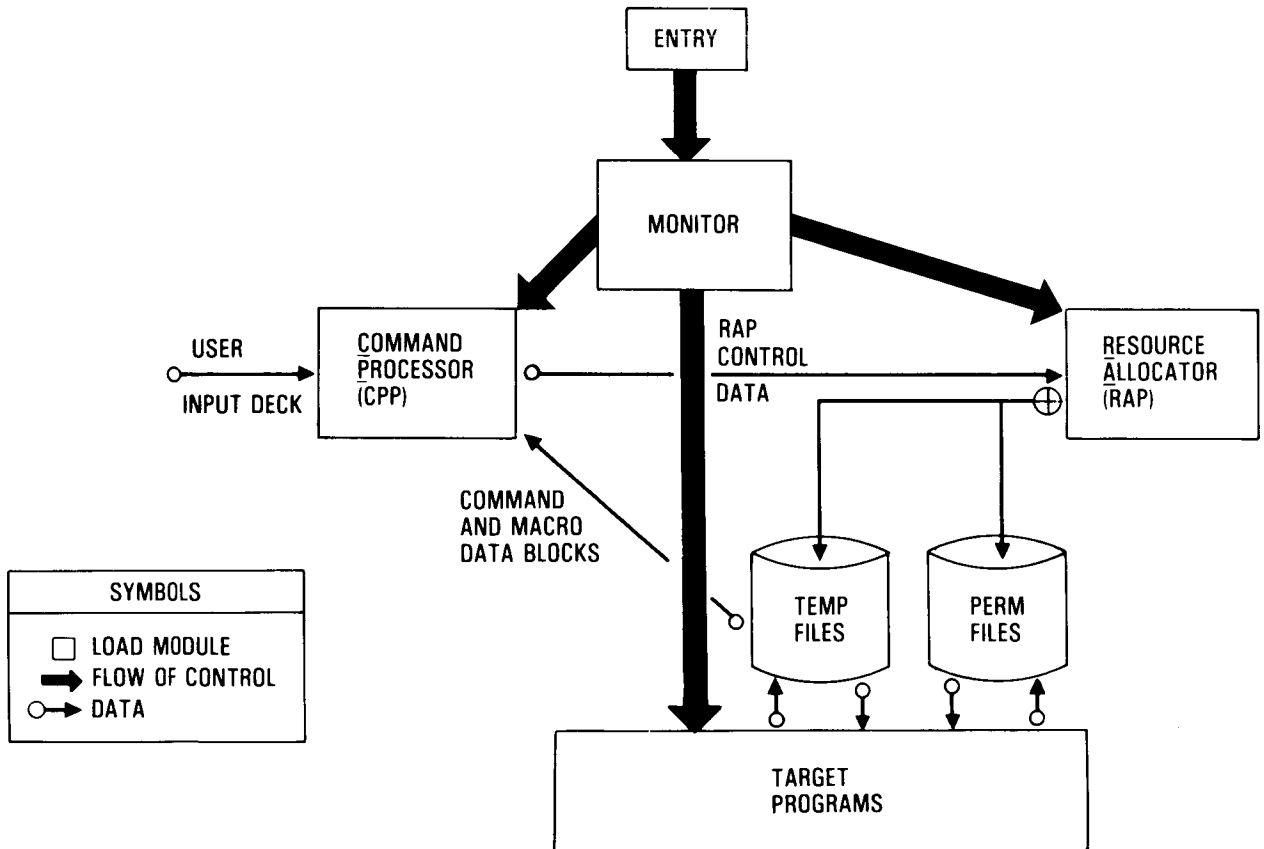


Figure 7

464

The user interfaces with the CBUS operating system through commands and through the command processor language. A command specifies a process in a language which is interpretable by the CBUS command processor at the user input level. A process is a particular method of doing something, generally involving a number of computer programs and/or operations. A command contains all the defaults necessary for executing a process. The command processor recognizes four levels of macro configured data structures; namely, macro, subcommand, command, and supercommand. The different levels of macros, as illustrated in Figure 8, make possible the definition of primitive processes which can be used as building blocks for any number of higher level processes. The macro and subcommand are building blocks for commands while commands are building blocks for supercommands.

A subcommand is a self-contained instruction set which defines a process to be performed and is accessible in the CBUS operating system by the same naming convention as is available for a macro.

A command contains, in a fixed sequence, a collection of references to subcommands as well as all defaults for attributes associated with subcommands and macros.

A supercommand contains references to commands and supercommands, and includes all defaults necessary to perform its function. Supercommands, therefore, permit recursive operations because a supercommand can reference itself.
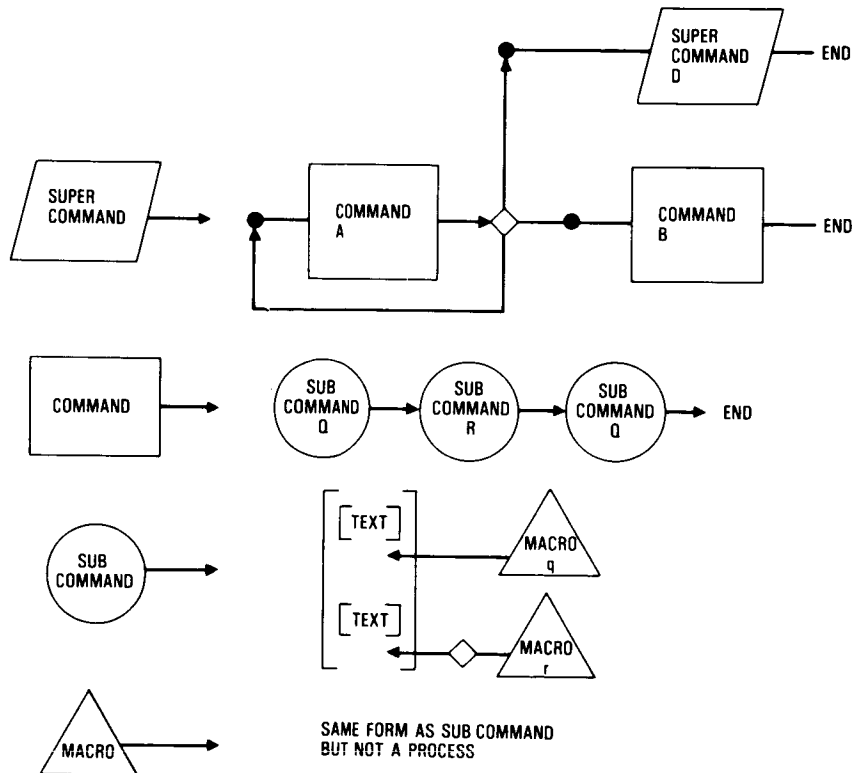


## MACRO STRUCTURE EXAMPLES

Figure 8

A command includes all instructions and attribute default assignments necessary for execution. The functionality concept requires that the user be able to alter the command's default attributes. Attributes which could be candidates for change are names of data sets to be incorporated into the process, constants to be used in the computations, and naming of output data sets associated with the process. The alter capability also permits the complete definition of the function with all defaults, while retaining the flexibility to generate a radically new version of the function without creating and storing a new version of an existing command/macro code.

As shown in Figure 9, an alter capability is made available at every level of the command/macro tier by providing an alter command card after the data line which is to be altered. The alter command line executes the prescribed alter function when the user supplies an altercard with the identical keyword which is also imbedded in the alter command line.

The altercards can be grouped into four categories: global, command user-supplied, subcommand default, and altermacro. Global altercards are those that the user can specify to apply to the entire run. Altercards supplied by the user under the command definition have the highest priority, and will override the global alter-cards. The altermacro, altercards imbedded in a macro, is placed below the global altercards and above the default cards supplied in the subcommand.
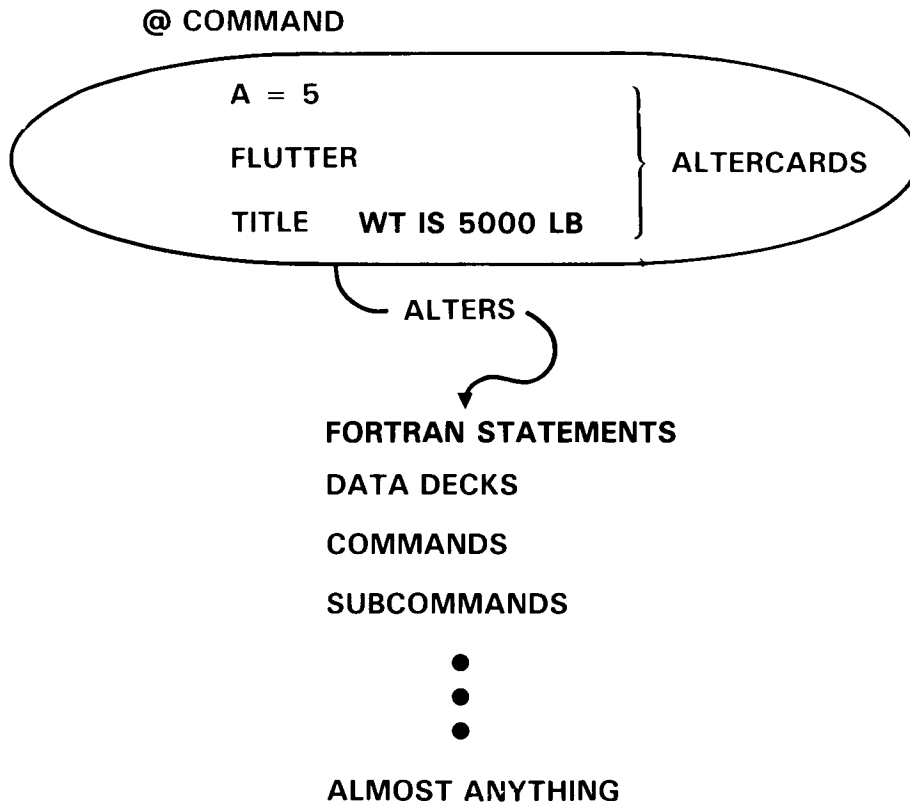
**@ COMMAND**

A = 5

FLUTTER

TITLE    WT IS 5000 LB    } ALTERCARDS

— ALTERS

FORTRAN STATEMENTS

DATA DECKS

COMMANDS

SUBCOMMANDS

•
•
•

ALMOST ANYTHING

Figure 9

## COMMAND PROCESSOR LANGUAGE

The user command language is a high level language which permits the typical user to define complex computing functions through commands and branch capabilities. Some of the essential features will be demonstrated by example.

Figure 10 shows the format for invoking a (super) command, executing an unconditional branch, a conditional branch, and a call to an internal procedure, and computing scalars, as well as a three level altercard capability. Each qualifier may contain up to eight characters. The altercard may be as simple as a name ABC.

**@ NAME;  INVOKES (SUPER) COMMAND**

**@ GO TO _____ ;**

**@ IF (A*B — 3.0. GT.R) THEN _____**

**@ CALL _____ ;  CALL TO INTERNAL PROCEDURE**

**A < 3.4 * 30 — B; CALCULATOR MODE**

**ABC __ DEF __ __ GHI __ __ __ JKL = _____ ; ALTERCARD**
**(THREE LEVELS)**

Figure 10

C-6

# THE DESIGN PROCESS

The first step in the design process is to define the objectives of the task and the necessary level of design detail required to satisfy those objectives. The design team must then review the requirements, cost out the project, and define a schedule. This is an iterative process between the customer and the design team as with any project with a specific amount of available resources. This phase is labelled "DESIGN OBJECTIVES" in Figure 11.

The next step is the generation of the structural finite element model, initial weight distributions, and initial entries into the various modules to generate geometry tables for each grid system to be used in the design.

The initial internal loads intensities are generated from static loads for a rigid airplane and uniform properties for those structural finite elements to be sized. A panel sizing and stress allowable (PSASA) process then generates from the load intensities the initial sizing for the specified margins of safety.

The computations for static loads and internal loads intensities are repeated using the sizing derived from rigid airplane loads.

The first flex sizing data provides a basis for updating the weight data and for generating dynamic loads input (gust, taxi, landing) along with the flutter minimum sizing constraints.
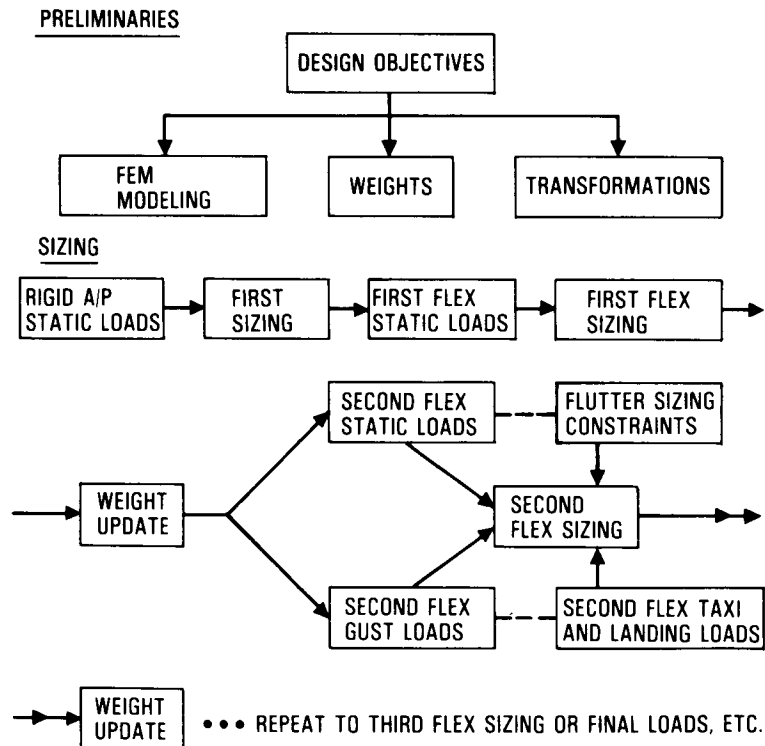


Figure 11

GRID TRANSFORMATIONS

The underlying premise to the development of PADS capability is the use of production tools and proven procedures to formulate the necessary analytical processes to be used in weight, flutter, loads, etc. This approach results in a general proliferation of grid/coordinate systems. A method was devised to generate systematically the transformations between the many grid systems without sacrificing flexibility (Figure 12).

The grid transformation process requires location and type-of-displacement labeling of the degrees of freedom (DOF) for the two grids involved in the transformation. However, certain sections of the airplane have special requirements concerning the transformation process; for example, aileron control surface mass elements should be beamed to flexibility degrees of freedom on the aileron and not to the degrees of freedom on the outer wing. So in addition to location and DOF information, the geometry table includes group identifications, such as inner wing, outer wing, aileron, pylon, and fuselage. The transformation between grids therefore is limited to boundaries defined by the airplane groups. The responsibility of generating geometry tables resides with the discipline which defines the grid.

## --THE KEY TO COMMUNICATION BETWEEN DISCIPLINES--

## AERODYNAMICS

## STRUCTURES (MODELLING AND STRESS)

## WEIGHT

## STATIC LOADS

## DYNAMIC LOADS

## FLUTTER

Figure 12

Each engineering discipline will define the modeling requirements according to its functions and responsibilities. There will be no outside constraints except where more than one discipline will be affected.

There are practical limits to reducing the elapsed time required to generate and checkout a 3-D finite element model. Experience gained with the use of user coded programs which generate, correct, and manipulate computer files led to the engineering development and coding of computer programs for rapid generation of principal parts of the finite element model using relatively few input variables.

A finite element model generator (Figure 13) will be assembled from this technology. Data for the model generator will be defined to represent a specific family of aircraft designs which may be generated using relatively simple inputs. The collection of model generator programs and the input data required to represent a particular family of aircraft designs will be referred to as a structural model generator (SMG).

Wing geometric data for input to the finite element model generator will consist of certain key variables that define the wing planform together with a 3-D parametric representation of the wing section shapes. The section shape representation is available from the aerodynamics department and serves as the input data for ASSET. This arrangement will permit variations in aspect ratio, t/c, planform, taper, sweep, and dihedral with relatively simple inputs.

# NASTRAN MODEL GENERATOR

Figure 13

There are two forms of finite element modeling: 1) that which is required for stress considerations, and 2) that which is required for structural flexibility/ stiffness considerations. The task here is to generate a finite element structural model computer data deck which will serve the objectives of both. Critical to the quick design concept as shown in Figure 14 is a structural model generator (SMG) which would generate a family of finite element models using relatively simple inputs. These inputs would primarily be a function of the airplane external geometry and generally not a function of model configuration arrangements.

The 3-D modeling of the structure begins with a "bones" drawing of critical geometric control points to be used in the programs which generate and assemble finite element program input decks. The 3-D description for the wing is derived from a data base which Aerodynamics generates as part of their aerodynamic configurations studies. Control surfaces, flaps, and the associated actuation systems are modeled as necessary. Leading and trailing edge surfaces are modeled for load carrying requirements and not stress sizing.

# STRUCTURAL MODEL GENERATOR

## --THE KEY TO QUICK DESIGN CONCEPT--

### GENERATES A FAMILY OF 3-D FINITE ELEMENT STRUCTURAL MODELS USING RELATIVELY SIMPLE INPUTS

- **AERODYNAMICS PARAMETRIC REPRESENTATION OF THE WING**

- **"BONES" DRAWING OF CRITICAL GEOMETRIC CONTROL POINTS**

### THE OBJECTIVE IS TO HAVE A STRUCTURAL MODEL GENERATOR FOR EACH CLASS OF AIRPLANES

- **JET TRANSPORT/ASW AIRPLANE (AVAILABLE)**

- **PROP DRIVEN TRANSPORTATION/ASW AIRPLANE (NOT AVAILABLE)**

- **FIGHTER (DELTA PLANFORM) (NOT AVAILABLE)**

Figure 14

471

# STRUCTURAL FINITE ELEMENT MODEL DEFINITION

The finite element model consists of three parts: 1) the wing, which is a full 3-D model (Figure 15) with a medium degree of detail, inculding control surfaces, flaps, gears, and leading and trailing edge structure; 2) the fuselage over the wing box, which is a full 3-D barrel section; and 3) the forward fuselage, aft fuselage, and the empennage, which are modeled with beam elements. There are 3,741 degrees of freedom in the NASTRAN F-set, 228 degrees of freedom for the definition of the structural influence coefficients, and 161 for the A-set stiffness matrix. The wing contour data base was obtained from the aerodynamics representation used in drag and lift studies. The ribs were modeled one model rib to two airplane ribs.
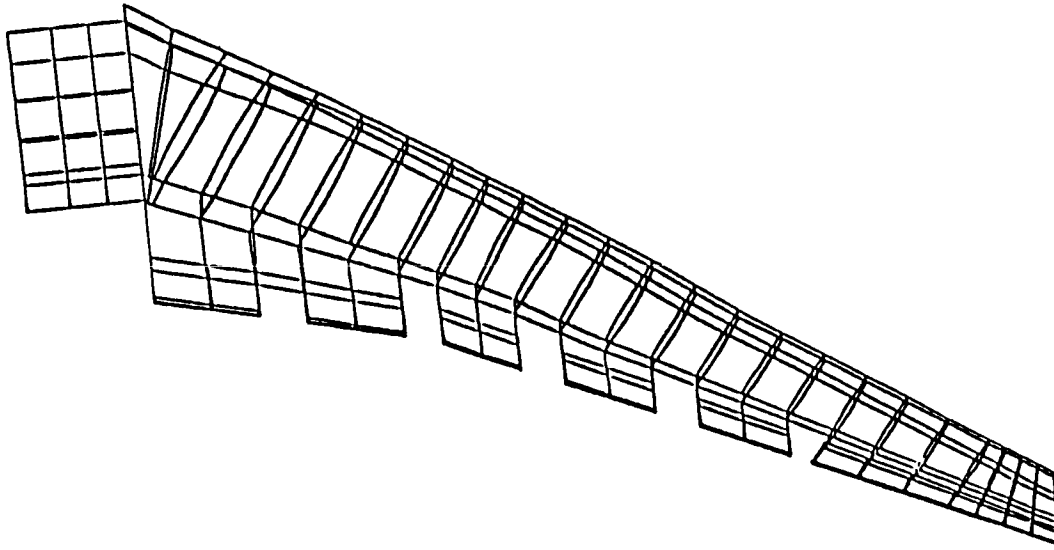


Figure 15

# FINITE ELEMENT MODEL GENERATOR

Generation of NASTRAN bulk data decks for families of high aspect ratio wing designs, in order to modify model parameters such as thickness ratio, sweep angle, aspect ratio, taper ratio, or wing area, has been automated and integrated into PADS. From the relatively simple inputs, key planform coordinates and cross-section definition datasets are created. Figure 16 shows an example of the program interfaces in the NASTRAN model generator for a typical high aspect ratio wing airplane design.

REWING generates the initial datasets which contain geometric keypoints and airfoil definition for a desired planform layout. From the datasets produced by REWING, a program called WBONES defines locations/orientations, such as spar and aileron layout, locations for planar grid points, and initial identification numbering for the production of NASTRAN grid cards. SLICE provides the airfoil definition for the three-dimensional finite element model. Input to SLICE consists of airfoil definition in the streamwise direction as well as outputs from REWING and WBONES. SLICE interpolates from the input airfoil definition to obtain the airfoil definition for the desired cuts.

Additional grid locations and connectivity necessary for structural elements between the fuselage and wing are created by a program called QUILT. PROCARD outputs a deck of wing grid cards which is in final form.

Program SICTAB generates additional NASTRAN bulk data cards such as ASETS, LDREF, FORCE, MOMENT, LMAT, and some of the MPC cards.
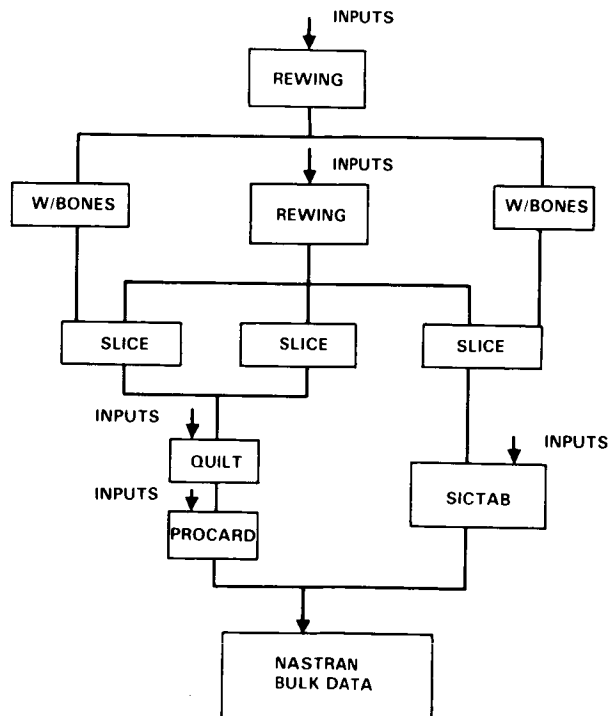
## NASTRAN MODEL GENERATOR PROGRAM INTERFACE



Figure 16

In the PADS system, the geometry of a wing is described by data files which contain the coordinates of the planform outline, the airfoil contour, and keypoints for major structural elements. With use of similarity transforms, the geometry description of new wings can be formed from existing wings. The layout of a new wing is defined by values of selected geometric parameters, such as aspect ratio, sweep, span, and thickness ratio. REWING creates the data files necessary for geometric description of wings. REWING allows creation of new planforms by variation of one or more geometric parameters.

Figure 17 displays creation of new planforms from existing planforms for subsonic and supersonic designs, respectively. The figure represents the creation of an aspect ratio 12 wing planform from an aspect ratio 7.64 wing planform. In this example, additional input to REWING included specifications to locate the 1/4 chord point of the MAC at the same fuselage location on the new planform as it was on the original. The location of this reference point is shown as an x for the original planform and as a + for the new planform. The figure shows a combined variation of sweep and taper angle for an arrow wing planform.
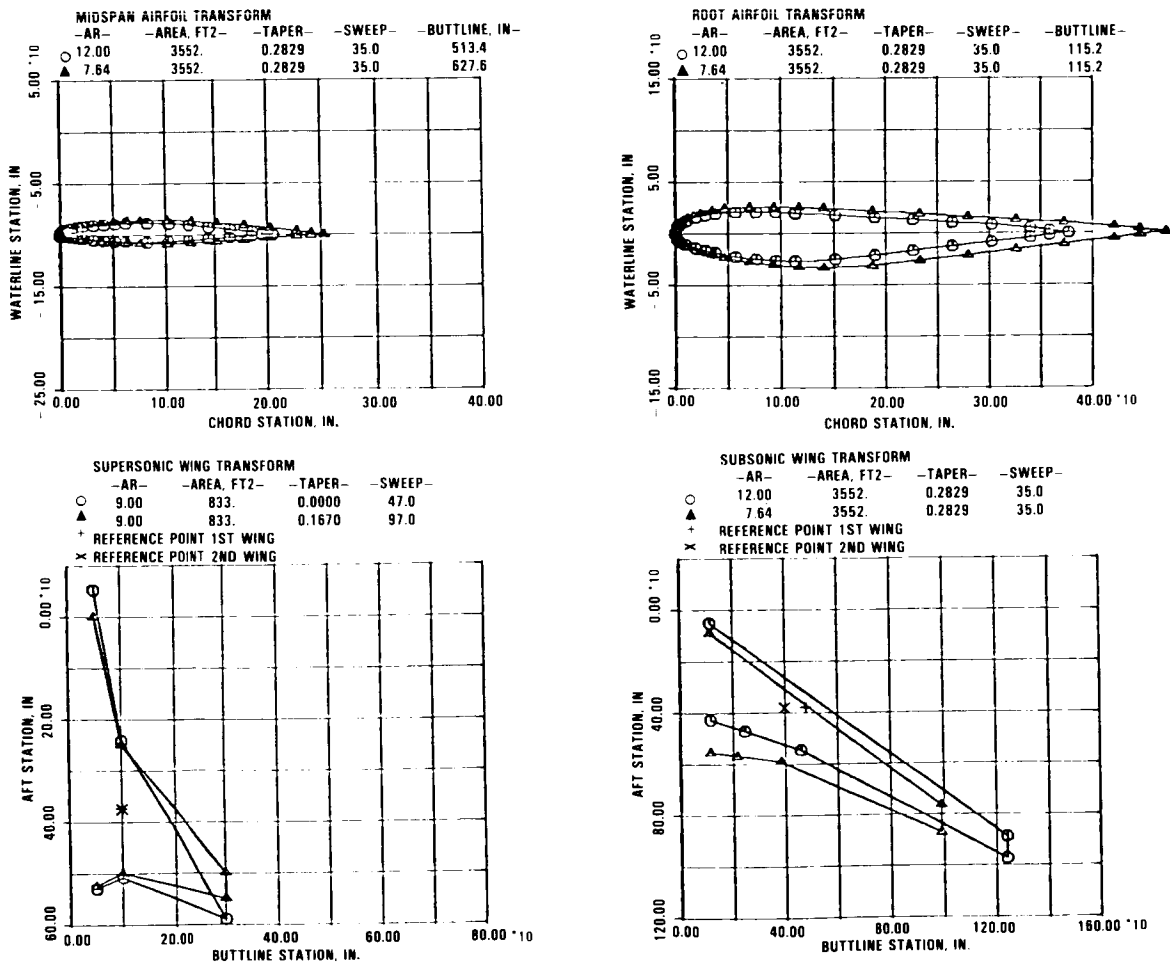


Figure 17

# STRUCTURAL MODEL GENERATOR CAPABILITIES

A summary of the NASTRAN model generator capabilities is shown in Figure 18. The quick response capability is derived from a flow of data and program executions that represents a family of aircraft configurations.

- **REPOSITIONS THE WING DUE TO ASPECT RATIO, SWEEP, AND AREA CHANGES**

- **FORMS THE EXTERNAL GEOMETRY FROM PARAMETRIC WING GEOMETRY SUPPLIED BY AERODYNAMICS**

- **GENERATES COMPLETE NASTRAN BULK DATA DECK WITHIN 2 DAYS FOR ASPECT RATIO, SWEEP, AND AREA CHANGES**

Figure 18

The procedures described above were used in the formulation of a NASTRAN model for aspect ratio 12 wing.  Figure 19 shows location of the wing and fuselage barrel section along with the stick model grid points for the fore and aft fuselage.
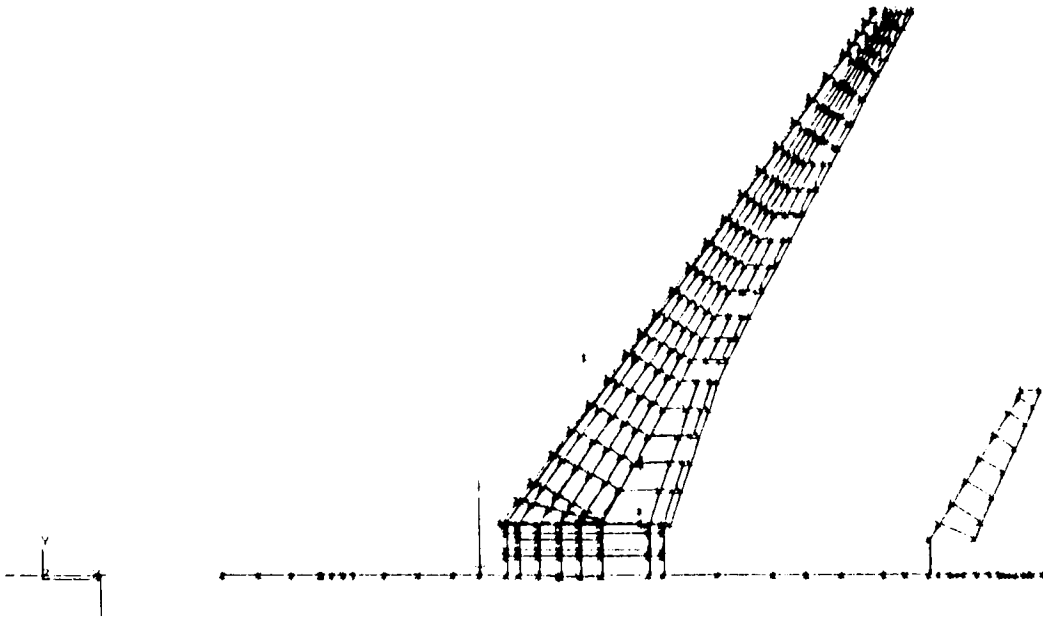


Figure 19

# AR12 SWEEP 35 NASTRAN MODEL WITHOUT WING

Figure 20 shows the NASTRAN model without wing. Fuselage attachments are more clearly seen in this figure. Gear up/down attachment points exist on the fuselage as well as on the wing.

VERTICAL FIN

GEAR UP/DOWN

HORIZONTAL FIN
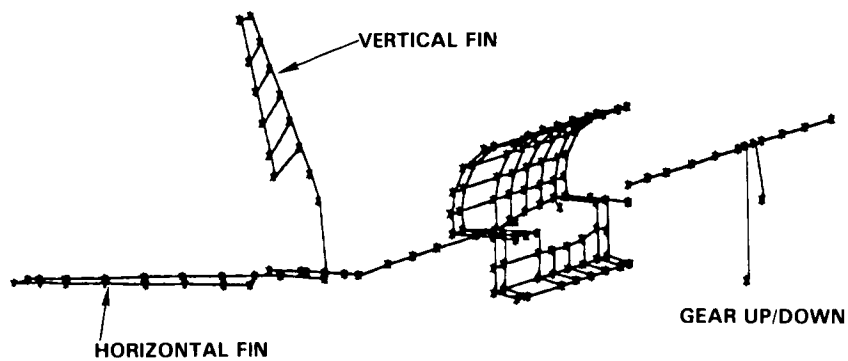
Figure 20

## NASTRAN MODEL BARREL SECTION DETAIL

   Figure 21 shows barrel section detail.  The fuselage stick model and the barrel
section interfaces are defined by multipoint constraint equations.  The wing carry-
through structure fits in the barrel section cavity.

**AR12 SWEEP 35**

NOSE

z

Figure 21

# GRID LOAD DISTRIBUTION

Complex aircraft such as the high aspect ratio wing design require a structural grid corresponding to a large number of degrees of freedom for the structural representation. Loads analyses, on the other hand, usually require a somewhat smaller grid. For this reason, application of external loads to a finite element model is normally performed through a load transformation process from a small t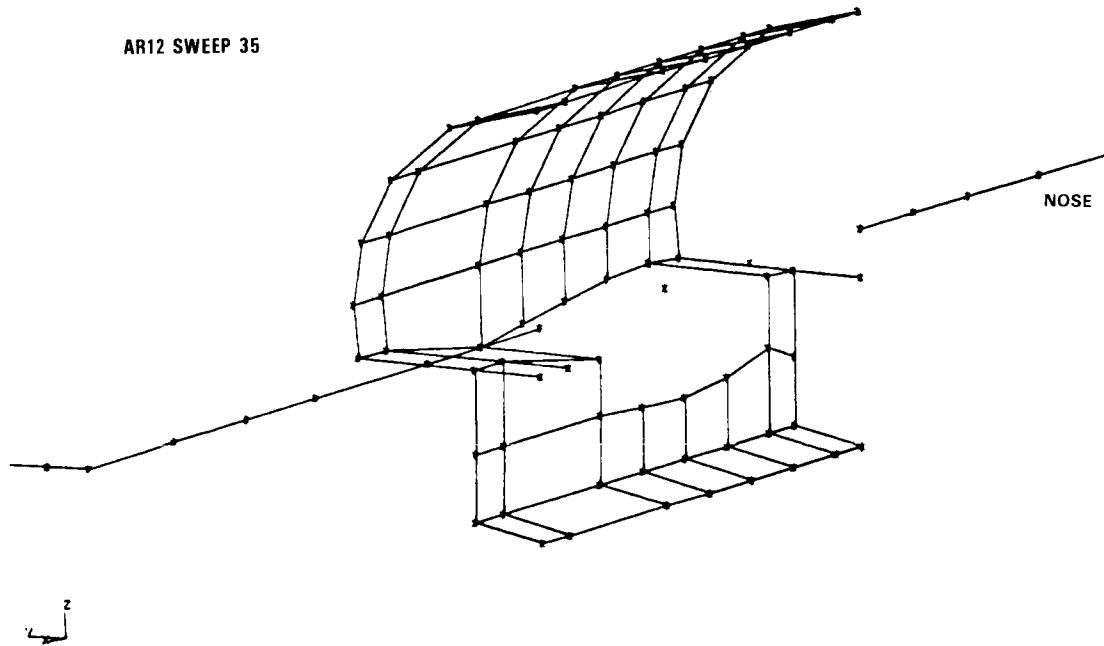o a large grid (Figure 22). In the PADS operation, the LDREF-LGROUP method is used. The LDREF cards contain load reference application information and the LGROUP cards contain information as to which grid points receive loads for a loaded reference point and how they are distributed. For changing planforms, the bulk data cards, for the LDREF-LGROUP method, are subject to change. For this reason, certain PADS modules were developed for purposes of automating the production of these cards.

```
   ┌─────────┐                                    ┌─────────┐
  (  ANALYSIS )      IS MAPPED INTO              (  NASTRAN )
  (  LOADS    )─────────────────────────────────>(  FEM    )
  (  GRID     )                                   (  GRID   )
   └─────────┘                                    └─────────┘
     SMALL                                           LARGE
     DOF                                             DOF
```
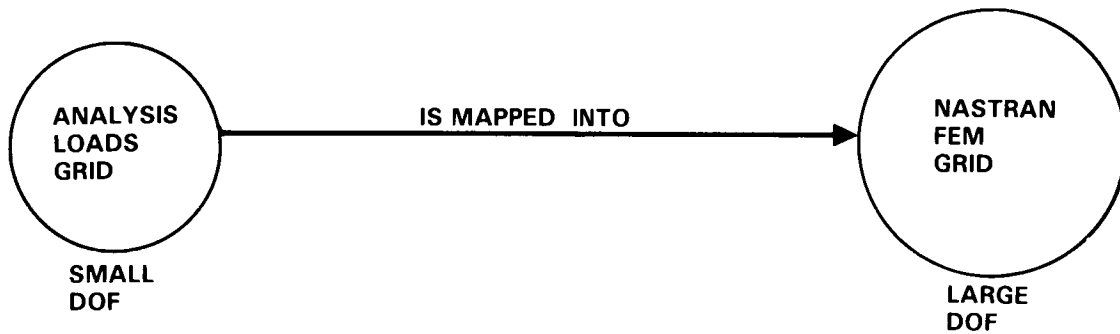
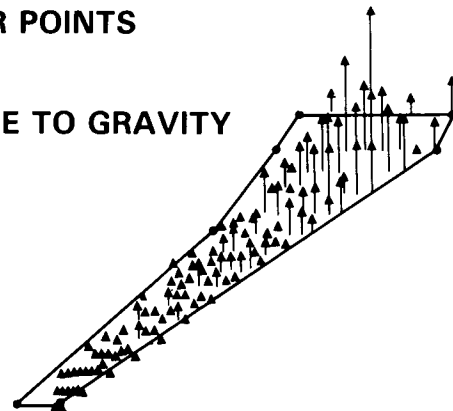Figure 22

# FUEL TANK LOADING PROCEDURE

With capabilities for changing planform and airfoil definitions in an automated procedure, a requirement surfaced to quickly form fuel tank weight distributions for changed planforms in an automated manner.  Issues to be addressed were 1) what will the new volume capacity be?  2) how can distributions for varying flight conditions be formed?  3) how can fuel tank weight distributions be entered into the model? A program  called TANK  was developed to automate computation of fuel tank loading distributions for preliminary design.

TANK receives inputs from other PADS modules  as well as inputs defining desired flight orientations and fuel loadings, and constructs a lumped fuel distribution which reflects the flight configurations considered in the design.  TANK computes definition of the tank boundaries from airfoil definition contained in the grid cards for the finite element model and corner point inputs.  With tank boundaries known, the fuel tank total volume can be computed.  Basic data input such as fuel density, attitude angles, and desired total fuel weight  allow TANK to form elementary fuel boxes and distribute the fuel weight as lumped fuel masses to the finite element grid locations.  Balance and center-of-gravity computation data, as well as the fuel distribution, are then supplied as output.

TANK, in the PADS environment, is called upon several times for aircraft with multiple tanks.  Then, a postprocessor combines the various fuel tank weight distributions and performs a transformation to other desired grids.  Typical plot output from the PADS fuel tank lumping procedure is shown in Figure 23.

An automated fuel tank weight distribution program was needed to complement the capabilities for quickly changing planform and airfoil contours.

- **FUEL VOLUME COMPUTED FROM FEM GEOMETRY DATA**
- **TANK BOUNDARIES DEFINED BY CORNER POINTS**
- **ACCEPTS LESS THAN FULL VOLUMES**
- **ACCEPTS TANK ORIENTATIONS RELATIVE TO GRAVITY**
- **BATCH ENTRY PROGRAM**

TYPICAL FUEL DISTRIBUTION

Figure 23

INTERLOP GUST PROGRAM

INTERLOP (INTERnal LOad Procedure) computes the internal loads combinations directly in the gust analysis. This requires the input of all internal loads of interest due to all unit loads at each structural grid point separately. Figure 24 shows the various elements of INTERLOP.

The advantages of the use of INTERLOP are substantial. Not only is the costly and time-consuming process of matching conditions avoided, but the internal vs. external loads matrix is used for other loads analyses besides gusts. Furthermore, since the internal loads are computed directly, no additional conservatisms need to be introduced, which is next to unavoidable if matching conditions are used.

Two new computer programs are created for this purpose: a preprocessor and a modified gust analysis program. The preprocessor forms the input to the gust analysis program defining the flexibility and the inertia properties (weights and moments of inertia of concentrated masses.) The new gust analysis program is a modified version of a standard gust loads program. The modifications include accepting as input the aerodynamic influence coefficients (AIC) which are also used in the flutter analysis. (These include AIC's at several reduced frequencies.) The program is extended to compute the 8 corners of the octagons of equal probability, and includes the bias formed by the 1-g steady loads. The latter is obtained using the 1-g (external) structural grid point loads computed by STATICS. The dimensions of the octagon are determined by an input value, which is the predicted gust intensity factor in feet/ second. This is based on the use of the design envelope approach rather than a mission profile analysis. The former, because of its simplicity, is considered to be more appropriate for a preliminary design effort, in particular because the missions may not yet be completely defined.
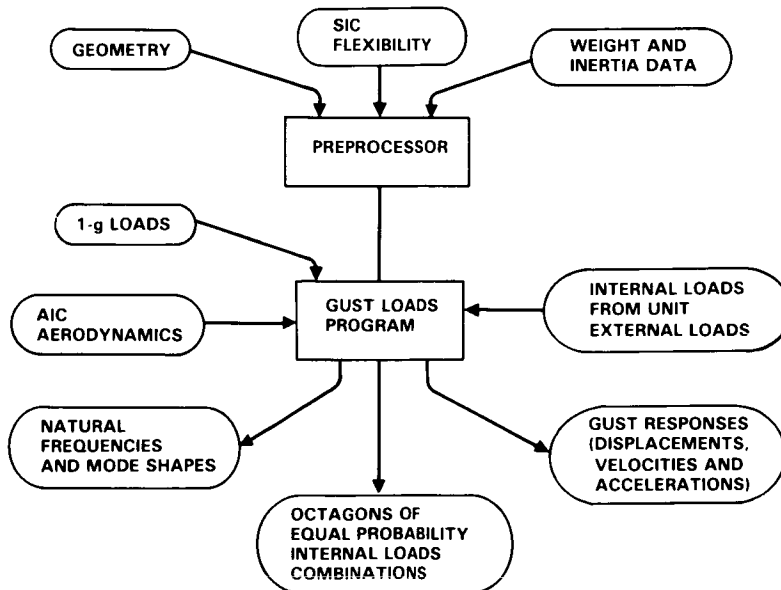
Figure 24

TYPICAL OCTAGONS OF EQUAL PROBABILITY - STRUCTURAL ELEMENT NO. 171 AND NO. 172
UPPER AND LOWER WING SURFACE

For a preliminary design, or in the absence of defined missions, the responses can be computed for a number of points of the design speed-altitude envelope, much in the same way that static gust analysis is done.

The design envelope contains the critical values of weight distribution, flight speed, and altitude. In this case the responses are found by multiplying the r.m.s. values of responses due to 1 ft/sec. gust by the gust intensity factor. This gust intensity factor is a function of altitude, comparable to specified gust velocities used in static analyses. In order to properly account for the phasing between the various responses, correlation coefficients between these responses are also computed. From these correlation coefficients and using the r.m.s. values of the responses, ellipses of equal probability of selected response combinations are formed. These are biased by the response due to 1-g steady flight for the pertinent design envelope point. In order to limit the number of conditions to be analyzed for stress, the ellipses are circumscribed by octagons. Thus each load combination results in 8 points of an octagon of equal probability.

Figure 25 shows a typical result of this new analysis approach. It consists of two equal probability ellipses and their circumscribing octagons. These are for one element of the upper wing surface and the corresponding element on the lower wing surface.
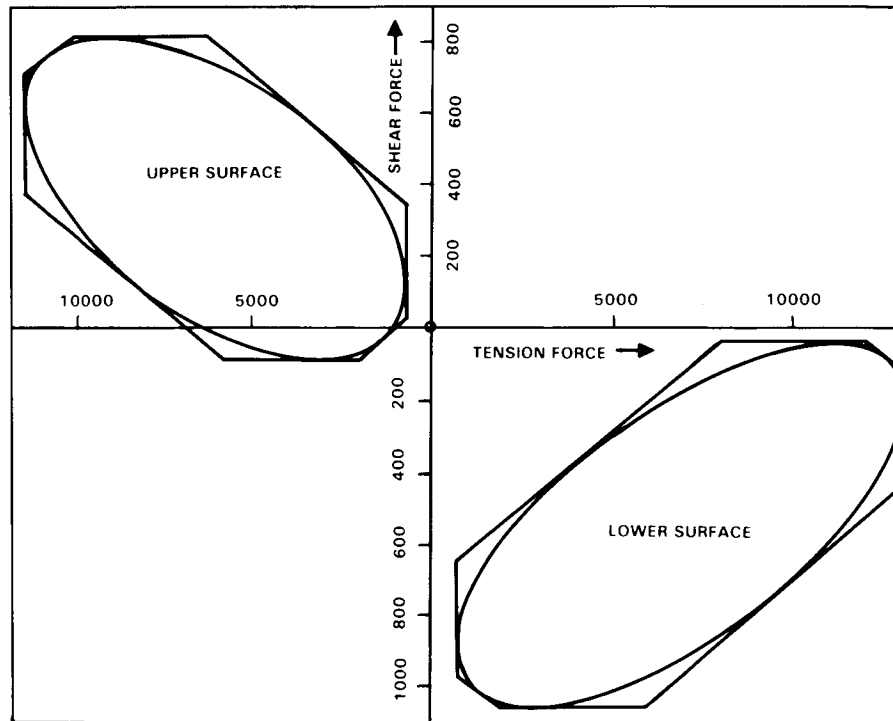


Figure 25

482

There were two requirements associated with structural sizing procedures (Figure 26) as applied to preliminary design: 1) the sizing must be based on project sizing procedures, and 2) the adoption of the production sizing procedures must accommodate the cost constraints of preliminary design.

A panel sizing and stress allowable process used internal load intensities from the finite element model to select the sizing necessary to satisfy strength, fatigue, and many other design criteria. This inhouse procedure is used to compute margins of safety for production designs. The process also makes use of a special data base to reduce the computer run times, an important factor in an iterative procedure. The data base is keyed to two configurations, namely Z-stringers for the upper surface and J-stringers for the lower surface. Materials for both configurations were 7075-T7651 plate for the skin and 7075-T6511 extrusion for the stringers.

The reference airplane production minimum margins of safety were taken from the stress reports. The grid in the stress report did not coincide with the panel layout. A linear interpolation was performed on the production margins of safety without regard to loading conditions compatibility. The margins of safety for the wing box, however, did not exist. The wing box margins of safety were therefore set to zero.

# SIZING PROCEDURES

Figure 26

## STRESS SIZING FUNCTION

Two tools are available at Lockheed to size structural elements based on strength criteria: the fully stressed design (FSD) program and the panel sizing and stress allowable (PSASA) program. Figure 27 shows the possible paths to structural sizing, 1) PSASA for stress allowables and FSD for sizing, and 2) PSASA for sizing.

PSASA generates the stress allowables and new sizings for use in the fully stressed design (FSD) program. PSASA is a complex array of programs which permit production level computations of stress interactions for a variety of conditions including panel buckling and several local buckling modes. If the design involves only panels, then sizing is possible using PSASA. PSASA is currently limited to combined uniaxial and shear loadings. However, PSASA does accept as input, margins of safety for each element being sized.

FSD requires a stress allowable for each element to be sized. The stress allowables remain constant within NASTRAN as the elements are sized to the internal loads. The internal loads are computed from the updated sizings and the external loads. Two to four iterations are necessary for the process to converge.
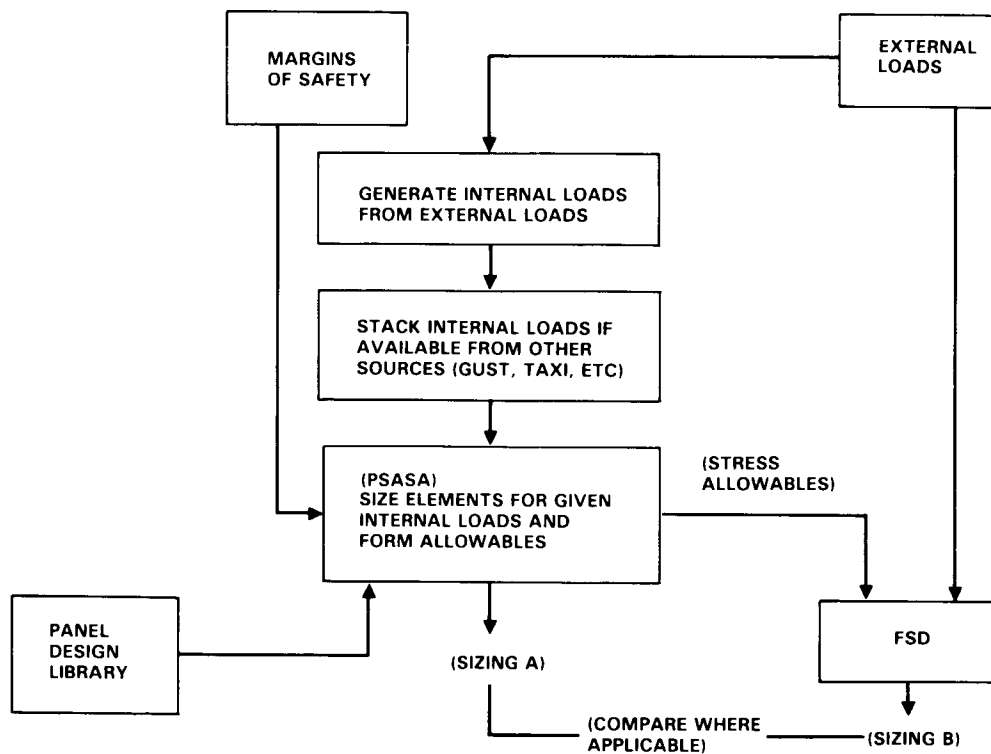


Figure 27

VALIDATION EFFORT

There are two phases to the process by which PADS is being evaluated: 1) the validation of CBUS operating system and the analysis programs, and 2) the validation of the design process for the objectives of preliminary design. Both phases require an existing production airplane design which has an extensive data base for weight, design loads, sizing, etc., for comparisons. These quantities are required not only for reasonableness checks but also to quantify the areas of design that may not be properly represented in the design process (Figure 28).

All major computing programs (FAMAS, NASTRAN, etc.) except the weight distribution program, the panel sizing and allowable program, the fully stressed design sizing program, and the program for structural resizing for flutter were used in the production design of the basic L-1011 and its derivatives.

The validation process reduces to the following tasks: 1) to verify that the existing computer programs and systems operate properly in the CBUS environment, 2) to verify that the many pre- and post-processor modules do what they were designed to do, 3) to verify that the CBUS data management systems properly function in their storing and retrieving modes, and 4) to generate comparative data for programs not extensively used.

The panel sizing and stress allowable procedure was checked against known allowable and sizing data for certain internal load conditions and the fully stressed design procedure was compared to the panel sizing procedure. The weight distribution program has internal checks for mass and moments of inertia quantities. The structural resizing for flutter programs also will contain internal checks in terms of reconciling the modules and sizing changes with the flutter results using the resized structural properties.

## ● CBUS

## ● NEW PROGRAMS

## ● DESIGN PROCESS

Figure 28

The airplane selected as a reference design is the L-1011-500 ACS. The airplane 3-view is shown in Figure 29. This configuration has a maximum gross weight of 504,000 pounds and a payload of 40,000 pounds at a range of 5200 nautical miles. The cruise Mach number is 0.83 and the cruise altitude is 37,000 feet. This version is a long-range derivative of the L-1011-1. Active control technology was used to minimize structural wing changes when the -500 wing span was extended to improve fuel economy. The maximum design zero fuel weight is 338,000 pounds. The typical operating empty weight is 252,000 pounds.



**L-1011-500 ACS THREE VIEW**

71 FT-7 IN. (21.82 M)

55 FT-4 IN. (16.87 M)

19 FT-7 IN. DIA (5.97 M)

164 FT-4 IN. (50.09 M)

164 FT-2 IN. (50.04 M)
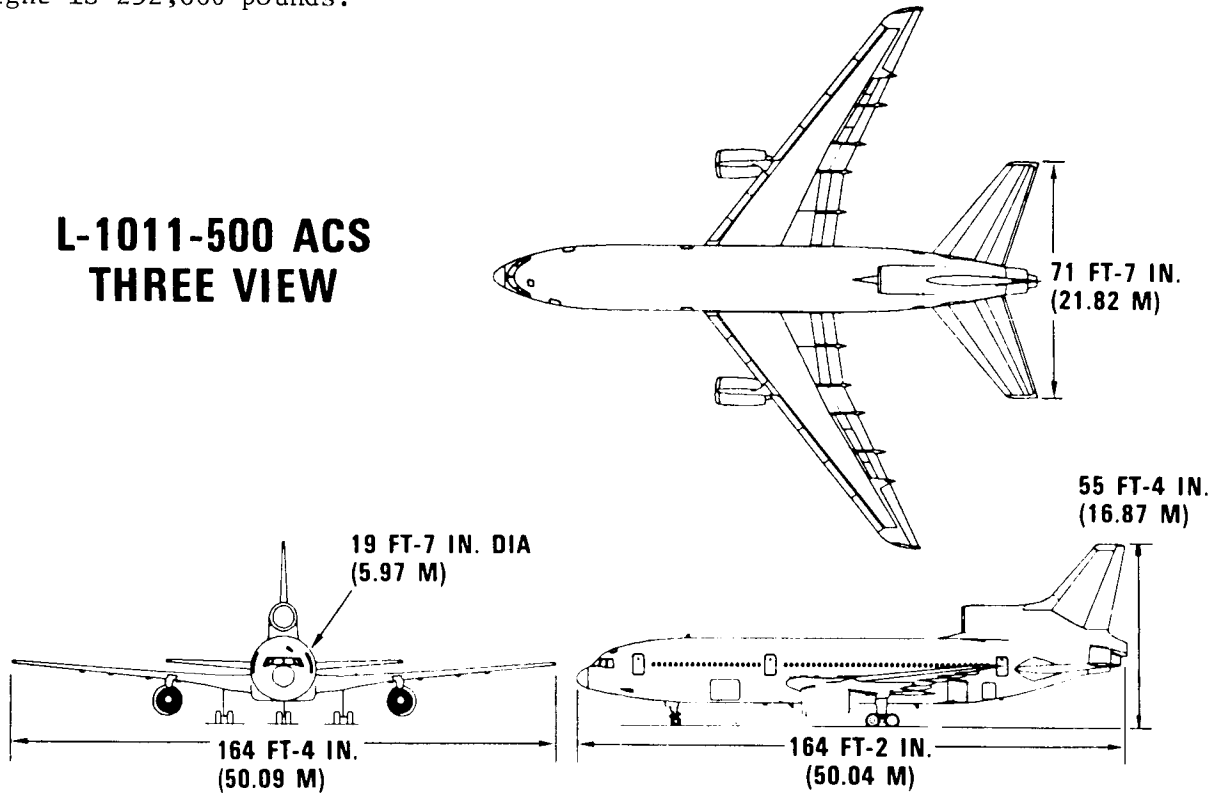
Figure 29

## WING UPPER SURFACE PANELS

The NASTRAN structural representation had 3741 degrees of freedom (DOF). The load reference or SIC locations numbered 228. The weight distribution module generated 500 panel weights and the static loads grid was defined with 289 load points. Weight and maneuver conditions were chosen to be a basis for the baseline design (Figure 30).
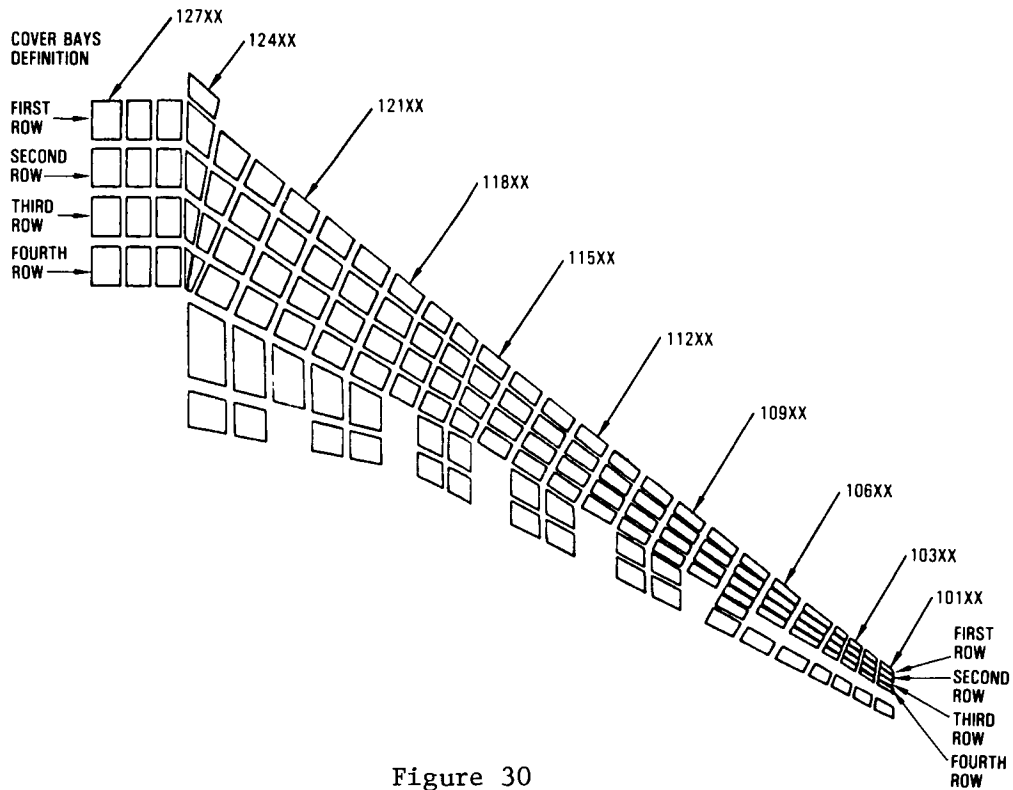
Figure 30

## STATIC LOADS

    Flight conditions were selected on the basis of a subset of the critical loads for the production airplane wing box. Both active controls on and active controls off conditions were used for symmetric manuevers. Ground handling (brake roll, etc.), and a pseudo taxi condition were also included. The airplane was trimmed for each flight condition, thereby producing net balanced airplane loads. The 25 load conditions are listed in Figure 31.

| LOAD COND. | A | B | C | D | E | F | G | H |
|---|---|---|---|---|---|---|---|---|
| FLIGHT COND. NO. | 1101 | 1102 | 1103 | 1104 | 1105 | LANDING | TAXI | BRAKE ROLL |
| WEIGHT – 1000 LB | 350.3 | 504.0 | 504.0 | 504.0 | 504.0 | 368.0 | 506.0 | 506.0 |
| C.G. – % MAC | 12.5 | 17.13 | 17.13 | 17.13 | 17.13 | 26.9 | 14.1 | 26.9 |
| FLIGHT COND. | MID-CRUISE | VA | VC | VD | FLAP | – | – | – |
| MACH NO. | 0.8 | .48 | .82 | .88 | .33 | .28 | – | – |
| VE – KEAS | 360.0 | 316.0 | 356.0 | 418.0 | 220.0 | 182.0 | – | – |
| ALTITUDE–1000 FT. | 20.0 | 0.0 | 21.3 | 17.3 | 0.0 | 0 | – | – |

| MANEUVER CONDITION | ACTIVE CONTROL (MLC) | LOAD CONDITION |
|---|---|---|
| 1G LEVEL FLIGHT – (BASIC) | ON | A |
| POSITIVE STEADY MANEUVER – (PSM) | ON | A THRU E |
| NEGATIVE STEADY MANEUVER – (NSM) | ON | A THRU E |
| POSITIVE STEADY MANEUVER – (PSM) | OFF | A THRU E |
| NEGATIVE STEADY MANEUVER – (NSM) | OFF | A THRU E |
| LANDING | ON | F |
| LANDING | OFF | F |
| TAXI | – | G |
| BRAKE ROLL | – | H |

Figure 31

# SUMMARY OF NUMERICAL RESULTS FOR VALIDATION DESIGN

There are many design details which can not practically be included in a preliminary design effort. However, if these details add significantly to weight and strength, then some accountability must be made in the design process. One objective of this numerical exercise is to quantify some of the detail design effects in terms of two approximate processes. The first process, model design factors, will account for model sizing increases required to accommodate design details which currently do not have any design criteria. Two PADS sizings will be presented in the study of the model design factors: 1) structure sized to zero margins of safety, and 2) structure sized to production margins of safety. The second process, model to hardware weight adjustments, will account for the differences between model weight derived from a finite element model representation of structural components and hardware weight derived from actual weighing of structural components.

Another objective of the design exercise is the evaluation of FSD in conjunction with the panel sizing (PSASA) program, which also produces stress allowables. Finally, the results of each engineering process will be checked for accuracy using the data base available for the reference airplane, namely the L-1011-500 ACS which is described in the validation section. The reference airplane has an active control system for maneuver load control (MLC). As part of exercising the PADS system, a wing panel sizing will be performed on the reference airplane with and without MLC for zero margins of safety. The results of the numerical study are summarized in Figure 32.

## PADS SIZINGS: NORMALIZED SURFACE WEIGHTS

|  | ZERO MARGINS | | | PRODUCTION MARGINS | | |
|---|---|---|---|---|---|---|
|  | UPPER SURFACE | LOWER SURFACE | BOTH SURFACES | UPPER SURFACE | LOWER SURFACE | BOTH SURFACES |
| REFERENCE AIRPLANE |  |  |  | 1 | 1 | 1 |
| PSASA SIZING W/MLC | .83 | .764 | .792 | .89 | .88 | .89 |
| FSD SIZING W/MLC | .845 | .781 | .808 | – | – | – |
| PSASA SIZING W/O MLC | .89 | .85 | .868 | – | – | – |

## WEIGHT FACTORS: HARDWARE WEIGHT/PRODUCTION MODEL WEIGHT = 1.2

Figure 32

# LOAD CONDITIONS YIELDING MINIMAL MARGINS OF SAFETY FOR STATIC
# AND DYNAMIC LOADS FOR REFERENCE AIRPLANE

New methodology development during 1983 made possible structural sizing for continuous turbulence in preliminary design. With techniques for computing panel octagons of equal probability for responses due to gust, static and dynamic loading conditions could be combined for purposes of determining aircraft sizing. In 1983, a sizing validation exercise, using combined gust and static loads, was performed on the PADS baseline design.

The design regions include the 1st through 4th rows of surface panels for both upper and lower surfaces. These panels were represented by a CALAC developed quadrilateral finite element (CMEMQ) in the structural model. Internal loads for the wing were computed in a NASTRAN static solution run. The Panel Sizing and Stress Allowable (PSASA) module was used for sizing of the surface panels. Optimized dimensions in PSASA are skin thickness, stringer web thickness, stringer flange thickness, and stringer height.

The loads applied to the structure for sizing include 21 static loads maneuver conditions, 4 ground handling conditions, and the 8 loads of equal probability which make up the octagons for the gust loads. Figure 33 shows the load conditions which have the minimal margin of safety for each panel for upper and lower surfaces. The margin of safety is the ratio of internal load which the panel can withstand over the applied internal load for an external load condition. Normally, this value is an input margin for the design. In cases when fail safe or fatigue conditions are imposed, the minimal margin may be somewhat greater. Gust conditions were found to be the designing factor for sections near the root rib and wing tip for both upper and lower surfaces. These areas are marked with Gs. Braking conditions determined the sizing around the main gear. Wing mid-section panels were designed by a 2.5g maneuver and these panels are indentified by the symbol x.

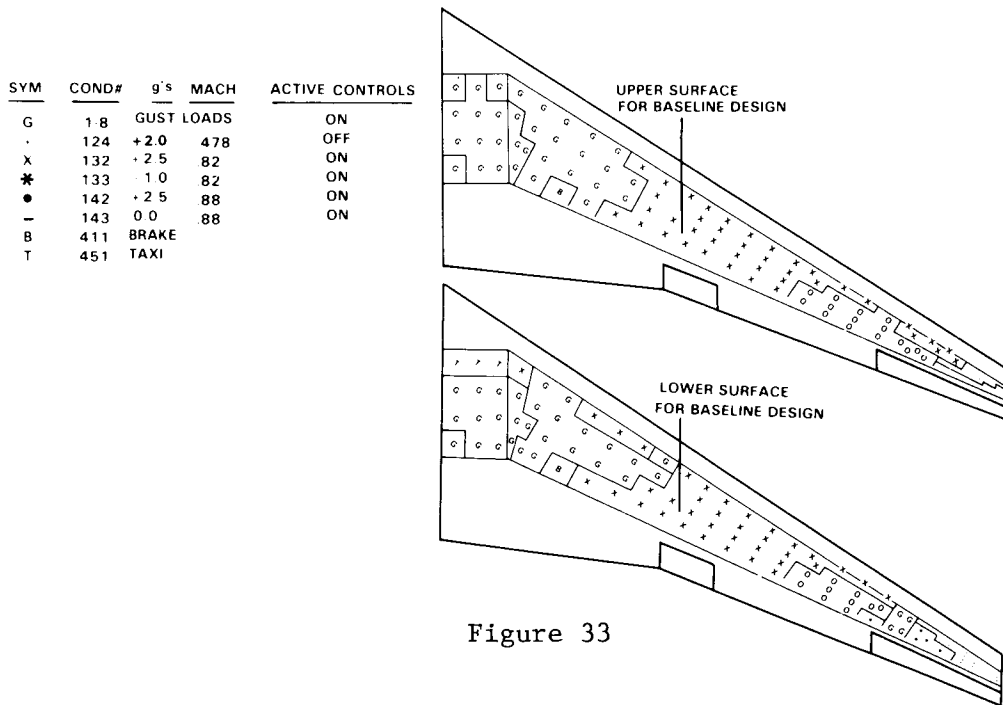| SYM | COND# | g's | MACH | ACTIVE CONTROLS |
|-----|-------|-----|------|-----------------|
| G | 1-8 | GUST LOADS | | ON |
| . | 124 | +2.0 | 478 | OFF |
| x | 132 | +2.5 | 82 | ON |
| * | 133 | -1.0 | 82 | ON |
| ● | 142 | +2.5 | 88 | ON |
| - | 143 | 0.0 | 88 | ON |
| B | 411 | BRAKE | | |
| T | 451 | TAXI | | |



Figure 33

A major portion of the work in 1982 dealt with the validation of the PADS modules by exercising them and making comparisons against a known database (baseline design). This exercise proved to be very fruitful for proposes of tuning the PADS system. In 1983 the PADS system was used to formulate an aeroelastic model of an aspect ratio 12 wing design (AR12) (Figure 34). With the incorporation of the new capabilities for the finite element generation, the grid load distribution scheme, and the fuel tank loading procedures, PADS built the necessary database and processed the high aspect ratio design through sizing for various MLC gains on the outboard aileron.

# ASPECT RATIO 12

# SWEEP 35°

# (NO GUST OR FLUTTER EFFECTS)

Figure 34

# AR12 MIDDLE 1/3 SECTION OF WING INTERNAL LOADS

The sizing procedure for the AR12 incorporated the methodology for computing the design element internal loads for applied unit external loads at the load reference points. The initial internal loads were formed for an arbitrary unit sizing. Internal loads due to the constructed 25 load conditions were formed by multiplying the load condition matrix and the internal load matrix for unit external loads. Figure 35 shows the intensity of the internal loads for the panels in the middle 1/3 section of the wingspan. Each square represents a combined normal (N) and shear (Q) internal load (lb/in) formed by one of the 25 load conditions in the middle 1/3 section of the wing.
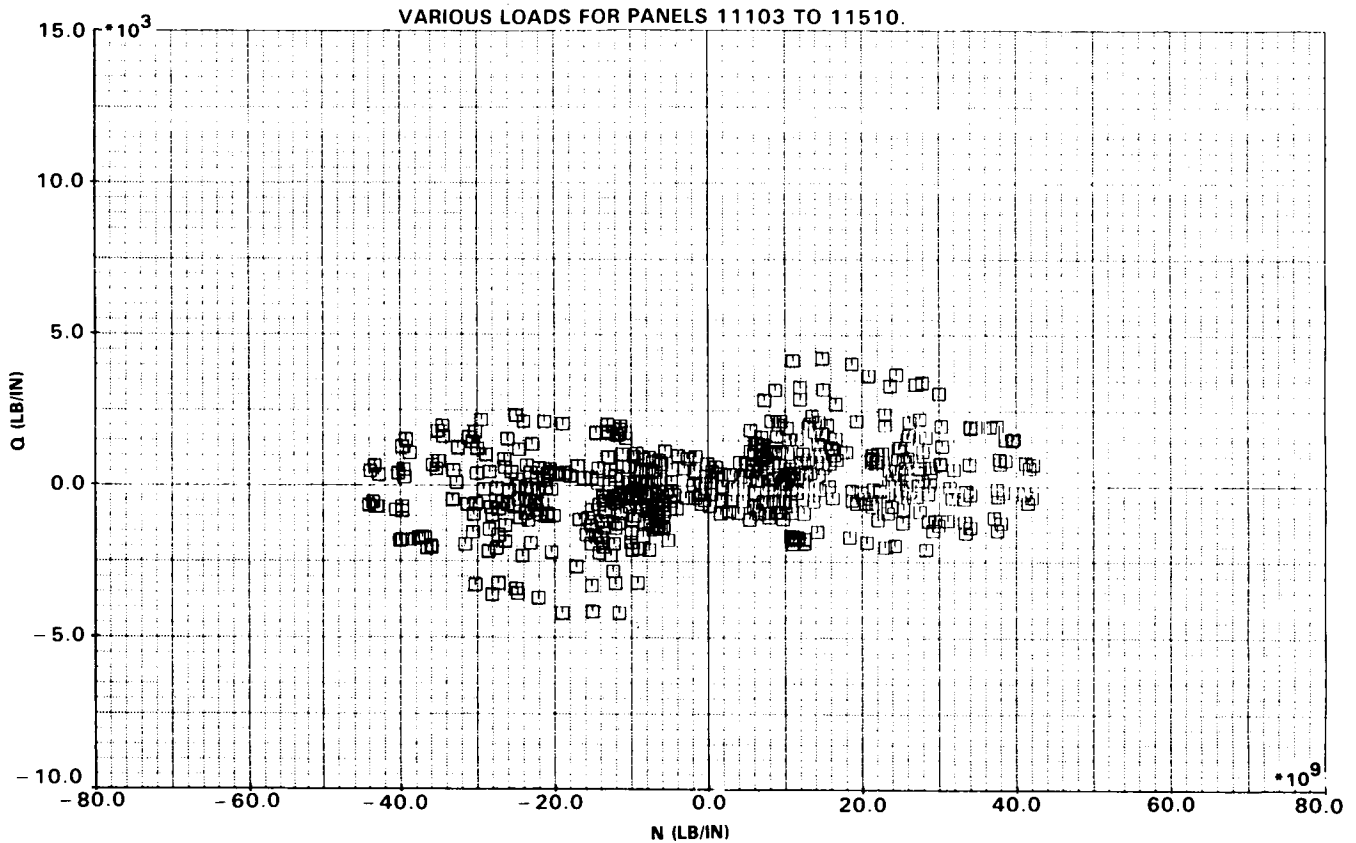


Figure 35

AR12 SWEEP 35 SIZING UPPER SURFACE 3RD FROM FRONT ROW
COMPARISON OF WEIGHT

Sizing for the internal loads was accomplished with the sized panel database approach for selection of optimal panel dimensions. The database approach consists of forming a database which contains families of optimized panels for various loading combinations. Each of the panel definitions in the database has a weight per unit area associated with it. From the database, the sizing routine selects two panels as a starting point for optimization of each panel in the design region of the airplane. The first panel is the lightest panel in the database which is sufficient to withstand all applied loads for that panel and the second is the next lightest panel in the database. These two panels are used to set the bounds on panel dimensions in the sizing procedure. The final optimized panel for each element in the design region is then computed. Variables for optimization are skin thickness, stringer web thickness, stringer flange thickness, and stringer overall height.

Figure 36 shows a comparison of the weight per unit area for upper surface panels in the third bay for rigid, first flex and second flex A/P loads.
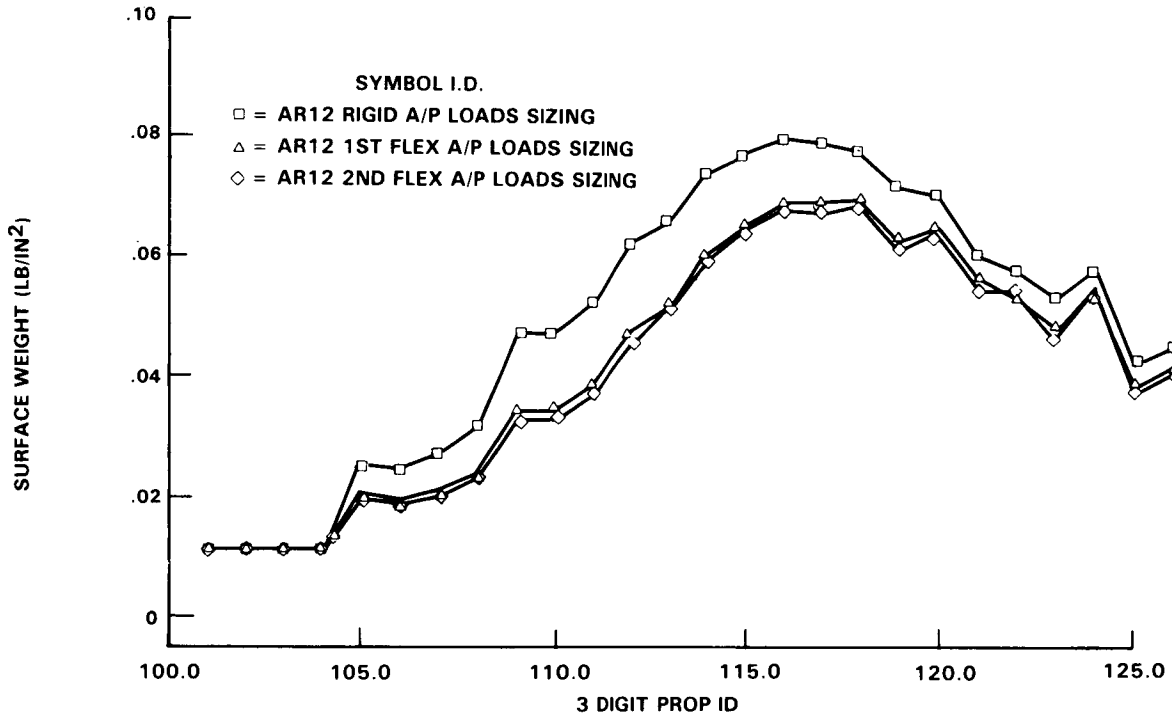


Figure 36

AR12 SWEEP 35 SIZING LOWER SURFACE 3RD FROM FRONT ROW
COMPARISON OF WEIGHT

Figure 37 shows the lower surface.  The 3-Digit Prop ID refers to the panel sta-
tion on the wing.  The layout of the panels is the same for both models with Figure 35
showing the baseline surface panel numbering convention.  The first 3 digits of the
numbers  along the 1st row represent the 3 Digit Prop ID.

ID 100 refers to panels on the wing tip while ID 125 refers to panels on the
wing box.
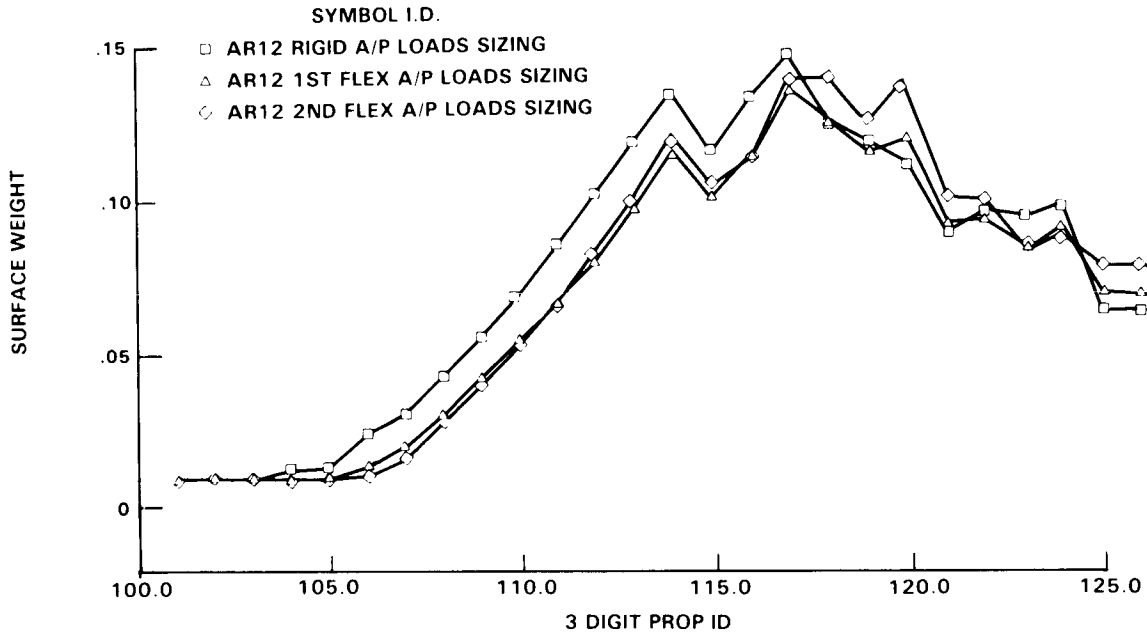
Figure 37

# STRUCTURAL SIZING ITERATIONS

Wing cover weights vs. number of structural sizing iterations is shown in Figure 38 for both upper and lower surfaces. This rapid convergence on wing cover weights has been the norm for both the baseline and the high aspect ratio designs.
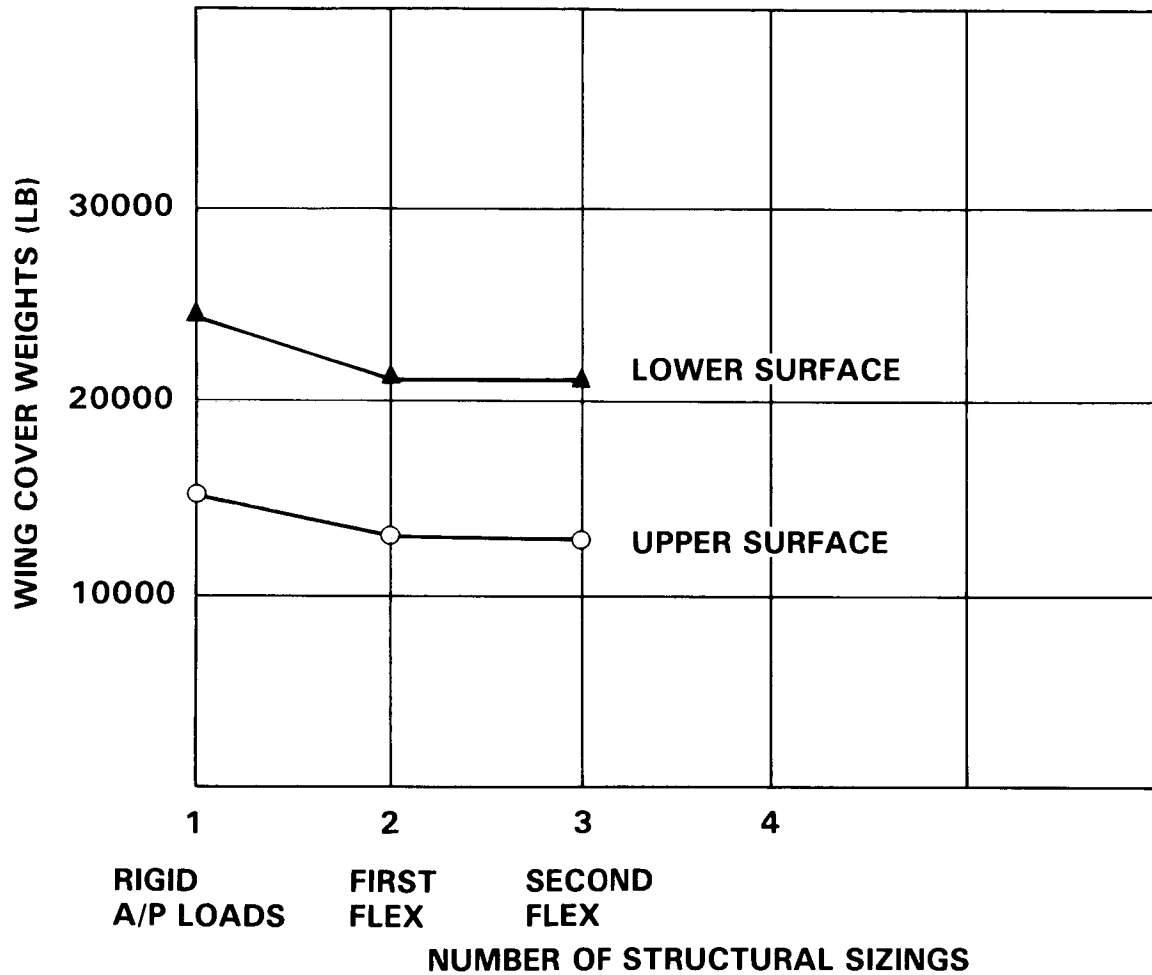


Figure 38

NET LOADS CASE 132 (X) 2ND FLEX A/P LOADS

Distribution for net loads, case 132 (X), are shown on Figure 39.

Load case 132 condition is defined by the following: GW/524354, CG/17.3, M/.82, V/356 KEAS, ALT/21300 ft., G/2.5, ACT/ON, FLAPS/0°. This case and the case shown in Figure 40 contribute to the design shown in Figure 41. The case shown in Figure 39 designs the upper and lower surface panels represented by (X) in Figure 41.
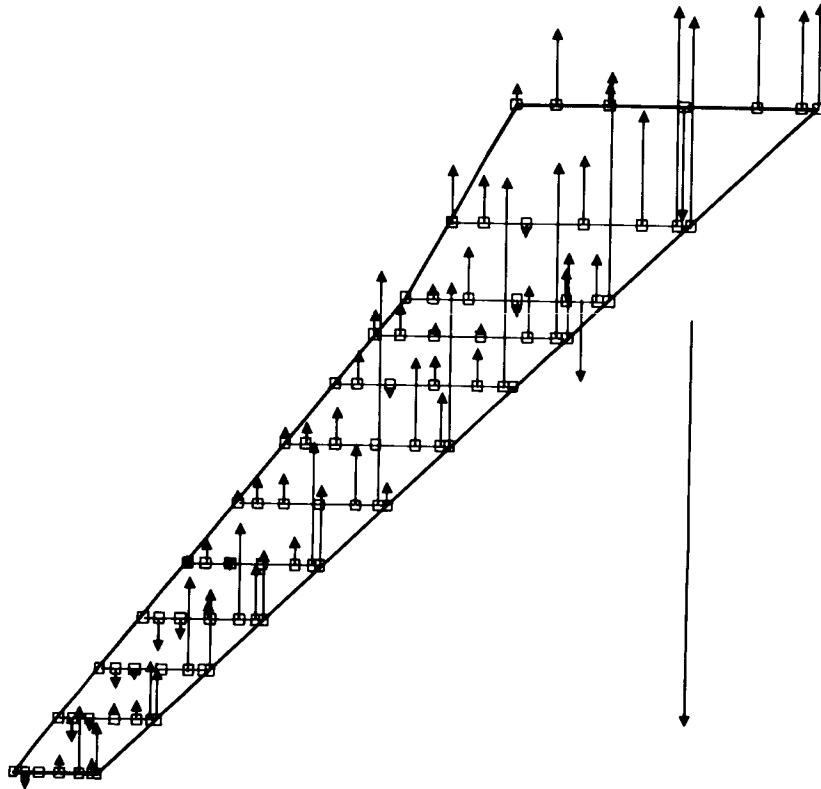
Figure 39

## NET LOADS CASE 124 (+) 2ND FLEX A/P LOADS

Distribution for net loads, case 124 (+), are shown in Figure 40. Load case 124 condition is defined by the following: GW/524354, CG/17.3, M/.478, V/316 KEAS, ALT/O FT, G/25, FLAPS/0$^{\circ}$. This case designs the upper and lower surface panels represented by (+) in Figure 41.
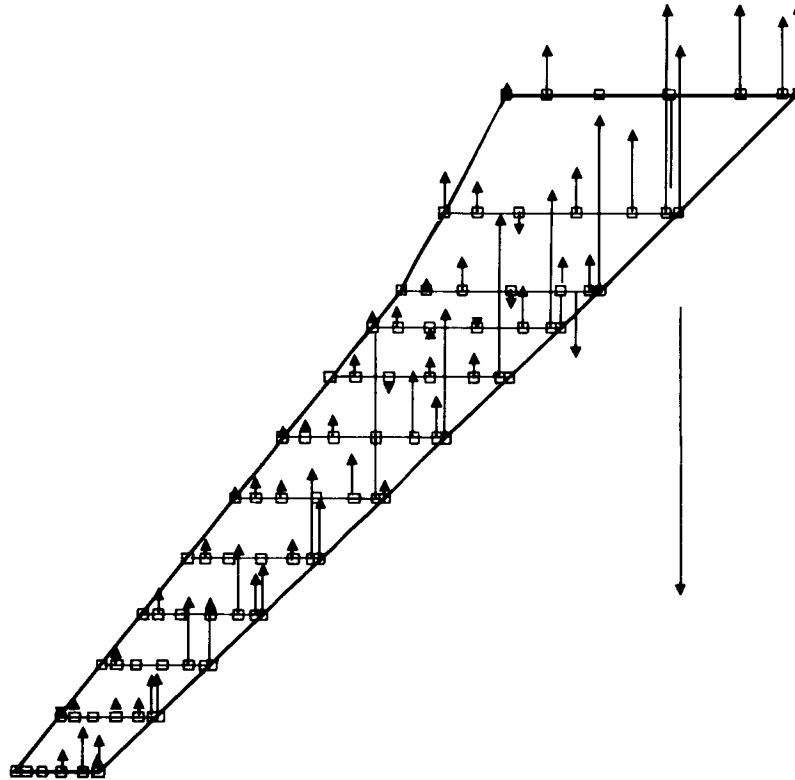


Figure 40

# LOAD CONDITIONS YIELDING MINIMUM MARGINS ON UPPER SURFACE
## PANELS AR12 SWEEP 35 2ND FLEX SIZING

Load cases which yield the minimal margin of safety after considerations in the optimization process for effects such as fatigue and fail safe conditions are shown in Figure 41. Each symbol corresponds to a load condition in the key. The symbol defines the load condition yielding the minimal margin for the corresponding panel.

| SYMBOL | COND# | g's | MACH | ACTIVE CONTROLS |
|--------|-------|-----|------|-----------------|
| # | 122 | 2.5 | .473 | ON |
| + | 124 | 2.0 | .473 | OFF |
| × | 132 | 2.5 | .82 | ON |
| * | 133 | - 1 | .82 | ON |
| ● | 142 | 2.5 | .88 | ON |
| . | 143 | 0 | .88 | ON |

UPPER SURFACE

LOWER SURFACE

Figure 41

498
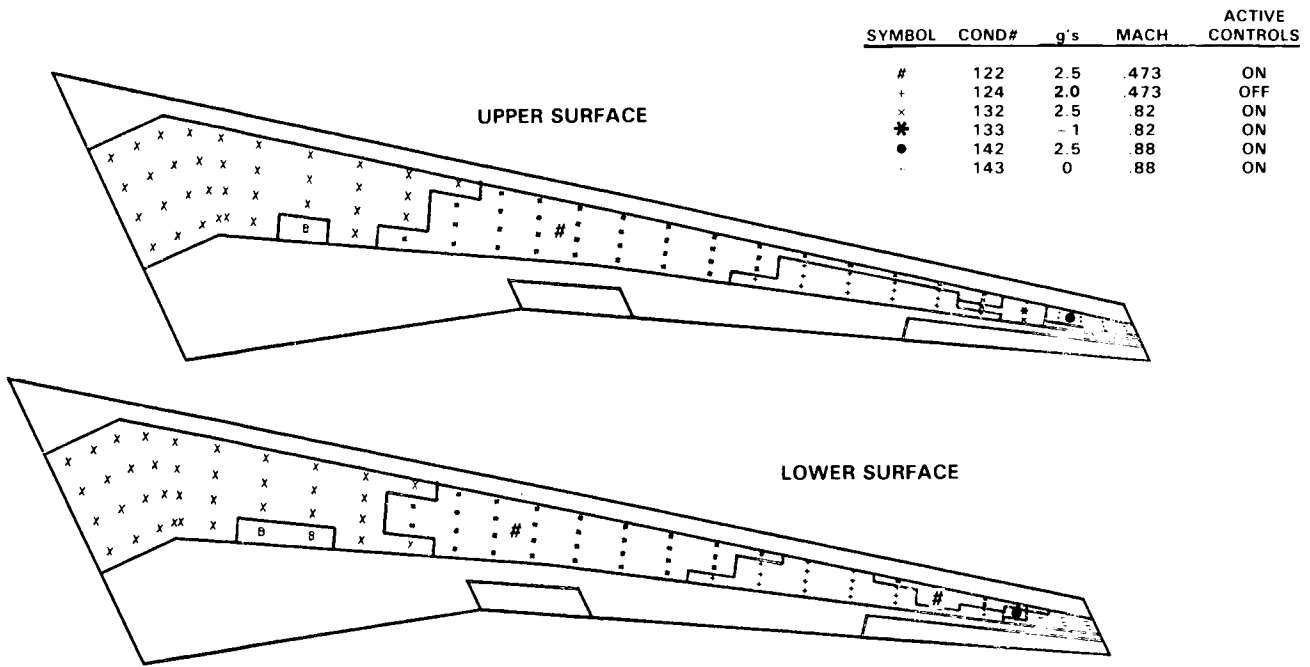
# COVER WEIGHTS FOR DIFFERENT MLC AILERON GAINS

    Different aileron-degree-per-g gains were used to generate the wing cover weights and indicate that a bucket exists for a gain of 20 degrees/g. If 20 degrees/g were selected, then the area around the aileron would have to be increased by almost a factor of 2 to reduce the gain around the 10 degrees/g. Eighty-six percent of the weight reduction takes place within 50 percent of the optimum gain factor (Figure 42). These results were produced for fixed spar web sizings.
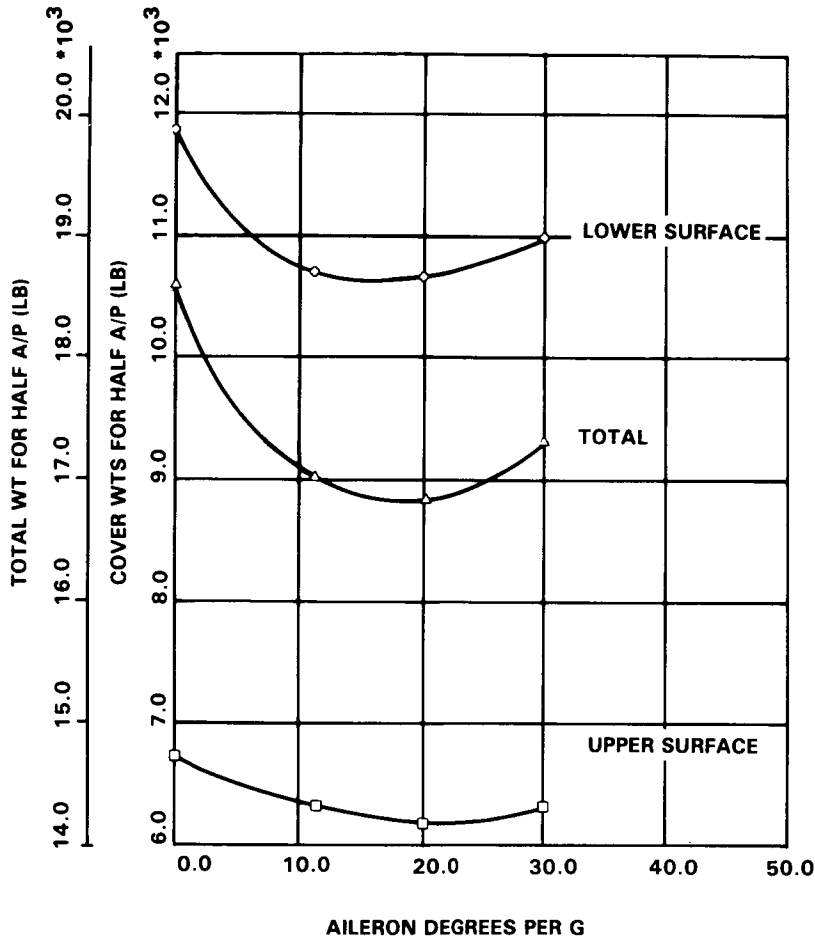


Figure 42

# WING WEIGHT PERCENT REDUCTION VS. LIMIT MANEUVER FACTOR

For an MLC gain of 11.33 degrees per g on the outboard aileron, wing weight percent reductions were computed for designs with and without MLC and for changing the limit maneuver load factor from 2.5 to 2.0 g's (Figure 43). The MLC increment is the percentage reduction of wing weight when MLC is added to the wing cover design. The maneuver limit increment is the percentage reduction of wing weight when the maneuver limit factor is reduced from 2.5 g to 2.0 g. Both columns are additive. For the AR12 SWEEP 35 design, the wing weight would be 16.8% less for a design incorporating both MLC and 2.0 g maneuver limit load factor than for a design with a maneuver limit factor of 2.5 g and no MLC.

| AIRCRAFT | MLC INCREMENT | MANEUVER LIMIT = 2 G INCREMENT FROM 2.5 G |
|---|---|---|
| REFERENCE AIRCRAFT AR 7.63 SWEEP 35 | 4.5 | |
| AR12 SWEEP 35 | 5.1 | 11.7 |

Figure 43

## PADS DESIGN ACTIVITY IN PROCESS

This Lockheed inhouse work is being coordinated with the NASA Langley Research Center multilevel design research activity under a cooperative effort to design an aircraft wing for fuel efficiency. The primary objective of this effort is to study and evaluate the multilevel and the PADS/ASSET approaches to aircraft wing design. Lockheed is providing a common design data base for this effort to NASA under the contract NAS1-16794. The contract technical monitor is Dr. J. Sobieski. The first phase of this study is projected for completion in December 1984 (Figure 44).

- **ASPECT RATIO 12 SWEEP 35**

  - **VERTICAL GUST LOADS**

  - **FLUTTER**

- **ASPECT RATIO 12 SWEEP 25**

  - **MANEUVER, BRAKE, LANDING LOADS**

  - **VERTICAL GUST LOADS**

  - **FLUTTER**

Figure 44

SUMMARY AND CONCLUSIONS

The following observations are provided as a summary review in support of the conclusions (Figure 45):

## CBUS Operating System

- An operating system has been defined and coded which provides the user with a continuous computing option without interfering with the standalone function of any participating program or system.

- The concept of a command has been developed as a driver for the data flow control and program execution requirements of an engineering process.

- The concept of altercards provides data paths into the command to change default attributes and/or to invoke other options.

- A command processor language has been developed which provides logical branching capabilities but leaves the naming of the commands/macros to the user.

- The concept of a supercommand provides the grouping of commands and other supercommands and includes all the command processor language capabilities.

## Data Management System

- All existing data management systems are available to provide retrieval and storage of permanent data blocks and communication with these systems is achieved by means of commands and subcommands.

- An internal data management system has been defined which supports the retrieval and storage of data by simple qualifiers so as to retain the simple functionality of a command.

## Design and Engineering Processes

- An aeroelastic design process has been defined in terms of production design computing tools and without violating the conceptual and early preliminary design phase elapsed time constraints.

- The design process has been modularized into specific engineering processes that closely followed the production design definitions.

- The concept of a finite element model generator for a family of aircraft structures has been formulated to satisfy the elapsed time constraints.

## Validation Using a Known Design Data Base

- The model to hardware weight ratios showed greater than expected variations with span.

- The engineering processes defined as the panel sizing and stress allowable generator, fully stressed design, weight, static loads, gust loads, and flutter were exercised and checked using a known aircraft design data base.

- The PADS wing panel sizing of a reference airplane design produced panel model weights that were 21 percent below the reference airplane values for zero structural margins of safety. The difference was reduced to 11 percent when production structural margins were used in sizing the panels.

502

SUMMARY AND CONCLUSIONS (Continued)

High Aspect Ratio Wing Designs

- Aspect ratio 12, sweep 35 design is almost complete.
- Aspect ratio 12, sweep 25 design has been started.

- **ACQUIRED A RAPID AEROELASTIC ANALYSIS AND DESIGN CAPABILITY**

- **DEMONSTRATED PADS CONCEPT OF USING EXISTING COMPUTER TOOLS TO GENERATE AEROELASTIC DESIGNS**

- **SATISFIED REQUIREMENTS OF FLEXIBILITY AND MODULARITY WITH CBUS**

- **VALIDATED CBUS OPERATION AND RUN DATA BASE MANAGEMENT SYSTEM**

- **VALIDATED SOME OF THE ENGINEERING PROCESSES; NOT COMPLETED**

- **DEMONSTRATED THE NEED FOR ADEQUATE DESIGN VISIBILITY AND CONTROL**

Figure 45

BIBLIOGRAPHY

Radovcich, N.A., "Preliminary Design of Structures [PADS], Methods Development and Application," AGARD paper, Conference Proceedings No. 354, presented at the 56th Structures and Materials Panel Meeting, London, United Kingdom, April 1983.

DESIGN ENHANCEMENT TOOLS
IN MSC/NASTRAN

D. V. Wallerstein
The MacNeal-Schwendler Corporation
Los Angeles, California

# DESIGN SENSITIVITY IN OPTIMIZATION

Design sensitivity (ref. 1) is the calculation of derivatives of constraint functions with respect to design variables. While a knowledge of these derivatives is useful in its own right, the derivatives are required in many efficient optimization methods. Constraint derivatives are also required in some reanalysis methods. Figure 1 shows where the sensitivity coefficients fit into the scheme of a basic organization of an optimization procedure (ref. 2). In the context of this paper the analyzer is to be taken as MSC/NASTRAN. The terminator program monitors the termination criteria and ends the optimization procedure when the criteria are satisfied. This program can reside in several places: in the optimzer itself, in a user written code, or as part of the MSC/EOS (Engineering Operating System) currently under development. Since several excellent optimization codes exist and since they require such very specialized technical knowledge, the optimizer under the new MSC/EOS is considered to be selected and supplied by the user to meet his specific needs and preferences. The one exception to this will be a fully stressed design (FSD) based on simple scaling. The gradients are currently supplied by various design sensitivity options now exisiting in MSC/NASTRAN's design sensitivity analysis (DSA).
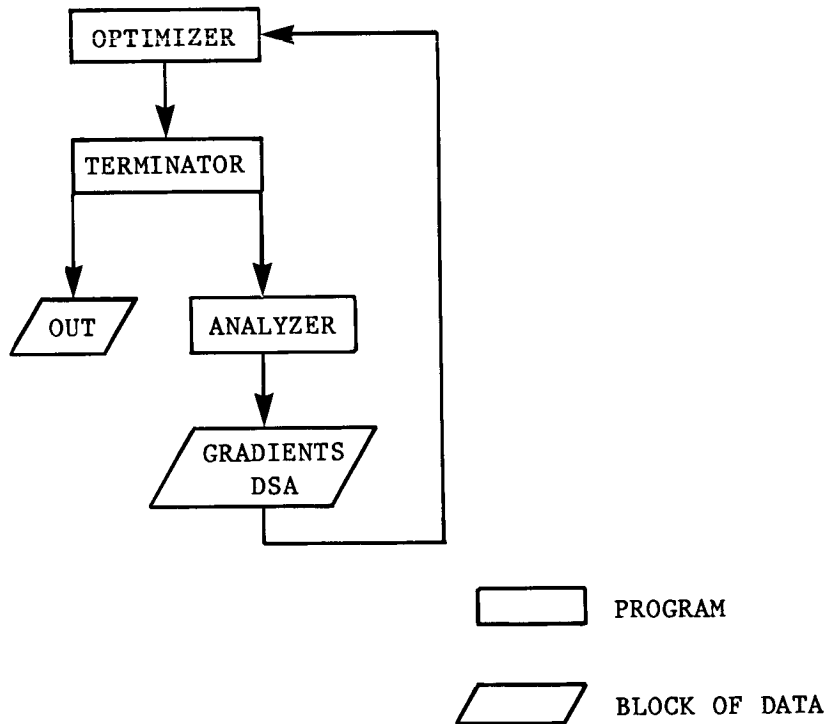


Figure 1

## DESIGN CONSIDERATIONS - USER ISSUES

Figure 2 outlines several implementation issues that were considered for the current MSC/DSA and are still valid for future enhancements.  From a user standpoint, the computations of the gradients should be a natural extension of the finite element analysis (FEM).  At the same time, the user should not be constrained by the FEM to the degree that he or she is forced to make unwanted adaptations of design requirements.  To this end, MSC/DSA has been designed to have generality in modeling complex designs and to allow for design variables which are not explicitly defined in terms of standard finite element properties such as area, second moments of area, and thickness.  By the same token, MSC/DSA must not and does not impose any size restrictions on the analysis.  On the other hand, through its ability to link many finite element property cards and material cards into a single design variable, MSC/DSA allows for computational efficiency by reducing the number of design variables needed for analysis.  The output is in two forms. A matrix is generated with both the current value of the constraint and the values of the gradients output to the data base and to a general FORTRAN file.  To aid the user in interpreting the results, this same information is output in table form with both numeric and user supplied BCD identifiers.

- EASE OF USE

- GENERALITY TO MODEL COMPLEX DESIGNS

- CAPACITY TO SOLVE LARGE PROBLEMS

- OUTPUT EASY TO COMPREHEND

Figure 2

507

## DESIGN CONSIDERATIONS - ANALYSIS ISSUES

Figure 3 gives the three prime issues considered in selecting the approach used for MSC/DSA. The general philosophy followed was that MSC/DSA be considered a post-processor to a standard MSC/NASTRAN analysis. This requirement was easily met through use of data-basing. Through the data base the LU decomposition of the stiffness matrix is recovered so that only backward operations are used to recover the solution vector needed to compute gradient terms. An important feature of the implementation is the table driven nature of MSC/DSA. Final recovery of all information needed to form gradients is handled by standard MSC/NASTRAN stress, force, displacement, or modal recovery modules. This means that the only new features added to MSC/NASTRAN are those which form the necessary correlation tables between constraints and their derivatives and the needed code to form the right hand side needed for solution vector recovery. The net result is ease and reliability in system maintenance.

- RESTART FROM PRIMARY ANALYSIS

- ONLY BACKWARD OPERATIONS USED TO RECOVER SOLUTION VECTOR

- DATA ORGANIZATION, ASSEMBLY AND RECOVERY

Figure 3

## DEFINITION OF TERMS

Figure 4 lists the meaning of some terms used in the following discussion. It is appropriate, however, to mention two things at this point. First, MSC/DSA does not impose any constraint equations. It merely returns the value of the constraint at the current point in design space. Second, the approach is the design space approach and not the adjoint method. The adjoint method is discussed only for comparison purposes. The two methods arise from the technique used to determine the value of the second term in the expression for $\delta\Psi_i$.

$\{b\}$ — Vector of Design Variables

$\{u\}$ — Vector of Displacements

$\{P\}$ — Vector of Loads

$[K]$ — Structural Stiffness

$\{\xi_i\}$ — Vector of Adjoint Variables

$$[H] = \left[\frac{\partial P}{\partial b}\right] - \left[\frac{\partial K}{\partial b} u\right]$$

$\Psi_i(b, u) \leq 0$ — Constraint Equation

$$\delta\Psi_i = \left\{\frac{\partial\Psi_i}{\partial b}\right\}^T \{\delta b\} + \left\{\frac{\partial\Psi_i}{\partial u}\right\}^T \{\delta u\} \quad \text{— Sensitivity Coefficient}$$

$B = b/b_0$ — Normalized Design Variable

$\Lambda_{ij}$ — Sensitivity Coefficient for $i^{th}$ Constraint and $j^{th}$ Design Variable

Figure 4

As mentioned in the previous figure, the difference between the adjoint method – sometimes called behavior space or state space and the design space method is how the $\{\delta u\}$ term is replaced by $\{\delta b\}$ in the expression for $\delta \Psi_i$. These two methods are depicted in figure 5. Notice that both require LU decompositions and formation of the $[H]$ matrix. The effect of the right hand sides is discussed in the next figure.

$$\{\delta u\} \longleftarrow \{\delta b\}$$

ADJOINT METHOD

$$[K]\{\xi_i\} = \left\{\frac{\partial \Psi_i}{\partial u}\right\}$$

$$\left\{\frac{\partial \Psi_i}{\partial u}\right\}^T \{\delta u\} = \{\xi_i\}^T [H]\{\delta b\}$$

DESIGN SPACE METHOD

$$[K]\left\{\frac{\partial u}{\partial b}\right\} = [H]$$

$$\{\delta u\} = \left\{\frac{\partial u}{\partial b}\right\}^T \{\delta b\}$$

Figure 5

# THEORY COMPARISONS OF TWO APPROACHES

Figure 6 gives a direct comparison of the two methods. The adjoint method uses the $\{\partial\Psi_i/\partial u\}$ vector to generate the right hand side. Only active constraints are used to generate this vector; hence, the number of unknown equations at any given point in design space is equal to the number of active constraints. In the design space method the right hand side is represented by the matrix $[H]$. This matrix is a true pertubation of the load vector for a change in each design variable and represents the perturbed equilibrium state of the structure. There is a column for each load vector perturbed by a design variable.

| Approach | Adjoint Method | Design Space |
|---|---|---|
| Unknowns | $\{\xi_i\}$ | $\left[\dfrac{\partial u}{\partial b}\right]$ |
| Set of equations to be solved | $[K]\{\xi_i\} = \left\{\dfrac{\partial\Psi_i}{\partial u}\right\}$ | $[K]\left[\dfrac{\partial u}{\partial b}\right] = [H]$ |
| Number of unknown vectors to be determined | Number of active constraints | Number of design variables times Number of load conditions |

Figure 6

Figure 7 compares the two methods from a different point of view. Generally, discussion of which method to use stems from the number of right hand side vectors. But such discussion rarely takes into consideration the efficiency of modern equation solvers. When this efficiency is taken into consideration the number of unknowns to solve for takes on less significances than other considerations. Two major advantages of the design space approach have already been alluded to. First, the [H] matrix represents a perturbation of equilibrium and its formulation fits neatly into an existing finite element code (also it must be formed in the adjoint method) and forms a natural load vector. Second, the formulation of the gradients fits in naturally with existing general purpose finite element code data recovery operations. Finally, a major expense in either method is the forming of the necessary correlation tables between constraints and design variables and the forming of the correlation between design variables and individual element properties.

| Item | Adjoint Method | Design Space |
|---|---|---|
| Few active constraints | Small advantage | -- |
| Many active constraints Few design variables | -- | Small advantage |
| Forming right hand side using existing code structure | -- | Major advantage |
| Forming gradients using existing code structure | -- | Major advantage |
| Forming necessary correlation tables relating element variables to design variables and response variables to constraints | Major expense | Major expense |

Figure 7

## THE DESIGN SPACE INCREMENTAL APPROACH

Figure 8 shows the necessary incremental equations required for the design space approach. Notice that perturbation to nodal equilibrium occurs from two sources, a change in stiffness arising from design variable perturbation of the element stiffness matrices and a change in the actual load vector arising from the same source. Also note that for accuracy and consistancy a total solution vector not an incremental one is formed.

$$[K^o]\{\Delta u_B\} = \{\Delta P_B\} - [\Delta K_B]\{u^o\}$$

$$\{\Delta P_B\} = \{\Delta P_{temp}\} + \left\{[\Delta M_B]\{Rigid\text{-}Body\ Acceleration\}\right\}$$

$$\{u\} = \{u^o\} + \{\Delta u_B\}$$

Figure 8

513

# SOME MORE DEFINITIONS

Figure 9 contains some definitions unique to this paper. These definitions are mostly self explanatory.

Q  - MSC/NASTRAN OUTPUT SUCH AS:

- Displacement

- Stress

- Force

$Q^B$ - OUTPUT VALUE USING NEW PROPERTY ORIGINAL SOLUTION VECTOR

$Q^U$ - OUTPUT VALUE USING ORIGINAL PROPERTY NEW SOLUTION VECTOR

$Q^O$ - OUTPUT VALUE USING BASE LINE RUN

Figure 9

## ACTUAL GRADIENT COMPUTATION

Figure 10 gives the actual gradient computation as used by the design space approach. The top equation is used for "element" type constraints (meaning element stress or force) with self terms. Self terms arise when a specific element is used as a constraint <u>and</u> one or more of its physical properties (such as area, second moment of area, etc.) is included in a design variable <u>and</u> the derivative of the constraint with respect to that specific design variable is required. The bottom equation is used for "element" type constraint without self terms and displacement type constraints. The incremental change in design variable is represented by $\Delta B_j$ and $Q_{Lim_i}$ are user supplied limit values used in constraint evaluations. The upper signs are associated with maximum type constraints and the lower signs are associated with minimum type constraints. The various values of Q come directly from stress, force, or displacement output files standard to MSC/NASTRAN.

$$\Lambda_{ij} = \pm \frac{Q_i^{B_j}}{\left\lceil Q_{Lim}\right\rceil_i \Delta B_j} \mp \frac{Q_i^o}{\left\lceil Q_{Lim}\right\rceil_i \Delta B_j} \pm \frac{Q_i^{u_j}}{\left\lceil Q_{Lim}\right\rceil_i \Delta B_j} \mp \frac{Q_i^o}{\left\lceil Q_{Lim}\right\rceil_i \Delta B_j}$$

or

$$\Lambda_{ij} = \pm \frac{Q_i^{u_j}}{\left\lceil Q_{Lim}\right\rceil_i \Delta B_j} \mp \frac{Q_i^o}{\left\lceil Q_{Lim}\right\rceil_i \Delta B_j}$$

Figure 10

Figure 11 gives the current user interface scheme. MSC/DSA is currently designed to run as a post-processor to the standard MSC/NASTRAN static solution sequence (SOL 61), modal solution sequence (SOL 63), and buckling solution sequence (SOL 65). The MSC/DSA solution sequence numbers correspond to each of the basic solution sequences. To aid in relating specific constraints to specific design variables two new case control cards have been defined. Constraints are defined via the DSCØNS cards and design variables are defined via the DVAR-DVSET cards.

SOL 51 ⎫
SOL 53 ⎬   EXECUTIVE
SOL 55 ⎭

SENSITY ⎫
        ⎬   CASE CONTROL
SET2    ⎭

DSCONS ⎫
DVAR   ⎬   BULK DATA
DVSET  ⎭

Figure 11

## RELATING CONSTRAINTS TO DESIGN VARIABLES

The user may be interested in the derivatives of every constraint with respect to every design variable. If this is so, just set SENSITIVITY = ALL. On the other hand, it may be more reasonable in analysis to relate specific constraints to specific design variables as depicted in figure 12. In this figure, structure located at A is considered far enough removed from structure located at B that derivatives of constraints at A with respect to design variables at B (or vice versa) would be meaningless. The SET, SET2, SENSITIVITY combination allows the user to define specific constraint design variable relationships. This combination shown relates in section A constraints 1 through 4 to design variables 70, 80, and 90. In section B the relationships are constraint 300 related to design variables 1 and 3; and constraints 100, 200, and 500 related to design variables 1, 3, and 4.
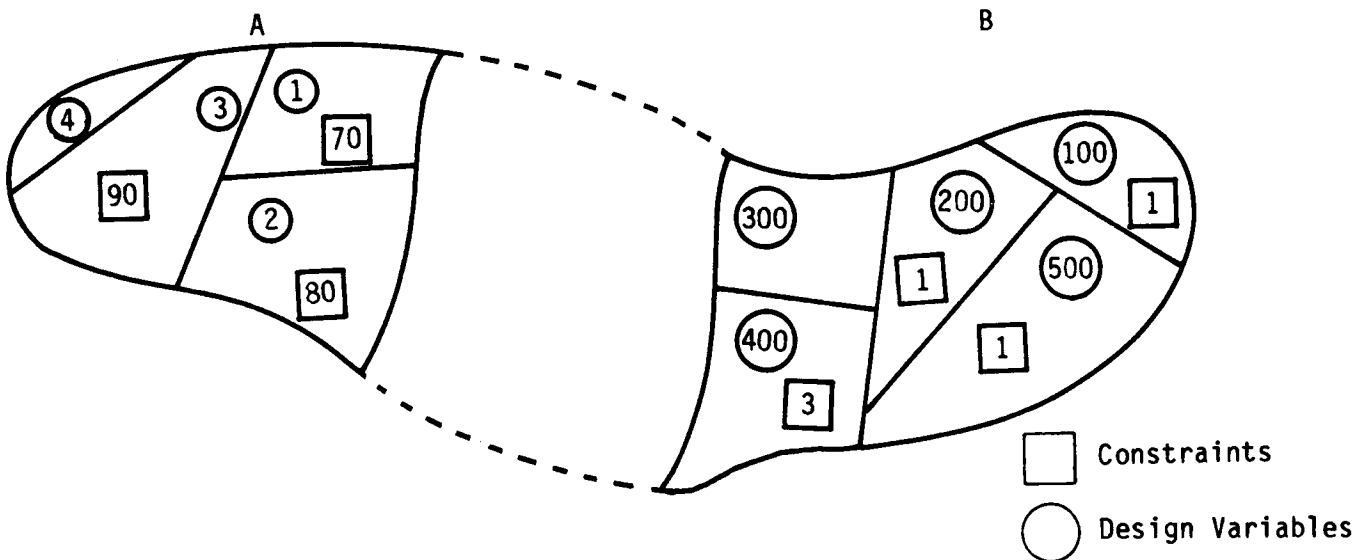


SET 1 = 1 THRU 4
SET 2 = 300                    Defines sets of DSCONS cards
SET 5 = 100, 200, 500

SET 30 = 70, 80, 90
SET 31 = 4                     Defines sets of DVAR cards

Then the following SET2 card may be defined:

SET2 = 18 (1,30), (2,33), ((5), (31,33))

and the following SENSITIVITY card is specified as:

**SENSITIVITY = 18**

Figure 12

Figure 13 shows how constraints are defined with the DSCØNS bulk data card. Each constraint must have a unique DSCID for internal and external identification. The LABEL is for user convenience in identification of output. TYPE is any one of the following: DISP, FØRCE, STRESS, LAMDA, or FREQ. ID identifies the actual grid element. CØMP identifies the specific displacement component or stress or force component. LIMIT and ØPT define the equations used for the constraint. If LIMIT = 0., then plus or minus the constraint value is returned depending on the value of ØPT.

| 1 | 2 | 3 | 4 | 5 | 6 | 7 | 8 | 9 | 10 |
|---|---|---|---|---|---|---|---|---|---|
| DSCONS | DSCID | LABEL | TYPE | ID | COMP | LIMIT | OPT | | |
| DSCONS | 21 | DOOR | DISP | 4 | 1 | .06 | MAX | | |

$$\text{(Upper Limit)} \quad \Psi_i = \frac{(\text{Constraint Value})^0}{|\text{Limit}|} - 1.0* \text{ Sign (Limit)}$$

or

$$\text{(Lower Limit)} \quad \Psi_i = 1.0* \text{ Sign (Limit)} - \frac{(\text{Constraint Value})^0}{|\text{Limit}|}$$

Figure 13

518

## DESIGN VARIABLE DEFINITION

Figure 14 shows the DVAR-DVSET cards needed for design variable definition. Each BID must be unique and define a design variable. Again, LABEL is a user convenience. DELTAB defines the incremental change in normalized design variables. VID points to a DVSET card or cards. The VID on the DVSET card need not be unique. TYPE defines the property being modified and FIELD defines the specific field on the property card being modified. PREF and ALPHA along with DELTAB define the actual change in property value. PID1 etc. define the specific property cards modified.

| 1 | 2 | 3 | 4 | 5 | 6 | 7 | 8 | 9 | 10 |
|---|---|---|---|---|---|---|---|---|---|
| DVAR | BID | LABEL | DELTAB | VID | VID | VID | VID | VID | ABC1 |
| DVAR | 10 | DOOR | .01 | 2 | 3 | 6 | 60 | 100 | |



$$P_o = P_o + \sum_{cards} Pref\left[(1 + \Delta B)^{\alpha} - 1\right]$$
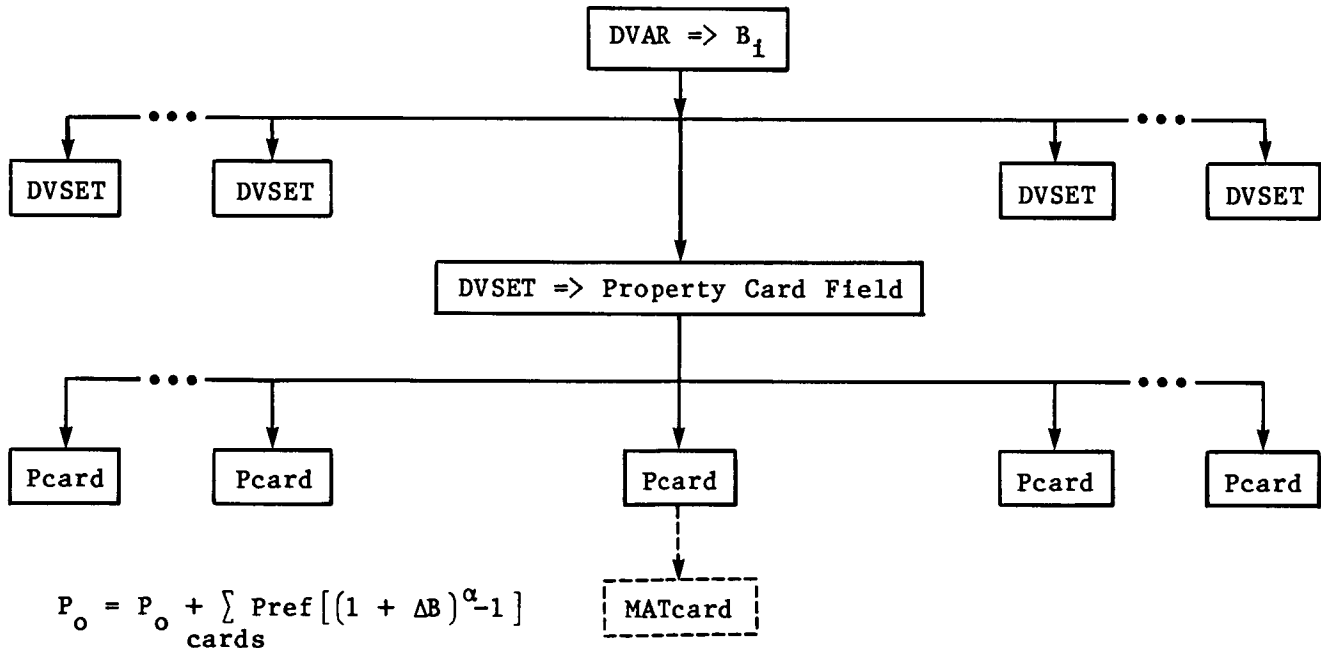
Figure 14

Output in MSC/DSA is of two types. Printed output gives the current constraint values and their derivatives along with all the user identifying labels and matrix output for use in optimization programs. The user will find the printed output so clean and self-explanatory that there is no need to discuss it. Figure 15 shows the form of the matrix output. The matrix is design constrained DC wide and its rows are grouped by design variables. The number of rows in each group is the total number of loads. The very first block gives the current constraint values.
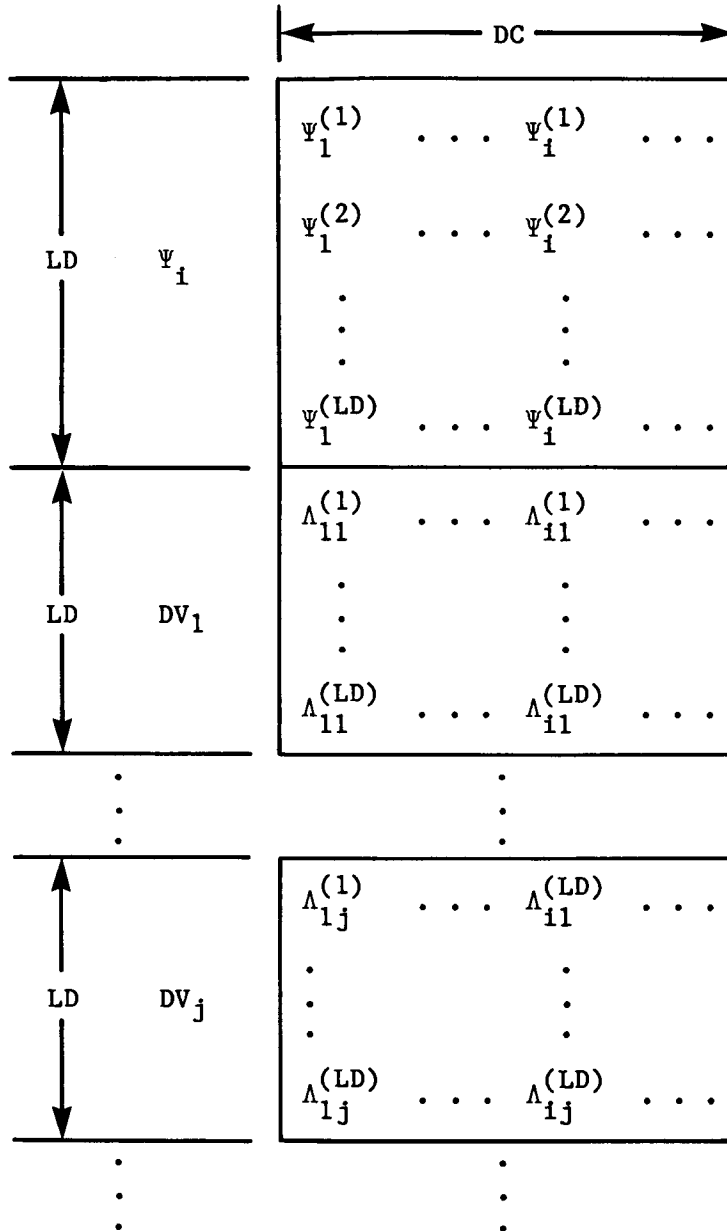


Figure 15

## SENSITIVITY COEFFICIENTS

The primary use of sensitivity coefficients is in optimization. However, it is often useful to look at them in their own right as tools that begin to give the analyst a "feel" of the structure. Figure 16 summarizes their meaning. For example, a positive sensitivity coefficient means that for an increase in design variable the value of the constraint will increase. This will move the design closer to a MAX constraint or further from a MIN constraint. Similar statements hold for a negative sensitivity coefficient.

$$\frac{\Delta \Psi}{\Delta B} > + \text{ B INCREASE } \Psi$$

$$\frac{\Delta \Psi}{\Delta B} < 0 + \text{ B DECREASE } \Psi$$

Figure 16

## EXTENSION TO SUPERELEMENT ANALYSIS

Currently MSC/DSA does not allow for substructuring or, as it is called in MSC/NASTRAN, superelement analysis. The inclusion of MSC/DSA into superelement analysis requires the establishment of ground rules as listed in figure 17. To this end, design variables are considered global in nature. This means the design variable must have a unique definition across all superelements. This requirement is necessary because design variables linking can extend across superelement boundaries. DSCØNS cards are local to superelements since they can define local quantities. DVSET cards are local to superelements since they point to property cards which (under current superelement development) are local to superelements. SENSITY cards are by superelement case control. ØBJF (structural weight) is accumulated for all superelements and its derivatives computed for all design variables.

- DVAR CARDS ARE GLOBAL


- DSCONS CARDS ARE LOCAL TO SUPERELEMENT


- DVSET CARDS ARE LOCAL TO SE


- SENSITY CARDS ARE BY SE CASE CONTROL


- OBJF CARD ABOVE SUBCASE LEVEL


Figure 17

# USER DEFINED CONSTRAINT RELATIONSHIPS

Currently, constraints are restricted to displacements, or specific stress or force output. It would be advantageous to define response values such as those depicted in figure 18. Here it is assumed that the constraint is related to the panel stress, either through the distortion energy relationship or through the utilization relationship.

$$\text{RESPONSE VALUE} = \text{MAX}\left(\beta_1, \ \beta_2\right)$$

$$\beta_1 = \sqrt{\left(\sigma_1^2 + \sigma_2^2 - \sigma_1 \sigma_2\right)/\bar{\sigma}_+} \qquad \text{(TENSION)}$$

$$\beta_2 = \frac{1}{2}\left(\frac{\sigma_L}{\bar{\sigma}_-} + \sqrt{\left(\frac{\sigma_L}{\bar{\sigma}_-}\right)^2 + 4\left(\frac{\tau_{XY}}{\bar{\tau}}\right)^2}\right) \qquad \text{(COMPRESSION)}$$

$$\sigma_L = \text{MIN}\left(o, \ \sigma_X, \ \sigma_Y\right)$$

Figure 18

Figure 19 demonstrates the proposed extension of the constraint card to include user defined relationships. Here the constraint points to a user defined equation rather than a specific stress component. Other than the first two fields, the EQN card is free field. The equations are written using standard FORTAN type nomenclature and include standard type functions such as MØD, MAX, MIN, SØRT etc. The Fi expressions are key word type expressions defined via the FUN1 card. The FUN1 card returns a value to Fi based on either the specified stress component directly or a table look-up relating the stress value to some functional relationship such as a current value of an allowable.

| 1 | 2 | 3 | 4 | 5 | 6 | 7 | 8 | 9 | 10 |
|---|---|---|---|---|---|---|---|---|---|
| DSCONS | DSCID | LABEL | TYPE | ID | COMP | LIMIT | OPT | EQUID | |
| DSCONS | 17 | SX123 | STRESS | 417 | | | MAX | 34 | |

| | | | | | | | | | |
|---|---|---|---|---|---|---|---|---|---|
| EQN | EQID | -- | FREE | FIELD | -- | -- | -- | -- | |
| EQN | 34 | MAX | (SQRT( | F1** | 2+F2* | *2- | F1*F | 3), | ABC |

| | ✕ | | | | | | | | |
|---|---|---|---|---|---|---|---|---|---|
| +BC | | (F4+ | SQRT( | F4** | 2+4.* | F5** | 2))) | | |

$$VALUE = EQN\ (F1,\ F2,\ \ldots\ F11)$$

$$VALUE = MAX\left(\sqrt{F1^2 + F2^2 - F1 * F3}\ ,\ \left(F4 + \sqrt{F4^2 + 4\ F\ 5^2}\right)\right)$$

| FUN1 | NAME | A | COMP | TID | ALPHA | BETA | B | | |
|---|---|---|---|---|---|---|---|---|---|
| FUN1 | F7 | | 2 | 32 | | | | | |

$$F_i = \left[A(Y)^\alpha + B\right]^\beta$$

Y = Function (Value of COMP)

Response Value = EQN (F1, F2, ... FN)

Figure 19

Figure 20 is a schematic of the MSC/EØS (Engineering Operating System) currently under development. The keys to this system are the MSC Data Base and the new (currently under code development) MSC/NDDL executive. The NDDL (Nastran Data Definition Language) provides the foundation for the development of a complete engineering data management system to support the various MSC analytical modules shown on the various spokes of figure 20. Since the NDDL provides a means of specifying a logical data structure definition it provides for the unique identification and addressability of the data and provides for the definition of the interdependencies of the data. Data Base managing will include such items as automatic storage and retrieval of data for ease of use; data recovery, integrity, and security procedures to insure data validity; and all current GINØ (general purpose input/output routines) calling sequences. Notice that the axle of the figure represents an extension of GINØ to include direct user interface between a user defined programming system (where for example the actual optimization programs will lie) and the NNDL and hence the Data Base. Through this interface new entry points into functional modules are provided so that the user's optimization routines can for example initiate new MSC/NASTRAN analysis or MSC/DSA analysis, or query the Data Base. Although the user is expected to supply his own optimization, note that one spoke includes a MSC/FSD (Fully Stressed Design) option. As envisioned, the user will have, through the interface module and the NNDL, access to any spoke or the rim or both.
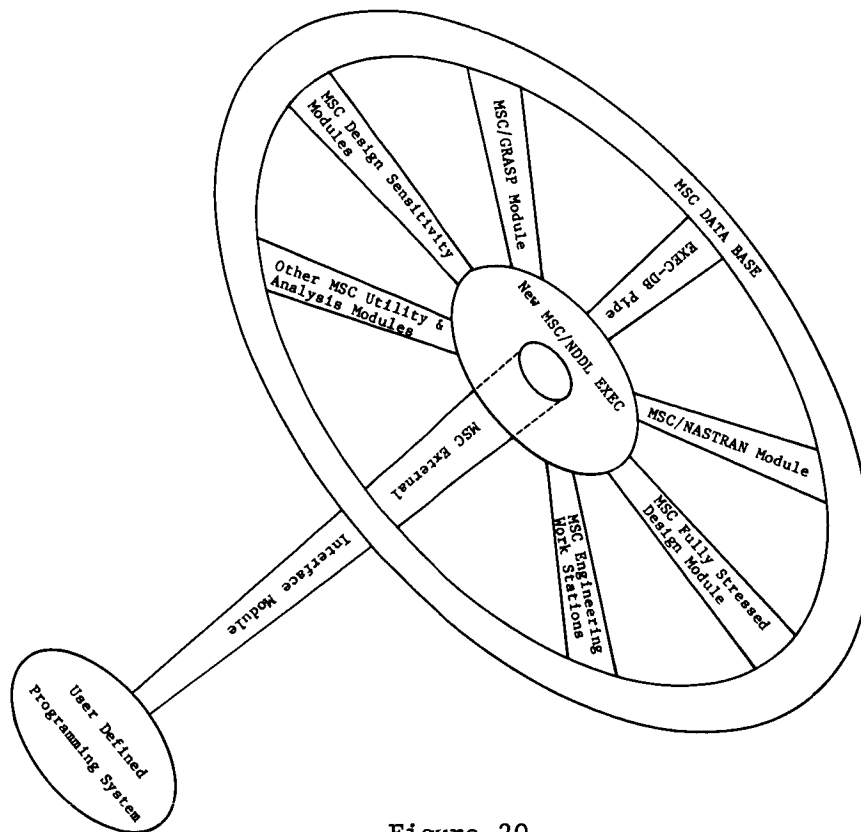


Figure 20

# REFERENCES

1. Arora, S.J.; and Haug, E.J.: Methods of Design Sensitivity Analysis in Structural Optimization. AIAA J., vol. 17, no. 9, 1979, pp. 970-974.

2. Sobieszczanski-Sobieski, Jaroslaw; and Rogers, James L.: A Programming System for Research and Applications in Structural Optimization. Proceedings International Symposium on Optimum Structural Design, 11th ONR Naval Structural Mechanics Symposium, Oct. 19-22, 1981, University of Arizona, Tuscon Arizona, pp. 11-9 to 11-21.

PROGRESS REPORT ON THE "AUTOMATED
STRENGTH-AEROELASTIC DESIGN OF AEROSPACE
STRUCTURES" PROGRAM

E. H. Johnson
Northrop Corporation, Aircraft Division
Hawthorne, California

V. B. Venkayya
Air Force Wright Aeronautical Laboratories
Wright-Patterson Air Force Base, Ohio

## INTRODUCTION

This paper describes an ongoing program whose goal is to develop an auto-mated procedure that can assist in the preliminary design of aircraft and space structures. As Figure 1 indicates, the program is sponsored by the Air Force Wright Aeronautical Laboratories with Northrop Corporation, Aircraft Division, as the prime contractor and Universal Analytics, Inc., a subcontractor.

The paper is entitled a "Progress Report" because it reports on an ongoing effort. The presentation will be limited to a discussion of the approach and capabilities that are to be included in the final procedures. An exception is that the Executive System is defined and tested to an extent sufficient to permit specific results to be included in the presentation.


CONTRACT NUMBER:        F33615-83-C-3232


SPONSOR:                AIR FORCE WRIGHT AERONAUTICAL LABORATORIES


PROGRAM MONITOR:        DR. V. B. VENKAYYA


CONTRACTOR:             NORTHROP CORPORATION, AIRCRAFT DIVISION


SUBCONTRACTOR:          UNIVERSAL ANALYTICS, INC.


PERFORMANCE PERIOD:     JULY 1983 - MARCH 1988


Figure 1

## MOTIVATION

The motivation for this program comes from a number of sources (Figure 2). First, there is a need for a procedure of this type that integrates the disciplines which drive structural design concepts with powerful optimization techniques. Existing procedures that approach this capability are deficient in their analysis techniques and their optimization methods and/or are not in the public domain. Additional motivating factors are to exploit the rapid advances that have been made in automated design algorithms, computer hardware and computer software. For instance, in the automated design area, recent research has shown the similarity of optimum criterion methods and mathematical programming approaches and has shown how approximate analyses can replace most of the detailed analyses formerly required in a design task (Ref. 1). It is hardly necessary to mention the revolutionary progress being made in computer hardware and, with modern data base concepts and structured programming, in software techniques.

- EXISTING PROCEDURES ARE CONSIDERED OUTDATED AND INADEQUATE

- IMPROVED UNDERSTANDING OF AUTOMATED DESIGN

- IMPROVED HARDWARE

- IMPROVED DATA HANDLING

- IMPROVED LANGUAGE - FORTRAN 77

Figure 2

## REQUIREMENTS

In developing the procedure, a number of basic requirements must be kept in mind (Figure 3). For instance, for the program to be useful, it must include analysis techniques from the technical disciplines that impact the preliminary design of aerospace structures. The procedure must also be efficient in its use of computer resources in order that its stated capabilities be affordable. It must also be recognized that a large array of related analysis procedures already exists in the environment this new procedure will enter. This program should, to the extent practicable, be compatible with these existing procedures. Finally, difficulties associated with the introduction of a new procedure must be minimized by providing well written and ample documentation.


- **INTERDISCIPLINARY**


- **EFFICIENT**


- **COMPATIBLE**


- **UNDERSTANDABLE**


Figure 3

## PROGRAM TASKS

The program is divided into six interrelated tasks (Figure 4). In the recently completed Design System Definition task, architecture of the procedure was defined and basic design issues were resolved. The current effort is focused on the development of the unique executive system and data base manager that will be used. The Module Development task, which is also under way, will integrate the engineering analysis techniques into the procedure. A "Pilot System," which will contain the key features of the final system, will be delivered in late 1985. Design studies will refine the procedure and apply it to practical design problems drawn from ongoing development activities. Under the User Guidelines task, comprehensive documentation of the procedure's structure, capabilities and input requirements will be developed. Results from applying the procedure and recommendations for its use will also be given.

## PHASE

| | |
|---|---|
| I | DESIGN SYSTEM DEFINITION |
| II | EXECUTIVE/DATA BASE CODING |
| III | MODULE DEVELOPMENT |
| IV | PILOT SYSTEM |
| V | DESIGN STUDIES |
| VI | USER GUIDELINES |

Figure 4

## SYSTEM ARCHITECTURE

The basic components of the system are identified in Figure 5. The Executive System is the heart of the software and directs program execution, data base control and system input and output. A new programming language entitled MAPOL (Matrix Analysis Problem Oriented Language) has been developed to drive the procedure. The Data Base System is a combination of a relational data base system (Ref. 2) which handles basic engineering data and a separate matrix handler to efficiently store and retrieve the matrix information using sophisticated packed formats. The functional modules perform the engineering tasks and are literally modularized for ease of program enhancement and modification. A utilities library will contain all basic matrix manipulation procedures and assorted miscellaneous operations such as search and sort routines. This will serve to eliminate redundant coding and help ensure its reliability.
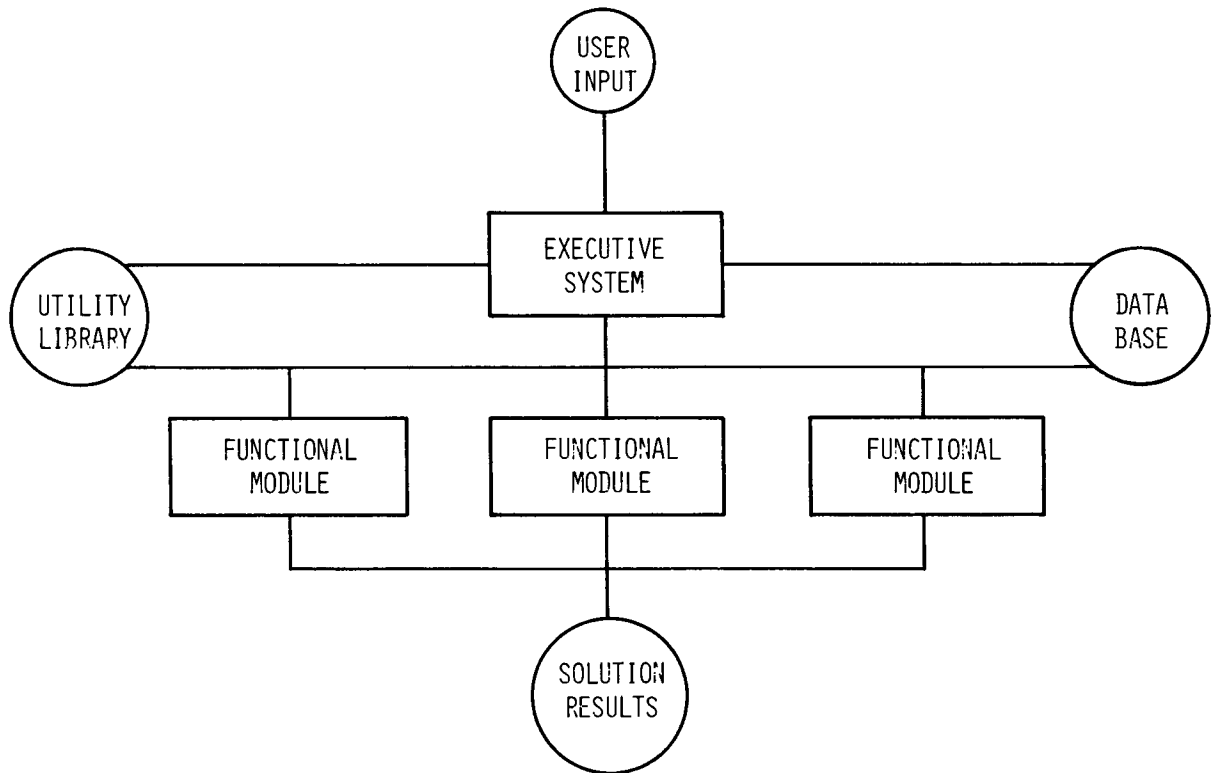
Figure 5

# EXECUTIVE SYSTEM

The Executive System is the heart of the software and performs four primary functions, as shown in Figure 6. Module sequence control is facilitated by a problem-oriented language called MAPOL. The actual execution of modules within the system will be performed by a "pseudo-machine," similar to the execution monitor concept of NASTRAN. This model is extremely flexible and powerful. Data management is a critical part of a large-scale analysis system both in terms of function and performance. The need to locally modify data while performing design optimization is ideally addressed by a relational data base system such as the RIM (Ref. 3) system. However, the need for the efficient manipulation of very large matrices requires that sophisticated packed formats, along with appropriate algorithms, be available. Therefore, the concept of a "partitioned data base" has been defined to satisfy both needs. The User-Interface includes simple, easy-to-use input data entry. Accurate, informative and user-friendly messages will be issued by the software instead of the often obscure programmer-oriented jargon often encountered. Solution results will be user-selectable and will be printed in a clear, easy to read manner. The allocation of computer resources and interfaces with the operating system of the procedure's host computer are also handled by the executive.

- **MODULE SEQUENCE CONTROL**

- **DATA MANAGEMENT CONTROL**

- **USER-INTERFACE CONTROL**

- **COMPUTER RESOURCE ALLOCATION**

Figure 6

## THE MAPOL LANGUAGE

The execution of the procedure is directed by a sophisticated control
language which can be most readily described as being an updating of the DMAP
language used in NASTRAN (Ref. 4).  Figure 7 provides a list of features of
the language.  The language recognizes scalars, vectors, matrices and relations
and has a number of intrinsic procedures to deal with each.  A user can also
construct special purpose procedures and structured programming features such
as IF-THEN-ELSE, DO-WHILE and DO-UNTIL are available.  With these features,
the user has considerable flexibility and power in directing the sequence
of the program's execution.  The language also simplifies the coding task by
substituting the higher level capability of MAPOL for detailed FORTRAN program-
ming.


● SPECIAL DATA TYPES FOR MATRICES AND RELATIONS


● PERMITS USER WRITTEN PROCEDURES


● CONTAINS STRUCTURED PROGRAMMING FEATURES


● INCLUDES A UTILITY LIBRARY


● CAN OPERATE DIRECTLY ON THE DATA BASE


Figure 7

Figure 8 provides a simple application of the MAPOL language in order to clearly illustrate some of its features.  The program reads in three matrices and operates on them in one of three different ways depending on whether the parameter ALPHA is negative, zero or positive.  The input matrices are printed after they are input while the output matrix and two scalar parameters are printed at the completion of the task.

```
PROGRAM MATRIX
MATRIX A, B, C, X;
REAL ALPHA, BETA;
CALL INPUT;
CALL PRINT (A, B, C);
IF (ALPHA < 0) THEN
    X : = A * B + C;
ELSE ·
    IF (ALPHA = 0) THEN
        X : = TRANS (BETA * A + B);
    ELSE
        X : = A * A * INV (C);
    ENDIF
ENDIF
CALL PRINT (ALPHA, BETA, X);
END;
```

Figure 8

# ENGINEERING MODULES

The scope of the engineering capabilities of the procedure is indicated by Figure 9, which lists the six distinct disciplines that are to be included to provide comprehensive preliminary design. In most cases, proven engineering software can serve as a resource for the various technologies. Candidate engineering analysis tools include NASTRAN, USSAERO (Ref. 5), Doublet Lattice (Ref. 6), and ADS (Ref. 7). The sensitivity module, which will provide gradient information, requires significant new coding while the other modules will be significantly altered to interact with the data base and the utilities library. The controls response analysis module is included in recognition of the increasingly important interactions between the control system and the structural response in the design of aerospace structures.

- STRUCTURAL ANALYSIS

- AERODYNAMIC LOADS

- AEROELASTIC STABILITY

- SENSITIVITY ANALYSIS

- OPTIMIZATION TECHNIQUES

- CONTROL RESPONSE ANALYSIS

Figure 9

MILESTONES

An indication of the scope of the project is given in Figure 10. The
entire project is slated to last for almost five years. As the figure indicates,
much of this time is to be spent in testing and debugging the procedure,
the rationale being that the eventual success of the procedure rests heavily
on making it as reliable and fully tested as practicable. Other milestones
include the recently completed design of the system architecture and the
implementation of this architecture by early next year. A pilot system,
which will incorporate the major design capabilities of the procedure, will
be delivered in early 1986. The final system delivery is scheduled for September
1987 with a training workshop for interested government and industry personnel
slated for early 1988.


PROGRAM GO-AHEAD                            JULY 1983

SYSTEM ARCHITECTURE DESIGNED                JANUARY 1984

DATABASE AND EXECUTIVE SYSTEM CODED         JANUARY 1985

PILOT SYSTEM DELIVERY                       JANUARY 1986

FINAL SYSTEM DELIVERY                       SEPTEMBER 1987

TRAINING WORKSHOP                           JANUARY 1988


Figure 10

## CONCLUSIONS

Because this presentation is a progress report, it is not possible to present conclusions in the usual sense. Instead, some summarizing comments on how the various attributes of the system will meet the goals set for the project will be offered. Firstly, by using proven engineering software as a basis for the project, a reliable and interdisciplinary procedure will be developed. The use of a control language for module sequencing and execution permits efficient development of the procedure and gives the user significant flexibility in altering or enhancing the procedure. The data base system will provide reliable and efficient access to the large amounts of interrelated data required in an enterprise of this sort. In addition, the data base will allow interfacing with existing pre- and post-processors in an almost trivial manner. Altogether, the procedure promises to be of considerable utility to preliminary structural design teams.

## REFERENCES

1. Fleury, C., and Schmit, L.A., Jr., "Dual Methods and Approximation Concepts in Structural Synthesis," NASA CR-3226, December 1980.

2. Date, C.J., An Introduction to Database Systems, Addison-Wesley Publishing Co., Reading, Massachusetts, 1977.

3. Gray, F.P., and Wahlstrom, S.O., "RIM-5 User's Guide," Boeing Commercial Airplane Company, 1981.

4. The NASTRAN Programmer's Manual (Level 17.4), NASA SP-223 (04), Section 4, December 1979.

5. Woodward, F.A., "An Improved Method for the Aerodynamic Analysis of Wing-Body-Tail Configurations in Subsonic and Supersonic Flow, Part I - Theory and Applications," NASA CR-2228, May 1973.

6. Giesing, J.P., Kalman, T.P., and Rodden, W.P., "Subsonic Steady and Oscillatory Aerodynamics for Multiple Interfering Wings and Bodies," Journal of Aircraft, Vol. 9, No. 10, October 1972, pp. 693-702.

7. Vanderplaats, G.N., Sugimoto, H., and Sprague, C.M., "ADS-1: A New General-Purpose Optimization Program" Proceedings of the AIAA/ASME/ASCE/ AHS 24th Structures, Structural Dynamics and Materials Conference, Part 1, Lake Tahoe, Nevada, May 1983.

| 1. Report No.<br>NASA CP-2327, Part 1 | 2. Government Accession No. | 3. Recipient's Catalog No. |
|---|---|---|
| 4. Title and Subtitle<br><br>RECENT EXPERIENCES IN MULTIDISCIPLINARY ANALYSIS AND OPTIMIZATION | | 5. Report Date<br>September 1984 |
| | | 6. Performing Organization Code<br>505-33-53-12 |
| 7. Author(s)<br><br>Jaroslaw Sobieski, Compiler | | 8. Performing Organization Report No.<br>L-15830 |
| | | 10. Work Unit No. |
| 9. Performing Organization Name and Address<br><br>NASA Langley Research Center<br>Hampton, Virginia 23665 | | 11. Contract or Grant No. |
| | | 13. Type of Report and Period Covered<br>Conference Publication |
| 12. Sponsoring Agency Name and Address<br><br>National Aeronautics and Space Administration<br>Washington, DC 20546 | | 14. Sponsoring Agency Code |

| 15. Supplementary Notes |
|---|
| |

16. Abstract

This conference publication contains the papers presented at the NASA Symposium on Recent Experiences in Multidisciplinary Analysis and Optimization, held at NASA Langley Research Center, Hampton, Virginia, April 24-26, 1984. The purposes of the symposium were to exchange information about the status of the application of optimization and the associated analyses in industry or research laboratories to real life problems, and to examine the directions of future developments. Within the broad statement of the symposium's purpose, information exchange has encompassed examples of successful application; identification of potential applications and benefits, even though no attempt to apply optimization may have been made as yet; synergistic effects of optimized interaction and trade-offs occurring among two or more engineering disciplines (e.g., structural engineering and aerodynamics) and/or subsystems in a system (e.g., propulsion and airframe in aircraft); and computer technology in the context of the foregoing. This information exchange has covered aerospace and other industries as well as universities and government agencies.

The goal of the meeting was to reach a better understanding of the extent to which optimization and the associated analyses are being used, development directions, the future potential, and actions that ought to be taken to realize the potential sooner. That goal was attained and there was a consensus that multidisciplinary analysis and optimization have an important potential as aids to human intellect in the design process, and that the cooperation of industry, academia, and government, under NASA leadership, is needed to realize that potential.

| 17. Key Words (Suggested by Author(s))<br><br>Optimization<br>Synthesis<br>Systems<br>Sensitivity<br>Computers | 18. Distribution Statement |
|---|---|

| 19. Security Classif. (of this report)<br>Unclassified | 20. Security Classif. (of this page)<br>Unclassified | 21. No. of Pages<br>546 | 22. Price |
|---|---|---|---|